



Climate change impacts on Caribbean coral reefs: reef accretion and scope for acclimation through symbiont genetic diversity

Submitted by **Emma Victoria Kennedy** to the University of Exeter
as a thesis for the degree of
Doctor of Philosophy in Biological Sciences
in April 2013

This thesis is available for Library use on the understanding that it is copyright material and that no quotation from the thesis may be published without proper acknowledgement.

I certify that all material in this thesis which is not my own work has been identified and that no material has previously been submitted and approved for the award of a degree by this or any other University.

Signature: *Emma Kennedy*

Abstract

Caribbean coral reefs are in crisis. Degradation of living coral and fish assemblages has accelerated during the past half century, with a suite of anthropogenic drivers –from local fishing pressure to unprecedented global scale climate change– implicated. Accompanying these losses is the physical disintegration of the three-dimensional calcium carbonate reef structure. Flattening of reefs, synonymous with loss of ecosystem function and provision of services, is caused by an imbalance in the carbonate budget: a trade-off between carbonate production and consolidation by calcifying organisms (principally coral-algal symbioses) and framework breakdown by bioeroding organisms and storms.

This thesis focuses on expanding our understanding of two functionally critical issues that strongly influence Caribbean coral reef community composition and dynamics, and which look likely to have a key bearing on the future state of reefs in the region: coral photosynthetic endosymbionts, and carbonate budgets. The former exert an important role in the production of the coral carbonate framework, whilst the latter reflect the dynamics of reef carbonate production and erosion. In the first part of the thesis, existing information on rates of carbonate production and erosion on Caribbean reefs is utilised to construct a detailed theoretical carbonate budget model. The model is used to chart historic changes in Caribbean carbonate budgets, tracking reef flattening across time and identifying key ecological drivers of these changes. This “eco-geomorphic” model is then coupled with state-of-the-art climate and ecological models, to project reef processes to the end of the century, asking the question ‘at what point will Caribbean reefs shift to net erosional regimes?’. The models are also used to explore the efficacy of local management and climate mitigation in altering the negative trajectory of reefs under projected warming and ocean acidification.

In the second part of the thesis, 632 corals from across the wider Caribbean are screened, to construct the largest recorded baseline of symbiont biogeography for the region’s key remaining reef framework builder, *Montastraea annularis*. Spatial patterns of symbiont diversity are explored in terms of environmental, geographic and genetic factors, contributing to the growing body of work currently in the early stages of cataloguing symbiont diversity and its ecological significance.

Although carbonate budget models forecast a bleak outlook for the Caribbean, detection of widespread low-level prevalence of thermally-tolerant endosymbionts in *M. annularis* provides a weak ‘nugget of hope’ for potential coral acclimation. Combined local management and aggressive mitigative action on carbon emissions are pre-requisites for maintenance of functioning reefs into the next century. Coral reef conservation efforts can be improved if we fully appreciate the contributions of *all* reef components –not just the enigmatic ones– to healthy reef functioning.

For the beautiful reefs of the Caribbean

And for Duncan

Patience is a virtue, and I'd wait forever

List of contents

	Page Number
Abstract	2
List of figures	12
List of tables	15
Authors declaration	17
Abbreviations	18
Acknowledgments	20
1. General Introduction	
1.1 Introducing Caribbean reefs	21
1.1.1 Geographic region	21
1.1.2 Coral reefs: founded on a symbiotic association	21
1.1.3 <i>Symbiodinium</i>	22
1.1.4 Reef building	23
1.1.5 <i>Montastraea</i> reefs	23
1.2 Value of reefs	25
1.3 The changing face of the Caribbean	26
1.3.1 Rising sea temperatures	28
1.3.2 Ocean acidification	29
1.3.3 Sea-level rise and storm activity	30
1.3.4 Future impacts	30
1.4 Research focus	31
1.4.1 Carbonate budgets	31
1.4.2 Zooxanthellae and bleaching thresholds	33
1.5 Thesis outline	34
1.6 References	37
2. Reef growth and erosion: a review of the major processes	
2.1 Reef construction	43
2.1.1 Colony scale building	44
2.1.1.1 <i>Coral calcification</i>	45
Calcium	46
Carbonate	46
Other inorganics	47
Organics	48
Skeleton formation	48
2.1.2 Reef growth at the community scale	49
2.1.2.1 <i>Scleractinian corals</i>	49
2.1.2.2 <i>Coralline crustose algae</i>	50
2.1.2.3 <i>Calcareous green algae</i>	51
2.1.2.4 <i>Non-burrowing sponges</i>	51
2.1.2.5 <i>Molluscs and echinoderms</i>	52
2.1.2.6 <i>Other reef encrusters</i>	52
2.1.3 Reef growth on a historic scale	52
2.1.4 Abiotic factors affecting reef growth	53
2.1.4.1 <i>Light intensity</i>	53
Light and depth	54

Light and turbidity	55
2.1.4.2 <i>Aragonite saturation state</i>	55
2.1.4.3 <i>Temperature</i>	57
2.1.4.4 <i>Water flow</i>	57
2.1.4.5 <i>Sedimentation</i>	58
2.1.4.6 <i>Nutrient availability</i>	59
2.1.4.7 <i>Temporal factors</i>	59
2.2 Reef bioerosion	60
2.2.1 Functional significance	60
2.2.1.1 <i>Reef modification</i>	61
2.2.1.2 <i>Reinforcement and fossilisation</i>	61
2.2.1.3 <i>Sediment production</i>	61
2.2.1.4 <i>Coral recruitment</i>	61
2.2.1.5 <i>Recycling nutrients</i>	61
2.2.1.6 <i>Asexual fragmentation</i>	62
2.2.1.7 <i>Enhancing biodiversity</i>	62
2.2.1.8 <i>A trophic role</i>	62
2.2.1.9 <i>Biogeochemical cycling</i>	62
2.2.2 Bioeroder guilds	63
2.2.2.1 <i>Microborers</i>	63
Algae	63
Fungi	64
Cyanobacteria	64
2.2.2.2 <i>Macroborers</i>	65
Porifera	65
Mollusca	66
Arthropoda	66
Polychaeta	67
Sipuncula	67
2.2.2.3 <i>Grazers</i>	67
Echinodermata	67
Bioeroding fish	71
Molluscs	74
2.2.3 Abiotic factors affecting reef bioerosion	74
2.2.3.1 <i>Temperature</i>	75
2.2.3.2 <i>Aragonite saturation state</i>	75
2.2.3.3 <i>Light intensity (and depth)</i>	75
Depth	76
2.2.3.4 <i>Nutrient availability</i>	77
2.2.3.5 <i>Sedimentation</i>	77
2.2.3.6 <i>Substrate type</i>	78
2.2.3.7 <i>Water flow</i>	78
2.3 Conclusion	79
2.4 References	80

3. Development of a theoretical carbonate budget model

3.1 Introduction	89
3.2 Chapter aims	92
3.3 Model parameterisation	92
1. <i>Terrigenous sedimentation rate</i>	92
922. <i>Aragonite saturation state</i>	92

3. Mean monthly sea surface temperature	98
4. Nutrient availability	98
5. Rugosity	99
6. Total living coral cover	100
7-13. Coral cover	100
14-20. Colony diameter	101
21-27. Colony height	101
28. <i>Porites porites</i> branch diameter	101
29. <i>Acropora</i> branch diameter	102
30. <i>Acropora</i> branches	102
31. <i>Agaricia</i> colony thickness	102
32-38. Linear extension rate	102
39-45. Bulk skeletal density	102
46-52. Optimal temperature	103
53-59. Temperature sensitivity	103
60-66. Aragonite sensitivity	104
67. CCA production	105
68. Microbioerosion rate	106
69-76. Clionaid bioerosion	106
77. Clionaid cover	106
78-84. Polychaete erosion	107
85. Bivalve cavity size	107
86-106. Parrotfish density	108
107. Parrotfish size	108
108. Damselfish territories	109
109. <i>Echinometra</i> density	109
110. <i>Diadema</i> density	109
111. <i>Echinometra</i> size	109
112. <i>Diadema</i> size	110
113. Urchin burrow size	110
114. Burrow excavation time	110
115. Hurricane return time	110
3.4 Defining model functions	111
A. Coral surface area	111
B. Colony calcification	114
C. Community calcification	114
D. Colony rugosity	114
E. OA effect on calcification	115
F. Temperature effect on calcification	116
G. Nutrient effect on calcification	117
H. Calcification feedback	117
I. Available substrate	118
J1. CCA cover	119
J2. CCA calcification	119
K. OA effect on CCA	119
L. Temperature effect on CCA	120
M1. <i>Echinometra</i> bioerosion	120
M2. <i>Diadema</i> bioerosion	120
M3. Urchin spine abrasion	121
N. Urchin community bioerosion	121
O ₁ Parrotfish bite rate	121
O ₂ . Bite volume	122
P. Framework density	122

<i>Q. Community parrotfish erosion</i>	123
<i>R. Nutrient effect on microbioerosion</i>	124
<i>S. Clionaid abundance</i>	125
<i>T. Nutrient effect on clionaid abundance</i>	125
<i>U. OA effect on clionaid erosion</i>	126
<i>V. Community sponge bioerosion</i>	127
<i>W. Polychaete bioerosion</i>	127
<i>X₁. Bivalve density</i>	128
<i>X₁. Bivalve erosion</i>	129
<i>Y. Reincorporated sediment</i>	129
<i>Z. Ecological model: Reefmod</i>	129
<i>Z₁. Bleaching mortality</i>	130
<i>Z₂. Hurricane mortality</i>	130
3.5 Model validation: a Jamaican case study	131
3.6 References	134

4. Caribbean carbonate budgets: responses to environmental perturbation

4.1 Summary	145
4.2 Highlights	145
4.3 Introduction	146
4.4 Methodology	147
4.4.1 Historical scenarios	147
4.4.2 Future forecasting	147
4.5. Results	149
4.6 Conclusions	154
4.6.1 Limitations	155
4.7 References	157

5. Biogeographic patterns of distribution and diversity of *Symbiodinium* in *Montastraea annularis* inhabiting shallow Caribbean reefs

5.1 Introduction	159
5.2 Chapter aims	161
5.2.1 Aim 1: Characterising <i>Symbiodinium</i> communities in <i>M. annularis</i>	161
5.2.2 Aim 2: Exploring spatial patterning in symbiont communities across the Caribbean and Bahamas	163
5.3 Methodology	165
5.3.1 Sample collection	165
5.3.2 Selection of a target gene region	167
5.3.3 Denaturing Gel Gradient Electrophoresis and sequencing analysis	168
5.3.4 Validation of DGGE using High Resolution Melt (HRM) analysis	171
5.3.5 Data analysis	171
5.4 Results	172
5.4.1 Local patterns in <i>Symbiodinium</i> ITS2 diversity	172
5.4.1.1 <i>Western Caribbean (Mesoamerican Barrier Reef System)</i>	172
Honduras (sites A, B and C)	173
Belize (sites D, E, F and G)	174
5.4.1.2 <i>The Bahamas</i>	175
Bahamas (sites L, K, P, CI, N and EN)	175
5.4.1.3 <i>The Greater Antilles</i>	177
Cuba (sites CA, CB and CC)	178

Dominican Republic (site DR)	179
Jamaica (sites JA and JB)	180
Cayman Islands (site X)	180
5.4.1.4 <i>The Southwestern Caribbean</i>	181
Nicaragua (sites NA and NB)	181
Columbia (site CM)	182
5.4.1.5 <i>The Lesser Antilles (Eastern and Southern Caribbean)</i>	183
British Virgin Islands (sites T and R)	184
Dominica (site DM)	185
Barbados (site BA)	186
5.4.1.6 <i>Southern Caribbean</i>	186
Tobago (site TB)	186
Venezuela (sites AV and BV)	187
Curaçao (sites VB, SB and Z)	187
5.4.2 Caribbean-wide spatial patterns in <i>Symbiodinium</i> diversity	188
5.4.2.1 <i>Cladal level patterns</i>	188
5.4.2.2 <i>Sub-cladal level patterns</i>	189
5.4.2.3 <i>Symbiodinium richness</i>	194
5.4.2.4 <i>Symbiodinium diversity</i>	197
5.4.2.5 <i>Species clustering</i>	197
5.4.2.6 <i>Spatial analyses</i>	198
PERMANOVA	198
Ordination	199
SADIE analysis	200
5.5 Discussion	204
5.5.1 Diversity of <i>Symbiodinium</i> ITS2 types hosted	204
5.5.1.1 <i>Sub-clade B1</i>	205
5.5.1.2 <i>Sub-clade B10</i>	206
5.5.1.3 <i>Sub-clade B17</i>	206
5.5.1.4 <i>Sub-clade B1j</i>	206
5.5.1.5 <i>Clade C</i>	207
5.5.1.6 <i>Clade A</i>	207
5.5.1.7 <i>Clade D</i>	207
5.5.2 Intra-site diversity	210
5.5.2.1 <i>Bahamas</i>	210
5.5.2.2 <i>Belize</i>	210
5.5.2.3 <i>Panama</i>	211
5.5.2.4 <i>Barbados</i>	211
5.5.3 Within-colony variation/Host-specificity	211
5.5.4 Spatial patterns of <i>Symbiodinium</i> distribution	212
5.5.6 Wider implications of the finding	213
5.6 References	214

6. Exploring environmental, geographic and genetic drivers of Caribbean symbiont biogeography in a key reef building coral

6.1 Introduction	219
6.2 Chapter Aims	220
6.3 Overview of statistical model variables	221
6.3.1 Dependent variables: symbiont community	221
6.3.2 Explanatory variables: geographic, environmental and genetic	221
6.3.2.1 <i>Geographic distance</i>	221
6.3.2.2 <i>Environmental conditions</i>	222
Temperature	222

Irradiance	222
Nutrients	224
Salinity	224
Mechanical disturbance regime	224
6.3.2.3 <i>Host population genetics</i>	225
6.3.2.4 <i>Confounding factors</i>	226
Collector	226
Collection month and year	226
6.4 Methodology	227
6.4.1 Dependent variables	227
6.4.2 DISTLM model explanatory variables	227
6.4.2.1 <i>Thermal stress metrics</i>	227
6.4.2.2 <i>Irradiance proxies</i>	228
6.4.2.3 <i>Salinity</i>	230
6.4.2.4 <i>Nutrients</i>	231
6.4.2.5 <i>Wave exposure</i>	231
6.4.2.6 <i>Enclosure</i>	232
6.4.2.7 <i>Hurricanes</i>	232
6.4.2.8 <i>Coral host metrics</i>	232
6.4.2.9 <i>Geographic distance measures</i>	232
6.4.3 Statistical methods	233
6.4.3.1 <i>Data exploration</i>	233
6.4.3.2 <i>DISTLM multiple regressions</i>	234
6.4.3.3 <i>Additional analyses</i>	235
PERMANOVA	235
RELATE	236
6.5 Results	236
6.5.1 DISTLM analyses	236
6.5.1.1 <i>Environmental vs genetic vs geographic variation</i>	238
6.5.2 Additional analyses	239
6.5.2.1 <i>PERMANOVA</i>	239
6.5.2.2 <i>RELATE (exploring host diversity)</i>	239
6.6 Discussion	243
6.6.1 Partitioning of symbiont communities by geographic distance	244
6.6.2 Environmental partitioning of symbiont communities	245
6.6.2.1 <i>Thermal stress</i>	245
6.6.2.2 <i>Nutrient concentrations</i>	248
6.6.2.3 <i>Other environmental factors</i>	248
6.6.2.4 <i>Latitude</i>	249
6.6.2.5 <i>Clade C</i>	250
6.6.3 Symbiont partitioning among coral hosts	250
6.6.4 Unexplained variation	252
6.7 Conclusion	253
6.8 References	255

7. Prevalence of cryptic *Symbiodinium D* in *Montastraea annularis*

7.1 Abstract	259
7.2 Introduction	260
7.2.1 <i>Symbiodinium D</i>	261
7.2.2 <i>Montastraea annularis</i>	262
7.2.3 Real-time PCR	263
7.2.4 Aims	263

7.3 Materials and Methods	263
7.3.1 Sample collection and DNA extraction	263
7.3.2 Symbiont screening using DGGE	264
7.3.3 RT-PCR analysis	264
7.3.4 Data analysis	266
7.4 Results	267
7.4.1 Assessment of symbiont communities by DGGE	267
7.4.2 Assessment of symbiont communities by RT-PCR	267
7.4.3 Quantifying background abundance of D	267
7.4.4 Spatial distribution of <i>Symbiodinium</i> D	269
7.5 Discussion	271
7.5.1 Dominance of B1 in <i>M. annularis</i> (DGGE)	271
7.5.2 Prevalence of low-abundance <i>Symbiodinium</i> D (RT-PCR)	271
7.5.3 Quantification of background abundance of D	272
7.5.4 Invasion of a competitive opportunist?	273
7.5.5 A mechanism for symbiont shuffling?	274
7.6 Conclusion	275
7.7 References	277

8. Temporal stability of *Montastraea annularis* symbioses: a Bahamian case study

8.1 Introduction	281
8.1.1 Stability of coral-algal symbioses over time: a contentious issue	281
8.1.2 Temporal dynamism of <i>M. annularis</i> ' symbiont communities?	282
8.2 Chapter aims	283
8.3 Methodology	284
8.3.1 Sampling sites	284
8.3.2 Sample collection	286
8.3.3 DNA extraction	287
8.3.4 DGGE and sequencing	287
8.3.5 Screening for <i>Symbiodinium</i> D	288
8.3.6 Statistical analyses	288
8.4 Results	288
8.4.1 Temporal stability of dominant symbionts	288
8.4.2 Temporal stability of cryptic <i>Symbiodinium</i> D	291
8.5 Discussion	292
8.5.1 Temporal stability of symbiont communities	292
8.5.2 Temporal stability of low abundance D	294
8.5.3 Study limitations	296
8.5.4 Conclusions	297
8.6 Acknowledgements	297
8.7 References	298

9. General Discussion

9.1 Project evaluation	301
9.1.1 Caribbean carbonate budgets and reef growth	301
9.1.1.1 Further work	302
9.1.2 <i>Symbiodinium</i> diversity	302
9.1.2.1 Further work	304
9.2 Synthesis of project strands	305
9.2.1 Linking symbiont diversity to <i>M. annularis</i> calcification rate	305
9.3 A 'nugget of hope' for the future?	307
9.5 References	310

Appendices

Chapter 4 Appendix	314
Chapter 5 Appendix	315
Chapter 6 Appendix	351
Chapter 7 Appendix	357
Chapter 8 Appendix	358
Chapter 9 Appendix	361

List of figures and illustrations

	Page number
General Introduction figures	
Figure 1.1 Map of the Wider Caribbean area.	22
Figure 1.2: <i>Montastraea annularis sensu stricto</i> , San Salvador, Bahamas.	24
Figure 1.3: Declining state of Caribbean reefs.	27
Figure 1.4: Photographs A-E document the decline of Caribbean reefs.	28
Figure 1.5: Thermal stress and coral bleaching.	29
Figure 1.6: <i>Oculina patagonica</i> experimental exposure to low seawater pH.	30
Figure 1.7: Diagram depicting the principal components of a coral reef carbonate budget.	32
Figure 1.8: Diagram depicting the equation used to estimate the rate of reef accretion	33
Chapter 2 figures	
Figure 2.1 Diagram summarizing the main functions of marine calcification at the colony level.	45
Figure 2.2 Diagram summarising transcellular pathways of calcium and DIC into the ECF.	47
Figure 2.3 <i>Montastraea annularis</i> calcification rate is related to depth.	54
Figure 2.4: Differential effects of SST on calcification of massive <i>Montastraea</i> and <i>Porites</i> .	57
Figure 2.5: Mean urchin test size (for a variety of species) plotted against bioerosion rate.	71
Figure 2.6: Relationship between bioerosion rates of different boring guilds and depth.	76
Chapter 3 figures	
Figure 3.1: Map of the Caribbean, including all published carbonate budget field studies to date.	90
Figure 3.2. Data flow diagram representing our carbonate budget algorithm.	93
Figure 3.3. Monthly aragonite saturation state, Ω_{ar} (A) and sea surface temperature, SST (B).	99
Figure 3.4. Three scales of coral reef rugosity.	100
Figure 3.5. Gaussian response of coral calcification to changing sea surface temperature.	104
Figure 3.6: Aragonite saturation state, Ω_{ar} , vs. coral reef community calcification.	105
Figure 3.7. Seawater aragonite saturation state (Ω_{ar}) and sponge bioerosion rates.	127
Figure 3.8. Validating the model: a Jamaican case study.	132
Chapter 4 figures	
Figure 4.1. Caribbean framework bioerosion vs. carbonate production over the past half century.	148
Figure 4.2. Sensitivity of model Caribbean reefs to simulated disturbance events.	150
Figure 4.3. Future carbonate budgets of a Caribbean fore-reef under climate change.	152
Figure 4.4. Alternative scenarios for future carbonate budgets.	153
Chapter 5 figures	
Figure 5.1: Geographic distribution of <i>Symbiodinium</i> types in <i>Montastraea annularis</i> .	165
Figure 5.2: Sampling methodology.	166
Figure 5.3: Diagram showing the target gene used to explore <i>Symbiodinium</i> diversity.	167
Figure 5.4: Denaturing Gel Gradient Electrophoresis.	169
Figure 5.5: Dominant symbiont types found at six sites across the MRBS ecoregion.	173
Figure 5.6: Dominant symbiont types, or pairs of types, in the Bahamian ecoregion.	176
Figure 5.7: Map showing location of sites in the Greater Antilles marine ecoregion.	178
Figure 5.8: Map showing location of sampling sites for the Southwestern ecoregion.	182
Figure 5.9: Map of the Lesser Antilles and symbiont types.	184
Figure 5.10: Map depicting absolute proportions of <i>Symbiodinium</i> clade B, C and D.	189
Figure 5.11: Bar chart reporting the relative proportions of symbionts hosted by <i>M. annularis</i> .	190
Figure 5.12: Pie-chart depicting the major symbionts, or pairs of symbionts found dominating	191

<i>Montastraea annularis</i> endosymbiont communities.	
Figure 5.13: Map showing the distribution of the dominant symbiont types hosted by <i>Montastraea annularis</i> at 33 sites across the Caribbean and Bahamas.	192
Figure 5.14: Bar chart describing the major symbiont sub-clades hosted by <i>Montastraea annularis</i> at 33 sites across the Caribbean and Bahamas.	193
Figure 5.15: Bar chart comparing total species richness between sites.	195
Figure 5.16: Red-blue plot showing clustering of data on <i>Symbiodinium</i> sub-cladal abundance, based on SADIE estimated indices of spatial clustering.	196
Figure 5.17: Bar graph representing symbiont diversity (Simpsons Reciprocal D) across the Caribbean.	197
Figure 5.18: <i>Montastraea annularis</i> symbionts.	198
Figure 5.19: Caribbean reefs, <i>Montastraea annularis</i> symbionts.	199
Figure 5.20: Red-blue plots highlighting areas and sites that showed significant positive (large red circles) and negative (large blue circles) clustering.	202
Figure 5.21: Red-blue plots for sub-cladal level.	204
Figure 5.22: Investigating <i>Symbiodinium</i> D.	209

Chapter 6 figures

Figure 6.1: Thermal stress metrics used to inform the statistical model.	228
Figure 6.2: Average chlorophyll-a concentration (mg m^{-3}) derived from MODIS satellite data.	230
Figure 6.3: Average salinity at the sea surface (psu), from the online world database 2009.	231
Figure 6.4: Mean inorganic nutrient concentrations of NO_3^- and PO_4^{3-} .	232
Figure 6.5: Draftsman plots of all environmental covariates.	234
Figure 6.6: RELATE output, showing the significant Spearman's ρ value (-0.12) generated for genetic and geographic matrix comparisons.	242
Figure 6.7: RELATE output, showing the significant Spearman's ρ value generated for distance and symbiont community matrix comparisons.	243
Figure 6.8: Scatter plots showing the relationship between symbiont community diversity.	247
Figure 6.9: Maximum monthly mean SST ($^{\circ}\text{C}$) by Caribbean eco-region.	248
Figure 6.10: Scatter graph showing the relationship between chronic temperature stress and number of colonies hosting clade C and B symbionts.	252

Chapter 7 figures

Figure 7.1: Standard curves for absolute quantification of <i>Symbiodinium</i> D DNA using RT-PCR.	266
Figure 7.2: Proportion of <i>M. annularis</i> population harbouring <i>Symbiodinium</i> D.	268
Figure 7.3: Relative quantities of <i>Symbiodinium</i> D gene copies found at each site (ratio of D:ITS2).	269

Chapter 8 figures

Figure 8.1 Map depicting partitioning of <i>Montastraea annularis</i> symbiont communities based on ordination.	285
Figure 8.2. Scatter plots showing the associations derived between specific symbiont strains and environmental parameters.	286
Figure 8.3. Linking east-west <i>Symbiodinium</i> partitioning to host calcification rates.	287
Figure 8.4 DGGE gel images revealing the most common banding patterns found at each site.	288
Figure 8.5 Pie charts representing dominant <i>Symbiodinium</i> types harboured by <i>M. annularis</i> colonies across four Bahamian reefs.	289
Figure 8.6 Pie charts displaying changes in the relative number of <i>Montastraea annularis</i> colonies found to host low abundances of <i>Symbiodinium</i> D, at four different sites in the Bahamas.	291
Figure 8.7. Bar chart showing accumulated degree heating weeks (a measure of thermal stress) in the Bahamas.	293
Figure 8.8. Maps showing SST anomalies, and DHWs (both measures of thermal stress) for the Bahamas during sampling months.	295

General Discussion figures

Figure 9.1. Partitioning of <i>Montastraea annularis</i> symbiont communities based on ordination	303
Figure 9.2. Scatter plots showing the associations derived between specific symbiont strains and environmental parameters (described in Chapter 5).	304
Figure 9.3. Linking east-west <i>Symbiodinium</i> partitioning to host calcification rates.	306

Appendices

Appendix Figure 4.1: Graphical abstract summarizing main finding of Chapter 4	314
Appendix Figure 5.1: HRM outputs for all sampled populations of <i>Montastraea annularis</i> endosymbionts.	317
Appendix Figure 5.2: DGGE gel images and HRM outputs for Belizean site D, Coral Gardens.	318
Appendix Figure 5.3: DGGE gel images and HRM outputs for Belizean site E, Eagle Ray.	319
Appendix Figure 5.4: DGGE gel images and HRM outputs for Belizean site G, Long Cay.	320
Appendix Figure 5.5: DGGE gel images and HRM outputs for Belizean site H, West Reef.	321
Appendix Figure 5.6: DGGE gel images and HRM outputs for Honduran site B, Sandy Bay.	322
Appendix Figure 5.7: DGGE gel images and HRM outputs for Honduran site C, Western Wall.	323
Appendix Figure 5.8: DGGE gel images and HRM outputs for Bahamian reef L, Snapshot.	324
Appendix Figure 5.9: DGGE gel images and HRM outputs for Bahamian reef K, Seahorse.	325
Appendix Figure 5.10: DGGE gel images and HRM outputs for Bahamian reef P, Propellor Reef.	326
Appendix Figure 5.11: DGGE gel images and HRM outputs for Bahamian reef N, Schoolhouse Reef	327
Appendix Figure 5.12: DGGE gel images and HRM outputs for Bahamian reef EN, from the Exhumas National Park. Inset shows image taken from another study, showing D1a and C31.	328
Appendix Figure 5.13: DGGE gel images and HRM outputs for Bahamian reef CI, from Conception Island.	329
Appendix Figure 5.14: DGGE gel images and HRM outputs for Cuban reef CA, Baracoa.	330
Appendix Figure 5.15: DGGE gel images and HRM outputs for Cuban reef CB, Bacunayagua.	331
Appendix Figure 5.16: DGGE gel images and HRM outputs for Cuban reef CC, Siboney. Inset: D1a banding from the Pacific, from LaJeunesse et al 2004.	332
Appendix Figure 5.17: DGGE gel images and HRM outputs for the Dominican Republic.	333
Appendix Figure 5.18: DGGE gel images and HRM outputs for the Jamaican site, Drunkenman's Cay (JA).	334
Appendix Figure 5.19: DGGE gel images and HRM outputs for Jamaican reef JB, Dairy Bull reef.	335
Appendix Figure 5.20: DGGE gel images and HRM outputs for Grand Cayman Reef X, Rum Point.	336
Appendix Figure 5.21: DGGE gel images and HRM outputs for Nicaraguan site NA, White Hole.	337
Appendix Figure 5.22: DGGE gel images and HRM outputs for Nicaraguan site NA, White Hole.	338
Appendix Figure 5.23: DGGE gel images and HRM outputs for Columbian site CM, Palo 1.	339
Appendix Figure 5.24: DGGE gel images and HRM outputs for BVI site T, Beef Island.	340
Appendix Figure 5.25: DGGE gel images and HRM outputs for BVI site R, Ginger Island.	341
Appendix Figure 5.26: DGGE gel images and HRM outputs for BVI site R, Ginger Island.	342
Appendix Figure 5.27: DGGE gel images and HRM outputs for Barbados site BA, Victors Reef.	343
Appendix Figure 5.28: DGGE gel images and HRM outputs for Tobago site TB, Buccoo Reef.	344
Appendix Figure 5.29: DGGE gel images and HRM outputs for Venezuelan site AV, Cayo de Agua.	345
Appendix Figure 5.30: DGGE gel images and HRM outputs for Venezuelan site BV, Dos Mosquises.	346
Appendix Figure 5.31: DGGE gel images and HRM outputs for Curaçao Z, Buoy 1.	347
Appendix Figure 5.32: DGGE gel images and HRM outputs for Curaçao site SB, Snake Bay.	348
Appendix Figure 5.33: DGGE gel images and HRM outputs for Curaçao site VB, Vaersenbay.	349
Appendix Figure 5.34: Dendrogram of square root transformed symbiont abundance data.	350
Appendix Figure 6.1: PCA ordination plot of Caribbean sites based on normalised temperature stress indices.	356
Appendix Figure 7.1: Red-blue plot indicating spatial clustering in the D distribution.	357
Appendix Figure 9.1: Scatter plot of published <i>Montastraea annularis</i> skeletal linear extension rates, taken from > 30 studies.	361

List of tables

Page number

General Introduction tables

Table 1.1: Summary of goods and ecological services provided by coral reef ecosystems.	26
---	----

Chapter 2 tables

Table 2.1: Summary of grazing impact of echinoid species.	69
Table 2.2: Summarising findings of fish bioerosion studies.	72

Chapter 3 tables

Table 3.1. Caribbean carbonate budget field studies attempted to date.	91
Table 3.2. A list of the parameters for the carbonate budget model.	94
Table 3.3. Explanations how planar surface was converted into 3-D volume of new skeletal material for each coral type to estimate gross carbonate production.	113

Chapter 5 tables

Table 5.1: Catalogue of known <i>Symbiodinium</i> diversity (based on ITS2 molecular marker) in the Caribbean <i>Montastraea annularis</i> .	164
Table 5.2. Primer pairs.	170
Table 5.3: Richness and diversity measures for <i>Symbiodinium</i> ITS2 at each of the 33 sites.	194
Table 5.4: Cluster indices generated by SADIE analysis for <i>Symbiodinium</i> clade distribution across sample sites.	201
Table 5.5: SADIE outputs.	203

Chapter 6 tables

Table 6.1: List of the environmental, geographic and genetic parameters .	226
Table 6.2: Summary of DISTLM population-scale marginal tests, examining the relationship between <i>Symbiodinium</i> communities and explanatory covariates.	235
Table 6.3: Summary of DISTLM population-scale outputs.	236
Table 6.4: Summary of DISTLM population-scale marginal test outputs.	237
Table 6.5: Summary of population-scale analyses for model selection to examine the relationship between <i>Symbiodinium</i> communities and environmental variables.	237
Table 6.6. Host genotype data by site.	239

Chapter 7 tables

Table 7.1. Clade-specific nuclear rDNA primer sets developed to amplify portions of the multi-copy ribosomal gene family in <i>Symbiodinium</i> clade D using qPCR.	264
Table 7.2: Summary of RT-PCR and DGGE outputs by site, grouped by marine eco-region.	270

Chapter 8 tables

Table 8.1 Results of Fisher's Exact Test comparing temporal changes in the dominant symbiont hosted.	290
Table 8.2 Results of Fisher's Exact Test comparing temporal changes in <i>Symbiodinium</i> D.	292

Appendix

Appendix Table 5.1: Summary of the number of identified sub-clades hosted by each individual sample.	315
Appendix Table 5.2: Outputs generated by the SADIE analyses, for <i>Symbiodinium</i> clade and species richness measures.	316
Appendix Table 5.3: Cluster indices generated by SADIE analysis for symbionts at each site.	316
Appendix Table 6.1: Hurricane frequency for each reef site.	351
Appendix Table 6.2. Pearson correlation between transformed environmental covariates.	352

Appendix Table 6.3. Geographic distances measures (km) between sites.	353
Appendix Table 6.4. Data on environmental variables (pre-transformation) included in the final model (see Table 6.1 for environmental covariate descriptors).	354
Appendix Table 6.5. PCA ordination plot of Caribbean sites based on normalised temperature stress indices.	355
Appendix Table 8.1: Database excerpt from GeoSymbio alignment file: records of <i>Symbiodinium</i> ITS2 gene isolated from <i>Montastraea annularis</i> corals only, <i>in hospite</i> .	358
Appendix Table 8.2: Percentage of <i>M. annularis</i> sampled colonies containing each symbiont taxa.	359
Appendix Tables 8.3: Contingency tables for the Fisher Exact Test for temporal variation across the Bahamas.	360
Appendix Table 8.4 Characterisation and PCR amplification conditions of the seven <i>Symbiodinium</i> clade B microsatellite loci, that could be used in future work.	360
Appendix Table 9.1: Data collated on <i>Montastraea annularis</i> skeletal linear extension rate.	362

Authors declaration

Nicola L. Foster and a team of researchers (J. Armando-Sanchez, C. Bastidas, S. Bejarano, S. Box, P. Bush, R. Ferrari, P. Gonzalez, S. Gore, R. Guppy, K. Kuran, C. McCoy, J. Mendes, J. Shears, P. Shears, S. Steiner and M. Vermeij) were responsible for the collection of all the *Montastraea annularis* used in the study (Chapters 5-8), with the exception of those sampled from Bahamian sites in 2010, 2011 and 2012 (Chapter 8). For these *M. annularis*, export and UK import licenses as well as scientific collection permits were obtained from CITES (Convention on International Trade in Endangered Species of wild fauna and flora) and the Bahamian Ministry of the Environment respectively, prior to sampling each year. All diving adhered to the University of Exeter code of conduct and complied with Gerace Research Centre scientific diving regulations. As part of her doctorate ('Population dynamics of the dominant Caribbean reef-building coral *Montastraea annularis*'), N. L. Foster also processed the samples she collected, and extracted and purified the DNA. Raw data on population genetics of the *M. annularis* host used to explore symbiont biogeography in Chapter 6 were also provided by N. L. Foster.

Chapters 3 and 4 make up a Report (Chapter 4) and Supplementary Information section (Chapter 3), "*Avoiding reef functional collapse requires combined local and global action*, Emma V. Kennedy, Chris T. Perry, Paul R. Halloran, Roberto Iglesias-Prieto, Christine H. L. Schönberg, Max Wisshak, Armin U. Form, Juan P. Carricart-Ganivet, Maoz Fine, C. Mark Eakin, Peter J. Mumby", accepted for publication in *Current Biology* the week of this thesis submission (published May 2013).

Although the hypothesis was conceived by P. J. Mumby, I led this study, developing the original carbonate budget model and historic scenarios. P. R. Halloran extracted the climate data to drive the model to 2100, and P. J. Mumby coupled the budget model to the Reefmod ecological model, from which future scenarios were generated. Subsequent versions of the model were tested and improved by myself and P. J. Mumby, with inputs from C. T. Perry. C. H. L. Schönberg, M. Wisshak and A. U. Form supplied the sponge bioerosion data and provided additional advice on the manuscript. R. Iglesias-Prieto and J. P. Carricart-Ganivet provided expert advice on calcification and commented on the manuscript. I wrote initial drafts of the Report and Supplementary Information. C. H. L. Schönberg helped me redraft the final version of the Supplementary Information. I wrote the final version of the manuscript with P. J. Mumby, with input from C. T. Perry and all other authors. I also co-ordinated the manuscript submission and drafted the response to reviewers comments, which were later edited by P. J. Mumby and C. T. Perry.

Iliana Chollett-Ordaz extracted all the environmental data used in Chapter 6 (Table 6.1) to explore environmental drivers of symbiont biogeography, and provided expert advice on data analysis.

The remainder of this thesis is my own work and that, to the best of my knowledge and belief, it contains no material which has been accepted or submitted for the award of any other degree or diploma.

Abbreviations

Ω_{ar} = Aragonite saturation state, a measure of the availability of carbonate ions in seawater.

AGRR = Atlantic and Gulf Rapid Reef Assessment Program, an international collaboration of scientists and reef managers aimed at determining regional condition of the reefs in the Western Atlantic and Gulf of Mexico, with an extensive online database of Caribbean coral reef condition.

ATP = Adenosine tri-phosphate, a coenzyme used as an energy carrier in the cells of all known organisms. Often called the "molecular unit of currency" of intracellular energy transfer.

CA = Carbonic anhydrase, a family of enzymes commonly found in animals that catalyse the reversible conversion of $\text{CO}_2 + \text{H}_2\text{O} \leftrightarrow \text{CO}_3^{2-} + \text{H}^+$.

CaCO_3 = The chemical formula of calcium carbonate, a white/clear mineral precipitated by calcifying organisms.

CARICOMP = Caribbean Coastal Marine Productivity Program, a regional scientific program to study coastal ecosystem productivity, produce monitoring data.

CCA = Coralline crustose algae, a heavily calcified, white-pink coloured encrusting reef algae.

CO_2 = The chemical formula for carbon dioxide.

DGGE = Denaturing gradient gel electrophoresis, a high-resolution acrylamide gel-based technique employed to separate DNA based on small differences in nucleic acid content using a chemical gradient to denature samples as they move across the gel. Commonly used in microbial ecology to assess mixed species assemblages.

DHW = Degree heating week, used to describe accumulated thermal stress experienced by coral reefs. One DHW is equivalent to 1 week of sea surface temperature at 1°C above the expected summertime maximum. Two DHWs can indicate either 1 week of 2°C above the expected summertime maximum or 2 weeks of 1°C above the expected summertime maximum.

DIC = Dissolved inorganic carbon.

DIN = Dissolved inorganic nitrogen.

DIP = Dissolved inorganic phosphorus.

ECF = Extracytoplasmic calcifying fluid, seawater-based fluid found in the calcicoblastic layer between a coral polyp and its skeleton.

G = Units describing carbonate accretion rate ($\text{kg CaCO}_3 \text{ m}^{-2} \text{ year}^{-1}$). Values of G can be positive (reef growth) or negative (indicating net erosion).

GBR = Great barrier reef, a >2000 km reef running parallel to the northeast coast of Queensland, Australia, the largest of its kind.

GHG = Greenhouse gas, any atmospheric gas that absorbs and emits thermal infrared radiation, e.g., water vapor, carbon dioxide, methane, nitrous oxide, ozone.

Gt = Gigatonne, a unit of mass.

HRM = High resolution melt analysis, a powerful and sensitive technique used in molecular biology to detect differences in double stranded DNA, based on monitoring of melting point of double stranded DNA using fluorescent markers.

I_a = Index of aggregation, a measure of spatial clustering of count data, generated as an output of SADIE analysis.

ITS2 = Internal transcribed spacer region II, a widely sequenced section of non-functional RNA that occurs in tandem repeats, commonly used in taxonomy to elucidate relationships among species.

LEC = Light enhanced calcification, a biogenic method of calcification adopted by scleractinian corals.

LER = Linear extension rate, refers to the vertical growth of coral skeletons.

LSU = Large ribosomal subunit, a component of ribosomal DNA commonly used for reconstructing evolutionary relationships between organisms, and for species identification in molecular ecology.

MPA = Marine protected area, an intertidal or subtidal area, together with its overlying water and associated flora, fauna, historical and cultural features, which has been reserved by law or other effective means to protect part or all of the enclosed environment.

MRBS = Mesoamerican barrier reef system, the second largest barrier reef system in the world after the GBR, running > 1000 km from the Yucatan peninsula in Mexico through Belize, Guatemala and Honduras.

MYA = Million years ago, a unit of historic time.

OTU = Operational taxonomic unit, a taxonomic level of sampling selected to be used in a study, such as individuals, populations, species, genera, or strains.

pCO₂ = Partial pressure of carbon dioxide, a measurement of concentration.

pH = a measure of the acidity or basicity of a solution, where acidic solutions have a pH < 7 and basic solutions > 7.

POM = particulate organic matter

RFLP = Restriction fragment length polymorphism, a DNA profiling technique based on restriction digest of DNA and subsequent separation by gel electrophoresis.

RFU = Relative fluorescence units, a unit of measurement used in HRM analysis which employs fluorescence detection.

SADIE = Spatial analysis by distance indices, a statistical approach designed for assessing the patterning of ecological count data from spatially referenced locations.

SI = Surface index, a factor used in scaling up planar area into three-dimensional surface area.

SSCP = Single-strand conformation polymorphism, a technique used to distinguish DNA strands based on conformational differences of identically sized single-stranded sequences, induced by certain experimental conditions (usually temperature), and an alternative to DGGE.

SST = Sea surface temperature, a measure of water temperature close (0-20 m) to the ocean's surface.

UVC = Underwater visual census, a field method for estimating the abundance of coral reef fishes.

Acknowledgements

This project would not have been possible without the training, funding, mentoring, advice, technical support and encouragement of many wonderful people, and three fantastic supervisors.

Thank you



1

General Introduction

1.1 Introducing Caribbean reefs

1.1.1 Geographic region

The Wider Caribbean region hosts 10.3% of the world's shallow tropical coral reefs (Wilkinson and Souter 2008). Covering 3.3 million km² of the western Atlantic Ocean, the marine realm encompasses the Bahamas and southern Florida, the Caribbean Sea (including the Lesser Antilles) and the Gulf of Mexico (Fig. 1.1). Ecologically, the region is divisible into 16 physio-chemical regimes, based on exposure and temperature and nutrient regimes (Chollett et al. 2012). Persistent subtropical trade winds, year-round sunshine, and consistent water exchanges result in little seasonal variation. Despite inputs from the Amazon and Orinoco, waters of the Wider Caribbean are oligotrophic: nutrient-poor currents enter through the east and are transported by the Caribbean current into the Gulf of Mexico (Heileman and Mahon 2009).

1.1.2 Coral reefs: founded on a symbiotic association

Extensive well-developed barrier systems and numerous bank and fringing reefs are among the Caribbean's 26,000 km² of coral reefs, in spite of the low productivity of the seawater. These include the Mesoamerican Barrier reef (the second largest reef system in the world), fringing reefs along the outer margins of the shallow sand banks of the Bahamas, and marginal reef systems at the regions limits in Bermuda (north) and Brazil (south) (Burke et al. 2011). The existence of these diverse reef systems are based on symbioses between hermatypic scleractinian corals (from the largest order of anthozoans, the Scleractinia), and single-celled coccoid phototropic dinoflagellates, known as zooxanthellae, found within membrane-bound vacuoles in their gastrodermal (inner) cell layers (Chalker et al. 1988, Rowan 1998, Gattuso et al. 1999, Hoegh-Guldberg 1999). The mutualistic association, established over 45 million years ago, facilitates tight recycling of nutrients, which enables the survival of the hermatypic scleractinia in a nutrient poor, clear water environment. This has ultimately driven the

ecological dominance of coral reefs in tropical shallow marine environments (Muscatine and Porter 1977, Rowan 1998).

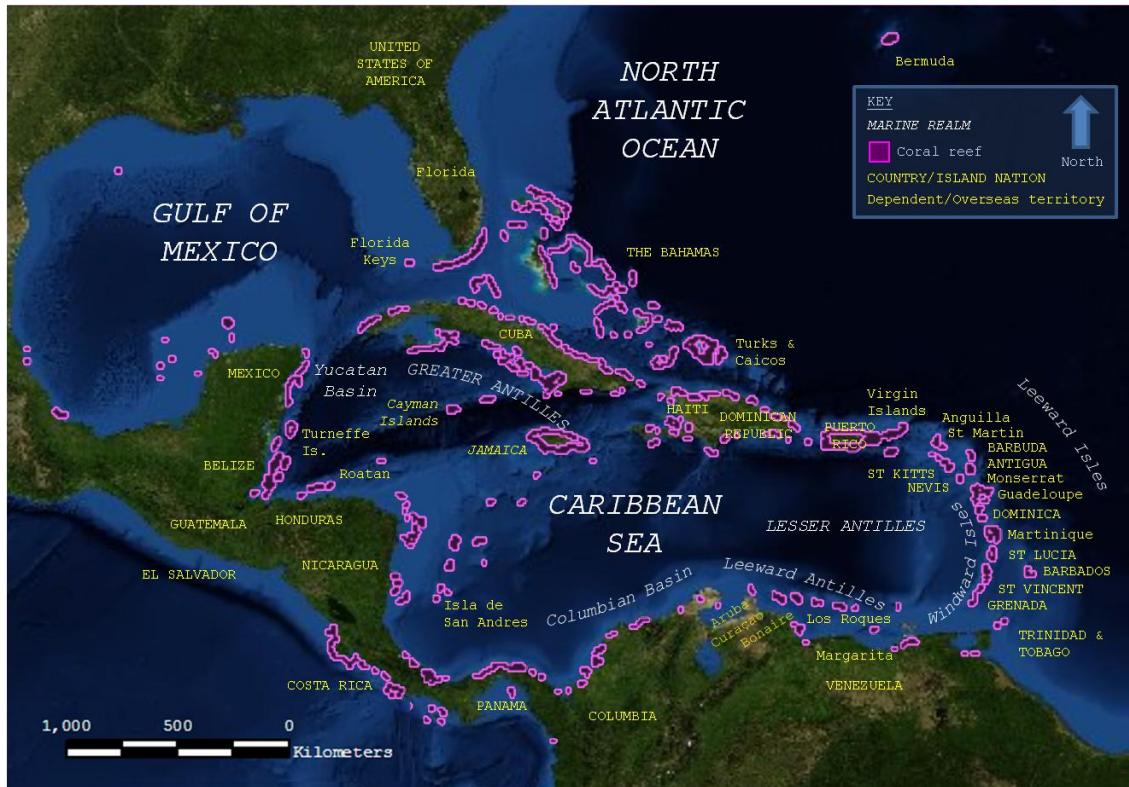


Figure 1.1 Map of the Wider Caribbean area, with locations of the 26,000 km² of coral reefs shown in pink. The region extends from Bermuda in the northwestern Atlantic down to the Amazon and Orinoco rivers on the north-eastern coast of South America. Polygon data on reef locations from UNEP-WCMC, (UNEP-WCMC)

1.1.3 *Symbiodinium*

Zooxanthellae, principally from the genus *Symbiodinium* (although some *Amphidinium*; Trench 1997) support their scleractinian hosts nutritionally, by translocating 78% of photosynthetically fixed carbon to the host, with the remainder used for their own respiration (21%) and growth (0.8%) (Edmunds and Davies 1986). *Symbiodinium* are found in extremely high densities (e.g., $1-5 \times 10^9$ cells cm⁻²; Fagoonee et al. 1999) within host cells, contributing 1-10% of coral tissue biomass and up to 50-70% of the entire reefs primary production. At these densities, the symbionts supply the bulk of the energy requirement for host cell maintenance (Muscatine et al. 1984), as well as conferring an archetypal brownish-yellow colour (derived from pigments chlorophyll a and c and dinoflagellate pigments diadinoxanthin and peridinin) to their hosts. Meanwhile, the host provides symbionts with protection, nutrients (nitrogen and phosphorus) and a constant supply of carbon dioxide (CO₂) required for photosynthesis.

Symbiodinium are as speciose as the scleractinians they inhabit (65 Caribbean coral species vs > 90 *Symbiodinium* taxa, or ‘clades’ hosted by Caribbean scleractinians), although this biodiversity has only recently been discovered using molecular techniques. Major

diversification occurred as early as 9-6 MYA, prior to the closure of the Isthmus of Panama, which isolated the Caribbean from the Pacific (LaJeunesse 2005). Different *Symbiodinium* types are thought to confer diverse physiological traits to their hosts, allowing acclimation of coral species to a variety of light conditions, bathymetries, temperatures and latitudes (Baker 2003). Some may even convey increased resistance to thermal stress (Jones et al. 2008, LaJeunesse et al. 2009) although this may incur physiological trade-offs (e.g., in growth rate; Little et al. 2004). The photosynthetic requirements of the symbiosis also restricts corals to the photic zone (i.e., shallow sunlit waters), and to temperatures in the range of 18 to 32°C (Cohen and McConnaughey 2003). This is what limits the global distribution of coral reef ecosystems to shallow, submarine platforms within the tropics (Trench 1997).

1.1.4 Reef building

Modern shallow water coral reef ecosystems are a product of the past 45–50 million years of evolution. Most reef-building scleractinia are colonial, constructed of multiple genetically identical anemone-like polyps, although solitary forms either with a single mouth exist (e.g., *Fungia* spp.). The coral-algal symbiosis facilitates rapid secretion of a calcium carbonate (CaCO_3) skeleton by each polyp (see Chapter 2; Gattuso et al. 1999, Allemand et al. 2004). Layers of skeleton build up annually over a coral's lifetime (which can last several centuries) to create large and topographically complex geological structures, bound together by calcareous algae (but see Chapter 2) and submarine lithification. These structures provide habitat for one quarter of all known marine species, despite taking up just 0.17% of the total marine benthic space (Allsopp et al. 2009). Since the closure of the Isthmus of Panama ~2.8 million years ago (Jackson et al. 1993, Schmidt 2007, Lessios 2008), the Wider Caribbean region¹ has been genetically isolated from the major coral areas of the Indo-Pacific (and Red Sea) and evolved to represent a biogeographically distinct region of coral reef development, with many endemics. This makes it important in terms of global biodiversity (Heileman and Mahon 2009).

1.1.5 *Montastraea* reefs

Caribbean reefs are dominated, both in terms of living cover and geographic coverage, by massive coral colonies from the *Montastraea annularis* species complex (Fig. 1.2; Goreau 1959, Knowlton et al. 1992). *M. annularis* (Ellis and Solander 1786), or mountain-star coral, which appears to have changed little over the last five million year period since its estimated origin (van Woesik et al. 2012) is the most intensively studied of the Caribbean corals. The species plays a key role in reef construction – particularly since the decline in abundance of the Caribbean's other major framework builder, *Acropora* spp. in the last two decades (Greer et al. 2009) – and is a common constituent of the fossil framework despite its relatively slow growth

¹ Henceforth referred to as 'Caribbean'

rate of $< 10 \text{ mm yr}^{-1}$ (Gladfelter et al. 1978). This is due to the species exceptional longevity (> 100 years), which allows it to progressively construct large dome-shaped colonies frequently over 1 m in diameter. This growth provides a 3-D framework that supports rich species assemblages: *Montastraea*-dominated forereefs contribute more to ecosystem processes and services (including tourism and fisheries) than other Caribbean reefs (Mumby et al. 2008).

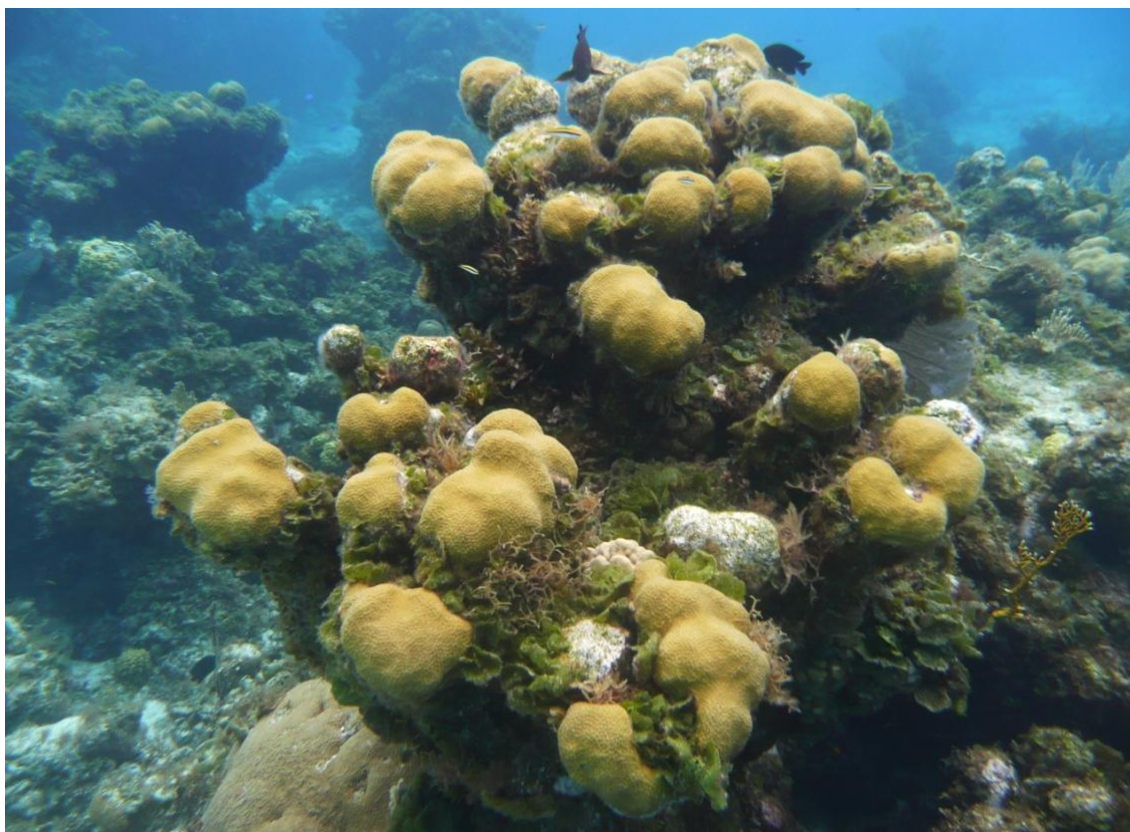


Figure 1.2: *Montastraea annularis sensu stricto*, San Salvador, Bahamas. Colonies exhibit columnar growth morphologies, with healthy colonies capable of creating large ($>2 \text{ m}^3$) reef structures.

Known to host multiple endosymbiotic dinoflagellate clades (Rowan 1998, Toller et al. 2001), the flexibility exhibited in *M. annularis* symbioses are thought to have facilitated its adaptation to a diverse range of habitats, including a depth range of 1-80 m, and a geographic range of $>4,000$ km (IUCN 2008). This flexibility may even enable colonies to avoid bleaching (LaJeunesse et al. 2009), although the species is generally considered highly-to-moderately susceptible to environmental perturbation (Oxenford et al. 2008, Yee et al. 2008). Until recently *M. annularis* was thought to be a generalist that exhibited plasticity in its growth forms (mounds, columns and plates) according to light conditions. However in the 1990s the different growth forms were designated as separate sibling species, *M. annularis sensu stricto*, *Montastraea faveolata* and *Montastraea franksi*, based on depth, ecology and behaviour (Weil and Knowlton 1994). The recent nature of this taxonomic revelation, means that the three species are sometimes still described as ‘*Montastraea annularis* complex’ or ‘*sensu lato*’².

² Henceforth, any reference to *Montastraea annularis* means the species in its strictest meaning, unless otherwise stated.

Subsequent reproductive and genetic studies have supported these divisions, although *M. annularis* and *M. franksi* are less genetically distinct than *faveolata* (Fukami et al. 2004) and able to hybridise (although reproductively isolated by the timing of their spawning; Szmant 1991, Levitan et al. 2004). In addition to reproduction through mass spawning events (Szmant 1991), *M. annularis* is capable of asexual fragmentation/fission and clonal reproduction (Foster et al. 2007).

Although not as severely depleted as key framework builders *Acropora palmata* and *A. cervicornis*, the abundance of this ecosystem engineer has recently declined across its range with some populations showing a 30% decrease in cover over an eleven year period (Bruckner and Bruckner 2006, Edmunds and Elahi 2007, Dupont et al. 2008, Miller et al. 2009), and many colonies showing declines in health (e.g., Fig. 2.1). The corals exhibit low growth rates and low recruitment (eggs and larvae are small, growth of recruits is slow and survivorship is lower than other coral species, e.g. *Acropora*), meaning any declines in adult populations reduces chance of successful population recovery.

1.2 Value of reefs

The ecosystem goods and services provided by coral reefs are of substantial economic and social value, with an annual global valuation estimate of US\$375 billion (Costanza et al. 1997). Key benefits associated with healthy reefs include high fishery yields, tourism-related incomes, protection from coastal erosion, and nutrition for local communities (Table 1.1). Abstract ‘option’, ‘bequest’ and ‘existence’ values (associated with high-biodiversity and aesthetic quality) also exist but are more challenging to quantify. Reef-based resources are the primary source of food, income and livelihood for an estimated 30 million people in coastal and island communities, and are critically important for the socio-economic wellbeing of a further 500 million (Wilkinson 2004, Burke et al. 2011).

The wide range of ecological goods and services provided by Caribbean reefs (estimated to be worth between US\$3.1 and 4.6 billion per year; Burke and Maidens 2004) diminish with coral reef degradation. As a consequence maintaining a healthy state of ecosystem functioning – through improved scientific understanding of the system and management – is a key priority (Moberg and Folke 1999). Since the ability of reefs to bind calcium and construct massive calcium carbonate frameworks is the pre-requisite for all the ecosystem goods and services described (Table 1.1), long term broad scale management goals should aim to maintain carbonate production (Moberg and Folke 1999). This requires a good scientific understanding of the reef building process, justifying the research basis of this thesis.

1.3 The changing face of the Caribbean

Caribbean reefs are experiencing unprecedented change. Recent studies have identified continuing long term declines in living coral cover over recent decades, with an 80% reduction since the mid-1970s (Fig. 1.3; Gardner et al. 2003). This has been accompanied by a retardation of reef growth rates (Perry et al. 2013) and an associated loss of architectural complexity (Fig. 1.2; Alvarez-Filip et al. 2009) and related benefits (Section 1.2).

Goods		Ecological services				
Renewable resources	Mining of reefs	Physical structure services	Biotic services	Biogeochemical	Information services	Social and cultural services
Sea food products <i>Support 9-12% of world fisheries; in the Caribbean, worth \$US312 million year⁻¹</i>	Coral blocks, rubble/sand for building <i>In the Maldives 20000 m³ coral mined year⁻¹</i>	Shoreline protection <i>Worth US\$0.7-2.2 billion year⁻¹ in the Caribbean, based on estimated cost of replacement</i>	Maintenance of habitats <i>Spawning, nursery, breeding and feeding areas for reef organisms</i>	Nitrogen fixation <i>High rate of nitrogen fixation allows systems to persist in oligotrophic conditions</i>	Monitoring and pollution record <i>e.g., coral skeletons record metals in seawater</i>	Recreation <i>In 1990 Caribbean tourism earned US\$900,000,000; Florida reefs alone attract US \$1.6 billion annually</i>
Raw materials and medicines <i>Bioprospecting in US is a multi-million dollar industry</i>	Raw materials for lime and cement production <i>e.g. for agricultural fertilizers</i>	Build up of land <i>e.g. 300,000 people in the Indian Ocean and 2.5 million Pacific islanders live on land built by reefs</i>	Biodiversity/genetic library <i>Over 60,000 new animals and plants described, harbour 1/3 of all marine species</i>	CO ₂ /Ca budget control <i>Reefs precipitate 50% of calcium delivered to the sea year⁻¹</i>	Climate records <i>e.g. density bands in corals allow reconstruction of tropical sea surface temperature and monsoonal flooding events</i>	Sustaining community livelihoods <i>Caribbean tourism employs over 350 000 people annually</i>
Other raw materials <i>e.g., Agar production (for ice-cream), coral skeletons and bone-grafting</i>	Mineral oil and gas <i>e.g. in Saudi Arabia and Australia</i>	Generation of coral sand <i>Production of white sandy beaches in the Caribbean</i>	Biological maintenance of resilience <i>Foodweb dynamics, e.g., grazing and predation</i>	Waste assimilation <i>Worth US\$ 58 per ha year⁻¹ in Galapagos</i>		Cultural, religious and spiritual values <i>e.g. for Pacific Islanders, Kenyans</i>
Curio and jewellery <i>Red coral worth US\$900 kg⁻¹</i>		Promoting growth of mangroves and seagrass beds <i>i.e. through dissipation of wave energy to produce lagoon environments</i>	Regulation of ecosystem processes and functions <i>CO₂ sinks (on geological timescales), construction of 3-D framework</i>			Aesthetic values and artistic inspiration <i>e.g. BBC's Blue Planet viewed by 6.7 million people; £10 million worth of DVDs sold</i>
Aquarium trade (live fish and coral) <i>Marine aquarium market US\$24-40 million year⁻¹</i>			Biological support through mobile links <i>e.g. transfer between mangroves and seagrass beds</i>			
			Export of organic production to pelagic food webs <i>Supporting local fisheries</i>			

Table 1.1: Summary of goods and ecological services provided by coral reef ecosystems.

Adapted from Moberg and Folke, 1999.

Although degradation of coral reefs is not a recent phenomenon (Pandolfi et al. 2003), deterioration has accelerated over the past 50 years (Wilkinson and Souter 2008). Prior to the 1980s, scleractinian corals dominated many Caribbean reefs and abundance of macroalgae was low, but a combination of natural and anthropogenic stressors have triggered transitions into states of persistent low coral and high macroalgal cover (Kramer 2003, Mumby and Steneck 2008), often described as ecological ‘phase-shifts’ (Done 1992, Bellwood et al. 2004). These

transitions to macroalgal-dominated states (“the slippery slope to slime”; Pandolfi et al. 2005), can be attributed to a suite of anthropogenic stressors (pollution, overfishing and degradation of water quality; Jackson et al. 2001) and natural hurricane activity, but have been particularly aggravated by the functional extinction of important echinoid herbivore *Diadema antillarum* (Lessios 1988, Levitan 1988) and severe bleaching events in 1998 and 2005 (Hoegh-Guldberg 1999, Wilkinson and Souter 2008, Eakin et al. 2010). Fourteen percent of Caribbean reefs are currently estimated to have <10% coral cover, a further 46% are considered threatened (20–90% loss of living corals), while the remaining 40% of reefs, which include the well-managed regions of Bonaire, Bermuda, and the Flower Garden Banks, are under no immediate local threat (Wilkinson 2008, Jackson et al. 2012).

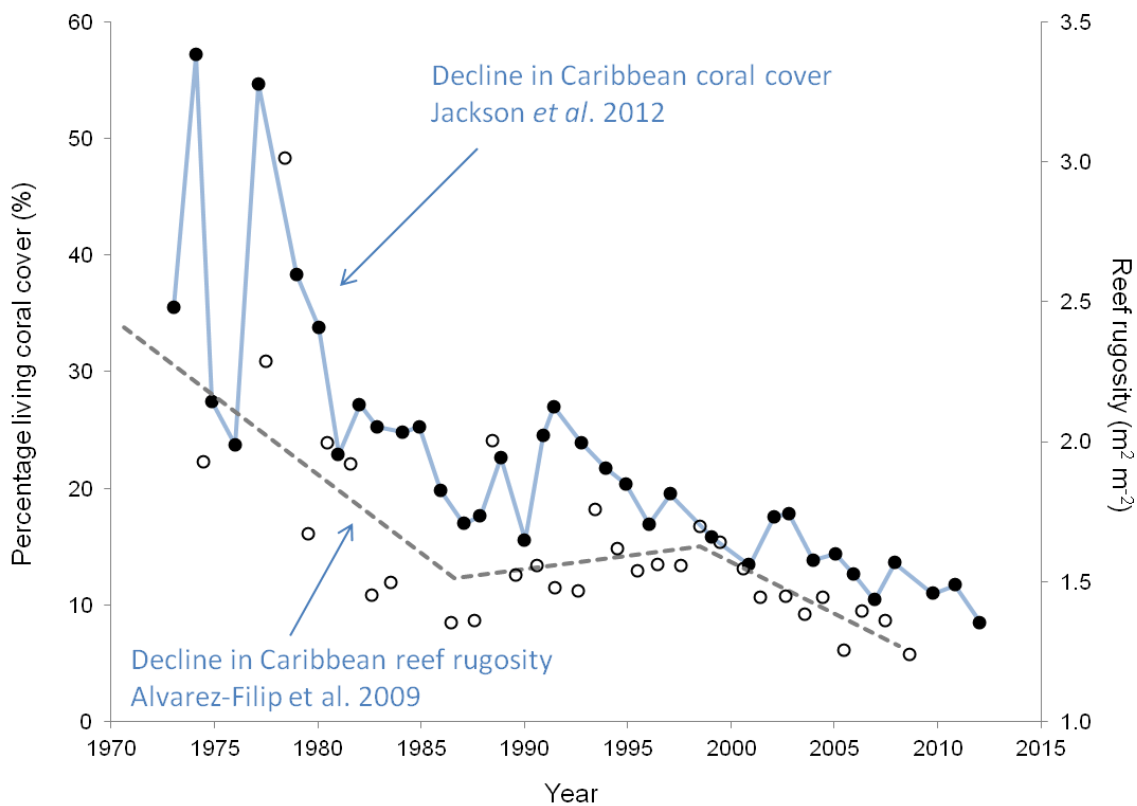


Figure 1.3: Declining state of Caribbean reefs. Chart summarises changes in living coral cover (●, from Jackson et al 2012) and reef rugosity, a measure of 3-D complexity (○, from Alvarez-Filip et al 2009) over the past half century. Weighted coral cover estimates from meta-analysis. Dashed line represents best fitting slope for rugosity loss.

These regional trends, indicative of deteriorating Caribbean coral reef ‘health’ and resilience (Hughes et al., 2003; Bellwood et al., 2004), are mirrored globally, with Pacific reef communities experiencing similar negative changes (Bruno and Selig 2007, De'ath et al. 2012).

A wide variety of extrinsic causes have been attributed to these changes in the Caribbean, both anthropogenic and natural. These include some that encourage macroalgal growth, such as fishing of herbivores (Aronson and Precht 2000, Mumby et al. 2006, Hughes et al. 2007), mass *D. antillarum* die-off due to disease (Levitan 1988) and eutrophication (Hallock and Schlager

1986, Fabricius 2005). Others reduce coral cover, such as hurricanes (Woodley et al. 1981, Gardner et al. 2005), coral disease (Gladfelter 1982, Aronson and Precht 2001), and more recently, coral bleaching (Mumby 1999, Cróquer and Weil 2009, Eakin et al. 2010).

Although the main drivers of Caribbean phase-shifts have largely been identified (Hughes 1994, Mumby and Steneck 2008), less is understood about interactive effects of the identified disturbances, which can operate over a confounding range of magnitudes, durations, frequencies and spatial distributions (Nyström et al. 2000). Additionally, anthropogenic threats are continually evolving. Emerging sources of disturbance (e.g., population explosion of the introduced Indo-Pacific lionfish, *Pterois volitans*, and Deep Water Horizon oil spill; Albins and Hixon 2011, White et al. 2012) are now accompanied by the global threat of climate change, mainly in the form of rising sea surface temperatures (SST) and ocean acidification (Hughes et al. 2003, Hoegh-Guldberg et al. 2007, Veron 2008). The immediacy of the climate threat was brought to the attention of the scientific community following increasingly destructive and extremely widespread mass bleaching events.

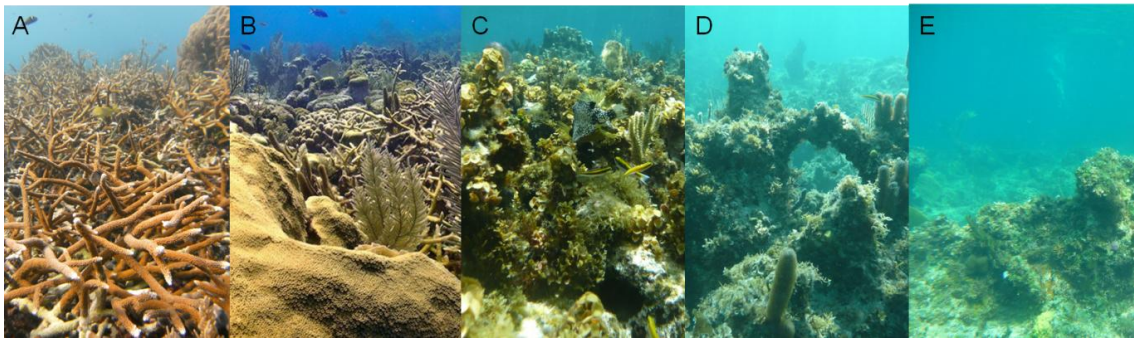


Figure 1.4: Photographs A-E document the decline of Caribbean reefs, from (A) highly structurally complex coral dominated systems through to (E) topographically flattened, algal dominated systems.

1.3.1 Rising sea temperatures

Anthropogenic activities, including deforestation, cement production, and burning of fossil fuels are releasing CO₂ into the atmosphere at an unprecedented rate (Caldeira and Wickett 2003). Since pre-industrial times, increases in CO₂ have brought about rises of 0.74°C global ocean surface temperature (IPCC, 2007), and if the current trend of accelerating global GHG emissions continues, increases of well over 2.0°C are possible. Thermal stress caused by rising SST is associated with coral bleaching (Fig. 1.5 B), the decoupling of the symbiotic relationship between scleractinian hosts and their endosymbiotic algae, which over prolonged periods can lead to reduced calcification and eventually partial or full colony mortality (Brown 1997). Degree heating weeks (DHW), a metric commonly used to characterize accumulated thermal stress, describe the number of consecutive weeks in which SSTs exceed (by > 1°C) the expected summertime SST maximum (Liu et al. 2006). Although the response of corals varies within and between species, one DHW can induce bleaching, thresholds of four DHW are generally

associated with mass bleaching events and eight with mortality (Eakin et al. 2010). The frequency and severity of bleaching events are predicted to increase over the coming decades (Donner et al. 2005), with climate projections forecasting the annual widespread bleaching events within 20-30 years (Donner et al. 2007) resulting in severe damage and world-wide mortality of corals (Nellman et al. 2008). Even non-lethal bleaching reduces the calcification of corals by up to 50% for six months, affecting the ability of a reef to effectively maintain structural growth. A significant time lag between changes in atmospheric CO₂ and temperature change means a period of committed warming even if emissions were reduced.

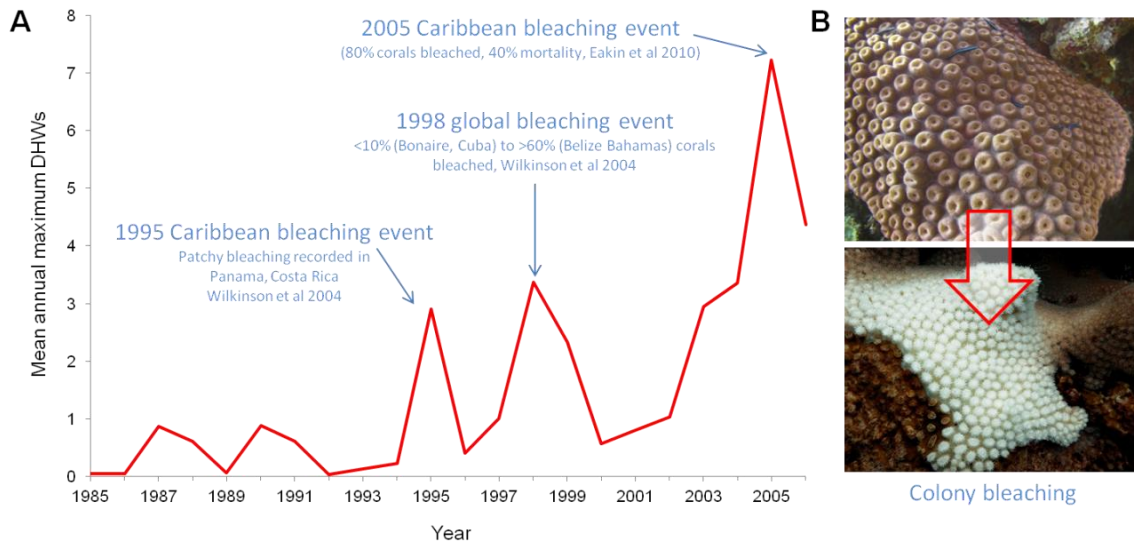


Figure 1.5: Thermal stress and coral bleaching. **A)** Graph of Caribbean-averaged annual maximum thermal stress (DHW) values 1985-2006, from Eakin et al 2010. 2005 was the warmest year in the Northern Hemisphere since records began (1880), previously 1998 has been the warmest. Both warming events caused massive coral losses with up to 95% of corals bleaching at some sites, and considerable post-bleaching mortality (Wilkinson and Souter 2008, Miller et al. 2009, Eakin et al. 2010). 2010 also saw a Caribbean mass bleaching event. **B)** *Montastraea cavernosa* colony exhibiting signs of bleaching. Photo credit: Renata Ferrari

1.3.2 Ocean acidification

Increasing atmospheric CO₂ concentrations are also associated with changes in ocean chemistry, principally reductions in ocean pH and carbonate ion concentrations (Caldeira and Wickett 2003). Availability of carbonate ions in seawater (denoted by the aragonite saturation state, Ω_{ar}) are thought to be tightly associated with corals ability to calcify (Langdon et al. 2000). This means ‘ocean acidification’ (OA) is predicted to become a considerable threat to corals by 2100 (Langdon et al. 2000, Hoegh-Guldberg et al. 2007, Silverman et al. 2009, Manzello 2010), primarily by negatively affecting reef calcification, but also coral recruitment (Morita et al. 2009, Doropoulos et al. 2012) and reproduction (Albright et al 2010). Caribbean seawater has already experienced a measurable decline of approximately -0.3 in the last 20 years in Ω_{ar} (Gledhill et al. 2008, Friedler et al. 2012), as unlike SST, ocean acidification does not lag behind changes in atmospheric CO₂ (equilibrium reached within a year). Although the response of calcifying organisms to OA is variable (Fabricius et al. 2011, McCulloch et al. 2012), both

experimental and modelling approaches suggest that predicted changes are likely to have net negative impact on the calcification of reef building communities (Fig. 1.6, Langdon et al. 2000, Orr et al. 2005, Hoegh-Guldberg et al. 2007, Silverman et al. 2009, Erez et al. 2011, Andersson and Gledhill 2013). The Caribbean currently experiences an Ω_{ar} of around 4.1 (HADSST2), with predictions suggesting that this value will decline to 3.4 at 490 ppm CO₂ and 3.2 at 550 ppm CO₂ (Simpson et al. 2009). The consensus opinion is that net calcification will decrease by 14–30% by 2100 (Gattuso et al., 1999; Kleypas et al., 1999), while another study suggests Caribbean coral reef calcification rates may have already declined by 15% since pre-industrial levels (Friedrich et al, 2012) In addition, changes in water chemistry may also enhance the natural chemical and mechanical breakdown of reef structural framework by bioeroding organisms (Wisshak et al. 2012). Comparable seawater changes in geological history resulted in complete disappearance of coral-reefs from the fossil record, for millions of years at a time (Veron 2008).

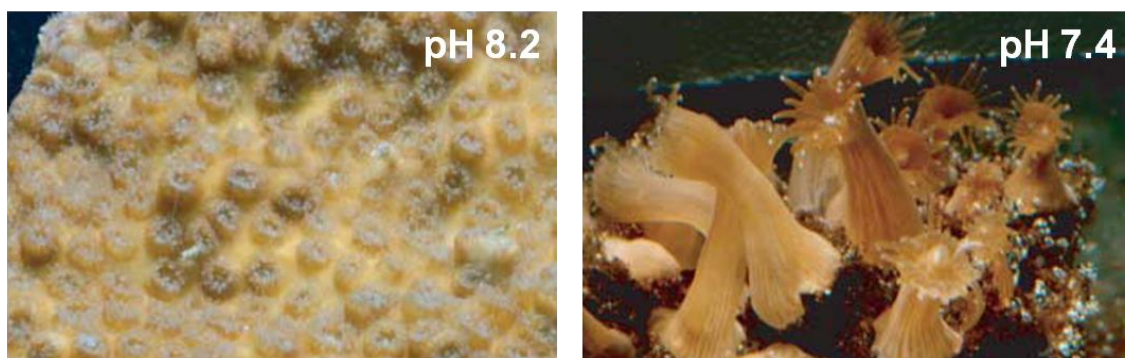


Figure 1.6: Mediterranean coral *Oculina patagonica* following 12 month exposure to standard (left) and depleted (right panel) seawater pH. The second panel shows complete skeletal dissolution (Fine and Tchenov 2007), although polyp biomass actually increases with pCO₂, confirming that competition for DIC between the processes of production (e.g., through zooxanthellae photosynthesis) and calcification (through coral skeletal production) exacerbates the problem when Ω_{ar} is low.

1.3.3 Sea-level rise and storm activity

Other predicted eventualities of rising CO₂ (besides the ‘evil twins’ of rising SST and increasing OA) include sea-level rise (Cazenave and Llovel 2010, Rahmstorf 2010) as well as an increase in severe weather events. Rising ocean surface temperatures are expected to amplify the frequency and severity of high-energy storm events (Emanuel 2005, Webster et al. 2005), leaving shorter windows of reef recovery while producing more widespread and severe impacts. Effects of extreme storm events could be exacerbated by weakening of reef structure through OA (Holland and Webster 2007). Combined, these multiple factors all have negative consequences for Caribbean reefs (Simpson et al. 2009).

1.3.4 Future impacts

The impacts of the changes on Caribbean reefs are already being experienced in terms of

economic losses. In 2007, the Caribbean suffered US \$10 billion in economic losses from weather related events representing over 13% of gross domestic product (GDP) (Frieler et al. 2013). One third of reef-building corals are considered to be at risk of extinction, with the Caribbean having the largest proportion in extinction risk categories (Carpenter et al. 2008). The ultimate driver of these anthropogenic effects is human population growth (described by coral scientists as the greatest threat to coral reefs, Kleypas and Eakin 2007), which has been positively correlated with macroalgal abundance, coral mortality, loss of herbivorous and piscivorous fish (Kleypas and Eakin 2007, Mora 2008), and increasing atmospheric concentrations of CO₂. With the intensity of human activities expected to increase (Cohen 2003), the outlook for the Caribbean appears bleak (Simpson et al. 2009).

1.4 Research focus

1.4.1 Carbonate budgets

Coral reef framework – the calcium carbonate structure underlying the living veneer of reefs – is a dynamic entity, continually being built and deconstructed by a diverse array of biological and geological processes (Fig. 1.7). Net reef growth rates are not simply a product of coral calcification, but also of bioerosion and storm damage, patterns of sediment storage within (or removal from) the reef and levels of secondary encrustation and cementation (Hubbard et al 1990).

The importance of these additional processes were illustrated by a study on Indonesian reefs, where degraded and polluted reefs maintained identical average coral skeletal extension growth rates to neighbouring healthy reef counterparts, despite rapid net erosion of their structural framework (Edinger et al. 2000). In order to fully understand the functioning of a reef, a holistic approach – one that considers bioerosion, sediment and the broad array of reef calcifiers – is required. Carbonate budgets provide a useful tool for achieving this, by examining the balance of reef accretory rates to those of erosional processes in order to assess the healthy functioning of a reef (in terms of ability to maintain architectural structure). Budgets attempt to quantify the many accretory and erosional processes of framework construction to provide an estimate of the net rate of reef accumulation, using a simplified equation $P_n = P_g - P_{SED}$ (Fig. 1.8).

P_g represents the gross production of carbonate by all reef calcifiers (blue box, Fig 1.7), P_{SED} is the total mechanically and chemically eroded carbonate removed from the reef and P_n is the net production of reef, conventionally measured in units of kilograms of CaCO₃ accumulated per planar unit reef area per year (sometimes referred to as ‘G’). Importantly, P_n can have a negative value if more carbonate is broken down and exported from the reef system is generated – this is when reefs may begin to lose structural complexity.

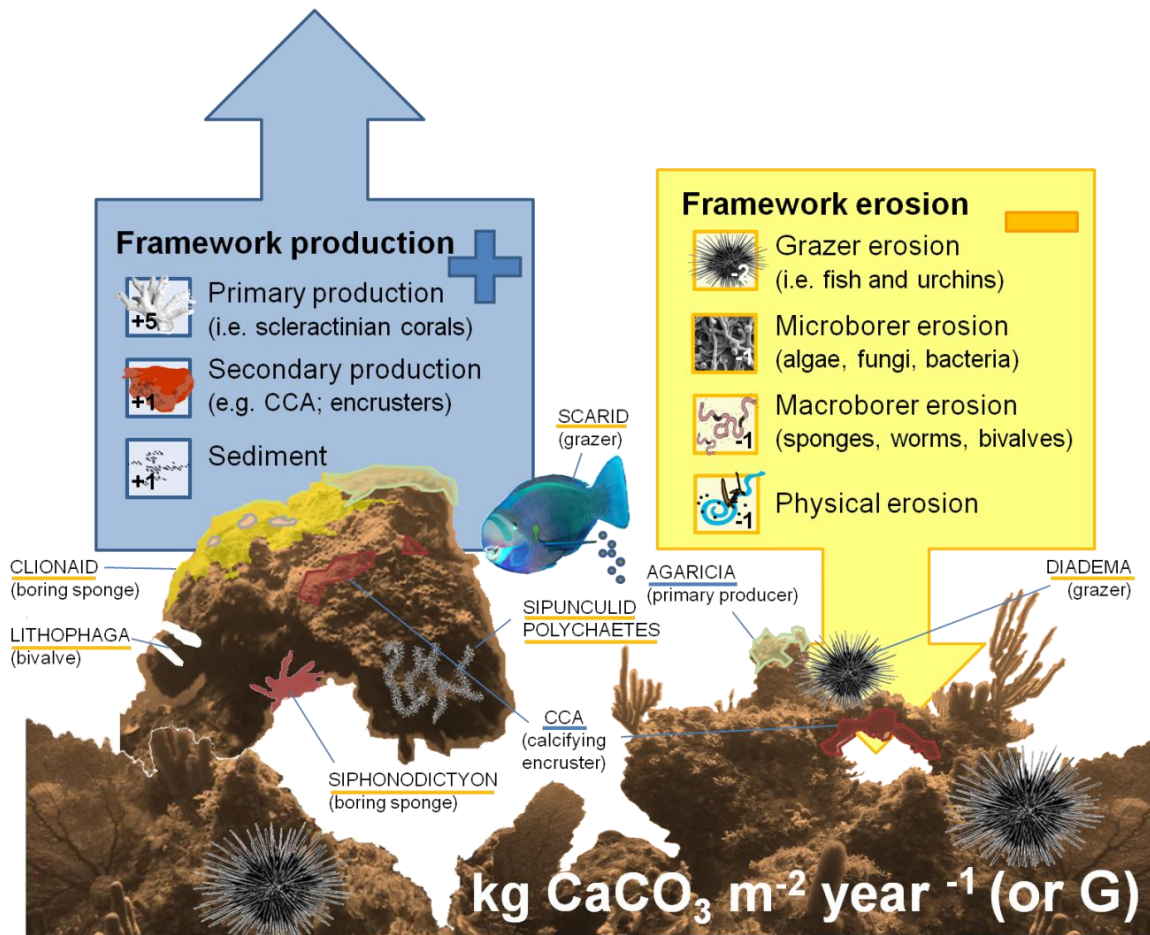


Figure 1.7: Diagram depicting the principal components of a coral reef carbonate budget. Carbonate budgets are a tool for estimating the net rate of accumulation of reef framework (in this case 2 kg CaCO₃ m⁻² year⁻¹, or ‘G’), but also provide useful information on the functioning of a reef in terms of bioerosion and accretion. Boxed values indicate typical figures of CaCO₃ accumulation/removal that contribute towards framework construction (blue box) and erosion (yellow box) in G. If summed, these values give a net rate of CaCO₃ accumulation of 2 G: a typical value for a healthy *Montastraea* reef.

Carbonate budgets need to remain positive to keep reefs positioned within the photic zone, and to maintain healthy ecosystem functioning (maximising provision of ecological services): a reef that cannot maintain a positive carbonate budget will eventually die (Edinger et al. 2000). For Caribbean reefs, measurable ecosystem tipping points include the point at which reefs stop accreting carbonate and start physically eroding (Hoegh-Guldberg et al. 2007, Silverman et al. 2009). A cessation of reef accretion (reef ‘turn-off’) and net erosion of reef structures (by bioeroders and storms) is argued by many as the ultimate and imminent trajectory (Perry and Smithers 2011), having occurred multiple times throughout geologic history; with ‘boom and bust’ growth and extinction events, usually associated with changes in carbon dioxide (Veron 2008).

Despite this, little is known about the effects of environmental change – and particularly future changes in OA and SST – on contemporary rates of Caribbean reef growth. Bioeroding organisms increase in diversity in degraded and dead framework (Enochs and Manzello 2012a), and with coral cover declining the potential implication of this increase – as well as effects of

various environmental factors on reef calcifying and bioeroding communities – requires urgent quantification. A critical issue facing coral reef managers and conservationists is fully understanding – and maintaining – the balance between reef structural growth (through coral calcification) and erosion (by bioeroders and storms), under changing environmental conditions. The requirement for a thorough exploration of Caribbean reef carbonate budgets in the context of local and global environmental change provides the basis for the first part of the thesis.

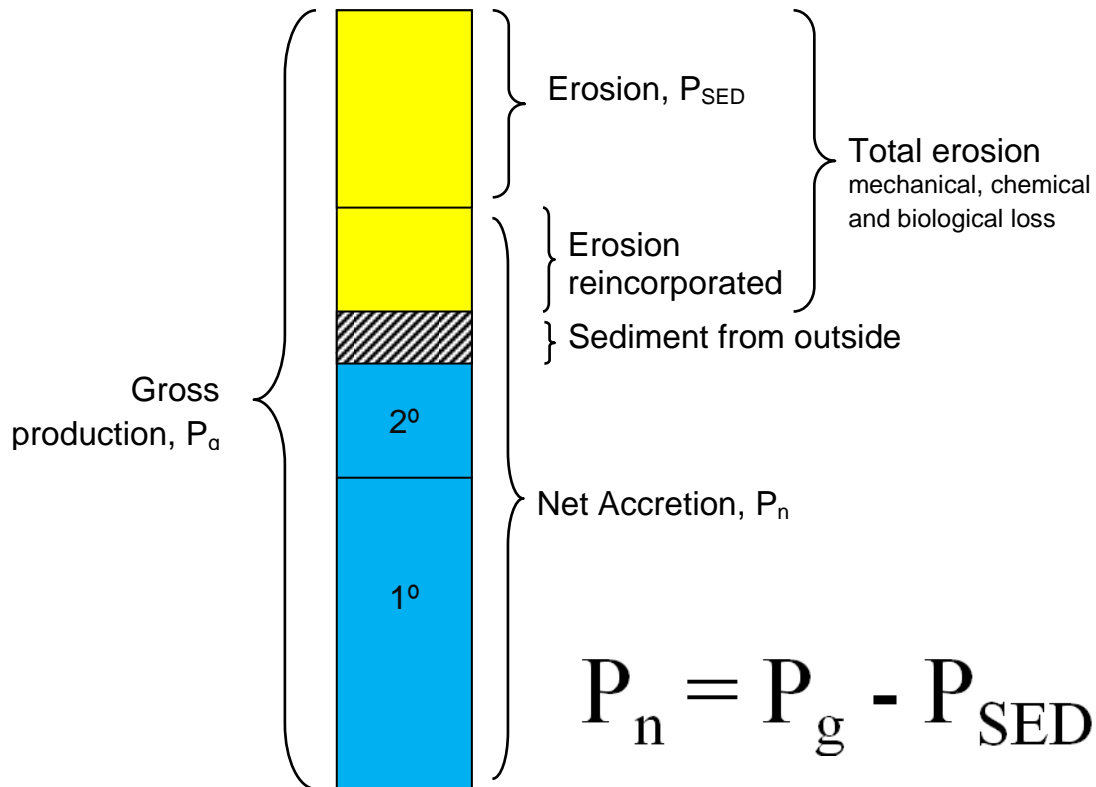


Figure 1.8: Diagram depicting the equation used to estimate the rate of reef accretion. P_g represents the gross production of carbonate by all reef calcifiers, P_{SED} is the total mechanically and chemically eroded carbonate removed from the reef and P_n is the net production of reef.

1.4.2 Zooxanthellae and bleaching thresholds

Zooxanthellae are the most abundant eukaryotes found in shallow water tropical marine environments, but were only formally described in the 1960s (Freudenthal 1962), and until the application of molecular techniques in the 1990s their diversity was severely underestimated (Rowan and Powers 1991). The true taxonomy and diversity of *Symbiodinium* are still in the process of being determined (Pochon et al. 2001, Silverstein et al. 2011), but OTUs are now known to number in their hundreds, and are split across nine taxonomic groupings (called clades). Diversity of *Symbiodinium* assemblages are thought to be particularly high (relative to host diversity) in the Caribbean (LaJeunesse 2005). An improved understanding of the critical role played by endosymbionts in calcification (Allemand et al. 2004) – and thereby reef growth, as well their influence in acclimation of coral hosts to varied and changing environments have recently made the study of these coral-algal symbioses more pertinent. Meanwhile, the growing

intensification in both the frequency and severity of reef-wide bleaching incidences (section 1.3.1), have brought *Symbiodinium* to the attention of reef scientists, with an urgent focus on understanding the newly emerging threat of symbiosis-degeneration to reef functioning.

Gaps in the knowledge regarding the functional diversity of types, the physiological traits they infer to their coral hosts, and the flexibility of the symbiotic partnership – particularly in the face of rising SST – need to be addressed in order to assess the ability of corals to survive future warming events and contribute towards reef building. Revealing bleaching ‘tipping points’ in corals, both at the coral colony (Fitt et al. 2001) and ecosystem level (Donner et al. 2005) is a critical step in predicting reef responses to global climate change. However, the ecological and biogeographic distributions of *Symbiodinium* diversity remains poorly characterised for much of the world (Finney et al. 2010). A better understanding of *M. annularis* holobiont diversity across the Caribbean will help inform researchers about the resilience of reefs to future environmental change. A better understanding of the specific environmental drivers of *Symbiodinium* biogeography is fundamental for prediction of coral community responses to a changing climate. To achieve this, comprehensive studies that examine the influence of multiple predictors are required. Addressing this issue becomes the focal point of the second part of the thesis.

However, the relatively recent discovery of diversity within *Symbiodinium* has meant that the field is still at the stage of categorisation of symbiont diversity and distribution. A comprehensive cataloguing of diversity is a necessary pre-requisite to full exploration of the extent of variation and flexibility regarding the ability of corals to host different *Symbiodinium* clades, and the subsequent ecological significance of this, before possibility of adaptation can be fully assessed.

1.5 Thesis outline

Caribbean coral reefs are rapidly approaching state of ecosystem dysfunction, driven by a complex suite of environmental threats, of which global climate change plays an important role (section 1.3). In this thesis I address two separate issues that will likely play a major role in determining the future behaviour of Caribbean reefs under projected climate change. In the first strand, the main aim is to pull together rates of the major biological, ecological and geological processes regarding CaCO₃ construction/breakdown in order to estimate the ability of *Montastraea* forereefs to positively generate carbonate framework (thereby maintaining ecosystem function) under an array of past and future environmental conditions.

A theoretical approach will be adopted - incorporating ecological, carbonate budget, and climate models into a single modelling framework- to reconstruct the patterns and drivers of carbonate

budgets for Caribbean reefs over the past 50 years. The model, parameterized and bounded using published empirical data on both bioeroders and reef calcifiers (described in Chapter 3), will be used to produce outputs that can be validated using published carbonate budgets from the region.

Chapter 3 describes the selection and full parameterisation of the carbonate budget mode with the most relevant factors that could affect carbonate production and/or erosion (115 parameters in total). Selection of model parameters and assignment of value limits for each parameter are determined using both published and unpublished empirical data.

In the second part of the thesis I focus on one aspect of reef functioning: *Symbiodinium* diversity. This was selected as a study focus because of the potential importance of genetic diversity in providing a ‘nugget of hope’ for acclimation of reefs to projected global climate change (Berkelmans and van Oppen 2006). The advent of molecular techniques has shifted recent research focus onto *Symbiodinium*, but much work needs to be done to characterise their full diversity, and further uncovering functional diversity is a major research goal of the field.

In Chapter 5 I aim to explore the flexibility of *M. annularis*, one of the most important reef building corals (Section 1.1.5), in hosting a diverse array of *Symbiodinium*. I categorise the symbionts found, elucidating significant biogeographic patterns which can be summarised as a broad Caribbean east-west divide in community dominance from less speciose clade B to richer clade C dominated communities in the Lesser Antilles. In Chapter 6 I attempt to explain these observed patterns in terms of environmental heterogeneity (including regional SSTs, Ω_{ar} , salinity) across the region, to analyse symbiont communities at different spatial scales and finally compare *Symbiodinium* community with established population genetic structuring of the host across the region.

In Chapter 7 I choose to focus in on one topical aspect of the *Symbiodinium* community composition: the presence of low abundance *Symbiodinium* D. This is discussed in the context of global climate change. Characterising the prevalence of this ecologically important symbiont, which confers bleaching resilience to its host - helps us to better understand the potential for adaptation and is a key requirement of conservation strategies (Mumby et al. 2011)

In Chapter 8, I explore the temporal stability of the symbioses described in Chapter 5, by means of a small scale investigation into Bahamian *M. annularis* colonies.

These disparate but topical subjects, as well as having a strong *Montastraea*-focus, are linked by the core involvement of communities of organisms (e.g., bioeroders, zooxanthellae) that play a vital role in the healthy reef functioning yet might be described as ‘cryptic’. Critically, this has meant that these communities have attracted less research effort. Investigation of both these

issues are core to predicting behaviour of Caribbean reefs under projected climate change, yet – probably as a result of the cryptic nature - gaps in the knowledge that surround these areas, particularly in regard to future response to climate change. In the final discussion chapter I synthesise the two strands, discussing potential impacts of *Symbiodinium* diversity on healthy reef growth.

1.6 References

- Albins M, Hixon M (2011) Worst case scenario: potential long-term effects of invasive predatory lionfish (*Pterois volitans*) on Atlantic and Caribbean coral-reef communities. *Environmental Biology of Fishes* **3**:1-7
- Allemand D, Ferrier-Pages C, Furla P, Houlbreque F, Puverel S, Reynaud S, Tambutte E, Tambutte S, Zoccola D (2004) Biomineralisation in reef-building corals: from molecular mechanisms to environmental control. *Comptes Rendus Palevol* **3**:453-467
- Allsopp M, Pambuccian S, Johnston P, Santillo D (2009) *State of the world's oceans*, Vol. Springer
- Alvarez-Filip L, Dulvy NK, Gill JA, Côté IM, Watkinson AR (2009) Flattening of Caribbean coral reefs: region-wide declines in architectural complexity. *Proceedings of the Royal Society B-Biological Sciences* **276**:3019-3025
- Andersson AJ, Gledhill D (2013) Ocean acidification and coral reefs: effects on breakdown, dissolution, and net ecosystem calcification. *Annual Review of Marine Science* **5**:321-348
- Aronson RB, Precht WF (2000) Herbivory and algal dynamics on the coral reef at Discovery Bay, Jamaica. *Limnology and Oceanography* **45**:251-255
- Aronson RB, Precht WF (2001) White-band disease and the changing face of Caribbean coral reefs. *Hydrobiologia* **460**:25-38
- Baker AC (2003) Flexibility and specificity in coral-algal symbiosis: Diversity, ecology, and biogeography of *Symbiodinium*. *Annual Review of Ecology Evolution and Systematics* **34**:661-689
- Bellwood DR, Hughes TP, Folke C, Nystrom M (2004) Confronting the coral reef crisis. *Nature* **429**:827-833
- Berkelmans R, van Oppen MJH (2006) The role of zooxanthellae in the thermal tolerance of corals: a 'nugget of hope' for coral reefs in an era of climate change. *Proceedings of the Royal Society B-Biological Sciences* **273**:2305-2312
- Brown BE (1997) Coral bleaching: causes and consequences. *Coral Reefs* **16**:S129-S138
- Bruckner AW, Bruckner RJ (2006) The recent decline of *Montastraea annularis* (complex) coral populations in western Curaçao: cause for concern? *Revista de Biología Tropical* **54**:45-58
- Bruno JF, Selig ER (2007) Regional decline of coral cover in the Indo-Pacific: timing, extent, and subregional comparisons. *PLoS ONE* **2**:e711
- Burke L, Maidens J (2004) *Reefs at risk in the Caribbean*, Vol. World Resources Institute
- Burke L, Reyta K, Spalding M, Perry A (2011) *Reefs at Risk Revisited*. Report No. ISBN 978-1-56973-762-0
- Caldeira K, Wickett ME (2003) Oceanography: anthropogenic carbon and ocean pH. *Nature* **425**:365-365
- Carpenter KE, Abrar M, Aeby G, Aronson RB, Banks S, Bruckner A, Chiriboga A, Cortes J, Delbeek JC, DeVantier L, Edgar GJ, Edwards AJ, Fenner D, Guzman HM, Hoeksema BW, Hodgson G, Johan O, Licuanan WY, Livingstone SR, Lovell ER, Moore JA, Obura DO, Ochavillo D, Polidoro BA, Precht WF, Quibilan MC, Reboton C, Richards ZT, Rogers AD, Sanciangco J, Sheppard A, Sheppard C, Smith J, Stuart S, Turak E, Veron JEN, Wallace C, Weil E, Wood E (2008) One-third of reef-building corals face elevated extinction risk from climate change and local impacts. *Science* **321**:560-563
- Cazenave A, Llovel W (2010) Contemporary sea level rise. *Annual Review of Marine Science* **2**:145-173
- Chalker BE, Barnes DJ, Dunlap WC, Jokiel PL (1988) Light and reef-building corals. *Interdisciplinary Science Reviews* **13**:222-237
- Chollett I, Mumby PJ, Muller-Karger FE, Hu C (2012) Physical environments of the Caribbean Sea. *Limnology and Oceanography* **54**:1233-1244
- Cohen A, McConnaughey TA (2003) Geochemical perspectives on coral mineralisation. *Reviews in Mineralogy and Geochemistry* **54**:151-187
- Cohen JE (2003) Human population: the next half century. *Science* **302**:1172-1175
- Costanza R, d'Arge R, deGroot R, Farber S, Grasso M, Hannon B, Limburg K, Naeem S, O'Neill RV, Paruelo J, Raskin RG, Sutton P, van den Belt M (1997) The value of the worlds ecosystem services and natural capital. *Nature* **387**:253-260
- Cróquer A, Weil E (2009) Changes in Caribbean coral disease prevalence after the 2005 bleaching event. *Diseases of aquatic organisms* **87**:33-43
- De'ath G, Fabricius KE, Sweatman H, Puotinen M (2012) The 27-year decline of coral cover on the Great Barrier Reef and its causes. *Proceedings of the National Academy of Sciences* **109**:17995-17999
- Done TJ (1992) Phase shifts in coral reef communities and their ecological significance. *Hydrobiologia* **247**:121-132

- Donner SD, Knutson TR, Oppenheimer M (2007) Model-based assessment of the role of human-induced climate change in the 2005 Caribbean coral bleaching event. *Proceedings of the National Academy of Sciences* **104**:5483-5488
- Donner SD, Skirving WJ, Little CM, Oppenheimer M, Hoegh-Guldberg OVE (2005) Global assessment of coral bleaching and required rates of adaptation under climate change. *Global Change Biology* **11**:2251-2265
- Doropoulos C, Ward S, Diaz-Pulido G, Hoegh-Guldberg O, Mumby PJ (2012) Ocean acidification reduces coral recruitment by disrupting intimate larval-algal settlement interactions. *Ecology Letters* **15**:338-346
- Dupont J, Jaap WC, Hallock P (2008) A retrospective analysis and comparative study of stony coral assemblages in Biscayne National Park, Florida (1977-2000). *Caribbean Journal of Science* **44**:334-344
- Eakin CM, Morgan JA, Heron SF, Smith TB, Liu G, Alvarez-Filip L, Baca B, Bartels E, Bastidas C, Bouchon C, Brandt M, Bruckner AW, Bunkley-Williams L, Cameron A, Causey BD, Chiappone M, Christensen TRL, Crabbe MJC, Day O, de la Guardia E, Díaz-Pulido G, DiResta D, Gil-Agudelo DL, Gilliam DS, Ginsburg RN, Gore S, Guzmán HcM, Hendee JC, Hernández-Delgado EA, Husain E, Jeffrey CFG, Jones RJ, Jordán-Dahlgren E, Kaufman LS, Kline DI, Kramer PA, Lang JC, Lirman D, Mallela J, Manfrino C, Maréchal J-P, Marks K, Mihaly J, Miller WJ, Mueller EM, Muller EM, Orozco Toro CA, Oxenford HA, Ponce-Taylor D, Quinn N, Ritchie KB, Rodríguez Sn, Ramírez AR, Romano S, Samhuri JF, Sánchez JA, Schmahl GP, Shank BV, Skirving WJ, Steiner SCC, Villamizar E, Walsh SM, Walter C, Weil E, Williams EH, Roberson KW, Yusuf Y (2010) Caribbean corals in crisis: record thermal stress, bleaching, and mortality in 2005. *PLoS ONE* **5**:e13969
- Edinger EN, Limmon GV, Jompa J, Widjatmoko W, Heikoop JM, Risk MJ (2000) Normal coral growth rates on dying reefs: Are coral growth rates good indicators of reef health? *Marine Pollution Bulletin* **40**:404-425
- Edmunds PJ, Davies PS (1986) An energy budget for *Porites porites* (Scleractinia). *Marine Biology* **92**:339-347
- Edmunds PJ, Elahi R (2007) The demographics of a 15-year decline in cover of the Caribbean reef coral *Montastraea annularis*. *Ecological Monographs* **77**:3-18
- Ellis J, Solander D (1786) *The natural history of many curious and uncommon zoophytes, collected from various parts of the globe*. Accessed through: World Register of Marine Species at <http://www.marinespecies.org/aphia.php?p=taxdetails&id=207479>
- Emanuel K (2005) Increasing destructiveness of tropical cyclones over the past 30 years. *Nature* **436**:686-688
- Enochs IC, Manzello DP (2012) Responses of cryptofaunal species richness and trophic potential to coral reef habitat degradation. *Diversity* **4**:94-104
- Erez J, Reynaud S, Silverman J, Schneider J, Allemand D (2011) Coral calcification under ocean acidification and global change. In: Dubinsky Z, Stambler N (eds) *Coral Reefs: An Ecosystem in Transition*. Springer, Berlin, p 151-176
- Fabricius KE (2005) Effects of terrestrial runoff on the ecology of corals and coral reefs: review and synthesis. *Marine Pollution Bulletin* **50**:125-146
- Fabricius KE, Langdon C, Uthicke S, Humphrey C, Noonan S, De'ath G, Okazaki R, Muehllehner N, Glas MS, Lough JM (2011) Losers and winners in coral reefs acclimatized to elevated carbon dioxide concentrations. *Nature Climate Change* **1**:165-169
- Fagoonee I, Wilson HB, Hassell MP, Turner JR (1999) The dynamics of zooxanthellae populations: a long-term study in the field. *Science* **283**:843-845
- Finney J, Pettay D, Sampayo E, Warner M, Oxenford H, LaJeunesse T (2010) The relative significance of host-habitat, depth, and geography on the ecology, endemism, and speciation of coral endosymbionts in the genus *Symbiodinium*. *Microbial Ecology* **60**:250-263
- Fitt W, Brown B, Warner M, Dunne R (2001) Coral bleaching: interpretation of thermal tolerance limits and thermal thresholds in tropical corals. *Coral Reefs* **20**:51-65
- Foster NL, Baums IB, Mumby PJ (2007) Sexual vs. asexual reproduction in an ecosystem engineer: the massive coral *Montastraea annularis*. *Journal of Animal Ecology* **76**:384-391
- Freudenthal HD (1962) *Symbiodinium* gen. nov. and *Symbiodinium microadriaticum* sp. nov., a zooxanthella: taxonomy, life cycle and morphology. *Journal of Protozoology* **9**:45-49
- Friedrich T, Timmermann A, Abe-Ouchi A, Bates NR, Chikamoto MO, Church MJ, Dore JE, Gledhill DK, Gonzalez-Davila M, Ilyina T, Jungclaus JH, McLeod E, Mouchet A, Santana-Casiano JM (2012) Detecting regional anthropogenic trends in ocean acidification against natural variability. *Nature Climate Change* **2**:167-171

- Frieler K, Meinshausen M, Golly A, Mengel M, Lebek K, Donner SD, Hoegh-Guldberg O (2013) Limiting global warming to 2°C is unlikely to save most coral reefs. *Nature Climate Change* **3**:165-170
- Fukami H, Budd AF, Levitan DR, Jara J, Kersanach R, Knowlton N (2004) Geographic differences in species boundaries among members of the *Montastraea annularis* complex based on molecular and morphological markers. *Evolution* **58**:324-337
- Gardner TA, Côté IM, Gill JA, Grant A, Watkinson AR (2003) Long-term region-wide declines in Caribbean corals. *Science* **301**:958-960
- Gardner TA, Côté IM, Gill JA, Grant A, Watkinson AR (2005) Hurricanes and Caribbean coral reefs: impacts, recovery patterns and role in long-term decline. *Ecology* **86**:174-184
- Gattuso J-P, Allemand D, Frankignoulle M (1999) Photosynthesis and calcification at cellular, organismal and community levels in coral reefs: a review on interactions and control by carbonate chemistry. *American Zoologist* **39**:160-183
- Gladfelter EH, Monahan RK, Gladfelter WB (1978) Growth rates of five reef-building corals in the Northeastern Caribbean. *Bulletin of Marine Science* **28**:728-734
- Gladfelter WB (1982) White-band disease in *Acropora palmata*: implications for the structure and growth of shallow reefs. *Bulletin of Marine Science* **32**:639-643
- Gledhill DK, Wanninkhof R, Millero FJ, Eakin M (2008) Ocean acidification of the Greater Caribbean Region 1996-2006. *Journal of Geophysical Research-Oceans* **113**:C10031
- Goreau TF (1959) The Ecology of Jamaican Coral Reefs I. Species Composition and Zonation. *Ecology* **40**:67-90
- Greer L, Jackson JE, Curran HA, Guilderson T, Teneva L (2009) How vulnerable is *Acropora cervicornis* to environmental change? Lessons from the early to middle Holocene. *Geology* **37**:263-266
- Hallock P, Schlager W (1986) Nutrient excess and the demise of coral reefs and carbonate platforms. *Palaios* **1**:389-398
- Heileman S, Mahon R (2009) Caribbean Sea: LME. In: Sherman K, Hempel G (eds) *The UNEP Large Marine Ecosystems Report: a perspective in changing conditions in LMEs of the worlds regional seas*. United Nations Environment Programme, Nairobi, Kenya
- Hoegh-Guldberg O (1999) Climate change, coral bleaching and the future of the world's reefs. *Marine Freshwater Research* **50**:839-866
- Hoegh-Guldberg O, Mumby PJ, Hooten AJ, Steneck RS, Greenfield P, Gomez E, Harvell CD, Sale PF, Edwards AJ, Caldeira K, Knowlton N, Eakin CM, Iglesias-Prieto R, Muthiga N, Bradbury RH, Dubi A, Hatzitolos ME (2007) Coral reefs under rapid climate change and ocean acidification. *Science* **318**:1737-1742
- Holland GJ, Webster PJ (2007) Heightened tropical cyclone activity in the North Atlantic: natural variability or climate trend? *Philosophical Transactions of the Royal Society A: Mathematical, Physical and Engineering Sciences* **365**:2695-2716
- Hughes TP (1994) Catastrophes, phase-shifts and large-scale degradation of a Caribbean coral reef. *Science* **265**:1547-1551
- Hughes TP, Baird AH, Bellwood DR, Card M, Connolly SR, Folke C, Grosberg R, Hoegh-Guldberg O, Jackson JBC, Kleypas J, Lough JM, Marshall P, Nyström M, Palumbi SR, Pandolfi JM, Rosen B, Roughgarden J (2003) Climate change, human impacts, and the resilience of coral reefs. *Science* **301**:929-933
- Hughes TP, Rodrigues MJ, Bellwood DR, Ceccarelli D, Hoegh-Guldberg O, McCook L, Moltschanivskyj N, Pratchett MS, Steneck RS, Willis B (2007) Phase shifts, herbivory, and the resilience of coral reefs to climate change. *Current Biology* **17**:360-365
- IUCN (2008) *Montastraea annularis*. In: IUCN 2012 *IUCN Red List of Threatened Species Version 2012*
- Jackson JBC, Cramer K, Donovan M, Friedlander A, Hooten AJ, Lam V (2012) *Tropical Americas coral reef resilience workshop*. GCRMN Report, April 29 - May 5, Panama City
- Jackson JBC, Jung P, Coates AG, Collins LS (1993) Diversity and extinction of tropical American mollusks and emergence of the Isthmus of Panama. *Science* **260**:1624-1626
- Jackson JBC, Kirby MX, Berger WH, Bjorndal KA, Botsford LW, Bourque BJ, Bradbury RH, Cooke R, Erlandson J, Estes JA, Hughes TP, Kidwell S, Lange CB, Lenihan HS, Pandolfi JM, Peterson CH, Steneck RS, Tegner MJ, Warner RR (2001) Historical overfishing and the recent collapse of coastal ecosystems. *Science* **293**:629-637
- Jones AM, Berkelmans R, van Oppen MJH, Mieog JC, Sinclair W (2008) A community change in the algal endosymbionts of a scleractinian coral following a natural bleaching event: field evidence of acclimatization. *Proceedings of the National Academy of Sciences* **275**:1359-1365
- Kleypas J, Eakin CM (2007) Scientists perceptions of the threats to coral reefs: results of a survey of coral reef researchers. *Bulletin of Marine Science* **80**:419-436

- Knowlton N, Weil E, Weigt LA, Guzman HM (1992) Sibling species in *Montastraea annularis*, coral bleaching, and the coral climate record. *Science* **255**:330-333
- Kramer PA (2003) Synthesis of coral reef health indicators for the western Atlantic: results of the AGRRA program (1997-2000). In: Status of Coral Reefs in the Western Atlantic: Results of Initial Surveys, Atlantic and Gulf Rapid Reef Assessment (AGRRA) Program. *Atoll Res. Bull.*, **496**:1-55
- Lajeunesse TC (2005) "Species" radiations of symbiotic dinoflagellates in the Atlantic and Indo-Pacific since the miocene-pliocene transition. *Molecular Biology and Evolution* **22**:570-581
- Lajeunesse TC, Smith RT, Finney J, Oxenford H (2009) Outbreak and persistence of opportunistic symbiotic dinoflagellates during the 2005 Caribbean mass coral 'bleaching' event. *Proceedings of the Royal Society B-Biological Sciences* **276**:4139-4148
- Langdon C, Takahashi T, Sweeney C, Chipman D, Goddard J (2000) Effect of calcium carbonate saturation state on the rate of calcification of an experimental coral reef. *Global Biogeochemical Cycles* **14**:639-654
- Lessios HA (1988) Mass mortality of *Diadema antillarum* in the Caribbean: what have we learned? *Annual Review of Ecology and Systematics* **19**:371-393
- Lessios HA (2008) The Great American schism: divergence of marine organisms after the rise of the Central American Isthmus. *Annual Review of Ecology, Evolution, and Systematics* **39**:63-91
- Levitan DR (1988) Algal-urchin biomass responses following mass mortality of *Diadema antillarum* Philippi at Saint John, U.S. Virgin Islands. *Journal of Experimental Marine Biology and Ecology* **119**:167-178
- Levitan DR, Fukami H, Jara J, Kline D, McGovern TM, McGhee KE, Swanson CA, Knowlton N (2004) Mechanisms of reproductive isolation among sympatric broadcast-spawning corals of the *Montastraea annularis* species complex. *Evolution* **58**:308-323
- Little AF, van Oppen MJH, Willis BL (2004) Flexibility in algal endosymbioses shapes growth in reef corals. *Science* **304**:1492-1494
- Liu G, Strong AE, Skirving WJ, Arzayus LF (2006) Overview of NOAA Coral Reef Watch Program's near-real-time satellite global coral bleaching monitoring activities. *Proceedings of the 10th International Coral Reef Symposium*, Okinawa, Japan, p 1738-1793
- Manzello D (2010) Coral growth with thermal stress and ocean acidification: lessons from the eastern tropical Pacific. *Coral Reefs* **29**:749-758
- McCulloch M, Falter J, Trotter J, Montagna P (2012) Coral resilience to ocean acidification and global warming through pH up-regulation. *Nature Climate Change* **2**:623-627
- Miller J, Muller E, Rogers C, Waara R, Atkinson A, Whelan KRT, Patterson M, Witcher B (2009) Coral disease following massive bleaching in 2005 causes 60% decline in coral cover on reefs in the US Virgin Islands. *Coral Reefs* **28**:925-937
- Moberg F, Folke C (1999) Ecological goods and services of coral reef ecosystems. *Ecological Economics* **29**:215-233
- Mora C (2008) A clear human footprint in the coral reefs of the Caribbean. *Proceedings of the Royal Society B-Biological Sciences* **275**:767-773
- Mumby PJ (1999) Bleaching and hurricane disturbances to populations of coral recruits in Belize. *Marine Ecology Progress Series* **190**:27-35
- Mumby PJ, Broad K, Brumbaugh DR, Dahlgren C, Harborne AR, Hastings A, Holmes KE, Kappel CV, Micheli F, Sanchirico JN (2008) Coral reef habitats as surrogates of species, ecological functions, and ecosystem services. *Conservation Biology* **22**:941-951
- Mumby PJ, Dahlgren CP, Harborne AR, Kappel CV, Micheli F, Brumbaugh DR, Holmes KE, Mendes JM, Broad K, Sanchirico JN, Buch K, Box S, Stoffle RW, Gill AB (2006) Fishing, trophic cascades, and the process of grazing on coral reefs. *Science* **311**:98-101
- Mumby PJ, Elliott IA, Eakin CM, Skirving W, Paris CB, Edwards HJ, Enríquez S, Iglesias-Prieto R, Cherubin LM, Stevens JR (2011) Reserve design for uncertain responses of coral reefs to climate change. *Ecology Letters* **14**:132-140
- Mumby PJ, Steneck RS (2008) Coral reef management and conservation in light of rapidly evolving ecological paradigms. *Trends in Ecology and Evolution* **23**:555-563
- Muscantine L, Falkowski PG, Porter JW, Dubinsky Z (1984) Fate of photosynthetic fixed carbon in light and shade-adapted colonies of the symbiotic coral *Stylophora pistillata*. *Proceedings of the Royal Society of London Series B, Biological Sciences* **222**:181-202
- Muscantine L, Porter JW (1977) Reef corals: mutualistic symbioses adapted to nutrient-poor environments. *BioScience* **27**:454-460
- Nellman C, Hain S, Alder J (2008) *In dead water: merging of climate change with pollution, over-harvest, and infestations in the world's fishing grounds*, UNEP Report Norway

- Nyström M, Folke C, Moberg F (2000) Coral reef disturbance and resilience in a human-dominated environment. *Trends in Ecology and Evolution* **15**:413-417
- Orr JC, Fabry VJ, Aumont O, Bopp L, Doney SC, Feely RA, Gnanadesikan A, Gruber N, Ishida A, Joos F, Key RM, Lindsay K, Maier-Reimer E, Matear R, Monfray P, Mouchet A, Najjar RG, Plattner GK, Rodgers KB, Sabine CL, Sarmiento JL, Schlitzer R, Slater RD, Totterdell IJ, Weirig MF, Yamanaka Y, Yool A (2005) Anthropogenic ocean acidification over the twenty-first century and its impact on calcifying organisms. *Nature* **437**:681-686
- Oxenford H, Roach R, Brathwaite A (2008) Large scale coral mortality in Barbados: a delayed response to the 2005 bleaching episode. *Proceedings of the 11th International Coral Reef Symposium, Florida*
- Pandolfi JM, Bradbury RH, Sala E, Hughes TP, Bjorndal KA, Cooke RG, McArdle D, McClenachan L, Newman MJH, Paredes G, Warner RR, Jackson JBC (2003) Global trajectories of the long-term decline of coral reef ecosystems. *Science* **301**:955-958
- Pandolfi JM, Jackson JBC, Baron N, Bradbury RH, Guzman HM, Hughes TP, Kappel CV, Micheli F, Ogden JC, Possingham HP, Sala E (2005) Are U.S. Coral Reefs on the Slippery Slope to Slime? *Science* **307**:1725-1726
- Perry CT, Murphy GN, Kench PS, Smithers SG, Edinger EN, Steneck RS, Mumby PJ (2013) Caribbean-wide decline in carbonate production threatens coral reef growth. *Nature Communications* **4**:1402
- Perry CT, Smithers SG (2011) Cycles of coral reef 'turn-on', rapid growth and 'turn-off' over the past 8500 years: a context for understanding modern ecological states and trajectories. *Global Change Biology* **17**:76-86
- Pochon X, Pawlowski J, Zaninetti L, Rowan R (2001) High genetic diversity and relative specificity among *Symbiodinium*-like endosymbiotic dinoflagellates in soritid foraminiferans. *Marine Biology* **139**:1069-1078
- Rahmstorf S (2010) A new view on sea level rise. *Nature Climate Change* **4**:44-45
- Rowan R (1998) Diversity and ecology of zooxanthellae on coral reefs. *Journal of Phycology* **34**:407-417
- Rowan R, Powers DA (1991) Molecular genetic identification of symbiotic dinoflagellates (zooxanthellae). *Marine Ecology-Progress Series* **71**:65-73
- Schmidt D (2007) The closure history of the Panama Isthmus: evidence from isotopes and fossils to models and molecules. In: Haywood WM, Gregory FJ, Schmidt DN (eds) *Deep-time perspectives on climate change: marrying the signal from computer models and biological proxies*. The Geological Society, London, p 429-444
- Silverman J, Lazar B, Cao L, Caldeira K, Erez J (2009) Coral reefs may start dissolving when atmospheric CO₂ doubles. *Geophysical Research Letters* **36**:L05606
- Silverstein R, Correa A, LaJeunesse T, Baker A (2011) Novel algal symbiont (*Symbiodinium* spp.) diversity in reef corals of Western Australia. *Marine Ecology Progress Series* **422**:63-75
- Simpson MC, Scott D, New M, Sim R, Smith D, Harrison M, Eakin CM, Warrick R, Strong AE, Kouwenhoven P, Harrison S, Wilson M, Nelson GC, Donner S, Kay R, Gledhill DK, Liu G, Morgan JA, Kleypas JA, Mumby PJ, Palazzo A, Christensen TR, Baskett ML, Skirving WJ, Elrick C, Taylor M, Magalhaes M, Bell J, Burnett JB, Ruttly MK, Overmas M, Robertson R (2009) *An overview of modelling climate change impacts in the Caribbean region with contribution from the Pacific Islands* United Nations Development Programme (UNDP), Barbados, West Indies
- Szmant AM (1991) Sexual reproduction by the Caribbean reef corals *Montastrea annularis* and *M. cavernosa*. *Marine Ecology-Progress Series* **74**:13-25
- Toller WW, Rowan R, Knowlton N (2001) Zooxanthellae of the *Montastraea annularis* species complex: Patterns of distribution of four taxa of *Symbiodinium* on different reefs and across depths. *Biological Bulletin* **201**:348-359
- Trench RK (1997) Diversity of symbiotic dinoflagellates and the evolution of microalgal-invertebrate symbiosis. In: Lessios HA, Macintyre IG (eds) *Proceedings of the 8th International Coral Reef Symposium, STRI, Panama*
- UNEP-WCMC *Millennium Coral Reef Mapping Project* validated maps provided by the Institute for Marine Remote Sensing, University of South Florida (IMaRS/USF) and Institut de Recherche pour le Développement (IRD, Centre de Nouméa), with support from NASA
- van Woerik R, Franklin EC, O'Leary J, McClanahan TR, Klaus JS, Budd AF (2012) Hosts of the Plio-Pleistocene past reflect modern day coral vulnerability. *Proceedings of the Royal Society B: Biological Sciences* **279**:2448-2456
- Veron J (2008) Mass extinctions and ocean acidification: biological constraints on geological dilemmas. *Coral Reefs* **27**:459-472

- Webster PJ, Holland GJ, Curry JA, Chang HR (2005) Changes in tropical cyclone number, duration, and intensity in a warming environment. *Science* **309**:1844-1846
- Weil E, Knowlton N (1994) A multi-character analysis of the Caribbean coral *Montastraea annularis* (Ellis and Solander, 1786) and its two sibling species, *M. faveolata* (Ellis and Solander, 1786) and *M. franksi* (Gregory, 1895). *Bulletin of Marine Science* **55**:151-175
- White HK, Hsing P-Y, Cho W, Shank TM, Cordes EE, Quattrini AM, Nelson RK, Camilli R, Demopoulos AWJ, German CR, Brooks JM, Roberts HH, Shedd W, Reddy CM, Fisher CR (2012) Impact of the Deepwater Horizon oil spill on a deep-water coral community in the Gulf of Mexico. *Proceedings of the National Academy of Sciences* **109**:20303-20308
- Wilkinson C (2004) *Status of coral reefs of the world: 2004*. GCRMN Report, 316 pp
- Wilkinson C (2008) *Status of coral reefs of the world: 2008*. GCRMN Report 405 pp
- Wilkinson C, Souter D (2008) *Status of Caribbean coral reefs after bleaching and hurricanes in 2005*. Global Coral Reef Monitoring Network, and Reef and Rainforest Research Centre, 152p, ISSN 1447 6185, Townsville, Australia
- Wisshak M, Schönberg CHL, Form A, Freiwald A (2012) Ocean acidification accelerates reef bioerosion. *PLoS ONE* **7**:e45124
- Woodley JD, Chornesky EA, Clifford PA, Jackson JBC, Kaufman LS, Knowlton N, Lang JC, Pearson MP, Porter JW, Rooney MC, Rylaarsdam KW, Tunnicliffe VJ, Wahle CM, Wulff JL, Curtis ASG, Dallmeyer MD, Jupp BP, Koehl MAR, Neigel J, Sides EM (1981) Hurricane Allen's impact on Jamaican coral reefs. *Science* **214**:749-755
- Yee SH, Santavy DL, Barron MG (2008) Comparing environmental influences on coral bleaching across and within species using clustered binomial regression. *Ecological Modelling* **218**:162-174

2

Reef growth and erosion: a review of the major processes

2.1 Reef construction

The term ‘reef’, “*a ridge of jagged rock, coral, or sand just above or below the surface of the sea*” has maritime origins (‘ryffe’), and originally referred to any sub-surface build-up that might potentially cause a hazard to ships (Oxford English Dictionary 2013). Scleractinian corals are not the only reef-building order: modern reefs include oyster and mussel beds (Hall-Spencer and Moore 2000), serpulid worm reefs (Moore et al. 2009) and deep water ahermatypic reefs (of which the Caribbean hosts the greatest diversity in the western hemisphere; Mullins et al. 1981, Etnoyer et al. 2011). All of these varied reef systems are founded on a common fundamental principle: the ability to generate three-dimensional framework through a combination of biological and geological processes and extend into the hydrodynamic regime. In tropical coral reefs, framework construction is predominantly calcium carbonate (CaCO₃) based. The prime mechanism of CaCO₃ generation is coral skeletogenesis through calcification, the deposition of calcium into mineral building blocks. This can be described by the following equation.



Reef construction is important for several reasons: firstly, the spatial complexity and depth gradients generated create habitat that supports substantial biodiversity; secondly, growth allows reefs to keep up with sea level rise (ensuring their survival as well as protection for coastal communities), and thirdly the topographic structure influences the hydrodynamic regime, enabling efficient filtering of nutrients from seawater. The process of alteration of the surrounding environment and creation of habitat for other organisms, makes corals ‘ecosystem engineers’ (Erez et al. 2011).

Reef growth operates at various temporal and spatial scales (Perry et al. 2008). In the following section reef construction is examined at the colony (2.1.1) and reef level (2.1.2), and on ecological to geomorphic to geological timescales (2.1.3). In the final part of this section (2.1.4) the main environmental factors that affect reef building are discussed, before moving onto an examination of reef bioerosion (2.2).

2.1.1 Colony scale building

Biogenic calcification arose in marine organisms as an evolutionary response to increasing seawater calcium, Ca^{2+} (a detoxification mechanism as high Ca^{2+} damages cellular processes) (Kleypas and Langdon 2007). The innovation of active pumps that promote CaCO_3 precipitation (by creating a super saturated carbonate environment) make the calcification process more efficient than geological calcification: since the onset of biological calcification, most of the carbon in the biosphere has been converted into carbonates (McConnaughey and Whelan 1997).

Calcification in modern scleractinians differs from other reef builders, in that a substantial part of the process is stimulated by endosymbiosis with photosynthetic dinoflagellates of the genus *Symbiodinium*. The mechanistic basis for this is uncertain (Gattuso et al. 1999, Moya et al. 2008), but is known to involve energetic subsidies from photosynthesis (Pearse and Muscatine, 1971) and changes in carbonate equilibrium resulting from photosynthesis (Goreau, 1959). This zooxanthellae-mediated calcification, termed light enhanced calcification (LEC), means coral reef framework generation is closely associated with irradiance. LEC also confers a rate of carbonate production in corals more rapid than that of other calcifying animals and over 100-fold faster than that of inorganic calcification (Cohen and McConnaughey 2003). This makes scleractinians the most industrious bioconstructors on the planet. Modern coral reefs are estimated to generate approximately 0.8 Gt of CaCO_3 per year (Rees 2006), playing a significant role in biogeochemical cycles, with roughly half the calcium entering the sea each year is taken up and temporarily bound into coral reefs (Smith 1978, Milliman and Droxler 1995). Meanwhile corals living in the Tethys sea 250 mya (Permian) accumulated entire mountain-ranges of CaCO_3 , constructing the Dolomites in the southern alps. However, reliance on zooxanthellae can also limit calcification. Disruption of the symbiosis (e.g., coral bleaching) leads to a cease in calcification, while some endosymbiont clades are associated with slower calcification rates (Little et al. 2004), indicating the critical role zooxanthellae play in the formation of massive reef framework.

Marine organisms use biogenic CaCO_3 for a diverse range of functions, from skeletal support to buoyancy regulation (summarised in Fig 2.1). For filter feeding corals one of the fundamental evolutionary drivers of skeletal growth is the need to extend into the hydrodynamic regime. This allows reefs to filter plankton out of seawater, gaining nutrients and carbon to support their high gross production, ecological diversity and evolutionary success in oligotrophic waters (Erez et

al. 2011). Harboured photosynthetic endosymbionts mean that competition for space and light modification to maximise harvesting are also crucial to survival (Fig. 2.1).

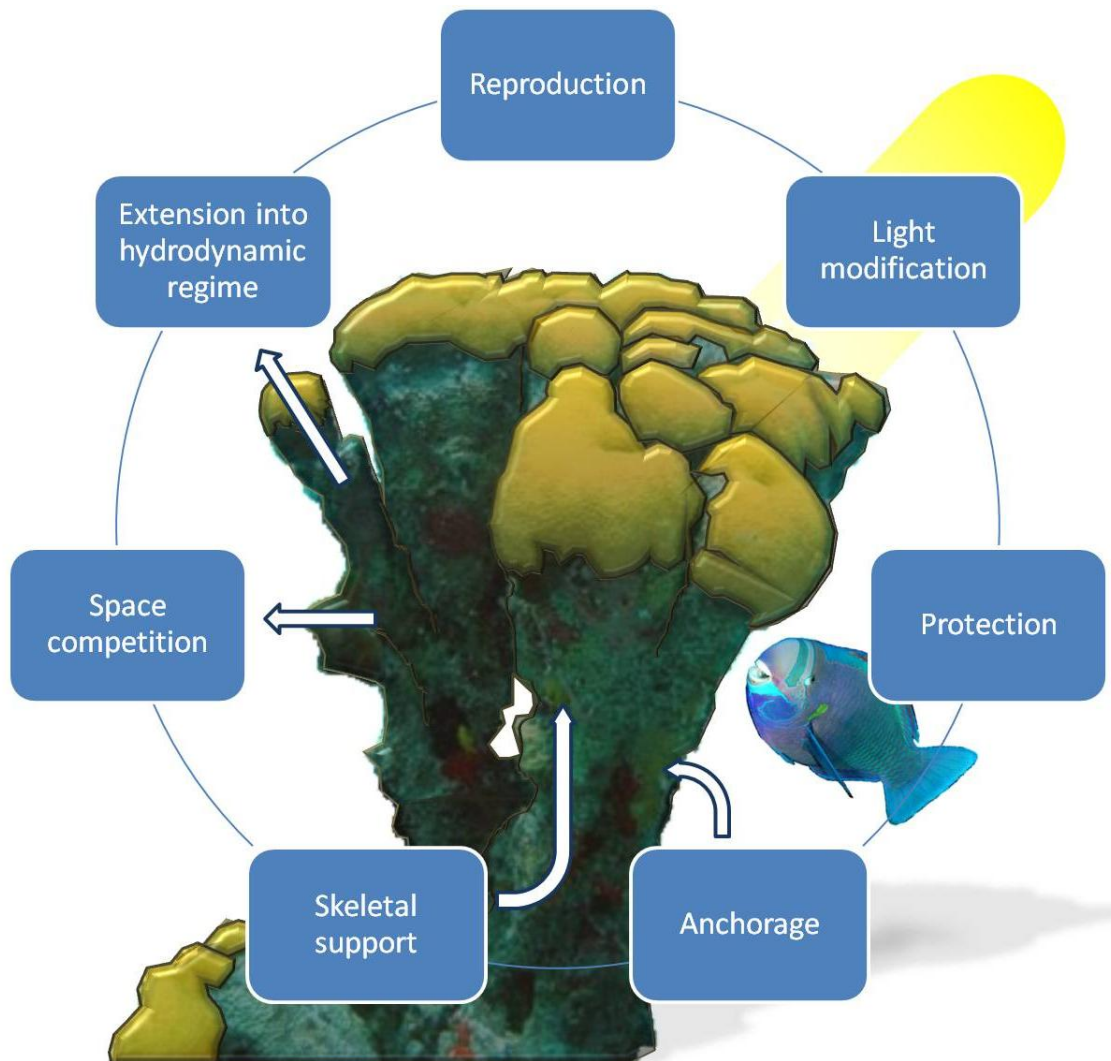


Figure 2.1 Diagram summarizing the main functions of marine calcification at the colony level: including protection (e.g., from desiccation, predation or in the case of corals, wave damage), anchorage to the substrate and competition for space and light with other colonies.

1.2.1.1 Coral calcification

Coral skeletogenesis occurs externally in a $< 1 \mu\text{m}$ thick fluid layer (the calciblastic layer) sandwiched between the lower epidermal layer (called the calciblastic epidermis) of the two-cell layer polyp and the coral skeleton (Fig. 2.2). This extracytoplasmic calcifying fluid (ECF) is composed of seawater, but requires extremely elevated concentrations of Ca^{2+} and carbonate to initiate CaCO_3 precipitation (Gattuso et al. 1999, Venn et al. 2011). Calcium (Ca^{2+}) ions occur in abundance in seawater (10 mM), but carbonate (CO_3^{2-}) ions are rare which is why the process of rapid biogenic calcification requires energy (Cohen and Holcomb, 2009).

Calcium

High seawater concentration of Ca^{2+} enables passive diffusion of the ions (mediated by voltage dependent calcium channels) down a concentration gradient into the two cell layers of the polyp (Fig. 2.2 A; Gattuso et al. 1999). From the lower (calicoblastic epidermal) cell layer, active transport is required to pump Ca^{2+} into the ECF against a concentration gradient of more than $10,000 \times$ (McConnaughey and Whelan 1997). Adenosine-triphosphate (ATP), provided by the oxidation of carbohydrates produced by zooxanthellae during photosynthesis, fuels this energetically expensive transport, and consequently the pump is light activated, shutting down at night. As each Ca^{2+} ion is pumped out of the cell, 2 H^+ ions are brought in, increasing the pH of the ECF to ~ 0.5 and ~ 0.2 pH units above seawater, usually at pH 8.15 (Venn et al. 2011). Importantly, this enhances the CaCO_3 saturation state, both encouraging crystal precipitation and preventing dissolution of new skeleton (excess H^+ ions in the ECF react with any free carbonate, CO_3^{2-} to form bicarbonate HCO_3^- , providing room for more carbonate to dissociate from the CaCO_3). An additional benefit of transporting protons back into the cell is that they help boost the availability of CO_2 for zooxanthellar photosynthesis (McConnaughey and Whelan 1997), see equation below. Recently, an alternative paracellular pathway for Ca^{2+} has been observed under lab conditions, with ions travelling through tight junctions *between* cells (Fig 2.2 B; Tambutté et al. 2012) rather than through.

Carbonate

The carbonate pathway into the ECF is more complicated. Unlike Ca^{2+} ions, dissolved inorganic carbon (DIC) exhibits multiple forms in seawater: carbonic acid [H_2CO_3]; bicarbonate [HCO_3^-] and carbonate [CO_3^-], along with carbon dioxide [CO_2_{aq}] (Gattuso et al. 1999). These four chemical states remain in equilibrium:



At the normal pH of seawater, levels of CO_2 are low (<1% DIC): the majority of carbon exists as HCO_3^- (89.8%), with approximately 6.7% as CO_3^- , meaning the calcification process is carbon-limited. Temperature, pH and any chemical reactions that use up one form of DIC will affect the DIC equilibrium: for example high temperatures and salinities and low pressure can reduce solubility of CO_2 , in turn influencing proportions of DIC, so that daily temperature fluctuations continuously alters the state of equilibrium.

A suite of enzymes known as carbonic anhydrases (CA) are involved in inter-converting inorganic carbon species and play a critical role in the calcification process (Moya et al. 2008),

giving the coral biotic control over skeletogenesis (Cohen and McConnaughey 2003). One theory suggests that these enzymes facilitate the conversion of CO_2 (that freely diffuses through cells from seawater through to the ECF) into HCO_3^- ready for precipitation (diffusion theory, Fig 1.3 D; McConnaughey and Whelan 1997). As CO_2 is relatively rare in seawater, it is likely that bulk (70-75%) of DIC involved in calcification may be generated by metabolic cell processes (i.e. respiration) rather than derived externally (Fig 2.2 E; Furla et al. 2000). Another theory suggests that HCO_3^- ions are actively pumped from the calicoblastic layer into the ECF using an anion exchange, where negatively charged anions (e.g., Cl^-) are pumped back across the membrane, in addition to CO_2 diffusion (active-transport theory, Fig 2.2 C; Furla et al. 2000).

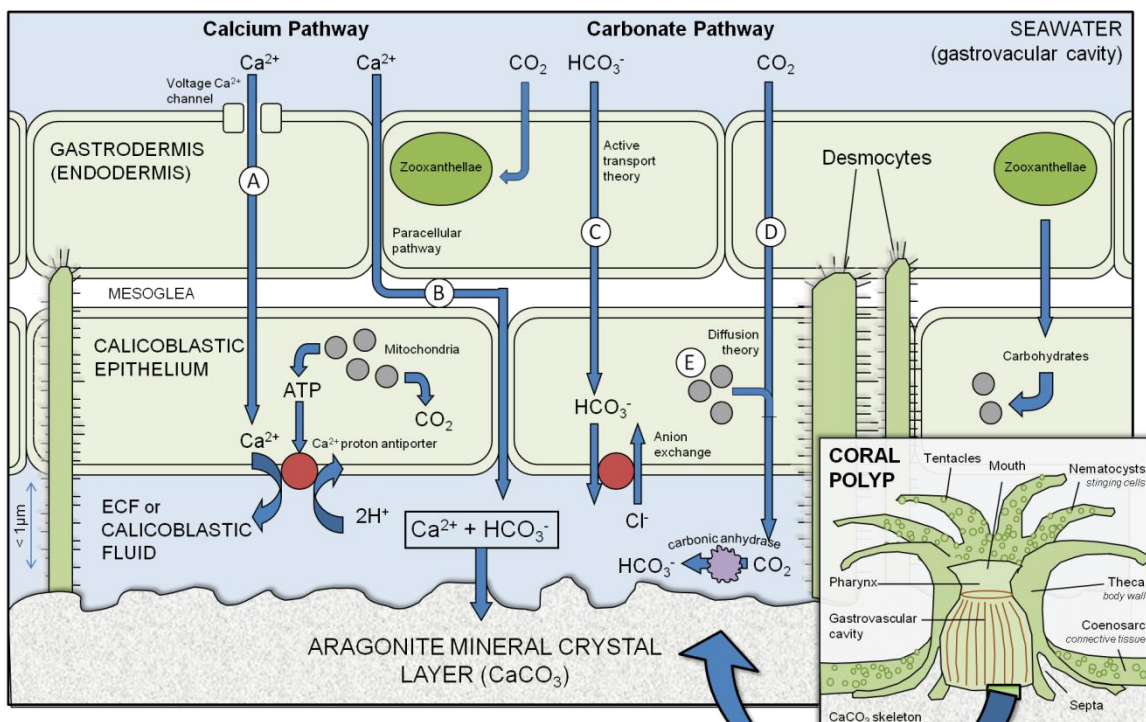


Figure 2.2 Diagram summarising transcellular pathways of calcium and DIC into the ECF. Calcium pathways include A) transcellular active transport and B) paracellular pathways. DIC pathways include C) active transport and D) diffusion. E) Up to 75% of DIC used in calcification is generated by cell respiration, with substantially more CO_2 becoming available during daylight. Desmocytes covered in short fibres attach the skeleton to the mesoglea (a thin connective layer between the two cell layers), but can become detached and reattached during calcification (see ‘Skeleton formation’. **Inset:** One coral polyp. Polyp walls consist of two single-cell-thick epithelial layers, the ectoderm (epidermis) and the endoderm (gastrodermis), separated by the mesoglea.

Other inorganics

Strontium, and occasionally other seawater metals (cadmium, manganese, lead, uranium and barium) are frequently incorporated into growing skeletons, exhibiting similar pathways to uptake as Ca^{2+} (Reynaud et al. 2004). Metals and other inorganics (e.g., siliclastic mud, quartz and feldspar) found in skeletons often reflect the composition of the seawater at the time of growth, and can be useful indicators of pollution events (Edinger et al. 2000), while others (e.g., uranium) can be used to age skeletons for climate reconstruction.

Organics

An organic matrix of proteins, glycoproteins, mucopolysaccharides and phospholipids synthesised by the coral play an important role in skeletogenesis (Allemand et al 1998). The organic component of scleractinian skeletons is minor compared to that of mollusc shells (~1% of total skeletal mass; Cohen and McConnaughey 2003), and is generally poorly understood (Weis and Allemand 2009). Proteins involved have high levels of aspartic acid, an amino acid that binds to calcium, and are likely to play a role in directing, controlling, inhibiting or boosting calcification rates in the ECF. This provides another mechanism by which CaCO_3 precipitation may be mediated by the coral host, rather than determined by external biotic processes (e.g., SST or Ω_{ar} , see section 2.1.4) (Cohen and McConnaughey 2003).

Skeleton formation

Organisms commonly secrete CaCO_3 either in the form of calcite (stable rhombohedral crystals) or aragonite (structurally stronger but less thermodynamically-stable orthorhombic crystals) (Doney et al. 2009). Today's coral skeletons are exclusively aragonitic (Stanley, 2006). The process of skeletal formation is tied to diurnal cycles, with daylight calcification promoted by photosynthesis to many times that of night rates (Goreau 1963). This is due to elevated ATP (levels 35% higher in light-incubated colonies) derived from carbohydrate synthesis; because uptake of CO_2 by zooxanthellae increases tissue pH levels, facilitating aragonite deposition, and because the $\text{Ca}^{2+}/\text{H}^+$ pump is light activated.

Every coral polyp constructs a CaCO_3 cup, known as a calyx, with the base plate containing radiating septa (or scleroseptum) which project upwards into the polyp gastrovascular base. At night, polyps contract base tissues incrementally, stretching upwards to create uninhabited space. Between each lift, organic matrix is secreted, encouraging the deposition of CaCO_3 into horizontal calcified dissepiments (Le Campion-Alsumard et al. 1995b). Needle-like aragonite crystals (ranging in width from several hundred nanometers in fast growing species, to a few micrometers in slower growing genera; Barnes 1970) form fan-like aggregates (similar to inorganically grown crystals) called sclerodermites as they precipitate out of solution around organic carbonate nucleation centres (Barnes 1970, Gladfelter 1983). The crystals amalgamate below the polyp tissue, producing nocturnal vertical, apical linear extension (Vago et al. 1997). The following day, rapid nucleation of new crystals into the framework thickens the extended scaffold, increasing skeletal density (Marubini and Thake 1999). Aragonite may continue to be deposited slowly (but abiotically) within the porous space previously occupied by the gastrovascular canals once the polyp has vacated, although the morphology, growth rate and chemical composition is very different to that biologically mediated coral growth (Cohen and McConnaughey 2003).

Coral skeletal growth is ultimately a biotic process (mediated by CA activity, zooxanthellar photosynthesis and organic matrix production rates). Skeletogenesis requires light, CO₂ and inorganic nutrients (for photosynthesis), organic food (to support tissue growth and organic matrix synthesis) and Ca²⁺ and CO₃²⁻ ions (for skeleton formation). Water movement (flow), temperature and pH, iron, zinc and dissolved oxygen are important factors that further facilitate coral metabolism. Beyond this, various abiotic controls may also influence calcification, and are discussed in 2.1.4.

2.1.2 Reef growth at the community scale

Scleractinian corals are unquestionably the most important producers of CaCO₃ - responsible for an estimated 60% to 97% of reef accretion on Jamaican reefs (Land 1979, Mallela and Perry 2007) but a large number of other calcifying reef organisms also contribute to reefal framework construction. These include calcifying macroalgae (calcareous green and coralline red), and molluscs and echinoderms as well as cryptic benthic foraminifera and bryozoans. These 'secondary' CaCO₃ producers play a critical role in stabilizing, consolidating and strengthening reef framework (Fabricius and De'ath 2001, Tribollet et al. 2002, Mallela 2007), but also contribute to the gross production of carbonate.

The total amount of CaCO₃ produced on a reef is a function of a) the abundance of calcifying organisms, b) the total surface area these organisms occupy and c) production rates of each organism (Hubbard et al. 1990). The roles played by the major calcifying reef organisms are described below.

2.1.2.1 Scleractinian corals

The important role of scleractinians in reef calcification mean that total living coral cover is an influential determinant of the ability of a reef to grow structurally: major declines in coral cover can result in cessation of reef growth, or even negative growth (Eakin 1996). However, this can be confounded by variation in the calcification ability of different scleractinian species caused by the biogenic nature of LEC. Estimates of linear extension rate (LER) of skeleton vary from <0.5 cm year⁻¹ (e.g., in platy agaricid corals) to >10 cm year⁻¹ in branching *Acropora* spp. Furthermore, colony morphology physically dictates the living area over which calcification can occur: branching species (e.g., *Acropora* spp) have faster LERs while massive corals accrete more slowly (Lewis et al. 1968, Gladfelter et al. 1978). Calcification is a function not just of LER of skeleton, but the bulk skeletal density (Dodge and Brass 1984), and this too varies between species (see Chapter 3). Both LER and bulk density can vary *within* a species too, depending on colony condition, environmental heterogeneity, and time (e.g., diurnal and seasonal changes). *Montastraea* spp. respond to environmental stress by investing calcification resources to build thicker skeletons, while *Porites* strategy is to invest in extension (Carricart-

Ganivet and Merino 2001, Carricart-Ganivet et al. 2012). Seasonal fluctuations in accretion rate produce ‘density banding’ (Weber et al. 1975, Highsmith 1979) mediated by changes in zooxanthellae density. These are related to environmental oscillation in SST (Weber et al. 1975, Carricart-Ganivet et al. 2000) as well as being linked to rainfall, light levels and coral reproduction (Mendes and Woodley 2002).

Studies have shown that variation in coral community composition can account for $\pm 1.78 \text{ kg m}^{-2} \text{ year}^{-1}$ in total reef carbonate productivity (Hart and Kench 2007). For example, eastern Pacific reefs dominated by *Pocillopora* spp. show low rates of carbonate accumulation compared to more speciose Caribbean reefs (Eakin 1996). However, the dominant producer of framework at each reef zone is not always the dominant cover type (Hart and Kench 2007), and reefs hosting greater coral diversity do not necessarily accrete faster (Perry 1996). On present-day reefs, it is generally the massive mound-like corals (*Porites* colonies in the Pacific and *Montastraea* in the Caribbean) that ‘exert a dominant control on rates of reef’ (Bosscher and Schlager 1992).

2.1.2.2 Coralline crustose algae

Crustose coralline algae (CCA), also known as lithothamnioid algae (Goreau 1963) play a primary role in the cementation and consolidation of reef matrix (MacIntyre 1997, Montaggioni et al. 1997). This function is particularly apparent in shallow, high wave-energy reef crest settings, and on mature, sea-level reef flats (MacIntyre 1997, Perry et al. 2008). Here, CCA (including *Porolithon onkodes* and various species of *Hydrolithon*, *Lithophyllum*, *Sporolithon* and *Neogoniolithon*) build encrustations through the construction of high-magnesium calcite skeletons (Goreau 1963). This has led to some authors describing CCA as ‘dominant calcareous encrusters’ (Goreau 1963, Bak 1976, Montaggioni et al. 1997) and they are frequently grouped with corals as “the most important calcifying element in the reef framework” (Bak 1976).

However, others contest that the role of CCA – particularly on Caribbean reefs - is insignificant (MacIntyre 1997, Perry 1999), the contributions of their thin (e.g., 2-3 mm; Perry 1999) crusts outweighed by that of physical processes of submarine lithification. Their significance is frequently ‘overemphasised and over-reported’ (MacIntyre 1997), causing some confusion for Caribbean researchers: in a St Croix study (Hubbard et al. 1990), the authors discuss the possibility that they underestimated the growth rate for coralline algae, when they found it to be two orders of magnitude below that of corals, compared to one order of magnitude found in a comparable Barbados study (Stearn and Scoffin 1977).

Difficulties faced by researchers in quantifying production rates of CCA (Chisholm et al. 1990) means that accurately estimating the relative contribution is a challenge. Although the evidence clearly suggests that on Caribbean coral reefs, at least, contribution of CCA to framework

production is unlikely to be of significance in carbonate budgets: environmental changes may make future consideration of CCA more important (Nash et al. 2013).

2.1.2.3 *Calcareous green algae*

Unlike the majority of reef calcifying organisms that create conditions suitable for calcification through ion transport (=trans-calcification, Fig. 2.2), calcareous green algae (including *Udotea*, *Penicillus* and *Halimeda*) calcify near sites of photosynthetic carbon uptake, naturally increasing the alkalinity of the surrounding water and promoting supersaturation and carbonate precipitation (=cis-calcification; McConnaughey and Whelan 1997, Demes et al. 2009). Calcareous green algae, whose biomass is mainly (60-80%) aragonitic CaCO₃ (with about 20% calcite; Borowitzka and Larkum 1976), originated in the Cretaceous and since that time have made substantial contributions to reef sediment (Rees et al. 2007). *Halimeda* grow by addition of new segments, with apical segments displaying 50% faster growth rates than basal segments, which mean continuously grazed *Halimeda* contribute more carbonate than standing crops (Borowitzka and Larkum 1976). Production of CaCO₃ by common Caribbean genera *Halimeda* spp. and *Penicillus* spp. has been estimated as 10 kg m⁻² year⁻¹ (Chave et al. 1972), while on a global scale, it has been suggested that stands of *Halimeda* accumulate approximately 0.15 and 0.40 Gt CaCO₃ year⁻¹ globally: 83% of coral reef carbonate production (Milliman and Droxler 1995, Hillis 1997). *Halimeda* make up 3 – 63% of the sand fraction in the Bahamas, suggesting that calcareous green algae are important carbonate producers (Hoskin et al. 1986). However on reefs the relative contribution to total carbonate production is limited by *Halimeda* abundance, which is usually <15% of living cover (Shulman and Robertson 1996, Williams and Polunin 2001). Additionally, the brittle nature of the algae means that any contribution to framework building will come from infilling by small particles, rather than production of framework blocks.

2.1.2.4 *Non-burrowing sponges*

Sponges have historically been a dominant contributor to reef growth, with the order *Stromatoporoidea* (capable of producing fused, calcareous skeletons) alternating with corals as the major framework producers throughout the Paleozoic era (Wilkinson 1983). Today, the role played by sponges in framework building is limited: just one group, the calcareous sclerosponges (found in the recesses and deep caverns of Caribbean reefs) contributing to reef CaCO₃ production through the formation of calcareous spicules (Wilkinson 1983). Like CCA, sponges play a secondary role in framework consolidation; physically supporting corals preventing collapse after basal structures have been bioeroded, reinforcing framework against wave action and binding coral rubble together during sediment infilling and lithification (Wulff and Buss 1979). However quantification of this role in terms of contributions to framework construction is challenging and few estimates of carbonate production exist.

2.1.2.5 Molluscs and echinoderms

Although their shells often comprise a significant proportion of reef sediments, most carbonate production estimates omit mollusc calcification (e.g., Stearn et al. 1977, Sadd 1984, Eakin 1996, Vecsei 2001). Chave *et al* (1972) were one of the first to suggest that the accretory potential of molluscs ($10 \text{ kg CaCO}_3 \text{ m}^{-2} \text{ year}^{-1}$; based on turnover rates of 10 year^{-1} , a mean shell size of 10^{-2} cm^2 and average mass of 10^{-3} g) could match the rest of the reef community and that molluscs should be considered in reef growth estimates. However, estimating their contribution is problematic: most approximations are derived from the abundance of shells in sediment (e.g., Hubbard et al. 1990, Yamano et al. 2000), but it has been argued that this is a poor proxy for live assemblages of reef molluscs (Hart and Kench 2007). Hart and Kench (2007) apply a rate of $100 \text{ g CaCO}_3 \text{ m}^{-2} \text{ yr}^{-1}$ to indicate mollusc production for their reef production study.

Echinoderms were additionally estimated to produce CaCO_3 at a rate of order of magnitude about $10 \text{ kg m}^{-2} \text{ year}^{-1}$, based on them living for several years in the tropics (turnover 0.1 per year), having a cross sectional area of 10 cm^2 and a skeletal mass of about 100 g (Chave et al. 1972).

2.1.2.6 Other reef encrusters

Several forms of calcareous encrusting foraminifera are important secondary framework constituents (Perry and Hepburn 2008b), with forams responsible for a reported 1-33% of the sand fraction in the Bahamas (Hoskin et al. 1986). Typically inhabiting protected cavities and sheltered undersides (Perry 1999), production estimates have been as high as $10 \text{ kg CaCO}_3 \text{ m}^{-2} \text{ year}^{-1}$ (based on a turnover of 10 year^{-1} , a size of 10^{-2} cm^2 and a mass of 10^{-3} g ; Chave et al. 1972). However, encrusting organisms are unlikely to play significant roles (aside from those of stabilization) due to their small size (Hubbard et al. 1990). Bryozoans and serpulids – common calcareous encrusters on reefs – make an even smaller contribution. These organisms are often incorporated into carbonate budget CCA estimates.

2.1.3 Reef growth on a historic scale

Holocene community reef growth estimates propose coral reef calcification as $4 \text{ kg m}^{-2} \text{ CaCO}_3 \text{ year}^{-1}$ (Smith and Kinsey 1976), with vertical accretion rates varying from $0.6 - 10 \text{ mm yr}^{-1}$ (e.g., 0.61 mm yr^{-1} St Croix (Hubbard et al. 1990), 11 mm yr^{-1} Barbados (Stearn and Scoffin 1977), and general rates of 3 mm yr^{-1} and 10 mm yr^{-1} (Smith 1983, Buddemeier and Smith 1988). Shallow Caribbean forereefs display the fastest growth rates, driven by high light availability and abundance of fast-growing branching corals (Huston 1985, Perry 1999, Vecsei 2001). Longer term rates of accretion for forereefs range from 1 m per 1000 years in Jamaica (Land 1974), to $3-5 \text{ m}$ in Panama (Macintyre and Glynn 1976) and 4.62 m in Antigua (Macintyre et al. 1985) in comparison to 0.84 , 0.67 and 1.63 m for the respective adjacent

backreefs. However, growth operates on different timescales (Perry et al. 2008), and the above carbonate accretion rates are likely to be far from constant (Hubbard 2009): evidence strongly suggests that Caribbean reefs experienced rapid accretion to catch up with sea level rise during the Holocene transgression, before entering phases of slow or negative accretion, characterised by reduced coral cover (Perry and Smithers 2011).

Sea-level rise is thought to be an important driver of reef growth (Chave et al. 1972, Hubbard 2009), with Caribbean reefs experiencing higher net carbonate production rates than their Pacific counterparts, due to a need to ‘keep up’ with 14 mm year⁻¹ rises in sea level. Reefs able to maintain framework extension rates similar to that of sea level rise have steadily accumulated 13 – 17 m thick framework over the past 7000 years while remaining close to the sea surface; while high amounts of fast accreting *A. cervicornis* enabled a growth spurt of 12 m per 1000 years on Alacran reef in the Yucatan in order to ‘catch up’ with surface (Neumann and Macintyre 1985). However, recent evidence suggests that Holocene rates of accumulation in the Caribbean are nearly an order of magnitude greater than present day (Perry et al. 2013). Today’s reef forming corals have persisted for the last 240 million years (Veron 2008) but disappearance from the fossil record on several occasions in geologic history have demonstrated that understanding the factors that control reef growth are vital to predictions about survival of reefs into the future.

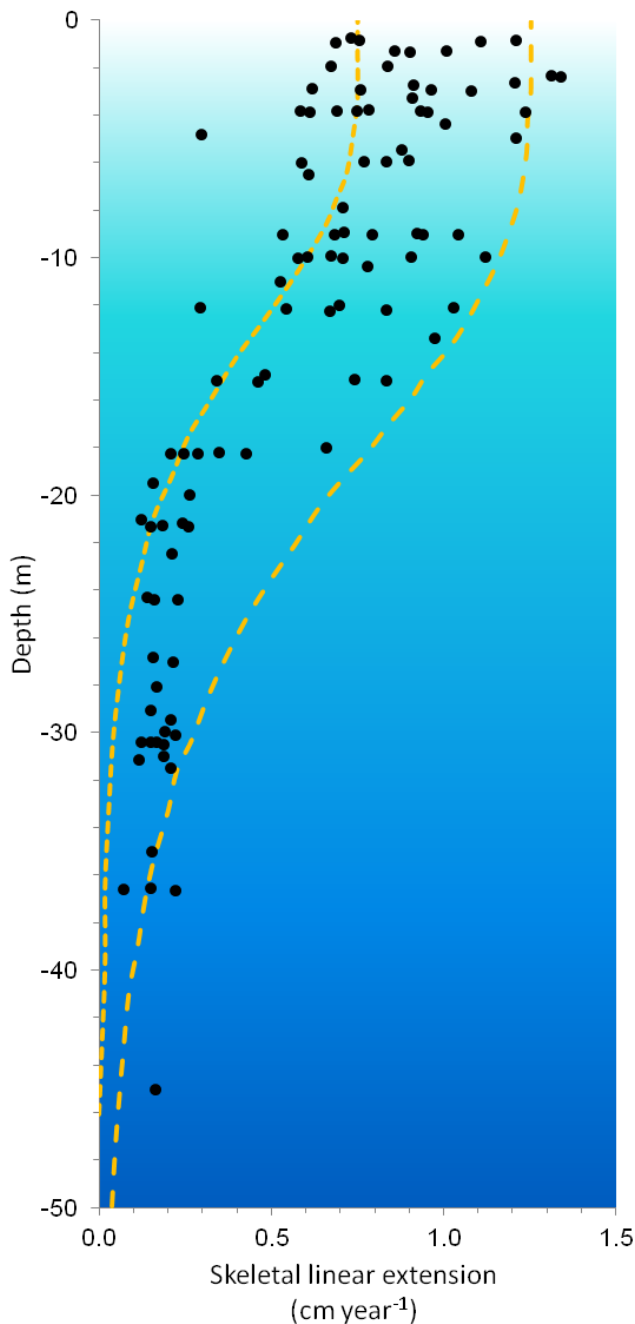
2.1.4 Abiotic factors controlling reef growth

Despite being a biotic process (mediated at the colony-level by organic matrix synthesis and zooxanthellae activity, see section 2.1.1), a variety of abiotic factors can affect reef carbonate production. Unlike biotic controls, many of these environmental factors (e.g., light) are operational at multiple scales, affecting reef growth from calcification at the cellular level, to creation of depth zones at the community level. The ultimate mechanistic driver in most cases is the effect of the environmental factor on endosymbiotic *Symbiodinium* as any abiotic factor (e.g., light, temperature, nutrient availability and turbidity) that influences rates of photosynthesis will affect the rate of the calcium pump driving changes in skeletal calcification rates, as well as the amount of carbohydrates generated and energy levels of the coral (including ability to synthesise organic matrix). In the following section we explore some of the major influential environmental variables and their effects on carbonate budgets.

2.1.4.1 Light intensity

Irradiance is the primary determinant of coral calcification. Light intensity varies spatially (e.g. with turbidity and depth) and temporally (diurnally and seasonally), affecting carbonate production rates on a variety of scales from influencing the global distribution of reefs, to generating reef depth zonation (based on attenuation of light in seawater) down to calcification rates of individual colonies (Bosscher and Schlager 1992, Hubbard 2009). Over short timescales

calcification rates of corals vary on diurnal scales, with faster (3-5 times) LEC calcification during the day, involving ‘strengthening’ of the coral skeleton, and slower vertical growth at night (Cohen and McConnaughey 2003). Over longer time periods, variation in annual rates of calcification, displayed as density bands in most scleractinians, have been attributed to seasonal changes in light level. Light can also influence the distribution of secondary calcifiers (although not their calcification rates; Agegian 1985). CCA is associated with high light environments, while shade loving or ‘sciaphilic’ encruster assemblages (of foraminifera and bryozoans) are typically found in low light areas.



Light and depth

Light attenuates with depth (Bosscher and Schlager 1992), and consequently scleractinian LEC rates decline exponentially with depth, e.g., *M. annularis* calcification declines from 0.6 – 1.0 cm year⁻¹ in shallow (<10 m) water to <0.2 cm year⁻¹ in deeper (>20 m) water (Baker and Weber 1975, Dustan 1975, Hubbard and Scaturro 1985, Huston 1985; see also Fig. 2.3).

Depth also affects colony morphology, with shallow high light habitats supporting faster growing branching or sub-massive colonies, massive colonies of *M. annularis* dominating deeper reefs or flattened or platy morphologies at deeper depths (Dullo 2005).

Figure 2.3: *Montastraea annularis* calcification rate is related to depth (data from Bosscher and Schlager, 1992). Growth rate determined by X-radiography of 108 colonies. Yellow lines indicate predicted max and min growth rates for that depth.

It has largely been assumed that light/depth has a similar effect on whole-reef accretion at the community level (albeit an order of magnitude slower than coral growth due to few reefs hosting high coral cover; Hubbard 2009). Net reef CaCO_3 production is often described as a function of sea-level rise (Chave et al. 1972). Although differences in the estimates of shallow (< 5 m) reef accretion (1 – 20 m / 1000 years), compared to < 2 m accreted for deep reefs (10–20m) support this supposition (Schlager 1981, Bosscher and Schlager 1992), recently this concept has been challenged (Gischler 2008, Hubbard 2009). Several studies report no difference between accretion rates between deep and shallow reefs, despite marked differences in coral calcification rates. This has been attributed to increased bioerosion (Hubbard 2009) and physical storm damage (Gischler 2008) in shallow regions, retarding reef growth (see Bioerosion section 2.2).

Light and turbidity

The attenuation coefficient of seawater (k), a measure of water turbidity, is also associated with the depth distribution (i.e., more massive species at depth) and growth rates of corals (Fig. 2.3). Reported k for coral reef-inhabited waters range from 0.04 to 0.16, with k increasing with turbidity, the lowest values (e.g., in Pacific atolls) allowing reef growth up to 140 m below the sea surface. Estimates of reef carbonate productivity on several reefs around Java demonstrated that mean coral extension rates fell with mean chlorophyll-a concentration (a proxy for turbidity) (Edinger et al. 2000). As well as more rapid coral extension in clear water, reefs that were actively accreting in deeper areas resided in clearer waters (Edinger et al. 2000).

However, recent work suggests the relationship between turbidity and carbonate production may be less clear cut than first assumed, with Middle Reef in Australia displaying both high turbidity and evidence of rapid accretion (Perry et al. 2012b) – see section on nutrient availability 2.1.4.6.

2.1.4.2 Aragonite saturation state

CO_2 solubility increases with depth, and with declines in temperature and salinity, meaning warm shallow Caribbean waters encourage CaCO_3 precipitation (equation 1, section 2.1). In the Bahamas, the aragonite saturation state, Ω_{ar} (a measure of the availability of CO_3^{2-} ions in seawater, ranging between 0–4.5 units) is so high under the shallow, warm and salty conditions that spontaneous abiotic precipitation of CaCO_3 can sometimes be viewed from space as ‘whitings’ (Broecker and Takahashi 1966, Dierssen et al. 2009).

A number of studies have shown that coral calcification rate is largely controlled by the degree Ω_{ar} (reviewed by Kleypas et al. 2006), which currently ranges from 4.0 to 4.2 in the Caribbean (Simpson et al, 2009), a region where Ω_{ar} does not fluctuate much Josie loves you!!!!!!!!!!!!.

Despite this, Ω_{ar} is estimated to be declining at a rate of -0.09 units per decade (Friedrich et al. 2012). Generally, coral reefs require an Ω_{ar} of >3.5 for optimal growth (Guinotte et al. 2003). As a result, coral calcification may be expected to deteriorate, with experiments documenting total coral skeletal dissolution under elevated acidity (Chapter 1, Fig 1.6; Fine and Tchernov 2007). Experimental doubling of CO_2 have caused declines in coral calcification from 9–56% (Guinotte and Fabry 2008), in the field, unprecedented reductions in linear extension of 92% of *Porites* colonies between 1990 and 2005 observed on the GBR have been attributed to 16% global decline in Ω_{ar} (De'ath et al. 2009), while climate modelling work suggests a decline of ~15% in Caribbean reef calcification since pre-industrial times (Friedrich et al. 2012). Conversely, addition of HCO_3^- to experimental corals may increase calcification rates (Marubini and Thake 1999).

At the reef-level Ω_{ar} has shown to be one of the primary controls of reef accretion (Broecker and Takahashi 1966, Langdon et al. 2000), with rates of gross community calcification directly correlated with rate of inorganic precipitation of CaCO_3 in seawater (Silverman et al. 2009). The consensus opinion is that net reef calcification will decrease by 14–30% by 2100 (Kleypas et al. 1999, Hoegh-Guldberg et al. 2007). However, the reliability of reef-scale predictions are undermined by substantial variability of the responses to elevated pCO_2 reported so far (declines in calcification range from 3% to 79%, Kleypas and Langdon 2007). Since the process of calcification is energy dependent (Andersson and Gledhill 2013), the response of coral calcification to changes in Ω_{ar} is species-specific and highly variable (but also see Marubini et al. 2003). This can make predicting reef-scale responses challenging, although ultimately past marine extinction events have been associated with periods of elevated pCO_2 over geologic timescales (Veron 2008).

Interestingly, rising pCO_2 is also associated with increased productivity of corals, as zooxanthellae up-regulate photosynthesis (Fig 1.6 B; Fine and Tchernov 2007, Anthony et al. 2008). This is believed to increase competition for DIC between calcification and photosynthesis (see section on nutrients, 2.1.4.6).

Other calcifiers are also negatively affected by rising CO_2 : in experiments, *Halimeda* net calcification rates fell as Ω_{ar} dropped from 2.0 to 0.7, and the algae also experienced a 18-43% reduction in CaCO_3 crystal size under low pH treatments (pH 8.1 vs 7.5). Foraminifera experienced three times greater mortality and dissolution of tests under the same conditions (forreviews, see Guinotte and Fabry 2008, Andersson and Gledhill 2013). CCA calcification is also negatively (-30-35%) impacted (Agegian 1985, Hall-Spencer et al. 2008, Kuffner et al. 2008), with rises from 400 to 750 ppm pCO_2 (Tribollet et al. 2006a, Anthony et al. 2008). CCA may be particularly vulnerable to changes in seawater chemistry, given its high-Mg calcite skeletons are more soluble at high pCO_2 (Anthony et al. 2008). Indirect effects of reduced

secondary carbonate production include increased fragility of reef framework, making reefs more sensitive to storm events (Manzello et al. 2008).

2.1.4.3 Temperature

Temperature is an important determinant of scleractinian calcification rate, with most species displaying a Gaussian-shaped response; typically increasing calcification with SST, plateauing at or below the normal peak summer temperature (normally around 26-27°C but fundamentally determined by the ambient temperature of the coral's environment), and finally declining with further SST increases beyond that (Jokiel and Coles 1977, Gladfelter 1984, Marshall and Clode 2004, Carricart-Ganivet et al. 2012). Field data on Pacific *Porites* spp. showed 1°C increases in SST (from 23 to 29°C) correlated with a 33% increase in calcification ($R^2=0.80$; Lough and Barnes 2000), while *M. annularis* calcification was found to be almost twice as sensitive to SST (0.57 g cm⁻² year⁻¹ for each 1°C; Carricart-Ganivet 2004). As with seawater alkalinity, responses are not only genera-specific (Carricart-Ganivet et al. 2012), but can vary within a species (Fig. 2.4; Carricart-Ganivet 2004).

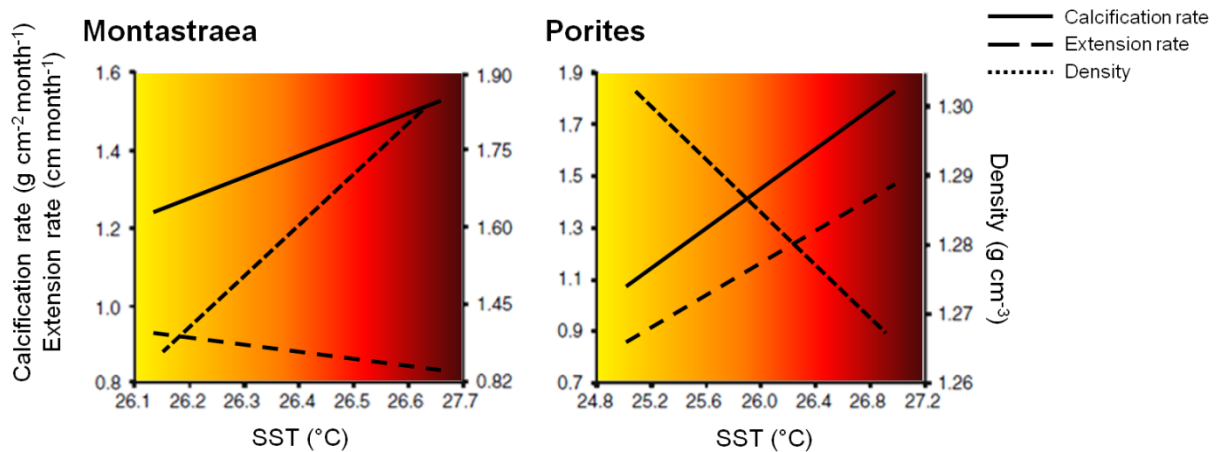


Figure 2.4: Differential effects of temperature on calcification of massive *Montastraea* and *Porites* (from Carricart-Ganivet, 2007).

Temperature also can drive temporal changes in calcification rates within an individual colony, with alternate high density bands displayed by most scleractinian species associated with higher summer temperatures (Weber et al. 1975). This relationship is driven by enhancements in coral metabolism and/or increases in photosynthetic rates of their symbiotic algae during summer (Buddemeier et al. 2004).

2.1.4.4 Water flow

Water movement (flow) is an important factor in coral growth. Flow enhances the exchange of gasses (O₂, CO₂) and dissolved compounds (nutrients, metabolic waste products) between the coral and its environment. The concept that water motion over a reef is linked to carbonate production rates was first proposed in 1978 (Smith and Kinsey 1976). Although the mechanism

remains unclear, this theory is used to explain the differential between lagoonal and forereef carbonate production rates (0.8 vs 4.0 kg m⁻² year⁻¹ respectively) calculated using alkalinity techniques. The opposite was observed in Bonaire, where leeward (sheltered) reefs were shown to be more productive in terms of coral growth than windward counterparts (Perry et al. 2012). At the colony scale, exposure may be linked to variation in skeletal density among colonies, with *Montastraea* spp. constructing denser skeletons in exposed areas (Carricart-Ganivet and Merino 2001).

Wave exposure and turbulence are additionally important in determining species composition and distribution (Perry and Hepburn 2008b) with exposed habitats dominated by CCA and fast growing branching corals.

2.1.4.5 Sedimentation

Coral production is limited by sediment loading, due to reduction in light levels and smothering of polyps (Rogers 1990, Edinger et al. 2000). In *M. annularis*, several studies link sedimentation with reduced growth rates, and occasionally colony mortality (for a review see Rogers 1990). Evidence suggests that these effects may be relayed to reef scale, with highly sedimented reefs suffering reduced coral diversity, cover and accretion (Rogers 1990), while periods of high turbidity throughout the Holocene are associated with reduced framework accretion, and in some cases death, of eastern Caribbean reefs (Davies and Hutchings 1983, Edinger and Risk 1994).

Counter-intuitively, some studies have shown primary calcification to be maintained (e.g., *Porites* skeletal extension rates of 16.3 mm year⁻¹ compared to 13.8 mm year⁻¹ in sedimented sites, Edinger et al. 2000) or even elevated (e.g. reef accretion of 1.02 kg m⁻² year⁻¹ compared to 1.83 kg m⁻² year⁻¹ at a sedimented site, Mallela and Perry 2007) at sites with high terrigenous inputs. This may occur when sedimentation is combined with eutrophication which can boost coral metabolism and skeletogenesis (Edinger et al. 2000, Mallela and Perry 2007, Perry et al. 2012b). Corals may adopt increased rates of feeding under sedimented conditions (Anthony and Fabricius 2000). However in many of these studies, LER was used as a proxy for calcification (Carricart-Ganivet 2011): a study into *M. annularis* growing under high sedimentation regimes showed that skeletal density was reduced, allowing corals to maintain extension rates (Carricart-Ganivet and Merino 2001). Carbonate production by secondary encrusters is also reduced at sites with elevated sediment inputs, as sediment can obscure substrate for settlement, in addition to impairing feeding, respiration and growth (Fabricius and De'ath 2001, Mallela and Perry 2007).

2.1.4.6 Nutrient availability

A range of responses have been recorded for the effect of dissolved inorganic nitrogen (DIN) and phosphate (DIP) on coral calcification, from 50% reductions in calcification, to increases in linear extension rates (Ferrier-Pagés et al. 2000, Fabricius 2005). Although negative effects on coral growth and calcification are recorded with prolonged exposure to DIN and DIP, moderate eutrophication generally has a positive effect on coral LER (which may not be the best proxy for calcification, despite being widely used; Carricart-Ganivet 2011). Research has documented increased skeletal extension rates by sewage outfalls (Lough and Barnes 2000), and along eutrophication gradients (Tomascik and Sander 1985, Edinger et al. 2000). Positive responses to nutrients are understood to be brought about by increased coral feeding on dissolved and particular matter (Tomascik and Sander 1985), and/or enhanced zooxanthellar photosynthesis facilitated by increased dissolved organic nutrients (Dubinsky et al. 1990, Edinger et al. 2000). Several studies provide evidence for increases in zooxanthellae density, chlorophyll-*a* per cell and photosynthetic rates with nutrients (Marubini and Davies 1996, Ferrier-Pagés et al. 2000). However, studies also show reductions in coral calcification with increasing zooxanthellae densities and cellular respiration (Marubini and Davies 1996) under elevated DIN levels. It has been proposed that zooxanthellae increases demand extra DIC, reducing the amount available to calcicoblastic cells for calcification (later demonstrated by adding bicarbonate to re-establish calcification; Marubini and Thake 1999). Interestingly, DIP appears to have little effect on tissue growth or zooxanthellae densities, and negative effects only recorded when exposures also contained DIN (Fabricius 2005). Nutrient levels also affect other reef calcifiers, with production by encrusters found to be greater at low impact sites ($69\text{--}159\text{ g m}^{-2}\text{ year}^{-1}$) compared to highly polluted sites ($2\text{--}29\text{ g m}^{-2}\text{ year}^{-1}$) (Mallela 2007).

Eutrophication has several additional indirect effects on reef-scale calcification. Firstly, the associated declines in water transparency (Hallock 1988) may negatively affect coral calcification rates (see section 2.4.1.1 on turbidity, Huston 1985). Secondly, overfeeding of corals due to increased plankton can cause disease. and thirdly eutrophication can be linked to reduced coral recruitment (though increased competition of coral planulae in the plankton) over longer periods of exposure (Hallock 1988).

2.1.4.7 Temporal factors

A variety of temporal factors (associated with temporal heterogeneity in environmental variables, e.g. daylight) affect ability of reefs to grow. At the shortest timescales, daily cycles affect calcification rates at the colony-level, with zooxanthellate corals experiencing higher net calcification rates during late afternoon/evening, and minima near sunrise (Conand et al. 1997). For example, marked differences in the site of deposition and crystal structure, as well as more rapid linear extension at night has been described in Acroporids (see section on skeleton

formation; also Gladfelter 1983). Similar patterns have been observed in CCA, with net dissolution at night (Chisholm et al. 1990). Lunar cycles have also been implicated in mediating *M. annularis* calcification (Davalos-Dehullu et al. 2008).

On seasonal scales, daily winter calcification is 57% of that of summer rates (Conand et al. 1997), with alternating bands of high and low density skeleton laid down associated with seasonal changes in light (Buddemeier 1974, Dodge and Thompson, 1974) or temperature (Weber et al. 1975; see also section on 'skeletal formation'). This means that at a reef-scale, carbonate accretion may not be a continual process, but characterised by episodic growth, and reef cores reflect these patterns (Hubbard et al. 1990). Large scale disturbances, such as El Nino events can change accretory state of reefs (Eakin 1996).

Colony age influences calcification rate (Lough 2008), with older *M. annularis* and *A. palmata* colonies accumulating carbonate faster than younger (smaller colonies) (Bak 1976). Over geologic time periods, the evolutionary stage of reefs may prove more important than factors such as pollution or turbidity in controlling the growth rate of the reef, with shallower more developed reefs less able to persist than geologically younger reefs with high growth potential (Perry et al. 2012b).

2.2 Reef bioerosion

Bioerosion is a critical but typically understudied aspect of healthy reef functioning (Hutchings 1986, Hatcher 1997). The term, coined by Neumann (1966), refers to “corrosion of hard substrates by living agents” (Perry and Hepburn 2008b), and its role can be as important as that of reef accretion, accounting for at least 50% the carbonate balance on some reefs. Bioeroders employ two main (but not mutually exclusive) methods to modify reef structure: chemical dissolution ('biocorrosion') and mechanical destruction ('bioabrasion') (Hutchings 1986). Although many bioeroding species are small in size and inhabit cryptic reef areas, it has been suggested that their combined reef biomass may equal or exceed that of surface biota (Ginsburg 1983).

2.2.1 Functional significance

Bioeroders are of extreme functional importance in breaking down reef structure as fast (and sometimes faster) than it can accumulate (Hutchings 1986, Eakin 1992, 1996). They also perform numerous other roles critical to the healthy functioning of a coral reef. Although some species directly degrade corals and calcifying algae, the bioerosion process should really be viewed as a type of mutual symbiosis rather than a parasitism (Fonseca et al. 2006).

2.2.1.1 Reef modification

The most perceptible function of bioeroders is modification of the reef framework created by calcifiers, through weakening of reef substrata by endolithic borers (section 2.2.2.1) and by the erosion of critical supporting structures (e.g., bases of corals by *Diadema*). Reef modification can determine coral colony size and vulnerability of framework to physical erosion by wave action, as well as setting depth limits for reefs (leading to development of reef zonation), and affecting coral recovery. Furthermore, bioerosion facilitates the formation of characteristic reef structures such as boulder tracts, eroded reef flats and algal cup reefs (Hutchings 1986).

2.2.1.2 Reinforcement and fossilisation

Calcium carbonate redistributed by bioeroders can eventually become incorporated back into the internal reef framework (Eakin 1996). Cavities produced by internal borers trap faecal matter and sediment, through wave action, gravity or by the feeding and respiratory currents set up by boring fauna. Carbonate sediments are eventually crystallised and cemented in the cavity system, strengthening the reef substrate (Ginsburg 1983, Hallock 1988). As much as 50% of internal reef framework can be made up of reincorporated sediments (Hubbard, 1990). These sedimentary facies have been shown to be important in maintaining reef structure (Davies 1983, Perry 1999) as well as fossilising patch reefs (Hutchings 1983).

2.2.1.3 Sediment production

A major ecological service provided by mechanical bioeroders is the generation of sediment, a large proportion of which will be exported to make sandy beaches (Sadd 1984). An estimated 20-40% of fine sediment in Belizean patch reefs, 2-3% of all sediment in the Persian Gulf and up to 30% of lagoonal sediments of Fanning Island, Pacific Line Islands, have been identified as chips eroded from reef substrate by bioeroding sponges (Wilkinson 1983). As well as contributing to biogeochemical cycles, sediment production can create new habitats, such as cays and lagoonal sediment habitats, and support the biodiversity of sediment-associated fauna, which make up a significant proportion of the reef ecosystem (Hutchings 1986).

2.2.1.4 Coral recruitment

Grazing (by external bioeroders such as parrotfish and urchins) can aid coral and coralline algae recruitment by exposing the substrate for settlement at the time of coral reproduction (Brock 1979, Steneck 1994). Increased abundances of the grazing urchin *Diadema* in Jamaica are associated with improved juvenile scleractinian recruitment (Carpenter and Edmunds 2006).

2.2.1.5 Recycling nutrients

Tight nutrient recycling is the key to reef survival in oligotrophic environments. Many bioeroders recycle detritus and organic material on the reef, including waste products from

surface biota such as mucus produced by corals and fish excrement (Hutchings 1983).

2.2.1.6 Asexual fragmentation

Boring organisms can benefit the coral community by aiding asexual fragmentation: coral propagation by breakage of branching, platy and delicate corals (Scott et al. 1988). The role of boring sponges has been shown to be significant in aiding weakening and breakage of branches in *A. cervicornis* (Wilkinson 1983).

2.2.1.7 Enhancing biodiversity

Bioderoders increase habitat complexity and the reef surface area, enabling support of a greater variety and biomass of organisms, with the constant background level of natural disturbance keeping the framework structure changing, maintaining high reef diversity (Hallock 1988). Brittlestars and clingfish have been shown to inhabit urchin burrows in Columbia (Schoppe and Werding 1996), while other reef fish species pass developmental stages in bored cavities, or use them as refugia during the day.

As well as creating new habitat, bioeroders are themselves taxonomically diverse, especially the cryptic biota (Glynn 1997), with >300 macroboring species found on one Jamaican reef (Buss and Jackson 1979). The wide range of bioeroding species found on reefs contribute substantially to coral reef biodiversity.

2.2.1.8 A trophic role

Many macro- and microborers are an important food source for holocentrid fish and predatory gastropods. The excretions of bioeroders, their larvae and the demersal plankton living in the cavities contribute to the food chain that sustains the surface biota (Ginsburg 1983). It has been suggested that corals consume nutrients such ammonium from the waste products of the borers (Mokady *et al.* 1998). Meanwhile grazing urchins and parrotfish play a key role as reef herbivores, in addition to bioeroder role (Mumby 2009).

2.2.1.9 Biogeochemical cycling

Biocorrosion (chemical breakdown of carbonates) aids carbon cycling by releasing carbonate back into the water, important for uptake by corals. It was shown in laboratory experiments that corals living in aquaria completely depleted carbonate content of seawater ($3.7 \text{ g m}^{-2} \text{ day}^{-1}$), without the presence of bioeroders to restore levels. On a wider scale, breakdown of reef framework by bioeroders, combined with sediment transport off reef is important in carbon biogeochemical cycles.

2.2.2 Bioeroder guilds

The importance of boring organisms within coral reefs has been recognised since the 1800s (Perry and Hepburn 2008b), and since this time numerous attempts have been made to categorise bioeroders into guilds, including epiliths, chasmoliths and endoliths (Golubic et al. 1975), boprint, burrowing and nektonc (Ginsburg 1983) and etchers, borers and grazers (Hutchings 1986). Today, reef bioeroders can be most sensibly divided into three groupings: grazers, macroborers and microborers, defined by Perry (1999).

2.2.2.1 Microborers

Microborers, defined by creation of borings <100 µm in diameter, are small, commonly autotrophic euendolithic microorganisms or microendoliths (Golubic et al. 1975, Vogel et al. 2000, Tribollet 2008b). An ancient group of organisms found as far back as the Precambrian, they have been detected on almost every available carbonate substrate on earth, both living (e.g., mollusc shells) and dead, and exist across a diverse range of ecosystems (from Arctic coastlines to freshwater ecosystems; Tribollet 2008a). They incorporate a diverse range of species: experimental blocks in Belize attracted 14 microboring species including six cyanobacteria species, three species of green algae, four fungi and one unidentified heterotroph (Carreiro-Silva et al. 2005). Microboring communities colonise reef substrate more rapidly than any other bioeroding group (arriving on freshly exposed substrate within four to nine days of exposure; Chazottes et al. 1995), and use chemical dissolution to penetrate (Tribollet et al. 2011) while exploiting fissures and colonising cavities in porous substrates (Tudhope and Risk 1985). Dissolution of framework can occur directly (through the production of organic acids and chelating fluids from terminal cells) or indirectly by increasing CO₂ during respiration (Tribollet et al. 2006b). Microborers are frequently present in elevated numbers, with one study estimating more than half a million euendolithic filaments per cm² on a marine limestone coast (Tribollet 2008a). Despite being prolific bioeroders (capable of erosion rates of up to 600 g m⁻² year⁻¹; Vogel et al. 2000) microbioerosion is generally considered difficult to quantify meaning this key process is often overlooked in carbonate budget studies (e.g., Mallela and Perry 2007).

Algae

Algal microborers ('euendolithic algae' or microflora) have been described as the most important bioeroders after sponges, due to their high rates of destruction and rapid chemical dissolution (Hein and Risk 1975). The most commonly described is a chlorophyte, *Ostreobium queketti*, which produces distinctive green banding, called the 'Ostreobium band' running parallel just 2-3 cm below the depositional surface of living coral colonies (Odum and Odum 1955, Carreiro-Silva et al. 2005). These dense networks of green filamentous algae, made of 10-20 µm thick borings, are present in almost all living corals in the Atlantic and Pacific, and may

in fact represent several algal genera, such as *Codiolum*, *Entocladia*, *Eugomontia*, *Phaeophila* (Risk and MacGeachy 1978, Glynn 1997). In the green banded zones, *O. queketti* is capable of removing up to 25% of the skeletal material, although deeper the filaments thin out, becoming grey as they lose chloroplasts and eventually dying (Le Campion-Alsumard et al. 1995a). *O. queketti* is unusual among microborers for its ability to bore living coral, for which it must negotiate a protective layer of polyp tissue and maintain rapid growth in the direction of the coral skeletal extension in order to absorb the light filtered by zooxanthellae in living tissue (Le Campion-Alsumard et al. 1995a). *O. queketti* is a low light specialist, found as deep as 275 m (Vogel et al. 2000). It is outcompeted at shallower depths by another common Caribbean chlorophyte *Phaeophila densdriodes* (Carreiro-Silva et al. 2005), which also dominates the GBR (Kiene 1997). In dead substrates, algal boring rates have been estimated as $0.6 \text{ kg m}^{-2} \text{ yr}^{-1}$ at their peak (Chazottes et al. 1995), but usually *O. queketti*, which bores deeper than the cyanobacterial assemblages that invade the top 1 mm of surface in the first six months of exposure, only establish community dominance after several years of exposure.

Fungi

Boring fungi are speciose, with >20 taxa isolated from coral reefs (Kendrick et al. 1982), dominated by *Lithophythium gangliiforme* and *Dodgella priscus* (Carreiro-Silva et al. 2005). Information is scarce on fungal microboring rates (Le Campion-Alsumard et al. 1995b), particularly as their cylindrical tunnel-like borings (~1-2 μm in diameter) are difficult to distinguish from algal borings (Glynn 1997). Despite this, they are known to be abundant in mollusc shells and other marine carbonates (Kendrick et al. 1982, Hutchings 1983), and have been observed growing out of living *Porites lobata* in French Polynesia (Le Campion-Alsumard et al. 1995a). Unlike other microborers, they are thought to attack live polyps, penetrating the surface and exiting adjacent to polyps prompting immune-like response in *Porites*. Boring fungi are heterotrophic, meaning they can penetrate deeper into coral skeletons than *O. quekettii*, in addition to etching surfaces. Fungi have been shown to parasitise euendolithic algae, attacking *O. quekettii* before expanding along its tunnels (Le Campion-Alsumard et al. 1995b).

Cyanobacteria

Cyanobacteria make up a substantial proportion of the microboring community in non-living substrates, particularly at depth, with over 15 species found in the Bahamas (Vogel et al. 2000). *Mastigocoleus testarum* and *Plectonema terebrans* are the most common boring heterotrophic cyanobacteria species (in the Caribbean and Pacific; Perry 1999, Tribollet et al. 2002), colonising experimental carbonate blocks rapidly following exposure (from the surface inwards) although remaining shallower than algae, and decreasing with time (Chazottes et al. 1995, Le Campion-Alsumard et al. 1995a). *Plectonema* produces borings of about 2-6 μm diameter, and

Mastigocoleus 8-15 μm (Chazottes et al. 1995). Both species are capable of rapid dissolution, removing 80% of *Acropora* skeletal material (Zubia and Peyrot-Clausade 2001), and responsible for 18-30% of bioeroded reef sediment on the GBR (Tudhope and Risk 1985).

2.2.2.2 Macroborers

Macroborers, including sponges, bivalves, polychaetes and sipunculans, contribute substantially to reef bioerosion, although their typically patchy distribution (determined by recruitment pulses; Hutchings 1986) means that, with the exception of sponges, on many reefs they take ‘secondary importance’ to grazers and microborers (e.g., in Jamaica; Perry 1999).

Porifera

Bioeroding sponges have been described as ‘the most important...organisms on reefs in terms of rates of destruction of substrate’ (Wilkinson 1983), responsible for 90% of the internal bioerosion in Barbados (MacGeachy 1977, Stearn and Scoffin 1977) and on the GBR (Risk et al. 1995), and capable of erosion rates that exceed mean reef carbonate production rates (Smith and Kinsey 1976, Nava and Carballo 2008). Of the major boring sponge genera (e.g., *Cliona*, *Anthosigmella*, *Sphaciospongia* and *Siphonodictyon*; Wilkinson 1983), the Clionoids are the most prolific and effective framework bioeroders in the Caribbean (Hein and Risk 1975, Hudson 1977, MacGeachy 1977, Scoffin et al. 1980), comprising 20 of the 36 Caribbean bioeroding species (>600 Caribbean sponges in total) (Diaz and Rützler 2001, Zea and Weil 2003). These sponges rival hermatypic scleractinians in biomass (Rützler 2002), and estimates for boring rates have been as high as 21-25 $\text{kg m}^{-2} \text{year}^{-1}$ (Neumann 1966), although this estimate is extreme (Hein and Risk 1975, Bak 1976). Caribbean boring sponges erode reef framework both directly, through excavation of dead substrate (e.g., *Cliona aprica*; Rützler 1975) and by encrusting and killing living coral tissue (e.g., *Cliona delitrix* and *Cliona lampa*; Ward-Paige et al. 2005), and indirectly by compromising structural integrity of the skeleton (MacGeachy and Stearn 1976). Excavation involves a combination of mechanical erosion (96%) and chemical ‘etching’ (5%) (Rützler 1975), although dissolution by etching has recently been shown to be more important than previously thought (Nava and Carballo 2008). Filopodia, 0.2 μm thick pseudopodial sheets which exude acid from the tips (regulated by carbonic anhydrase) are extended into reef substrate, dissolving the carbonate and organic matrix in a concave pattern. This produces distinctive hemispherical-shaped silt sized ‘sponge chips’ which are then removed by ameobiod transport (Hein and Risk 1975, Rose and Risk 1985, López-Victoria and Zea 2005). Sponge chips are identifiable in sediments, and make up to 41% of the sand in Belizean beaches (Rützler 1975, Glynn 1997). Boring rates vary with time: initial rates of penetration (2-3 years after substrate exposure) are extremely high (accounting for Neumann's high estimates, 1966) but sponges rarely penetrate further than 2 cm (Wilkinson 1983), with erosion rates eventually levelling off at $\sim 7 \text{ kg m}^{-2} \text{year}^{-1}$ (Rutzler and Rieger 1973, Hutchings

1986). Based on average Caribbean sponge abundance this would mean a reef-rate of $0.25 \text{ kg m}^{-2} \text{ year}^{-1}$. Despite available information on boring rates, it remains challenging to convert these values into reef based rates based on the extent of sponge infestation, given that usually only a small proportion of tissue (contains the inhalant and exhalent papillae) are exposed above the surface.

Mollusca

Three main bivalve families – Pholadidae (angelwings), Gastrochaenidae (clams) and Mylittidae (mussels) - have developed the ability to bore into reef substrate (beyond the shallow etchings of intertidal chitons, limpets and snails). Of these, the mylittid *Lithophaga* spp. is the best studied, leaving large 10-15 cm deep cavities in coral skeletons (Perry and Hepburn 2008b). *Lithophaga* are thought to enlarge their borings using a combination of initial chemical softening (excreting acid from glands along the edge of the mantle) and a mechanical ‘grinding’, involving rotation of the shell which is anteriorly thickened (Hein and Risk 1975, Kleemann 1980, Glynn 1997). Combined dissolution and boring can remove up to 40% of coral skeletons (Lazar and Loya 1991), although the role of bivalves in destabilizing coral heads is thought to be more important than removing large amounts of carbonate. Although considered minor contributors to reef bioerosion (particularly in the Pacific: Kiene 1988, Chazottes et al. 1995, Risk et al. 1995, but also see Highsmith et al. 1983, Perry 1998) as suspension feeders, bivalves can thrive under sedimented conditions (Macdonald and Perry 2003). For example in Jamaican back-reefs abundances of up to 500-10,000 individuals per m^2 have been reported (Scott et al. 1988), making them dominant members of the Jamaican boring community (Perry 1998).

Arthropoda

Boring crustaceans, including barnacles, shrimp and some grazing hermit crabs (Scott 1985), are not generally considered significant bioeroders; accounting for just 0.1% of boring on Jamaican reefs (Perry 1998). The barnacle *Lithotrya*, an endolithic borer, mechanically excavates 2-10 cm long cylindrical chambers in coral skeletons, usually on the underside of reefs (Scott 1985). These chambers are connected, so that heavily infested substrate can become fragile. Pairs of *Alpheus simus* (pistol shrimp) excavate 10-15 mm diameter chambers using chemical dissolution (Cortes et al. 1984). In Costa Rica, these shrimp have been observed to burrow up to 15 cm into dead coral, removing an estimated 950 cm^3 carbonate substrate, although once bored these shrimp will continue to live in the burrows without boring for several years.

Polychaeta

Several polychaete families contain boring species: Eunicidae, Lumbrineridae, Dorvilleidae, Spionidae, Cirratulidae and Sabellidae employ combinations of mechanical and chemical bioerosion to various extent (Hutchings 1986). Eunicid worms use well developed mandibles to excavate twisting, branching networks (Hutchings 1986), while spionid worms like *Polydora* create narrow (0.3-0.5mm) u-shaped borings using chemical dissolution (Hein and Risk 1975, Risk and MacGeachy 1978). Cirratulids and sabellid worms are also thought to employ chemical methods, although polychaete boring is generally not well studied. Polychaete abundances tend to be higher on Indian Ocean (Chazottes et al. 1995) and Pacific reefs (e.g., up to 80,000 boring polychaetes per m² in experimental blocks; Davies and Hutchings 1983). In the Caribbean polychaetes are considered less important bioeroders (Bak 1976, MacGeachy and Stearn 1976, Highsmith 1981), although like *Lithophaga* spp., in high densities (and particularly at polluted or disturbed sites; Zubia and Peyrot-Clausade 2001) they can contribute substantially to reef-scale bioerosion (12% of Jamacian boring community; Perry 1998).

Sipuncula

There is little agreement in the literature on the boring contribution of sipunculans (unsegmented marine worms), with huge variation between reefs and regions (Hein and Risk 1975, Davies and Hutchings 1983, Chazottes et al. 1995, Fonseca et al. 2006). The mechanism of bioerosion is unknown, although many species exhibit a variety of hooks spines and papillae which may be used in mechanical boring (Hutchings 1986). They create cylindrical pencil sized borings, which vary in depth with species, and while in most regions they are reported to associate with dead substrate (Chazottes et al. 1995) in the Caribbean they have been found in live *Porites* (Scott 1985), and at densities of up 1,200 individuals m⁻² in Belize (Rice and Macintyre 1982).

2.2.2.3 Grazers

Principally comprised of echinoids and fish, the external framework grazers (also known as epiliths) main method of erosion is to scrape carbonate substrate (including both live and dead coral substrates and encrusting coralline algae) off the reefal surface, typically as a unintentional consequence of herbivory (Hutchings 1986). Grazers contribute substantially to total reef bioerosion (Bak et al. 1984, Kiene 1988, Kiene and Hutchings 1994), sometimes accounting for up to 70% of reef bioerosion (Pari et al. 2002, Tribollet et al. 2002).

Echinodermata

Urchin bioerosion plays a critical role in carbonate budgets of the Caribbean, eastern and central Pacific; even in areas where parrotfish or sponges are significant contributors (Bak 1994). Pre-

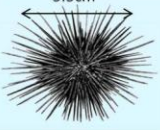
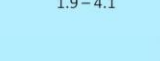
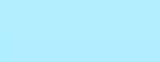
Diadema die-off, > 75% of total reef bioerosion has been accredited to urchins: Barbados studies in 1977 and 1980 reported 79.4% (18.7 g CaCO₃ m⁻² day⁻¹) to 89% (9.7 kg m⁻² year⁻¹) of total erosion effort was attributable to urchins (Hunter 1977, Scoffin et al. 1980), vastly outweighing contributions by fish (0.1-0.2 kg) and sponges (0.5-1.0 kg) in the same region (Hunter 1977), while in Curaçao they were estimated to be responsible for 87.8% of bioerosion (9.0 g CaCO₃ m⁻² day⁻¹; Bak et al. 1984). Published echinoid erosion rates - usually in the range of 3-9 kg m⁻² year⁻¹ (depending on the species, intensity of grazing, and population density; Mokady et al. 1996) - are often comparable to records for gross carbonate production by corals (1-4 kg CaCO₃ m⁻² year⁻¹), suggesting urchin erosion is capable of equalling or exceeding reef carbonate production (Bak 1994). One study in Pacific Panama showed that urchin densities as high as 50 ind per m² were responsible for driving reefs into net negative carbonate accumulation, dramatically altering the structure to the extent that they became increasingly exposed to predation (Eakin 1996).

Urchins bioerode in two ways: directly through grazing, and indirectly via abrasion of their structural environment using spines (Bak 1994). Grazing is aided by a powerful jaw apparatus (the Aristotle's lantern), consisting of five radially arranged calcified plates ('teeth') located on the ventral side of the body. Crystalline calcite teeth are capable of grinding limestone, with recent evidence suggesting that teeth are designed to break sporadically along deliberately positioned layers of weaker organic material sandwiched between the crystal, keeping them razor sharp (Killian et al. 2011). Urchins also excavate 'home cavities', shallow surface depressions - used as burrows - using spine abrasion (Hutchings 1986). Attempts have been made to quantify erosion by urchin spines; with estimates for *Diadema* revealing a size dependent contribution of ~13-24% to total urchin erosion (0.06 g day⁻¹ for a >3 cm *Diadema*; Herrera-Escalante et al. 2005). These estimates are comparable Bahamian *Echinometra lucunter* estimates, where cavity excavation takes between 0.7 and 10.3 years (mean=2.9), and cavities measure 72 cm³ on average (17 - 126 cm³) (Hoskin and Reed 1984).

Despite numerous reported high rates, urchin erosion estimates vary more widely than for any other bioeroder guild. This is because the pace of echinoid erosion is very sensitive to three dynamic factors (Bak 1994): population density, size frequency distribution and taxonomic composition - all of which may be subject to rapid change as well as natural variation. For example variation in the abundance of *Diadema mexicanum*, from 0.06 ind m⁻² on a Panamanian reef flat, to 18.8 ind m⁻² on the adjacent fore-reef, translate into an 100-fold increase in bioerosion (0.01 - 1.04 kg CaCO₃ m⁻² year⁻¹ respectively) (Eakin 1996).

Meanwhile in the Caribbean, *D. antillarum* community bioerosion estimates of 5.2 kg (St Croix, Ogden 1977), 5.1 kg (Venezuela, Weil 1980) and 8.9 kg CaCO₃ m⁻² year⁻¹ (Barbados, Stearn

Table 2.1: Summary of grazing impact of echinoid species

	Species name, common name and mean test size	Abundance (ind m ⁻²)	Mean test size (cm)	Reef scale erosion (g m ⁻² yr ⁻¹)	Individual erosion rate (g ind ⁻¹ day ⁻¹)	Study site	Published source
Western Atlantic	 <i>Diadema antillarum</i> (long-spined sea urchin) 5.5cm	23	2.2	8878	0.31 – 7.41*	Bellairs reef, Barbados	Stearn & Scoffin, 1977
		71	n/a	n/a	n/a	Discovery Bay, Jamaica	Sammarco, 1982
		1	n/a	1.6	0.54 [‡]	Rio Bueno, Jamaica	Mallela & Perry, 2007
	 <i>Echinometra lucunter</i> (rock boring urchin) 3cm	92 - 176	3	3,900	0.12	St Croix, US Virgin Isles	Ogden, 1977
		37	n/a	3,000	0.242	Little Bahama Bank, Bahamas	Hoskin & Reed 1984
	 <i>Echinometra viridis</i> (red sea urchin)	0.8 – 62.6	2.0 – 2.4	80 – 4,140	0.181	La Parguera, Puerto-Rico	Griffin <i>et al.</i> , 2003
Tropical Eastern Pacific	 <i>Eucidaris thouarsii</i> (needle urchin) 2.9 – 4.0	10 - 50 (abundant)	4.3 – 6.3 (large)	1,700	0.67	Galapagos	Glynn <i>et al.</i> , 1979
		5 - 150	2.0	3,470 – 10,400	0.19	Uva Island, Panama	Glynn, 1988
		0.06 - 48.3	2.0	10 - 4,380	0.27 – 0.32	Uva Island, Panama	Eakin, 1996
		1.0 - 6.8	2.9 – 4.0	170 – 3,280	0.54 – 3.88*	Bahias de Huatulco, Mexico	Herrera-Escalante <i>et al.</i> , 2005
	 <i>Centrostephanus coronatus</i> (crowned urchin)	6.86	1.0 - 1.5	190	0.075	Playa Blanca, Columbia	Toro-Farmer <i>et al.</i> , 2004
Indo-Pacific	 <i>Diadema savignyi</i> (needle urchin)	6 (large)		3870	4.7	Moorea, French Polynesia	Bak, 1990
		0.4 – 11.8	2 – 6.5	1640 - 5500	0.99	Gulf of Thailand	Ruengsawang & Yeemin, 2000
	 <i>Diadema setosum</i> (needle urchin)	0.1 – 6.4	3.01	409 - 736	0.31	Gulf of Eilat, Red Sea	Mokady <i>et al.</i> , 1996
		 <i>Echinothrix diadema</i> (needle urchin)	0.65 – 0.93	6 - 7.5 (large)	796 – 1,783	3.3 - 7	Moorea, French Polynesia
			6 (large)		7.4	Kenya	McClanachan & Shafir, 1990
	 <i>Echinometra mathaei</i> (needle urchin) 1.9 – 4.1	7 - 10		600 – 7,500	0.14	French Polynesia	Peyrot-Clausade <i>et al.</i> , 2000
		2 - 7	1.95	8	0.11	Marshall Islands	Russo, 1980
		0.04	1.93	29	0.14	Moorea, French Polynesia	Bak, 1990
		3.8 - 73.6	3.5 – 4.0	425 - 8320	~0.3*	La Reunion,	Conand <i>et al.</i> , 1997
			4.08	372 - 8,300	0.7	Kenya	McClanachan & Shafir, 1990
		3.7 – 10.5	2.31	160 - 500	0.12	Gulf of Eilat, Red Sea	Mokady <i>et al.</i> , 1996
		30	3.71		0.9 - 1.4	Arabian Gulf	Downing & El-Zahr, 1987
	 <i>Echinostrephus molaris</i> (very low)	0.2 (very low)					Bak, 1990
 <i>Echinostrephus aciculatus</i>		1.7 – 2.4		0.15 – 0.4*	Marshall Islands	Russo, 1980	
 <i>Echinothrix calamaris</i> (few)	<0.01 – 1.1 (few)				Zanzibar, Kenya	McClanachan & Shafir, 1990, Herring, 1972	
	<i>Echinometra spp.</i>	0.133	n/a	3600	7.3	Kailua Bay, Hawaii	Harney & Fletcher, 2003

and Scoffin 1977), fell to just 0.002 kg (Jamaica, Mallela and Perry 2007) following the 1983 mass mortality event. Variation in body size can be as significant as density in determining total bioerosion effort, with larger individuals making more effective bioeroders (Fig 2.5; Bak 1994, Conand et al. 1997). In Moorea the largest *Diadema savignyi* (6.7 cm diameter) were able to consume >500 times more carbonate than their 1.2 cm counterparts (Bak 1990). When individual rates are extrapolated to reef-scale level, this translates into sizable variation in bioerosion: the order of magnitude difference between *Echinometra mathei* erosion estimates of 0.9-1.4 g day⁻¹ in the Arabian Gulf (Downing and El-Zahr 1987) and 0.14 g day⁻¹ in French Polynesia (Bak 1990) were explained by differences in test diameter of 3.71 cm compared to 1.93 cm (Bak 1994). Experimental work revealed that stocking density of echinoderms influences mean body size, with mean test diameter inversely related to population density (Levitan 1988). Field evidence – with smaller urchins during plagues and larger following die-offs support the fact that erosive ability due to size is as sensitive to change as population density is.

Finally, as well as intra-species variation in body size and abundance, species differences are influential in explaining bioerosion. For example, in the Red Sea, despite *Echinometra mathaei* outnumbering *Diadema setosum*, these urchins are responsible for only ~18% of total echinoid erosion on the reef slope, due to their more limited ability to erode substrate (Mokady et al. 1996). Behavioural differences will also affect rates: for example *Echinometra* exhibit patchy grazing (*Echinometra mathaei* is a typically small species, found in high densities and grazes in close proximity to its burrow, Bak 1990), while *Diadema* and *Echinothrix* have larger home ranges, and erode uniformly (Sammarco 1982).

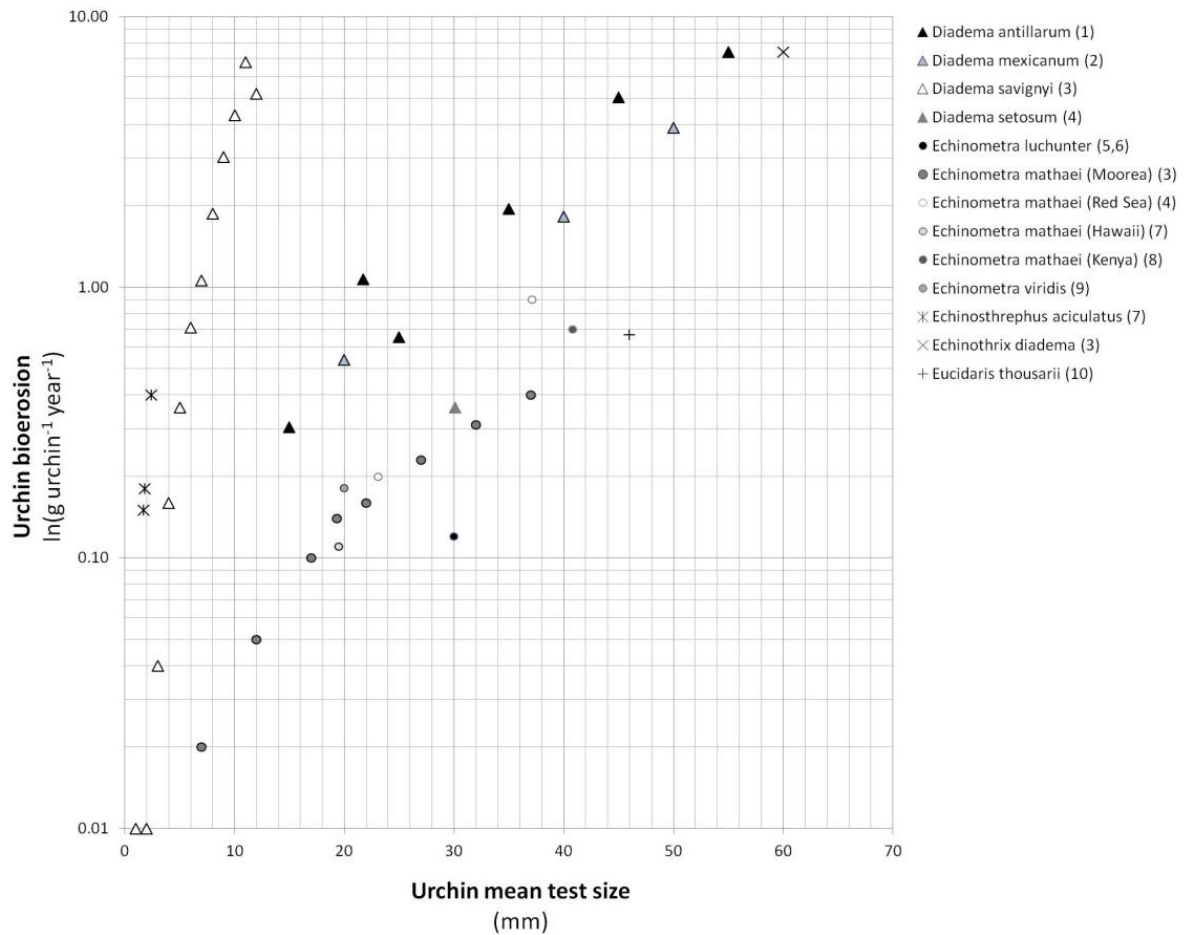


Figure 2.5: Published values for mean urchin test size for a variety of species are plotted against bioerosion rate to demonstrate the importance of test size in explaining erosivity. Data sourced from: 1. Stearn and Scoffin, 1977; 2. Herrera-Escalante et al., 2005; 3. Bak, 1990; 4. Mokady et al. 1996; 5. Ogden, 1977; 6. Hoskin and Reed, 1984; 7. Russo, 1980; 8. McClanahan and Muthiga, 1988; 9. Griffin et al., 2003; 10. Glynn et al., 1979

Of the echinoderms, only the echinodea (e.g., *Diadema*, *Echinometra*, *Echinostrephus* and *Eucidaris*) are usually considered significant bioeroders. However, recently the contributions of deposit feeding sea cucumbers (Holothuroidea) have been reported, with a populations processing of sand and rubble accounting for 50% of night-time CaCO_3 dissolution at a site on the GBR (Schneider et al. 2011).

Bioeroding fish

A number of reef fish families (Scaridae, Acanthuridae, Chaetodontidae, Pomacentridae, Gobiidae, Balistidae, Mullidae, Labridae, Tetradontidae) process significant amounts of carbonate in their digestive tracts (Bardach 1961), and more still (Monacanthidae, Blennidae, Pomacanthidae, Zanclidae) are corallivores (Rotjan and Lewis 2008). However, the Scaridae (parrotfish) alone dominate reef carbonate erosion (Ogden 1977, Kiene 1988, Bruggeman et al. 1996), cropping framework with ‘beaks’ of fused teeth made of dahllite or francolite (minerals harder than CaCO_3 ; Hutchings 1986).

Parrotfish were recently identified as the dominant bioeroders on reefs around Bonaire (Perry et al. 2012a), primarily because they comprise a major component of the fish community (e.g. *Arothron meleagris* erodes 20 g of coral per day but total reef loss is only 30 g CaCO₃ m⁻² year⁻¹ due to low population size of 40 individuals per ha; Guzman and Robertson 1989), but also because of their tendency to target convex surfaces – removing the tops off colonies so smooth coral off – decreasing height and reducing rugosity of reefs (Bellwood and Choat, 1990).

Parrotfish species fall into one of two categories – scrapers and excavators– based on feeding mode (Bellwood and Choat 1990). *Scarus vetula*, with broad-edged teeth worn to an even cutting edge, but small jaw muscles, exhibits a ‘scraping’ feeding mode, while *Sparisoma viride*, which has a crenate cutting edge due to alternately protruding teeth on the vertical tooth row, forages by deliberately excavating the substrate in short, powerful bites, removing up to five times more carbonate (Bellwood and Choat 1990, Bruggeman 1995).

Pharyngeal bones grind carbonate into a paste, and in place of a stomach, a thin walled alimentary tract, containing high levels of carbonic anhydrase (Smith and Paulson 1975) is adapted for carbonate digestion (Glynn 1997). Parrotfish are efficient at processing carbonate,

Bioeroding fish	Bioerosion rate g CaCO ₃ m ⁻² year ⁻¹	Location	Reef type	Data source
All bioeroding fishes	400-600	Bermuda	coral reef	Bardach, 1959
grazing fish ***	230	Bermuda	patch reef	Bardach 1961
<i>Sparisoma viride</i>	209	Bermuda		Gygi, 1975
<i>Sparisoma viride</i>	35	Barbados		Gygi, 1969
All Scaridae	20	St Croix		Hubbard et al 1990
<i>Scarus croicensis</i>	490	St Croix		Ogden, 1977
<i>Scarus iserti</i>	490	Panama		Ogden, 1977
All Scaridae	61	Barbados	fringing reef	Frydl & Stearn, 1978
All Scaridae	40	Barbados	bank reef	Frydl & Stearn, 1978
All Scaridae	168	Barbados	moorings	Frydl & Stearn, 1978
<i>Scarus iserti</i>	490	Barbados	patch reef	Frydl & Stearn, 1978
<i>Sparisoma viride</i>	16	Jamaica	clear fringing reef	Malella & Perry, 2007
<i>Sparisoma viride</i>	7	Jamaica	turbid fringing reef	Malella & Perry, 2007
<i>Sparisoma viride</i>	34	Barbados		Scoffin et al 1980
<i>Scarus vetula</i>	2,341	Bonaire	shallow reef zone	Bruggeman et al 1996
<i>Sparisoma viride</i>	4,692	Bonaire	shallow reef zone	Bruggeman et al 1996
<i>Scarus vetula</i>	1,363	Bonaire	gorgone zone	Bruggeman et al 1996
<i>Sparisoma viride</i>	1,495	Bonaire	gorgone zone	Bruggeman et al 1996
<i>Scarus vetula</i>	611	Bonaire	drop off	Bruggeman et al 1996
<i>Sparisoma viride</i>	880	Bonaire	drop off	Bruggeman et al 1996
<i>Scarus vetula</i>	259	Bonaire	reef slope	Bruggeman et al 1996
<i>Sparisoma viride</i>	503	Bonaire	reef slope	Bruggeman et al 1996
<i>Sparisoma viride</i>	36	Barbados	fringing reef	Stearn and Scoffin 1977
<i>Sparisoma viride</i>	61	GBR	fringing reef	Kiene, 1988
Scarids + gastropods	105	GBR	windward reef slope (10m)	Kiene, 1988
Scarids + gastropods	1,573	GBR	reef flat	Kiene, 1988
Scarids + gastropods	8,929	GBR	lagoon (4m)	Kiene, 1988
Scarids + gastropods	1,150	GBR	windward reef slope (10m)	Kiene, 1988

Scarids + gastropods	604	GBR	reef flat	Kiene, 1988
Scarids + gastropods	859	GBR	lagoon (3m)	Kiene, 1988
Scarids + gastropods	3,361	GBR	windward reef slope, 10m (Wreck Reef)	Kiene, 1988
Scarids + gastropods	1,002	GBR	reef flat (Wreck Reef)	Kiene, 1988
Scarids + gastropods	166	GBR	Lagoon, 0.5m (Wreck Reef)	Kiene, 1988
All bioeroding fishes	280 ± 40	GBR	turbid, nearshore (Snapper Island)	Tribollet et al 2002
All bioeroding fishes	320 ± 120	GBR	turbid, nearshore reef (Low Isles)	Tribollet et al 2002
All bioeroding fishes	2,770 ± 330	GBR	Turbid reef (Lizard Island)	Tribollet et al 2002
All bioeroding fishes	2,800 ± 530	GBR	Clear offshore reef (Ribbon Reef)	Tribollet et al 2002
All bioeroding fishes	1,240 ± 190	GBR	Clear offshore reef (Harrier Reef)	Tribollet et al 2002
All bioeroding fishes	1,370 ± 580	GBR	Oceanic site (Osprey Reef)	Tribollet et al 2002
<i>Chlorurus spp.</i>	925 – 5,576	GBR	fringing reef (Heron Island)	Bellwood, 1995*
<i>Chlorurus spp.</i>	1,990 – 3,538	GBR	fringing reef (Lizard Island)	Bellwood, 1995**
All Scaridae	900-3,800	GBR	inner-shelf reefs	Hoey & Bellwood 2008
All Scaridae	5,200-8,400	GBR	inner-shelf reefs	Hoey & Bellwood 2008
All Scaridae	32,300	GBR	outer-shelf reef crest	Hoey & Bellwood 2008
All Scaridae	23,100	GBR	outer-shelf reef flat	Hoey & Bellwood 2008
All Scaridae	1,800	GBR	outer-shelf reef slope	Hoey & Bellwood 2008
All Scaridae	800	GBR	outer-shelf reef back	Hoey & Bellwood 2008
<i>S. rubroviolaceus, C. perspicillatus</i>	1080 ± 160	Hawaii	fore reef (Hanauma Bay)	Ong & Holland, 2010
<i>S. rubroviolaceus, C. perspicillatus</i>	710 ± 130	Hawaii	reef shelf (Hanauma Bay)	Ong & Holland, 2010
<i>Scarus sordidus</i>	57	Reunion	outer reef flat (La Saline Reef)	Conand et al. 1997
<i>Scarus sordidus</i>	135	Reunion	inner reef flat (La Saline Reef)	Conand et al. 1997
<i>Scarus sordidus</i>	37	Reunion	back reef zone (La Saline Reef)	Conand et al. 1997
All Scaridae	50	Reunion	outer reef flat	Peyrot-Clausade et al 2000
All Scaridae	120	Reunion	inner reef flat	Peyrot-Clausade et al 2000
All Scaridae	30	Reunion	back reef zone	Peyrot-Clausade et al 2000
All Scaridae	3,900	Moorea	barrier reef front	Peyrot-Clausade et al 2000
All Scaridae	700	Moorea	barrier reef flat	Peyrot-Clausade et al 2000
All Scaridae	700	Moorea	barrier reef flat	Peyrot-Clausade et al 2000
All Scaridae	3,300	Moorea	fringing reef	Peyrot-Clausade et al 2000
All Scaridae	100-9000	Mariana Is.	reef flat, slope and lagoon	Cloud, 1959
Scarids + Echinometra	1,270 ± 270	Moorea		Pari et al 2002
Scarids + Echinometra	1,580 ± 270	Atimaonao		Pari et al 2002
Scarids + Echinometra	1,420 ± 330	Tikehau		Pari et al 2002
Scarids + Echinometra	2,490 ± 830	Tikehau 2		Pari et al 2002
Scarids + Echinometra	1,680 ± 670	Takapoto 1		Pari et al 2002
Scarids + Echinometra	1,480 ± 100	Takapoto 2		Pari et al 2002
All Scaridae	3,148 - 3213	Red Sea	reef flat and slope	Alwany et al 2009
All bioeroding fishes	20	Panama	back reef zone (Uva Island)	Eakin, 1996
All bioeroding fishes	1,150	Panama	reef flat (Uva Island)	Eakin, 1996
All bioeroding fishes	1,280	Panama	fore reef (Uva Island)	Eakin, 1996
All bioeroding fishes	1,250	Panama	reef base (Uva Island)	Eakin, 1996
<i>Arothron meleagris</i>	30	Panama	pocilloporid reef (Las Perlas)	Glynn et al, 1972

Table 2.2: Summary of reef fish bioerosion studies.

which is ingested either as coral/CCA substrate ('eroded') or old sediment trapped in algal turfs ('reworked' carbonates) and have an estimated digestive processing time of 75 minutes (Frydl and Stearn 1978). It has been argued (Bellwood 1995) that reef carbonate ingested by the

scrapers is primarily comprised of reworked carbonates (Frydl and Stearn 1978, Bruggeman et al. 1996), and as a result their contribution to actual framework erosion is negligible.

Few other reef fish display these specialist features, although other adaptations – such as a thick-walled gizzard in surgeonfish stomachs for grinding – aid carbonate ingestion, helping release nutritionally important organic material from the carbonate matrix (Smith and Paulson, 1974). As scarid excavation in the Caribbean is largely restricted to one, heavily fished species, *Sparisoma viride*, fish bioerosion is thought to be more limited than in the Red Sea (three excavating genera *Chlorurus*, *Cetosaurus* and *Scarus* spp.; Alwany et al. 2009) and Indo-Pacific (16 bioeroding species in three abundant genera *Bolbometopon*, *Cetoscarus* and *Chlorurus* spp.; Bellwood 1995). *Bolbometopon muricatum* is a particularly voracious bioeroder, with schools of 30-50 individuals estimated to ingest up to 32 kg m⁻² year⁻¹ in the outer reefs of the GBR (Hoey and Bellwood 2008).

Molluscs

Mollusc bioerosion is less effectual than that of fish or echinoids due to their smaller size and population density. Most mollusc erosion occurs as a by-product of feeding on epilithic, epidendolithic and shallow endolithic algae whose growth has weakened substrate (Trudgill 1976, Glynn 1997). The limpets *Acmaea*, *Cellana* and *Patelloida* spp. have radulae made of calcite (denser than the aragonite/high magnesium calcite coral skeletons) that gently remove substrate, and may also employ acid secretions excavate a home scar (having recorded pH values of 5.7 – 7.5 on underside of limpets). Snails (e.g., *Cittarum*, *Littorina*, *Nerita*, *Nodilittorina*) also use radula used to scrape rock surface, but possess weaker proteinaceous teeth (Glynn 1997).

Chitons (e.g. *Acanthopleura*, *Chiton*) possess magnetite capped radula and abrade substrate while grazing algae (Lowenstam and Weiner, 1989). They also erode their homing site depression, processing a significant proportion of CaCO₃ daily (Trudgill 1976). *Acanthopleura granulata* are responsible for an estimated 104.2 g of carbonate erosion m⁻² year⁻¹ in the Bahamas, while snails were reported as eroding 155 g m⁻² year⁻¹ at the same site (Hoskin et al. 1986).

2.2.3 Abiotic factors affecting reef bioerosion

Boring, like calcification, is a biotically-mediated process. Factors like population density, recruitment, disease, abundance and predation all affect net reef bioerosion rates. Much less is known about the abiotic controls on bioerosion (especially compared to calcification, section 2.1.4). It is becoming increasingly important to understand the bioeroder responses to environmental change, both as the borer abundances increase and the reefs face mounting environmental threats (Chapter 1, Section 1.3). Boring is expected to increase on reefs in the

future, firstly as widespread Caribbean coral mortality increases habitat availability (i.e. more exposed framework for colonisation), and secondly in response to local environmental change. For example, abundance of macroboring filter feeders (sponges, bivalves and worms) have been shown to increase under eutrophied conditions (Ward-Paige et al. 2005), while sponge bioerosion rates have been shown to increase under OA (Wisshak et al. 2012). In the past, fluctuations in bioeroder abundances have had significant effects on reef carbonate budgets (e.g., Eakin 1996, Chapter 4). In the following section some of the known abiotic controls on reef bioerosion are discussed.

2.2.3.1 Temperature

Little information is available about response of bioerosion rates to SST. Indirectly, rising SST can increase community boring through coral mortality (Eakin 2001). The 1982/1983 El Niño Southern Oscillation event led to 50-99% coral mortality in the tropical eastern Pacific (TEP), with *Diadema* erosion subsequently increasing five-fold, producing negative carbonate budgets in Panama and the Galapagos (Glynn 1988, Eakin 1996). Some evidence suggests that microborer activity could be retarded by thermal stress (Fine and Loya 2002).

2.2.3.2 Aragonite saturation state

Little research has been conducted on the effects of OA on reef bioerosion. It has been hypothesised that low pH conditions might promote bioerosion indirectly by weakening CaCO₃ framework, or making the cost of acidic excretions less metabolically costly in chemical borers (Glynn 1997). However, many eroding organisms (e.g., echinoids, molluscs) have calcium carbonate shells and therefore might be expected to be negatively affected. Microboring activity is not negatively affected: studies have shown that reef cyanobacteria grow under extremely high pCO₂ (Thomas et al. 2005) and that *O. queketti* photosynthesis, growth and bioerosion were increased (by 48%) under doubled pCO₂ (Tribollet et al. 2009). Recently, experiments have shown that bioerosion rate of the boring sponge *Cliona orientalis* are elevated under high pCO₂ conditions (Wisshak et al. 2012).

2.2.3.3 Light intensity (and depth)

Organisms living within the coral framework receive minimal light, which is why most macro and micro-borers are heterotrophic filter feeders rather than autotrophs. Microborers, however, are predominantly phototrophs and consequently light is the main controlling factor for their abundance, with clear depth-gradients in microbioerosion (Vogel et al. 2000, Tribollet and Golubic 2002). In the Bahamas, microbioerosion rates were shown to decline progressively from around 0.25 kg m⁻² year⁻¹ at 2 m to virtually nothing at 477 m (Hoskin et al. 1986). High

irradiance has been shown to inhibit boring, e.g., by damaging *O. queketti* (Fine and Loya 2002), a shade specialist.

Many Clionaid sponges harbour zooxanthellae (Weisz et al 2010), and these species demonstrate faster boring rates, increased depth of penetration and more rapid tissue growth under high light conditions. They also show faster rates of bioerosion than azooxanthellae sponges (Hill 1996, Schonberg 2006). Interestingly, light has also been suggested to stimulate sponge boring rates of azooxanthellate *Cliona lampa* and *Anthosigmella varians* (Rützler 1975) although the mechanism for this is uncertain (Wilkinson 1983). Other studies show no relationship between depth and macroborer (mainly Cliona) erosion (Hubbard et al. 1990). Turbidity has been positively correlated with bioerosion, although this may be confounded by sediment and nutrients (Edinger et al. 2000).

Depth

Parrotfish bioerosion in Bonaire is affected by depth (being greater on reef slopes than shallow reef crest) although this is related to accessibility rather than light levels (Bruggemann et al. 1996), with declines in grazing rate with depth noted in Jamaica (Steneck 1994). As well as affecting parrotfish density, a study in Hawaii documented larger parrotfish bite volumes at depth (Ong and Holland 2010).

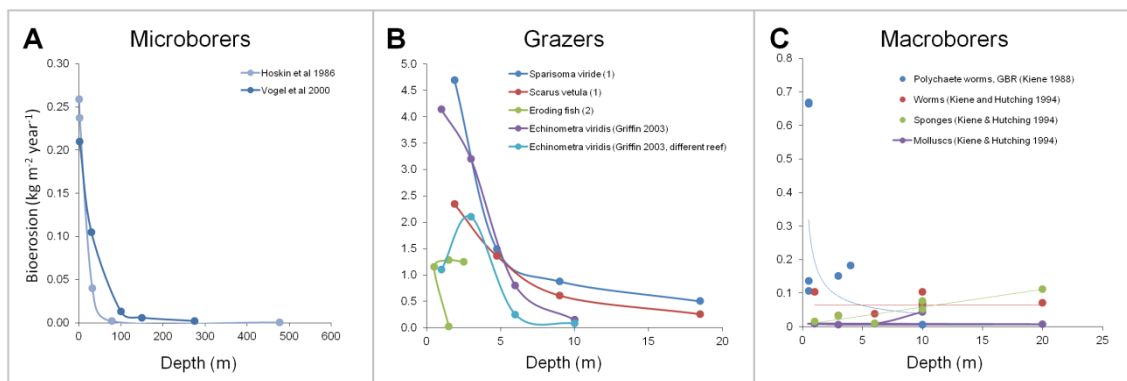


Figure 2.6: Relationship between bioerosion rates of different boring guilds and depth **A)** shows change in microbioerosion rates with increasing depth from two Bahamian studies **B)** changes in bioerosion rate (kg) with depth in grazers) and **C)** in macroborers.

Urchin distributions are depth-linked, with *Diadema setosum* bioerosion decreasing with depth in Thailand as abundance changes (Ruengsawang and Yeemin 2000). In Puerto-Rico, as well as declines in abundance, mean *Echinometra* urchin size was shown to decrease with depth, with highest bioerosion rates at 1-3 m (Griffin et al. 2003). Depth zonation was also observed among macroborers in Jamaica, with Clionaid sponges found at mid-depth fore-reef sites (> 12 m), while the siphunculan *Phascolosoma perlucens* and the bivalve *Lithophaga bisulcata* dominated shallow sites (Perry 1998). Other authors agree that bivalve densities decline with depth (Scott

1985). Depth has shown to be closely correlated ($r^2=0.89$) with sponge abundance, with mean boring sponge densities increasing (9-18 fold) on deep forereefs compared to back and patch reefs, but declining after ~19 m (Chiappone et al. 2007). The opposing influences of depth on bioerosion (Fig. 2.6) and on net reef calcification (section 2.1.4.1) may explain similar net framework growth rates recorded for deep and shallow reefs despite greater gross productivity of shallow reefs (Hubbard et al 2009).

2.2.3.4 Nutrient availability

Increased availability of nutrients are associated with increased net bioerosion (Rose and Risk 1985, Sammarco 1996, Holmes et al. 2000), because the majority of endolithic bioeroders are suspension or filter feeders (Highsmith 1980, Holmes 1997). Several Caribbean studies show a strong positive association between organic pollution and sponge abundance (Risk and MacGeachy 1978, Calahan 2005), sponge size (Ward-Paige et al. 2005) and sponge boring rates (Rose and Risk 1985, Holmes 2007). For example, abundances of the boring sponge *Cliona delitrix* increased fivefold in an area exposed to untreated fecal sewage (Rose and Risk 1985). Other authors that found that sponge abundances increase on eutrophied Caribbean reefs: in Cuba (Alcolado and Herrera 1987); Curaçao (Meesters et al. 1991) and Jamaica (Goreau 1992). Incidences where sponge abundance declines with eutrophication have been attributed to the confounding negative effect of sedimentation (López-Victoria and Zea 2005). Other macroborers (e.g., *Polydora* spp.) increase in relative abundance at polluted sites (Zubia and Peyrot 2001). Microbioerosion is also positively associated with eutrophication (Chazottes 1994, Peyrot-Clausade et al. 1995, Zubia and Peyrot 2005, Carreiro-Silva et al. 2009). Microboring rates increased by a factor of nine following experimental addition of DIN and DIP on Belize reefs, while the total area of experimental carbonate substrate colonised was three times higher in treatments with added inorganic nutrients (Carreiro-Silva et al. 2009). However, the association between microboring and eutrophication is not as evident on Pacific reefs (Vogel et al. 2000, Kiene 1997). Clear positive associations between net reef bioerosion rates and borer abundances and eutrophication have led to the assertion that nutrient availability is the most important abiotic control of bioerosion (Hallock 1988). This holds true on geo-ecological timescales: more intense sponge boring observed on ancient Miocene reefs has been linked to enhanced nutrient availability, due to upwelling (Edinger and Risk 1994).

2.2.3.5 Sedimentation

While nutrients typically have a positive effect on boring sponge growth and abundance, sedimentation has the opposite effect, inhibiting growth (Holmes 1997, Lopez-Victoria and Zea 2005, Maldonado et al. 2007). Sediment smothers reef surfaces, and removal is energy-intensive, leading to reduced sponge pumping rates and even preventing feeding for extended periods (Wilkinson 1983, MacDonald and Perry 2003). At high levels sedimentation can bury

dead corals preventing colonisation by framework eroders (Perry 1996). However, mild sedimentation may promote bivalve and polychaete erosion by providing heterotrophic nutrition. Boring communities may change from sponge to bivalve dominated under chronic sedimentation (MacDonald and Perry 2003). Microboring dominated reef bioerosion at a sedimented site in Jamaica, suggesting that microborers may be less sensitive to sediment than macroborers, who were found in greater abundance at a nearby clear-water site (Mallela and Perry 2007).

2.2.3.6 Substrate type

Properties of the reef framework may determine bioerosion rates, with surface area, volume, ratio of dead to living coral, macroalgal cover and substrate density all influencing boring rates (Hutchings 1983). Low density substrate is thought to increase parrotfish bioerosion rates (Bruggeman et al. 1994, Tribollet et al. 2002, Ong and Holland 2010), although other authors have noted the opposite in macroborers, with denser substrate stimulating bioerosion (Tribollet and Golubic 2005).

Macroborers are more abundant and efficient in dense substrate (Highsmith 1981), with *Cliona orientalis* shown to grow faster in corals with denser skeletons, fewer pores and more structural barriers (Schonberg 2002). Field evidence supports higher rates of sponge bioerosion in denser materials (Neumann 1966, Highsmith 1981, Highsmith et al. 1983, Rose and Risk 1985), although exceptions exist (Edinger and Risk 1997, Ward and Risk 1977), and low substrate porosity aids quicker and deeper penetration, although no more material is removed per unit time (Rutzler 1975, Neumann 1966). Many macroborers show preferential tendencies toward certain species (e.g., *Agaricia* was bored over *Montastraea* and *Siderastrea* in Jamaica, MacDonald & Perry 2003; while *Montastraea* and *Siderastrea* were preferred by sponges in the Florida Keys, Chiappone et al. 2007). Stearn and Scoffin (1977) further found sponges eroded different coral skeletons to different extents in Barbados.

While macroborers prefer a substrate free of encrusting organisms, and a framework that is deep, physically stable, remote from grazers and excess sediment, substrate type is not so important for microbial euendolithic communities (Le Campion-Alsumard et al. 1995). Several studies have shown that density is unrelated to microbioerosion rates (Zubia and Peyrot 2001, Tribollet et al. 2002) although abundances were shown to vary between branching and mound coral skeletons due to differences in surface area available for colonisation (Zubia and Peyrot 2001).

2.2.3.7 Water flow

Endolithic borers (particularly sponges) generally require high water flow to provide nutrients

(Wilkinson 1983), with a requirement of ambient flow rates of 15 cm s^{-1} for efficient filter feeding in sponges, and flow rates of $>45 \text{ cm s}^{-1}$ increasing filter feeding 3-8 fold (Leys et al. 2011). Clionads increase bioerosion rates under flowing currents (Naumann 1966, Rützler 1975) although this effect can be variable (Holmes et al. 2009). Sponge abundances tend to be higher on exposed forereefs (Lopez-Victoria and Zea 2005, Chiappone et al. 2007). However, leeward reefs in Bonaire exhibited greater parrotfish erosion ($>2 \text{ kg}$) compared to 0.95 kg at windward sites (Perry et al. 2012).

2.3 Conclusion

This review has illustrated the complex multi-component nature of net reef growth, which is further complicated by differential responses of each contributing component to environmental variation. Understanding the environmental drivers of net reef growth may help explain recent reported declines in Caribbean calcification (Castillo et al. 2011). Preconceptions about how reefs grow on geo-ecological timescales, extrapolated from established relationships between coral calcification and environmental factors such as light, turbidity and depth, are increasingly being challenged (Gischler 2008, Hubbard 2009, Perry et al. 2012b). In most cases, this is because bioerosion has not been accounted for. Bioerosion is of increasing relevance as boosted erosion in areas of nutrient enrichment, coupled with reduced coral growth, skeletal densities and recruitment rates can lead to conditions where reef erosion exceeds calcium carbonate accretion (Perry et al. 2012). Not only is preservation of a dynamic reef structure critical to the maintenance of reef ecosystem services (Section 2.2.1 and Chapter 1, Section 1.2), but with sea level rise projected to increase during the 21st century (due to thermal expansion, melting glaciers and loss of Greenland and West Antarctic ice sheets) the ability of reefs to ‘keep up’ depends on calcifier and bioeroder activity and how these organisms respond to environmental changes. Addressing gaps in the knowledge – particularly regarding sensitivity of bioeroders and calcifiers to environmental variation – is a fundamental to the answer to the question ‘at what point will coral reefs stop growing?’.

2.4 References

- Agegian CR (1985) The biogeochemical ecology of *Porolithon gardineri* (Foslie). Ph.D thesis, University of Hawaii
- Alwany MA, Thaler E, Stachowitsch M (2009) Parrotfish bioerosion on Egyptian Red Sea reefs. *Journal of Experimental Marine Biology and Ecology* **371**:170-176
- Andersson AJ, Gledhill D (2013) Ocean acidification and coral reefs: effects on breakdown, dissolution, and net ecosystem calcification. *Annual Review of Marine Science* **5**:321-348
- Anthony KRN, Fabricius KE (2000) Shifting roles of heterotrophy and autotrophy in coral energetics under varying turbidity. *Journal of Experimental Marine Biology and Ecology* **252**:221-253
- Anthony KRN, Kline DI, Diaz-Pulido G, Dove S, Hoegh-Guldberg O (2008) Ocean acidification causes bleaching and productivity loss in coral reef builders. *Proceedings of the National Academy of Sciences of the United States of America* **105**:17442-17446
- Bak RPM (1976) The growth of coral colonies and the importance of crustose coralline algae and burrowing sponges in relation with carbonate accumulation. *Netherlands Journal of Sea Research* **10**:325-337
- Bak RPM (1990) Patterns of echinoid bioerosion in two Pacific coral reef lagoons. *Marine Ecology Progress Series* **66**:267-272
- Bak RPM (1994) Sea-urchin bioerosion on coral reefs - place in the carbonate budget and relevant variables. *Coral Reefs* **13**:99-103
- Bak RPM, Carpay MJE, de Ruyter van Steveninck ED (1984) Densities of the sea urchin *Diadema antillarum* before and after mass mortalities on the coral reefs of Curaçao. *Marine Ecology Progress Series* **17**:105-108
- Baker PA, Weber JN (1975) Coral growth rate: variation with depth. *Earth and Planetary Science Letters* **27**:57-61
- Bardach JE (1961) Transport of calcareous fragments by reef fishes. *Science* **133**:98-99
- Barnes DJ (1970) Coral skeletons: an explanation of their growth and structure. *Science* **170**:1305-1308
- Bellwood DR (1995) Direct estimate of bioerosion by two parrotfish species, *Chlorurus gibbus* and *C. sordidus* on the Great Barrier Reef, Australia. *Marine Biology* **121**:419-429
- Bellwood DR, Choat JH (1990) A functional analysis of grazing in parrotfishes (family Scaridae): the ecological implications. *Environmental Biology of Fishes* **28**:189-214
- Bellwood DR, Hughes TP, Folke C, Nystrom M (2004) Confronting the coral reef crisis. *Nature* **429**:827-833
- Borowitzka MA, Larkum AWD (1976) Calcification in the green alga *Halimeda*. *Journal of Experimental Botany* **27**:864-878
- Bosscher H, Schlager W (1992) Computer simulation of reef growth. *Sedimentology* **39**:503-512
- Brock RE (1979) An experimental study on the effects of grazing by parrotfishes and role of refuges in benthic community structure. *Marine Biology* **51**:381-388
- Broecker WS, Takahashi T (1966) Calcium carbonate precipitation on the Bahama Banks. *Journal of Geophysical Research* **71**:1575-1602
- Bruckner AW (2002) Life-saving products from coral reefs. *Issues in Science and Technology* **18**:39-44
- Bruggeman JH (1995) *Parrotfish grazing on reefs: a trophic novelty*. Ph.D thesis, University of Groningen
- Bruggeman JH, van Kessel AM, van Rooij JM, Breeman AM (1996) Bioerosion and sediment ingestion by the Caribbean parrotfish *Scarus vetula* and *Sparisoma viride*: implications of fish size, feeding mode and habitat use. *Marine Ecology-Progress Series* **134**:59-71
- Bruno JF, Sweatman H, Precht WF, Selig ER, Schutte VGW (2009) Assessing evidence of phase shifts from coral to macroalgal dominance on coral reefs. *Ecology* **90**:1478-1484
- Buddemeier RW, Baker AC, Fautin DG, Jacobs JR (2004) The adaptive hypothesis of bleaching. In: Rosenberg E, Loya Y (eds) *Coral health and disease*. Springer-Verlag, Berlin, Germany
- Burke L, Maidens J (2004) *Reefs at risk in the Caribbean*, Vol 3. World Resources Institute
- Buss LW, Jackson JBC (1979) Competitive networks: nontransitive competitive relationships in cryptic coral reef environments. *The American Naturalist* **113**:223-234
- Carreiro-Silva M, McClanahan TR, Kiene WE (2005) The role of inorganic nutrients and herbivory in controlling microbioerosion of carbonate substratum. *Coral Reefs* **24**:214-221
- Carricart-Ganivet JP (2004) Sea surface temperature and the growth of the West Atlantic reef-building coral *Montastraea annularis*. *Journal of Experimental Marine Biology and Ecology* **302**:249-260
- Carricart-Ganivet JP (2011) Coral skeletal extension rate: An environmental signal or a subject to inaccuracies? *Journal of Experimental Marine Biology and Ecology* **405**:73-79

- Carricart-Ganivet JP, Beltrán-Torres AU, Merino M, Ruiz-Zárate MA (2000) Skeletal extension, density and calcification rate of the reef building coral *Montastraea annularis* (Ellis and Solander) in the Mexican Caribbean. *Bulletin of Marine Science* **66**:215-224
- Carricart-Ganivet JP, Cabanillas-Terán N, Cruz-Ortega I, Blanchon P (2012) Sensitivity of calcification to thermal stress varies among genera of massive reef-building corals. *PLoS ONE* **7**:e32859
- Carricart-Ganivet JP, Merino M (2001) Growth responses of the reef-building coral *Montastraea annularis* along a gradient of continental influence in the southern Gulf of Mexico. *Bulletin of Marine Science* **68**:133-146
- Castillo KD, Ries JB, Weiss JM (2011) Declining coral skeletal extension for forereef colonies of *Siderastrea siderea* on the Mesoamerican Barrier Reef system, southern Belize. *PLoS ONE* **6**:e14615
- Chave KE, Smith SV, Roy KJ (1972) Carbonate production by coral reefs. *Marine Geology* **12**:123-129
- Chazottes V, Le Campion-Alsumard T, Peyrot-Clausade M (1995) Bioerosion rates on coral reefs: interactions between macroborers, microborers and grazers (Moorea, French Polynesia). *Palaeogeography Palaeoclimatology Palaeoecology* **113**:189-198
- Chisholm JRM, Collingwood JC, Gill EF (1990) A novel in-situ respirometer for investigating photosynthesis and calcification in crustose coralline algae. *Journal of Experimental Marine Biology and Ecology* **141**:15-29
- Cohen A, McConnaughey TA (2003) Geochemical perspectives on coral mineralisation. *Reviews in Mineralogy and Geochemistry* **54**:151-187
- Conand C, Chabanet P, Cuet P, Letourneur Y (1997) The carbonate budget of a fringing reef in La Reunion Island (Indian Ocean): sea urchin and fish bioerosion and net calcification. *Proceedings of the 8th International Coral Reef Symposium*. p 953-958
- Cortes J, Murillo MM, Guzman HM, Acuña J (1984) Pérdida de zooxantelas y muerte de corales y otros organismos arrecifales en el Caribe y Pacífico de Costa Rica. *Revista de Biología Tropical* **32**:227-231
- Davalos-Dehullu E, Hernandez-Arana H, Carricart-Ganivet JP (2008) On the causes of density banding in skeletons of corals of the genus *Montastraea*. *Journal of Experimental Marine Biology and Ecology* **365**:142-147
- Davies PJ (1983) Reef Growth. In: Barnes DJ (ed) *Perspectives on coral reefs*. Australian Institute of Marine Science, Townsville
- Davies PJ, Hutchings PA (1983) Initial colonization, erosion and accretion of coral substrate. *Coral Reefs* **2**:27-35
- De'ath G, Lough JM, Fabricius KE (2009) Declining coral calcification on the Great Barrier Reef. *Science* **323**:116-119
- Demes KW, Bell SS, Dawes CJ (2009) The effects of phosphate on the biomineralization of the green alga, *Halimeda incrassata* (Ellis) Lam. *Journal of Experimental Marine Biology and Ecology* **374**:123-127
- Diaz MC, Rützler K (2001) Sponges: An essential component of Caribbean coral reefs. *Bulletin of Marine Science* **69**:535-546
- Dierssen HM, Zimmerman RC, Burdige DJ (2009) Optics and remote sensing of Bahamian carbonate sediment whittings and potential relationship to wind-driven Langmuir circulation. *Biogeosciences* **6**:487-500
- Dodge RE, Brass GW (1984) Skeletal extension, density and calcification of the reef coral, *Montastrea annularis*: St. Croix, U.S. Virgin Islands. *Bulletin of Marine Science* **34**:288-307
- Doney SC, Fabry VJ, Feely RA, Kleypas JA (2009) Ocean acidification: the other CO₂ problem. *Annual Review of Marine Science* **1**:169-192
- Donner SD, Potere D (2007) The inequity of the global threat to coral reefs. *BioScience* **57**:214-215
- Donner SD, Skirving WJ, Little CM, Oppenheimer M, Hoegh-Guldberg OVE (2005) Global assessment of coral bleaching and required rates of adaptation under climate change. *Global Change Biology* **11**:2251-2265
- Downing N, El-Zahr CR (1987) Gut Evacuation and filling rates in the rock-boring sea urchin, *Echinometra mathaei*. *Bulletin of Marine Science* **41**:579-584
- Dubinsky Z, Stambler N, Ben-Zion M, McCloskey LR, Muscatine L, Falkowski PG (1990) The effect of external nutrient resources on the optical properties and photosynthetic efficiency of *Stylophora pistillata*. *Proceedings of the Royal Society of London B Biological Sciences* **239**:231-246
- Dullo WC (2005) Coral growth and reef growth: a brief review. *Facies* **51**:33-48

- Dustan P (1975) Growth and form in the reef-building coral *Montastrea annularis*. *Marine Biology* **33**:101-107
- Eakin CM (1992) Post-El Niño Panamanian reefs: less accretion, more erosion and damselfish protection *Proceedings of the 7th International Coral Reef Symposium*, Guam, p 387-396
- Eakin CM (1996) Where have all the carbonates gone? A model comparison of calcium carbonate budgets before and after the 1982-1983 El Niño at Uva Island in the eastern Pacific. *Coral Reefs* **15**:109-119
- Edinger EN, Limmon GV, Jompa J, Widjatmoko W, Heikoop JM, Risk MJ (2000) Normal coral growth rates on dying reefs: Are coral growth rates good indicators of reef health? *Marine Pollution Bulletin* **40**:404-425
- Edinger EN, Risk MJ (1994) Oligocene-Miocene extinction and geographic restriction of Caribbean corals: Roles of turbidity, temperature, and nutrients. *Palaeos* **9**:576-598
- Erez J, Reynaud S, Silverman J, Schneider J, Allemand D (2011) Coral calcification under ocean acidification and global change. In: Dubinsky Z, Stambler N (eds) *Coral Reefs: An Ecosystem in Transition*. Springer, Berlin, p 151-176
- Etnoyer PJ, Shirley TC, Lavelle KA (2011) *Deep coral and associated species: taxonomy and ecology* (DeepCAST) II Expedition Report
- Fabricius K, De'ath G (2001) Environmental factors associated with the spatial distribution of crustose coralline algae on the Great Barrier Reef. *Coral Reefs* **19**:303-309
- Fabricius KE (2005) Effects of terrestrial runoff on the ecology of corals and coral reefs: review and synthesis. *Marine Pollution Bulletin* **50**:125-146
- Ferrier-Pagés C, Gattuso JP, Dallot S, Jaubert J (2000) Effect of nutrient enrichment on growth and photosynthesis of the zooxanthellate coral *Stylophora pistillata*. *Coral Reefs* **19**:103-113
- Fine M, Tchernov D (2007) Scleractinian coral species survive and recover from decalcification. *Science* **315**:1811-1811
- Fonseca AC, Dean HK, Cortés J (2006) Non-colonial coral macroborers as indicators of coral reef status in the south Pacific of Costa Rica. *Revista de Biología Tropical* **54**:101-115
- Friedrich T, Timmermann A, Abe-Ouchi A, Bates NR, Chikamoto MO, Church MJ, Dore JE, Gledhill DK, Gonzalez-Davila M, Ilyina T, Jungclaus JH, McLeod E, Mouchet A, Santana-Casiano JM (2012) Detecting regional anthropogenic trends in ocean acidification against natural variability. *Nature Climate Change* **2**:167-171
- Frieler K, Meinshausen M, Golly A, Mengel M, Lebek K, Donner SD, Hoegh-Guldberg O (2013) Limiting global warming to 2°C is unlikely to save most coral reefs. *Nature Climate Change* **3**:165-170
- Furla P, Galgani I, Durand I, Allemand D (2000) Sources and mechanisms of inorganic carbon transport for coral calcification and photosynthesis. *Journal of Experimental Biology* **203**:3445-3457
- Gattuso J-P, Allemand D, Frankignoulle M (1999) Photosynthesis and calcification at cellular, organismal and community levels in coral reefs: a review on interactions and control by carbonate chemistry. *American Zoologist* **39**:160-183
- Ginsburg RN (1983) Geological and biological cavities in coral reefs. In: Barnes DJ (ed) *Perspectives on coral reefs*. AIMS, Clouston, Manuka, p 148-153
- Gischler E (2008) Accretion patterns in Holocene tropical coral reefs: do massive coral reefs in deeper water with slowly growing corals accrete faster than shallower branched coral reefs with rapidly growing corals? *International Journal of Earth Sciences* **97**:851-859
- Gladfelter E (1983) Skeletal development in *Acropora cervicornis* II. Diel patterns of calcium carbonate accretion. *Coral Reefs* **2**:91-100
- Gladfelter EH (1984) Skeletal development in *Acropora cervicornis* III. A comparison of monthly rates of linear extension and calcium carbonate accretion measured over a year. *Coral Reefs* **3**:51-57
- Gladfelter EH, Monahan RK, Gladfelter WB (1978) Growth rates of five reef-building corals in the northeastern Caribbean. *Bulletin of Marine Science* **28**:728-734
- Glynn PW (1997) Bioerosion and coral reef growth: a dynamic balance. In: Birkeland C (ed) *Life and death of coral reefs*. Chapman and Hall, p 69-98
- Golubic S, Perkins R, Lukas K (1975) Boring microorganisms and microborings in carbonate substrates. In: Frey RW (ed) *The study of trace fossils*. Springer Berlin Heidelberg, p 229-259
- Goreau TF (1963) Calcium carbonate deposition by coralline algae and corals in relation to their roles as reef-builders. *Annals of the New York Academy of Sciences* **109**:127-129
- Guinotte JM, Fabry VJ (2008) Ocean acidification and its potential effects on marine ecosystems. *Year in Ecology and Conservation Biology* **1134**:320-342
- Hall-Spencer JM, Moore PG (2000) *Limaria hians* (Mollusca: Limacea): a neglected reef-forming keystone species. *Aquatic Conservation: Marine and Freshwater Ecosystems* **10**:267-277

- Hall-Spencer JM, Rodolfo-Metalpa R, Martin S, Ransome E, Fine M, Turner SM, Rowley SJ, Tedesco D, Buia MC (2008) Volcanic carbon dioxide vents show ecosystem effects of ocean acidification. *Nature* **454**:96-99
- Hallock P (1988) The role of nutrient availability in bioerosion: Consequences to carbonate buildups. *Palaeogeography, Palaeoclimatology, Palaeoecology* **63**:275-291
- Hart DE, Kench PS (2007) Carbonate production of an emergent reef platform, Warraber Island, Torres Strait, Australia. *Coral Reefs* **26**:53-68
- Harvell CD, Kim K, Burkholder JM, Colwell RR, Epstein PR, Grimes DJ, Hofmann EE, Lipp EK, Osterhaus ADME, Overstreet RM, Porter JW, Smith GW, Vasta GR (1999) Emerging marine diseases - climate links and anthropogenic factors. *Science* **285**:1505-1510
- Hatcher BG (1997) Organic production and decomposition. In: Birkeland C (ed) *Life and death of coral reefs*. Chapman and Hall, New York
- Hein FJ, Risk MJ (1975) Bioerosion of coral heads: inner patch reefs, Florida reef tract. *Bulletin of Marine Science* **25**:133-138
- Herrera-Escalante T, López-Pérez RA, Leyte-Morales GE (2005) Bioerosion caused by the sea urchin *Diadema mexicanum* (Echinodermata: Echinoidea) at Bahias de Huatulco, Western Mexico. *Revista De Biología Tropical* **53**:263-273
- Highsmith RC (1979) Coral growth rates and environmental control of density banding. *Journal of Experimental Marine Biology and Ecology* **37**:105-125
- Highsmith RC (1981) Coral bioerosion: damage relative to skeletal density. *American Naturalist* **117**:193-198
- Highsmith RC, Lueptow RL, Schonberg SC (1983) Growth and bioerosion of three massive corals on the Belize barrier reef. *Marine Ecology Progress Series* **13**:261-271
- Hillis L (1997) Coralgall reefs from a calcareous green alga perspective, and a first carbonate budget. In: Lessios HA, MacIntyre IG (eds) *Proceedings of the 8th International Coral Reef Symposium*, Panama
- Hoegh-Guldberg O, Mumby PJ, Hooten AJ, Steneck RS, Greenfield P, Gomez E, Harvell CD, Sale PF, Edwards AJ, Caldeira K, Knowlton N, Eakin CM, Iglesias-Prieto R, Muthiga N, Bradbury RH, Dubi A, Hatziohos ME (2007) Coral reefs under rapid climate change and ocean acidification. *Science* **318**:1737-1742
- Hoey A, Bellwood D (2008) Cross-shelf variation in the role of parrotfishes on the Great Barrier Reef. *Coral Reefs* **27**:37-47
- Hoskin CM, Reed JK (1984) Carbonate sediment produced by rock-boring urchin, *Echinometra lucunter*, and infauna, Black Rock, Little Bahama Bank. *American Association of Petroleum Geologists* **68**:487-487
- Hoskin CM, Reed JK, Mook DH (1986) Production and off-bank transport of carbonate sediment, Black Rock, southwest Little Bahama Bank. *Marine Geology* **73**:125-144
- Hubbard DK (2009) Depth-related and species-related patterns of Holocene reef accretion in the Caribbean and western Atlantic: a critical assessment of existing models. In: Swart PK, Eberli GP, McKenzie JA, Jarvis I, Stevens T (eds) *Perspectives in Carbonate Geology*. John Wiley & Sons, Ltd, p 1-18
- Hubbard DK, Miller AI, Scaturro D (1990) Production and cycling of calcium-carbonate in a shelf-edge reef system (St. Croix, United States Virgin Islands): applications to the nature of reef systems in the fossil record. *Journal of Sedimentary Petrology* **60**:335-360
- Hubbard DK, Scaturro D (1985) Growth rates of seven species of scleractinian corals from Cane Bay and Salt River, St Croix, USVI. *Bulletin of Marine Science* **36**:325-338
- Hudson JH (1977) Long-term bioerosion rates on a Florida reef tract: a new method. In: Taylor DL (ed) *Proceedings of the 3rd International Coral Reef Symposium*, Miami, Florida
- Hunter IG (1977) Sediment production by *Diadema antillarum* on a Barbados fringing reef. *Proceedings of the 3rd International Coral Reef Symposium*, Miami, Florida
- Huston M (1985) Variation in coral growth rates with depth at Discovery Bay, Jamaica. *Coral Reefs* **4**:19-25
- Hutchings PA (1983) Cryptofaunal communities of coral reefs. In: Barnes DJ (ed) *Perspectives on coral reefs*, AIMS, Townsville, p 200-208
- Hutchings PA (1986) Biological destruction of coral reefs - a review. *Coral Reefs* **4**:239-252
- Jokiel PL, Coles SL (1977) Effects of temperature on the mortality and growth of Hawaiian reef corals. *Marine Biology* **43**:201-208
- Kendrick B, Risk MJ, Michaelides J, Bergman K (1982) Amphibious microborers: bioeroding fungi isolated from corals. *Bulletin of Marine Science* **32**:862-867

- Kiene WE (1988) A model of bioerosion on the Great Barrier Reef *Proceedings of the 6th International Coral Reef Symposium*, Australia, p 449-454
- Kiene WE (1997) Enriched nutrients and their impact on bioerosion: results from ENCORE. In: Lessios H, MacIntyre I (eds) *Proceedings of the 8th International Coral Reef Symposium*, Panama
- Kiene WE, Hutchings PA (1994) Bioerosion experiments at Lizard Island, Great Barrier Reef. *Coral Reefs* **13**:91-98
- Killian CE, Metzler RA, Gong Y, Churchill TH, Olson IC, Trubetskoy V, Christensen MB, Fournelle JH, De Carlo F, Cohen S, Mahamid J, Scholl A, Young A, Doran A, Wilt FH, Coppersmith SN, Gilbert PUPA (2011) Self-sharpening mechanism of the sea urchin tooth. *Advanced Functional Materials* **21**:682-690
- Kleemann KH (1980) Boring bivalves and their host corals from the Great Barrier Reef. *Journal of Molluscan Studies* **46**:13-54
- Kleypas JA, Buddemeier RW, Archer D, Gattuso JP, Langdon C, Opdyke BN (1999) Geochemical consequences of increased atmospheric carbon dioxide on coral reefs. *Science* **284**:118-120
- Kleypas JA, Feely RA, Fabry VJ, Langdon C, Sabine CL, Robbins LL (2006) *Impact of ocean acidification on coral reefs and other marine calcifiers: a case guide for future research*. St Petersburg, Florida
- Kleypas JA, Langdon C (2007) Chapter 5: Coral reefs and changing seawater chemistry. In: Phinney J, Skirving W, Kleypas J, Hoegh-Guldberg O, Strong AE (eds) *Coral Reefs and Climate Change: Science and Management*, Vol **61**. Coastal and Estuarine Studies, p 73-109
- Kuffner IB, Andersson AJ, Jokiel PL, Rodgers KS, Mackenzie FT (2008) Decreased abundance of crustose coralline algae due to ocean acidification. *Nature Geoscience* **1**:114-117
- Land LS (1974) Growth rate of a West Indian (Jamaican) reef. In: Cameron AM, Cambell BM, Cribb AB, Edean R, Jell JS, Jones OA, Mather P, Talbot FH (eds) *Proceedings of the 2nd International Symposium on Coral Reefs*, Brisbane, Australia, p 409-412
- Land LS (1979) Fate of reef-derived sediment on the north Jamaican island slope. *Marine Geology* **29**:55-71
- Langdon C, Takahashi T, Sweeney C, Chipman D, Goddard J (2000) Effect of calcium carbonate saturation state on the rate of calcification of an experimental coral reef. *Global Biogeochemical Cycles* **14**:639-654
- Lazar B, Loya Y (1991) Bioerosion of coral reefs- a chemical approach. *Limnology and Oceanography* **36**:377-383
- Le Campion-Alsumard T, Golubic S, Hutchings P (1995a) Microbial endoliths in skeletons of live and dead corals: *Porites lobata* (Moorea, French Polynesia). *Marine Ecology Progress Series* **117**:149-157
- Le Campion-Alsumard T, Golubic S, Priess K (1995b) Fungi in corals: symbiosis or disease? Interaction between polyps and fungi causes pearl-like skeleton biomineralisation. *Marine Ecology Progress Series* **117**:137-147
- Levitan DR (1988) Algal-urchin biomass responses following mass mortality of *Diadema antillarum* Philippi at Saint John, U.S. Virgin Islands. *Journal of Experimental Marine Biology and Ecology* **119**:167-178
- Lewis JB, Axelsen F, Goodbody I, Cynthia P, Chrislett G (1968) *Comparative growth rates of some reef corals in the Caribbean*. Marine Sciences Centre Report McGill University, Montreal (Quebec), 27 pp
- Leys SP, Yahel G, Reidenbach MA, Tunnicliffe V, Shavit U, et al. (2011) The sponge pump: the role of current induced flow in the design of the sponge body plan. *PLoS ONE* **6**:e27787
- Little AF, van Oppen MJH, Willis BL (2004) Flexibility in algal endosymbioses shapes growth in reef corals. *Science* **304**:1492-1494
- López-Victoria M, Zea S (2005) Current trends of space occupation by encrusting excavating sponges on Colombian coral reefs. *Marine Ecology* **26**:33-41
- Lough J (2008) Coral calcification from skeletal records revisited. *Marine Ecology-Progress Series* **373**:257-264
- Lough JM, Barnes DJ (2000) Environmental controls on growth of the massive coral *Porites*. *Journal of Experimental Marine Biology and Ecology* **245**:225-243
- Macdonald IA, Perry CT (2003) Biological degradation of coral framework in a turbid lagoon environment, Discovery Bay, north Jamaica. *Coral Reefs* **22**:523-535
- MacGeachy JK (1977) Factors controlling sponge boring in Barbados reef corals. In: Taylor DL (ed) *Proceedings of the 3rd International Coral Reef Symposium*, Miami, Florida
- MacGeachy JK, Stearn CW (1976) Boring by macroorganisms in the coral *Montastraea annularis* on Barbados reefs. *Internationale Revue der gesamten Hydrobiologie* **61**:715-746

- MacIntyre IG (1997) Re-evaluating the role of crustose algae in the construction of coral reefs. In: Lessios HA, Macintyre IG (eds) *Proceedings of the 8th International Coral Reef Symposium*, Panama
- Mallela J (2007) Coral reef encruster communities and carbonate production in cryptic and exposed coral reef habitats along a gradient of terrestrial disturbance. *Coral Reefs* **26**:775-785
- Mallela J, Perry CT (2007) Calcium carbonate budgets for two coral reefs affected by different terrestrial runoff regimes, Rio Bueno, Jamaica. *Coral Reefs* **26**:129-145
- Manzello DP, Berkelmans R, Hendee JC (2007) Coral bleaching indices and thresholds for the Florida Reef Tract, Bahamas, and St. Croix, US Virgin Islands. *Marine Pollution Bulletin* **54**:1923-1931
- Manzello DP, Kleypas JA, Budd DA, Eakin CM, Glynn PW, Langdon C (2008) Poorly cemented coral reefs of the eastern tropical Pacific: Possible insights into reef development in a high-CO₂ world. *Proceedings of the National Academy of Sciences* **105**:10450-10455
- Marshall AT, Clode P (2004) Calcification rate and the effect of temperature in a zooxanthellate and an azooxanthellate scleractinian reef coral. *Coral Reefs* **23**:218-224
- Marubini F, Davies PS (1996) Nitrate increases zooxanthellae population density and reduces skeletogenesis in corals. *Marine Biology* **127**:319-328
- Marubini F, Ferrier-Pagés C, Cuif J-P (2003) Suppression of skeletal growth in scleractinian corals by decreasing ambient carbonate-ion concentration: a cross-family comparison. *Proceedings: Biological Sciences* **270**:179-184
- Marubini F, Thake B (1999) Bicarbonate addition promotes coral growth. *Limnology and Oceanography* **44**:716-720
- McConnaughey TA, Whelan JF (1997) Calcification generates protons for nutrient and bicarbonate uptake. *Earth-Science Reviews* **42**:95-117
- Mendes JM, Woodley JD (2002) Effect of the 1995-1996 bleaching event on polyp tissue depth, growth, reproduction and skeletal band formation in *Montastraea annularis*. *Marine Ecology Progress Series* **235**:93-102
- Milliman JD, Droxler AW (1995) Calcium carbonate sedimentation in the global ocean: linkages between the neritic and pelagic environments. *Oceanography* **8**:92-94
- Mokady O, Lazar B, Loya Y (1996) Echinoid bioerosion as a major structuring force of Red Sea coral reefs. *Biological Bulletin* **190**:367-372
- Montaggioni LF, Cabioch G, Camoin GF, Bard E, Ribaud Laurenti A, Faure Gérard, Déjardin P, Récy J (1997) Continuous record of reef growth over the past 14 k.y. on the mid-Pacific island of Tahiti. *Geology* **25**:555-558
- Moore CG, Richard Bates C, Mair JM, Saunders GR, Harries DB, Lyndon AR (2009) Mapping serpulid worm reefs (Polychaeta: Serpulidae) for conservation management. *Aquatic Conservation: Marine and Freshwater Ecosystems* **19**:226-236
- Moya A, Tambutté S, Bertucci A, Tambutté E, Lotto S, Vullo D, Supuran CT, Allemand D, Zoccola D (2008) Carbonic anhydrase in the scleractinian coral *Stylophora pistillata*: characterisation, localisation and role in biomineralisation. *Journal of Biological Chemistry* **283**:25475-25484
- Mullins HT, Newton CR, Heath K, Vanburen M (1981) Modern deep-water coral mounds north of Little Bahama Bank: criteria for recognition of deep water coral bioherms in the rock record. *Journal of Sedimentary Research* **51**:999-1013
- Mumby P (2009) Herbivory versus corallivory: are parrotfish good or bad for Caribbean coral reefs? *Coral Reefs* **28**:683-690
- Mumby PJ, Hastings A, Edwards HJ (2007) Thresholds and the resilience of Caribbean coral reefs. *Nature* **450**:98-101
- Nash MC, Opdyke BN, Troitzsch U, Russell BD, Adey WH, Kato A, Diaz-Pulido G, Brent C, Gardner M, Prichard J, Kline DI (2013) Dolomite-rich coralline algae in reefs resist dissolution in acidified conditions. *Nature Climate Change* **3**:268-272
- Nava H, Carballo JL (2008) Chemical and mechanical bioerosion of boring sponges from Mexican Pacific coral reefs. *Journal of Experimental Biology* **211**:2827-2831
- Nellman C, Hain S, Alder J (2008) *In dead water: merging of climate change with pollution, over-harvest, and infestations in the world's fishing grounds*. Report, Norway
- Neumann AC (1966) Observations on coastal bioerosion in Bermuda and measurements of boring rate of sponge *Cliona lampa*. *Limnology and Oceanography* **11**:92-98
- Neumann AC, Macintyre IG (1985) Reef response to sea level rise: keep-up, catch-up or give-up. In: Gabrie C, Toffart JL, Salvat B (eds) *Proceedings of the 5th International Coral Reef Congress*, Tahiti
- Norström AV, Norström M, Lokrantz J, Folke C (2009) Alternative states on coral reefs: beyond coral-macroalgal phase shifts. *Marine Ecology Progress Series* **376**:295-306

- Odum HT, Odum EP (1955) Trophic structure and productivity of a windward coral reef community on Eniwetok Atoll. *Ecology* **25**:291-320
- Ogden JC (1977) Carbonate sediment production by parrotfish and sea urchins on Caribbean reefs: reef biota. *American Association of Petroleum Geologists* **4**:281-288
- Oxford English Dictionary (2013) "reef, n.2", Vol. Oxford University Press
- Pari N, Peyrot-Clausade M, Hutchings PA (2002) Bioerosion of experimental substrates on high islands and atoll lagoons (French Polynesia) during 5 years of exposure. *Journal of Experimental Marine Biology and Ecology* **276**:109-127
- Perry CT (1996) Distribution and abundance of macroborers in an upper Miocene reef system, Mallorca, Spain: Implications for reef development and framework destruction. *Palaios* **11**:40-56
- Perry CT (1998) Macroborers within coral framework at Discovery Bay, north Jamaica: species distribution and abundance, and effects on coral preservation. *Coral Reefs* **17**:277-287
- Perry CT (1999) Reef framework preservation in four contrasting modern reef environments, Discovery Bay. *Jamaica Journal of Coastal Research* **15**:796-812
- Perry CT, Edinger EN, Kench PS, G. M, S.G. S, Steneck RS, Mumby PJ (2012) Estimating rates of biologically driven coral reef framework production and erosion: a new census-based carbonate budget methodology and applications to the reefs of Bonaire. *Coral Reefs* **31**:853-868
- Perry CT, Hepburn LJ (2008b) Syn-depositional alteration of coral reef framework through bioerosion, encrustation and cementation: Taphonomic signatures of reef accretion and reef depositional events. *Earth-Science Reviews* **86**:106-144
- Perry CT, Murphy GN, Kench PS, Smithers SG, Edinger EN, Steneck RS, Mumby PJ (2013) Caribbean-wide decline in carbonate production threatens coral reef growth. *Nature Communications* **4**:1402
- Perry CT, Smithers SG (2011) Cycles of coral reef 'turn-on', rapid growth and 'turn-off' over the past 8500 years: a context for understanding modern ecological states and trajectories. *Global Change Biology* **17**:76-86
- Perry CT, Smithers SG, Gulliver P, Browne NK (2012b) Evidence of very rapid reef accretion and reef growth under high turbidity and terrigenous sedimentation. *Geology* **40**:719-722
- Perry CT, Spencer T, Kench PS (2008) Carbonate budgets and reef production states: a geomorphic perspective on the ecological phase-shift concept. *Coral Reefs* **27**:853-866
- Reaka-Kudla ML (1997) Chapter 7. The global biodiversity of coral reefs: a comparison with rainforests. In: Reaka-Kudla ML, Wilson DE, Wilson EO (eds) *Biodiversity II: understanding and protecting our biological resources*. National Academies Press
- Reaka-Kudla ML, Feingold JS, Glynn W (1996) Experimental studies of rapid bioerosion of coral reefs in the Galapagos Islands. *Coral Reefs* **15**:101-107
- Rees SA (2006) *Coral reefs of the Indo-Pacific and changes in global Holocene climate*. University of Southampton, PhD thesis, 315 pp.
- Rees SA, Opdyke BN, Wilson PA, Henstock TJ (2007) Significance of *Halimeda* bioherms to the global carbonate budget based on a geological sediment budget for the Northern Great Barrier Reef, Australia. *Coral Reefs* **26**:177-188
- Reynaud S, Ferrier-Pagés C, Boisson F, Allemand D, Fairbanks RG (2004) Effect of light and temperature on calcification and strontium uptake in the scleractinian coral *Acropora verweyi*. *Marine Ecology Progress Series* **279**:105-112
- Risk MJ, MacGeachy JK (1978) Aspects of bioerosion of modern Caribbean reefs. *Revista de Biologia Tropical* **26**:85-125
- Risk MJ, Sammarco PW, Edinger EN (1995) Bioerosion in *Acropora* across the continental shelf of the Great Barrier Reef. *Coral Reefs* **14**:79-86
- Rogers CS (1990) Response of coral reefs and reef organisms to sedimentation. *Marine Ecology Progress Series* **62**:185-202
- Rose CS, Risk MJ (1985) Increase in *Cliona delitrix* infestation of *Montastraea cavernosa* heads on an organically polluted portion of the Grand Cayman fringing reef. *Marine Ecology* **6**:345-363
- Rotjan RD, Lewis SM (2008) Impact of coral predators on tropical reefs. *Marine Ecology-Progress Series* **367**:73-91
- Rützler K (1975) Role of burrowing sponges in bioerosion. *Oecologia* **19**:203-216
- Rützler K (2002) Impact of crustose clinoid sponges on Caribbean coral reefs. *Acta Geologica Hispanica* **37**:61-72
- Rützler K, Rieger G (1973) Sponge burrowing: fine structure of *Cliona lampa* penetrating calcareous substrata. *Marine Biology* **21**
- Sadd JL (1984) Sediment transport and CaCO₃ budget on a fringing reef, Cane Bay, St. Croix, United States Virgin Islands. *Bulletin of Marine Science* **35**:221-238

- Sammarco PW (1982) Echinoid grazing as a structuring force in coral communities: Whole reef manipulations. *Journal of Experimental Marine Biology and Ecology* **61**:31-55
- Schlager W (1981) The paradox of drowned reefs and carbonate platforms. *Geological Society of America Bulletin* **92**:197-211
- Schneider K, Silverman J, Woolsey E, Eriksson H, Byrne M, Caldeira K (2011) Potential influence of sea cucumbers on coral reef CaCO₃ budget: a case study at One Tree Reef. *Journal of Geophysical Research: Biogeosciences* **116**:G04032
- Schoppe S, Werding B (1996) The boreholes of the sea urchin genus *Echinometra* (Echinodermata: Echinoidea: Echinometridae) as a microhabitat in tropical South America. *Marine Ecology* **17**:181-186
- Scoffin TP, Stearn CW, Boucher D, Frydl P, Hawkins CM, Hunter IG, Macgeachy JK (1980) Calcium-carbonate budget of a fringing reef on the west coast of Barbados. Part 2: Erosion, sediments and internal structure. *Bulletin of Marine Science* **30**:475-508
- Scott PJB (1985) Aspects of living coral associates in Jamaica. *Proceedings of the 5th International Coral Reef Symposium*, Tahiti
- Scott PJB, Moser KA, Risk MJ (1988) Bioerosion of concrete and limestone by marine organisms: A 13 year experiment from Jamaica. *Marine Pollution Bulletin* **19**:219-222
- Shulman MJ, Robertson DR (1996) Changes in the coral reefs of San Blas, Caribbean Panama: 1983 - 1990. *Coral Reefs* **15**:231-236
- Silverman J, Lazar B, Cao L, Caldeira K, Erez J (2009) Coral reefs may start dissolving when atmospheric CO₂ doubles. *Geophysical Research Letters* **36**: L05606
- Simpson MC, Scott D, New M, Sim R, Smith D, Harrison M, Eakin CM, Warrick R, Strong AE, Kouwenhoven P, Harrison S, Wilson M, Nelson GC, Donner S, Kay R, Gledhill DK, Liu G, Morgan JA, Kleypas JA, Mumby PJ, Palazzo A, Christensen TRL, Baskett ML, Skirving WJ, Elrick C, Taylor M, Magalhaes M, Bell J, Burnett JB, Ruttly MK, Overmas M, Robertson R (2009) *An overview of modelling climate change impacts in the Caribbean region with contribution from the Pacific Islands*. United Nations Development Programme (UNDP), Barbados, West Indies
- Smith SV (1978) Coral reef area and contributions of reefs to processes and resources of the worlds oceans. *Nature* **273**:225-226
- Smith SV, Kinsey DW (1976) Calcium-carbonate production, coral reef growth and sea-level change. *Science* **194**:937-939
- Stearn CW, Scoffin TP (1977) Carbonate budget of a fringing reef, Barbados. *Proceedings of the 3rd International Coral Reef Symposium*, Miami, Florida
- Stearn CW, Scoffin TP, Martindale W (1977) Calcium carbonate budget of a fringing reef on the west coast of Barbados. Part 1: Zonation and Productivity. *Bulletin of Marine Science* **27**:479-510
- Steneck RS (1994) Is herbivore loss more damaging to reefs than hurricanes? Case studies from two Caribbean reef systems (1978-1988). In: Ginsburg RN (ed) *Global aspects of coral reefs: health, hazards and history*. University of Miami, Miami, Florida, USA, p C32-C37
- Tambutté E, Tambuté S, Segonds N, Zoccola D, Venn A, Erez J, Allemand D (2012) Calcein labelling and electrophysiology: insights on coral tissue permeability and calcification. *Proceedings of the Royal Society B: Biological Sciences* **279**:19-27
- Tomascik T, Sander F (1985) Effects of eutrophication on reef-building corals: I. Growth rate of the reef building coral *Montastraea annularis*. *Marine Biology* **87**:143-155
- Tribollet A (2008a) The boring microflora in modern coral reef ecosystems: a review of its roles. In: Wisshak M, Tapanila L (eds) *Current developments in bioerosion*. Springer-Verlag, p 67-94
- Tribollet A (2008b) Dissolution of dead corals by euendolithic microorganisms across the northern Great Barrier Reef. *Microbial Ecology* **55**:569-580
- Tribollet A, Atkinson MJ, Langdon C (2006a) Effects of elevated pCO₂ on epilithic and endolithic metabolism of reef carbonates. *Global Change Biology* **12**:2200-2208
- Tribollet A, Decherf G, Hutchings PA, Peyrot-Clausade M (2002) Large-scale spatial variability in bioerosion of experimental coral substrates on the Great Barrier Reef (Australia): importance of microborers. *Coral Reefs* **21**:424-432
- Tribollet A, Golubic S, Dubinsky Z, Stambler N (2011) Reef Bioerosion: Agents and Processes. In: *Coral Reefs: An Ecosystem in Transition*. Springer Netherlands, p 435-449
- Tribollet A, Langdon C, Golubic S, Atkinson M (2006b) Endolithic microflora are major primary producers in dead carbonate substrates of Hawaiian coral reefs. *Journal of Phycology* **42**:292-303
- Trudgill S (1976) The marine erosion of limestones on Aldabra Atoll, Indian Ocean. *Zeitschrift für Geomorphologie* **26**:164-200

- Tudhope AW, Risk MJ (1985) Rate of dissolution of carbonate sediments by microboring organisms, Davies Reef, Australia. *Journal of Sedimentary Petrology* **55**:440-447
- van Hoodonk RJ, Manzello DP, Moyer J, Brandt ME, Hendee JC, McCoy C, Manfrino C (2012) Coral bleaching at Little Cayman, Cayman Islands 2009. *Estuarine, Coastal and Shelf Science* **106**:80-84
- Vecsei A (2001) Fore-reef carbonate production: development of a regional census-based method and first estimates. *Palaeogeography Palaeoclimatology Palaeoecology* **175**:185-200
- Venn A, Tambutté E, Holcomb M, Allemand D, Tambutté S (2011) Live tissue imaging shows reef corals elevate pH under their calcifying tissue relative to seawater. *PLoS ONE* **6**:e20013
- Veron J (2008) Mass extinctions and ocean acidification: biological constraints on geological dilemmas. *Coral Reefs* **27**:459-472
- Vogel K, Gektidis M, Golubic S, Kiene WE, Radtke G (2000) Experimental studies on microbial bioerosion at Lee Stocking Island, Bahamas and One Tree Island, Great Barrier Reef, Australia: implications for paleoecological reconstructions. *Lethaia* **33**:190-204
- Ward-Paige CA, Risk MJ, Sherwood OA, Jaap WC (2005) Clionid sponge surveys on the Florida Reef Tract suggest land-based nutrient inputs. *Marine Pollution Bulletin* **51**:570-579
- Weber J, N. , White EW, Weber PH (1975) Correlation of density banding in reef coral skeletons with environmental parameters: the basis for interpretation of chronological records preserved in the coralla of corals. *Paleobiology* **1**:137-149
- Weil E (1980) Papel del erizo *Diadema antillarum Philippi* en la regulació n de la estructura de las comunidades coralinas. Universidad Central de Venezuela, PhD thesis
- Weis VM, Allemand D (2009) What determines coral health? *Science* **324**:1153-1155
- Wilkinson CR (1983) Role of sponges in coral reef structural processes. In: Barnes DJ (ed) *Perspectives on coral reefs*. Australian Institute of Marine Science, Townsville, Australia, p 263-274
- Williams ID, Polunin NVC (2001) Large-scale associations between macroalgal cover and grazer biomass on mid-depth reefs in the Caribbean. *Coral Reefs* **19**:358-366
- Wisshak M, Schönberg CHL, Form A, Freiwald A (2012) Ocean acidification accelerates reef bioerosion. *PLoS ONE* **7**:e45124
- Wulff JL, Buss LW (1979) Do sponges help hold coral reefs together? *Nature* **281**:474-475
- Yee SH, Santavy DL, Barron MG (2008) Comparing environmental influences on coral bleaching across and within species using clustered binomial regression. *Ecological Modelling* **218**:162-174
- Zea S, Weil E (2003) Taxonomy of the Caribbean excavating sponge species complex *Cliona caribbea* - *C. aprica* - *C. langae* (Porifera, Hadromerida, Clionadiae). *Caribbean Journal of Science* **39**:348-370
- Zubia M, Peyrot-Clausade M (2001) Internal bioerosion of *Acropora formosa* in Reunion (Indian Ocean): microborer and macroborer activities. *Oceanologica Acta* **24**:251-262

3

Development of a theoretical carbonate budget model

3.1 Introduction

Consideration of the carbonate balance of any given reef is important, both as a measure of health status (Perry et al. 2012), and because much of the value of reefs (biodiversity, coastal protection) is a by-product of their three-dimensional complexity (Moberg and Folke 1999). A carbonate budget, defined as the “*sum of gross carbonate production from corals and calcareous encrusters as well as sediment produced within or imported into the reef minus that lost through biological or physical erosion, dissolution or sediment export*” (Chave et al. 1972) provides a quantitative estimate of framework growth that takes into account both accretion and erosion processes (Chapter 1, Fig. 1.8). Carbonate budgets provide a holistic approach to reef health assessment, that may be favourable to conventional measures that focus on superficial surface-related factors such as coral or algal cover; methods which lack consideration of the internal effects of bioeroders and encrusters on the framework functioning (Perry et al. 2008). Increasingly, maintenance of ‘bioconstruction’ is viewed as a key ecological goal for reef managers (Done 1995).

Only a handful of comprehensive carbonate budgets have been attempted in the field, due to the wide variety of contributing factors and difficulties associated with their quantitative assessment. Of these budgets, the different methodological approaches (Smith 1978) adopted (e.g., geological assessment of drill cores to assess vertical framework growth (Moore and Shedd 1977); hydrochemical techniques such as the alkalinity anomaly method (Smith and Kinsey 1976); and biological census-based approaches (Harney and Fletcher 2003, Perry et al. 2012)) and the diverse range of temporal and spatial scales over which budgets were assessed (Fig. 3.1), has meant that the majority of published carbonate budgets are not directly comparable. Few time series have been attempted, and with multiple factors to account for, even inclusive budgets often overlooked contributing components –for example, most failed to quantify encruster carbonate production due to its cryptic nature (Sadd 1984, Mallela 2007).

Finally, many published budgets rely on flawed assumptions, such as temporally uniform rates of calcification, or fixed skeletal density of corals (Edinger et al. 2000).

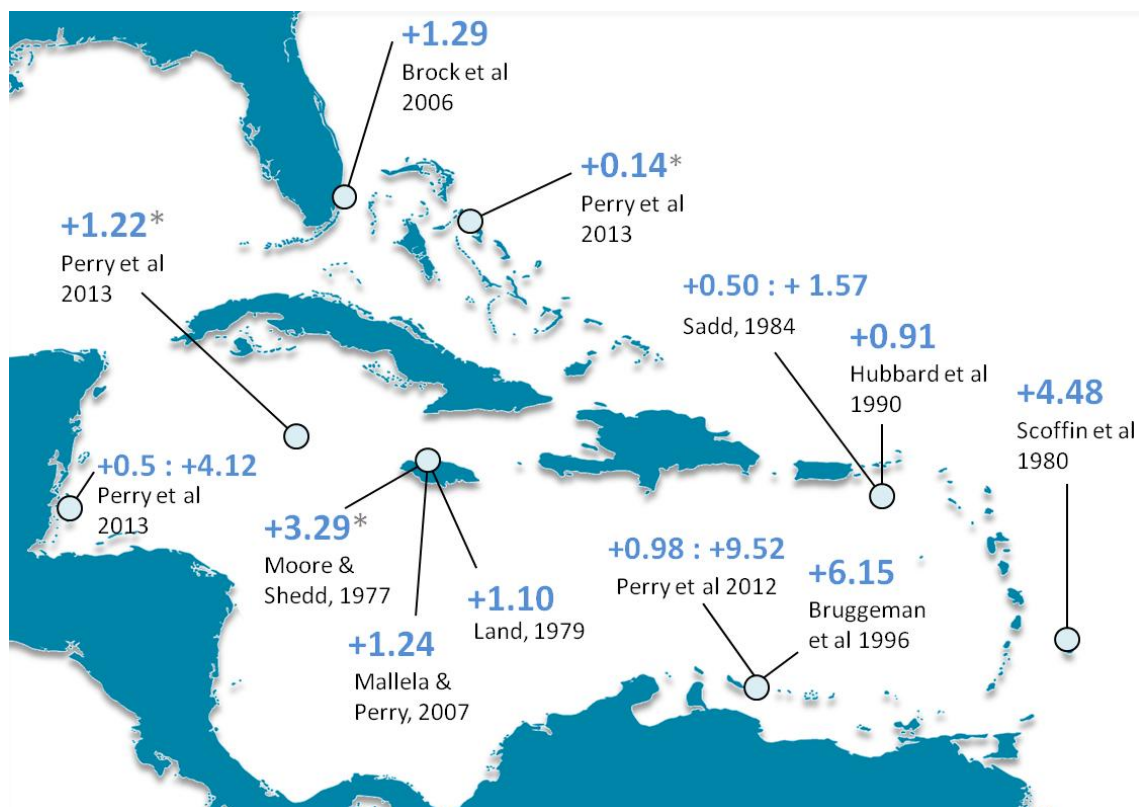


Figure 3.1: Map of the Caribbean, including all published carbonate budget field studies to date. Values (in blue) show the estimated net productivity of a reef, in kg CaCO₃ m⁻² year⁻¹, and publication reference is noted below. At the beginning of the current study, only five comprehensive studies existed for the Caribbean: thanks to Perry et al this number has now doubled. Asterisks denote an average value where the carbonate budget for more than one reef was calculated (for full details see Table 3.1).

Early budget studies focused only on pristine reefs (Stearn and Scoffin 1977, Land 1979, Hubbard et al. 1990). Later comparative budgets of reefs growing under sub-optimal environmental conditions with healthy reefs emerged (Eakin 1996, Edinger et al. 2000, Mallela and Perry 2007). Several of these demonstrated that small changes in rates of processes attributing to the budget can have large impacts on the rate of net framework production, in some cases pushing it from a positive to a negative budgetary state. Recent evidence has shown that Caribbean reefs have been losing architectural structure since the 1960's, with the near disappearance of the most complex reefs over the last 40 years (Alvarez-Filip et al. 2009). The mechanisms behind recent rugosity loss have not been fully explored: although rapid declines of hard coral cover (Gardner et al. 2003) is assumed to be a major driver (Alvarez-Filip et al. 2009), a lack of recovery following mortality events suggests it is accompanied by disruption to the carbonate balance causing bioerosion to exceed accretion (Sheppard et al. 2002). Traditionally, research on environmental disturbance has focused more on how change affects aspects of framework production-associated processes, namely coral productivity and mortality. The scarcity of published carbonate budget studies demonstrates that approaches to assessing reef health that consider both bioerosion and production are rarely adopted.

Reef location	Depth (m)	Accretion (kg m ⁻² yr ⁻¹)	Bioerosion (kg m ⁻² yr ⁻¹)	Net budget (kg m ⁻² yr ⁻¹)	Method used	Reef type	Study
Jamaica, Discovery Bay	< 20	5.20	1.20	1.10	sediment transport	fringing reef	Land, 1979
Jamaica, East Forereef	15	3.90	1.26	2.65	geological; cores	fore-reef terrace	Moore & Shedd 1977
Jamaica, East Forereef	27	0.80	0.25	0.55	geological; cores	base forereef escarpment	Moore & Shedd 1977
Jamaica, Zingoro	27	2.00	0.63	1.37	geological; cores	base forereef escarpment	Moore & Shedd 1977
Jamaica, Zingoro	40	0.70	0.22	0.48	geological; cores	forereef slope	Moore & Shedd 1977
Jamaica, Pear Tree Bottom	15	5.80	1.86	3.94	geological; cores	forereef terrace	Moore & Shedd 1977
Jamaica, Pear Tree Bottom	27	5.40	1.72	3.69	geological; cores	forereef escarpment	Moore & Shedd 1977
Barbados, Bellairs Reef	< 10	8.87	6.72	4.48	census-based	fringing reef	Scoffin <i>et al.</i> 1980
St Croix, Cane Bay	10	3.10	0.50*	1.00	sediment transport	shallow reef	Sadd, 1984
St Croix, Cane Bay	10-15	5.00	0.16*	1.57	sediment transport	coral gardens	Sadd, 1984
St Croix, Cane Bay	10-12	0.85	0.64*	0.34	sediment transport	sand flat	Sadd, 1984
St Croix, Cane Bay	15 - 30	5.00	1.06*	0.50	sediment transport	coral gardens (deep)	Sadd, 1984
St Croix, Cane Bay	12 - 18	0.85	3.20*	0.11	sediment transport	sand slope	Sadd, 1984
St Croix, Cane Bay	<30	1.00	1.26*	0.50	sediment transport	deep reef	Sadd, 1984
St Croix, Cane Bay	3 - 39	1.21	0.71	0.91**	census-based/cores	exposed fringing reef	Hubbard <i>et al.</i> 1990
Bonaire, Karpata (shallow reef)	0.3 - 3	3.82	6.8***	-2.98	census-based/theoretical	shallow reef	Bruggeman <i>et al.</i> 1996
Bonaire, Karpata (drop off)	6 - 12	7.75	1.6***	6.15	census-based/theoretical	drop off	Bruggeman <i>et al.</i> 1996
Bonaire, Karpata (reef slope)	12 - 25	2.95	0.7***	2.25	census-based/theoretical	reef slope	Bruggeman <i>et al.</i> 1996
Jamaica, Rio Bueno (OE)	< 20	1.21	0.13	1.24	census-based	fringing reef (clean site)	Mallela & Perry 2007
Jamaica, Rio Bueno (CE)	< 20	1.88	0.27	1.89	census-based	fringing reef (poor water quality)	Mallela & Perry 2007
Bonaire, NDR-5	5	6.75	3.12	3.63	census-based	leeward fringing reef	Perry <i>et al.</i> 2012
Bonaire, NDR-10	10	12.27	2.75	9.52	census-based	leeward fringing reef	Perry <i>et al.</i> 2012
Bonaire, Calabas	10	4.68	2.38	2.30	census-based	leeward fringing reef	Perry <i>et al.</i> 2012
Bonaire, Cai	5	0.26	1.24	-0.98	census-based	windward fringing reef	Perry <i>et al.</i> 2012
Bonaire, White Hole	10	3.03	2.05	0.98	census-based	windward fringing reef	Perry <i>et al.</i> 2012
Bahamas, Ski Slopes	20	1.91	1.20	0.71	census-based	shelf edge <i>Montastraea</i> reef	Perry <i>et al.</i> 2013
Bahamas, Cathedral Rock	19	1.74	1.52	0.22	census-based	shelf edge <i>Montastraea</i> reef	Perry <i>et al.</i> 2013
Bahamas, Hole-in-the-Wall	17	1.17	1.69	-0.52	census-based	shelf edge <i>Montastraea</i> reef	Perry <i>et al.</i> 2013
Belize, Southwater Caye	10	5.09	0.97	4.12	census-based	forereef <i>Montastraea</i> zone	Perry <i>et al.</i> 2013
Belize, Columbus Reef	10	2.44	0.96	1.48	census-based	forereef <i>Montastraea</i> zone	Perry <i>et al.</i> 2013
Belize, Tobacco Reef	5	3.27	1.88	1.39	census-based	relict <i>A. palmata</i> zone	Perry <i>et al.</i> 2013
Belize, Columbus Reef	5	3.15	2.08	1.07	census-based	relict <i>A. palmata</i> zone	Perry <i>et al.</i> 2013
Belize, Tobacco Reef	10	1.72	1.22	0.50	census-based	forereef <i>Montastraea</i> zone	Perry <i>et al.</i> 2013
Belize, Southwater Caye	5	2.28	2.27	0.01	census-based	relict <i>A. palmata</i> zone	Perry <i>et al.</i> 2013
Grand Cayman, Spotts Reef	10	3.90	2.58	1.32	census-based	forereef <i>Montastraea</i> zone	Perry <i>et al.</i> 2013
Grand Cayman, Don Fosters Reef	10	4.91	3.67	1.24	census-based	forereef <i>Montastraea</i> zone	Perry <i>et al.</i> 2013
Grand Cayman, Babylon Reef	10	2.98	1.88	1.10	census-based	shallow forereef slope	Perry <i>et al.</i> 2013
Grand Cayman, Pallas Reef	5	1.94	2.08	-0.14	census-based	relict <i>A. palmata</i> zone	Perry <i>et al.</i> 2013
Grand Cayman, Don Fosters Reef	5	0.88	2.65	-1.77	census-based	shallow hardground	Perry <i>et al.</i> 2013

*=estimate based on sediment transport, **0.41 kg reincorporated; **=parrotfish estimates only; all Perry *et al* estimates based on average of 3-6 transects per site.

Table 3.1. Caribbean carbonate budget field studies attempted to date.

3.2 Chapter aims

The aim of this chapter was to produce a theoretical carbonate budget model that ultimately could be used to improve understanding of past and future changes in CaCO_3 productivity in Caribbean reefs (see Chapter 4 for model outputs). Prior to model creation an in-depth literature review was carried out, where data on rates of bioerosion and reef construction by the major Caribbean reef organisms under as many environmental conditions as possible were collated, along with abundances of these organisms at different time points in recent ecological history. This allowed full parameterisation of the model using empirical data, gathered from over 200 published studies; amounting to thousands of hours worth of dedicated research by coral ecologists and geomorphologists from the 1950's (when the advent of scuba first allowed detailed exploration of Caribbean reefs) to the present day. This chapter describes the development of the model: specifically its parameterisation (in section 3.3) and the algorithms employed in driving outputs (section 3.4) based on best available empirical data. Finally, model validation is outlined (section 3.5).

3.3 Model parameterisation

The carbonate budget algorithm required 115 input parameters (Table 3.2). A brief description of each model parameter ([1] to [115]) is listed in this section. Parameters, listed in **blue**, are assigned a number [*n*] that can be referenced back to Figure 3.2, and Table 3.2. Parameters are used to inform model algorithms, listed in the next section, *Defining model functions*, and are referred to by letters, e.g., [X] in the text.

[1] **SedRate**: *Terrigenous sedimentation rate* ($\text{mg cm}^{-3} \text{ day}^{-1}$). External sediment inputs are a key contributor to the carbonate budget (MacIntyre 1978), and Caribbean rates range from 0.3–37 $\text{mg cm}^{-2} \text{ day}^{-1}$ (Pastorek and Bilyard 1985, Mallela et al. 2004). High sedimentation rates ($> 10 \text{ mg cm}^{-2} \text{ day}^{-1}$) may actively inhibit coral reef framework growth (Rogers 1990) by reducing extension rates (Dodge et al. 1974, Torres and Morelock 2002), as well as often negatively affecting the bioeroding community (Fabricius 2005, Maldonado et al. 2008). Model arguments were taken from a Jamaican carbonate study (Mallela and Perry 2007), and correlate with the rate of framework infilling. Carbonate sedimentation (a product of reef carbonate production, including bioerosion and other benthically produced carbonate) is estimated separately (see section on **SedRetention**, [Y], under *Defining model functions*).

[2] **Arag**: *Aragonite saturation state* (Ω_{ar}). Aragonite saturation state (Ω_{ar}) is an essential model parameter as it influences calcification rates (Gattuso et al. 1998a, Langdon and Atkinson 2005), with reef communities able to thrive where Ω_{ar} ranges from 3.1 to 4.1 (Fine and Tchernov 2007). The seawater Ω_{ar} is a proxy for ocean acidification ($\Omega = [\text{Ca}^{2+}] [\text{CO}_3^{2-}] / \lambda$, where λ is the

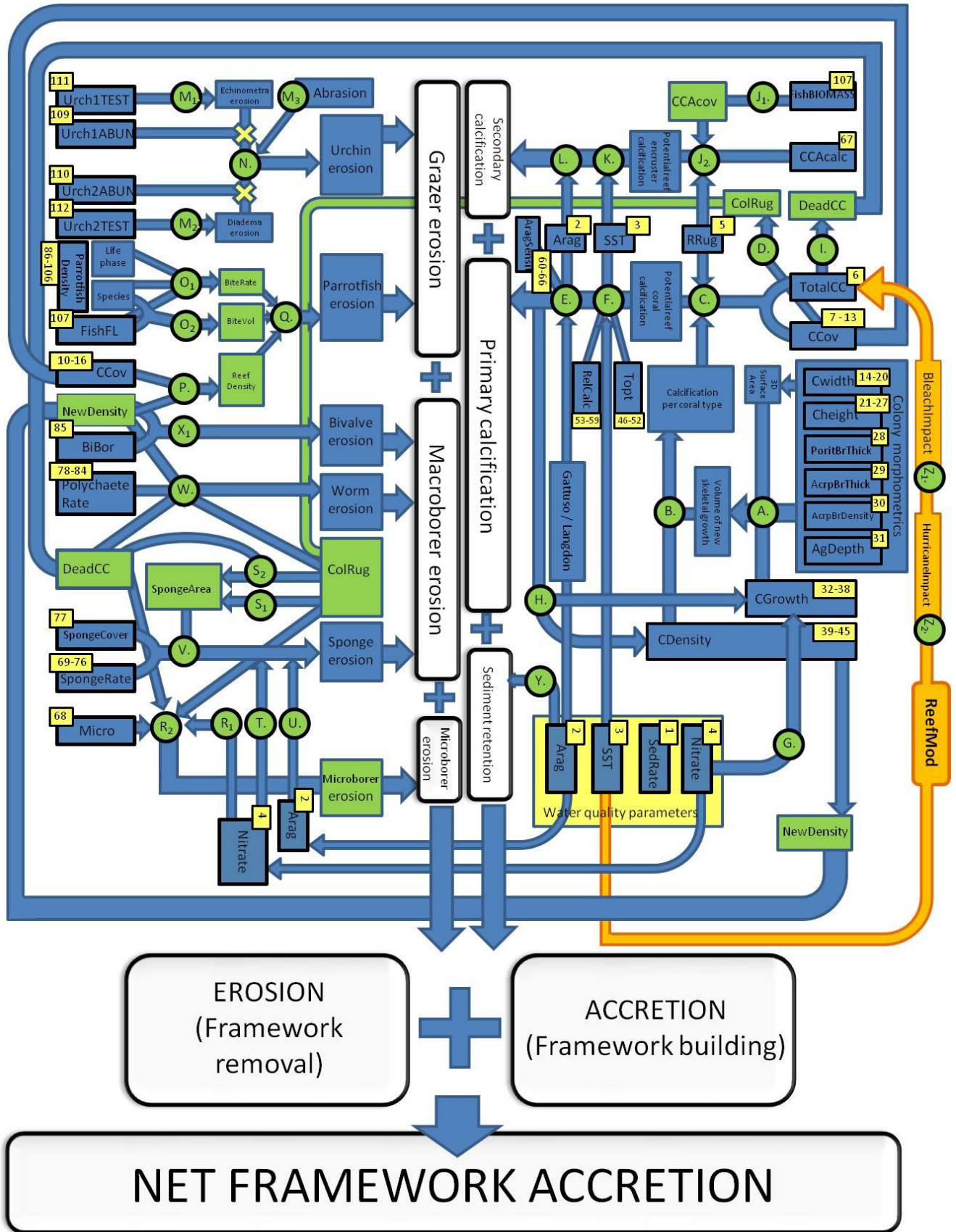


Figure 3.2. Data flow diagram representing the carbonate budget algorithm: Rectangular boxes with bold borders show inputs, while major process operations are represented by green circles, and arrows represent the flow of data. **Numbered boxes** (parameters, see *Model parameterisation*) and **letters** (relationships, see *Defining model relationships* section) can be related back to the coloured terms in the text.

Parameters		Code	Units	1		2		3		4		5		Future value	SD	Main data source	
				Value	SD	Value	SD	Value	SD	Value	SD	Value	SD				
1	Environmental variables	Sedimentation rate	SedRate	mg cm ⁻² day ⁻¹	7.1	2.4	7.1	2.4	7.1	2.4	17	4	17	4	17	4	Pastorok & Bilyard, 1985; Mallela & Perry, 2007
2		Aragonite saturation state	Arag	n/a	4.48	0.04	4.39	0.02	4.3	0.02	4.22	0.02	4.22	0.02	variable		HadGEM-2ES model AR5 data; Gledhill <i>et al.</i> 2008
3		Sea surface temperature	SST	°C	27.98	1.47	27.69	1.47	27.77	1.47	27.88	1.47	27.88	1.47	variable		HadGEM-2ES model AR5 data;
4		Nutrient availability	Nitrate	μmol l ⁻¹	0.24	0.12	0.24	0.12	0.3	0.12	0.4	0.12	0.4	0.12	0.4	0.12	Carreiro-Silva <i>et al.</i> 2005, Rogers 1990
5	Reef factors	Rugosity (Scale 1 - reef scale)	RRug	m ² m ⁻²	2.5	0.5	1.5	0.15	1.5	0.15	1.2	0.05	1.2	0.05	1.2	0.05	Alvarez-Filip <i>et al.</i> 2009; Holmes, 2008; Crabbe <i>et al.</i> 2009
6		Total living coral cover	TotalCC	%	55	5	55	5	30	2	25	2	10	2	25 or 10	0.02	Gardner <i>et al.</i> 2002; Hughes 1994; Stearn & Scoffin, 1977,
7		<i>Acropora</i> spp. living cover	Ccov [1]	relative %	45.7	30.1	45.7	30.1	8.9	10.6	8.9	10.6	8.9	10.6	8.9	10.6	Stearn & Scoffin (1977); Hughes, 1989; AGGRA data
8		<i>Montastraea</i> spp. living cover	Ccov [2]	relative %	36.4	29.4	36.4	29.4	40.3	21.2	40.3	21.2	40.3	21.2	40.3	21.2	Mallela & Perry 2007; Hughes, 1989; AGGRA database
9		<i>Agaricia</i> spp. living cover	Ccov [3]	relative %	2.1	1.1	2.1	1.1	14.1	11.6	14.1	11.6	14.1	11.6	14.1	11.6	Hughes, 1989; AGGRA database (Kramer, 2003)
10		<i>P. porites</i> living cover	Ccov [4]	relative %	4.7	3	4.7	3	7.2	6.3	7.2	6.3	7.2	6.3	7.2	6.3	Hughes, 1989; AGGRA database (Kramer, 2003)
11		<i>P. asteroides</i> living cover	Ccov [5]	relative %	3.2	1.9	3.2	1.9	10	6.8	10	6.8	10	6.8	10	6.8	Hughes, 1994; AGGRA database (Kramer, 2003)
12		<i>Diploria</i> spp. living cover	Ccov [6]	relative %	5	3.4	5	3.4	10.6	16.5	10.6	16.5	10.6	16.5	10.6	16.5	Hughes, 1994; AGGRA database (Kramer, 2003)
13		<i>Siderastrea</i> spp. living cover	Ccov [7]	relative %	2.9	2.2	2.9	2.2	8.9	7	8.9	7	8.9	7	8.9	7	Hughes, 1994; AGGRA database (Kramer, 2003)
14	Colony morphometrics	<i>Acropora</i> colony diameter	Cwidth [1]	cm	95.2	1	95.2	1	95.2	1	95.2	1	95.2	1	100	0	AGGRA database; Bythell <i>et al.</i> 2001; Courtney <i>et al.</i> 2007
15		<i>Montastraea</i> colony diameter	Cwidth [2]	cm	54.6	16	54.6	16	54.6	16	54.6	16	54.6	16	52.57	0	AGGRA database (query: Jamaican forereef)
16		<i>Agaricia</i> colony diameter	Cwidth [3]	cm	31.2	1	31.2	1	31.2	1	31.2	1	31.2	1	100	0	AGGRA database; Bythell <i>et al.</i> 2001
17		<i>P. porites</i> colony diameter	Cwidth [4]	cm	36.8	1	36.8	1	36.8	1	36.8	1	36.8	1	100	0	AGGRA database: Jamaican forereef); Courtney <i>et al.</i> 2007
18		<i>P. asteroides</i> diameter	Cwidth [5]	cm	24.2	6.95	24.2	6.95	24.2	6.95	24.2	6.95	24.2	6.95	26.26	0	AGGRA database); Bythell <i>et al.</i> 2001
19		<i>Diploria</i> colony diameter	Cwidth [6]	cm	35.9	11.38	35.9	11.38	35.9	11.38	35.9	11.38	35.9	11.38	35.8	0	Bythell <i>et al.</i> 2001 (mean size range of <i>Diploria</i>)
20		<i>Siderastrea</i> colony diameter	Cwidth [7]	cm	36.3	18.11	36.3	18.11	36.3	18.11	36.3	18.11	36.3	18.11	45.55	0	AGGRA database (query: Jamaican forereef)
21		<i>Acropora</i> colony height	Cheight [1]	cm	31.2	1	29.64	1	28.16	1	26.75	1	26.75	1	100	0	AGGRA database; Alvarez-Filip <i>et al.</i> 2009
22		<i>Montastraea</i> colony height	Cheight [2]	cm	44.9	13.57	42.66	13.57	40.52	13.57	38.49	13.57	38.49	13.57	46.39	0	AGGRA database; Alvarez-Filip <i>et al.</i> 2009
23		<i>Agaricia</i> colony height	Cheight [3]	cm	17.7	1	16.82	1	15.97	1	15.18	1	15.18	1	100	0	AGGRA database; Alvarez-Filip <i>et al.</i> 2009
24		<i>P. porites</i> colony height	Cheight [4]	cm	18.4	1	17.48	1	16.06	1	15.77	1	15.77	1	100	0	AGGRA database; Alvarez-Filip <i>et al.</i> 2009
25		<i>P. asteroides</i> colony height	Cheight [5]	cm	11.5	3.65	10.92	3.65	10.38	3.65	9.86	3.65	9.86	3.65	9.53	0	AGGRA database; Alvarez-Filip <i>et al.</i> 2009
26		<i>Diploria</i> colony height	Cheight [6]	cm	24.2	11.98	22.99	11.98	21.84	11.98	20.75	11.98	20.75	11.98	23.37	0	AGGRA database; Alvarez-Filip <i>et al.</i> 2009
27		<i>Siderastrea</i> colony height	Cheight [7]	cm	19.8	7.79	18.81	7.79	17.87	7.79	16.98	7.79	16.98	7.79	23.16	0	AGGRA database; Alvarez-Filip <i>et al.</i> 2009
28		<i>P. porites</i> branch diameter	PoritBrThick	cm	1.3	fixed	1.3	fixed	Unpublished data								
29		<i>Acropora</i> branch diameter	AcprBrThick	cm	1.62	0.51	1.62	0.51	1.62	0.51	1.62	0.51	1.62	0.51	1.62	0.51	Unpublished data
30	<i>Acropora</i> branch density	AcprBrDensity	branches m ⁻²	121.1	49.7	121.1	49.7	121.1	49.7	121.1	49.7	121.1	49.7	121.1	49.7	Stearn & Scoffin 1977	

Table 3.2. A list of the parameters for the carbonate budget model. Parameters are numbered to correspond with figure 3.2 and parameter descriptions (listed in blue) in the text. ‘Code’ is the Matlab reference for the parameter used in the text. ‘1’– ‘5’ denote values used in the five historical scenarios (parameter mean value and standard deviation used to inform each scenario) and ‘Future value’ the argument used in model projections. ‘Data source’ denotes the main papers from which the parameters were taken. More detailed explanations of each parameter (with reference number [n] and code) are in the text above.

Parameters (continued)		Code	Units	1		2		3		4		5		Future value	SD	Main data source			
				Value	SD	Value	SD	Value	SD	Value	SD	Value	SD						
31		<i>Agaricia</i> growth edge depth	AgDepth	cm	1	0.6	1	0.6	1	0.6	1	0.6	1	0.6	1	0.6	Estimate		
32	Coral growth rates	<i>Acropora</i> extension rate	Cgrowth [1]	cm year ⁻¹	3.25	0.36	3.25	0.36	3.25	0.36	3.25	0.36	3.25	0.36	10.78	1.6	Crabbe, 2009; Tunnicliffe 1983		
33		<i>Montastraea</i> extension rate	Cgrowth [2]	cm year ⁻¹	0.97	0.28	0.97	0.28	0.97	0.28	0.97	0.28	0.97	0.28	0.97	0.72	Stearn & Scoffin 1977; Davies 1983; Carricart-Ganivet 2000		
34		<i>Agaricia</i> extension rate	Cgrowth [3]	cm year ⁻¹	0.11	0.02	0.11	0.02	0.11	0.02	0.11	0.02	0.11	0.02	0.12	0.01	Huston 1985		
35		<i>P. porites</i> extension rate	Cgrowth [4]	cm year ⁻¹	1.23	0.36	1.23	0.36	1.23	0.36	1.23	0.36	1.23	0.36	3.77	0.31	Davies 1983; 1.23 (sd 0.7) Huston, 1985		
36		<i>P. asteroides</i> extension rate	Cgrowth [5]	cm year ⁻¹	0.32	0.11	0.32	0.11	0.32	0.11	0.32	0.11	0.32	0.11	0.32	0.15	Huston 1985; 0.88 (sd 0.74) Vaughn 1916 Florida		
37		<i>Diploria</i> linear extension rate	Cgrowth [6]	cm year ⁻¹	0.4	0.14	0.4	0.14	0.4	0.14	0.4	0.14	0.4	0.14	0.53	0.06	Edmunds 2007		
38		<i>Siderastrea</i> extension rate	Cgrowth [7]	cm year ⁻¹	0.55	0.2	0.55	0.2	0.55	0.2	0.55	0.2	0.55	0.2	0.55	0.2	Mallela & Perry 2007		
39	Coral density	<i>Acropora</i> skeletal density	Cdensity [1]	g cm ⁻³	1.7	0.09	1.7	0.09	1.7	0.09	1.7	0.09	1.7	0.09	1.7	0.09	1.7	0.09	Bruggeman 1994; Mallela & Perry 2007
40		<i>Montastraea</i> skeletal density	Cdensity [2]	g cm ⁻³	1.7	0.09	1.7	0.09	1.7	0.09	1.7	0.09	1.7	0.09	1.7	0.09	1.7	0.09	Carricart-Ganivet et al. 2000; Mallela & Perry 2007
41		<i>Agaricia</i> skeletal density	Cdensity [3]	g cm ⁻³	1.5	0.09	1.5	0.09	1.5	0.09	1.5	0.09	1.5	0.09	1.5	0.09	1.5	0.09	Mallela & Perry 2007
42		<i>P. porites</i> skeletal density	Cdensity [4]	g cm ⁻³	1.7	0.09	1.7	0.09	1.7	0.09	1.7	0.09	1.7	0.09	1.7	0.09	1.7	0.09	Mallela & Perry 2007
43		<i>P. asteroides</i> skeletal density	Cdensity [5]	g cm ⁻³	1.1	0.09	1.1	0.09	1.1	0.09	1.1	0.09	1.1	0.09	1.1	0.09	1.1	0.09	Mallela & Perry 2007
44		<i>Diploria</i> skeletal density	Cdensity [6]	g cm ⁻³	1.2	0.09	1.2	0.09	1.2	0.09	1.2	0.09	1.2	0.09	1.2	0.09	1.2	0.09	Mallela & Perry 2007
45		<i>Siderastrea</i> skeletal density	Cdensity [7]	g cm ⁻³	1.1	0.09	1.1	0.09	1.1	0.09	1.1	0.09	1.1	0.09	1.1	0.09	1.1	0.09	Mallela & Perry 2007
46	Coral calcification	Opt. temp. for <i>Acropora</i>	Topt [1]	°C	24	n/a	1985 temp.	0	Roberto Iglesias, pers. comm										
47		Opt. temp. for <i>Montastraea</i>	Topt [2]	°C	27.2	n/a	1985 temp	0	Roberto Iglesias, pers. comm										
48		Opt. temp. for <i>Agaricia</i>	Topt [3]	°C	24	n/a	1985 temp	0	Roberto Iglesias, pers. comm										
49		Opt. temp. for <i>P. porites</i>	Topt [4]	°C	24	n/a	1985 temp	0	Roberto Iglesias, pers. comm										
50		Opt. temp. for <i>P. asteroides</i>	Topt [5]	°C	23	n/a	1985 temp	0	Roberto Iglesias, pers. comm										
51		Opt. temp. for <i>Diploria</i>	Topt [6]	°C	24	n/a	1985 temp	0	Roberto Iglesias, pers. comm										
52		Opt. temp. for <i>Siderastrea</i>	Topt [7]	°C	24	n/a	1985 temp	0	Roberto Iglesias, pers. comm										
53		<i>Acropora</i> SD relative calc.	RelCalc [1]	°C	5.6	n/a	5.6	n/a	5.6	n/a	Roberto Iglesias, pers. comm								
54		<i>Montastraea</i> SD relative calc.	RelCalc [2]	°C	3.35	n/a	3.35	n/a	3.35	n/a	Roberto Iglesias, pers. comm; Carricart-Ganivet et al. 2000								
55		<i>Agaricia</i> SD relative calc.	RelCalc [3]	°C	5.6	n/a	5.6	n/a	5.6	n/a	Roberto Iglesias, pers. comm								
56		<i>P. porites</i> SD relative calc.	RelCalc [4]	°C	5.6	n/a	5.6	n/a	5.6	n/a	Roberto Iglesias, pers. comm, Lough & Barnes, 2000								
57		<i>P. asteroides</i> SD relative calc.	RelCalc [5]	°C	3.35	n/a	3.35	n/a	3.35	n/a	Roberto Iglesias, pers. comm								
58		<i>Diploria</i> SD relative calc.	RelCalc [6]	°C	3.35	n/a	3.35	n/a	3.35	n/a	Roberto Iglesias, pers. comm								
59	<i>Siderastrea</i> SD relative calc.	RelCalc [7]	°C	3.35	n/a	3.35	n/a	3.35	n/a	3.35	n/a	3.35	n/a	3.35	n/a	3.35	n/a	Roberto Iglesias, pers. comm	
60	<i>Acropora</i> OA sensitivity	AragSensit [1]	n/a	0.2	n/a	0.2	n/a	0.2	n/a	0.2	n/a	0.2	n/a	0.2	n/a	0.2	n/a	Chris Langdon, pers. comm	

Table 3.2. Section 2, parameters [31]–[60] (continued from previous page).

Parameters (continued)		Code	Units	1		2		3		4		5		Future value	SD	Main data source			
				Value	SD	Value	SD	Value	SD	Value	SD	Value	SD						
61	Coral calcification	<i>Montastraea</i> OA sensitivity	AragSensit [2]	n/a	0.11	n/a	0.11	n/a	0.11	n/a	0.11	n/a	0.11	n/a	0.11	n/a	Chris Langdon, pers. comm		
62		<i>Agaricia</i> OA sensitivity	AragSensit [3]	n/a	0.23	n/a	0.23	n/a	0.23	n/a	0.23	n/a	0.23	n/a	0.23	n/a	Chris Langdon, pers. comm		
63		<i>P. porites</i> OA sensitivity	AragSensit [4]	n/a	0.28	n/a	0.28	n/a	0.28	n/a	0.28	n/a	0.28	n/a	0.28	n/a	Chris Langdon, pers. comm		
64		<i>P. asteroides</i> OA sensitivity	AragSensit [5]	n/a	0.33	n/a	0.33	n/a	0.33	n/a	0.33	n/a	0.33	n/a	0.33	n/a	Albright <i>et al.</i> 2008;		
65		<i>Diploria</i> OA sensitivity	AragSensit [6]	n/a	0.28	n/a	0.28	n/a	0.28	n/a	0.28	n/a	0.28	n/a	0.28	n/a	Chris Langdon, pers. comm		
66		<i>Siderastrea</i> OA sensitivity	AragSensit [7]	n/a	0.44	n/a	0.44	n/a	0.44	n/a	0.44	n/a	0.44	n/a	0.44	n/a	Chris Langdon, pers. comm		
67		Encruster	CCA calcification rate	CCAcalc	kg CaCO ₃ m ⁻² yr ⁻¹	2.74	2.51	2.74	2.51	2.74	2.51	2.74	2.51	2.74	2.51	2.74	2.51	McClanachan <i>et al.</i> 2001; O'Leary 2010	
68	Micro	Microbioerosion rate	Micro	kg CaCO ₃ m ⁻² yr ⁻¹	0.47	0.4	0.47	0.4	0.47	0.4	0.47	0.4	0.47	0.4	0.47	0.4	Tribollet <i>et al.</i> 2002, 2006; Tudhope & Risk, 1985; Chazottes <i>et al.</i> 1995		
69	Macrobioerosion	Sponge erosion in <i>Acropora</i>	SpongeRate [1]	kg CaCO ₃ m ⁻² yr ⁻¹	0.35	fixed	0.2	fixed	0.2	fixed	0.2	fixed	0.2	fixed	0.2	fixed	Risk <i>et al.</i> 1995		
70		Sponge erosion: <i>Montastraea</i>	SpongeRate [2]	kg CaCO ₃ m ⁻² yr ⁻¹	0.38	fixed	0.38	fixed	0.38	fixed	0.38	fixed	0.38	fixed	0.38	fixed	0.38	fixed	Stearn & Scoffin 1977
71		Sponge erosion in <i>Agaricia</i>	SpongeRate [3]	kg CaCO ₃ m ⁻² yr ⁻¹	0.38	fixed	0.38	fixed	0.38	fixed	0.38	fixed	0.38	fixed	0.38	fixed	0.38	fixed	Stearn & Scoffin 1977
72		Sponge erosion in <i>P. porites</i>	SpongeRate [4]	kg CaCO ₃ m ⁻² yr ⁻¹	0.2	fixed	0.2	fixed	0.2	fixed	0.2	fixed	0.2	fixed	0.2	fixed	0.2	fixed	Stearn & Scoffin 1977
73		Sponge erosion in <i>P.asteroides</i>	SpongeRate [5]	kg CaCO ₃ m ⁻² yr ⁻¹	0.15	fixed	0.15	fixed	0.15	fixed	0.15	fixed	0.15	fixed	0.15	fixed	0.15	fixed	Stearn & Scoffin 1977
74		Sponge erosion in <i>Diploria</i>	SpongeRate [6]	kg CaCO ₃ m ⁻² yr ⁻¹	0.08	fixed	0.08	fixed	0.08	fixed	0.08	fixed	0.08	fixed	0.08	fixed	0.08	fixed	Derived from Stearn & Scoffin 1977
75		Sponge erosion in <i>Siderastrea</i>	SpongeRate [7]	kg CaCO ₃ m ⁻² yr ⁻¹	0.08	fixed	0.08	fixed	0.08	fixed	0.08	fixed	0.08	fixed	0.08	fixed	0.08	fixed	Stearn & Scoffin 1977
76		Sponge erosion in dead coral	SpongeRate[Dead]	kg CaCO ₃ m ⁻² yr ⁻¹	0.51	n/a	0.51	n/a	0.51	n/a	0.51	n/a	0.51	n/a	0.51	n/a	0.51	n/a	Stearn & Scoffin 1977
77		Bioeroding sponge cover	SpongeCover	%	10	fixed	10	fixed	10	fixed	10	fixed	10	fixed	10	fixed	10	fixed	Ward-Paige <i>et al.</i> 2005; Chiappone <i>et al.</i> 2007; Rützler 2002
78		Polychaetes in <i>Acropora</i>	PolychaeteRate [1]	cm ³ year ⁻¹	0	fixed	0	fixed	0	fixed	0	fixed	0	fixed	0	fixed	0	fixed	Hein and Risk 1975
79	Polychaetes in <i>Montastraea</i>	PolychaeteRate [2]	cm ³ year ⁻¹	2.23	fixed	2.23	fixed	2.23	fixed	2.23	fixed	2.23	fixed	2.23	fixed	2.23	fixed	Hein and Risk 1975	
80	Polychaetes in <i>Agaricia</i>	PolychaeteRate [3]	cm ³ year ⁻¹	0	fixed	0	fixed	0	fixed	0	fixed	0	fixed	0	fixed	0	fixed	Hein and Risk 1975	
81	Polychaetes in <i>P. porites</i>	PolychaeteRate [4]	cm ³ year ⁻¹	0	fixed	0	fixed	0	fixed	0	fixed	0	fixed	0	fixed	0	fixed	Hein and Risk 1975	
82	Polychaetes in <i>P.asteroides</i>	PolychaeteRate [5]	cm ³ year ⁻¹	0	fixed	0	fixed	0	fixed	0	fixed	0	fixed	0	fixed	0	fixed	Hein and Risk 1975	
83	Polychaetes in <i>Diploria</i>	PolychaeteRate [6]	cm ³ year ⁻¹	4.36	fixed	4.36	fixed	4.36	fixed	4.36	fixed	4.36	fixed	4.36	fixed	4.36	fixed	Hein and Risk 1975	
84	Polychaetes in <i>Siderastrea</i>	PolychaeteRate [7]	cm ³ year ⁻¹	3.43	fixed	3.43	fixed	3.43	fixed	3.43	fixed	3.43	fixed	3.43	fixed	3.43	fixed	Hein and Risk 1975	
85	Bivalve burrow volume	BiBor	cm ³	47	fixed	47	fixed	47	fixed	47	fixed	47	fixed	47	fixed	47	fixed	Perry 1998	
86	Grazing	<i>Sc. taeniopterus</i> (juv) density	pr juv	ind 100m ⁻²	10.12	0.001	0.76	0.001	0.76	0.001	0.76	0.001	0.76	0.001	variable	variable	Mumby <i>et al.</i> 2006		
87		<i>Sc. taeniopterus</i> (IP) density	pr ip	ind 100m ⁻²	3.93	0.001	2.35	0.001	2.35	0.001	2.35	0.001	2.35	0.001	variable	variable	Mumby <i>et al.</i> 2006		
88		<i>Sc. taeniopterus</i> (TP) density	pr tp	ind 100m ⁻²	0.95	0.001	0.91	0.001	0.91	0.001	0.91	0.001	0.91	0.001	variable	variable	Mumby <i>et al.</i> 2006		
89		<i>Scarus vetula</i> (juv) density	qu juv	ind 100m ⁻²	0	0.001	0	0.001	0	0.001	0	0.001	0	0.001	variable	variable	Mumby <i>et al.</i> 2006		
90		<i>Scarus vetula</i> (IP) density	qu ip	ind 100m ⁻²	2.5	0.001	2.97	0.001	2.97	0.001	2.97	0.001	2.97	0.001	variable	variable	Mumby <i>et al.</i> 2006		

Table 3.2. Section 3, parameters [61]–[90] (continued from previous page).

Parameters (continued)	Code	Units	1		2		3		4		5		Future value	SD	Main data source		
			Value	SD	Value	SD	Value	SD	Value	SD	Value	SD					
91	Grazing parameters	<i>Scarus vetula</i> (TP) density	qu tp	ind 100m ⁻²	1.19	0.001	0	0.001	0	0.001	0	0.001	0	0.001	variable	variable	Mumby <i>et al.</i> 2006
92		<i>Sp. aurofrenatum</i> (j) density	rb juv	ind 100m ⁻²	6.43	0.001	0.12	0.001	0.12	0.001	0.12	0.001	0.12	0.001	variable	variable	Mumby <i>et al.</i> 2006
93		<i>Sp. aurofrenatum</i> (IP) density	rb ip	ind 100m ⁻²	10.48	0.001	1.11	0.001	1.11	0.001	1.11	0.001	1.11	0.001	variable	variable	Mumby <i>et al.</i> 2006
94		<i>Sp. aurofrenatum</i> (TP) density	rb tp	ind 100m ⁻²	1.55	0.001	2.00	0.001	2.00	0.001	2.00	0.001	2.00	0.001	variable	variable	Mumby <i>et al.</i> 2006
95		<i>Sp. rubripinne</i> (juv) density	rp juv	ind 100m ⁻²	0	0.001	0	0.001	0	0.001	0	0.001	0	0.001	variable	variable	Mumby <i>et al.</i> 2006
96		<i>Sp. rubripinne</i> (IP) density	rp ip	ind 100m ⁻²	0	0.001	0	0.001	0	0.001	0	0.001	0	0.001	variable	variable	Mumby <i>et al.</i> 2006
97		<i>Sp. rubripinne</i> (TP) density	rp tp	ind 100m ⁻²	0.36	0.001	0	0.001	0	0.001	0	0.001	0	0.001	variable	variable	Mumby <i>et al.</i> 2006
98		<i>Sp. chrysopterym</i> (j) density	rt juv	ind 100m ⁻²	0	0.001	0	0.001	0	0.001	0	0.001	0	0.001	variable	variable	Mumby <i>et al.</i> 2006
99		<i>Sp. chrysopterym</i> (IP) density	rt ip	ind 100m ⁻²	0.24	0.001	0	0.001	0	0.001	0	0.001	0	0.001	variable	variable	Mumby <i>et al.</i> 2006
100		<i>Sp. chrysopterym</i> (TP) density	rt tp	ind 100m ⁻²	0.71	0.001	0	0.001	0	0.001	0	0.001	0	0.001	variable	variable	Mumby <i>et al.</i> 2006
101		<i>Sparisoma viride</i> (j) density	sp juv	ind 100m ⁻²	6.90	0.001	0.20	0.001	0.20	0.001	0.20	0.001	0.20	0.001	variable	variable	Mumby <i>et al.</i> 2006
102		<i>Sparisoma viride</i> (IP) density	sp ip	ind 100m ⁻²	7.74	0.001	2.22	0.001	2.22	0.001	2.22	0.001	2.22	0.001	variable	variable	Mumby <i>et al.</i> 2006
103		<i>Sparisoma viride</i> (TP) density	sp tp	ind 100m ⁻²	1.55	0.001	0.65	0.001	0.65	0.001	0.65	0.001	0.65	0.001	variable	variable	Mumby <i>et al.</i> 2006
104		<i>Scarus iserti</i> (juv) density	st juv	ind 100m ⁻²	0	0.001	23.0	0.001	23.0	0.001	23.0	0.001	23.0	0.001	variable	variable	Mumby <i>et al.</i> 2006
105		<i>Scarus iserti</i> (IP) density	st ip	ind 100m ⁻²	0	0.001	0	0.001	0	0.001	0	0.001	0	0.001	variable	variable	Mumby <i>et al.</i> 2006
106	<i>Scarus iserti</i> (TP) density	st tp	ind 100m ⁻²	0	0.001	2.23	0.001	2.23	0.001	2.23	0.001	2.23	0.001	variable	variable	Mumby <i>et al.</i> 2006	
107	Parrotfish size (fork length)	FishFL	ind 100m ⁻²	n/a	n/a	n/a	n/a	n/a	n/a	n/a	n/a	n/a	n/a	variable	variable	Kramer, 2003; Bruggeman 1994; Paddock <i>et al.</i> 2009	
108	Damselfish territories	Damself	%	0.02	fixed	0.02	fixed	0.02	fixed	0.02	fixed	0.02	fixed	0.02	fixed	Eakin 1988, 1991, 1992; Zubia & Peyrot-Clausade, 2001	
109	<i>Echinometra</i> sp. density	Urch1ABUN	ind m ⁻²	25.5	7	25.5	7.5	4.5	3.1	4.5	3.1	0.73	0.1	0.73	0.1	Sammarco, 1982; Ogden, 1977; Hughes <i>et al.</i> 1987; Hoskin & Reed 1984	
110	<i>Diadema</i> sp. density	Urch2ABUN	ind m ⁻²	3.2	1.36	12.5	4.02	0.09	0.005	0.09	0.001	0.029	0.001	0.029	0.001	Hay, 1984; Bak <i>et al.</i> 1984; Hughes, 1987; Hughes, 1994; Kramer, 2003	
111	<i>Echinometra</i> sp. test size	Urch1TEST	mm	30	2	30	2	30	2	30	2	30	2	30	2	Ogden, 1977;	
112	<i>Diadema</i> sp. test size	Urch2TEST	mm	36	2.32	30	2.32	60.4	2.32	60.4	2.32	60.4	2.3	60.4	2.3	Leviton, 1988; Stearn & Scoffin 1977	
113	<i>Echinometra</i> cavity volume	volBurrow	cm ³	72	fixed	72	fixed	72	fixed	72	fixed	72	fixed	72	fixed	Hoskin & Reed 1984	
114	<i>Echinometra</i> cavity build time	tBurrow	years	2.9	fixed	2.9	fixed	2.9	fixed	2.9	fixed	2.9	fixed	2.9	fixed	Hoskin & Reed 1984	
115	Hurricane return time	tHurricane	years	n/a	n/a	n/a	n/a	n/a	n/a	n/a	n/a	n/a	n/a	17	fixed	Edwards <i>et al.</i> .2011; Mumby, unpublished data	

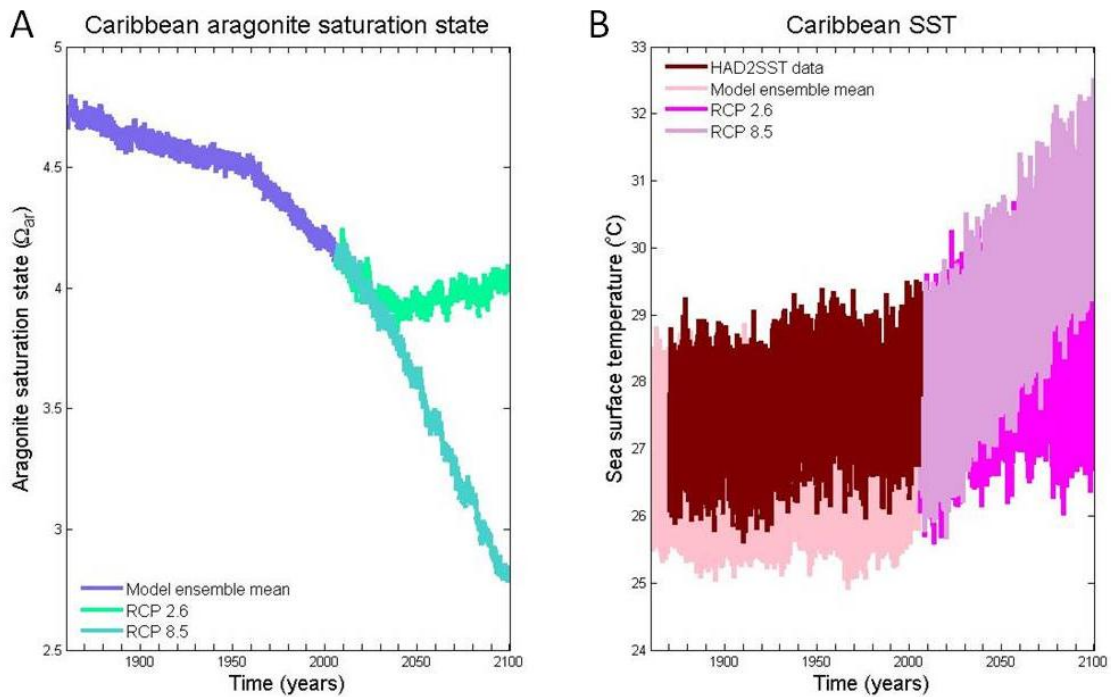
Table 3.2. Section 4, parameters [91]–[115] (continued from previous page).

solubility coefficient for different dissolved forms of CaCO_3). Because Ca^{2+} is abundant in seawater, changes in Ω tend to be controlled by variations in the carbonate ion CO_3^{2-} concentrations, which are affected by dissolved CO_2 . Surface waters exhibiting $\Omega_{\text{ar}} > 4$ have previously been described as ‘optimal’ for reef growth, 3.5–4.0 as ‘adequate’, 3.0–3.5 as ‘low’, and <3.0 considered ‘extremely marginal’, although calcification still occurs at marginal carbonate saturation (Guinotte et al. 2003). Caribbean Ω_{ar} is currently falling at a rate of $-0.012 \pm 0.001 \Omega_{\text{ar}} \text{ yr}^{-1}$ ($r^2 = 0.97$) (Gledhill et al. 2008), and this is reflected in a range of **Arag** values being used in present scenarios. Historical arguments for scenarios 1 to 5 (Chapter 4, Fig. 4.1) were derived from HadGEM–2ES earth system model (1800–2006) from the Met Office (Figure 3.3). Monthly saturation state data averaged across the Caribbean area were derived from corrected SST values (see **SST**): Ω_{ar} shows seasonal and spatial variability (Gledhill et al. 2008), and was validated using Hawaii Ocean Time Series and Bermuda Atlantic Time Series data. Future scenarios were populated with **Arag** values driven by either HadGEM–2ES RCP 2.6 or RCP 8.5 models (Jones et al. 2011).

[3] **SST**: *Mean monthly sea surface temperature ($^{\circ}\text{C}$)*. Sea surface temperature (SST) determines coral and secondary encruster calcification in the model (see sections [F] and [L] under *Defining model functions*), as well as mortality through bleaching events in future scenarios (see [Z]). HADSST2 archived monthly SST data for the Caribbean region (1860–2006) were retrieved and compared to AR5 model data. Model and observational data were time-averaged over the period 1970–2000, for which observations are known to be robust. A difference was calculated to provide the offset, which was then applied to the model data for the same region. Once corrected, annual AR5 model values for the past were used to populate the historical scenarios (averaged for each time period, Fig. 3.3), as well as to calculate **Arag**. Annual SST data from RCP 2.6 and RCP 8.5 were used to inform future models, with monthly data used to predict bleaching events.

[4] **Nitrate**: *Nutrient availability ($\mu\text{mol l}^{-1}$)*. Nitrate level was chosen as a proxy for nutrient pollution or eutrophication on reefs. Parameter values ranging from low ($0.24 \mu\text{mol l}^{-1}$) to high ($0.46 \mu\text{mol l}^{-1}$) were taken from the literature (Carreiro-Silva et al. 2005). Healthy fore-reefs habitually thrive under oligotrophic conditions (nitrate concentrations typically $0.1 - 0.5 \mu\text{mol l}^{-1}$; ammonium $0.2-0.5 \mu\text{mol l}^{-1}$ and phosphorus $< 0.3 \mu\text{mol l}^{-1}$) (Ferrier-Pagés et al. 2000). Overall, eutrophication is likely to be highly influential to the balance between carbonate production and destruction (Hallock and Schlager 1986). Calcification is mostly – but not always (Anthony 1999a) – negatively influenced by eutrophication, reducing coral skeletal growth rates, e.g., indirectly by shading through algal blooms (Kinsey and Davis 1979, Hallock 1988, Marubini and Davies 1996, Ferrier-Pagés et al. 2000), see [G] in *Defining model relationships* section. This effect of stunted growth is expected to be enhanced by increased bioerosion: many macrobioeroders are filter feeders with increased fitness in more eutrophic

conditions, such as molluscs and sponges (Highsmith 1981, Rose and Risk 1985, Hallock 1988, Holmes 1997, Ward-Paige et al. 2005), see [R], and microendoliths are enhanced as well from the occurrence of otherwise limited nutrients (Carreiro-Silva et al. 2005), [T].



Decade	Historic scenario	Ω_{ar} corrected model average	SST (°C) corrected model average	Nitrogen ($\mu\text{mol l}^{-1}$) model average
1960's	1	4.46 ± 0.029	27.59 ± 0.19	0.029 ± 0.0029
1970's	2	4.39 ± 0.018	27.64 ± 0.16	0.027 ± 0.0017
1980's	3	4.31 ± 0.023	27.75 ± 0.08	0.029 ± 0.0016
1990's	4	4.24 ± 0.015	27.90 ± 0.21	0.027 ± 0.0030
2000's	5	4.20 ± 0.020	28.30 ± 0.06	0.030 ± 0.0046

Figure 3.3. Monthly aragonite saturation state, Ω_{ar} (A) and sea surface temperature, SST (B) AR5 model data for the wider Caribbean area, showing historical data (1860–2006), and for both, the RCP 2.6 and RCP 8.5 scenarios. These data were used to drive the carbonate budget model toward the end of the century. Decadal averages (table) were used to inform historical scenarios (1a–5d).

[5] **RRug:** *Scale 1 (reef scale) rugosity ($m^2 m^{-2}$)*. Early budget calculations failed to incorporate macro relief (Fig. 3.4A), leading to budget underestimation (Odum and Odum 1955, Sadd 1984). Later, ‘correction factors’ were introduced in order to generate more realistic estimates (reviewed by Holmes, 2008). The approximation of gross reef morphology is now acknowledged to be important in calculating total reef carbonate growth (Dahl 1973), and published reef scale rugosity values are widely available (Holmes 2008). Arguments for historic scenarios 1 to 5 follow the documented decline of Caribbean reef architectural complexity, attributed to acroporid loss and the functional disappearance of *Diadema* (Alvarez-Filip et al. 2009). Values used to determine suitable parameters for the present model corresponded with

those found for specific Caribbean reefs (Dahl 1973, Klumpp and Polunin 1989, Holmes 2008, Crabbe 2009).

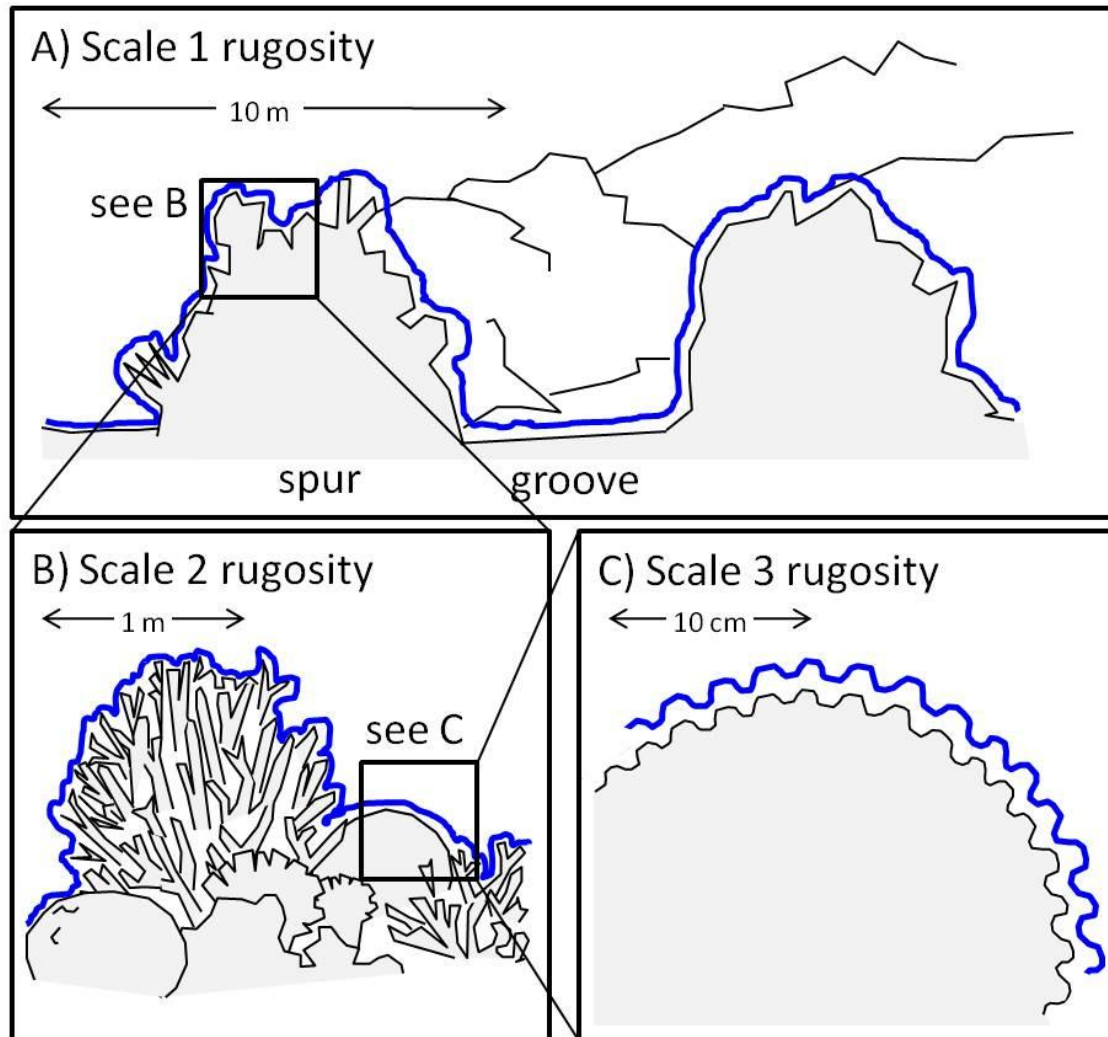


Figure 3.4. Three scales of rugosity (after Dahl 1973, diagram based on Stearn et al. 1977). **A)** Scale 1, or reef scale, rugosity – in the model parameter [5], **RRug**; **B)** Scale 2, or colony scale, rugosity (generated by function [D], **ColRug**) and **C)** Scale 3, or microscale, rugosity, not included in the model.

[6] **TotalCC**: *Total living coral cover (%)*. Coral CaCO_3 production is the most influential component in most carbonate budgets, responsible in some cases for 97% of net carbonate production (Sadd 1984, Mallela and Perry 2007). Percentage cover arguments for historic scenarios 1–5 were selected from Gardner’s 2003 meta-analysis on Caribbean coral cover (Gardner et al. 2003), supported by other studies (Hughes 1994, Wilkinson 2004). In future scenarios, **TotalCC** is set at either 25% (‘high’) or 10% (‘low’) for the year 2000, and is determined in subsequent steps by coral mortality in the preceding time phase.

[7-13] **CCov**: *Relative coral cover/community composition (%)*. Seven representative coral taxa were selected based on coral cover data from Belize (Ferrari et al. 2012), Jamaica (Hughes 1994) and the Western Atlantic (Lang et al. 2010). A mix of commonly occurring corals were

chosen and classified according to their reproductive strategies: brooders with high recruitment and mortality (the genera *Agaricia*, *Siderastrea*, and the species *Porites asteroides*); broadcasters with low recruitment and mortality (*Montastraea* and *Diploria* spp.), and those relying primarily on asexual reproduction (*Acropora* spp., *Porites porites*). Community composition in the Caribbean has shifted in recent decades (Allard 1994, Green et al. 2008), and the **CCov** parameter was modified between scenarios to reflect these changes. In early scenarios (1–2), framework building corals of the genera *Acropora* and *Montastraea* dominate the reefs (46% and 36% of total coral community), while in scenarios 3–5 and future scenarios *Acropora* and *Montastraea* spp. populations declined, while non-framework building corals such as *Agaricia* and *Porites* spp. increased their relative abundance (30% and 28%).

[14–20] **Cwidth**: *Mean colony diameter for each coral taxon (cm)*. Colony diameter helps to determine colony size and thus area over which skeletal growth can occur (Bak 1976). Inclusion of colony dimensions in the model allows accurate surface area (SA) estimation of several model taxa (*Diploria* and *Montastraea* spp.) using log-linear models (Courtney et al. 2007) (rather than the traditional, but less precise, scaling factors) – which influence both bioerosion and accretion (Bak and Meesters 1998) see section [A] and [D] in *Defining model functions*. The models were shown to generate more accurate SA measurements than several other techniques and could presently be extended to cover *Siderastrea* spp. and *P. asteroides*. However, log linear models cannot be applied accurately to *Acropora* spp., *Agaricia* spp. or *P. porites* (Holmes 2008), therefore simple geometric techniques using alternative parameters (see [28]–[31]) were adopted for these taxa (Dahl 1973), see section [A]. **Cwidth** mean and variance parameters for all remaining model coral taxa were populated using the report of an AGGRA database query for Jamaican fore-reef colonies (Kramer 2003), and supported by data collected from Belize in 2009 (Ferrari et al. 2012). Where more than one species existed, datasets were combined. The mean and stdev **Cwidth** values assigned to each species (Table 3.2) and were fixed across historical scenarios.

[21–27] **Cheight**: *Mean colony height for each coral taxon (cm)*. Inclusion of a second colony dimension increased the accuracy of log-linear models, from $r^2=0.95$ to $r^2=0.99$ (see [A]) (Courtney et al. 2007). It also provided a means by which height of colonies above the reef can be reduced for modelling purposes, e.g., to simulate hurricane activity. **Cheight** parameters were generated in the same way as **Cwidth**. Arguments for historic scenarios 1–5 allowed for a conservative 10% decline in **Cheight** over time (Alvarez-Filip et al. 2009).

[28] **PoritBrThick**: **P. porites* branch diameter (cm)*. For branching model coral taxa, growth and accumulation of CaCO_3 are almost entirely restricted to the tips (Stearn et al. 1977). Therefore neither planimetric area nor SA of living tissue are suitable proxies for area of growth. A mean value for branch thickness was required for estimation of the cylindrical volume of growing tips, which was then scaled up by colony branch density to give a measure

of carbonate accumulation. Branch diameter values for *P. porites* were taken from field measurements for a published carbonate budget (Stearn et al. 1977).

[29] **AcrpBrThick**: *Acropora cervicornis* branch diameter (cm). (See above). *Acropora* spp. branch thickness values were taken from field measurements collected at Glovers Reef, Belize ($x=1.62$ cm; $stdev = 0.51$, $n=47$).

[30] **AcrpBrDensity**: Mean abundance of *Acropora* branches per unit area (branches m^{-2}). Mean *Acropora* branch ‘density’ (number of growing branch tips per m^2 of living *Acropora* spp.) was estimated by analysis of 10×10 m photoquadrat data in Vidana (MSEL, University of Exeter) from Glovers Reef, Belize in 2005 (121 branches m^{-2} , $SE=0.11$, $n=21$). No relationship was found between abundance ($r^2=0.005$) and colony size ($r^2=0.03$), or colony branch number.

[31] **AgDepth**: Colony thickness at growing edge of encrusting *Agaricia* sp. (cm). A parameter for mean thickness (cm) at the growing edge (cm) of the colony allows estimation of volume of new platy *Agaricia* skeletal growth. Our modelled *Agaricia* is our only representative of an encrusting colony, and carbonate accumulation is estimated assuming horizontal extension of the colony rather than growth strategies as in other corals: branch extension (*Acropora*), upward growth (*P. porites*) or outward growth over a hemispherical area (*Diploria*, *Siderastrea*), see [A]. Inclusion of the **AgDepth** parameter adds a morphometric element to the calculation, allowing the budget for *Agaricia* to vary with colony size, even when growth rate and density do not.

[32-38] **CGrowth**: Linear extension rate (LER) for each coral taxon ($cm\ year^{-1}$). Coral skeletal extension is widely used as an environmental proxy (Carricart-Ganivet 2011); the decline in coral LERs over the last 30 years is well documented both in the Pacific and North Atlantic Oceans (Bak et al. 2009, Manzello 2010). Skeletal extension rate is dependent on available energy for active deposition of calcareous material (i.e., calcification rate) and the way in which this material is used to construct the skeleton (density and porosity) (Carricart-Ganivet and Merino 2001). Inter-specific variation in LER is large, and some species also demonstrate individual variation (e.g., reported LER values for *Acropora cervicornis* ranged from 4.5 to 26 $cm\ yr^{-1}$; Lewis et al. 1968, Davies 1983). LER values previously used in Jamaican carbonate budgets were taken from the literature to parameterise the model (Huston 1985). Although input arguments remained fixed across scenarios, during model runtime LER was assumed to be altered by seawater nutrient level, carbonate saturation and temperature (see *Defining model function* section, [E–G]).

[39-45] **CDensity**: Bulk skeletal density for each coral taxon ($g\ cm^{-3}$). The **CDensity** parameter describes meso-architecture of the skeletal volume including the porosity, as opposed to skeletal micro density (Bucher et al. 1998). Bulk skeletal density varies threefold among coral species

(Hughes 1987) and demonstrates limited intra-specific geographic variation (Carricart-Ganivet et al. 2000), but may vary with exposure, turbidity (Hallock 1988), depth (Baker and Weber 1975), nutrient enrichment (Scoffin et al. 1989, Risk and Sammarco 1991), Ω_{ar} or SST (Krief et al. 2010). Species specific bulk density means and variances were gleaned from the literature and assigned to the seven model taxa (Bruggeman 1994, Carricart-Ganivet et al. 2000, Mallela and Perry 2007). As well as being critical in estimating calcification, coral density may influence erosion rates (Carricart-Ganivet 2007), with porosity affecting resistance to mechanical damage (Scott and Risk 1988, Bucher et al. 1998), boring (Highsmith 1981, Schönberg 2002) and grazing activity (Bruggeman et al. 1996). Despite its importance, early budget attempts failed to include species specific density estimates (Chave et al. 1972); or broad assumptions were made (Land 1974), with critical impacts on budget estimations. Evidence suggests Pacific coral densities have declined over recent timescales at some sites (De'ath et al. 2009), however this has not been confirmed in Caribbean corals, and as a result arguments remain fixed throughout scenarios 1–5. During future simulations **CDensity** values have been designed to respond to changes in calcification rates (see [H]).

[46-52] **Topt**: *Optimal temperature for coral growth (°C)*. The model assumes that corals are acclimated to a specific temperature (**Topt**), an assumption which determines the effect of **SST** on calcification rates. Evidence suggests that optimal temperature for coral growth lies below the normal peak summer temperatures (Jokiel and Coles 1977, Marshall and Clode 2004). **Topt** data for *Montastraea faveolata* and *P. asteroides* from the Mexican Caribbean were adopted (Carricart-Ganivet 2004, Carricart-Ganivet et al. 2012). For the future model runs, **Topt** is given as the SST at the start of the time series, or in 1985.

[53-59] **sdRelCalc**: *Sensitivity of coral calcification to SST*. This parameter describes the sensitivity of coral calcification to temperature change, by defining the width of the temperature response curve (Fig. 3.5). Values extrapolated from *Montastraea annularis* (Carricart-Ganivet et al. 2000) and *Porites* spp. (Lough 2008) were applied to model taxa – as the relationship has only been characterised for these two species (Carricart-Ganivet et al. 2012).

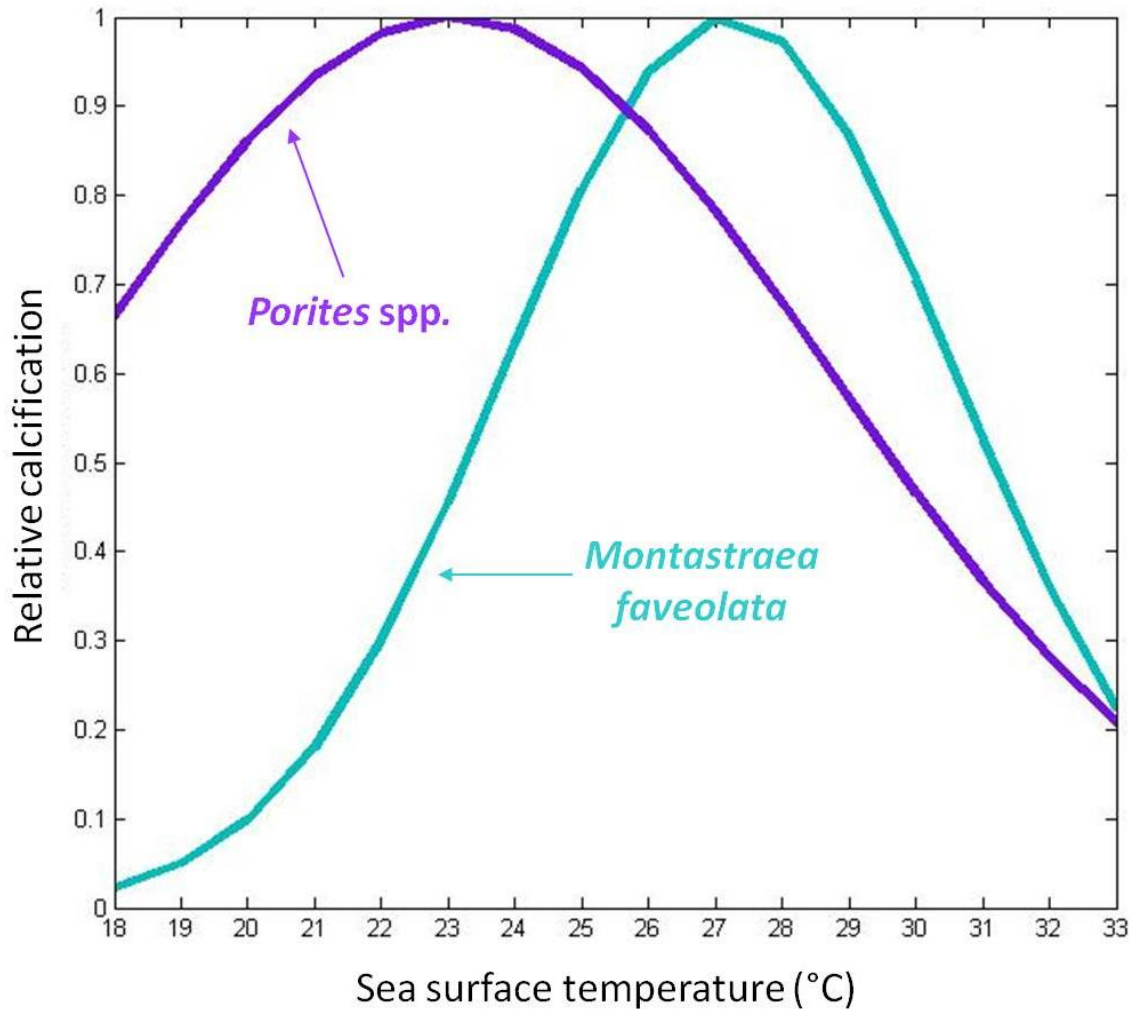


Figure 3.5. Gaussian response of coral calcification to changing sea surface temperature, employed to estimate community CaCO_3 production in the carbonate budget model.

[60-66] **AragSensit:** *Species specific sensitivity to changes in Ω_{ar} .* Coral calcification is a biogenic activity, suggesting species are likely to exhibit differential sensitivity to changes in factors such as Ω_{ar} (Marubini et al. 2003). Unpublished data on the calcification responses of five Caribbean coral species to changing seawater alkalinity enabled the derivation of different equations to describe the response of each model species (Fig. 3.6), e.g., *M. faveolata* proved fairly insensitive (slope = 0.11), while *Siderastrea radians* was more sensitive (slope = 0.44). This corresponds to empirical data from Chinchorro Bank, Mexico that showed little measurable effect of Ω_{ar} on *M. faveolata* and a mild effect on *P. asteroides* (Carricart-Ganivet et al. 2012). The derived equations are used to inform the applied linear reduction in calcification in response to changing Ω_{ar} . We assumed that at Ω_{ar} 4.6 all corals demonstrate a relative calcification of 1 (Fig. 3.6). When the model is run using the alternative ('Gattuso') calcification algorithm (curved rather than linear response between Ω_{ar} and calcification; Gattuso et al. 1998a), lack of published data means all coral taxa are treated identically.

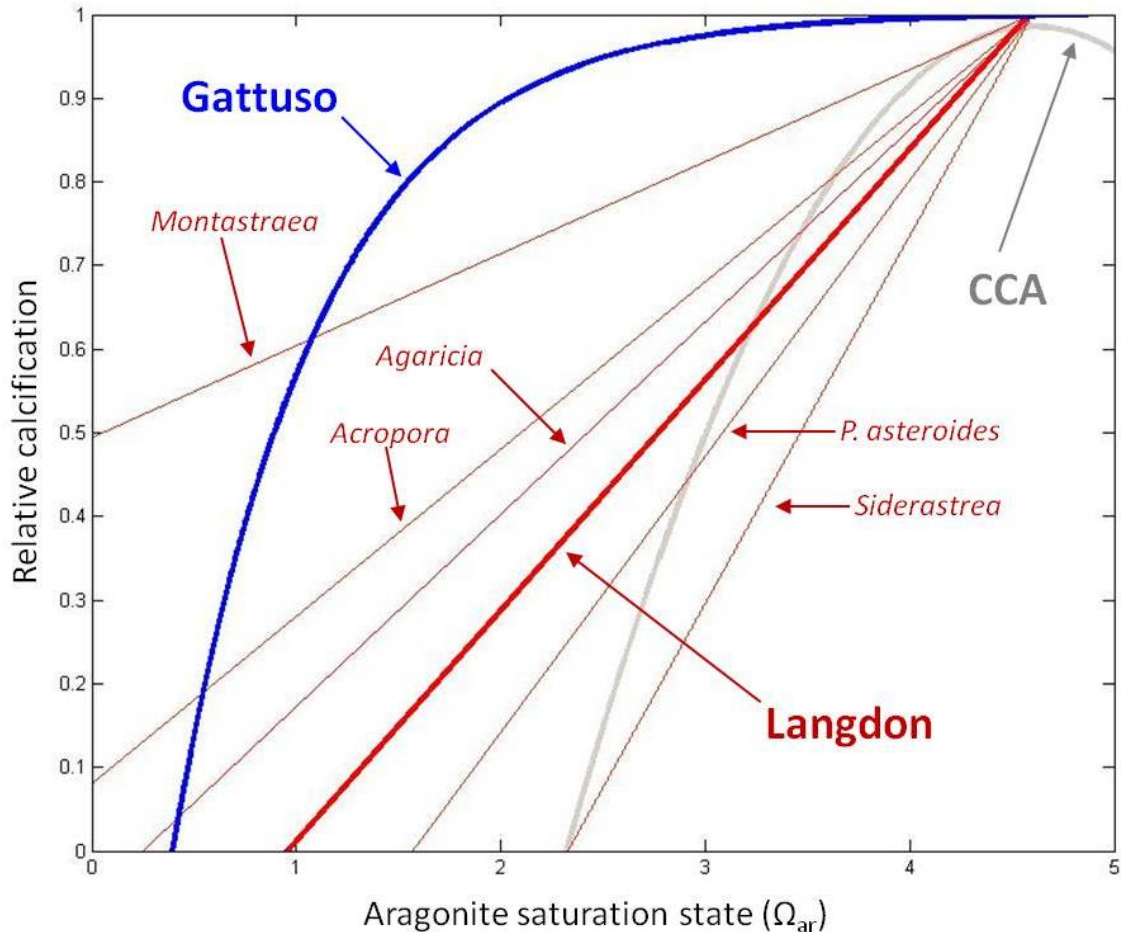


Figure 3.6: Aragonite saturation state, Ω_{ar} , vs. coral reef community calcification. Comparison between the main two response curves presently described (red, linear (Langdon et al. 2000); blue, non-linear (Gattuso et al. 1998a)), used to define the relationship between aragonite saturation state (Ω_{ar}) and coral community calcification in the model (see [E] in *Defining model functions* section). The Langdon relationship is employed as default: linear variations are adopted for different coral species (thin red lines). *Diploria* is assumed to behave similarly to *Siderastrea*, and *P. porites* to *Agaricia*. See Fig. 4.4 (Chapter 4) for effect of application of the Gattuso (curved) relationship on model outcomes. Grey curve shows the relationship between Ω_{ar} and CCA the described *Porolithon onkodes* response to ocean acidification (Anthony et al. 2008), see [K].

[67] **CCAcalc:** Carbonate production rate of secondary framework builders ($\text{kg CaCO}_3 \text{ m}^{-2} \text{ year}^{-1}$). Previous carbonate budgets have frequently overlooked the contribution of secondary framework builders due to the difficulty associated with measuring CaCO_3 production rates (Conand et al. 1997, Edinger et al. 2000). Disentangling calcification rates of individual taxa is associated with errors, but the **CCAcalc** parameter aims to describe the combined carbonate production rate of crustose coralline algae (CCA), encrusting foraminifera, bryozoans and other encrusting communities which colonise the substrate (Perry 1999) – see also [J]. Published CCA calcification rates vary widely, and a mean value of $2.74 \text{ kg m}^{-2} \text{ year}^{-1}$ (SD 2.51) was derived from a range of Caribbean estimates (Adey and Vassar 1975, Martindale 1976, Stearn and Scoffin 1977, Stearn et al. 1977, Hubbard et al. 1990, Friele and Hillis 1997). Input arguments are fixed across scenarios, although susceptible to changes in carbonate chemistry during runtime (see section [K]).

[68] **Micro**: *Microbioerosion rate* ($\text{kg CaCO}_3 \text{ m}^{-2} \text{ yr}^{-1}$). Worldwide estimations of community microbioerosion by fungi, bacteria and algae range from ~ 0.02 to $\sim 1.34 \text{ kg m}^{-2} \text{ yr}^{-1}$ (Kiene 1997, Tribollet et al. 2002). A mean of five estimates taken from the Bahamas, Belize and Jamaica, gave a value of $0.47 (\pm 0.44) \text{ kg m}^{-2} \text{ yr}^{-1}$ that was fixed throughout scenarios (Hoskin et al. 1986, Vogel et al. 2000, Carreiro-Silva et al. 2005, Mallela and Perry 2007, Carreiro-Silva et al. 2009). Microbioerosion rates are, in many cases, strongly influenced by availability of light (Vogel et al. 2000), but also affected by substrate type (Vogel et al. 2000), ocean acidification (Tribollet et al. 2009) and in cases nutrient level (Carreiro-Silva et al. 2005), and this is accounted for in the model (see *Defining model functions* section, [R]).

[69-75; 76] **SpongeRate**: *Clionaid bioerosion rates in different materials* ($\text{kg CaCO}_3 \text{ m}^{-2} \text{ yr}^{-1}$). Boring sponges are usually the dominant internal bioeroders on Caribbean reefs (Goreau 1963, Hein and Risk 1975, MacGeachy and Stearn 1976, Highsmith et al. 1983, Perry 1998). In cases they may be responsible for $> 90\%$ of all macrobioerosion (Stearn and Scoffin 1977, Mallela and Perry 2007), sometimes eroding faster than local skeletogenesis (Hein and Risk 1975, Hudson 1977, Nava and Carballo 2008). Being highly diverse (Pulitzer-Finali 1986, Van Soest 2001) and abundant (Perry 1998) they are an important component of the fore-reef macroboring community, and bioerosion rates are a crucial model parameter. Boring rates are substrate dependant (Neumann 1966): they are far more prevalent and rapid bioeroders in dead coral as well as displaying varying bioerosion rates according to bulk density of corals. A single erosion rate (**SpongeRate[Dead]**) for the sum of a local sponge community inhabiting dead amorphous framework was acquired from Stearn and Scoffin's budget (Stearn and Scoffin 1977), and applied to estimate the bulk of reef bioerosion. In addition, slightly lower boring values for specific Caribbean corals skeletons (**SpongeRate**) were adopted from the same study (Stearn and Scoffin 1977), where boring was calculated by planimetric area, taking into account reef topography, and also accounting for substrate bias. Data were unavailable for two of the seven modelled species: given the similar skeletal morphology and density for *Diploria*, an identical rate as for *Siderastrea* was adopted while **SpongeRate** values for *Acropora* were derived from Great Barrier Reef (GBR) *Acropora* which are known to be two to three times that of *Porites* (Risk et al. 1995). All rates used were long term averages, and so account for reported faster initial penetration during first 6 months (Rützler 1975).

[77] **SpongeCover**: *Clionaid cover* (% cover). Evidence of increasing bioeroding sponge abundance in the Caribbean has in part been linked to coral mortality and increased area for settlement (Glynn 1997, Williams et al. 1999, Rützler 2002, López-Victoria and Zea 2005, Ward-Paige et al. 2005, Schönberg and Ortiz 2008), hence a parameter expressing such trends becomes essential. As only a proportion of living and dead colonies will be infested by bioeroding sponges, a sponge cover value was assigned to the model reef to provide a more conservative estimate of sponge bioerosion (unit: percentage cover). Living *Cliona* spp. cover

has been reported as 1.8–6.8% in Belize (Rützler 2002), and 4.1–34.9% and 7.6–10.4% in Florida (Ward-Paige et al. 2005, Chiappone et al. 2007). A 10% value for infestation of available dead substrate (**DeadCC**) was assigned.

[78-84] **PolychaeteRate**: *Rate of polychaete bioerosion in various substrates ($\text{cm}^{-2} \text{CaCO}_3 \text{yr}^{-1}$)*. Bioeroding worms (polychaetes and sipunculans) occur exclusively in dead coral (Hein and Risk 1975, Peyrot-Clausade et al. 1992, Hutchings 2008) and represent only a minor component of the Caribbean macroboring community (~8.5%, less than in the Pacific; Perry 1998). They were overlooked by many carbonate budget studies; partly due to worms frequently being considered unimportant (Bak 1976, MacGeachy and Stearn 1976, Highsmith 1981), partly due to being poorly studied (i.e. little data on Caribbean bioerosion rates exist), and finally due to high spatial variability in abundance and diversity (Perry and Hepburn 2008b). All the above make the contribution of worms to local bioerosion difficult to estimate, with sponge bioerosion often used as a key proxy for internal macrobioerosion. However, evidence suggests that polychaete contribution can be significant in budget calculations (Hein and Risk 1975, Bak 1976, MacGeachy and Stearn 1976, Klein et al. 1991, Perry 1998, Macdonald and Perry 2003) with reported rates of up to $1-3 \times 10^{-3} \text{ kg m}^{-2} \text{ yr}^{-1}$ (Mallela 2007, Mallela and Perry 2007). Data on the volume of skeleton removed by spionid worms in different dead coral substrates (*Diploria*, *Montastraea*, *Siderastrea* spp.) were derived from a Florida study (Hein and Risk 1975), and bioerosion rates ($\text{cm}^3 \text{ year}^{-1}$) for these substrates inferred using substrate age data. The fact that in Florida worms were only found in these particular coral species may suggest a preference for certain substrates. In contrast, a Jamaican study was unable to find consistent trends in substrate susceptibility to worm bioerosion, with polychaetes found in most substrates (Macdonald and Perry 2003), and we thus used a conservative estimate, i.e. bioerosion in taxa other than *Diploria*, *Montastraea*, *Siderastrea* spp. was assumed to be nil.

[85] **BiBor**: *Bivalve excavation volume (cm^3)*. Evidence considers molluscs significant bioeroders (Jones and Pemberton 1988a), in terms of direct substrate attrition (Highsmith 1981, Perry 1999) – e.g., bivalves erode from 20% to 40% of coral skeletons (Lazar and Loya 1991) – but also in undermining coral heads and destabilizing reef structure (Macdonald and Perry 2003). Bivalves are among the larger of these macroborers, forming long, wide, excavations (Scott et al. 1988, Perry 1998). Here, a parameter describing cavity width is used to determine bivalve bioerosion (Perry 1998). Boring size estimates for *Lithophaga* spp. in Jamaica are $15 \times 2 \text{ cm}$ (Perry 1998) and $10 \times 2 \text{ cm}$ (Scott et al. 1988), which corresponded to other published estimates (Jones and Pemberton 1988b). Based on these values, the volume of a cylinder ($\pi r^2 h$) was estimated for a boring 2 cm in diameter and 15 cm long resulting in a value of 47 cm^3 , following a concept of morphometric measurements to estimate bioerosion (Schiaparelli et al. 2005). Bivalve abundance is linked to substrate type (associated with *Siderastrea* and *Madracis* spp.; Scott 1985, Perry 1999), and is positively correlated with substrate density (Highsmith

1981) and reef sedimentation (Macdonald and Perry 2003). The cavity volume estimate remains fixed across scenarios.

[86-106] **ParrotfishDensity**: Mean density of different parrotfish species and life stages (individuals m^{-2}). Parrotfish feeding mode is important in determining bioerosion contribution, with different species adopting strategies that have varied impacts on the budget. *Scarus* spp. are ‘scrapers’ and *Sparisoma* spp. ‘excavators’, which means they erode different volumes of reef framework (Bellwood and Choat 1990, Bruggeman et al. 1996). Fish density also directly affects bioerosion, but Caribbean reef fish abundance has declined over the last 50 years (Paddock et al. 2009), with overfishing influencing community composition and size (see **FishFL**), as well as abundance. To incorporate the effects of abundance/community structure into the model, parameters were drawn from real datasets and used to inform published grazing algorithms: 227 underwater visual census (UVC) 30×4 m transects were surveyed across 30 different fished and unfished sites (Mumby, unpublished data). The grazing algorithm used is based on seven parrotfish species (Mumby et al. 2006); three scraping *Scarus* spp. (*Scarus taeniopterus* ‘pr’: princess parrotfish, *S. vetula* ‘qu’: queen, *S. iseri* ‘st’: striped) and four excavating *Sparisoma* spp. (*Sparisoma aurofrenatum* ‘rb’: redband, *S. rubripinne* ‘rp’: yellowtail, *S. chrysopterus* ‘rt’: red tail and *S. viride* ‘sp’: stoplight). For each species, mean density (individuals m^{-2}) for juvenile (juv), intermediate phase (IP) and terminal phase (TP) individuals in cm size classes was obtained (see **FishFL**). For historic scenarios 1 and 2a, data representing an ‘unfished’ population was extracted from the database of UVC data taken from the protected Glovers Reef Reserve, Belize (Mumby et al. 2012). It has been suggested that many Caribbean fish (especially top level predators) were depleted by fishing long before the first scientific surveys (Jackson et al. 2001, McClanachan et al. 2010). For scenarios 2b–5d and future scenarios, data from the nearby fished region of Southwater Cay, Belize was used to inform the model (Mumby et al. 2012), with the exception of ‘unfished’ projections – which used the Glovers Reef data.

[107] **FishFL**: Body size of seven parrotfish species in different life stages (cm). Body size of parrotfish (fork length, FL = measured from the snout to the tail fork) is a parameter used in estimating both grazing bite rate and bite volume, together important in determining parrotfish erosion contribution (Ong and Holland 2010). Fishing influences parrotfish abundance (see parameters 91–111, **ParrotfishDensity**) but also affects the community structure; both the mean size of individuals and the representation by different species in the community (Mumby et al. 2006). Smaller-bodied species (<23 cm e.g., *S. iseri*) are found at comparable densities in unfished and fished communities, but mean body size is significantly reduced in unfished areas, due to greater predation. Larger species (e.g., *S. vetula*) show little size variation due to fishing, but their mean density is doubled in unfished communities (Mumby et al. 2006). **FishFL** values were drawn from 227 fished and unfished Caribbean site 30×4 m UVC datasets and used to

inform published grazing models (Mumby et al. 2012). For historic scenarios 1 and 2a, and projections involving local conservation action (fig. 3B, D, F and H), data representing an ‘unfished’ population were extracted from the database of UVCs taken from the protected Glovers Reef Reserve, Belize (Mumby et al. 2012) while for remaining ‘fished’ scenarios data came from nearby Southwater Cay.

[108] **Damsel**: *Percentage cover of damselfish territory (% cover)*. Territorial damselfish protect small areas of the reef from urchin and parrotfish grazing, resulting in reduced bioerosion rates (Eakin 1988, 1991, 1992, Zubia and Peyrot-Clausade 2001). Therefore the percentage of reef area covered in damselfish lawns (**Damsel**) is included in the model.

[109] **Urch1ABUN**: *Density of Echinometra urchins (ind m⁻²)*. This parameter describes density of the rock-boring urchin *Echinometra* sp., the first of two modelled urchins, and an important framework bioeroder. Historic scenario 1–2a (Chapter 4, Fig. 4.1) values were taken from Sammarco (1982), whose values were comparable to those in published studies from the 1970s, but more conservative than Ogden’s values in St. Croix (Ogden 1977). Variation is expected to be high due to the patchy distribution of *Echinometra*. We conserved values in scenario 2b and 3b due to lack of evidence for an effect of reef overfishing on *Echinometra* populations in the 1980s, e.g. associated reduction in predation pressure and competition. Although *Echinometra* was largely unaffected by the *Diadema* mortality event, a decline in abundance was still found in 1986 compared to earlier surveys (Hughes et al. 1987). An estimate used by us was supported by the findings of other studies (Griffin et al. 2003) and adopted in scenarios 3–5 and into the future scenarios.

[110] **Urch2ABUN**: *Density of Diadema urchins (ind m⁻²)*. In the Caribbean the important bioeroding urchin *Diadema* showed densities ranging from 1 – 8 individuals m⁻² prior to disease outbreak and heavy fishing (Bak et al. 1984, Hay 1984). Population densities responded positively to overfishing (Hay 1984, Hughes 1994), leading to Caribbean urchin densities increasing to a point where they became ‘the most important grazing animals in reef environments’ (Levinton 1982). Values for fished scenarios 2b and 3b were drawn from a study that compared fished and overfished sites (Hay 1984). Following the outbreak of *Diadema* disease in 1983, abundance decreased considerably, e.g., from 9 to 0.09 ind m⁻² at 14 sites around Jamaica (Hughes 1994), again being consistent with density reductions reported at other Caribbean sites (Panama: 95–99% reduction (Lessios et al. 1984); Curacao: 98–100% (Bak et al. 1984); Jamaica: 98–100% (Hughes et al. 1985); Barbados: 87–100% (Hunte et al. 1986); US Virgin Islands, 99% (Levitan 1988)). *Diadema* abundance has shown limited recovery since this time (Lang et al. 2010), and was entered as ‘uncommon’ in scenario 5 and into future scenarios.

[111] **Urch1TEST**: *Mean test diameter of Echinometra urchins (mm)*. Urchin test size is a parameter used to calculate an individual’s bioerosion ability, with larger urchins having a

greater bioerosion rate. *Echinometra* is a smaller, less mobile urchin than *Diadema* (Sammarco 1982): historic and future test size values were taken from *Echinometra lucunter* estimates from St. Croix (Ogden 1977), and remain fixed throughout scenarios, as other estimates of *Echinometra* test size agree (Russo 1980, McClanahan and Muthiga 1989, Griffin et al. 2003). The parameter '**Urch1TEST**' describes the average test diameter for the present population in mm.

[112] **Urch2TEST**: Mean size of *Diadema* urchins (mm). *Diadema* demonstrates ecological plasticity, with a population's mean test size converging in response to food or density limitation (Levitan 1989). A combination of field studies (Stearn and Scoffin 1977) and stocking experiments (Levitan 1989) provided values to inform this part of the model. Prior to the 1983 disease outbreak, *Diadema* size was inversely proportional to population density (Carpenter 1981, Hunte et al. 1986, Levitan 1988), with mean test size decreasing in scenario 2b and 3b where overfishing reduced competition and predation pressure on urchins (McClanahan et al. 2001), causing specimen numbers to rise. Reflecting the mass mortality event the mean and maximum test size of individuals increased significantly in the 4th suite of scenarios, while individuals in smaller size classes became less frequent (Levitan 1988, Hughes 1994). With little or no recovery of numbers these values are adopted in scenario 5 and into future scenarios.

[113] **volBurrow**: *Echinometra* home cavity volume (cm^3). A frequently overlooked component of grazer bioerosion is enlargement of excavations in the framework by the spines of reef echinoids (Bak 1994). **volBurrow**, taken from a Bahamas study, describes the mean volume of *Echinometra lucunter* home cavities (Hoskin and Reed 1984). This fixed value, along with average reef density (**ReefDensity**, see [P]) and length of time required to create a burrow, **tBurrow**, (from the same study: see [M₃]) is required to estimate *Echinometra* sp. spine abrasion.

[114] **tBurrow**: Time taken for *Echinometra* to excavate home cavity (years). Taken from a Bahamas study (Hoskin and Reed 1984). See parameter [113].

[115] **tHurricane**: Hurricane frequency (return time: in years). Storms and hurricanes result in major changes to the reef framework, namely via destruction of branched (and other) coral species (Foster et al. 2007); reducing complexity **RRug** and percentage living coral cover **CCov**, but also indirectly through sediment flushing (affecting **SedRetention**), and turnover of *Halimeda* and CCA communities (Perry 1999). Longer term effects include sustained mortality levels (Knowlton et al. 1981), increased incidence of coral disease (Bythell et al. 1993) reduction in settlement of coral larvae, as well as beneficial effects like asexual reproduction through fragmentation (Foster et al. 2007). Few studies have attempted direct estimation of hurricane impact on carbonate budgets – although values of $0.06 \text{ kg m}^{-2} \text{ yr}^{-1}$ erosion by mechanical abrasion were measured in the Bahamas (Hoskin et al. 1986). The effect of storm

damage will depend on a variety of factors, including reef depth (most damage occurring between 0–20 m deeper reefs having greater protection; Brown 1997), community structure (mound-like species, e.g., *M. annularis* more likely to survive intact (Woodley et al. 1981, Grigg 1995), while framework fragility is also linearly related to skeletal density and porosity (Scott et al. 1988)), reef zone and positioning (impact more severe on reef crest and reef terrace; Perry 1999), as well as wave height and energy (Madin and Connolly 2006) and wind speeds ($>200 \text{ km h}^{-1}$ causing severe damage; Stoddart 1985). However, previous budget studies have generally considered erosion due to physical storm events of less significance than low level constant bioerosion (e.g., 440 kg storm erosion vs. 2,800 kg sediment generated by bioerosion in Hawaii; Harney and Fletcher 2003), and physical reef damage frequently remains unquantified. The model uses **tHurricane** to estimate coral mortality, but not instant framework/sediment removal caused by hurricanes (which is both poorly quantified and unlikely to outweigh the indirect impact of coral mortality on the carbonate budget). Hurricane frequency was simulated using a binomial model employed by **ReefMod** (see [Z]), which when implemented approximates a Poisson random distribution (Edwards et al. 2011). Hurricane return time (17 years) was derived from historical data from Belize, an intermediate for the Caribbean. Over the next few decades, hurricane severity is expected to increase (Emanuel 2005).

3.4 Defining model functions

Relationships between the parameters (listed in the *Model parameterisation* section) are described below, including background and information on the data source. Each section (A–Z) describes one model function (see Fig. 3.2). Functions, listed in **green**, are assigned a letter of the alphabet so that they can be cross-referenced back to the green ‘process’ circles in the data flow diagram (Fig. 3.2). Functions utilize various input parameters, in **blue**, which can be referred back to the previous section on *Model parameterisation*.

[A] **SurfaceArea**: *Estimating volume of new skeletal material generated ($\text{cm}^3 \text{ cm}^{-2}$)*. Simple geometric techniques were used to estimate the volume of new skeletal framework produced per areal cover of each coral taxon, based on morphometric input parameters (**Cheight**, **Cwidth**, **AcrpBrDensity**, **AgDepth**, **PoritBrThick**, **AcrpBrThick**; see Table 3.2, parameters [14–31]) and published LERs (parameters [32–38], **CGrowth**). Standard surface index (SI) factors (often employed in scaling up planar area into 3D surface area (Dahl 1973, Holmes 2008)) fail to take account of the effects of colony size on reef topography (independent of living cover), and are associated with errors – especially for more complex coral morphologies. As colony surface increases as a power function with size (Bak and Meesters 1998), inputting colony dimensions

means this effect can be controlled for, as well as being used to explore the effects on the budget of altering mean colony size.

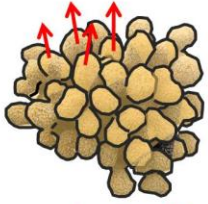
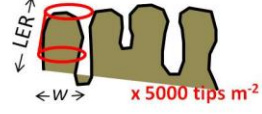
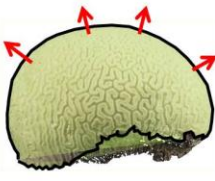
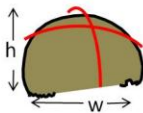
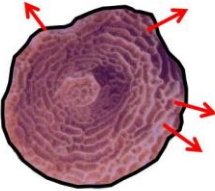
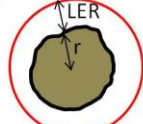
A.i) Massive/submassive corals: For model taxa with hemispherical shapes, published log-linear scaling models (Courtney et al. 2007) were used to estimate mean colony surface area based on both height (*Siderastrea*, *Diploria*, *Montastraea* spp. and *P. asteroides* parameter 21; **Cheight**) and diameter input parameters (parameter 14; **Cwidth**; see Table 3.2):

$$\text{SurfaceArea} = 0.904 \log(\text{Cheight}) + 1.165 \log\left(\frac{1}{2} \text{Cwidth}\right) + 0.610$$

In trials, this method was able to predict colony surface area with an accuracy of $r^2=0.95$ compared to computer tomography for colonies with hemispherical morphologies (Courtney et al. 2007). Assuming growth occurs equally over the entire colony surface, surface area estimates were then multiplied by annual LERs (**Cgrowth**, Table 3.2; parameters [32–38]) to give an estimate of volume of skeleton laid down per massive colony per year (Table 3.3). The surface area estimates could also be divided by the colony planimetric area (based on **Cwidth**) to generate a scaling factor, similar to published SI estimates, but specific to model runs depending on the colony dimension input values (see [D]).

A.ii) Branching corals: Branching corals grow upwards from tips rather than evenly across the colony surface (Stearn et al. 1977); surface area-estimates were thus not suitable for quantifying growth volume. In addition, log-linear models were shown to be less accurate when applied to non-hemispherical colonies (Courtney et al. 2007). Estimates for *P. porites* were derived from photoquadrat data using the methodology employed in a Barbados carbonate budget, which assumed that only $76\% \pm 0.86$ of any given colony surface is actively accreting (Stearn et al. 1977). For our second branching taxon, *Acropora* spp., cylindrical volume of branch tips was estimated (branch width, **AcrpBrThick** x LER, **CGrowth**) and multiplied by the number of growing tips found per meter squared (see parameter [30], **AcrpBrDensity**), resulting in a value of new *Acropora* colony volume ($\text{m}^{-2} \text{year}^{-1}$; see Table 3.3).

A.iii) Platy corals: *Agaricia* spp., often flat or leaf-like, represents the encrusting/platy coral component, for which assumed growth is in a two- rather than a three-dimensional process (Table 3.3). Lateral radial growth rates of encrusting colonies, such as encrusting forms of *P. asteroides*, have been shown to exceed any vertical growth in the same colony (Chornesky and Peters 1987). Colony growth planimetric area was estimated by subtracting the original colony area (area of a circle, based on colony

Morphology		Carbonate accumulation estimate	Calcification function	Data source
Branching coral <i>Porites porites</i>		Branch tip density x volume x LER x skeletal density x planimetric living coral cover 	$Agaricia = (CCov * TotalCC * ((\pi * (PoritBrThick / 2)^2 * CLER) * CDensity) * (10000 / PoritBrThick^2) / 1000)) * (10^{(0.904 * \log_{10}(CHeight) + 1.165 * \log_{10}(CWidth / 2) + 0.610)}) / (\pi * ((CWidth / 2)^2))) * RRug$	Stearn <i>et al.</i> 1977; based on <i>Porites</i> calcification estimates
Branching coral <i>Acropora</i>		Branch tip density x tip volume x skeletal density x planimetric living coral cover 	$Acropora = CCov * TotalCC * (\pi * (AcrpBrThick / 2)^2 * CLER * CDensity * AcrpBrDensity / 1000) * RRug$	Geometric techniques and parameters taken from unpublished data
Hemispherical coral <i>Diploria</i>		SA (log linear model estimation based on colony dimensions) x LER x skeletal density x planimetric living coral cover 	$MassiveCoral = CCov * TotalCC * (10^{(0.904 * \log_{10}(CHeight) + 1.165 * \log_{10}(CWidth / 2) + 0.610)}) / (\pi * ((CWidth / 2)^2))) * CDensity * CLER * rRRug$	Courtney <i>et al.</i> 2007. Log-linear models
Encrusting coral <i>Agaricia</i>		(New growth area – original colony area) x colony height x skeletal density x planimetric living coral cover 	$Agaricia = CCov * TotalCC * (\pi * (CLER + CWidth / 2)^2) / (\pi * (CWidth / 2)^2) - (CCov * TotalCC) * 10000 * AgDepth * CDensity / 1000 * RRug$	Based on geometric techniques

→ = direction of colony growth
LER = linear extension rate (cm year⁻¹)

Table 3.3. Explanations how planar surface was converted into 3-D volume of new skeletal material for each coral type to estimate gross carbonate production. *Agaricia* sp. and massive coral estimates involve a scaling factor specific to colony dimensions input for each taxon (branching coral estimates give new skeleton per m²). The scaling factor is later used in coral calcification calculations.

width **Cwidth**) from the new area (LER plus colony radius used to calculate new circle area):

$$New\ volume\ (cm^3\ year^{-1}) = \left(\pi \left(\frac{Cwidth}{2} + LER \right)^2 - \pi \left(\frac{Cwidth}{2} \right)^2 \right) \times AgDepth$$

The height of the growing edge of the colony was represented by parameter **AgDepth** (parameter [31]), which was then used to estimate the volume of new skeleton. An assumption was made that the colony was roughly circular in shape, and that colony extension was equal in all directions. As with massive corals, division of the new surface area by the old gave a scaling factor (Dahl 1973, Holmes 2008), but specific to the mean colony size in each run (see [D]).

[B] **CoralCalc**: *Estimating colony calcification ($\text{kg CaCO}_3 \text{ m}^{-2} \text{ yr}^{-1}$)*. In order to estimate colony scale calcification of the seven model taxa, density parameters (**CDensity**, Table 3.2; parameters [39–45]) were multiplied by volume of new skeletal material (see [A]) to give colony calcification (**CoralCalc**).

[C] **CommunityCalc**: *Estimating total coral community calcification ($\text{kg CaCO}_3 \text{ m}^{-2} \text{ yr}^{-1}$)*. The rate of calcification by corals per m^2 of reef area is directly determined by: coral abundance (taking 3D shape of reef into account), coral species (and their varying calcification rates), coral colony size (diameter and height - relationships [A] and [B]). Total calcification is also influenced by external factors: e.g., depth, temperature, alkalinity (relationships [E] and [F]). Although many published calcification rates exist for Caribbean corals, rates vary (due to variation in skeletal growth rates caused by environmental stochasticity), and so the model generates its own calcification estimates, based on annual extension rate per coral taxon (parameter [32–38], **Cgrowth**) and the average density of the skeleton (parameter [39–45], **CDensity**; Dodge and Brass 1984, Carricart-Ganivet et al. 2000), an approach adopted by other carbonate budget studies (Sadd 1984, Mallela and Perry 2007).

A final estimate for reef calcification ($\text{kg CaCO}_3 \text{ m}^{-2} \text{ year}^{-1}$) was derived by summing the colony calcification (**CoralCalc**; generated by relationship [B]) under consideration of relative cover of each species (**CCov**; parameters [7–13]), multiplying by reef total living coral cover (**TotalCC**; [6]), and finally again by reef topography (**Rrug**; [5]; Stearn et al. 1977).

[D] **ColRug**: *Estimating scale II (colony scale) rugosity ($\text{cm}^2 \text{ cm}^{-2}$)*. Colony types can be loosely classified into ‘simple’ (e.g., hemispherical *Diploria* and *Siderastrea* spp.); ‘moderate’ (e.g., *Agaricia* and *Montastraea* spp.) and ‘complex’ (e.g., branching *Acropora* and *Porites* spp.) morphologies (Bythell et al. 2001). Although published budgets have often attempted to include a mean rugosity measure, most have failed to account for differential rugosity of species types (Sadd 1984, Mallela and Perry 2007), Fig 3.4B. The 3D surface area of a reef framework plays a role as important as planimetric cover (**CCov**; parameters [7–13]) in determining both accretion and bioerosion rates (Stearn et al. 1977). A problem identified in early carbonate budget studies was the “lack of correlation between the abundance, or standing crop of a [coral] species, and the volume of skeletal detritus it produces” (Goreau 1963), due to wide variation in species surface areas and contribution to community make-up. Colony scale rugosity (**ColRug**) was generated from species specific coral cover and colony dimension inputs and is a factor that can later be used to estimate the available dead framework surface area over which bioerosion can potentially occur. Unlike other published studies that have attempted to incorporate fixed rugosity values (Hubbard et al. 1990, Mallela and Perry 2007), our estimate takes into account coral community composition and individual colony dimensions (see [A]), and is thus able to reflect changes in the coral community (as some species are more rugose than others).

$$ColRug \text{ (colony scale rugosity)} = \sum (CCov_{(i)} \times SurfaceArea_{(i)})$$

For all seven corals, a **SurfaceArea** factor was calculated in step [A] by dividing estimated hemispherical or flat colony surface area by planimetric area. **SurfaceArea** parameters were then multiplied by **CCov** ([7–13]) to give a taxon-specific value for 3D surface area (rugosity). The colony scale rugosity value can then be generated by summing the taxon-specific values, providing a measure of overall framework surface area ($m^2 m^{-2}$). In other functions taxon values can be treated independently (e.g. for sponge bioerosion estimates, see ‘[T]').

[E] **OAReduc**: *Relationship between ocean acidification and community calcification*. Calcification rates for many calcareous marine organisms are reduced under acidified conditions, through inhibition of aragonite or calcite formation (Gattuso et al. 1998b, Marubini and Atkinson 1999, Langdon et al. 2000, Leclercq et al. 2000, Marubini et al. 2003, Silverman et al. 2007, Fabry 2008, Silverman et al. 2009), and increased dissolution (Langdon et al. 2000, Yates and Halley 2006, Fine and Tchernov 2007). Although evidence of an effect of decreasing aragonite saturation state on community calcification in the field is still scarce, coral community calcification has been predicted to decline by 11–44% in the next 100 years (Borowitzka and Larkum 1976, Agegian 1985, Langdon et al. 2000, Leclercq et al. 2002), or on average by 32% due to the decrease of CO_3^{2-} by 30% to 36% (Langdon et al. 2000). Two published relationships describe the association between alkalinity and community calcification rate (Gattuso et al. 1998a, Langdon et al. 2000); in our model we run both the linear (‘**Lang**’) and non-linear (‘**Gatt**’) relationships to allow for related uncertainty (see figure 3.5). The relationships are described by:

$$\begin{aligned} \text{Langdon: Relative calcification} &= -0.2647 + (0.2758 \times Arag) \\ \text{Gattuso: Relative calcification} &= 1.732 \times \left(1 - \exp\left(\frac{-Arag}{0.72}\right) - 0.73\right) \end{aligned}$$

The degree of aragonite sensitivity may vary among species, with some taxa demonstrating enhanced calcification at CO_2 levels projected to occur over the 21st century (Iglesias-Rodriguez et al. 2008, Ries et al. 2009). Parameters 60–66 (**AragSensit**) describe the degree of sensitivity of model taxa, with the genus *Siderastrea* being more sensitive to changes in **Arag** (parameter [2]) than *Montastraea* (see Fig. 3.6). These data are only applicable to the linear response curve, and so are not implemented when the model is running using ‘**Gatt**’.

The model assumes no local adaptation or acclimation to availability of carbonate ions. Experiments have suggested that corals reared under acidified conditions may switch to utilize less soluble calcite as an alternative to aragonite (Ries et al. 2006), and the effect is additive, but not interactive with other parameters (e.g. temperature, nutrients etc. – see [F]). Studies have correlated Ω_{ar} to seasonal changes in temperature, light and nutrients (Silverman et al. 2007,

Silverman et al. 2009), but OA remains independent in the model. No other mitigation – for example the increased weathering of terrestrial carbonates providing is considered (Gattuso et al. 1998b). OA may have other effects on benthic calcifiers, particularly on early developmental stages and reproduction, resulting in negative consequences for population size and dynamics and community structure of calcifying populations (Kurihara 2008). These effects are not included in the current model.

[F] **TempReduc**: *Relationship between temperature and community calcification*. Coral calcification shows a Gaussian response to temperature change (Vaughan 1916, Kemp et al. 2011). Coral growth typically increases with rising temperature (Lough and Barnes 1997, 2000, Carricart-Ganivet 2004), peaking just below the normal summer high temperature, and declining rapidly beyond that (Jokiel and Coles 1977, Marshall and Clode 2004, Carricart-Ganivet et al. 2012) (Fig. 3.5). The optimum temperature (parameter 46–52, **Topt**) to which corals are acclimated varies according the ambient temperature of the coral’s environment (Marshall and Clode 2004). The curve describing the relationship between SST and relative calcification is defined as:

$$\text{Relative calcification} = A \times \exp\left(-0.5 \times \frac{(\text{SST} - \text{Topt})^2}{\text{sdRelCalc}}\right)$$

Where A is 1 (amplitude of curve), 0.5 is the standard for hump-shaped functions, **SST** is scenario surface water temperature (see parameter 3), **Topt** (parameters [46–52]) is the temperature of optimal calcification and **sdRelCalc** (parameter [53–59]) is the standard deviation of the optimal temperature curve (Fig. 3.5). Response to the same temperature change varies between genera, e.g., in the Caribbean, *P. asteroides* is more sensitive to increasing temperature than *M. faveolata* (Carricart-Ganivet et al. 2012). The relationship was derived from calcification data from *M. faveolata* in Puerto Morelos, and four *Porites* species from Heron Island, GBR (Lough and Barnes 2000, Carricart-Ganivet 2004).

The model considers the effect of temperature and alkalinity on calcification separately, as an additive effect:

$$\text{Total relative calcification} = 1 - (1 - \text{TempReduc}) - (1 - \text{OAReduc})$$

However, some evidence suggests that calcification response may be more complicated, with temperature potentially masking, offsetting or reinforcing the effect of elevated partial pressure of carbon dioxide, $p\text{CO}_2$ (Reynaud et al. 2003, Anthony et al. 2008). A synergistic effect would mean that the predicted decline in calcification might be worse than expected under high temperatures, but less dramatic if temperatures remain low. However, Langdon and Atkinson observed little or no interaction of temperature and alkalinity on calcification (Langdon and Atkinson 2005). Lack of quantitative data on possible synergistic effects or effect interactions

between changing **SST** and **Arag** meant that an additive effect – likely to give a more conservative measure under predicted climate change – was assumed. As for OA (see [E]) a further assumption of the model is no physiological acclimation or adaptation by corals to changing temperature, although this can be simulated by changing the **Topt** values.

[G] **CLER**: *Relationship between nutrient availability or shading and coral LERs*. Nutrifaction may directly affect calcification by providing nutrition for corals (Hallock and Schlager 1986), and by heightening competition for carbon between photosynthesis and calcification (Dubinsky et al. 1990, Marubini and Thake 1999); see **Nitrate**; [4]). However, the increase in nitrate level must be large before a significant response is observed (Marubini and Atkinson 1999). Nutrient availability also influences seawater transparency (primarily controlled by plankton densities), hence eutrophication can indirectly affect coral calcification rates by shading, reducing the benefits of the photosynthetic symbiosis with the zooxanthellae (Hallock 1988). Other budget studies have assumed reduction in calcification rate associated with depth/light is uniform across species (Sadd 1984) – an assumption that is now corrected, accepting that responses vary among species (Huston 1985). Relationships have been described for *Acropora* (Tunncliffe 1983), *Montastraea* (Dustan 1975, Huston 1985), *Porites* (Huston 1985), *Diploria* (Logan et al. 1994) and *Siderastrea* spp. (Huston 1985). *Agaricia* shows little change in skeletal growth rate with depth (Bak 1976, Huston 1985). With more data available on light affecting calcification (Baker and Weber 1975, Huston 1985) than on direct effect of nutrients, the relationships listed above were used to inform the model of the relationship between nutrient level and growth.

The model takes published coral extension rates (see **CGrowth**, parameters 32–38) and applies a reduction factor for shading, extrapolated from the above relationships (assuming that a ‘high’ nitrate level of $0.46 \mu\text{mol l}^{-1}$ will equal a decrease in light level equivalent to a depth increase of 10 m, and any nutrient level of $0.24 \mu\text{mol l}^{-1}$ nitrate or below will result in 100% initial growth rate) to generate a new set of values for coral LER, called **CLER**. The recalculated growth estimates (**CLER** values) inform reef calcification (see [A]).

[H] **NewDensity/NewCLER**: *Calcification feedback into coral LER/density*. A reduction in calcification rate brought about by changes in **Arag** and **SST** (see [E] and [F]) will tend to manifest itself either as a) a reduction in linear extension (**CGrowth**), while also allowing corals to maintain skeletal density, b) a reduction of skeletal density (**CDensity**) in order to maintain extension, c) both reduction of linear extension and skeletal density, or d) by maintenance of the status quo by investing more in calcification, impacting on other physiological processes. Coral species employ different growth strategies: for example, *Porites* spp. invest increased calcification in extension, and slower calcification rates correlate with a decrease in extension rate rather than a decrease in density (Lough and Barnes 2000). In contrast, *Montastraea* spp. use their increased calcification resources to construct denser skeletons, and skeletal extension rate is maintained despite a reduction in calcification rate (Carricart-Ganivet 2004). Therefore,

extension rate can be considered the primary control of calcification rate in Pacific *Porites* (Lough and Barnes 2000, Lough 2008), and density can be considered the primary control of calcification rate in Caribbean *Montastraea* (Carricart-Ganivet 2007). Using a given growth strategy in the model will affect the framework budget, with reduction of extension potentially resulting in less growth and spatial complexity of the reef (by reducing a coral's ability to compete for space (Eakin 1992)), and reduction of density potentially facilitating mechanical bioerosion (although some internal bioeroders show faster rates in denser substrates) and may cause greater fragility in the face of storms (Kleypas and Langdon 2007). Lack of information on growth strategies of Caribbean coral species and whether they favour extension of skeletal density meant that in our model only *Montastraea* density will be affected.

Model taxa new LERs and densities were estimated by application of reduction factors: in *Acropora*, *Agaricia*, *Porites*, *Diploria* and *Siderastrea* sp. this will be a percentage reduction of normal linear extension equivalent to the reduction in calcification experienced by the community (the reduction in linear extension brought about by eutrophication - see [H] - will already have been applied at this stage). In *Montastraea* this will be instead a percentage reduction in normal density equivalent to the reduction in community calcification. The new vectors generated, 'NewDensity' and 'NewCLER', were used later in the model to inform on polychaete and parrotfish erosion. Meanwhile, linear extension will increase rugosity (ColRug, see [D]) increasing the potential area over which bioerosion can take place.

An assumption of the model is that a proportional reduction in calcification translates into a similar proportional reduction in density or linear extension (Carricart-Ganivet 2004): This is supported by evidence from Carricart and colleagues (Carricart-Ganivet 2004) who demonstrated that calcification/temperature and density/temperature slopes were not significantly different in *M. annularis*. However, while we assume this relationship also holds true for the other corals, we do not have comparable data.

[I] **DeadCC**: *Estimating available substrate (% cover)*: The amount of bare substrate available for colonisation by encrusters and bioeroders is an important component of the carbonate model. Atlantic and Gulf Rapid Reef Assessment (AGRRA; Lang et al. 2010) data suggest that standing dead colonies constitute 13.5% of reef area at shallow sites in the Caribbean and adjacent seas. In contrast, the Caribbean Coastal Marine Productivity Program (CARICOMP 2001) data gave a value of 23.6% for "abiotic material without sand", but all such values are associated with high variance and were averaged across the Caribbean. Values for cover of dead calcium carbonate materials (including rubble) ranged from 37% (± 12) to 51% (± 11) in Jamaica (Mumby et al. 2007), and 33% (± 15) in the Dominican Republic (Lang et al. 2010). However, employing numbers from published studies cannot reflect any change of **DeadCC** associated with coral mortality, so **DeadCC** was simply estimated as a proportion of the remaining cover once living cover is accounted for:

$$DeadCC = 0.6 \times (1 - TotalCC)$$

Where **TotalCC** is a model parameter [6], and 0.6 is an estimate of available dead substrate given an assumed sand/algal cover.

[J₁] **CCAcov**: *Estimating encruster cover (% cover)*. CCA and other secondary encrusting calcifiers (combined with CCA owing to the difficulty of distinguishing contribution of encrusting organisms within a CCA matrix) have been described as “key elements of the binder guild” and “the most important calcifying elements of the reef framework [after corals]” (Perry and Hepburn 2008b). CCA are likely to comprise the majority of this group (CCA accounted for 82% of calcareous growth on experimental substrates; Eakin 1992), but play a smaller role in Caribbean framework construction compared to the Pacific (Agegian 1985, MacIntyre 1997). Published estimates of Caribbean CCA cover ranged from 1 – 80% (Chave et al. 1972, Stearn et al. 1977, Liddell and Ohlhorst 1987, Bruggeman et al. 1996, Shulman and Robertson 1996) but were unsuitable as input values due to extremely large variation, both geographically as well as over time (Shulman and Robertson 1996). CCA cover also varied depending on OA (Kuffner et al. 2008), urchin abundance (Steneck 1994) and macroalgal cover (Williams and Polunin 2001). As a result, the strong, positive, Caribbean-wide relationship between percentage cover CCA and scarid biomass (Williams and Polunin 2001), was adopted to generate a value of CCA cover to inform the model:

$$CCA\ cover = 1.706 \times Parrotfish\ biomass^{0.9707}$$

The value of scarid biomass was estimated using density and length values (see [U]). When tested, this method of estimating CCA cover produced similar percentage cover values and temporal trends across historic scenarios compared to other published studies (Steneck 1994).

[J₂] **CCAcalcification**: *Estimating encruster calcification (kg CaCO₃ m⁻² yr⁻¹)*. To generate an estimate for the contribution of CCA to gross reef carbonate production, percentage cover of CCA (see [J]) was multiplied by available substrate, **DeadCC** (see [I]) and CCA calcification rate (parameter [67], **CCAcalc**):

$$CCA\ contribution = CCAcov \times CCAcalc \times RRug \times DeadCC$$

[K] **CCAReduc(OA)**: *Relationship between ocean acidification and encruster calcification*. Although the high-Mg calcite produced by CCA is not thought to be as sensitive as aragonite to changes in seawater alkalinity (Kroeker et al. 2010), evidence from Hawaii suggests that CCA carbonate production may be strongly inhibited by increasing OA (Agegian 1985, Tribollet et al. 2006). The modelled calcification response of CCA to changing seawater alkalinity is based on the described *Porolithon onkodes* response to OA (Anthony et al. 2008; see also Fig. 3.6):

$$CCA\ reduction\ factor = -18.869 \times Arag^2 + 173.92 \times Arag - 302.21$$

This assumes that a 3.2% monthly gain in mass reaches CCA maximum calcification potential. The CCA reduction factor gives a measure of the percentage of mass increase compared to the potential increase. As the **Arag** value falls below $\Omega_{ar}=2$, CCA will dissolve, contributing to framework erosion. This is unlikely to have a large effect on the overall budget as the projected alkalinity is unlikely to become that low, and sensitivity tests showed the maximum erosive effect to be negligible.

Values generated by application of the calcification reduction factor to **CCAcalc** (parameter [67]) appear to be comparable to published findings (Kuffner et al. 2008). If calcification is negative CCA cover is reduced by this amount (Kuffner et al. 2008).

[L] **CCAReduc(Temp)**: Relationship between SST and encruster calcification. CCA and encrusting community calcification was shown to be sensitive to temperature rises of only a few degrees above ambient (Agegian 1985). CCA are thought to respond in a similar way to corals to temperature change (see [F]), with responses following a Gaussian distribution. Hence, SST curves applied in step [F] were also employed at this step.

[M₁] **Urch1BIO**: Estimating *Echinometra* individual bioerosion ($kg\ CaCO_3\ ind^1\ yr^{-1}$). The bioerosive ability of urchins is dependent on size. The relationship between *Echinometra* spp. test diameter (parameter [111]) and bioerosion was recorded by researchers in Moorea (Bak 1990, Conand et al. 1997) but correspond to Caribbean values for *Echinometra* spp. bioerosion, e.g., $0.24\ g\ ind^{-1}\ day^{-1}$ (Hoskin and Reed 1984) and $0.12\ g\ m^{-2}\ day^{-1}$ (Ogden 1977).

The non-linear relationship between test size and erosion rate was used to derive the equation:

$$Urch1BIO = \frac{0.0002 \times Urch1TEST^2 + 0.0029 \times Urch1TEST - 0.0098}{1000g} \times 365\ days$$

Where **Urch1TEST** (parameter [111]) is the mean diameter (mm) of *Echinometra* tests for the present population in that scenario. This can then be used to estimate *Echinometra* bioerosion in terms of $kg\ eroded\ individual^{-1}\ yr^{-1}$.

[M₂] **Urch2BIO**: Estimating *Diadema* individual bioerosion ($kg\ CaCO_3\ ind^1\ yr^{-1}$). The relationship between *Diadema* test diameter and bioerosion was derived from the exponential function described in Stearn and Scoffin's carbonate budget (Stearn and Scoffin 1977) and was used to inform the model:

$$Diadema\ erosion, Urch2BIO = \frac{0.1229e^{0.779 \times Urch2TEST}}{1000g} \times 365\ days$$

Where **Urch2TEST** is the mean test diameter of the *Diadema* population (parameter [112]). Previous carbonate budget studies have included a correction factor (CF) of -43 to -50% to allow for reworked carbonate sediment (where a proportion of the urchin gut contents used to estimate bioerosion was not from direct framework erosion (Ogden 1977, Mallela and Perry 2007)). However, a correction factor was already applied to raw data prior to derivation of the function, so application of an independent correction factor is not required.

[M₃] **UrchABRASION**: *Estimating total echinoid substrate abrasion by spines (kg CaCO₃ m⁻² yr⁻¹)*. Framework erosion via mechanical movement of urchin spines was reported to contribute to between 13 and 24% of total bioerosion caused by the urchin *Diadema mexicanum* (Herrera-Escalante et al. 2005). In the model, *Echinometra* spine abrasion was estimated using mean home cavity volume (**volBurrow**, parameter [113]), average reef density (**ReefDensity** see [P]) and length of time required to create a burrow (**tBurrow**, [114]):

$$\text{Urch1ABRASION} = \frac{\text{volBurrow} \times \text{ReefDensity}}{\text{tBurrow}} / 365 \text{ days}$$

Diadema spine abrasion (ranging from 0.06 to 0.91 g urchin⁻¹ day⁻¹) was derived directly from mean test size (**Urch2TEST**, parameter [112]), and is based on data from Mexico (Herrera-Escalante et al. 2005). *Echinometra* (**Urch1ABRASION**) and *Diadema* (**Urch1ABRASION**) abrasion values were then summed, to give **UrchABRASION**, a measure for total urchin community abrasion (kg CaCO₃ m⁻² yr⁻¹).

[N] **Urchin**: *Estimating total echinoid community bioerosion (kg CaCO₃ m⁻² year⁻¹)*. In order to estimate total urchin contribution to the carbonate budget, erosion rates for both model taxa (see [M]; **Urch1BIO**, **Urch2BIO**) derived from test size (parameters [111–112]; **Urch1TEST**, **Urch2TEST**) were multiplied by respective urchin abundance (parameters [109–110]; **Urch1ABUN**, **Urch2ABUN**) to generate an estimate for total carbonate erosion (kg CaCO₃ m⁻² year⁻¹). Added to these were the values for total community urchin spine abrasion (**UrchABRASION** [M₃]), generating the total community contribution to the budget (**Urchin**), in kg CaCO₃ m⁻² year⁻¹.

[O₁] **BiteRate**: *Estimating parrotfish bite rates (bites)*. An adapted version of Mumby’s scard grazing model was adopted to generate parrotfish grazing rates, the first step in estimating fish bioerosion (Mumby et al. 2006). The Mumby model is based on allometric relationships between fork length and both bite rate and mouth size for the genera *Sparisoma* and *Scarus* and uses the following equations to estimate grazing rate (Mumby et al. 2006):

$$\begin{aligned} \text{For Scarus: } \text{BiteRate}, r &= CSp((3329 - (33.00 \text{ FishFL})) - \text{Species offset}) \\ \text{For Sparisoma: } \text{BiteRate}, r &= CSc((1088 - (17.12 \text{ FishFL})) - \text{Species offset}) \end{aligned}$$

Where hourly bite rate, r , is calculated as a function of species (Species offset) using **FishFL** as the fork length (parameter [107]; in cm) In the above equation C is a weighting factor for life phase, such that values for the genus *Scarus* (Sc) are 0.85 for terminal phase (TP) and 1 for initial phase (IP) fish and juveniles. Those for *Sparisoma* (Sp) are 0.80 for TP, 1 for IP and 0.84 for juveniles. Species-level offsets in the genus *Scarus* are 0 for *Sc. vetula*, 1196 for *Sc. taeniopterus*, and 1714 for *Sc. iserti*. Offsets in the genus *Sparisoma* are 260 for *Sp. aurofrenatum*, 142 for *Sp. rubripinne*, 264 for *Sp. chrysopterum*, and 56 for *Sp. viride*. Offsets were based on 20 minute observations of grazing intensity in Belize (Mumby et al. 2006). Morphometric data were entered as a $3 \times 4 \times 7$ three-dimensional matrix, with rows (TP, IP, juv) defining life phase, the columns fork-length size in cm (5, 15, 25, 35), the layers representing species (qu, st, pr, sp, rb, rp, rt, see [86–106]), and abundance is given for each species in individuals 120 m^{-2} .

[O₂.] **BiteVol**: *Estimating parrotfish single bite volume ($\text{cm}^3 \text{ ind}^{-1}$)*. To estimate carbonate removal by fish, the bite volume (cm^3) for each species and life phase was estimated, using the method of Bruggeman et al. (1996) who documented a linear relationship between grazing scar volume and fork length (FL):

$$\begin{aligned} \text{For Scarus: Volume (BiteVol)} &= 0.193 \times 10^{-6} \times \text{FishFL}^3 \\ \text{For Sparisoma: Volume (BiteVol)} &= 1.295 \times 10^{-6} \times \text{FishFL}^3 \end{aligned}$$

Scarus and *Sparisoma* spp. are treated independently, because of the different way they erode, with *Scarus* spp. ‘scraping’ and *Sparisoma* spp. ‘excavating’ framework, and bite method affecting volumes taken. *Sparisoma* spp. have also been observed to take shallower bites at water depths exceeding 3 m compared to shallower depths (Bruggeman 1995). We used this information to correct the volume of *Sparisoma* bites for our modelled depth, which involved a 42% reduction of bite volume (Bruggeman 1995).

[P] **ReefDensity**: *Estimating mean reef framework density (g cm^{-3})*. Mean density of the framework can be estimated by multiplying the density of each coral taxon (once effects of OA and temperature are taken into account – see [H]), by its proportional cover (**CCov**):

$$\text{Framework density} = \text{sum}(\text{NewDensity} \times \text{CCov})$$

This generates a framework density representative of the coral community in the scenario. However, it assumes that corals die and contribute skeletal material to the framework in the same proportions in which they are found living (i.e., no differential mortality of species and no differential speed in material break-down).

Using one value for mean substrate density assumes that parrotfishes are biting randomly across the reef. However, bite volume on turf algae is greater than on CCA, and live coral is rarely bitten (Ong and Holland 2010). Framework density is also important in estimating bivalve

bioerosion (see [X]) and erosion by urchin spinal abrasion. This level of complexity is not included in the study, and the model relies on the simplified assumption of a uniform framework density for bioerosion.

[Q] **ParrotErosion**: *Estimating total community parrotfish bioerosion (kg CaCO₃ m⁻² yr⁻¹).* Total parrotfish bioerosion is expressed as mass of framework eroded per area of reef per unit time (kg CaCO₃ m⁻² year⁻¹) and was calculated as a function of size- and species-specific bite rates (see **BiteRate** [O₁]), bite volumes (**BiteVol** [O₂]) and substrate skeletal density (**ReefDensity**, [P]):

$$\text{ParrotErosion} = \frac{\text{ParrotfishDensity}}{120 \text{ m}^2} \times \text{BiteRate} \times \text{BiteVol} \times \text{ReefDensity}$$

For each species, life phase and size class, total parrotfish bioerosion was estimated as species- and size-specific density (individuals 120 m⁻², parameters [86–106]), multiplied by bite rate and bite volume to give volume of framework removed (cm³ CaCO₃ m⁻² hour⁻¹). Fish bioerosion rates were then calculated by multiplying the above volume measure by mean substrate density (g cm⁻³, i.e. average density of substrate per m² depending on the coral community in that particular scenario), to give an estimate in g CaCO₃ m⁻² hour⁻¹ (**ReefDensity**).

Values were then converted into kg, and annual rates estimated by multiplying the result by 9.33 hrs, a value taken from Bruggeman's measure of parrotfish feeding rate (Bruggeman 1995) and 365 days (parrotfishes do not take holidays). According to Bruggeman's value we assume that parrotfishes feed almost continuously during the day (Mumby 2006); with the duration of daily foraging period equalling the length of daylight period -0.65 hours, increasing steadily from early morning to noon, where it peaks until an hour before dusk, not changing significantly between 12:00 and 17:00 hours, during which time feeding rate is not significantly affected by time of day:

$$\text{ParrotErosion} = \frac{\text{sum}(\text{ParrotErosion}) \times 9.33 \text{ hours} \times 365 \text{ days}}{1000 \text{ g}}$$

Parrotfish erosion also a) reduces the amount of CCA, which is preferentially grazed by parrotfishes (Ong and Holland 2010) and b) exposes bare substrate (~4% in unfished parrotfish populations) which enables coral recruitment. However, neither of these effects were quantified more than once, and are thus not included in this paper.

For estimates of parrotfish biomass, fish lengths (parameter [107], **FishFL**) were converted to biomass using the genus-specific allometric relationships of Bohnsack and Harper (Bohnsack and Harper 1988).

[R₁] **MicroEnFac**: *Relationship between microboring rates and nutrient levels.* Nutrient levels affect microbioerosion rates positively (Chazottes et al. 1995, Zubia and Peyrot-Clausade 2001). Field studies reported an 80% increase in microbioerosion at eutrophied sites (Mallela and Perry 2007), (although on the GBR nitrification was shown to have a negative effect when combined with high turbidity; Tribollet and Golubic 2005) and experimental doubling of nitrates enhanced microbioerosion by a factor of nine (Carreiro-Silva et al. 2009). This is likely due to microborer (algae, bacteria and fungi) density being nutrient limited. A linear relationship between microbioerosion rates and the model proxy for nutrient availability, concentration of NO₃⁻ in seawater, μmol l⁻¹ (parameter [4], **Nitrate**) was extrapolated from a published association (Carreiro-Silva et al. 2009):

$$\text{Enhancement factor, } \mathbf{MicroEnFac} = 36.364 \times \mathbf{Nitrate} - 7.7273$$

Presently assumed microbioerosion rates (**Micro**, parameter [68]) were then multiplied by the enhancement factor to give improved estimates of bioeroder contribution under conditions of eutrophication.

[R₂] **Microbioerosion**: *Estimating microborer abundance and erosion (kg CaCO₃ m⁻² yr⁻¹).* Microborer activity is regulated primarily by the abundance of available dead coral substrate (**DeadCC**, see [I]), but is also affected by light availability, nutrient levels (see above, [R₁]), grazing intensity and substrate density (**ReefDensity**, see [P]). The influence of light is here ignored, because in the model microbioerosion is only estimated for one water depth. The surface area available for microborer colonisation is important in determining boring rates, with infestation 36% greater in branching compared to massive corals (Zubia and Peyrot-Clausade 2001). To account for variation in the amount of available substrate with different ratios of branching to massive corals, rates are multiplied by coral framework rugosity (dependent on proportional cover and mean dimensions of different coral taxa). The final value is multiplied by scale I (macro) rugosity:

$$\text{Microbioerosion rate} = \mathbf{Micro} \times \mathbf{DeadCC} \times \mathbf{RRug} \times \sum \mathbf{ColRug} \times \mathbf{EnFac}$$

Where **Micro** (parameter [68]) is the microbioerosion rate (kg CaCO₃ m⁻² yr⁻¹); **RRug** (parameter [5]) is a reef topography measure, **DeadCC** (see [I]) is the available dead substrate, and **ColRug** (see [D]) is the framework scale II rugosity (Fig 3.4). Our calculation of microbioerosion rate is only valid when grazing levels are low (Mallela and Perry 2007). In scenarios where nitrate levels are increased (for example in the ‘polluted’ (b) scenarios, Chapter 4, Figure 4.1), grazing was reduced through urchin die-off and overfishing of parrotfish. The total value was multiplied by the enhancement factor (**EnFac**, see [R₁]), which allowed modelled microbioerosion rates to increase under high nutrient conditions.

[S] **SpongeArea**: *Estimating boring sponge abundance*. Actively eroding clionoids live within the substrate, with most of their biomass hidden below the surface, making abundance of these sponges difficult to estimate (Rützler 1975). Yet boring sponge abundance in the Caribbean has increased in recent decades, with increases linked to eutrophication (see [T]) (Rose and Risk 1985, Holmes 1997, Ward-Paige et al. 2005), as well as coral mortality (Rützler 2002, López-Victoria and Zea 2005). Direct relationships between dead substrate availability (specifically available dead substrate (Glynn 1997, Rützler 2002, López-Victoria and Zea 2005)) and coral colony size (Rützler 1975, MacGeachy 1977, Alvarez et al. 1990) and sponge abundance have been reported. Sponge abundance in the model is estimated based on substrate availability (**DeadCC**, see [I]). In addition, our estimate of colony scale rugosity (**ColRug**, see [D]) was linked to colony morphometric inputs (**Cwidth**, **Cheight**, parameters [14–27]) in a way that variation in mean colony size will influence the area of each taxon over which sponge boring can occur. The following was the simplest way to recreate the effect of colony size/surface area on sponge boring estimates:

$$\text{SpongeArea} = \text{DeadCC} \times \text{ColRug}_{(i)} \times \text{SpongeCover}$$

Where **DeadCC** [I] is the percentage of available substrate for colonisation, **ColRug** [D] gives the proportional 3D cover of each coral taxon ‘*i*’, that comprises the framework (essentially topography), and these are multiplied by **SpongeCover** [77], a parameter describing infestation of this available space. The advantage of this method is that the actual surface area provided by different coral taxa (*Acropora*, *Montastraea*, *Agaricia* spp., *P. porites*, *P. asteroides*, *Diploria* and *Siderastrea* spp.) is estimated independently, allowing differential bioerosion rates in each coral type by using substrate specific boring data (based on *Pione lampa*, *Cliona delitrix* and *Siphonodictyon* spp. along with zooxanthellate clionoids, including *C. caribbaea*, *C. tenuis*, *C. apica*, *C. varians*; Stearn and Scoffin 1977). This was implemented, because vigour of sponge invasion varies (along with coral type, angle of attack, season) according to substrate density (Highsmith et al. 1983, Scoffin and Bradshaw 2000); see **SpongeRate**, parameters [69–76]).

[T] **SpongePollution**: *Relationship between percentage infestation and eutrophication*. As filter feeders, bioeroding sponges can significantly benefit from anthropogenic eutrophication (Rose and Risk 1985, Tomascik and Sander 1985, Hallock and Schlager 1986, Holmes 1997, Holmes et al. 2000, Ward-Paige et al. 2005), which boosts particulate organic matter (POM) and bacterioplankton, to the extent that a greater sponge biomass in the Caribbean compared to the Pacific has been explained by elevated POM (Wilkinson 1987). Numerous Caribbean studies link sponge bioerosion rates with nutrient levels above other habitat qualities (Risk and MacGeachy 1978, Hallock 1988, Holmes 1997, Holmes et al. 2000, Ward-Paige et al. 2005) with examples from Curaçao and Bonaire (Meesters et al. 1991), Jamaica (Goreau 1992), and Grand Cayman (Rose and Risk 1985) demonstrating increased abundance (and implied

bioerosion, few studies link directly) with increasing nutrient levels. Macrobioerosion rates have also been linked to factors associated with turbidity and rates of sedimentation (Tudhope and Risk 1985). The model relationship between sponge infestation and nitrate levels (**Nitrate**, parameter [4]) was based on a curve derived from data describing a doubling of clionoids in coral rubble in Barbados as nitrate levels were raised from 0.52 to 4.45 $\mu\text{g l}^{-1}$ (Holmes 2000), assuming that the larger, more aggressive sponge species usually occurring in massive substrates react in analogue (Holmes et al. 2000). The nitrate measurements in $\mu\text{g l}^{-1}$ were converted to $\mu\text{mol l}^{-1}$, and the relationship between % infestation and nitrate level were described as:

$$\text{Increase in infestation, } \mathbf{SpongePollution} = 55.045 \times \mathbf{Nitrate} + 23.586$$

The value generated gives a 'eutrophication factor' (**SpongePollution**) which provides a percentage increase in areal sponge cover driven by elevated nutrient levels, by which sponge abundance (**SpongeArea**, see [S]) can be multiplied. For example, at 0.48 $\mu\text{mol l}^{-1} \text{NO}_3^-$ an additional 50% **SpongeArea** would be infested. The **SpongePollution** factor generates an increase in sponge infestation from around 36 to 50% for the range of **Nitrate** values used in the model, an estimate which corresponds to other published findings (Hein and Risk 1975).

[U] **SpongeOAEffect**: *Relationship between sponge boring rates and seawater carbonate saturation*. Recent experimental evidence suggests that clionaid bioerosion rates are linearly related to $p\text{CO}_2$ (Wisshak et al. 2012). A regression provided by Wisshak *et al.* (Wisshak et al. 2012) is based on perturbation experiments with *Cliona orientalis* exposed to four different $p\text{CO}_2$ treatments (mean pH levels: 8.10, 8.05, 7.91, 7.57 on the total scale). The relationship between Ω_{ar} clionaid bioerosion and $p\text{CO}_2$ (converted to Ω_{ar}) is expressed as follows:

$$\text{Bioerosion rate} = -0.6214 \times \Omega_{\text{ar}} + 4.3406$$

The relative increase in total bioerosion was derived from mean weight changes (total bioerosion), and the pH was converted into Ω_{ar} using the CO2SYS Macro (Lewis and Wallace 1998). The well-supported ($P < 0.001$, $r^2 = 0.97$) relationship between relative bioerosion (%increase from present levels) and Ω_{ar} was described as:

$$\text{SpongeOA Effect (\% increase)} = -28.113 \times \mathbf{Arag} + 195.07$$

SpongeOAEffect is the percentage increase in bioerosion rate from normal (e.g. 100% = normal bioerosion under current $p\text{CO}_2$ conditions). **Arag** is Ω_{ar} (parameter [2]). Sponge bioerosion estimates were multiplied by **SpongeOAEffect** to give the rate of sponge bioerosion enhanced by OA (see [V]).

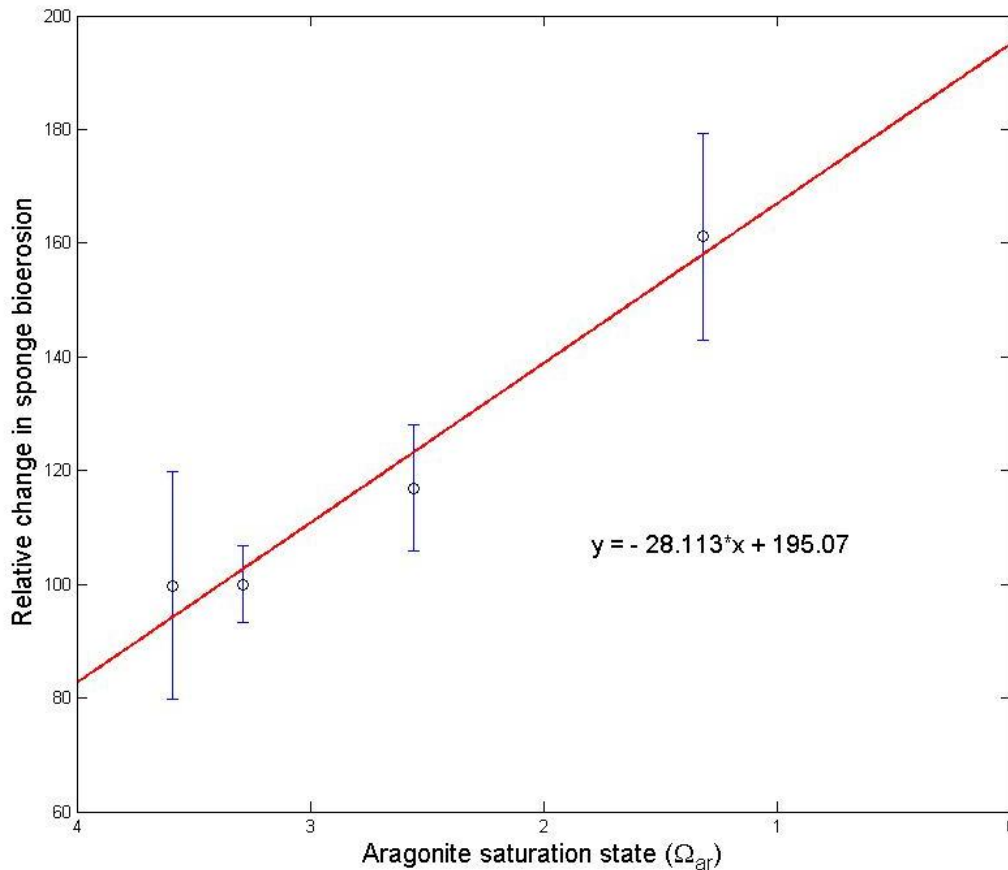


Figure 3.7. Relationship between seawater aragonite saturation state (Ω_{ar}) and sponge bioerosion rates, as described by Wisshak *et al.* (Wisshak *et al.* 2012).

[V] **SpongeBioerosion**: *Estimating sponge bioerosion ($kg\ CaCO_3\ m^{-2}\ yr^{-1}$)*. The value **SpongeBioerosion** gives the final boring sponge contribution, having taken into account aragonite saturation (see [U]), nutrient loading (see [T]), availability of substrate (see [S]), clionaid cover (see parameter [82]) and different bioerosion rates in different substrate types (parameters [69–76]):

$$SpongeBioerosion = SpongeRate_i \times (SpongeArea_i + SpongePollution) \times SpongeOAEffect \times RRug$$

Where **SpongeRate** (see [69–76]) is the rate of bioerosion in a range of substrates (dead framework and model coral species, i (Stearn and Scoffin 1977)); **SpongeArea** [S] is the infestation of sponges in each of these substrates, derived from available potential area ($DeadCC \times ColRug$) and percentage sponge cover (**SpongeCover** [77]); **SpongePollution** [T] is additional infestation based on **Nitrate** levels ($\mu mol\ l^{-1}$) (Holmes 2000); **SpongeOAEffect** is a percentage change in sponge bioerosion rate driven by changes in **Arug** [2], and **RRug** [5] is the reef topography and affects to the reference unit m^2 .

[W] **PolychaeteErosion**: *Estimating polychaete bioerosion rate ($kg\ CaCO_3\ m^{-2}\ yr^{-1}$)*. The parameter **PolychaeteRate** provides polychaete bioerosion rates in three model coral taxa: *Diploria* ($4.4\ cm^3\ yr^{-1}$), *Montastraea* ($2.2\ cm^3\ yr^{-1}$) and *Siderastraea* spp. ($3.3\ cm^3\ yr^{-1}$), with no

infestation of remaining coral taxa (Hein and Risk 1975); see parameter [78–84]. In order to convert estimates into mass of CaCO₃ removed per unit area, rates (cm³ yr⁻¹) were multiplied by respective skeletal densities for these three species as affected by environmental conditions (**NewDensity**; see [H]), applied to the percentage dead cover of these coral types, then summed to give a value in kg of framework eroded m⁻² yr⁻¹.

$$PolychaeteErosion = \frac{\sum [PolychaeteRate_{(i)} \times NewDensity_{(i)} \times (ColRug_{(i)} \times DeadCC)] \times RRug}{1000 \text{ g}}$$

Little quantitative evidence exists for Caribbean polychaete bioerosion rates changing under different circumstances (although some evidence for nutrient effect; Fonseca et al. 2006), but at present the model does not allow polychaete bioerosion to vary with anything except for available substrate (**DeadCC**, see [I]).

[X₁] **BivalveDensity**: Relationship between bioeroding bivalve abundance and substrate density. Bivalves (mainly *Lithophaga* spp.) show patchy distribution (Perry and Hepburn 2008b), making abundance per unit area difficult to estimate. Field studies demonstrate a high degree of infestation across all depths (Jones and Pemberton 1988a, Macdonald and Perry 2003), and in some cases *Lithophaga* spp. were found in abundances of 500 to 10,000 individuals m⁻² (Scott et al. 1988), thus representing a significant part of the macroboring community. Patterns of occurrence appear to represent substrate preferences (Kleemann 1980, Lazar and Loya 1991), suggesting that *Lithophaga* spp. associate only with specific corals e.g., the live coral boring bivalve, *Lithophaga bisulcata* was only found within *Siderastrea siderea* heads (Perry 1998), and *Lithophaga madracensis* only found in *Madracis* (Scott 1985). To comply with these findings, modelled bivalve distribution was associated with living and dead *Siderastrea* cover only (n.b., *Madracis* is not in the model). This also enabled simulation of patchiness. Macborer activity tends to be greater in higher density skeleton, both in the Caribbean and Pacific, with the number of boring bivalves per coral head increasing with increasing skeletal density (MacGeachy and Stearn 1976, Highsmith 1981). The published relationship between bivalve abundance and skeletal density (Highsmith 1981) was used to estimate bivalve abundance per *Siderastrea* colony:

$$BivalveDensity = 0.55e^{2.2096 \times NewDensity}$$

With **NewDensity** being the skeletal density value for *Siderastrea* after considering environmental effects on calcification (see [H]). This equation produces between 0–33 individuals per coral head (given a maximum coral density of 2.93 g cm⁻³), consistent with published observations e.g., 1.5 in small heads (James 1970); 75–100 in large heads (Jones and Pemberton 1988a).

[X₂] **BivalveErosion**: *Estimating total bioerosion by bivalves (kg CaCO₃ m⁻² yr⁻¹).* In order to scale boring bivalve abundance from colony scale up to reef scale, **BivalveDensity** was multiplied by **SidColony**, the number of *S. siderea* colonies per m² reef area, a parameter generated using total *Siderastrea* cover (**CCov**[7], parameter [13]) and mean *Siderastrea* colony size (**CWidth**, parameter [23]). Reef scale bivalve abundance was then multiplied by mean bivalve cavity volume (see parameter [90], **BiBor**), to give an estimate of total bivalve bioerosion (kg CaCO₃ m⁻² year⁻¹):

$$\text{BivalveErosion} = \frac{(0.055 \times e^{2.209 \times \text{NewDensity}} \times \text{SidColony}) \times \text{CCov}_7 \times \text{BiBor} \times \text{NewDensity}}{1000 \text{ g}}$$

Where **NewDensity** is a measure of amended mean *Siderastrea* density after considering the effects of OA and SST (see [H]). **SidNumber** is the number of *Siderastrea* colonies per m² assuming 100% cover (i.e. 1 m² divided by the mean area of one *Siderastrea* colony (πr^2), based on the given **CWidth** value in that scenario). **BiBor** is a fixed estimate of the volume of bivalve excavated cavity based on published estimates (Scott et al. 1988, Perry 1998) and **CCov** is the percentage cover (living and dead) of *Siderastrea* colonies on the reef.

[Y] **SedRetention**: *Estimating the proportion of reincorporated sediment (%).* Sediment retention is an essential part of framework building: a high proportion of bioeroded material remains near the site of origin. As much as 50% of sediments generated by bioerosion on St. Croix reefs (Hubbard et al. 1990) were estimated to be reincorporated into the reef framework instead of being removed. The remainder was deposited in sand channels that cross deeper sections of the reef, with periodic export by storms (Hubbard et al 1991). Cores have revealed that 3.15% of reef framework may be composed of biogenically reworked sediment (Moore and Shedd 1977). Finer silts, as produced by sponges (Rützler 1975), fill cavities in the framework, and may be cemented to harden. As well as being dependent on abiotic factors (e.g., reef slope, wave action, framework porosity) the volume of sediment recaptured by the framework is defined by the bioeroders present, e.g., fine-grained material produced by echinoids is defecated directly onto framework, while fish only spend part of the time defecating over a reef and produce larger grains (Eakin 1996). Eakin developed a retention model based on grain size and bioeroder movements, demonstrating that if it was assumed 30% of sediment produced was reworked, model outputs resembled field measurements that suggested that 21% (Land 1979) to 30% (Eakin 1996) of all bioeroded material was absorbed back into the reef structure.

Application of this 30% value in the model allows a fixed of reef-generated sediment to be added to the carbonate budget model. This is combined with the fixed terrigenous sedimentation rate, to give a total rate of sedimentation.

[Z] **ReefMod**: *Coupling an ecological model to the carbonate budget model.* ReefMod, a dynamic Caribbean fore-reef ecological model (Mumby et al. 2007), was linked to the static

carbonate budget model in order to project future net accretion to the end of the century. This simulation model, based on a square lattice of 0.25 m² reef patches, follows the dynamics of individual coral colonies in discrete six month steps. The model follows coral recruitment and growth, reproduction and mortality, as well as macroalgal growth and grazing by fish and urchins. Macroalgae (*Dictyota* and *Lobophora* spp.) compete and interact with coral by larval settlement as well as by vegetative growth. Algae can additionally be grazed, with an unexploited community of parrotfishes maintaining up to 40% of the reef area in a grazed state, implemented for every 6 months in the model, and *Diadema antillarum* grazing affecting 53% of reef area. Estimation of coral mortality due to 1) temperature-induced bleaching [**BleachMortality**, Z₁] and 2) hurricanes [**HurrMortality**, Z₂] produced the most important **ReefMod** outputs. These **ReefMod** generated coral mortality values were then used to inform the carbonate budget model at six monthly timesteps, specifically dictating the values of parameters [6] (**Total CC**) and [7–13] (**CCov**) for future scenarios (Table 3.2). Bleaching did not occur in the model if a hurricane occurred that year.

[Z₁] **BleachMortality**: *Relationship between SST and coral mortality*. The relationship between SST and mortality of entire coral colonies is based on a linear regression relating coral mortality to degree heating weeks (DHWs) (Edwards et al. 2011), taken from the most extensive bleaching event in the Caribbean to date (Eakin et al. 2010). Degree heating months (DHMs) represent the cumulative heating stress on a coral reef throughout the year, and are equal to one month of SST 1°C greater than the maximum in the monthly climatology. DHMs predicted by HadGEM–2ES (see **SST** parameter [3]) were converted to DHWs (by multiplying by 4: one DHM being a good proxy for four DHWs, two DHMs for eight DHWs; Donner et al. 2005) for the purposes of estimating mortality. Bleaching was modelled to occur at a range of temperatures, but with mortality dependent on the extent and duration of thermal stress. Partial mortality (defined by **ReefMod** as colonies reduced in area by 30%) was also calculated from DHWs, with brooders (e.g. *Acropora*, *Montastraea*, *Diploria* spp. and *Siderastraea siderea*) at greater risk of partial mortality than spawners (*Agaricia*, *Porites* spp. and *Siderastrea radians*) (McField 1999). Some level of adaptation was included, with corals previously exposed to elevated SSTs modelled to have a lower risk of mortality during subsequent bleaching events (McField 1999).

[Z₂] **HurrMortality**: *Relationship between hurricane impact and coral mortality*. The impact of hurricanes (described by parameter [115] **tHurricane**) on coral mortality was derived from a published relationship, based on colony size and storm strength (Madin and Connolly 2006). Intermediate-sized colonies were most impacted: small adult colonies were less frequently dislodged due to drag, while large colonies were heavy enough to avoid dislodgement. Up to 80% of juvenile colonies (1–60 cm²) were killed by scouring during this severe hurricane event. Mature corals (>250 cm²) suffered partial colony mortality during storms, the extent of which

was based on a Gaussian distribution dependent on storm strength (derived from Mumby, unpubl. data). Hurricane events also caused macroalgal reduction of 90% (Mumby et al. 2005).

3.5 Model validation: a Jamaican case study.

Early model calibration was carried out by checking the suite of outputs against published values to look for discrepancies. On the whole, model outputs agree with published data, e.g., recent carbonate field budgets measured in Bonaire revealed similar estimates of erosion and accretion in comparison to model generated outputs (Perry et al. 2012; Fig. 1.4, Chapter 4).

For three reasons Jamaica's Rio Bueno reef provides a useful case study against which to test the model. Firstly, because it is the site of a pair of comprehensive carbonate budget field studies which straddle two decades of ecological change (Land 1979, Mallela and Perry 2007). Secondly, because it has been subject to various well-documented ecological disturbances: Hurricane Allen in 1980 (Woodley et al. 1981), loss of *Diadema* in 1983 (Hughes et al. 1985, Steneck 1994) and Hurricane Gilbert in 1988 (Hughes 1994), making it interesting from a carbonate budget perspective. Thirdly, these reefs are among the Caribbean's most intensively studied, with a good time series of data available on coral cover, urchin numbers and other parameters needed to inform the carbonate budget model (Liddell and Ohlhorst 1992).

Using 17 time series of ecological data from Rio Bueno and Discovery Bay, from six published studies (Land 1979, Hughes et al. 1987, Liddell and Ohlhorst 1992, Hughes 1994, Steneck 1994, Aronson and Precht 2000), we were able to reconstruct and run 17 historic carbonate budgets. Available parameters used to inform model runs included coral, macroalgal (Fig. 3.8A), CCA and encruster cover, sedimentation rates, *Diadema* and parrotfish abundances, and site specific coral growth rates (Huston 1985). Model outputs, in terms of CaCO₃ production, bioerosion, and net accretion (Fig. 3.8B), followed a trajectory that varied over the 24-year time period, in agreement with the key finding of Chapter 4 that Caribbean carbonate budgets experienced dramatic changes over recent ecological timescales (Chapter 4, Fig. 1). In the late 1970s, accretion remained high (10.2 ± 1.9 kg), comparable with theoretical scenario 1 (Chapter 4, Fig. 4.1) estimates. Hurricane Allen in 1980 caused coral mortality (Fig. 3.8A) reducing the accretion potential of the reef down to ~ 3 kg, where it remained until the 2000s. Although parrotfish numbers are low throughout, at the beginning of the time series bioerosion (mainly by urchins) was 3.9 ± 1.0 kg. Bioerosion exceeded carbonate production, as accretion was reduced into the early 80s, pushing the carbonate budget into the negative. The loss of *Diadema* in 1983 reduced the bioeroder impact on the surface of the reef, allowing the budget to recover, where it

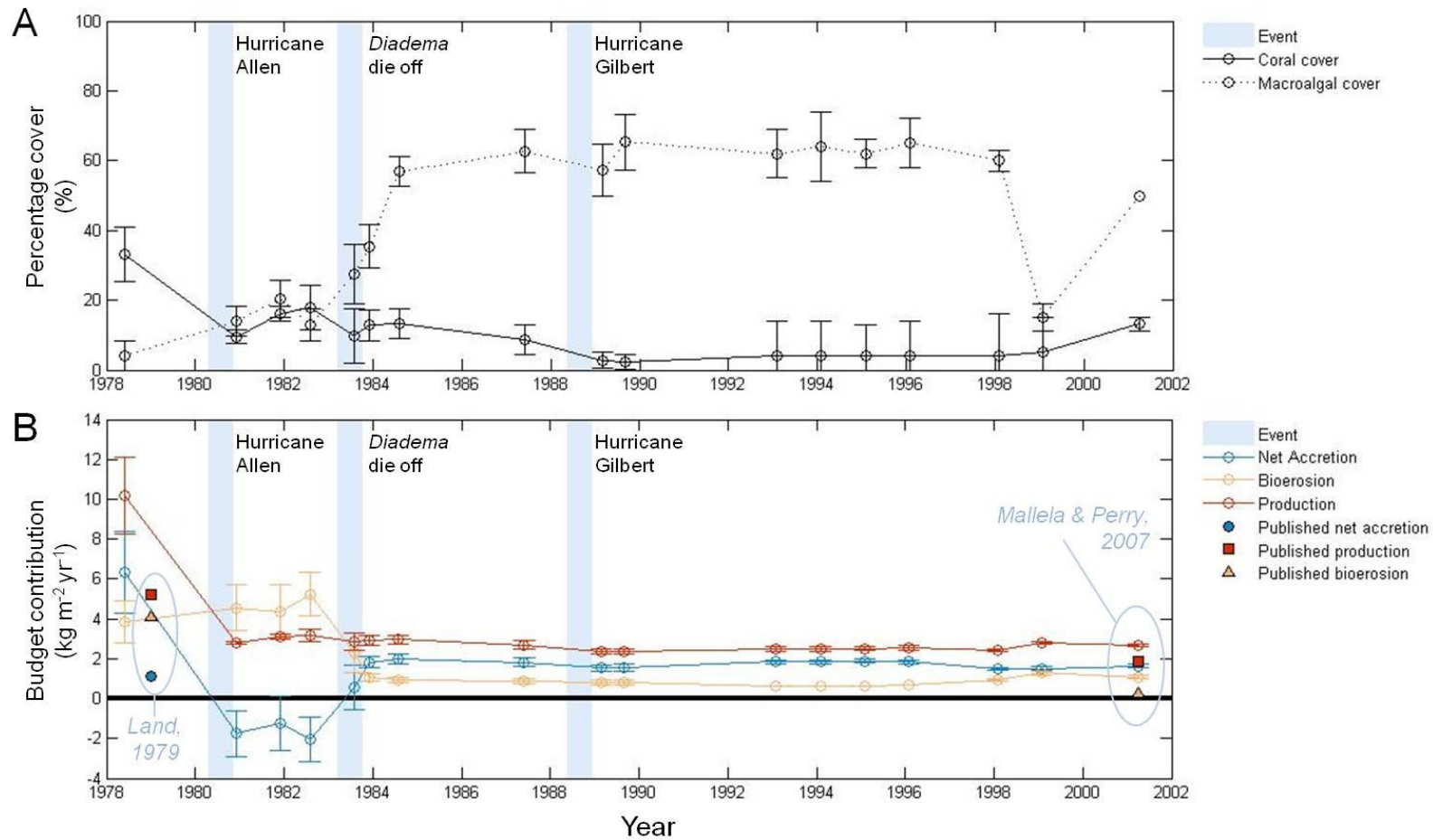


Figure 3.8. Validating the model: a Jamaican case study. **(A)** Published coral and macroalgal cover recorded in Rio Bueno, Jamaica, at 17 different points in time. **(B)** Calcium carbonate production (red), bioerosion (yellow) and net accretion (blue) values generated when ecological parameters from (A) (along with additional site specific data on CCA and encruster cover, sedimentation, coral linear extension rates, *Diadema* and parrotfish abundance) were used to inform the carbonate budget model. Model outputs can be compared to published field carbonate budget values (coloured data points) from two papers spanning the time period

remained at a low rate until surveyed April 2001 (Mallela and Perry 2007). The 2001 study corroborates with our theoretical model, with no significant difference between model outcomes (budget, carbonate production, bioerosion, urchin and parrotfish) and published field measurements (paired two-tail t-test, $t=1.518$, $p=0.203$, $df=4$). Land's 1979 budget produced a net carbonate accumulation value of $1.1 \text{ kg CaCO}_3 \text{ m}^{-2} \text{ yr}^{-1}$ compared to our estimated model budget of 6.3 kg (Figure 3.8). Erosion estimates proved similar (Land: 4.1 , model: $3.9 \text{ kg CaCO}_3 \text{ m}^{-2} \text{ yr}^{-1}$), indicating that above discrepancy was produced by carbonate production estimates. Land's carbonate production calculations employed a fixed linear extension rate for all coral species (with the exception of *Acropora* spp.), based on *Montastraea* sp. linear extension rates. It is now known that *Montastraea* is a relatively slow growing coral (Huston 1985). This assumption is the likely reason for observed differences, and when a similar assumption was made for the present model (i.e., *Montastraea* linear extension rates applied to all species) a similar CaCO_3 production value ($1.4 \pm 0.3 \text{ kg}$) was generated. As well as aiming to demonstrate the validity of the model, this exercise served to highlight the difficulties involved in not only calculating but comparing carbonate budgets from different sources.

3.6 References

- Adey WH, Vassar JM (1975) Colonization, succession and growth rates of tropical crustose coralline algae (Rhodophyta, Cryptonemiales). *Phycologia* **14**:55-69
- Agegian CR (1985) *The biogeochemical ecology of Porolithon gardineri (Foslie)*. Ph.D thesis, University of Hawaii
- Allard P (1994) *Effects of eutrophication and grazing on coral community changes*. Ph.D thesis, McGill University
- Alvarez-Filip L, Dulvy NK, Gill JA, Côté IM, Watkinson AR (2009) Flattening of Caribbean coral reefs: region-wide declines in architectural complexity. *Proceedings of the Royal Society B-Biological Sciences* **276**:3019-3025
- Alvarez B, Diaz MC, Laughlin RA (1990) The sponge fauna on a fringing reef in Venezuela, I: composition, distribution and abundance. In: Rützler K (ed) *New perspectives in sponge biology*. Smithsonian Institution Press, Washington, DC, p 358-366
- Anthony KRN (1999) Coral suspension feeding on fine particulate matter. *Journal of Experimental Marine Biology and Ecology* **232**:85-106
- Anthony KRN, Kline DI, Diaz-Pulido G, Dove S, Hoegh-Guldberg O (2008) Ocean acidification causes bleaching and productivity loss in coral reef builders. *Proceedings of the National Academy of Sciences of the United States of America* **105**:17442-17446
- Aronson RB, Precht WF (2000) Herbivory and algal dynamics on the coral reef at Discovery Bay, Jamaica. *Limnology and Oceanography* **45**:251-255
- Bak RPM (1976) The growth of coral colonies and the importance of crustose coralline algae and burrowing sponges in relation with carbonate accumulation. *Netherlands Journal of Sea Research* **10**:325-337
- Bak RPM (1990) Patterns of echinoid bioerosion in two Pacific coral reef lagoons. *Marine Ecology Progress Series* **66**:267-272
- Bak RPM (1994) Sea-urchin bioerosion on coral reefs - place in the carbonate budget and relevant variables. *Coral Reefs* **13**:99-103
- Bak RPM, Carpay MJE, de Ruyter van Steveninck ED (1984) Densities of the sea urchin *Diadema antillarum* before and after mass mortalities on the coral reefs of Curaçao. *Marine Ecology Progress Series* **17**:105-108
- Bak RPM, Meesters EH (1998) Coral population structure: the hidden information of colony size-frequency distributions. *Marine Ecology Progress Series* **162**:301-306
- Bak RPM, Nieuwland G, Meesters HWG (2009) Coral growth rates revisited after 31 years: what is causing lower extension rates in *Acropora palmata*? *Bulletin of Marine Science* **84**:287 - 294
- Baker PA, Weber JN (1975) Coral growth rate: variation with depth. *Earth and Planetary Science Letters* **27**:57-61
- Bellwood DR, Choat JH (1990) A functional analysis of grazing in parrotfishes (family Scaridae): the ecological implications. *Environmental Biology of Fishes* **28**:189-214
- Bohnsack JA, Harper DE (1988) *Length-weight relationships of selected marine reef fishes from the southeastern United States and the Caribbean*. Report, National Oceanic and Atmospheric Administration, National Marine Fisheries Service, Southeast Fisheries Center, Miami, Florida
- Borowitzka MA, Larkum AWD (1976) Calcification in the green alga *Halimeda*. *Journal of Experimental Botany* **27**:864-878
- Brown BE (1997) Disturbances to reefs in recent times. In: Birkeland C (ed) *Life and Death of Coral Reefs*. Chapman & Hall, NY, USA, p 354-379
- Bruggeman JH (1994) Foraging by the stoplight parrotfish *Sparisoma viride*. II. Intake and assimilation of food, protein and energy. *Marine Ecology Progress Series* **106**:57-71
- Bruggeman JH (1995) *Parrotfish grazing on reefs: a trophic novelty*. Ph.D thesis, University of Groningen
- Bruggeman JH, van Kessel AM, van Rooij JM, Breeman AM (1996) Bioerosion and sediment ingestion by the Caribbean parrotfish *Scarus vetula* and *Sparisoma viride*: implications of fish size, feeding mode and habitat use. *Marine Ecology Progress Series* **134**:59-71
- Bucher DJ, Harriott VJ, Roberts LG (1998) Skeletal micro-density, porosity and bulk density of acroporid corals. *Journal of Experimental Marine Biology and Ecology* **228**:117-136
- Bythell JC, Gladfelter EH, Bythell M (1993) Chronic and catastrophic natural mortality of three common Caribbean reef corals. *Coral Reefs* **12**:143-152
- Bythell JC, Pan P, Lee J (2001) Three-dimensional morphometric measurements of reef corals using underwater photogrammetry techniques. *Coral Reefs* **20**:193-199

- CARICOMP (2001) *CARICOMP: manual of methods for mapping and monitoring of physical and biological parameters in the coastal zone of the Caribbean*. Report, University of West Indies, Jamaica
- Carpenter RC (1981) Grazing by *Diadema* (Itillarlul (Philippi)) and its effects on the benthic algal community. *Journal of Marine Research* **39**:749-765
- Carreiro-Silva M, McClanahan TR, Kiene WE (2005) The role of inorganic nutrients and herbivory in controlling microbioerosion of carbonate substratum. *Coral Reefs* **24**:214-221
- Carreiro-Silva M, McClanahan TR, Kiene WE (2009) Effects of inorganic nutrients and organic matter on microbial euendolithic community composition and microbioerosion rates. *Marine Ecology Progress Series* **392**:1-15
- Carricart-Ganivet JP (2004) Sea surface temperature and the growth of the West Atlantic reef-building coral *Montastraea annularis*. *Journal of Experimental Marine Biology and Ecology* **302**:249-260
- Carricart-Ganivet JP (2007) Annual density banding in massive coral skeletons: result of growth strategies to inhabit reefs with high microborers' activity? *Marine Biology* **153**:1-5
- Carricart-Ganivet JP (2011) Coral skeletal extension rate: An environmental signal or a subject to inaccuracies? *Journal of Experimental Marine Biology and Ecology* **405**:73-79
- Carricart-Ganivet JP, Beltrán-Torres AU, Merino M, Ruiz-Zárate MA (2000) Skeletal extension, density and calcification rate of the reef building coral *Montastraea annularis* (Ellis and Solander) in the Mexican Caribbean. *Bulletin of Marine Science* **66**:215-224
- Carricart-Ganivet JP, Cabanillas-Terán N, Cruz-Ortega I, Blanchon P (2012) Sensitivity of calcification to thermal stress varies among genera of massive reef-building corals. *PLoS ONE* **7**:e32859
- Carricart-Ganivet JP, Merino M (2001) Growth responses of the reef-building coral *Montastraea annularis* along a gradient of continental influence in the southern Gulf of Mexico. *Bulletin of Marine Science* **68**:133-146
- Chave KE, Smith SV, Roy KJ (1972) Carbonate production by coral reefs. *Marine Geology* **12**:123-127
- Chazottes V, Le Campion-Alsumard T, Peyrot-Clausade M (1995) Bioerosion rates on coral reefs: interactions between macroborers, microborers and grazers (Moorea, French Polynesia). *Palaeogeography Palaeoclimatology Palaeoecology* **113**:189-198
- Chiappone M, Rutten LM, Milleri SL, Swanson DW (2007) Large-scale distributional patterns of the encrusting and excavating sponge *Cliona delitrix* Pang on Florida Keys coral substrates. In: Custódio MR, Hajdu E, Lôbo-Hajdu G, Muricy G (eds) *Proceedings of the 7th International Sponge Symposium*, Rio de Janeiro, p 255-263
- Chornesky EA, Peters EC (1987) Sexual reproduction and colony growth in the scleractinian coral *Porites astreoides*. *Biological Bulletin* **172**:161-177
- Conand C, Chabanet P, Cuet P, Letourneur Y (1997) The carbonate budget of a fringing reef in La Reunion Island (Indian Ocean): sea urchin and fish bioerosion and net calcification. *Proceedings of the 8th International Coral Reef Symposium*, Panama City, p 953-958
- Courtney LA, Fisher WS, Raimondo S, Oliver LM, Davis WP (2007) Estimating 3-dimensional colony surface area of field corals. *Journal of Experimental Marine Biology and Ecology* **351**:234-242
- Crabbe MJC (2009) Scleractinian coral population size structures and growth rates indicate coral resilience on the fringing reefs of North Jamaica. *Marine Environmental Research* **67**:189-198
- Dahl AL (1973) Surface area in ecological analysis: quantification of benthic coral-reef algae. *Marine Biology* **23**:239-249
- Davies PJ (1983) Reef Growth. In: Barnes DJ (ed) *Perspectives on coral reefs*. Australian Institute of Marine Science, Townsville
- De'ath G, Lough JM, Fabricius KE (2009) Declining coral calcification on the Great Barrier Reef. *Science* **323**:116-119
- Dodge RE, Brass GW (1984) Skeletal extension, density and calcification of the reef coral, *Montastrea annularis*: St. Croix, U.S. Virgin Islands. *Bulletin of Marine Science* **34**:288-307
- Done TJ (1995) Ecological criteria for evaluating coral reefs and their implications for managers and researchers. *Coral Reefs* **14**:183-192
- Donner SD, Skirving WJ, Little CM, Oppenheimer M, Hoegh-Guldberg OVE (2005) Global assessment of coral bleaching and required rates of adaptation under climate change. *Global Change Biology* **11**:2251-2265
- Dubinsky Z, Stambler N, Ben-Zion M, McCloskey LR, Muscatine L, Falkowski PG (1990) The effect of external nutrient resources on the optical properties and photosynthetic efficiency of *Stylophora pistillata*. *Proceedings of the Royal Society of London B Biological Sciences* **239**:231-246
- Dustan P (1975) Growth and form in the reef-building coral *Montastrea annularis*. *Marine Biology* **33**:101-107

- Eakin CM (1988) Avoidance of damselfish lawns by the sea urchin *Diadema mexicanum* at Uva Island, Panama. *Proceedings of the 6th International Coral Reef Symposium*, Australia, p 21-26
- Eakin CM (1991) *The damselfish-algal lawn symbiosis and its influence on the bioerosion off an El Niño impacted coral reef, Uva Island, Pacific Panama*. PhD thesis, University of Miami
- Eakin CM (1992) Post-El Niño Panamanian reefs: less accretion, more erosion and damselfish protection *Proceedings of the 7th International Coral Reef Symposium*, Guam, p 387-396
- Eakin CM (1996) Where have all the carbonates gone? A model comparison of calcium carbonate budgets before and after the 1982-1983 El Niño at Uva Island in the eastern Pacific. *Coral Reefs* **15**:109-119
- Eakin CM, Morgan JA, Heron SF, Smith TB, Liu G, Alvarez-Filip L, Baca B, Bartels E, Bastidas C, Bouchon C, Brandt M, Bruckner AW, Bunkley-Williams L, Cameron A, Causey BD, Chiappone M, Christensen TRL, Crabbe MJC, Day O, de la Guardia E, Díaz-Pulido G, DiResta D, Gil-Agudelo DL, Gilliam DS, Ginsburg RN, Gore S, Guzmán HCM, Hendee JC, Hernández-Delgado EA, Husain E, Jeffrey CFG, Jones RJ, Jordán-Dahlgren E, Kaufman LS, Kline DI, Kramer PA, Lang JC, Lirman D, Mallela J, Manfrino C, Maréchal J-P, Marks K, Mihaly J, Miller WJ, Mueller EM, Muller EM, Orozco Toro CA, Oxenford HA, Ponce-Taylor D, Quinn N, Ritchie KB, Rodríguez Sn, Ramírez AR, Romano S, Samhoury JF, Sánchez JA, Schmahl GP, Shank BV, Skirving WJ, Steiner SCC, Villamizar E, Walsh SM, Walter C, Weil E, Williams EH, Roberson KW, Yusuf Y (2010) Caribbean corals in crisis: record thermal stress, bleaching, and mortality in 2005. *PLoS ONE* **5**:e13969
- Edinger EN, Limmon GV, Jompa J, Widjatmoko W, Heikoop JM, Risk MJ (2000) Normal coral growth rates on dying reefs: Are coral growth rates good indicators of reef health? *Marine Pollution Bulletin* **40**:404-425
- Edwards HJ, Elliott IA, Eakin CM, Irikawa A, Madin JS, McField M, Morgan JA, Van Woesik R, Mumby PJ (2011) How much time can herbivore protection buy for coral reefs under realistic regimes of hurricanes and coral bleaching? *Global Change Biology* **17**:2033-2048
- Emanuel K (2005) Increasing destructiveness of tropical cyclones over the past 30 years. *Nature* **436**:686-688
- Fabricius KE (2005) Effects of terrestrial runoff on the ecology of corals and coral reefs: review and synthesis. *Marine Pollution Bulletin* **B**:125-146
- Fabry VJ (2008) Marine calcifiers in a high-CO₂ ocean. *Science* **320**:1020-1022
- Ferrari R, Gonzalez-Rivero M, Ortiz JC, Mumby PJ (2012) Interaction of herbivory and seasonality on the dynamics of Caribbean macroalgae. *Coral Reefs* **31**:683-692
- Ferrier-Pages C, Gattuso JP, Dallot S, Jaubert J (2000) Effect of nutrient enrichment on growth and photosynthesis of the zooxanthellate coral *Stylophora pistillata*. *Coral Reefs* **19**:103-113
- Fine M, Tchernov D (2007) Scleractinian coral species survive and recover from decalcification. *Science* **315**:1811-1811
- Fonseca AC, Dean HK, Cortés J (2006) Non-colonial coral macroborers as indicators of coral reef status in the south Pacific of Costa Rica. *Revista de Biología Tropical* **54**:101-115
- Foster NL, Baums IB, Mumby PJ (2007) Sexual vs. asexual reproduction in an ecosystem engineer: the massive coral *Montastraea annularis*. *Journal of Animal Ecology* **76**:384-391
- Friele D, Hillis L (1997) Carbonate production by *Halimeda incrassata* in a land proximal lagoon, Pico Feo, San Blas, Panama. *Proceedings of the 8th International Coral Reef Symposium*, Panama, p 767-772
- Gardner TA, Côté IM, Gill JA, Grant A, Watkinson AR (2003) Long-term region-wide declines in Caribbean corals. *Science* **301**:958-960
- Gattuso JP, Frankignoulle M, Bourge I, Romaine S, Buddemeier RW (1998a) Effect of calcium carbonate saturation of seawater on coral calcification. *Global and Planetary Change* **18**:37-46
- Gattuso JP, Frankignoulle M, Wollast R (1998b) Carbon and carbonate metabolism in coastal aquatic ecosystems. *Annual Review of Ecology and Systematics* **29**:405-434
- Gledhill DK, Wanninkhof R, Millero FJ, Eakin M (2008) Ocean acidification of the Greater Caribbean Region 1996-2006. *Journal of Geophysical Research-Oceans* **113**:C10031
- Glynn PW (1997) Bioerosion and coral reef growth: a dynamic balance. In: Birkeland C (ed) *Life and death of coral reefs*. Chapman and Hall, p 69-98
- Goreau TF (1963) Calcium carbonate deposition by coralline algae and corals in relation to their roles as reef-builders. *Annals of the New York Academy of Sciences* **109**:127-129
- Goreau TF (1992) Bleaching and reef community change in Jamaica: 1851-1991. *American Zoologist* **32**:683-695

- Green DH, Edmunds PJ, Carpenter RC (2008) Increasing relative abundance of *Porites astreoides* on Caribbean reefs mediated by an overall decline in coral cover. *Marine Ecology Progress Series* **359**:1-10
- Griffin SP, García RP, Weil E (2003) Bioerosion in coral reef communities in southwest Puerto Rico by the sea urchin *Echinometra viridis*. *Marine Biology* **143**:79-84
- Grigg RW (1995) Coral reefs in an urban embayment in Hawaii: a complex case history controlled by natural and anthropogenic stress. *Coral Reefs* **14**:253-266
- Guinotte JM, Buddemeier RW, Kleypas JA (2003) Future coral reef habitat marginality: temporal and spatial effects of climate change in the Pacific basin. *Coral Reefs* **22**:551-558
- Hallock P (1988) The role of nutrient availability in bioerosion: Consequences to carbonate buildups. *Palaeogeography, Palaeoclimatology, Palaeoecology* **63**:275-291
- Hallock P, Schlager W (1986) Nutrient excess and the demise of coral reefs and carbonate platforms. *Palaios* **1**:389-398
- Harney JN, Fletcher CH (2003) A budget of carbonate framework and sediment production, Kailua Bay, Oahu, Hawaii. *Journal of Sedimentary Research* **73**:856-868
- Hay ME (1984) Patterns of fish and urchin grazing on Caribbean coral reefs: are previous results typical? *Ecology* **65**:446-454
- Hein FJ, Risk MJ (1975) Bioerosion of coral heads: inner patch reefs, Florida reef tract. *Bulletin of Marine Science* **25**:133-138
- Herrera-Escalante T, López-Pérez RA, Leyte-Morales GE (2005) Bioerosion caused by the sea urchin *Diadema mexicanum* (Echinodermata: Echinoidea) at Bahias de Huatulco, Western Mexico. *Revista De Biología Tropical* **53**:263-273
- Highsmith RC (1981) Coral bioerosion: damage relative to skeletal density. *American Naturalist* **117**:193-198
- Highsmith RC, Lueptow RL, Schonberg SC (1983) Growth and bioerosion of three massive corals on the Belize barrier reef. *Marine Ecology Progress Series* **13**:261-271
- Holmes G (2008) Estimating three-dimensional surface areas on coral reefs. *Journal of Experimental Marine Biology and Ecology* **365**:67-73
- Holmes KE (1997) Eutrophication and its effect on bioeroding sponge communities. In: Lessios HA, MacIntyre IG (eds) *Proceedings of the 8th International Coral Reef Symposium*, Panama City, Panama
- Holmes KE (2000) Effects of eutrophication on bioeroding sponge communities with the description of new West Indian sponges, *Cliona* spp. (Porifera: Hadromerida: Clionidae). *Invertebrate Biology* **119**:125-138
- Holmes KE, Edinger EN, Hariyadi, Limmon GV, Risk MJ (2000) Bioerosion of live massive corals and branching coral rubble on Indonesian coral reefs. *Marine Pollution Bulletin* **40**:606-617
- Hoskin CM, Reed JK (1984) Carbonate sediment produced by rock-boring urchin, *Echinometra lucunter*, and infauna, Black Rock, Little Bahama Bank. *American Association of Petroleum Geologists* **68**:487-487
- Hoskin CM, Reed JK, Mook DH (1986) Production and off-bank transport of carbonate sediment, Black Rock, southwest Little Bahama Bank. *Marine Geology* **73**:125-144
- Hubbard DK, Miller AI, Scaturro D (1990) Production and cycling of calcium-carbonate in a shelf-edge reef system (St. Croix, United States Virgin Islands): applications to the nature of reef systems in the fossil record. *Journal of Sedimentary Petrology* **60**:335-360
- Hudson JH (1977) Long-term bioerosion rates on a Florida reef tract: a new method. In: Taylor DL (ed) *Proceedings of the 3rd International Coral Reef Symposium*, Miami, Florida
- Hughes TP (1987) Skeletal density and growth form of corals. *Marine Ecology Progress Series* **35**:259-266
- Hughes TP (1994) Catastrophes, phase-shifts and large-scale degradation of a Caribbean coral reef. *Science* **265**:1547-1551
- Hughes TP, Keller BD, Jackson JBC, Boyle MJ (1985) Mass mortality of the echinoid *Diadema antillarum* Philippi in Jamaica. *Bulletin of Marine Science* **36**:377-384
- Hughes TP, Reed DC, Boyle MJ (1987) Herbivory on coral reefs: community structure following mass mortalities of sea urchins. *Journal of Experimental Marine Biology and Ecology* **113**:39-59
- Hunte W, Côté I, Tomascik T (1986) On the dynamics of the mass mortality of *Diadema antillarum* in Barbados. *Coral Reefs* **4**:135-139
- Huston M (1985) Variation in coral growth rates with depth at Discovery Bay, Jamaica. *Coral Reefs* **4**:19-25
- Hutchings P (2008) Role of polychaetes in bioerosion of coral substrates. In: Wisshak M, Tapanila L (eds) *Current Developments in Bioerosion*. Springer Berlin Heidelberg, p 249-264

- Iglesias-Rodriguez MD, Halloran PR, Rickaby REM, Hall IR, Colmenero-Hidalgo E, Gittins JR, Green DRH, Tyrrell T, Gibbs SJ, von Dassow P, Rehm E, Armbrust EV, Boessenkool KP (2008) Phytoplankton calcification in a high-CO₂ world. *Science* **320**:336-340
- Jackson JBC, Kirby MX, Berger WH, Bjorndal KA, Botsford LW, Bourque BJ, Bradbury RH, Cooke R, Erlandson J, Estes JA, Hughes TP, Kidwell S, Lange CB, Lenihan HS, Pandolfi JM, Peterson CH, Steneck RS, Tegner MJ, Warner RR (2001) Historical overfishing and the recent collapse of coastal ecosystems. *Science* **293**:629-637
- James NP (1970) Role of boring organisms in the coral reefs of the Bermuda Platform. In: Ginsberg RN, Stanley SM (eds) *Organism-sediment interrelationships*. Bermuda Biological Station
- Jokiel PL, Coles SL (1977) Effects of temperature on the mortality and growth of Hawaiian reef corals. *Marine Biology* **43**:201-208
- Jones B, Pemberton SG (1988a) Lithophaga borings and their influence on the diagenesis of corals in the Pleistocene ironshore formation of Grand Cayman Island, British West Indies. *Palaios* **3**:3-21
- Jones CD, Hughes JK, Bellouin N, Hardiman SC, Jones GS, Knight J, Liddicoat S, O'Connor FM, Andres RJ, Bell C, Boo K-O, Bozzo A, Butchart N, Cadule P, Corbin KD, Doutriaux-Boucher M, Friedlingstein P, Gornall J, Gray L, Halloran PR, Hurtt G, Ingram WJ, Lamarque J-F, Law RM, Meinshausen M, Osprey S, Palin EJ, Parsons Chini L, Raddatz T, Sanderson MG, Sellar AA, Schurer A, Valdes P, Wood N, Woodward S, Yoshioka M, Zerroukat M (2011) The HadGEM2-ES implementation of CMIP5 centennial simulations. *Geoscientific Model Development* **4**:543-570
- Kemp DW, Oakley CA, Thornhill DJ, Newcomb LA, Schmidt GW, Fitt WK (2011) Catastrophic mortality on inshore coral reefs of the Florida Keys due to severe low-temperature stress. *Global Change Biology* **17**:3468-3477
- Kiene WE (1997) Enriched nutrients and their impact on bioerosion: results from ENCORE. In: Lessios H, MacIntyre I (eds) *Proceedings of the 8th International Coral Reef Symposium*, Panama City, Panama
- Kinsey DW, Davis PJ (1979) Effect of elevated nitrogen and phosphorus on coral reef growth. *Limnology and Oceanography* **25**:935-940
- Kleemann KH (1980) Boring bivalves and their host corals from the Great Barrier Reef. *Journal of Molluscan Studies* **46**:13-54
- Klein R, Mokady O, Loya Y (1991) Bioerosion in ancient and contemporary corals of the genus *Porites*: patterns and palaeoenvironmental implications. *Marine Ecology Progress Series* **77**:245-251
- Kleypas JA, Langdon C (2007) Chapter 5: Coral reefs and changing seawater chemistry. In: Phinney J, Skirving W, Kleypas J, Hoegh-Guldberg O, Strong AE (eds) *Coral Reefs and Climate Change: Science and Management*, Vol 61. Coastal and Estuarine Studies, p 73-109
- Klumpp DW, Polunin NVC (1989) Partitioning among grazers of food resources within damselfish territories on a coral reef. *Journal of Experimental Marine Biology and Ecology* **125**:145-169
- Knowlton N, Lang JC, Rooney MC, Clifford P (1981) Evidence for delayed mortality in hurricane-damaged Jamaican staghorn corals. *Nature* **294**:251-252
- Kramer PA (2003) Synthesis of coral reef health indicators for the western Atlantic: results of the AGRRA program (1997-2000). In: *Status of Coral Reefs in the Western Atlantic: Results of Initial Surveys, Atlantic and Gulf Rapid Reef Assessment (AGRRRA) Program*, Vol 496. Atoll Res. Bull., p 1-55
- Krief S, Hendy EJ, Fine M, Yam R, Meibom A, Foster GL, Shemesh A (2010) Physiological and isotopic responses of scleractinian corals to ocean acidification. *Geochimica et Cosmochimica Acta* **74**:4988-5001
- Kroeker KJ, Kordas RL, Crim RN, Singh GG (2010) Meta-analysis reveals negative yet variable effects of ocean acidification on marine organisms. *Ecology Letters* **13**:1419-1434
- Kuffner IB, Andersson AJ, Jokiel PL, Rodgers KS, Mackenzie FT (2008) Decreased abundance of crustose coralline algae due to ocean acidification. *Nature Geoscience* **1**:114-117
- Kurihara H (2008) Effects of CO₂-driven ocean acidification on the early developmental stages of invertebrates. *Marine Ecology Progress Series* **373**:275-284
- Land LS (1974) Growth rate of a West Indian (Jamaican) reef. In: Cameron AM, Cambell BM, Cribb AB, Endean R, Jell JS, Jones OA, Mather P, Talbot FH (eds) *Proceedings of the 2nd International Symposium on Coral Reefs*, Brisbane, Australia, p 409-412
- Land LS (1979) Fate of reef-derived sediment on the north Jamaican island slope. *Marine Geology* **29**:55-71
- Lang JC, Marks KW, Kramer PA, Kramer PR, Ginsburg RN, Reef AaGR (2010) *Atlantic and Gulf Rapid Reef Assessment Methodology v 54*, <http://www.agrra.org/method/methodology.html>

- Langdon C, Atkinson MJ (2005) Effect of elevated pCO₂ on photosynthesis and calcification of corals and interactions with seasonal change in temperature/irradiance and nutrient enrichment. *Journal of Geophysical Research-Oceans* **110**:C09S07
- Langdon C, Takahashi T, Sweeney C, Chipman D, Goddard J (2000) Effect of calcium carbonate saturation state on the rate of calcification of an experimental coral reef. *Global Biogeochemical Cycles* **14**:639-654
- Lazar B, Loya Y (1991) Bioerosion of coral reefs- a chemical approach. *Limnology and Oceanography* **36**:377-383
- Leclercq N, Gattuso J-P, Jaubert J (2002) Primary production, respiration, and calcification of a coral reef mesocosm under increased CO₂ partial pressure. *Limnology and Oceanography* **47**:558-564
- Leclercq N, Gattuso JP, Jaubert J (2000) CO₂ partial pressure controls the calcification rate of a coral community. *Global Change Biology* **6**:329-334
- Lessios HA, Robertson DR, Cubit JD (1984) Spread of *Diadema* mass mortality through the Caribbean. *Science* **226**:335-337
- Levinton JS (1982) *Marine Ecology*, Vol. Prentice-Hall, New Jersey
- Levitan DR (1988) Algal-urchin biomass responses following mass mortality of *Diadema antillarum* Philippi at Saint John, U.S. Virgin Islands. *Journal of Experimental Marine Biology and Ecology* **119**:167-178
- Levitan DR (1989) Density-dependent size regulation in *Diadema antillarum*: effects on fecundity and survivorship. *Ecology* **70**:1414-1424
- Lewis E, Wallace DWR (1998) *Program Developed for CO₂ System Calculations*, Carbon Dioxide Information Analysis Center, Oak Ridge National Laboratory, U.S. Department of Energy, Oak Ridge, Tennessee
- Lewis JB, Axelsen F, Goodbody I, Cynthia P, Chrislett G (1968) *Comparative growth rates of some reef corals in the Caribbean*. Report, McGill University, Montreal (Quebec)
- Liddell WD, Ohlhorst SL (1987) Patterns of reef community structure, North Jamaica. *Bulletin of Marine Science* **40**:311-329
- Liddell WD, Ohlhorst SL (1992) Ten years of disturbance and change on a Jamaican fringing reef *Proceedings of the 7th International Coral Reef Symposium*, Guam
- Logan A, Yang L, Tomascik T (1994) Linear skeletal extension rates in two species of *Diploria*; from high-latitude reefs in Bermuda. *Coral Reefs* **13**:225-230
- López-Victoria M, Zea S (2005) Current trends of space occupation by encrusting excavating sponges on Colombian coral reefs. *Marine Ecology* **26**:33-41
- Lough J (2008) Coral calcification from skeletal records revisited. *Marine Ecology Progress Series* **373**:257-264
- Lough JM, Barnes DJ (1997) Several centuries of variation in skeletal extension, density and calcification in massive *Porites* colonies from the Great Barrier Reef: A proxy for seawater temperature and a background of variability against which to identify unnatural change. *Journal of Experimental Marine Biology and Ecology* **211**:29-67
- Lough JM, Barnes DJ (2000) Environmental controls on growth of the massive coral *Porites*. *Journal of Experimental Marine Biology and Ecology* **245**:225-243
- Macdonald IA, Perry CT (2003) Biological degradation of coral framework in a turbid lagoon environment, Discovery Bay, north Jamaica. *Coral Reefs* **22**:523-535
- MacGeachy JK (1977) Factors controlling sponge boring in Barbados reef corals. In: Taylor DL (ed) *Proceedings of the 3rd International Coral Reef Symposium*, Miami, Florida
- MacGeachy JK, Stearn CW (1976) Boring by macroorganisms in the coral *Montastraea annularis* on Barbados reefs. *Internationale Revue der gesamten Hydrobiologie* **61**:715-746
- MacIntyre IG (1978) Distribution of submarine cements in a modern Caribbean fringing reef, Galeta Point, Panama - reply. *Journal of Sedimentary Petrology* **48**:669-670
- MacIntyre IG (1997) Re-evaluating the role of crustose algae in the construction of coral reefs. In: Lessios HA, Macintyre IG (eds) *Proceedings of the 8th International Coral Reef Symposium*, Panama City, Panama
- Madin JS, Connolly SR (2006) Ecological consequences of major hydrodynamic disturbances on coral reefs. *Nature* **444**:477-480
- Maldonado M, Giraud K, Carmona C (2008) Effects of sediment on the survival of asexually produced sponge recruits. *Marine Biology* **154**:631-641
- Mallela J (2007) Coral reef encruster communities and carbonate production in cryptic and exposed coral reef habitats along a gradient of terrestrial disturbance. *Coral Reefs* **26**:775-785

- Mallela J, Perry CT (2007) Calcium carbonate budgets for two coral reefs affected by different terrestrial runoff regimes, Rio Bueno, Jamaica. *Coral Reefs* **26**:129-145
- Mallela J, Perry CT, Haley MP (2004) Reef morphology and community structure along a fluvial gradient, Rio Bueno, Jamaica. *Caribbean Journal of Science* **40**:299-311
- Manzello D (2010) Coral growth with thermal stress and ocean acidification: lessons from the eastern tropical Pacific. *Coral Reefs* **29**:749-758
- Marshall AT, Clode P (2004) Calcification rate and the effect of temperature in a zooxanthellate and an azooxanthellate scleractinian reef coral. *Coral Reefs* **23**:218-224
- Martindale W (1976) *Calcareous encrusting organisms of the recent and Pleistocene reefs of Barbados, West Indies*. Ph.D thesis, University of Edinburgh, Scotland
- Marubini F, Atkinson MJ (1999) Effects of lowered pH and elevated nitrate on coral calcification. *Marine Ecology Progress Series* **188**:117-121
- Marubini F, Davies PS (1996) Nitrate increases zooxanthellae population density and reduces skeletogenesis in corals. *Marine Biology* **127**:319-328
- Marubini F, Ferrier-Pagés C, Cuif J-P (2003) Suppression of skeletal growth in scleractinian corals by decreasing ambient carbonate-ion concentration: a cross-family comparison. *Proceedings: Biological Sciences* **270**:179-184
- Marubini F, Thake B (1999) Bicarbonate addition promotes coral growth. *Limnology and Oceanography* **44**:716-720
- McClanahan, McField, Huitric, Bergman, Sala, Nyström, Nordemar, Elfving, Muthiga (2001) Responses of algae, corals and fish to the reduction of macroalgae in fished and unfished patch reefs of Glovers Reef Atoll, Belize. *Coral Reefs* **19**:367-379
- McClanahan TR, Muthiga NA (1989) Patterns of preedation on a sea urchin, *Echinometra mathaei* (de Blainville), on Kenyan coral reefs. *Journal of Experimental Marine Biology and Ecology* **126**:77-94
- McClenahan L, Hardt M, Jackson JBC, Cooke R (2010) Mounting evidence for historical overfishing and long-term degradation of Caribbean marine ecosystems: comment on Julio Baisre's "Setting a baseline for Caribbean fisheries". *Journal of Island and Coastal Archaeology* **5**:165-169
- McField MD (1999) Coral response during and after mass bleaching in Belize. *Bulletin of Marine Science* **64**:155-172
- Meesters EH, Knijn R, Willemsen P, Pennartz R, Roberts G, van Soest RWM (1991) Sub-rubble communities of Curaçao and Bonaire coral reefs. *Coral Reefs* **10**:189-197
- Moberg F, Folke C (1999) Ecological goods and services of coral reef ecosystems. *Ecological Economics* **29**:215-233
- Moore CH, Shedd WW (1977) Effective rates of sponge bioerosion as a function of carbonate production. In: Taylor DL (ed) *Proceedings of the 3rd International Coral Reef Symposium*, Miami, Florida, p 499-505
- Mumby PJ (2006) The impact of exploiting grazers (Scaridae) on the dynamics of Caribbean coral reefs. *Ecological Applications* **16**:747-769
- Mumby PJ, Dahlgren CP, Harborne AR, Kappel CV, Micheli F, Brumbaugh DR, Holmes KE, Mendes JM, Broad K, Sanchirico JN, Buch K, Box S, Stoffle RW, Gill AB (2006) Fishing, trophic cascades, and the process of grazing on coral reefs. *Science* **311**:98-101
- Mumby PJ, Foster NL, Glynn Fahy EA (2005) Patch dynamics of coral reef macroalgae under chronic and acute disturbance. *Coral Reefs* **24**:681-692
- Mumby PJ, Hastings A, Edwards HJ (2007) Thresholds and the resilience of Caribbean coral reefs. *Nature* **450**:98-101
- Mumby PJ, Steneck RS, Edwards AJ, Ferrari R, Coleman R, Harborne AR, Gibson JP (2012) Fishing down a Caribbean food web relaxes trophic cascades. *Marine Ecology Progress Series* **445**:13-24
- Nava H, Carballo JL (2008) Chemical and mechanical bioerosion of boring sponges from Mexican Pacific coral reefs. *Journal of Experimental Biology* **211**:2827-2831
- Neumann AC (1966) Observations on coastal bioerosion in Bermuda and measurements of boring rate of sponge *Cliona lampa*. *Limnology and Oceanography* **11**:92-99
- Odum HT, Odum EP (1955) Trophic structure and productivity of a windward coral reef community on Eniwetok Atoll. *Ecology* **25**:291-320
- Ogden JC (1977) Carbonate sediment production by parrotfish and sea urchins on Caribbean reefs: reef biota. *American Association of Petroleum Geologists* **4**:281-288
- Ong L, Holland K (2010) Bioerosion of coral reefs by two Hawaiian parrotfishes: species, size differences and fishery implications. *Marine Biology* **157**:1313-1323

- Paddock MJ, Reynolds JD, Aguilar C, Appeldoorn RS, Beets J, Burkett EW, Chittaro PM, Clarke K, Esteves R, Fonseca AC, Forrester GE, Friedlander AM, J. G-S, González-Sansón G, Jordan LKB, McClellan DB, Miller MW, Molloy PP, Mumby PJ, Nagelkerken I, Nemeth M, Navas-Camacho R, Pitt J, Polunin NVC, Reyes-Nivia MC, Robertson DR, Rodríguez-Ramírez A, Salas E, Smith SR, Spieler RE, Steele MA, Williams ID, Wormald CL, Watkinson AR, Côté IM (2009) Recent region-wide declines in Caribbean reef fish abundance. *Current Biology* **19**:1 - 6
- Pastorek RA, Bilyard GR (1985) Effects of sewage pollution on coral reef communities. *Marine Ecology Progress Series* **21**:175-189
- Perry CT (1998) Macroborers within coral framework at Discovery Bay, north Jamaica: species distribution and abundance, and effects on coral preservation. *Coral Reefs* **17**:277-287
- Perry CT (1999) Reef framework preservation in four contrasting modern reef environments, Discovery Bay, Jamaica. *Journal of Coastal Research* **15**:796-812
- Perry CT, Edinger EN, Kench PS, G. M, S.G. S, Steneck RS, Mumby PJ (2012) Estimating rates of biologically driven coral reef framework production and erosion: a new census-based carbonate budget methodology and applications to the reefs of Bonaire. *Coral Reefs* **31**:853-868
- Perry CT, Hepburn LJ (2008b) Syn-depositional alteration of coral reef framework through bioerosion, encrustation and cementation: Taphonomic signatures of reef accretion and reef depositional events. *Earth-Science Reviews* **86**:106-144
- Perry CT, Spencer T, Kench PS (2008) Carbonate budgets and reef production states: a geomorphic perspective on the ecological phase-shift concept. *Coral Reefs* **27**:853-866
- Peyrot-Clausade M, Hutchings P, Richard G (1992) Temporal variations of macroborers in massive *Porites lobata* on Moorea, French Polynesia. *Coral Reefs* **11**:161-166
- Pulitzer-Finali G (1986) A collection of West Indian Demospongiae (Porifera). In Appendix, a list of the Demospongiae hitherto recorded from the West Indies. *Estratto dagli Annali del Museo Civico di Storia Naturale di Genova* **86**:65-216
- Reynaud S, Leclercq N, Romaanie-Lioud S, Ferrier-Pagés C, Jaubert J, Gattuso JP (2003) Interacting effects of CO₂ partial pressure and temperature on photosynthesis and calcification in a scleractinian coral. *Global Change Biology* **9**:1660-1668
- Ries JB, Cohen AL, McCorkle DC (2009) Marine calcifiers exhibit mixed responses to CO₂-induced ocean acidification. *Geology* **37**:1131-1134
- Ries JB, Stanley SM, Hardie LA (2006) Scleractinian corals produce calcite, and grow more slowly, in artificial Cretaceous seawater. *Geology* **34**:525-528
- Risk MJ, MacGeachy JK (1978) Aspects of bioerosion of modern Caribbean reefs. *Revista De Biologia Tropical* **26**:85-125
- Risk MJ, Sammarco PW (1991) Cross-shelf trends in skeletal density of the massive coral *Porites lobata* from the Great Barrier Reef. *Marine Ecology Progress Series* **69**:195-200
- Risk MJ, Sammarco PW, Edinger EN (1995) Bioerosion in *Acropora* across the continental shelf of the Great Barrier Reef. *Coral Reefs* **14**:79-86
- Rogers CS (1990) Response of coral reefs and reef organisms to sedimentation. *Marine Ecology Progress Series* **62**:185-202
- Rose CS, Risk MJ (1985) Increase in *Cliona delitrix* infestation of *Montastraea cavernosa* heads on an organically polluted portion of the Grand Cayman fringing reef. *Marine Ecology* **6**:345-363
- Russo AR (1980) Bioerosion by two rock boring echinoids (*Echinometra mathaei* and *Echinostrephus aciculatus*) on Enewetak Atoll, Marshall Islands. *Journal of Marine Research* **38**:99-110
- Rützler K (1975) Role of burrowing sponges in bioerosion. *Oecologia* **19**:203-216
- Rützler K (2002) Impact of crustose clinoid sponges on Caribbean coral reefs. *Acta Geologica Hispanica* **37**:61-72
- Sadd JL (1984) Sediment transport and CaCO₃ budget on a fringing reef, Cane Bay, St. Croix, United States Virgin Islands. *Bulletin of Marine Science* **35**:221-238
- Sammarco PW (1982) Echinoid grazing as a structuring force in coral communities: Whole reef manipulations. *Journal of Experimental Marine Biology and Ecology* **61**:31-55
- Schiaparelli S, Giada F, Albertelli G, Cattaneo-Vietti R (2005) A nondestructive method to evaluate population structure and bioerosion activity of the boring bivalve *Gastrochaena dubia*. *Journal of Coastal Research* **21**:383-386
- Schönberg CHL (2002) Substrate effects on the bioeroding demosponge *Cliona orientalis*. 1. Bioerosion Rates. *Marine Ecology* **23**:313-326
- Schönberg CHL, Ortiz JC (2008) Is sponge bioerosion increasing? *Proceedings of the 11th International Coral Reef Symposium*, Fort Lauderdale, Florida

- Scoffin TP, Bradshaw C (2000) The taphonomic significance of endoliths in dead-versus live-coral skeletons. *Palaios* **15**:248-254
- Scoffin TP, Tudhope AW, Brown BE (1989) Fluorescent and skeletal density banding in *Porites lutea* from Papua New Guinea and Indonesia. *Coral Reefs* **7**:169-178
- Scott PJB (1985) Aspects of living coral associates in Jamaica. *Proceedings of the 5th International Coral Reef Symposium*, Tahiti
- Scott PJB, Moser KA, Risk MJ (1988) Bioerosion of concrete and limestone by marine organisms: A 13 year experiment from Jamaica. *Marine Pollution Bulletin* **19**:219-222
- Scott PJB, Risk MJ (1988) The effect of *Lithophaga* (Bivalvia: Mytilidae) boreholes on the strength of the coral *Porites lobata*. *Coral Reefs* **7**:145-151
- Sheppard CRC, Spalding M, Bradshaw C, Wilson S (2002) Erosion vs. recovery of coral reefs after 1998 El Niño: Chagos reefs, Indian Ocean. *Ambio* **31**:40-48
- Shulman MJ, Robertson DR (1996) Changes in the coral reefs of San Blas, Caribbean Panama: 1983 - 1990. *Coral Reefs* **15**:231-236
- Silverman J, Lazar B, Cao L, Caldeira K, Erez J (2009) Coral reefs may start dissolving when atmospheric CO₂ doubles. *Geophysical Research Letters* **36**:L05606
- Silverman J, Lazar B, Erez J (2007) Effect of aragonite saturation, temperature, and nutrients on the community calcification rate of a coral reef. *Journal of Geophysical Research* **112**:C05004
- Smith SV (1978) Coral reef area and contributions of reefs to processes and resources of the worlds oceans. *Nature* **273**:225-226
- Smith SV, Kinsey DW (1976) Calcium-carbonate production, coral reef growth and sea-level change. *Science* **194**:937-939
- Stearn CW, Scoffin TP (1977) Carbonate budget of a fringing reef, Barbados. *Proceedings of the 3rd International Coral Reef Symposium*, Miami, Florida
- Stearn CW, Scoffin TP, Martindale W (1977) Calcium carbonate budget of a fringing reef on the west coast of Barbados. Part 1: Zonation and Productivity. *Bulletin of Marine Science* **27**:479-510
- Steneck RS (1994) Is herbivore loss more damaging to reefs than hurricanes? Case studies from two Caribbean reef systems (1978-1988). In: Ginsburg RN (ed) *Global aspects of coral reefs: health, hazards and history*. University of Miami, Miami, Florida, USA, p C32-C37
- Stoddart DR (1985) Hurricane effects on coral reefs. In: Gabrie C, Toffart JL, Salvat B (eds) *Proceedings of the 5th International Coral Reef Symposium*, Tahiti, p 349-350
- Tomascik T, Sander F (1985) Effects of eutrophication on reef-building corals: I. Growth rate of the reef building coral *Montastraea annularis*. *Marine Biology* **87**:143-155
- Tribollet A, Atkinson MJ, Langdon C (2006) Effects of elevated pCO₂ on epilithic and endolithic metabolism of reef carbonates. *Global Change Biology* **12**:2200-2208
- Tribollet A, Decherf G, Hutchings PA, Peyrot-Clausade M (2002) Large-scale spatial variability in bioerosion of experimental coral substrates on the Great Barrier Reef (Australia): importance of microborers. *Coral Reefs* **21**:424-432
- Tribollet A, Godinot C, Atkinson M, Langdon C (2009) Effects of elevated pCO₂ on dissolution of coral carbonates by microbial euendoliths. *Global Biogeochemical Cycles* **23**:GB3008
- Tribollet A, Golubic S (2005) Cross-shelf differences in the pattern and pace of bioerosion of experimental carbonate substrates exposed for 3 years on the northern Great Barrier Reef, Australia. *Coral Reefs* **24**:422-434
- Tudhope AW, Risk MJ (1985) Rate of dissolution of carbonate sediments by microboring organisms, Davies Reef, Australia. *Journal of Sedimentary Petrology* **55**:440-447
- Tunncliffe VJ (1983) Caribbean staghorn coral populations: pre-Hurricane Allen conditions in Discovery Bay, Jamaica. *Bulletin of Marine Science* **33**:132-151
- Van Soest RWM (2001) Porifera. In: Costello MJ, Emblow C, White R (eds) *European register of marine species: a check-list of the marine species in Europe and a bibliography of guides to their identification*. Vol 50, p 85-103
- Vaughan TW (1916) The results of investigations of the ecology of the Floridian and Bahamaian shoal-water corals. *Proceedings of the National Academy of Sciences* **2**:95-100
- Vogel K, Gektidis M, Golubic S, Kiene WE, Radtke G (2000) Experimental studies on microbial bioerosion at Lee Stocking Island, Bahamas and One Tree Island, Great Barrier Reef, Australia: implications for paleoecological reconstructions. *Lethaia* **33**:190-204
- Ward-Paige CA, Risk MJ, Sherwood OA, Jaap WC (2005) Clionid sponge surveys on the Florida Reef Tract suggest land-based nutrient inputs. *Marine Pollution Bulletin* **51**:570-579
- Wilkinson C (2004) Status of coral reefs in the Northern Caribbean and Western Atlantic node of the GCRMN. In: Wilkinson C (ed) *Status of Coral Reefs of the World*

- Wilkinson CR (1987) Inter-ocean differences in size and nutrition of coral reef sponge populations. *Science* **236**:1654-1657
- Williams EH, Bartels PJ, Bunkley-Williams L (1999) Predicted disappearance of coral-reef ramparts: a direct result of major ecological disturbances. *Global Change Biology* **5**:839-845
- Williams ID, Polunin NVC (2001) Large-scale associations between macroalgal cover and grazer biomass on mid-depth reefs in the Caribbean. *Coral Reefs* **19**:358-366
- Wisshak M, Schönberg CHL, Form A, Freiwald A (2012) Ocean acidification accelerates reef bioerosion. *PLoS ONE* **7**:e45124
- Woodley JD, Chornesky EA, Clifford PA, Jackson JBC, Kaufman LS, Knowlton N, Lang JC, Pearson MP, Porter JW, Rooney MC, Rylaarsdam KW, Tunnicliffe VJ, Wahle CM, Wulff JL, Curtis ASG, Dallmeyer MD, Jupp BP, Koehl MAR, Neigel J, Sides EM (1981) Hurricane Allen's impact on Jamaican coral reefs. *Science* **214**:749-755
- Yates KK, Halley RB (2006) CO_3^{2-} concentration and pCO_2 thresholds for calcification and dissolution on the Molokai reef flat, Hawaii. *Biogeosciences Discussions* **3**:123-154
- Zubia M, Peyrot-Clausade M (2001) Internal bioerosion of *Acropora formosa* in Reunion (Indian Ocean): microborer and macroborer activities. *Oceanologica Acta* **24**:251-262

4

**Caribbean carbonate budgets:
responses to environmental
perturbation**

Kennedy EV, Perry CT, Halloran PR, Eakin CM, Fine M, Carricart-Ganivet JP, Iglesias-Prieto R, Wisshak M, Schönberg CHL, Form AU, Mumby PJ (2013)
Avoiding coral reef functional collapse requires local and global action
Current Biology **23**(10):912-918

4.1 Summary

Caribbean coral reefs face multiple anthropogenic threats, from pollution and overfishing, to the dual effects of greenhouse gas emissions: rising sea temperature and ocean acidification (Hoegh-Guldberg et al. 2007). Most reef functions are founded upon an ability to maintain a three-dimensional structure through net carbonate accumulation. This ability may be compromised by ecological disturbances, ultimately threatening reef structural resilience and associated ecosystem function (Perry et al. 2008a). Here, we integrate ecological models with carbonate budgets and drive their dynamics with the latest generation of climate models. We first reconstruct well-known ecological perturbations on Caribbean reefs and find that their combined impact can drive reefs into net erosional regimes. We then project the current state of reefs into the future and find that action is needed at both local and global scales to maintain positive carbonate budgets to at least 2100. Local action, including conservation of herbivorous fishes and avoidance of pollution, can delay the onset of reef loss by two decades under 'business as usual' greenhouse gas emissions, although the benefits will only work on the few remaining reefs with > 10% coral cover, and the duration is ecologically and socially trivial. A low carbon economy (RCP 2.6) is needed to ensure maintenance of reef structure and associated functionality.

4.2 Highlights

- Many Caribbean reefs are expected to experience continued structural decline by 2080
- Avoiding decline necessitates local management and significantly reduced CO₂ emissions
- Reconstructed carbonate budgets reveal high sensitivity to ecological perturbations
- Climate policy should aim for the most aggressive IPCC emission scenario (RCP2.6)

4.3 Introduction

Coral reefs provide a wealth of ecosystem services, including the provision of coastal protection, commercial fishing, tourism, animal protein, sand production and the highest biodiversity in the oceans (Knowlton et al. 2010). Many of these services are ultimately founded on the healthy functioning of living corals and the habitat structures they create. Through their growth, corals generate skeletons of calcium carbonate (limestone) that provide a natural breakwater and the complex three-dimensional habitat needed to sustain biodiversity. Erosion of this carbonate substrate generates sand accumulating on beaches and islands. The long-term maintenance of reef structures requires that the production of carbonate exceeds its rate of erosion; i.e., that the carbonate budget is positive (Perry et al. 2012). However, carbonate budgets are acutely threatened by the combined effects of climate change and local anthropogenic stressors (Perry et al. 2008b). Rates of coral production may decline because of a suite of detrimental processes including coral bleaching (Donner et al. 2005), ocean acidification (Hoegh-Guldberg et al. 2007), diseases (Harvell et al. 1999), and a reduction in reef resilience (Mumby et al. 2007). Further, rates of erosion are projected to increase as ocean acidification weakens coral skeletons (Manzello et al. 2008), and enhances the capacity of chemical bioerosion (Wisshak et al. 2012).

Here, we couple models of climate change, ecosystem dynamics and carbonate processes to ask whether reefs could shift to net erosional states, and consider how mitigative action at global and local scales might avoid this undesirable trajectory. We focus on Caribbean reefs for three reasons. Firstly, much of the pioneering research on carbonate budgets was carried out in this region (Stearn & Scoffin 1977, Land 1979, Hubbard et al. 1990, Perry et al. 2012), thereby providing a benchmark to develop models and gauge changes in budgets over recent decades. Secondly, the low diversity of this region simplifies the challenge of modelling reef dynamics and carbonate budgets (Mumby et al. 2007). Thirdly, Caribbean reefs have experienced profound levels of disturbance and degradation (Gardner et al. 2003) and (De'ath et al. 2012) there is an urgent need to understand future trajectories of ecosystem functioning.

Recent evidence suggests that Caribbean reefs have been losing architectural structure since the late 1970s (Fig. 4.1A) (Alvarez-Filip et al. 2009). These changes have been caused by widespread coral mortality, and whilst the drivers of mortality differ among sites, coral disease, hurricanes, overfishing, urchin die-off and episodic bleaching events have all contributed. To explore the implications of these well-documented ecological events on the dynamics of reef structures (Hoegh-Guldberg et al. 2007), we developed several characteristic scenarios (Fig. 4.1, A and C) ranging from 'healthy' intact ecosystems documented in the 1960s through to the present-day [model specification provided in supporting online material (SOM)]. Key

ecological events are: (i) depletion of reef fish by fishing; (ii) loss of large branching *Acropora*, primarily because of disease; (iii) plagues of the urchin *Diadema antillarum* when its predators were overfished; (iv) loss of *Diadema* because of disease; (v) poor watershed management leading to eutrophication, and (vi) on-going climate change from the 1960s onward. We also model the effects of recuperating some ecological processes through improved reef management or natural recovery (Hughes et al. 2010).

4.4 Methodology

A simulation model was created in Matlab (MATLAB 7.1, The MathWorks Inc., Natick, MA, 2000). Model parameters were drawn from published literature on Caribbean reefs, some unpublished data and climate data from IPCC AR5 earth system models (see Chapter 3 for full methodology). 115 parameters were defined in total, and each assigned a mean value and a standard deviation (Table 3.2, Chapter 3). Parameters included a wide range of ecological variables (e.g., mean *Diadema* test size, *Montastraea* abundance), physiological rates (e.g., linear extension rate of *Acropora*, bioerosion rate of azooxanthellate clionaid sponges in dead coral) and water quality parameters (e.g., aragonite saturation state, nitrate concentration). Shallow (6-8 m depth) fore-reef specific data were used wherever available. A full description of parameters can be found in Chapter 3, section 3.4 *Defining model parameters*.

4.4.1 Historical scenarios

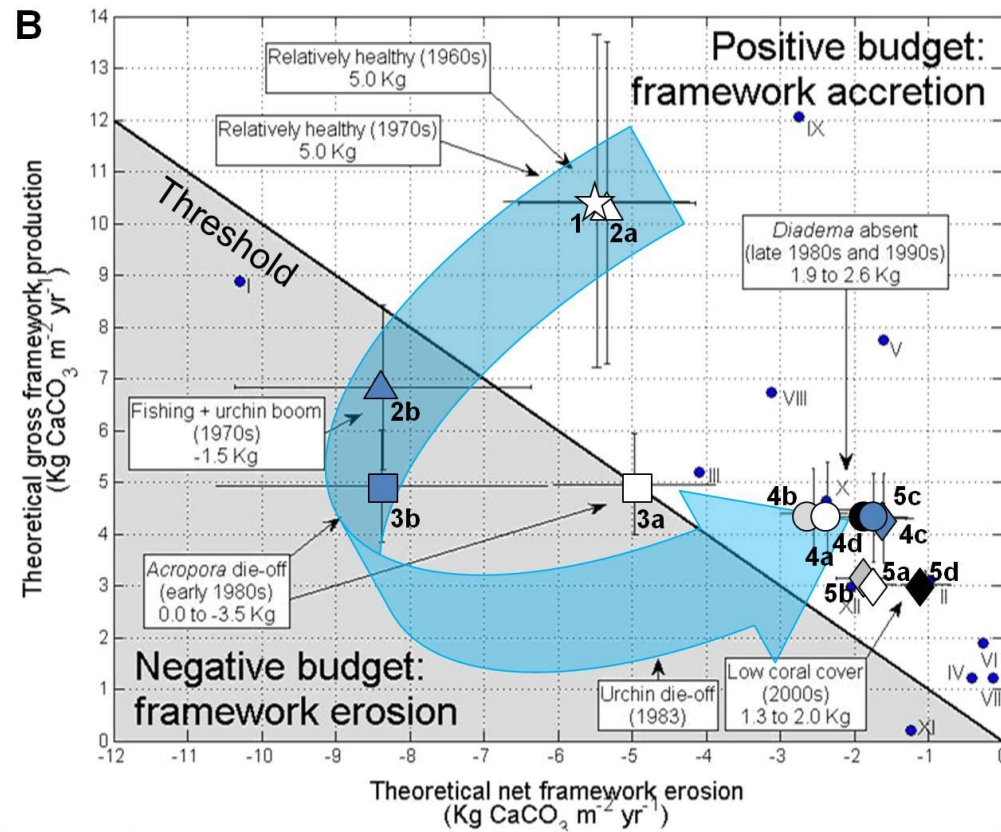
For each parameter, arguments were defined for a suite of ‘historical’ scenarios (Fig 4.1), named 1-5, representing decadal changes in Caribbean ecology. Parameter inputs were assigned a random value in each model run, generated from the normal distribution provided by the given mean and standard deviation (derived from published variability estimates). Some normal distributions were truncated. Each scenario was run 250 times, and data on the mean net production of calcium carbonate framework (in kg CaCO₃ m⁻² year⁻¹) generated, along with gross framework production, gross erosion and net erosion estimates (also in kg). Outputs were compared to published carbonate budgets (Fig 4.1). A sensitivity analysis was run with carbonate budget as the output variable, to identify factors important in driving the model. Adjustments were made to the script to correct for abnormalities, and the process repeated until we had confidence in the model inputs, processes and outputs. The model was then validated by testing its consistency to empirical published studies (Chapter 3, section 3.5).

4.4.2 Future forecasting

HadGEM-2ES (the Hadley Centre Global Environmental Model version 2 Earth System configuration) (Collins et al. 2011) AR5 climate model data for sea surface temperatures (SSTs)



Figure 4.1. Changes in Caribbean framework bioerosion vs. carbonate production over the past half century. **(A)** Photographs of Caribbean reefs typifying states of degradation used to inform the development of historical scenarios (1 to 5). From L-R: Scenario 1, a relatively healthy reef (considered typical of the 1960s/early 1970s) with high abundance and diversity of corals and fish; Scenario 2 (1970s) in some cases overfished; Scenario 3 (1970s/early 1980s), reefs have lost most branching Acroporids and are often heavily fished with reduced coral cover; Scenario 4, *Diadema* free reef with low coral cover and diversity from the mid-1980s to 1990s; Scenario 5, 2000s, a degraded reef with low coral cover. **(B)** Main plot displaying model generated outputs (scenarios 1 to 5), with mean net accretion values ($\text{kg CaCO}_3 \text{ m}^{-2} \text{ year}^{-1}$). Scenarios were run 250 times. Parameter values were varied randomly within set limits, based on stdevs. Arrow shows chronological trajectory of net reef budget states on Caribbean fore-reefs since the 1960's through to the present (2000's). For comparison, other published reef carbonate budgets from the Caribbean region are plotted. **(C)** Table lists plotted scenarios and their descriptors: '-' = absent, '+' = present, '++' = plague. *'Ac' = *Acropora*, 'Mo' = *Montastraea*.



Decade:	☆ 1960s	△ 1970s	□ 1980s	○ 1990s	◇ 2000s
State:	a 'healthy'	b polluted	c fished	d polluted + fished	● Published studies

Scenario	Historic era	Carbonate budget (Kg CaCO ₃ m ⁻² yr ⁻¹) and reef scenario description	Coral Cover (%)	Urchin abundance	Acropora cover	Parrotfish density	Nutrient (μmol l ⁻¹ NO ₃ ⁻)	Dominant coral*
1	1960s	5.0 Relatively healthy ecosystem	55	+	+	+	0.2	Ac
2a	1970s	5.0 Healthy ecosystem + 10 years climatic change	55	+	+	+	0.2	Ac
2b		-1.5 Healthy ecosystem + heavily fished	55	++	+	-	0.2	Ac
3a	early 1980s	-0.0 Acropora loss + lightly fished	30	+	-	+	0.2	Mo
3b		-3.5 Acropora loss + heavily fished	30	++	-	-	0.2	Mo
4a	mid 1980s and 1990s	2.1 <i>Diadema</i> die-off + lightly fished	25	-	-	+	0.2	Mo
4b		2.7 <i>Diadema</i> die-off + heavily fished	25	-	-	-	0.2	Mo
4c		1.9 <i>Diadema</i> die-off + polluted	25	-	-	+	0.4	Mo
4d		2.6 <i>Diadema</i> die-off + polluted and heavily fished	25	-	-	-	0.4	Mo
5a	2000s	1.3 Low coral cover + lightly fished	10	-	-	+	0.2	Mo
5b		2.0 Low coral cover + heavily fished	10	-	-	-	0.2	Mo
5c		1.3 Low coral cover + polluted	10	-	-	+	0.4	Mo
5d		2.0 Low coral cover + polluted and heavily fished	10	-	-	-	0.4	Mo

Published studies								
I	1977	1.4	Barbados, Bellairs Reef, fringing reef	37	Stearns & Scoffin, 1977			
II	1977	2.1	Jamaica, fore reef terrace (15m)	n/a	Moore & Shedd, 1977			
III	1979	1.1	Jamaica, Discovery Bay	3.1	Land, 1979			
IV	1990	0.9	St Croix, Cane Bay, fringing reef	10-50	Hubbard <i>et al.</i> , 1990			
V	1996	6.2	Bonaire, Karpata, reef slope (6-12m)	31	Bruggeman <i>et al.</i> , 1996			
VI	2007	1.2	Jamaica, Discovery Bay, clear water	13	Mallela & Perry, 2007			
VII	2007	1.9	Jamaica, Discovery Bay, polluted fringing reef	16	Mallela & Perry, 2007			
VIII	2012	3.6	Bonaire, leeward fringing reef, MPA (5m)	24	Perry <i>et al.</i> , 2012			
IX	2012	9.5	Bonaire, leeward MPA (10m), high complexity	28	Perry <i>et al.</i> , 2012			
X	2012	2.3	Bonaire, leeward fringing reef (10m)	25	Perry <i>et al.</i> , 2012			
XI	2012	-1.0	Bonaire, windward fringing reef (5m)	3	Perry <i>et al.</i> , 2012			
XII	2012	1.0	Bonaire, windward fringing reef (10m)	17	Perry <i>et al.</i> , 2012			

for the Caribbean Sea were retrieved for RCP 2.6 and 8.5, and compared to observational data from the HADSST2 data set for the same area (1870-2006). Model and observational data were time-averaged over the period 1970-2000, for which observations are known to be robust, and the difference calculated to provide the offset, which was then applied to the model data. Monthly alkalinity data averaged across the Caribbean area were derived from ‘corrected’ SST values. Model carbonate chemistry data were validated using Hawaii Ocean Time Series and Bermuda Atlantic Time Series. Aragonite saturation state (Ω_{ar}) and SST model forecasts (RCP 2.6 and RCP 8.5) were used to drive scenario 1 to 5 carbonate budget models into the future, with 140 model runs representing 6-monthly time steps between 2010 and 2080 populated with Ω_{ar} and SST data (Fig. 3.3, Chapter 3). Most other parameters remained fixed, according to scenario 1 (if driving a healthy reef into the future) or 5 (poor quality reef). The carbonate budget model was coupled to ReefMod (Mumby 2006, Edwards et al. 2011), an ecological model, allowing coral mortality and algal cover to be affected in a stepwise fashion and fed back into the carbonate budget model. Bleaching events were simulated when degree heating months (DHMs) accumulate (where anomaly exceeds 1°C). Carbonate budgets were estimated at six monthly intervals, from 2010 to 2080. Future forecasting simply measured the effects of climate change and overfishing on coral reefs.

4.5 Results

Although reef ecosystems were not pristine in the 1960s, our reconstruction of the environment and ecological structure yielded high mean rates of net carbonate production at 5.0 (± 3.2) kg $\text{CaCO}_3 \text{ m}^{-2} \text{ y}^{-1}$, and a maximum of 17.7 kg $\text{CaCO}_3 \text{ m}^{-2} \text{ y}^{-1}$ (Fig. 4.1B, scenario 1). All subsequent budgets will be expressed simply in kg. Moving forward to the 1970s, carbonate budgets show little difference when only greenhouse gas-driven changes in temperature and ocean acidification (OA) were added (Fig. 4.1B, scenario 2a). These hind-casted budgets of net reef carbonate production are almost identical to those rates measured in several classic studies from the 1970s, which found that Caribbean reefs existed in positive budgetary states, primarily because of high rates of production by the species *Acropora palmata* and *cervicornis*. Measured rates ranged from 4.5 kg (Stearn & Scoffin 1977) to 2.1 kg (Moore & Shedd 1977) in Barbados, and 1.1 kg in Jamaica (Land 1979). Similarly, a synthesis of regional fore-reef carbonate production measures from this period suggested that gross carbonate production rates in the region ranged from ~10-17 kg (Vecsei 2001).

Many reefs had already experienced heavy fisheries exploitation by the 1960s and 1970s, resulting in depauperate fish communities and plagues of urchins, that were freed from their predators (Hughes 1994). Under these circumstances, we found that the hyperabundance of bioeroding urchins shifted many reefs towards a net loss of reef structure (-1.5 kg; Fig. 4.1B, scenario 2b).

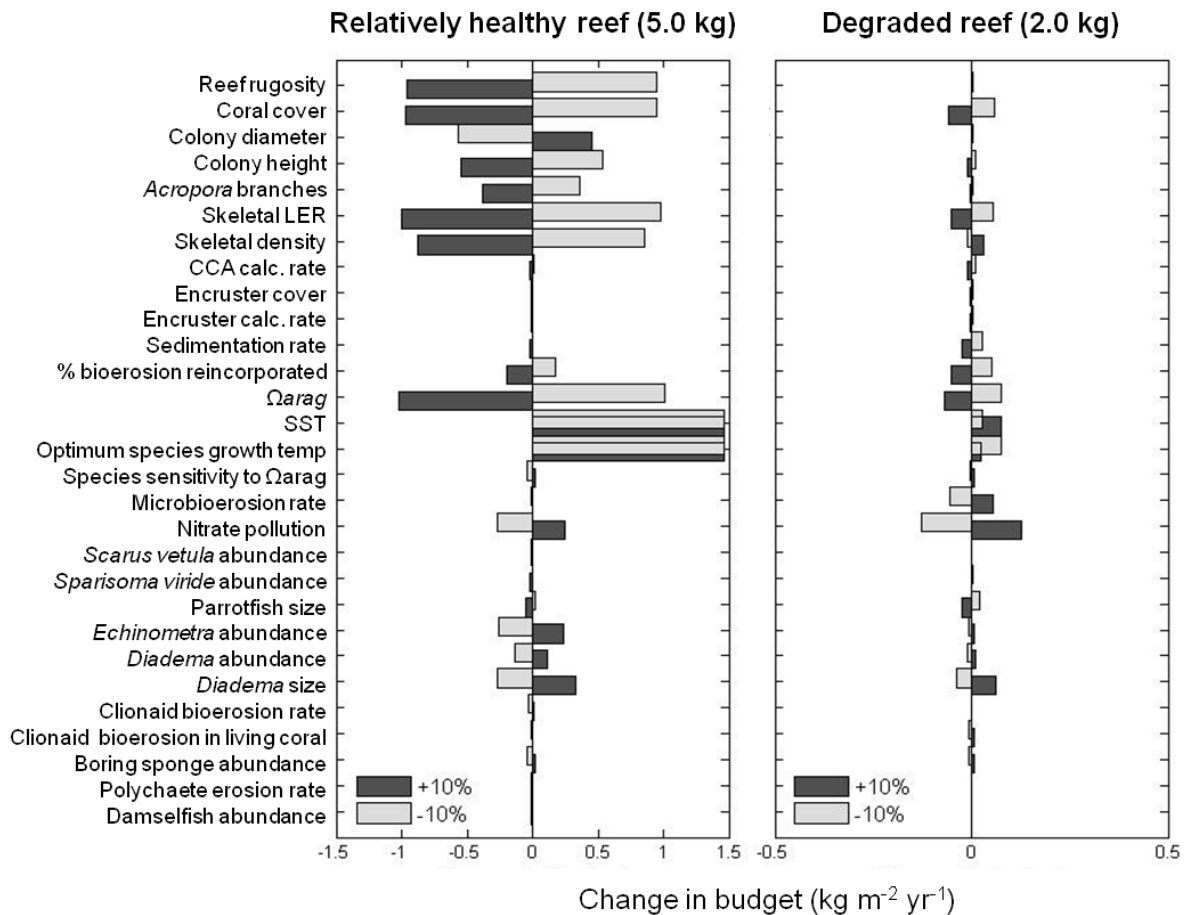


Figure 4.2. Sensitivity of model Caribbean reefs to simulated disturbance events. Absolute change in carbonate budget output (x-axis) brought about by 10% change in selected variable (y-axis). The model was tested using relatively healthy reef scenario 1 (55% coral cover, high urchin and fish densities), which generates a reference budget of 5.0 kg CaCO₃ m⁻² year⁻¹, and a present-day degraded Caribbean reef (10% coral cover, low diversity, few fish or urchins) accreting at 2.0 kg CaCO₃ m⁻² year⁻¹. Water quality parameters such as aragonite saturation state, sea surface temperature (SST) and nitrate content remain important determinants of carbonate budget. Note x-axes differ between panels.

In the 1980s two events shaped the ecology of Caribbean reefs dramatically. First, both species of the branching coral, *Acropora*, experienced region-wide decline because of white band disease. Our early 1980s scenarios reflect this event through significant reductions in net carbonate production, such that even lightly fished reefs were pushed close to carbonate equilibrium (Fig. 4.1B, scenario 3a, -0.01 kg). Fished reefs in the 1980s show the most negative budget of -3.5 kg, driven by high urchin bioerosion (-11.1 kg) and reduced coral productivity (2.6 kg). This budget is similar to that calculated on heavily exploited reefs in the tropical Eastern Pacific (-0.6 to -3.6 kg) (Eakin 1996): sites at which extensive reef structural disintegration was also documented.

The second major occurrence in the 1980s was the regional mass mortality of the urchin *D. antillarum* in 1983/4 (Lessios 1988). The modelled impact of this change was to drive carbonate budgets back into positive states, albeit with lower net accretion than in the 1960s because of the switch in dominant coral species towards slower-growing massive species and overall

reductions in coral cover (Fig. 4.1B, scenarios 4a-d). Although internal bioerosion doubled under polluted scenarios (Fig. 4.1B, scenarios 4c and d), the increase was insufficient to shift the system into net erosion (net budget +0.30 kg). Again modelled values of net carbonate (1.9 to 2.7 kg) were comparable to empirical estimates at the time, such as that from St Croix (0.9 kg) (Hubbard et al. 1990).

Net carbonate budgets in stylised reefs of the 1990s are positive but the decline in coral after bleaching events in 1998 and 2005 (Eakin et al. 2010) led to increasingly marginal carbonate production in the 2000s (Fig. 4.1B). However, although net production remained positive, it is important to recognise that absolute levels of carbonate production and bioerosion have declined, principally because of reduced coral production and a loss of urchin and sometimes parrotfish bioerosion. The ecosystem therefore has diminished fluxes of carbonate processes (Fig. 4.2). In accordance with previous decades, modelled budget estimates are comparable to recent studies from Jamaica (Mallela & Perry 2007) and exposed sites of Bonaire (Perry et al. 2012).

To identify how the key drivers of carbonate dynamics have changed over time, we ran model sensitivity analyses for the 'healthy' reefs of scenario 1a and unhealthy reefs of scenario 5d (Fig. 4.2). Each sensitivity analysis calculated the difference in budget associated with a $\pm 10\%$ change in the mean value of each of the 115 input variables. Healthy, coral-dominated reefs were most sensitive to changes in coral production brought about by variability in the physical drivers of calcification (sea surface temperature and carbonate saturation state) as well as intrinsic skeletal density and linear extension rate (Fig. 4.2). Once corals no longer dominated reefs, the system became less sensitive to drivers of calcification and responded to drivers of bioerosion such as nitrate level (a proxy for eutrophication), sponge bioerosion rate, and the size and abundance of urchins. Indeed, nitrate level was ranked the most important factor for degraded reef budgets such that a 10% increase led to a 33% decline in net carbonate production.

The maintenance of a positive carbonate budget is a fundamental pre-requisite to sustain many reef functions such as the provision of habitat for biodiversity and fisheries. To assess the action needed to sustain net carbonate production, we separated location interventions from global efforts to mitigate greenhouse gas emissions. Our first analysis considered the local action of protecting grazing parrotfishes which have been found to reduce levels of seaweed on fore-reefs (Mumby et al. 2006) and assist coral recovery (Mumby & Harborne 2010). We also contrasted a 'business as usual' scenario of greenhouse gas emissions (Representative Concentration Pathway, RCP 8.5) with a progressive move towards a low carbon economy (RCP 2.6). In this first analysis we assumed that the catastrophic losses of *Acropora* and the urchin *Diadema* persist and also compare the outlook for reefs with a 'relatively healthy' 20% coral cover and a

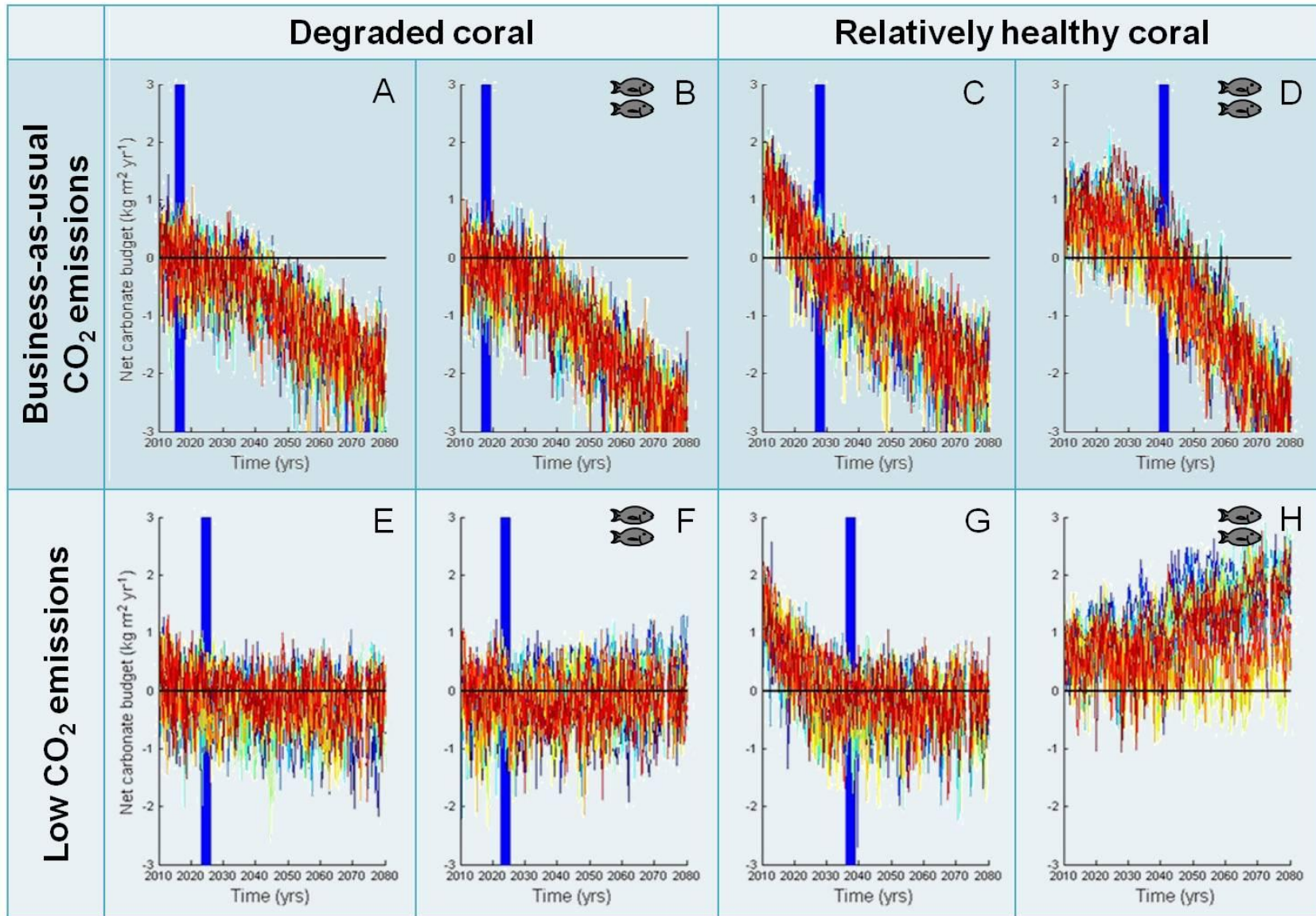


Figure 4.3. Future carbonate budgets of a stylised Caribbean fore-reef under climate change and ocean acidification. Degraded reefs begin with 10% coral cover whereas ‘healthy’ reefs have 20% coral cover. Top panels display RCP8.5 realistic climate scenarios and bottom panels RCP2.6 optimistic climate scenarios. Each plot displays 20 simulations. Blue lines indicate point at which the

Fish protected in marine reserves

more degraded 10% cover. While scope exists for coral adaptation to rising stress (Van Oppen et al. 2011), the extent of adaptation is uncertain (Mumby et al. 2011) and we make the conservative assumption of no adaptation.

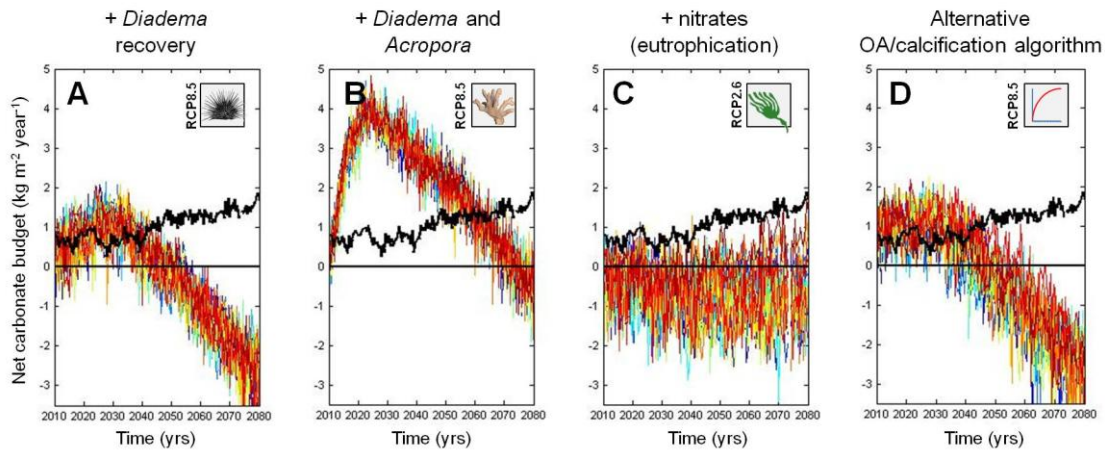


Figure 4.4. Alternative scenarios for future carbonate budgets. Plot comparing the effect of (A) simulated *Diadema* recovery, (B) combined *Diadema* and *Acropora* recovery, (C) chronic eutrophication event, and (D) alternative calcification effects with predicted future scenarios (black line shows original model output, mean of 20 runs: see Fig. 4.3, D and H).

Only one set of interventions maintained substantial positive carbonate budgets until the end of simulations in 2080: local maintenance of grazing by protecting parrotfishes and concerted global action to reduce greenhouse gas emissions (Fig. 4.3H). Moreover, clear positive budgets required reefs to start with relatively healthy coral as those starting with only 10% coral remained close to equilibrium (Fig. 4.3F). If greenhouse gas emissions follow the business as usual trend (RCP 8.5) then reefs eventually exhibit strong net erosion irrespective of local conservation measures (Fig. 4.3, A to D). However, conservation of parrotfish managed to delay the onset of net erosion by approximately a decade providing that the reef started with higher coral cover (Fig. 4.3, C and D). The non-linear benefit of parrotfish protection with initial coral cover occurred because of ecosystem hysteresis. For a given biomass of parrotfish a system with higher coral cover is more resilient, in part because higher coral cover intensifies grazing and reduces the cover of macroalgae, which are competitors of coral (Mumby et al. 2007). Under RCP 8.5, however, the increase in resilience is eventually overwhelmed by the frequency of coral bleaching.

The outlook for carbonate budgets improves when greenhouse gases are mitigated aggressively. Although only one scenario led to clear reef growth, the alternatives hovered above and below carbonate equilibrium (Fig. 4.3, E to G). The impact of parrotfish conservation on more degraded reefs clearly contrasts the positive role of herbivores in removing macroalgae with their 'negative' role in eroding reef substrate (Bruggeman 1994). When parrotfish stocks are heavily fished, rates of bioerosion are lower and net carbonate production is initially greater

(Fig. 4.1B, scenario 5a and b, Fig. 4.3, E and F). However, because coral cover declines rapidly in the functional absence of parrotfish, the long-term consequence of heavy fishing is worse for the reef because a decline in coral skeletal production leads to a lower overall carbonate budget (Fig. 4.3, E and F).

The benefits of local action are not confined to managing parrotfish. Nutrient availability affects both calcification and bioerosion (see Chapter 3), with eutrophication likely to be highly influential to the balance between carbonate production and destruction (Hallock 1988). We found qualitatively similar results simulating the effects of eutrophication in which an increase in nitrate concentration of $0.22 \mu\text{mol l}^{-1}$ prevented long-term net carbonate production even under RCP 2.6 (Fig. 4.4C). We also considered the potential impact of a full recovery of the fast-growing coral *A. cervicornis* and/or the urchin *Diadema* on fore-reefs at the modelled depth of 10 m. Recovery of either species is sufficient to allow positive reef growth even under RCP 8.5 (Fig. 4.4, A and B). Whether these key species make a full recovery is highly uncertain. Ambiguity also surrounds the effects of ocean acidification on coral net calcification and growth (Erez et al. 2011, Pandolfi et al. 2011). Most simulations assumed linear reductions in net calcification with falling aragonite saturation state. However, much less extreme reductions in calcification have also been reported (Gattuso et al. 1998). We repeated the business-as-usual greenhouse gas emissions but substituted a more benign impact of ocean acidification on net calcification (Fig. 4.4D). Although carbonate budgets improved, the overall result remained unchanged; even with parrotfish protection, no eutrophication, and an initial cover of 20% coral, carbonate budgets eventually became strongly negative.

The assessment and management of coral reefs has largely focused on ecological variables such as coral cover, coral size distribution, and fish abundance. Yet the ultimate goals of most management are founded on the functions delivered by reefs as three-dimensional geological structures. We propose that management directed towards positive carbonate budgets is a useful step towards realising both the biodiversity and livelihood goals of reef management. Our results suggest that local interventions are far from futile (Bradbury 2012), and indeed essential for assuring sustained ecosystem functioning. However, we also provide unambiguous evidence that local efforts must be accompanied by rigorous global action to mitigate climate change.

4.6 Conclusions

In this chapter, the models developed in Chapter 3 were employed to investigate Caribbean reef functioning in terms of carbonate production in the recent past and future. [A diverse range of scenarios were forecast to allow for uncertainty](#). Model outputs suggest that prevention of the structural collapse of coral reefs will require local action to avoid overfishing and pollution, along with concerted global action to reduce greenhouse gas concentrations.

During the process of data collection and model construction, gaps in the scientific knowledge – particularly concerning bioerosion rates – became apparent. Identification of these gaps could be beneficial in directing future research. Gaps highlighted included quantification of variations in sub-lethal responses among scleractinian taxa to Ω_{ar} and SST change, specifically in terms of density (linear extension often used as a proxy). Calcification responses of secondary carbonate producers also remain poorly quantified, with ambiguity still surrounding net responses of CCA to projected ocean acidification (Anthony et al. 2008, but also Nash et al. 2013). Although the geo-ecological model outputs suggest that the impact of rising Caribbean SST will outweigh those of OA, additional uncertainty surrounding synergistic effects of the dual effects of climate change. Lack of detailed data on response of bioeroders (with the exception of Clionaid; Wisshak et al. 2012) both directly to climate change and indirectly through alteration in substrate density have also hampered forecasting. Improved estimates of bioerosion rates, particularly for macro and micro-bioerosion, will become increasingly valuable as reefs become net-erosional, especially since responses to environmental perturbations are still not well understood. Construction of the model remains an ongoing process, and code can be updated and improved as new insights into coral reef functioning become available in the literature.

The production of the model itself (Chapter 3) has imparted a useful tool for exploring further patterns of reef growth, and can be taken in any number of future directions. Logical steps may include a more detailed examination of various parameters – particularly those identified as playing a critical role in net reef growth, such as *D. antillarum* size or abundance – the aim of exploring ecological relationships. The growing availability of empirical data on calcifier and bioeroder abundance following the launch of the ReefBudget project (doubling the number of published Caribbean field carbonate budgets; Perry et al. 2012), provides a unique opportunity: both to validate the model against the field studies, and to develop more specific carbonate budgets for individual reefs, possibly even projecting individual reef futures under climate and management scenarios (although care would have to be taken on the spatial scales of available climate data). Ultimately it could be developed into an online management tool for use by local reef workers to explore the effects of ecological relationships on reef functioning in their area.

4.6.1 Limitations

Parameterized and bounded using published empirical data (Chapter 3), the model allows for environmental stochasticity, and produces outputs that consistent with published Caribbean carbonate budgets (Fig. 4.1), giving us confidence in its predictive power. More recently, field studies have found that 21% of Caribbean reef sites are presently in net erosional states (n=19, range: -1.77 to -0.14 G), while a further 26% had positive budgets under 1 G, adding validity to historic conclusions (Perry et al. 2013). Another study by the same authors found that protected ‘No Dive Reserve’ sites in Bonaire had the most productive budgets, lending further credence to

the main conclusions of this chapter, that marine protected areas may (at least temporarily) assist with maintaining budgets (Perry et al. 2012). However, like any model, our theoretical model is only as good as the empirical data that it is founded on. Like many of the published reef carbonate budgets that came before it, this data could have flaws, and certainly has some gaps. Essentially it is a simplified version of a complex ecosystem, and necessarily contains assumptions. Real world environments may not respond predictably, meaning caution should always be taken when interpreting results.

One such model assumption is the inability of the seven scleractinian genera parameterised to acclimate or adapt to changing environmental conditions. Variation in the symbiont strains hosted by reef-building corals may affect calcification rates or bleaching susceptibility. Gaps in the knowledge regarding quantitative effects of hosting different strains on calcification rates currently make inclusion of symbionts in the model unfeasible. Subsequent chapters go on to explore symbiont diversity hosted by the most important contributor to reef calcification *M. annularis* (Chapter 5); to discuss this variation in terms of bleaching susceptibility (Chapter 7) and finally to link symbiont diversity to *M. annularis* calcification rates (Chapter 9).

4.7 References

- Alvarez-Filip L, Dulvy NK, Gill JA, Côté IM, Watkinson AR (2009) Flattening of Caribbean coral reefs: region-wide declines in architectural complexity. *Proceedings of the Royal Society B-Biological Sciences* **276**:3019-3025
- Anthony KRN, Kline DI, Diaz-Pulido G, Dove S, Hoegh-Guldberg O (2008) Ocean acidification causes bleaching and productivity loss in coral reef builders. *Proceedings of the National Academy of Sciences of the United States of America* **105**:17442-17446
- Bradbury RH (2012) *A world without coral reefs*. New York Times, Opinion pages
- Buggeman JH (1994) Foraging by the stoplight parrotfish *Sparisoma viride*. II. Intake and assimilation of food, protein and energy. *Marine Ecology Progress Series* **106**:57-71
- Collins WJ, Bellouin N, Doutriaux-Boucher M, Gedney N, Halloran P, Hinton T, Hughes J, Jones CD, Joshi M, Liddicoat S, Martin G, O'Connor F, Rae J, Senior C, Sitch S, Totterdell I, Wiltshire A, Woodward S (2011) Development and evaluation of an Earth-System model – HadGEM2. *Geoscientific Model Development* **4**:1051-1075
- De'ath G, Fabricius KE, Sweatman H, Puotinen M (2012) The 27-year decline of coral cover on the Great Barrier Reef and its causes. *Proceedings of the National Academy of Sciences USA* **109**:17995-17999
- Donner SD, Skirving WJ, Little CM, Oppenheimer M, Hoegh-Guldberg OVE (2005) Global assessment of coral bleaching and required rates of adaptation under climate change. *Global Change Biology* **11**:2251-2265
- Eakin CM (1996) Where have all the carbonates gone? A model comparison of calcium carbonate budgets before and after the 1982-1983 El Niño at Uva Island in the eastern Pacific. *Coral Reefs* **15**:109-119
- Eakin CM, Morgan JA, Heron SF, Smith TB, Liu G, Alvarez-Filip L, Baca B, Bartels E, Bastidas C, Bouchon C, Brandt M, Bruckner AW, Bunkley-Williams L, Cameron A, Causey BD, Chiappone M, Christensen TRL, Crabbe MJC, Day O, de la Guardia E, Diaz-Pulido G, DiResta D, Gil-Agudelo DL, Gilliam DS, Ginsburg RN, Gore S, Guzman HcM, Hendee JC, Hernandez-Delgado EA, Husain E, Jeffrey CFG, Jones RJ, Jordan-Dahlgren E, Kaufman LS, Kline DI, Kramer PA, Lang JC, Lirman D, Mallela J, Manfrino C, Marechal J-P, Marks K, Mihaly J, Miller WJ, Mueller EM, Muller EM, Orozco Toro CA, Oxenford HA, Ponce-Taylor D, Quinn N, Ritchie KB, Rodriguez Sn, Ramirez AR, Romano S, Samhoury JF, Sanchez JA, Schmahl GP, Shank BV, Skirving WJ, Steiner SCC, Villamizar E, Walsh SM, Walter C, Weil E, Williams EH, Roberson KW, Yusuf Y (2010) Caribbean Corals in Crisis: Record Thermal Stress, Bleaching, and Mortality in 2005. *PLoS ONE* **5**:e13969
- Erez J, Reynaud S, Silverman J, Schneider J, Allemand D (2011) Coral calcification under ocean acidification and global change. In: Dubinsky Z, Stambler N (eds) *Coral Reefs: An Ecosystem in Transition*. Springer, Berlin, p 151-176
- Gardner TA, Côté IM, Gill JA, Grant A, Watkinson AR (2003) Long-term region-wide declines in Caribbean corals. *Science* **301**:958-960
- Gattuso JP, Frankignoulle M, Wollast R (1998) Carbon and carbonate metabolism in coastal aquatic ecosystems. *Annual Review of Ecology and Systematics* **29**:405-434
- Hallock P (1988) The role of nutrient availability in bioerosion: Consequences to carbonate buildups. *Palaeogeography, Palaeoclimatology, Palaeoecology* **63**:275-291
- Harvell CD, Kim K, Burkholder JM, Colwell RR, Epstein PR, Grimes DJ, Hofmann EE, Lipp EK, Osterhaus ADME, Overstreet RM, Porter JW, Smith GW, Vasta GR (1999) Emerging marine diseases - climate links and anthropogenic factors. *Science* **285**:1505-1510
- Hoegh-Guldberg O, Mumby PJ, Hooten AJ, Steneck RS, Greenfield P, Gomez E, Harvell CD, Sale PF, Edwards AJ, Caldeira K, Knowlton N, Eakin CM, Iglesias-Prieto R, Muthiga N, Bradbury RH, Dubi A, Hatzitolos ME (2007) Coral reefs under rapid climate change and ocean acidification. *Science* **318**:1737-1742
- Hubbard DK, Miller AI, Scaturro D (1990) Production and cycling of calcium-carbonate in a shelf-edge reef system (St. Croix, United States Virgin Islands): applications to the nature of reef systems in the fossil record. *Journal of Sedimentary Petrology* **60**:335-360
- Hughes TP (1994) Catastrophes, phase-shifts and large-scale degradation of a Caribbean coral reef. *Science* **265**:1547-1551
- Hughes TP, Graham NAJ, Jackson JBC, Mumby PJ, Steneck RS (2010) Rising to the challenge of sustaining coral reef resilience. *Trends in Ecology and Evolution* **25**:633-642
- Knowlton N, Brainard RE, Fisher R, Moews M, Plaisance L, Caley MJ (2010) Coral Reef Biodiversity, Chapter 4. In: McIntyre A (ed) *Life in the World's Oceans*. Wiley-Blackwell

- Land LS (1979) Fate of reef-derived sediment on the north Jamaican island slope. *Marine Geology* **29**:55-71
- Lessios HA (1988) Mass mortality of *Diadema antillarum* in the Caribbean: what have we learned? *Annual Review of Ecology and Systematics* **19**:371-393
- Mallela J, Perry CT (2007) Calcium carbonate budgets for two coral reefs affected by different terrestrial runoff regimes, Rio Bueno, Jamaica. *Coral Reefs* **26**:129-145
- Manzello DP, Kleypas JA, Budd DA, Eakin CM, Glynn PW, Langdon C (2008) Poorly cemented coral reefs of the eastern tropical Pacific: Possible insights into reef development in a high-CO₂ world. *Proceedings of the National Academy of Sciences* **105**:10450-10455
- Moore CH, Shedd WW (1977) Effective rates of sponge bioerosion as a function of carbonate production. In: Taylor DL (ed) *Proceedings of the 3rd International Coral Reef Symposium*, Miami, Florida, p 499-505
- Mumby PJ, Dahlgren CP, Harborne AR, Kappel CV, Micheli F, Brumbaugh DR, Holmes KE, Mendes JM, Broad K, Sanchirico JN, Buch K, Box S, Stoffle RW, Gill AB (2006) Fishing, Trophic Cascades, and the Process of Grazing on Coral Reefs. *Science* **311**:98-101
- Mumby PJ, Elliott IA, Eakin CM, Skirving W, Paris CB, Edwards HJ, Enríquez S, Iglesias-Prieto R, Cherubin LM, Stevens JR (2011) Reserve design for uncertain responses of coral reefs to climate change. *Ecology Letters* **14**:132-140
- Mumby PJ, Harborne AR (2010) Marine Reserves Enhance the Recovery of Corals on Caribbean Reefs. *PLoS ONE* **5**:e8657
- Mumby PJ, Hastings A, Edwards HJ (2007) Thresholds and the resilience of Caribbean coral reefs. *Nature* **450**:98-101
- Nash MC, Opdyke BN, Troitzsch U, Russell BD, Adey WH, Kato A, Diaz-Pulido G, Brent C, Gardner M, Prichard J, Kline DI (2013) Dolomite-rich coralline algae in reefs resist dissolution in acidified conditions. *Nature Climate Change* **3**:268-272
- Pandolfi JM, Connolly SR, Marshall DJ, Cohen AL (2011) Projecting coral reef futures under global warming and ocean acidification. *Science* **333**:418-422
- Perry CT, Edinger EN, Kench PS, G. M, S.G. S, Steneck RS, Mumby PJ (2012) Estimating rates of biologically driven coral reef framework production and erosion: a new census-based carbonate budget methodology and applications to the reefs of Bonaire. *Coral Reefs* **31**:853-868
- Perry CT, Murphy GN, Kench PS, Smithers SG, Edinger EN, Steneck RS, Mumby PJ (2013) Caribbean-wide decline in carbonate production threatens coral reef growth. *Nature Communications* **4**:1402
- Perry CT, Spencer T, Kench PS (2008a) Carbonate budgets and reef production states: A geomorphic perspective on the ecological phase-shift concept. *Coral Reefs* **27**:853-866
- Perry CT, Spencer T, Kench PS (2008b) Carbonate budgets and reef production states: a geomorphic perspective on the ecological phase-shift concept. *Coral Reefs* **27**:853-866
- Roff G, Mumby PJ (2012) Global disparity in the resilience of coral reefs. *Trends in Ecology and Evolution* **27**:404-413
- Stearn CW, Scoffin TP (1977) Carbonate budget of a fringing reef, Barbados. *Proceedings of the 3rd International Coral Reef Symposium*, Miami, Florida
- Van Oppen MJH, Souter P, Howells EJ, Heyward A, Berkelmans R (2011) Novel genetic diversity through somatic mutations: fuel for adaptation of reef corals? *Diversity* **3**:405-423
- Vecsei A (2001) Fore-reef carbonate production: development of a regional census-based method and first estimates. *Palaeogeography Palaeoclimatology Palaeoecology* **175**:185-200
- Wisshak M, Schönberg CHL, Form A, Freiwald A (2012) Ocean acidification accelerates reef bioerosion. *PLoS ONE* **7**:e45124

5

Biogeographic patterns of distribution and diversity of *Symbiodinium* in *Montastraea annularis* inhabiting shallow Caribbean reefs

5.1 Introduction

The obligate symbiosis that exists between scleractinian corals and their unicellular dinoflagellate endosymbionts is undoubtedly the most fundamental inter-species association on a coral reef. This symbiosis forms the basis of a diverse and productive ecosystem, allowing tropical coral reefs to not only *exist* (by part-way solving Darwin's paradox), but to *persist* over time scales of several millions of years (LaJeunesse et al. 2004, Van Oppen and Gates 2006) and to flourish in oligotrophic tropical waters all over the world. The mutualism is productive in terms of generating organic compounds (symbiotic zooxanthallae account for 50-70% of total reef primary production; Muscatine and Porter 1977), but equally importantly promotes host calcium carbonate skeletal deposition, helping create the greatest bioconstruction in the world – the three-dimensional structural reef framework (described in Chapters 2 and 4). The resilience of the coral-endosymbiont relationship in the face of environmental change could be key to the fate of reefs in a rapidly changing world (Hoegh-Guldberg 1999, Baker et al. 2004). As a consequence, it has become necessary to consider the core living component of reefs – the coral – not as a stand-alone organism, but as a coral-endosymbiont 'holobiont' (Ortiz 2008).

Thanks to the advent of molecular genetics, endosymbiotic dinoflagellates – once thought to be a single pandemic species, *Symbiodinium microadriticum* (Freudenthal 1962) – are now known to number in excess of 400 taxa (the largest dinoflagellate group known to science). Nested within nine cladal groups (A-I), *Symbiodinium* have a genetic disparity comparable to distinct genera of free-living dinoflagellates (Rowan and Powers 1991a, Coffroth 2005, Pochon and Gates 2010). Scleractinian corals are predominantly associated with clade C, but also with A, D, F, G and, particularly in the Caribbean, B (LaJeunesse 2002). Although the molecular systematics are still decidedly blurred and ecologically relevant units of diversity still debated (LaJeunesse and Thornhill 2011), the genetic markers currently used for identification – nuclear ribosomal genes ITS1 and 2, SSU and LSU, mitochondrial cytochrome b, chloroplast 23s rDNA (Sampayo et al. 2009) and plastid psbA (LaJeunesse and Thornhill 2011) – are thought to be

capable of resolving reproductively isolated lineages. Mapping the distribution of these lineages has revealed major partitions based on geography (LaJeunesse et al. 2004), bathymetry, habitat and host (Finney et al. 2010), with further divisions driven by local environmental factors such as irradiance (Rowan et al. 1997), turbidity (Garren et al. 2006), salinity, temperature, coral ontogeny and stress. Observed partitioning, along with experimental manipulations, have allowed the formation of hypotheses concerning the various physiological traits of *Symbiodinium* operational taxonomic units (OTUs). It is thought that variation among OTUs may expand the functional diversity of the intact symbiotic association (holobiont). Importantly, some clades appear to have elevated thermal tolerance which can infer bleaching resistance to the coral holobiont (Berkelmans and van Oppen 2006). Coral bleaching, a phenomena first observed in the 1980's, involves a decoupling of the coral-endosymbiont relationship, through damage and/or loss of chlorophyll from within the alga (Warner et al. 1999), causing a waning in pigmentation, a drop in photosynthesis and calcification, increase in disease susceptibility and, depending on the duration and severity of the bleaching, partial or total mortality (Fitt et al. 2001, Buddemeier et al. 2004). Occurrences of bleaching have been increasing globally in both frequency and intensity, and temperature driven stress-induced coral bleaching, driven by global climate change, is now believed to be the single biggest threat facing reefs today (Hoegh-Guldberg et al. 2007). In 2005 the Caribbean experienced the most severe bleaching event on record, with over 80% of corals bleaching (Wilkinson and Souter 2008, Eakin et al. 2010). Our understanding of *Symbiodinium* diversity and it's ecological significance has direct consequences for reef conservation efforts under global climate change (Hoegh-Guldberg 1999).

Partitioning of *Symbiodinium* diversity has been observed at a range of spatial scales, from biogeographic (e.g., clade C dominates Pacific communities, while B and C share dominance in the Atlantic-Caribbean; LaJeunesse 2005, Finney et al. 2010), to latitudinal (B is typically found in high latitude environments; Rodriguez-Lanetty et al. 2001), to reef scale (symbiont communities commonly differ in adjacent inner vs. outer reef environments; LaJeunesse et al. 2004, Garren et al. 2006, LaJeunesse et al. 2010), to environmental gradients on a single reef as a function of depth or host (Baker 2003). By controlling for variables such as species (i.e., by focussing on a single host) and colony depth (sampling at <15 m), this study attempts to elucidate biogeographic patterns of *Symbiodinium* ITS2 (LaJeunesse 2001) diversity inhabiting shallow water corals across the Caribbean region. The *Montastraea annularis* species complex is the dominant coral in the tropical Western Atlantic in terms of distribution, abundance and scientific focus (Knowlton et al. 1992). As hermaphroditic broadcast spawners, all *Montastraea* species acquire their *Symbiodinium* horizontally – from the ocean environment – rather than inheriting them vertically, from parent to offspring (Leviton et al. 2004). Several studies have set out to catalogue the diversity of endosymbionts hosted by this key ecosystem engineer. *M. annularis* appears to be one of the most flexible coral hosts known in terms of symbiont

specificity, readily associating with a range of sub-cladal types, as well as showing substantial intra-colony zonation (Rowan et al. 1997).

In this chapter, I describe the geographic distribution of *M. annularis* endosymbiont communities across the Caribbean, at >30 shallow water sites stretching ~3,000 km from Barbados in the east to Belize in the west, and ~1,800 km from the Bahamas in the north, to Columbia in the south. Fundamental “gaps in the knowledge” regarding coral-endosymbiont relationships exist (Stat and Gates 2011), partly due to our relatively limited (albeit increasing) understanding of *Symbiodinium* ITS2 diversity and geographic distribution (LaJeunesse et al. 2004). Although much is already known about the *Symbiodinium* communities hosted by *M. annularis*, the large size and geographic spread of the dataset, along with the level of taxonomic resolution to which symbionts are catalogued in this study, offers new insights into arguably one of the most important symbiotic relationships on the planet. By helping elucidate emerging biogeographic patterns, the data will reinforce current understanding of coral reef resilience, and will contribute critical new information about *Symbiodinium* ITS2 diversity in the Caribbean’s most important coral. We hope the results will bolster current understanding by helping elucidate emerging biogeographic patterns, or contribute new information about *Symbiodinium* ITS2 diversity in the Caribbean’s most important coral.

5.2 Chapter aims

The aims of this chapter are twofold: the first is to describe local and Caribbean-wide community diversity, by cataloguing the communities of zooxanthellae hosted by shallow-water *M. annularis* across its Caribbean range to sub-cladal level. The second goal is to determine whether these symbiont communities exhibit any significant form of spatial structuring. This is achieved using analyses designed for spatial count data to identify local clustering patterns, to establish Caribbean-wide trends and to test for spatial associations between clades.

5.2.1 Aim 1: Characterising *Symbiodinium* communities in *M. annularis*

M. annularis is a species capable of hosting dynamic, multi-taxa communities of algal symbionts (Rowan et al. 1997). The widely acknowledged hypothesis that individual coral species were populated exclusively with a single *Symbiodinium* taxon (Trench 1993, Goulet 2007) was challenged when, along with other corals and invertebrates, it was demonstrated that *M. annularis* readily associated with four genetically distinct taxon: A, B, C and D (Rowan and Knowlton 1995, Rowan et al. 1997, Toller et al. 2001a). Regionally endemic *Symbiodinium* B (along with the less commonly occurring A) tend to be hosted by *M. annularis* in high-light environments (e.g., unshaded colony tops), while C was found in habitats with lower irradiance, typically in deeper reef areas or on the shaded sides of colonies (Rowan et al. 1997, Toller et al. 2001a). Not only has *M. annularis* proved capable of hosting a variety of zooxanthellae clades,

but the species is also frequently found harbouring multiple taxa at any one time (Rowan et al. 1997), with mixed A/C and B/C samples occurring at intermediate depths. *M. annularis* has additionally been observed to experience change in the composition of the symbiont communities, particularly during severe bleaching events (Toller et al. 2001b). More recent studies - from Barbados (LaJeunesse et al. 2009, Finney et al. 2010), Belize (Warner et al. 2006, Finney et al. 2010), the Florida Keys and the Bahamas (Thornhill et al. 2009) (see Table 5.1) – have been able to further resolve ‘species’ differences, identifying a total of 11 sub-cladal types that commonly associated with *M. annularis*. These studies showed *Symbiodinium* B1 to be the most prevalent sub-clade, occurring across the coral’s entire latitudinal range, while A13 and D1a (associated with acute thermal stress) were described as occurring at low and variable abundances.

As the sample size and geographic coverage of this study is considerably greater than any published study on *M. annularis* to date, and as *M. annularis* symbioses are thought to remain fairly stable over time (Toller et al. 2001b, Warner et al. 2006, Thornhill et al. 2006a but also see Chapter 8), it was predicted that the full range of *Symbiodinium* variety (as listed in Table 5.1) would be catalogued, and that *M. annularis* individuals would likely host multiple cladal types. As only shallow water corals (all sampling was carried out at an average depth of 5.95 m) were surveyed, we expected a substantial proportion of the symbiont communities to comprise *Symbiodinium* B, with C types occurring less frequently, and sporadic occurrences of D1a and A13.

H_0 = The *Symbiodinium* diversity hosted by *M. annularis* will not significantly differ from a null distribution of ITS2 types characterised in earlier studies on ITS2 diversity (e.g., Fig. 5.1). *M. annularis* from the Caribbean sea and Bahamas are expected to associate with a range of symbiont types from four clades, including A13, B1, B10, B17, B1j, C1, C12, C3, C7, C12 and D1a. Communities will be dominated largely by *Symbiodinium* B clades > C clades, and D1a and A13 will occur less frequently.

H_1 = The *Symbiodinium* diversity hosted by *M. annularis* will differ from previous studies on the holobiont. This may be a) because of temporal instability in *Symbiodinium* communities (evidence from Thornhill et al. 2006a show this unlikely) or b) due to the lack of coverage of previous studies.

H_0 = *M. annularis* will typically be associated with just one zooxanthalla clade (Goulet 2006).

H_1 = A major proportion of corals sampled will associate with more than one cladal type.

5.2.2 Aim 2: Exploring spatial patterning in symbiont communities across the Caribbean and Bahamas

Symbiodinium communities show clear evidence of biogeographic partitioning at spatial scales ranging from oceanic (e.g., Pacific vs. Atlantic; LaJeunesse 2005), to regional (along a latitudinal gradient; Rodriguez-Lanetty et al. 2001, LaJeunesse et al. 2004); and between reefs (back reef vs. fore reef, offshore vs lagoonal; LaJeunesse et al. 2004, Thornhill et al. 2009, LaJeunesse et al. 2010), colonies (Warner et al. 2006) and within colonies (Rowan et al. 1997). Despite this, *Symbiodinium* B has repeatedly been shown to be the dominant symbiont in *M. annularis* at sites across nearly the entire latitudinal range of the tropical western Atlantic, from the Bahamas (LaJeunesse 2002) to Panama (Rowan et al. 1997, Garren et al. 2006). Although *Symbiodinium* C is frequently hosted by *M. annularis*, unless co-dominant with B types these occurrences are almost exclusively in deeper reef habitats (i.e., >10-15 m) (LaJeunesse et al. 2009, Finney et al. 2010), most likely due to C's low tolerance to irradiance (Rowan et al. 1997). As this study is primarily concerned with geographic rather than bathymetric distribution of *Symbiodinium*, I chose to focus on shallow water colonies only. The current known geographic spread of different types does not provide conclusive evidence for spatial patterning (Fig. 5.1) within *M. annularis*. It seems unlikely that symbiont communities exhibit any form of spatial structuring at the sampling depth (~6 m), and subsequently we might expect to observe an almost uniform distribution of *Symbiodinium* B dominated communities across the *M. annularis* range (H_0).

- a. H_0 = Symbiont communities hosted by *M. annularis* exhibit spatial heterogeneity across the Caribbean region – distribution is not different from random. *Symbiodinium* B dominates communities.
- b. H_1 = Symbiont communities exhibit some degree of spatial structuring across the Caribbean, based on previous studies showing *M.annularis* hosting markedly different symbiont communities in Panama and Belize (Garren et al. 2006).

This chapter describes inter-colony variation in *Symbiodinium* ITS2 types, before examining inter-site variation. Intra-colony variation is also investigated.

Clade	ITS2 type	Genbank accession number	Locations sampled	Depth (m)		Pseudonyms	Published references
				Min	Max		
A	A13	AF333504	Barbados	0	15	A1.1; <i>Symbiodinium cariborum</i>	LaJeunesse <i>et al.</i> 2009
B	B1	AF333511	Bermuda; US Virgin Islands; Barbados; Bahamas; Florida	0	15	<i>Symbiodinium pulchrorum</i> ; <i>S. bermudense</i>	Savage <i>et al.</i> 2002; Correa <i>et al.</i> 2009; Finney <i>et al.</i> 2010; LaJeunesse, 2002; Thornhill <i>et al.</i> 2006; Thornhill <i>et al.</i> 2009
	B10	AF499787	Florida	3	4		Thornhill <i>et al.</i> 2009
	B17	AY074987	Panama	-	-		Savage <i>et al.</i> 2002
	B1j	GU907637	Barbados	0	10		Finney <i>et al.</i> 2010; LaJeunesse <i>et al.</i> 2009
C	C1	AF333515	US Virgin Islands	4	8	<i>Symbiodinium goreau</i>	Correa <i>et al.</i> 2009
	C3	AF499789	US Virgin Islands; Bahamas; Florida; Belize	1	4		Warner <i>et al.</i> 2006; Correa <i>et al.</i> 2009; LaJeunesse, 2002; Thornhill <i>et al.</i> 2006; Thornhill <i>et al.</i> 2009
	C7	AF499797	US Virgin Islands; Barbados; Belize	0	20		Warner <i>et al.</i> 2006; Correa <i>et al.</i> 2009; Finney <i>et al.</i> 2010; LaJeunesse <i>et al.</i> 2009
	C12	AF499801	Bahamas; Barbados	12	15	C7a	Thornhill <i>et al.</i> 2006; Thornhill <i>et al.</i> 2009; Finney <i>et al.</i> 2010; LaJeunesse <i>et al.</i> 2009
D	D1	AF334660	US Virgin Islands; Belize; Bahamas; Barbados; Florida	1	15		LaJeunesse <i>et al.</i> 2001; Correa <i>et al.</i> 2009; Finney <i>et al.</i> 2010; LaJeunesse 2002; Thornhill <i>et al.</i> 2006; LaJeunesse <i>et al.</i> 2009
	D1-4	AF499802	Bahamas; US Virgin Islands; Belize; Barbados; Florida	1	15	<i>Symbiodinium trenchii</i> Also known as D1b, D5, D1a	LaJeunesse 2002; Correa <i>et al.</i> 2009; Finney <i>et al.</i> 2010; LaJeunesse <i>et al.</i> 2009; Thornhill <i>et al.</i> 2006.

Table 5.1: Catalogue of known *Symbiodinium* diversity (based on ITS2 molecular marker) in the Caribbean *Montastraea annularis*

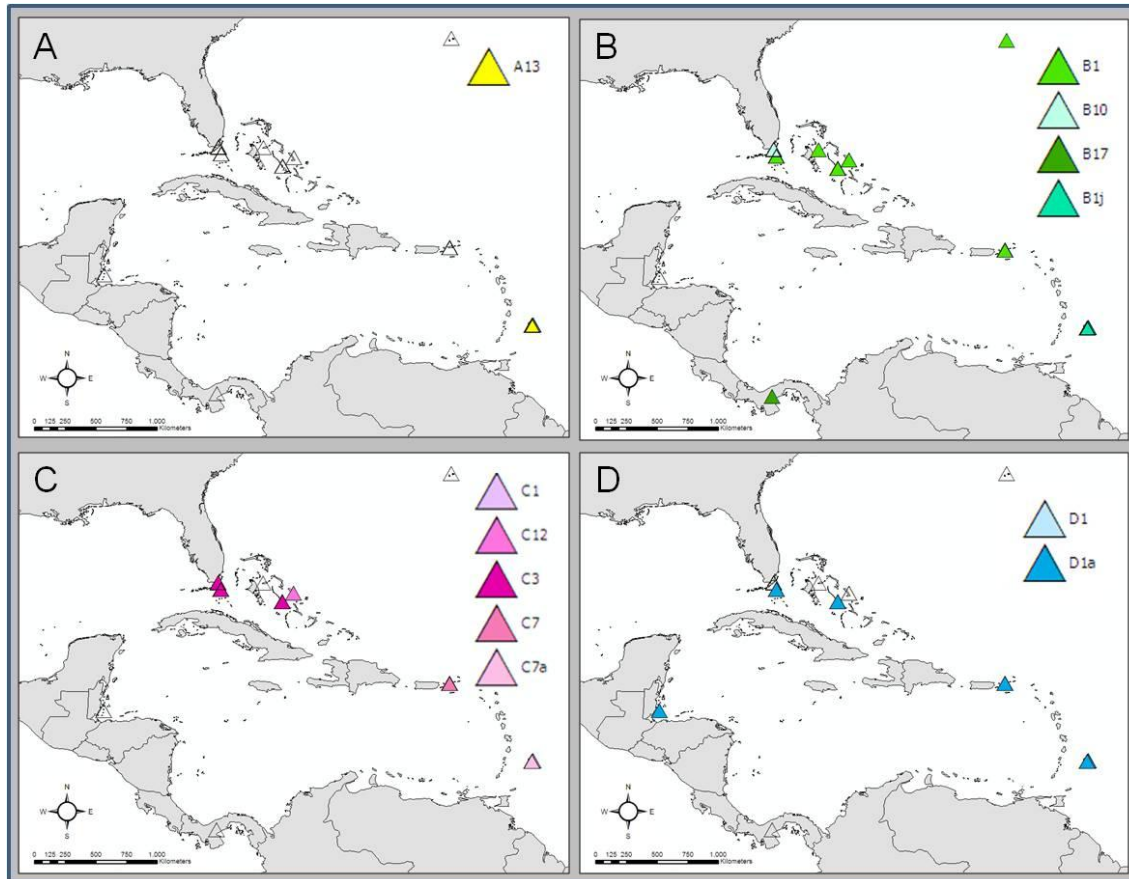
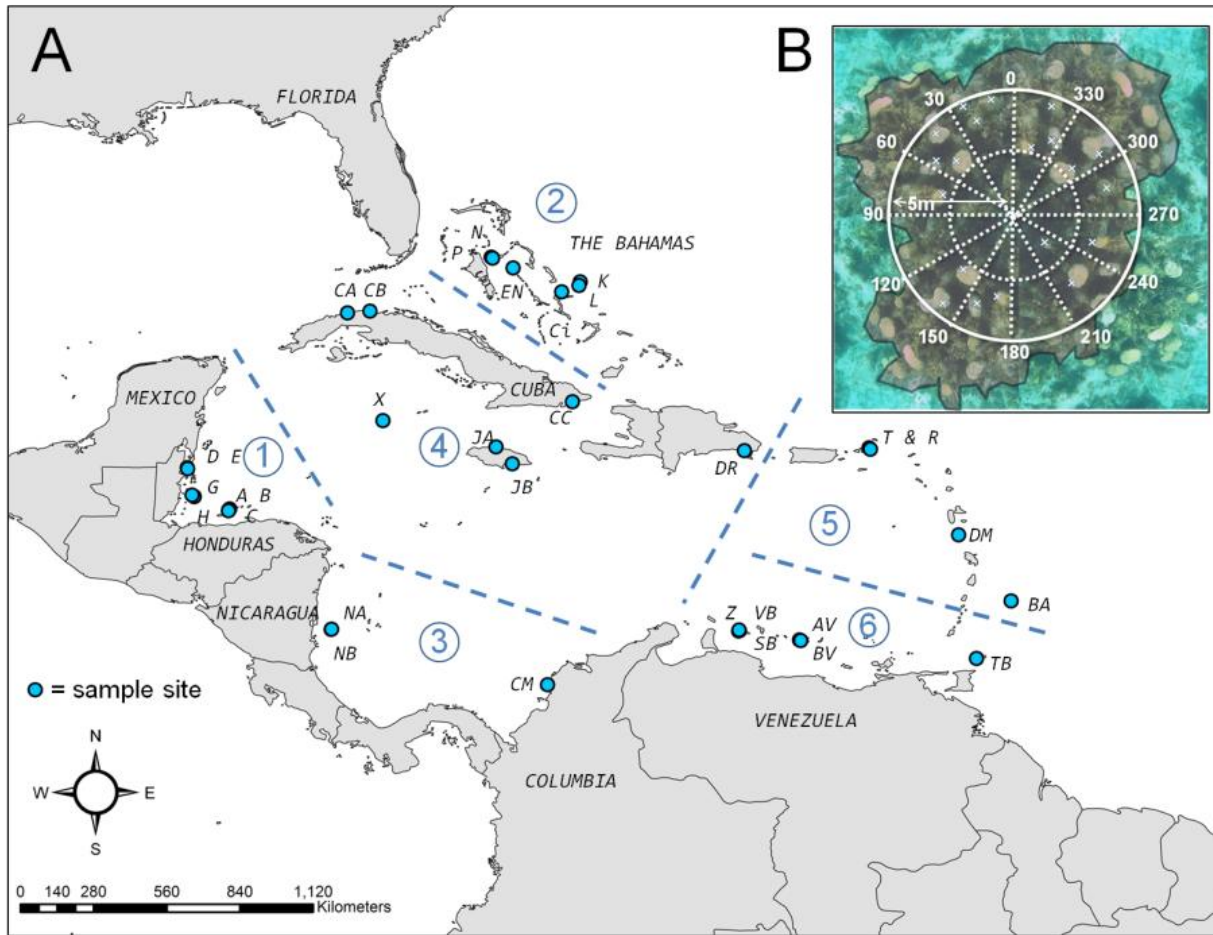


Figure 5.1: Current knowledge of geographic distribution of *Symbiodinium* types in *Montastraea annularis*. (A) Distribution of *Symbiodinium* A (A13, also known as A1.1 only A type found), (B) B types, (C) C types and (D) D-types. Data downloaded from online global *Symbiodinium* database GeoSymbio, October 2012 (Frankin et al. 2012).

5.3 Methodology

5.3.1 Sample collection and DNA extraction

Thirty-three field sites across a 3,000 by 1,800 km region encompassing the Caribbean Sea and Bahamas were sampled as part of a study into *M. annularis* host population genetics (Foster 2007) (Fig. 5.2). Sites, selected based on the presence of *M. annularis* reefs and the feasibility of sampling, fell into six broad marine ecoregions: the Bahamas (n=6 sites), Greater Antilles (7), Eastern Caribbean (4), Western Caribbean (7), Southern Caribbean (6) and Southwestern Caribbean (3) (Spalding et al. 2007). A 10 m wide circular sampling plot (Fig. 5.2B), was established at each sampling location *sensu* Foster 2007 using SCUBA (Foster 2007). The radius of the plot was extended beyond 5 m if less than 30 colonies were found in the initial plot. Thirty spatially independent *M. annularis* colonies within each plot were sampled. The location of each colony was mapped by recording distance (to the nearest 5 cm) from the centre of the sampling plot (marked with a stake), and bearing ($^{\circ}$) (Fig. 5.2B). A ~ 1 cm² sample was



C

Marine Ecoregion	Site ID	Site name	Location	Collection depth	Collection date
Western Caribbean	A	Seaquest	Honduras	4.0	Oct 2004
	B	Sandy Bay	Honduras	6.0	Oct 2004
	C	Western Wall	Honduras	4.5	Oct 2004
	D	Coral Gardens	Belize	4.5	Jan 2006
	E	Eagle Ray	Belize	2.0	Jan 2006
	G	Long Cay	Belize	6.0	Jan 2006
	H	West Reef	Belize	3.5	Jan 2006
	Bahamas	CI	Conception Island	Bahamas	18.6
EN		Exumas North	Bahamas	7.9	Apr 2007
K		Seahorse Reef	Bahamas	3.4	Jun 2006
L		Snapshot Reef	Bahamas	2.7	Jun 2006
N		School House Reef	Bahamas	3.5	Jun 2006
P		Propeller Reef	Bahamas	3.0	Jun 2006
South west	NA	White Hole	Nicaragua	9.0	Sep 2006
	NB	Chavo	Nicaragua	10.0	Sep 2007
	CM	Palo 1	Columbia	8.0	n/a
Greater Antilles	CA	Baracoa	Cuba	4.0	Sep 2007
	CB	Bacunayagua	Cuba	4.0	Sep 2007
	CC	Siboney	Cuba	4.0	Sep 2007
	X	Rum Point	Cayman	5.0	Jul 2007
	DR	Bayahibe	Dominican Rep	6.0	Oct 2007
	JA	Drunkenmans Cay	Jamaica	8.0	Sep 2007
	JB	Dairy Bull	Jamaica	8.0	Sep 2007
Eastern Caribbean	BA	Victor's Reef	Barbados	11.8	Jul 2007
	R	Ginger Island	BVI	4.0	Nov 2007
	T	Beef Island	BVI	4.0	Nov 2006
	DM	Grande Savane	Dominica	12.0	Aug 2007
Southern Caribbean	SB	Snakebay	Curacao	12.0	Oct 2005
	VB	Vaersenbay	Curacao	8.7	Oct 2005
	Z	Buoy 1	Curacao	8.5	Oct 2005
	TB	Buccoo Reef	Tobago	3.0	Sep 2007
	AV	Cayo de Agua	Venezuela	4.0	Aug 2007
	BV	Dos Mosquises	Venezuela	4.0	Aug 2007

Figure 5.2: Sampling methodology. (A) Map showing location of *M. annularis* sampling sites, with accompanying table (C) listing site names, locations and collection dates and depths. Blue lines divide different biogeographic marine ecoregions, 1-6. (B) aerial schematic of the circular survey protocol performed at each site (x denotes sample).

gently chipped from the edge of each lobe on each colony using a hammer and a chisel. It was essential to sample from the tops of colonies only, as evidence of intra-colony symbiont zonation *Symbiodinium* exists in *M. annularis* (Rowan et al. 1997, Toller et al. 2001a, Thornhill et al. 2009). Samples were placed in labelled plastic ziplock bags, and on returning to the shore preserved in 90% ethanol and stored at 4°C. A GPS waypoint, time, weather conditions and reef position of each sample were also recorded.

A 200 µl mix of coral host and symbiont DNA was purified from each 1 cm³ tissue sample using a spin-column protocol (DNeasy tissue kits, Qiagen), yield quality was assessed using a nanodrop, and extracted elution was stored at -20°C.

5.3.2 Selection of a target gene region

The Internal Transcribed Spacer 2 (ITS2) gene – a 320 base pair (bp) sequence in the nuclear ribosomal genome - was selected as the target region to explore *Symbiodinium* genetic diversity (Fig. 5.3). The molecular marker is commonly used to resolve symbiont sub-cladal types (LaJeunesse 2001), and is able to determine more species than alternative nuclear, mitochondrial and chloroplast markers (LSU, ITS1, psBA and cp23S), although there is high level of agreement between all (Sampayo et al. 2009). ITS2 was chosen as rDNA transcription tracts have a low rate of polymorphism among species, allowing phylogenetic relationships to be resolved, although ITS (which is non-coding) are more variable due to insertions, deletions and point mutations. Our primers begin in the adjacent 5.8S coding section as the ITS2 itself is very variable.

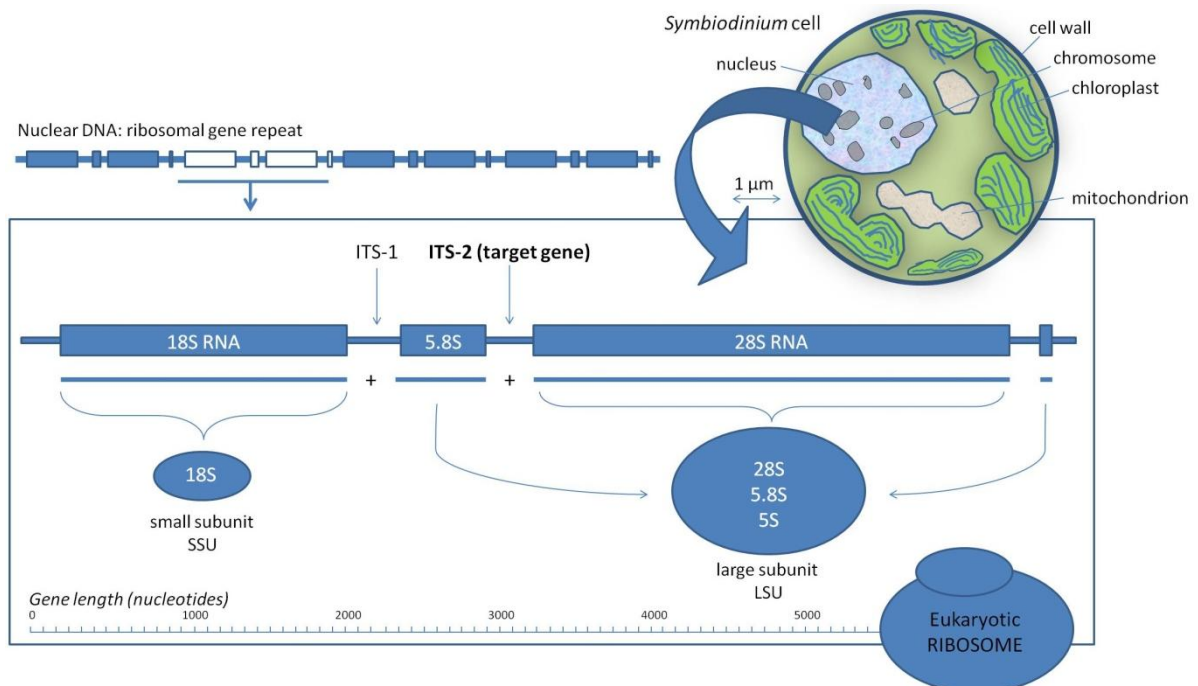


Figure 5.3: Diagram showing the target gene used to explore *Symbiodinium* diversity. The eukaryotic ribosome is a large (20-nm) complex of RNA and protein, that catalyses protein translation (production of proteins from amino acids using messenger RNA template).

5.3.3 Denaturing Gel Gradient Electrophoresis (DGGE) and sequencing analysis

Denaturing gel gradient electrophoresis ('DGGE') and direct sequencing were used to identify *Symbiodinium* ITS2 types within each individual *M. annularis* sample (Fig. 5.4). The technique involves electrophoresis of fragments of genetic material on a vertical acrylamide gel containing a gradient of increasing DNA denaturants (urea and formamide). It separates double-stranded DNA fragments that are identical in length, but differ in sequence, by exploiting the difference in stability of G-C ($3 \times$ H-bonds) and A-T ($2 \times$ H-bonds) pairing. G-C rich fragments will be more stable and remain double-stranded until reaching higher denaturant concentrations. Double stranded fragments migrate further in acrylamide gel; denatured DNA molecules become larger and slow or stop – in this way fragments are separated. DGGE was selected from a variety of available screening methods (reviewed by Sampayo et al. 2009), as it has been demonstrated to provide a higher and clearer level of resolution than other genetic analyses. In comparative tests, alternative methods such as SSCP (based folding rather than melting, like DGGE), LICOR size-analysis, cloning, direct sequencing of the LSU D1/D2 domain and restriction fragment length polymorphism (RFLP) were shown to resolve fewer than six *Symbiodinium* species (SSCP=6; RFLP=4, direct sequencing=5), while DGGE resolved eight. DGGE also produced considerably clearer profiles comprising bands that can be resolved and separated more precisely, compared to SSCP.

DGGE produces diagnostic fingerprints or 'profiles', consisting of high-melting-lower-migrating homoduplexes, and low-melting-higher-migrating-heteroduplexes (Fig 5.4). Homoduplexes correspond to the dominant sequence variants in the ribosomal array of each ITS2 type; heteroduplexes occur due to cross-hybridisation of fragments of different lengths (with homologous regions at the 3' and 5' ends) and have reduced electrophoretic mobility compared to homoduplexes, appearing higher on the gel. Bands were sequenced to confirm identity of subclades, and aligned, with the aim of designing primers to target specific cladal types. Zooxanthellae communities could subsequently be compared within and between sites, and between years.

The ITS2 region of the symbiont DNA was targeted using *Symbiodinium* specific primers 'ITSintfor2' and 'ITS2CLAMP' (LaJeunesse 2002), designed to amplify a 330-360 bp product containing the ITS2. The internal primer 'ITSintfor2' (5'-GAA TTG CAG AAC TCC GTG-3') anneals to a conserved region of the 5.8S rDNA and is paired with the conserved 3' flanking primer 'ITS-reverse', that has been modified by addition of a 39 bp GC clamp (underlined) (5'-CGC CCG CCG CGC CCC GCG CCC GTC CCG CCG CCC CCG CCC GGG ATC CAT ATG CTT AAG TTC AGC GGG T-3') and amplified using a 'touchdown' amplification protocol with annealing conditions 10°C above the final annealing temperature of 52°C, to ensure specificity. Reaction mix: 1 x PCR reaction buffer, 2.5 mM MgCl₂, 0.2 mM dNTPs, 2 U Taq DNA Polymerase, 0.6 µM primer in a 12.5 µl reaction.

Both INGENYphorU-2x2 system (Ingenu) and CBS Scientific (CBS) DGGE systems were used to run PCR products on denaturing gradient gels. In both cases, a 0% [20 ml of 40% acrylamide (37.5:1 acrylamide:bis-acrylamide), 2 ml of 50× TAE and 78 ml dH₂O] and a 100% [20 ml of 40%

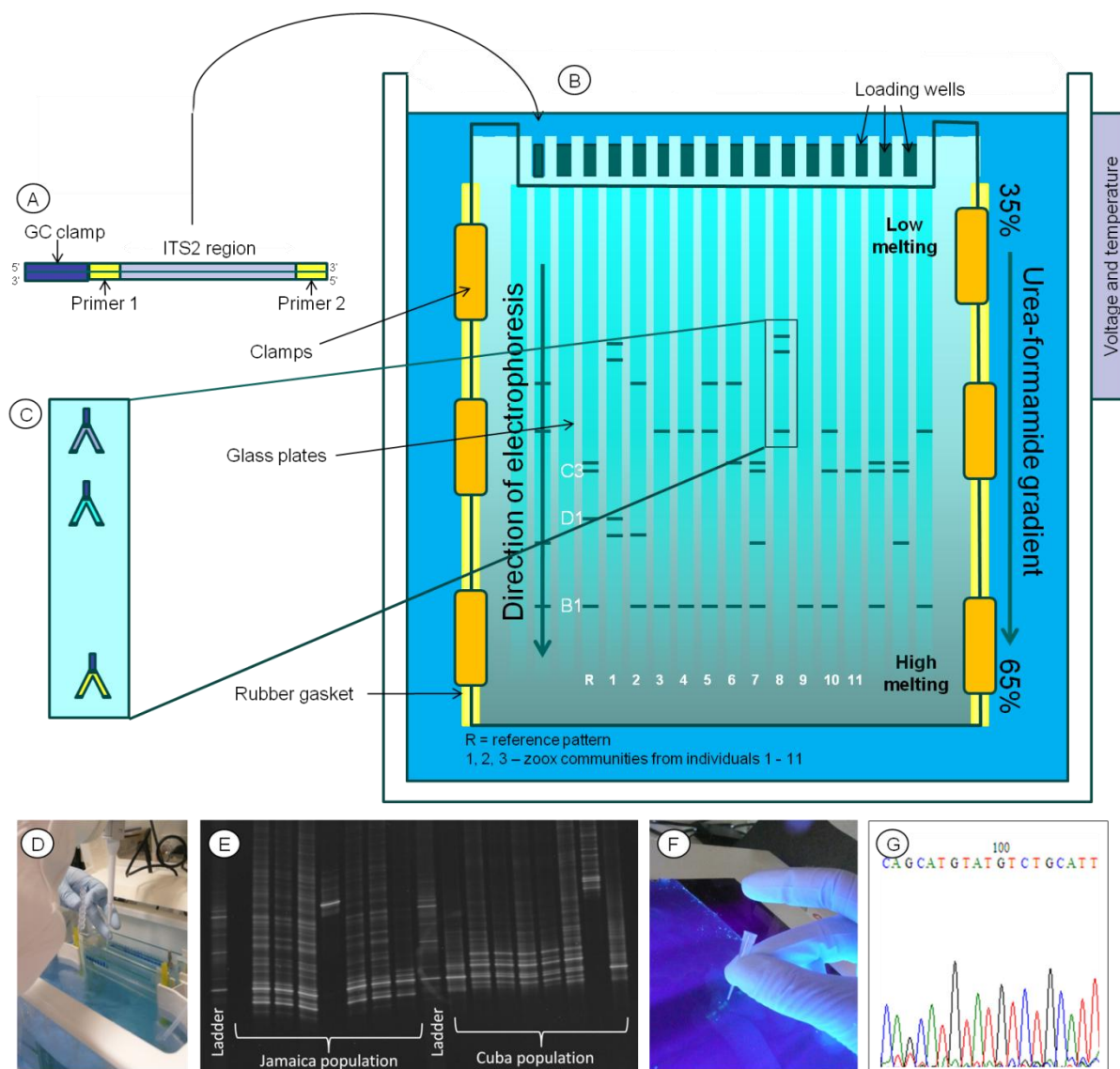


Figure 5.4: Denaturing Gel Gradient Electrophoresis: A) the target gene is amplified by PCR from a mix of holobiont genomic material using *Symbiodinium* specific primers, with a GC clamp. B) The mixed assemblage of PCR products are loaded into wells C) PCR product migrates down the gel, as double stranded fragments melt the GC clamp holds the denatured strands together. Final position of each band on the gel depends on the melting point of the fragment and conformation of the strands. Low migrating bands (homoduplexes) represent ITS2 types, while higher migrating bands (heteroduplexes) are a common by-product caused by hybridisation of different ITS2 variants. D) A mix of PCR product and blue loading dye being loaded into wells in polyacrylamide gel, in the pre-heated CBS tank. E) After running for 14 hours, gel is removed from the tank and exposed to SYBR-Green dye, before being imaged on a UV transilluminator, to reveal banding patterns. F) Bands are excised from the gel, using a 10 µm pipette tip, before being reamplified and then purified prior to sequencing G) The final step: the DNA from each excised band is sequenced, and an alignment performed.

acrylamide, 40 ml formamide, 42 g urea and 2 ml of 50× TAE] denaturant acrylamide. Both the INGENYphorU-2x2 system (Ingenu) and CBS Scientific (CBS) DGGE systems were used to run PCR products on denaturing gradient gels. In both cases, a 0% [20 ml of 40% acrylamide (37.5:1

acrylamide:bis-acrylamide), 2 ml of 50× TAE and 78 ml dH₂O] and a 100% [20 ml of 40% acrylamide, 40 ml formamide, 42 g urea and 2 ml of 50× TAE] denaturant acrylamide solution were prepared beforehand, and mixed to get a 60% (12.8 ml 0% solution: 19.2 ml 100% solution) and a 40% (12.8 ml 100% solution: 19.2 ml 0% solution). To each solution, 120 µl ammonium persulphate (APS) solution (0.1 g APS : 1 ml dH₂O), and 18 µl TEMED (Bio-Rad) were added. Gels (28 ×18 cm) were cast using a manual gradient mixer, and then left to set for 2 hours. PCR product (15 µl) from every individual was loaded into DGGE wells after mixing with 5 µl bromophenol blue loading buffer (15% Ficoll, 0.25% xylene cyanol FF, 0.25% bromophenol blue), and gels were run overnight for 14 hours at 114V, at a constant temperature of 60°C. An ITS2 standard (provided by the Hoegh-Guldberg lab, UQ) was run in the first lane of each gel. After the 14 hours, the gel was gently transferred to a staining bath and covered with SybrGreen I nucleic acid gel stain (stock was diluted 1:10,000 in 1 M TAE buffer). SybrGreen I (Invitrogen) was selected as it has a greater affinity for nucleic acids than ethidium bromide, as well as producing a fluorescent enhancement an order of magnitude greater, meaning it is a much (25 ×) more sensitive stain. The gel is covered with aluminium foil to protect from light, and incubated in the staining buffer at room temperature for 20 minutes. The gel was then imaged in a UV transilluminator.

Region	Primer	Primer sequence (5' to 3')	Size	T _m
ITS2 rDNA	ITSintfor2	GAATTGCAGAACTCCGTG	326 bp	59°C
	ITS2-reverse	GGGATCCATATGCTTAAGTTCAGCGGGT		
ITS2 rDNA (for DGGE)	ITS2CLAMP	<u>CGCCCGCCGCGCCCGTCCCGCCGCCCCGCCGGATCCATATGCTTAAGTTCAGCGGGT</u>	~360 bp	62-52°C (touchdown)
	ITSintfor2	GAATTGCAGAACTCCGTG		

Table 5.2. Primer pairs. Showing gene regions targeted for analyses, primer pairs used for PCR, approximate size of the amplified DNA fragment and annealing temperature used to examine diversity in the genus *Symbiodinium*. For analysis of ITS regions using denaturing gradient gel electrophoresis, a GC-rich area is attached to the reverse primer (underlined).

Gels were examined carefully by eye. There was usually a more prominently stained band (or bands) that were scored as the dominant symbiont (Warner et al. 2006). When two or more symbionts are abundant in a sample (> 10% of the population; Thornhill *et al.* 2006), the fingerprint profiles of each are identifiable in the same lane (LaJeunesse 2002). Gel images were compared with published profiles from other labs for identification. Representatives of every discreet, prominent band were excised under a UV-transilluminator using 10 µl tips and stored at 4°C overnight in 1.5 ml eppendorf tubes containing 30 µl RNase free water. Reamplification was performed with 1 µl eluate, using ITSinfor2 and ITS2-reverse lacking the GC-clamp. 2 µl of the PCR product was then cleaned using Exo-sap (per 100 samples: 5 µl Exonuclease 1 (20U µl⁻¹), 10 µl Exonuclease buffer and 85 µl dH₂O, along with 20 µl Antarctic phosphatase (5U µl⁻¹), 10 µl buffer and 70 µl dH₂O). 2 µl was added to each sample and put in the thermocycler at 37°C for 15 min and a further 15 min at 80°C. Following the determination of concentration of each sample on the nanodrop, samples were diluted to a suitable concentration (6-12 ng µl⁻¹) for sequencing. The product was sequenced in both directions using

both forward and reverse amplification primers separately (Macrogen). A sequence alignment was performed in Clustal X and checked by eye, prior to comparison against a database of all known Caribbean *Symbiodinium* types in Geosymbio database (Frankin et al. 2012).

5.3.4 Validation of DGGE using High Resolution Melt (HRM) analysis

High-resolution melting analysis is a relatively new method that has been used to successfully identify *Symbiodinium* to both clade (Correa et al. 2009) and sub-type level (Mieog et al. 2007, Granados-Cifuentes and Rodriguez-Lanetty 2011). It is increasingly being used as a method for detecting low levels (10-20% of the population) of symbionts (Silverstein et al. 2012). Limitations of DGGE are numerous, including limits on the permitted size of the DNA fragment; a requirement for technical expertise in the use of the equipment and gel preparation; and careful optimisation of the acrylamide and denaturant concentrations as well as electrophoresis times, which can vary according to gene region and brand of DGGE system. As well as heteroduplexes (similar sequences that migrate to different gel positions), co-migration can occur where dissimilar sequences with similar melting properties migrate together (April and Gates 2007), causing up to an estimated 6% of diversity to be missed (Pochon et al. 2007), although this can be avoided by sequencing. One of the problems associated with using a multi-copy and intra-genomically variable molecular marker is that genomes of some clades have a higher ribosomal copy number, making them easier to detect – for example clade C copy number is that is 3-5 times that of clade D (Smith, 2008). Finally, DGGE is only able to detect the most numerically abundant ITS2 types in a mixed sample.

HRM has several advantages over DGGE, in that: 1) it is 1000-fold more sensitive than DGGE (Correa et al. 2009), and thus able to detect low levels of ‘cryptic’ symbionts (i.e., DGGE shown to only detect ITS2 type D1 when it comprised at least 10-30% of the total community (LaJeunesse et al. 2009), 2) it can be used to quantify the relative abundance of types (Correa et al. 2009) and 3) it is quicker than DGGE (Granados-Cifuentes and Rodriguez-Lanetty 2011).

HRM was used to help validate and improve DGGE estimates of ITS2 diversity at each site. EvaGreen dye was selected to detect melting, as it is less inhibitory towards PCR and less likely to cause non-specific amplification, meaning it can be used at a higher concentration, resulting in a more robust PCR signal. Once a list of symbionts hosted by *M. annularis* had been established, each individual sample was scored on the presence and absence of each type. In addition to this, the ‘dominant’ bands on each gel were also recorded. See Chapter 7 (section 7.3) for full methodology for this technique.

5.3.5 Data analysis

Presence/absence data for ITS2 types at all sites were initially explored using pie and bar charts.

Symbiont diversity indices were calculated for each site, using Simpsons Reciprocal D Index [$D=1/\sum(n(n-1))/N-(N-1)$], where n is the number of symbiont ITS2 types and N is the total number of spatially independent colonies sampled. SADIE (Spatial Analysis by Distance IndicEs) - a statistical approach designed for assessing the patterning of count data from spatially referenced locations - were used to test quantify spatial patterns in the data, both at cladal and sub-cladal level (Perry 1995). SADIE measures the spatial pattern at each sampled unit using an index of clustering based on geographic distance – assigning each site either a positive patch cluster (v_i) or a negative gap cluster (v_j) value. These can then be mapped to produce a class post map representing local quantification of spatial patterning. Finally, a contour map is produced by interpolating between the datapoints (using a universal kriging method), and superimposed onto the classed post map to produce a red-blue plot indicating clustering of spatial data (Perry et al. 1999).

5.4 Results

5.4.1 Local patterns in *Symbiodinium* ITS2 diversity

In total, 76 DGGE gels were run, revealing approximately 22 different DGGE banding profiles (see Appendix section 5 for full profile descriptions). Over 300 bands were excised, and 120 of these successfully sequenced, providing information on ITS2 types. Results from each site within the six marine ecoregions (Fig. 5.2) are discussed in turn, with brief descriptions of the ITS2 diversity at each sampling location. More detailed descriptions of site characteristics, along with gel images and HRM outputs are provided in the Appendix (Appendix Figs. 5.2-5.33).

5.4.1.1 Western Caribbean (Mesoamerican Barrier Reef System)

The Mesoamerican Barrier Reef System (MBRS), the second largest reef system after the Australian Great Barrier Reef, stretches over 1000 km from the Yucatán Peninsula through Belize and Guatemala to the Bay Islands of Honduras (Fig. 5.5). The region is characterised by relatively warm (mean = 27.27°C) waters with high salinity and water clarity (Chollett et al. 2012). Although episodically exposed to hurricane disturbance (Hurricane Mitch and bleaching in 1998 saw a 50% reduction in coral cover; McField et al. 2008), the region generally experiences little influence from rainfall and land run off, except in the south which is exposed to the major watersheds of Honduras and Guatemala. Despite being one of the better preserved regions of reef (corals show low levels of bleaching and disease compared to other Caribbean sites) living coral cover has declined since 1990s records of 28% (Honduras, 1990) and 30% (Belize), and prior to sampling averaged 12% and 10% respectively (McField et al. 2008). Four of the sites (D, E, G and H), sampled in 2006, are located 100 km apart on the Belize barrier reef, which comprises 80% of the MBRS, the final three sampled in 2004 sited a further ~140

km away on Roatan, in Honduras (Fig. 5.5). This region exhibited the lowest symbiont diversity after the Bahamas (Simpsons $1/D = 3.13$), and was less diverse than the Caribbean average (5.79). This is partly due to finding a limited number (nine) of ITS2 types, and the high dominance of sub-clades B1 and B17 (Fig. 5.5), of which B17 appeared to be unique to the region.

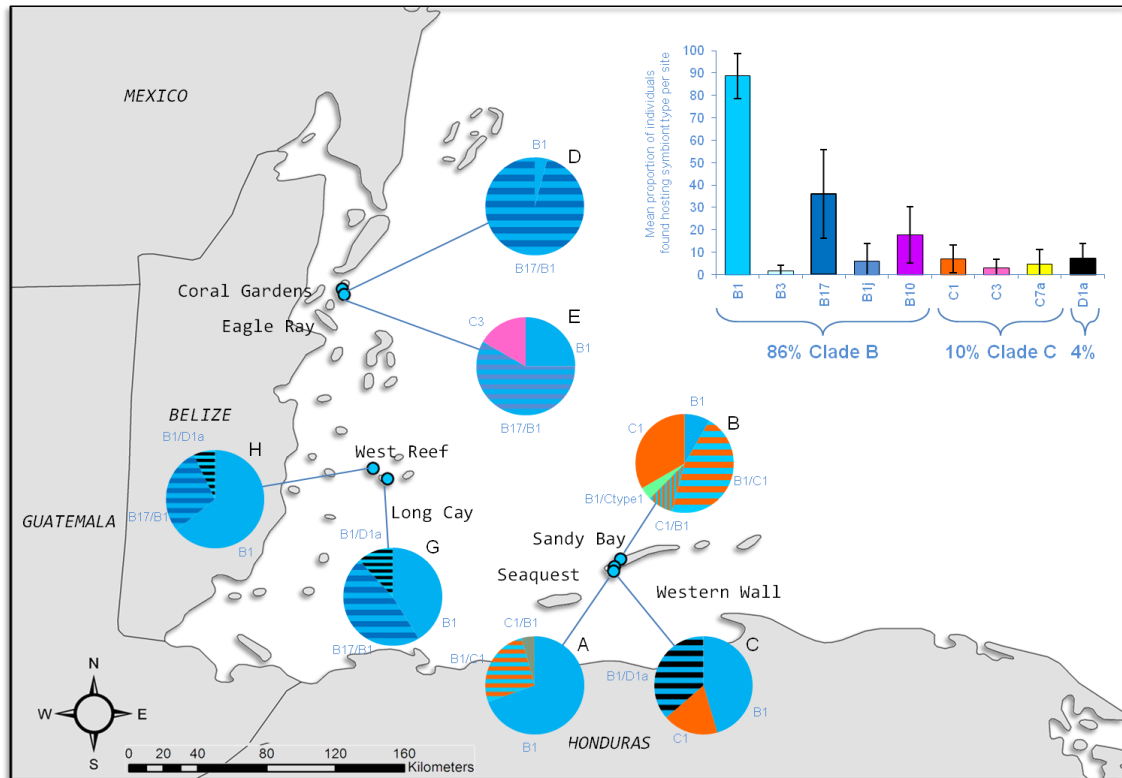


Figure 5.5: Map depicting dominant symbiont types found at six sites across the Mesoamerican Barrier Reef System. Pie charts represent the symbiont types that dominated communities at each site, while the bar chart (inset) represents *all* the individual sub-clades identified in this region, and their mean abundances. Some sub-clades depicted in the bar chart, e.g., D1a, were found in >30% of individuals yet were present in low amounts and never dominated communities, so do not appear in the pie charts. Meanwhile, B1 was found in over 80% of individuals, and made up the majority of communities in many sites.

Honduras (sites A, B and C)

The Honduran locality consisted of three sites off the northwest coast of Roatan. Western Wall (C), situated off the tip of the island was the most exposed site; the other two (Seaquest, A and Sandy Bay, B) were located in shallow sandy bays.

Sandy Bay (B), Roatan was the most diverse of the Honduran sites ($1/D = 4.99$). All coral colonies contained a C1 band: in 33% of cases this was the dominant band, and a further 54% shared co-dominance with another type (usually B1). Samples hosting C1 exclusively generated tall (>1000) HRM peaks at 84.0°C. Most of the remaining samples produced a second peak at 86.3°C – representing a co-dominant B1 band. One sample (B06) uniquely produced two even higher bands. Sequencing was not able to resolve this type, which has temporarily been named

Ctype1. HRM was unable to distinguish this unidentified band from C1, producing one identical melting peak, suggesting that this type is very similar to C1.

Most Seaquest (A) and Western Wall (C) corals were dominated by B1 (along with two B1 heteroduplexes, that were not always visible), supported by a clear melt peak at 86.1°C generated by HRM analysis. Several samples also had a C1 band, as seen at Sandy Bay. HRM analysis provided some further resolution, with some samples at site C generating additional melt peaks from those expected for B1 and C1. Further investigation revealed that samples producing these peaks were all individuals that were shown to contain D1a in a separate analysis (Chapter 7). Those that did not contain D1a did not have the second melt peak. Samples from Honduran site B were also shown to contain D1a but did not show these peaks – possibly D lay below the detection limit for this technique.

Belize (sites D, E, F and G)

Four sites were sampled in Belize. Coral Gardens (D) a sheltered, well developed lagoonal patch reef with high coral cover, and Eagle Ray (E), a shallow (2-3 m) patch reef, were situated on the eastern side of the island Caye Caulker (Foster 2007). Long Cay (G) and West Reef (H), were reef slope sites located 100 km south on the Glovers Atoll. Long Cay was located on the more exposed eastern side of the atoll, West Reef a slope on the leeward side of the atoll was shallower (Fig. 5.2).

The *M. annularis* sampled at Coral Gardens (D) consisted of large colonies with a high (90%) living tissue cover (Foster 2007). The majority of DGGE profiles presented a dominant low-migrating B17 band, and a slightly higher B1 band. Sequencing revealed just three SNP differences between the two ITS2 types. HRM analysis supported this, despite being able to distinguish between B1 and B17 (one 86.3°C melt peak produced) samples that hosted a B17/B1 mix produced a bigger fluorescent flare than the few samples that DGGE revealed just to exclusively host B1 (>2000 units compared to 500-800 units).

Neighbouring site Eagle Ray (E) shared the B17/B1 DGGE profiles of Coral Gardens. A few samples produced a higher migrating band, in the C3 position. HRM helped confirm that this was a C3 band, producing a melt peak (83.8°C) that differed from the B17/B1 peak (86.3°C).

The Long Cay site, the deepest of the four Belizean sites, had well developed reef with large colonies of *M. annularis*, although many of the colonies had less than 10% live tissue (Foster 2007). Long Cay (G) samples – most of which matched those occurring at nearby sheltered reef slope site West Reef (H) – were mostly dominated by a B1 band (and several higher migrating bands which sequencing revealed to be B1 heteroduplexes). A few samples also produced a band in the D1 position, and although sequencing was unable to confirm this as a D1, HRM

melt profiles produced peaks around 84.5°C for these samples, a similar temperature for sites known to host D1. Screening further samples from G using QPCR using more sensitive D-specific primers (Chapter 7) revealed a further 9/10 samples contained low levels of D1a. The remainder of the samples from Long Cay and West Reef were dominated by B17/B1 mix seen at the other Belizean sites.

5.4.1.2 The Bahamas

The Bahamas ecoregion consists of 13 major islands and >2000 smaller cays, with 3,580 km² of reefs distributed across two shallow sandbanks (Grand and Little Bahama Bank) that run 1400 km from Florida to Haiti (Fig. 5.2). They represent about 14% of the Wider Caribbean's reefs (Burke and Maidens 2004). A high number of hurricanes coupled with cooler water in the north and turbid, hypersaline waters on the leeward bank margins limits reef development, with coral cover ranging from 1% to 47%. High resolution classification approaches have delineated six distinct physiochemical within the Bahamas (Chollett et al. 2012). Three of our study sites (Conception Island, Seahorse and Snapshot reefs) were in a region (7) characterised by relatively warm waters with high salinity and high water clarity, while the other three were in an area of low average and minimum temperature but high seasonal maxima. The 2005 bleaching episode affected 17% of colonies over 25-50% of their surface, although monitoring suggests little to no mortality. Prior to sampling in June 2006 there would have been little apparent recent damage (Jones et al. 2008).

Data showed that the Bahamas ecoregion hosted a lower than average species richness (eight species- the second lowest after the West when corrected for sample size; Fig. 5.11) and lowest diversity out of all the regions (Simpsons 1/D = 2.34). Like the Western Caribbean ecoregion, the high prevalence of B1 best explains this low diversity: with the exception of the Exhumas (EN) (where only 50% of samples hosted B1), B1 was found in every single sample at all sites in the Bahamas.

Bahamas (sites L, K, P, CI, N and EN)

Snapshot reef (L) hosted the lowest *Symbiodinium* ITS2 diversity of all the sites sampled (Simpsons 1/D = 1.26) with every sample producing an identical DGGE ribotype with a dominant B1 band, and several fainter bands (two above, one below). These higher bands appeared to varying degrees, and sequencing of all bands in several samples revealed these bands to be B1 heteroduplexes. HRM analysis supported the DGGE evidence: all samples to produced a single melt peak at 86.1°C, confirming presence of B1 in all samples (Appendix Fig. 5.8).

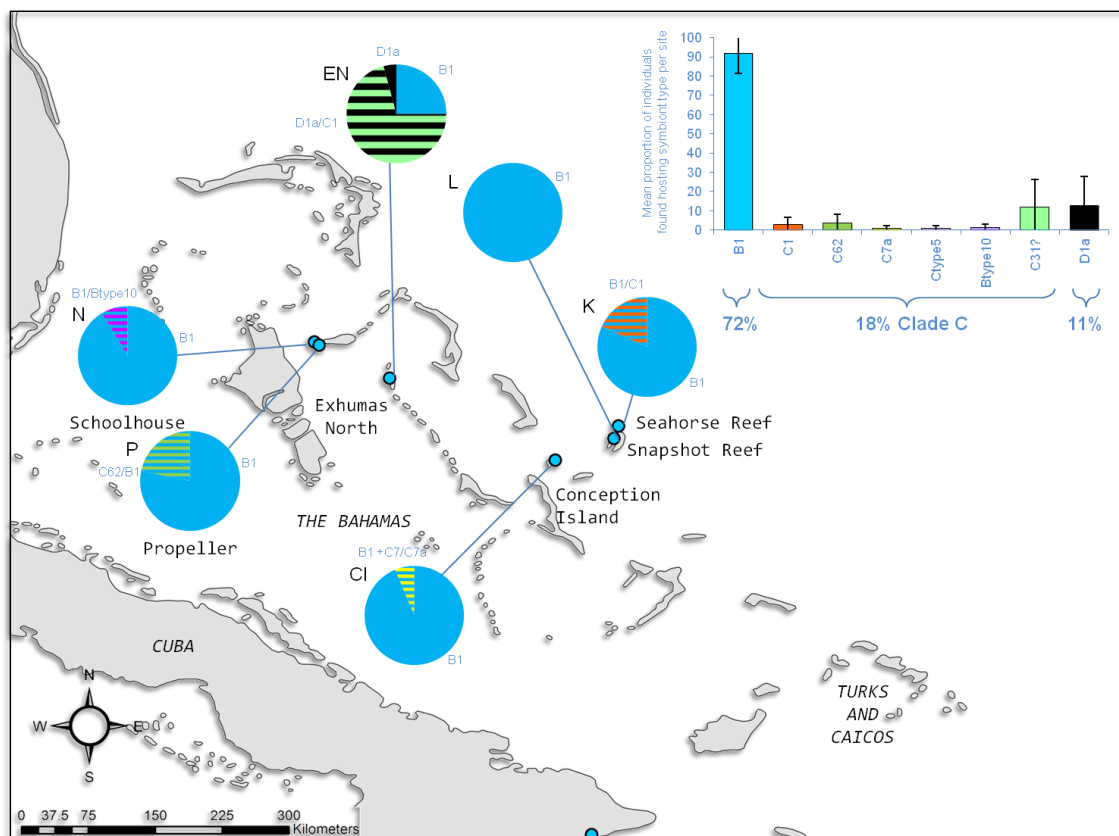


Figure 5.6: Map showing sample sites and the geographic diversity of dominant *Symbiodinium* ITS2 types, or pairs of types, in the Bahamian eco-region. Inset: bar chart showing the species richness across the region. 'C31' is an unidentified type, found co-existing with D1a in most Exhumas (EN) samples, along with other samples from Dominica and the BVI.

Seahorse reef (K) was the most exposed of the Bahamian sites, located off the north of San Salvador Island about 40 km from the more sheltered leeward Snapshot Reef (L). Along with Snapshot, B1 was dominant in all samples, with a few showing a co-dominant C1 band (Fig. 4.6). HRM produced melt curves at the B1 temperature, although no secondary melt peaks showing that HRM was unable to detect or distinguish C1 here (Appendix Fig. 5.9).

The majority of Propeller reef (P) samples adhered to a simple B1-dominated ribotype evident at Snapshot reef (L). When corrected for sample size this site hosted the lowest total Caribbean symbiont richness, along with Snapshot and Schoolhouse reefs. A slightly higher band in some samples was almost close to being a D1 band, but a combination of sequencing and direct comparison with EN samples revealed it to be a B1 heteroduplex, migrating further than D1. Three samples, produced additional higher migrating bands, which sequencing revealed to be an unknown type. The positioning of the band appeared similar to C12, but lay slightly higher on the gel and had seven SNPs different to the normal C1 sequence. An alignment with all major published ITS2 types extracted from the GeoSymbio database (Frankin et al. 2012) showed C62 to be the closest, but not perfect, match to this symbiont. For samples containing this type, HRM produced a second melt peak at 83.9°C (C62) as well as the 86.1°C corresponding to B1 (Appendix Fig. 5.10).

All Conception Island (CI) samples were dominated by the B1 band, displaying similar DGGE profiles to that of Propeller Reef. In one sample, three high bands were also observed: a pair that are comparable with the double C7/C7a bands – similar to some Barbadian communities - and a lower unidentified band (“Ctype5”). HRM supported the presence of a C-type in this instance (Appendix Fig. 5.13).

Almost all Schoolhouse reef (N) samples shared the common Bahamian B1 banding profile. A minority of samples showed a slightly different banding pattern, which was most similar to B8 (or B34) in an alignment, but could not be identified with confidence. HRM failed to distinguish between profiles 1 and 2 with all samples producing a single melt peak at the B1 position ($86.1 \pm 0.1^\circ\text{C}$) although closer inspection revealed samples potentially hosting B8 appeared to have a small peak around 84.9°C (Appendix Fig. 5.11).

The Exhumas (EN) samples displayed remarkably divergent profiles to other Bahamian sites, and had significantly higher species richness (Exhumas Simpsons $1/D = 4.92$, vs. Bahamian mean of 1.78 ± 0.31). The majority produced a fingerprint with a dominant band pair in the D1/D1a position, and a higher migrating pair of C-type bands above, just below C1. This DGGE fingerprint dominated a variety of other sites, including Dominican (DM) and BVI (R) sites. While most EN samples had a low amount of B1 present – a very faint band could just be observed in most lanes – some had a B1 dominated profile. HRM analysis showed a peak around $84.7 - 84.8^\circ\text{C}$ in most samples, corresponding to the DGGE profile containing D1/D1a/unknown C-type bands. This was also observed in the HRM output from Dominican (DM) and BVI (R) samples. Here, HRM was evidently unable to distinguish between the D1/D1a and slightly higher unidentified C-band (Appendix Fig. 5.12).

5.4.1.3 The Greater Antilles

The central Caribbean region once possessed high coral (50%) cover, despite overfishing around densely populated islands like Jamaica. Outbreaks of coral disease and *Diadema* mass mortality, along with severe coral bleaching and hurricanes in the 1980's (Chapter 4), has led to coral cover being eroded to 5-10%. The Greater Antilles ecoregion was found to host the greatest number of symbiont taxa (Fig. 5.7), and had a high spread of species richness and evenness, it hosted the second highest symbiont diversity in the Caribbean (Simpsons $1/D = 5.65$), after the Eastern Caribbean (7.54).

B1 was still the most important symbiont type in terms of frequency of occurrence, but was only exclusively dominant in 21% of cases; more often sharing dominance with other B (40.5%) or C types (6.0%). A scarcity of previous *Symbiodinium* studies in this central region (see Fig. 5.1) meant that few predictions could be made about the sub-types expected.

Cuba (sites CA, CB and CC)

Fringing and bank-barrier reefs border 98% of Cuba's 3,200 km shelf margin, and separation of these reefs by large lagoons and patch reefs mean they have been protected from most detrimental anthropogenic influences outside of heavy fishing, leading to estimates of 18-21% live coral cover prior to sampling (Jones et al. 2008). Two sampling sites, Baracoa (CA) and Bacunayagua (CB) were situated 82 km apart on the Archipiélago de los Colorados, a 100 km archipelago running along the northwest coast of the main island. The third site, Siboney (CC), lay 805 km away in the southeast. Cuba experienced widespread and intense bleaching in 2005 (reports of 50-100% of coral colonies experienced bleaching at 89% of sites) and, coupled with damage from hurricanes Wilma and Denis, suffered further widespread lower intensity bleaching in 2006, prior to sampling in September 2007 (Jones et al. 2008).

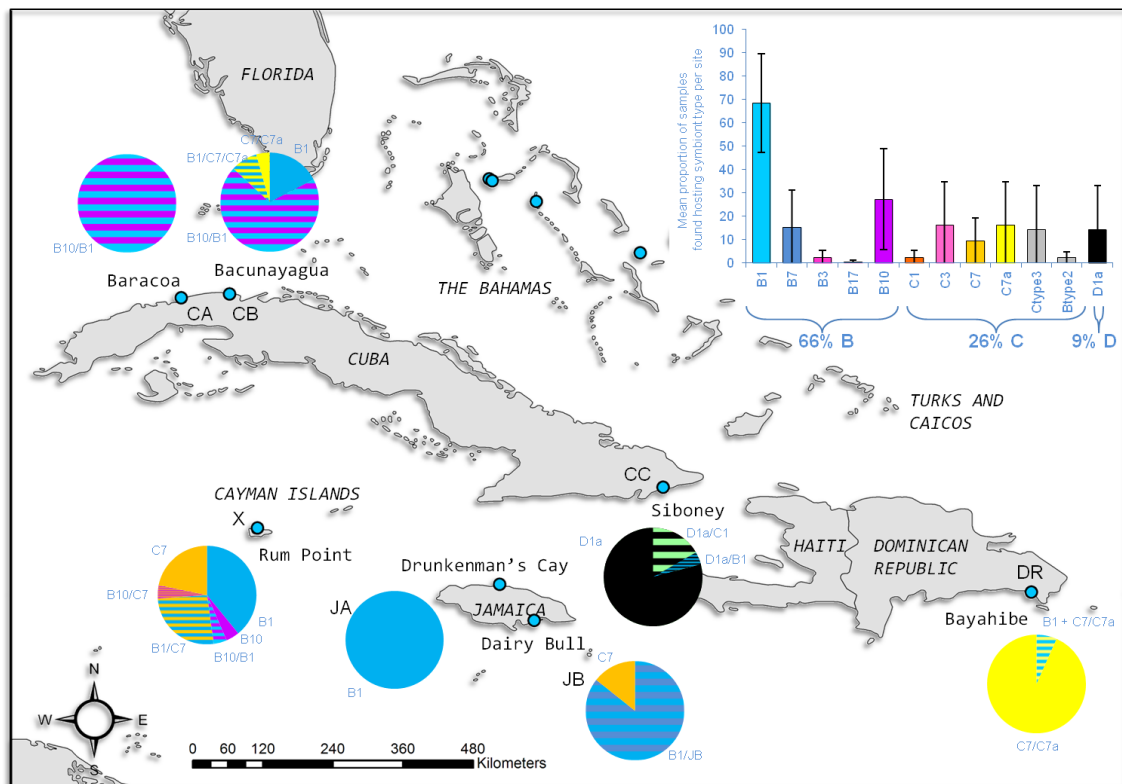


Figure 5.7: Map showing location of sites in the Greater Antilles marine ecoregion, along with data showing the diversity of symbionts found in this region (inset: bar graph) and their relative abundance (pie charts). B1 was the most common, hosted by over 50% of individuals. Pie charts depict the dominant symbiont, or pair of symbionts, hosted by individuals at each site (n=24).

Baracoa (CA) and Bacunayagua (CB) sites were almost uniformly composed of what sequencing revealed to be a B10 dominated fingerprint: a profile that appears to be unique to these sites. The only other place that B10 occurred in the dataset was at the Grand Cayman site, and in a background capacity in Honduras, although B10 appeared in *M. annularis* samples from nearby Floridian reefs 320 km due north of our Cuban sites in another study from 2003-2005 (Thornhill et al. 2009). Located just above the B1 band, the B10 sub-type was shown to

have just one base pair different to B1. In the majority of cases either B10 or a B10/B1 was dominant (Fig. 5.7). A few samples, particularly at Bacunayagua (CB), appeared to host just B1. One CB sample possessed a fingerprints with higher migrating bands. Sequencing revealed this community to be dominated by C7/C7a, with an unidentified band below ('Btype2'), and a C3 band above. Another sample had a combination of both this and the B10/B1 banding.

HRM analysis appeared to be unable to resolve the differences between closely related ITS2 sequences B1 and B10, with all samples producing a single melt peak at 85.8°C (± 0.1), representative of the B1/B10 mix. However, closer inspection of the plot revealed that the relative fluorescence of individuals hosting only B1 was almost 500 units higher, and more tapered, possibly causing a distinction between B1 profile, and smaller (1000 units), more skewed and flatter curves of B1/B10 mix. This might be explained by the fact a single melt curve was representing two similar ITS2 types. Finally, samples hosting C7/C7a produced a completely distinct peak at 84.1°C.

Siboney (CC) symbiont communities appeared very different to other Cuban (CA, CB) samples, perhaps unsurprisingly coming from over > 800 km away. None shared the unique B1/B10 Cuban profile, instead producing fingerprints with five faint bands. The brightest band in each case was a D1 band, with a D1a below, and three further bands above. In our dataset, this profile is shared by a BVI sample, a single Jamaican sample and seven Bahamian samples from one site in the Exhumas (EN). As well as the D1a band, a few samples showed additional bands: some in the B1 and B17 position, while several others produced a possible C-type band (C1?) above the main D1 that was unidentifiable. HRM melt profiles corroborated the DGGE ribotypes, with the majority showing a melt peak around 84.7°C, representing the dominant D1/D1a bands.

Dominican Republic (site DR)

The Dominican Republic possesses 166 km of mainly fringing reefs and 377 km of mangroves (Jones et al. 2008). Coral cover is shown to be slowly increasing, and was recorded as 19.4% at our sampling site in Bayahibe in 2004. Bleaching affected 68% of colonies in October 2005, and again in August 2006 (68-96% colonies). Colonies bleached over 50-95% of their surfaces, with a recorded mortality of 11%, so our sampling site may have been impacted at the time of survey, in October 2007.

Bayahibe (DR) samples all produced a banding pattern very similar to that described in Barbados (LaJeunesse et al. 2009). The profile is dominated by a pair of bright bands: C7 and C7a (also known as C12, Franklin et al 2012). Above this pair of bands lay several C7 heteroduplexes. Below the band pair lay a very faint C3 band. The difference between the published profile and ours is a bright C-type band between C3 and C7, which sequencing was

unable to identify. Sequencing revealed only one base pair difference between this new type ('Ctype5') and C3.

HRM analysis showed melt peaks for profiles at 83.8 – 84.0°C, for all samples where DGGE had shown a C7/C7a + C3 DGGE ribotype. This melt peak value lay halfway between recorded melt peak values for C7/C7a (e.g. 84.1°C) and C3 (83.9°C), perhaps reflecting the mix of types. Comparing melt profiles to those with similar DGGE fingerprints showed that the DR (with the additional unidentified C band) had a slightly lower melting peak, and also appeared skewed to the right, than those dominated by C7/C7a and C3 alone (e.g. Dominican samples). One sample showed an unusual double peak, with the second peak at 86.2°C. This was the only sample that contained D1a.

Jamaica (sites JA and JB)

Jamaica has well developed fringing reefs along the north and east coasts, with patch reefs around the south. Since records began, live coral cover of Jamaican reefs has been driven down to < 5 % by overfishing, hurricanes, *Diadema* and coral diseases, although both our study sites had higher than average live coral cover (JA=28.1%, JB=20%) (Jones et al. 2008). Widespread bleaching occurred in the area between August and October 2005, with *Montastraea* spp. being among the worst affected species, although many corals showed quick recovery, with 50% recovered within five months. At the time, our two Jamaican study sites, Drunkenman's Cay (JA) and Dairy Bull (JB) were among the most severely impacted, with more than 80% of the coral community bleaching (Jones et al. 2008). As a result of the bleaching event, coral mortality has increased, particularly in *Montastraea* due to increased incidence of white plague. Surveys at Drunkenman's Cay showed > 5% recently killed coral in November 2005 and again in May 2006. Sampling was carried out in September 2007.

Samples from Drunkenman's Cay (JA) displayed the lowest diversity in the Greater Antilles (Simpsons 1/D = 1.48) with all samples producing a B1 dominated fingerprint. The profile also harboured several higher-migrating B1 heteroduplexes, and a paler B7 band lying just below, in a similar, but slightly lower position than B17. The majority of Dairy Bull (JB) reef samples produced similar profiles, with a bright B1 band and a co-dominant B7 band, although here the B7 band is as bright as the B1 (Appendix Fig. 5.19). This B1/B7 mix was also found in Columbia (CM) samples. A few samples produced an alternative profile, which appears to host a single symbiont, C7. This profile is also common to all Curaçao sites and one of the Venezuelan sites (BV).

Cayman Islands (site X)

The Cayman Islands reefs – particularly those of Little Cayman - remain relatively unspoiled.

Rum Point, off the Northern side of Grand Cayman, exhibited a decline in coral cover from 25.7% to 15.4% between 1997 and 2001, prior to sampling in July 2007. This was partly attributed to nutrient pollution leached from populated areas increasing macroalgal abundance (Jones et al. 2008). *Montastraea*, the most abundant coral genera in the Caymans (46%) experienced a 30% decline in abundance (1999 to 2005), while more ‘weedy’ species *Porites* and *Agaricia* steadily increased over the same time period. White plague was thought to be culpable, increasing average *Montastraea* mortality from 29% to 42.7%. The bleaching event of 2005 produced partial bleaching recorded in most *M. annularis* colonies, although mortality appeared low, with total coral cover remaining relatively consistent between 2005 and 2006 (Jones et al. 2008). Further severe bleaching events in 2009 produced bleaching in almost 50% of the remaining corals, with *M. annularis* identified as the second most bleaching-sensitive species (van Hooidonk et al. 2012).

Rum Point samples hosted a variety of *Symbiodinium* types (see Appendix Fig. 5.20). All individuals hosted various combinations of C7, B1 or B10 – either exclusively, or co-dominantly. A faint band present in many samples appeared similar to the B7 band found present in Jamaican samples, although unfortunately this could not be confirmed. HRM analysis corroborated DGGE observations, although was not able to resolve B1/B10 differences conclusively. Samples hosting purely B1 had a higher melting temperature than those hosting B10 only (86.2°C for B1, compared to 85.8°C for B10), but most samples contained a mix of B10 and B1, leading to a mass of peaks at 86.0°C around 1500. Where samples contained both B1 and B10, melt peak of 86.0 was observed.

5.4.1.4 The Southwestern Caribbean

When corrected for sample size, the Southwestern Caribbean region hosted the second greatest species richness, after the Eastern Caribbean. This was also the only region in which B1 was not the most dominant symbiont, with C3 and C7 types appearing frequently.

Nicaragua (sites NA and NB)

Chavo (NB) hosted three DGGE ribotypes. Approximately 40% of the Chavo samples exclusively hosted B1, producing a simple profile that was shared by neighbouring site White Hole (NA), just 1.73 km away. A further 38% exclusively harboured C-types, including C7a/C7/C3 mix – this profile was found in one sample at White Hole. The remaining 22% were a mix of these profiles, harbouring roughly equal amounts of C and B types. These produced a double melt peak in HRM (86.1°C and 83.9°C). The majority of Nicaraguan samples, produced a single melt peak at 86.1°C, corresponding with the B1 band. However, while many of the 86.1°C melt peaks showed a neatly tapered peak up to 2,500 RFU units, some peaks displayed a shorter (~1000 units), broader peak, with a bulge to the left hand side (usually peaking around

83.9°C), perhaps indicative of a dominant B1 with some additional C7a/C7 banding. This phenomenon is also commonly found in nearby site NB.

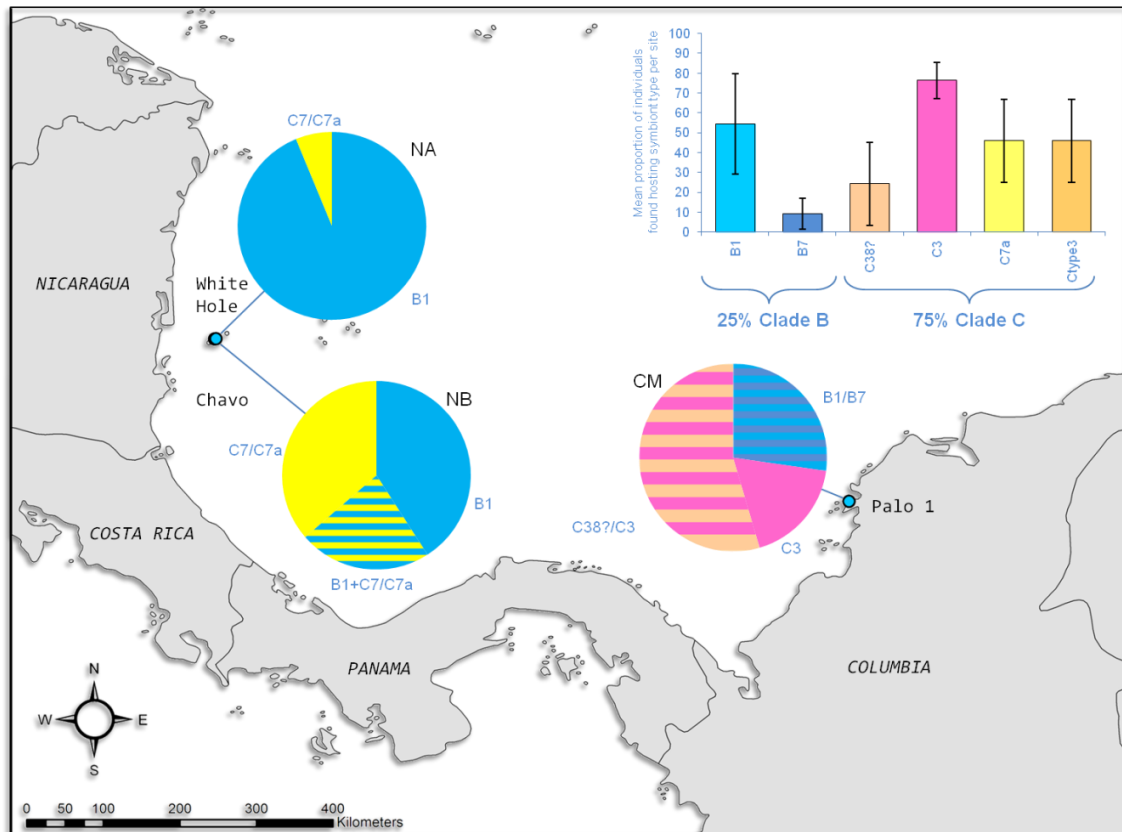


Figure 5.8: Map showing location of *Montastraea annularis* sampling sites for the Southwestern Caribbean marine ecoregion, along with diversity of dominant symbiont ITS2 symbiont types recorded (pie charts). Bar graph shows the species richness for the region, based on abundance of all types.

Columbia (site CM)

Columbia samples were dominated by a single high-migrating band, which sequencing revealed to be C3. The majority of samples showed a different, pale double band in a similar position that had migrated slightly higher on the gel. An alignment showed the closest type to this was C38 – previously only found in *Acropora* in the Eastern Caribbean (LaJeunesse 2005). A lower migrating band was present in CM35, the B7 band also present in Jamaican samples, and some samples displayed both the C38(?) and B7 band.

HRM analysis supported the DGGE outcome, with C3 dominated profiles producing an unmistakable fluorescent peak (2500) at 84.0°C, while the B7 dominated profile showed a similarly clear-cut fluorescent peak at 2000, at 86.4°C (a little higher than the melt peak for B1 of 86.1°C, as expected). Other samples that contained a mix of B7 and C38 – e.g., CM32 and CM27 – still generated a melt peak at the B-type melt temperature, but the curve was <1000 and spanned a broader temperature range. Samples harbouring exclusively C38(?) were almost indistinguishable from C3 in terms of melting point, this could be expected, given these ITS2

types travelled a similar distance on the gel. However C38 had a consistently lower melting point than C3 (83.6-83.8°C compared to 84.0-84.1°C) and could be differentiated by the fact they showed much less fluorescence and had a broader curve.

5.4.1.5 The Lesser Antilles (Eastern and Southern Caribbean)

Ten sites made up this final group of easterly Caribbean Islands: from the Leeward Antilles Curaçao and Venezuela, the Leeward Islands (British Virgin Isles and Dominica), and the Windward Islands of Tobago and Barbados (Fig. 5.9). These sites are all situated on the partly volcanic island arc that begin east of Puerto Rico and stretch round to the Venezuelan coastline. The Lesser Antilles reefs were severely impacted by the 2005 bleaching event, which began when a bleaching hotspot developed northeast of Barbados in June, spreading to cover the remainder of the region by August and covering most of the Caribbean Sea by October (Bouchon et al. 2005). The accumulated heating stress was the most extreme ever recorded in the Caribbean, but was particularly catastrophic for the Lesser Antilles, which experienced DHW's exceeding five for most of the summer, and a maximum of 13-14 DHW by November 2005 (Bouchon et al. 2005). Prolonged elevated temperatures caused the most severe mortality

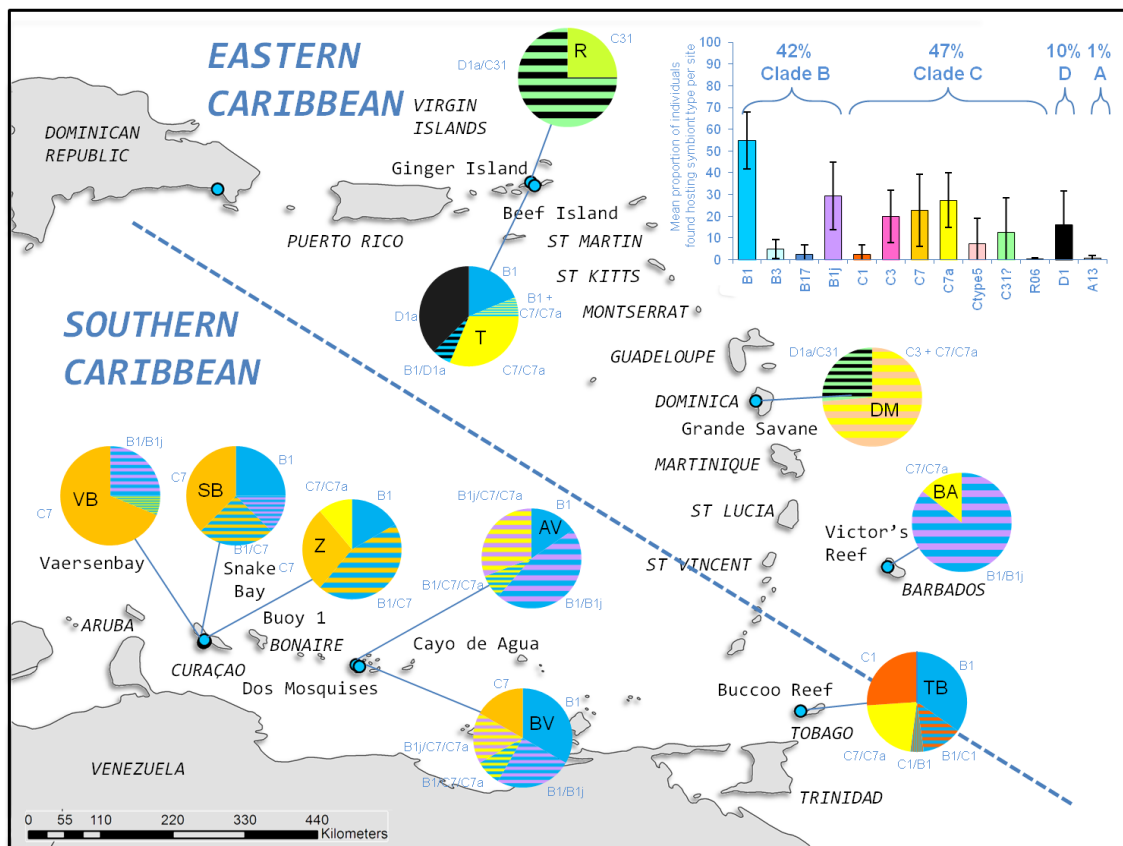


Figure 5.9: Map of the Lesser Antilles (including the Eastern Caribbean and Southern Caribbean marine ecoregions), showing *Montastraea annularis* sampling sites, along with relative dominance of *Symbiodinium* ITS2 types, or pairs of types (pie charts). Bar chart depicts the range of taxa found, with bars representing average abundance of the type, with error bars showing 1 s.d.

observed in this region; in Barbados all species on all reefs were bleached, while Guadeloupe and Martinique experienced 25-52% coral mortality (Bouchon et al. 2005). Reef sites have shown little sign of recovery, with *M. annularis* in the US Virgin Islands showing over 69% mortality since the event (Miller et al. 2009). Disease and bleaching were still evident in 2006 and *M. annularis* was among the species worst affected.

M. annularis of the Lesser Antilles appeared to host more *Symbiodinium* C than other regions: on average 50% of samples hosted C7 or C7/C12, compared to just 12% across the other sites. In addition to greater occurrences, clade C was more abundant, dominating endosymbiont communities more frequently (34% of samples compared to just 12% in other sites) – see Fig. 5.9. In direct contrast, B1 – the most commonly occurring symbiont, present on average in 70% of samples – was considerably less abundant in this region, arising in just 55% of individuals, (at >40% of sites surveyed outside the Lesser Antilles, B1 was found in every single sample) – as well as being less important, being the dominant clade in just 14% of individuals compared to 44%. With 11 symbiont sub-clades identified in this region, the Lesser Antilles corals also hosted a greater diversity of types – with three sites hosting seven symbiont types, and none hosting less than three. The Eastern Caribbean hosted the greatest symbiont richness (when corrected for sample size), with the Southern hosting a similar number of types to the Greater Antilles. The Lesser Antilles had the greatest *Symbiodinium* ITS2 diversity, at 8.26, above the survey average of 5.79. The region also hosted unique types - for example B1j was common in Barbados, Curaçao, Tobago and Venezuela, but not found in any other Caribbean areas. Dominica may also host an as yet unidentified type (Ctype5) not seen at any other sites.

British Virgin Islands, BVI (sites T and R)

Two sites were sampled from the BVI location, Beef Island (T) and Ginger Island (R). Prolonged exposure to elevated SSTs in 2005 had a severely detrimental impact on the British Virgin Isles, with colonies of *M. annularis* suffering high mortality from white plague in the southern BVI. This area was probably the hardest hit in the entire Caribbean, with all colonies > 10 cm showing at least 11% partial mortality. The damage continued long after the SSTs fell, and when sampling for this study began in 2006, 15% of colonies were reported as showing recent mortality (Bouchon et al. 2005).

Beef Island (T) samples showed more variable symbiont communities than their Ginger Island counterparts. Individuals fell into one of three main DGGE ribotypes, each dominated by a different clade type. The most frequently occurring consisted of a bright band that sequencing revealed to D1a, and a fainter band well spaced above (D1), and was identical to the principal ribotype found at the Cuban site (CC). Other samples appeared to show a B1 dominated banding profile, while a third presented a C7/C7a band, with a C3 and several heteroduplexes above. Ginger Island (R) samples were also dominated by D1/D1a, although the profile

generated was slightly different. Shared with a Bahamian site (EN) and a few samples from Dominica (DM), it consisted of a bright C band (thought to be C31) – present in all samples – which lies just below the C1 band, and a second, paler band is well spaced below, lying above the D1 band in several samples. In some samples a faint D1 band is also present in the usual place, with a D1a below.

All samples dominated by D1/D1a had a single melt peak at 84.7°C – this agrees with D1 dominated samples from Belize (G) and Cuba (CC) which produced similar sized melt peaks at 84.6°C and 84.8°C respectively. HRM analysis was unable to resolve differences in D1/D1a and C31 band mix seen at Ginger Island, the positioning of the melt peak suggests that the D1/D1a mix is masking the signal of the unidentified C-type (C31?). Beef Island communities dominated by B1 produced melt peaks as expected at 86.2°C. The final set of Beef Island samples produced a peak at 84.1°C, agreeing with other C-dominated samples.

Dominica (site DM)

Directly southeast of the BVI, the Dominican coral communities are subjected to high levels of rainfall, runoff sedimentation and river input plus grow on volcanic rock, meaning little build up of carbonate base framework. Dominica was unusual in being one of the only sites (along with Cuban CC site, and Ginger Island, R) that no individuals screened were dominated by a B-type – in most other sites at least one or two individuals were dominated by sub-clade B1. Only 5 of the 19 samples screened contained (weak) B1 bands (Fig. 5.9). Eight of the ten samples displayed a fingerprint is dominated by two bright C7 parallel bands (a C7 and C7a above), with a faint unidentified band ('Ctype5'), and a bright C3 band below this. This was also present in one Tobago, one Barbados, a Dominican Republic and several Nicaraguan samples. Sequencing revealed this new C-band, shared by the Dominican Republic, (where it was dominant), to have one base pair difference from C38 and from C7. Above the C7/C7a double bands, are a double C3 band, and an array of C7 heteroduplexes. This ribotype is very similar to the C7a profile previously been described in Barbados (Finney et al. 2010). A few samples had lower B1 bands and the brightest band in an unusual position, just below the C1, with a band below this, closer to the D1 (these bands are mostly likely to be a C-type (C31). Lower down, these profiles all contained the D1/D1a banding, as seen in Cuban (CC) and Bahamian (EN) sites. DGGE gels showed these DM profiles are identical to those found in the BVI (site R, Ginger Island) (see Appendix Fig 5.26).

HRM profiles fell into one of two melt peaks: 84.0°C and 84.7°C. DM01 and DM09 followed the 84.7°C, identical to the C31(?) melt peaks of Ginger Island samples, but also similar to the D1/D1a dominated samples (e.g., Cuban CC samples), which also contain D1/D1a mix but not the C above (C31). Evidently the D1/D1a signal is masking that of the other C bands. All other samples were between 84.0 and 84.1°C, corresponding to the C3/C7 declaration.

Barbados (site BA)

Barbados, the most easterly of the Lesser Antilles islands, is a fossil coral island surrounded by a 2-3 km wide shelf supporting a variety of reefs. Average live coral cover has been degraded to 10% (range 1-30%), due to coastal development, storms and overharvesting of fish and corals, though offshore bank reefs are less damaged (30% coral). Bleaching in 2005 was severe and widespread, with 59-86% of all colonies affected. Initially inshore reefs were impacted worse (80.6%), although with increasing time spent at elevated SSTs virtually all species bleached. *M. annularis* was among the most sensitive, with approximately 70% of all colonies bleaching. By June 2006, bleaching persisted in 17.2% of colonies and coral continued to die, recent mortality was evident in 18.7%, and partial mortality estimates trebled, probably due to reduced resistance to coral disease (Bouchon et al. 2005).

The majority of Barbados corals showed a B1j profile, consisting of a B1 band, a B1j band, and two B1 heteroduplexes above (Appendix Fig 5.27). One sample had a different profile with two bright parallel C7 and a C7a bands, and another also contained some in the A13 position, although it was too weak to be successfully sequenced. Most samples produced one HRM peak around 76°C, which probably represents the B1/B1j mix. The C7/C7a community produced a strong flare at 84.1°C.

5.4.1.6 Southern Caribbean

The Southern Caribbean ecoregion boasts sites with high coral cover, partly because of their location away from the paths of most hurricanes. Although the Lesser Antilles hosted the greatest *Symbiodinium* diversity, the Eastern Caribbean contributed more than the Southern Caribbean, which was more similar in diversity to the Southwest ecoregion (Simpsons 1/D = 4.94).

Tobago (site TB)

Tobago hosts extensive shallow water reefs, dominated by the *M. annularis* complex (37%). Reefs are healthy, boasting low macroalgal cover (3%), and few records of coral disease or tissue necrosis prior to 2005 (Bouchon et al. 2005). The 2005 bleaching event was both extensive, affecting > 85% of reefs, and severe with 66% of corals bleaching. 73% of *M. annularis* complex surveyed showed evidence of bleaching, although it exhibited high variability: at our Buccoo Reef site (TB), it was reported that one stand of *M. annularis* exhibited bleaching across 97% of its surface, while a neighbouring stand was showed minimal (6%) bleached tissue. The authors of the report note that this observation probably indicated the presence of bleaching resistant symbiont clades. Mortality increased since the event, particularly

among massive corals, so that it was likely that Buccoo Reef was less pristine at the time of sampling in September 2007 (Bouchon et al. 2005).

All Tobagan DGGE ribotypes contained what was understood to be a (usually dominant) C1 band, along with a lower, unidentified band (could be a C1 heteroduplex), identical to those found in Honduras site B. B1 was another frequently occurring band. An alternative profile with higher migrating C7/C7a double bands, often accompanied by C3, was also recorded (Appendix Fig. 5.28). These produced a single melt peak at 83.9°C. C1/B1 samples generated two equally sized melt peaks - one at 83.7°C (very similar to 83.9°C, but slightly lower fluorescence (e.g. 1500 compared to 2500 units) and one at 86.1°C (corresponding to *Symbiodinium* B1). Finally, some samples simply had the 86.1°C curve, exclusively hosting B1.

Venezuela (sites AV and BV)

The Los Roques islands, 128 km directly north of Venezuela, are a small archipelago of over 350 islands, and have been a National Park since 1972 and a RAMSAR site since 1996. Two westerly islands – Cayo de Agua and Dos Mosquises - were chosen as sampling sites. These sites both hosted the greatest symbiont richness observed in the entire study (BV slightly more than AV), when corrected for sample size. At both sites similar ITS2 ribotypes were observed, with DGGE revealed a mix of banding profiles.

In both Cayo de Agua (AV) and Dos Mosquises (BV) the most commonly occurring DGGE banding pattern was dominated by a bright B1j along with a double C7/C7a band, a pale B1 band, a double band below B1, and other pale banding throughout the profile. This tended to generate two melt peaks in the HRM: one representing the B1 (86.2°C) and the second the C7/C7a (84.0°C) strains. Most samples showed variations on this profile, some missing the C7/C7a, and some the B1. A few samples were dominated by B1, particularly in the Dos Mosquises samples. Although HRM was unable to distinguish between B1 and B1j dominated samples, the melting temperature was slightly lower for mixed samples reflecting the fact that the B1j band doesn't travel as far on the gel (Appendix Figs 5.29 and 5.30).

Curaçao (sites VB, SB and Z)

Curaçao is a small oceanic island 70 km north of Venezuela; with continuous *M. annularis* dominated reefs fringing the 60 km by 15 km island (Bouchon et al. 2005). The three sampling sites; Vaersenbay (VB), Snake bay (SB) and Buoy 1 (Z), were located off the western side of the island and spaced less than three kilometres apart. Reefs around Curaçao have been described as having living coral cover of 30-70%, this high abundance partly explicable by the islands location south of the path of most hurricanes (Bouchon et al. 2005). The collection date of these samples (October 2005) indicate that collections would have been made during the

height of the bleaching 2005 event. However, bleaching affected only 14% of colonies, with Curaçao and nearby Bonaire escaping relatively lightly compared to Eastern Caribbean sites (e.g. in St Maarten and Saba where 80% of colonies bleached). There was no apparent mortality and high coral cover was maintained between 2005 and 2006, with just 3% of colonies in bleaching again in November 2006 (Bouchon et al. 2005).

Curaçao samples were either dominated by B1 or C7, or some combination of these types (Fig. 5.9). In occasional samples at Buoy Z, a double C7/C7a band was apparent instead of the single C7. Several (although not all) of the samples dominated by B1 revealed a DGGE profile similar to that described previously in Barbados with a B1j above, and two heteroduplexes above that this (Finney et al. 2010), although others presented a single B1 band. At Snake Bay and Vaersenbay, a few samples appeared to show an additional bright band immediately above the B1, possibly representing B3.

HRM corroborated DGGE observations, although an amorphous peak in the B1 position (86.0°C) suggests that this melt profile reflects more than simply B1, but a B1/B1j mix (Appendix Figs. 5.31 and 5.32). Consistent tall (4000) peaks at 84.1°C were thought to contain only C7, while shorter, broader peaks hosted C7/C7a, although this could not be used reliably as a diagnostic tool. Double melt peaks occurred where both B1/B1j and C7 profiles were found, with peak size varying in proportion to the brightness of the DGGE band image were consistent with the DGGE results (Appendix Figs. 5.31 to 5.33).

5.4.2 Caribbean-wide spatial patterns in *Symbiodinium* diversity

The *Symbiodinium* communities of 632 coral colonies were successfully characterised (out of 792 attempted), across 33 sites, with an average of 18 holobiont communities resolved per site (n= 11 to 24). Twenty-two sub-clades were identified, nested within four clades: A, B, C and D. Clade B occurred most frequently, with 75% of the colonies sampled hosting B sub-types. Of this 75%, 72% hosted B-clades exclusively (Fig. 5.10: inset), with the remainder hosting a B/C mix, or occasionally combination of B/D or B/C/D. Forty-percent of colonies hosted clade C *Symbiodinium*, 14% hosted clade D and <1% were found to harbour clade A. Figure 5.10 shows the spatial distribution of clades across the Caribbean and Bahamas. Examination of the mapped data by eye appears to show a greater abundance of clade B (in blue) in the north-east, and more clade C (in yellow) in the southeast. This geographic patterning was later shown to be robust using SADIE analyses.

5.4.2.1 Cladal level patterns

The majority (74%) of *M. annularis* colonies possessed just one cladal type (though this often consisted of several sub-types), with the ratio of clades B : C : D being 7 : 2 : 1. Twenty-four

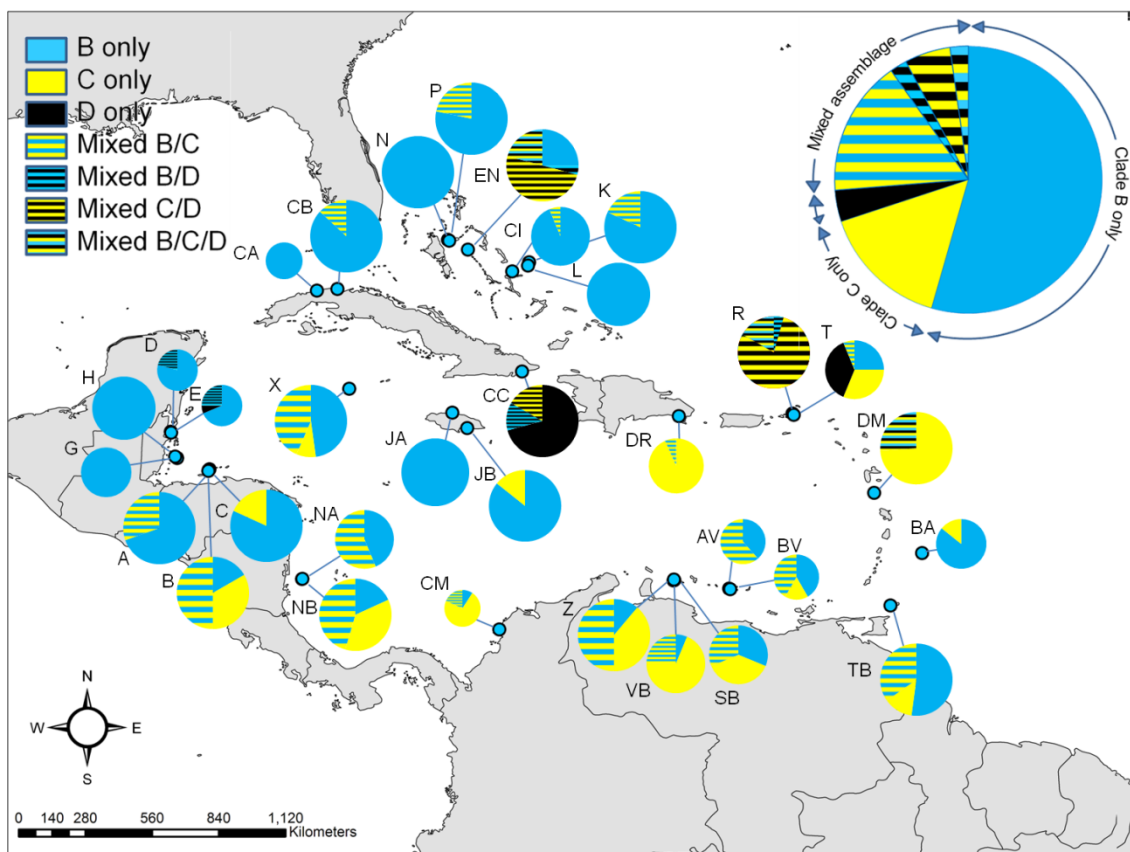


Figure 5.10: Map depicting absolute proportions of *Symbiodinium* clade B, C and D (and combinations of these clades) hosted by *Montastraea annularis* at 33 sites across the Caribbean and Bahamas, $n=632$. Pie chart size reflects actual sample size (minimum 11, max 24). **Inset:** Pie chart summarising the proportional composition of clades hosted.

percent of samples hosted two clades, with a B/C combination occurring most frequently, accounting for two-thirds of all ‘mixed’ types. Just 2% of samples were found to harbour a mix of B, C and D clades (Fig. 5.10).

5.4.2.2 Sub-cladal level patterns

Six *Symbiodinium* B ITS2 sub-clades (B1, B3, B7, B17, B1j and B10) were identified using DGGE and sequencing. A further two B-types (provisionally labelled ‘Btype2’ and ‘Btype10’) were detected but not recognised as a previously recorded type. B1 was the most prolific of the sub-clades: it was found in 72% of all samples, was harboured by corals at all but one site and accounted for more than half of all the clade B’s found (70%). The remaining four clades amounted to just 30% of all B’s found (Fig. 5.11). Seven *Symbiodinium* C sub-clades were detected (C1, C3, C7, C12 - also known as C7a, C31, C38 and C62) along with a further three types (‘Ctype3’, ‘Ctype5’ and ‘Ctype6’) that were again unable to be categorized. Clade C symbiont types showed less variation in their comparative abundances, with C12 (also known as C7a), C3 and C7 occurring most frequently (Fig. 5.11). Clade D sub-types consisted simply of

D1a, the only D clade *Symbiodinium* known to inhabit the Caribbean. One example of Clade A was found at a site in Barbados, this was identified as A13.

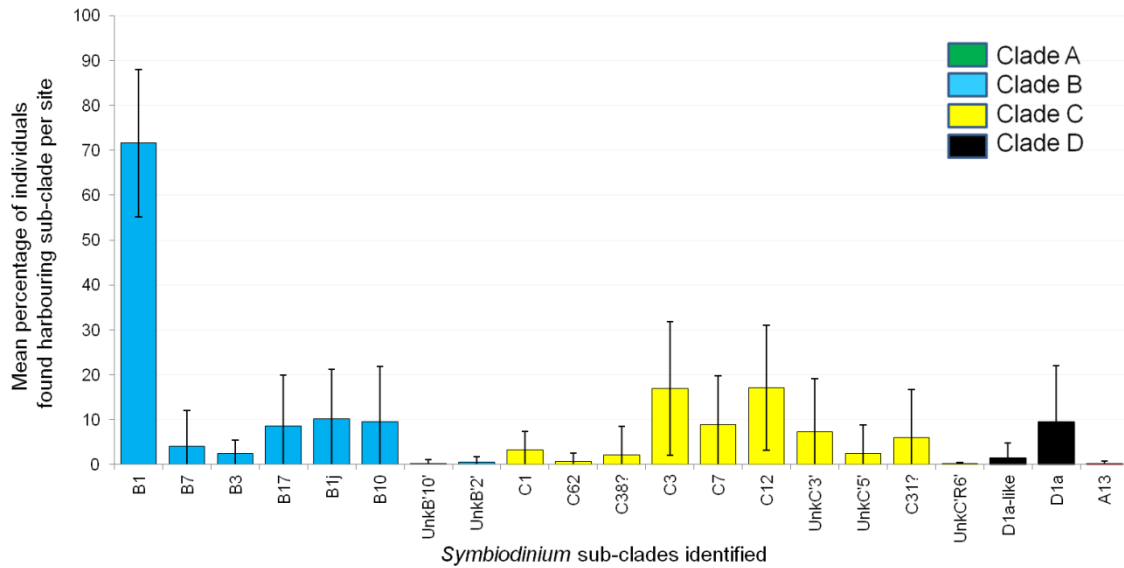


Figure 5.11: Bar chart reporting the relative proportions of symbionts (classified to sub-cladal level) hosted by *Montastraea annularis*. B1 was the most abundant symbiont, found in 72% of samples (457 individuals). Symbionts labelled ‘Unk’ were unable to be successfully identified to sub-cladal level.

Each *M. annularis* colony analysed hosted between one and five of these symbiont sub-clades. Most hosted just one (34%) or two (39%). Twenty percent of samples hosted three, and just 7% hosted four or more sub-clades. Species richness (per colony) ranged from 1.44 to 2.49 (Margalef’s richness), mean =1.63.

Although no attempt was made to quantitatively determine the abundances of symbiont sub-clades in corals hosting mixed assemblages, the brightness of each DGGE gel band is understood to infer a qualitative measure of relative abundance. As some bands were very pale compared to others, we were able to record the ‘dominant’ types in each sample. This method provided additional information besides beyond presence/absence species abundance data. For example, B1 was harboured by 72% of corals (Fig. 5.11), but was the dominant symbiont in the communities of just 35% (Fig. 5.12). In a further 32% of samples, B1 was co-dominant with

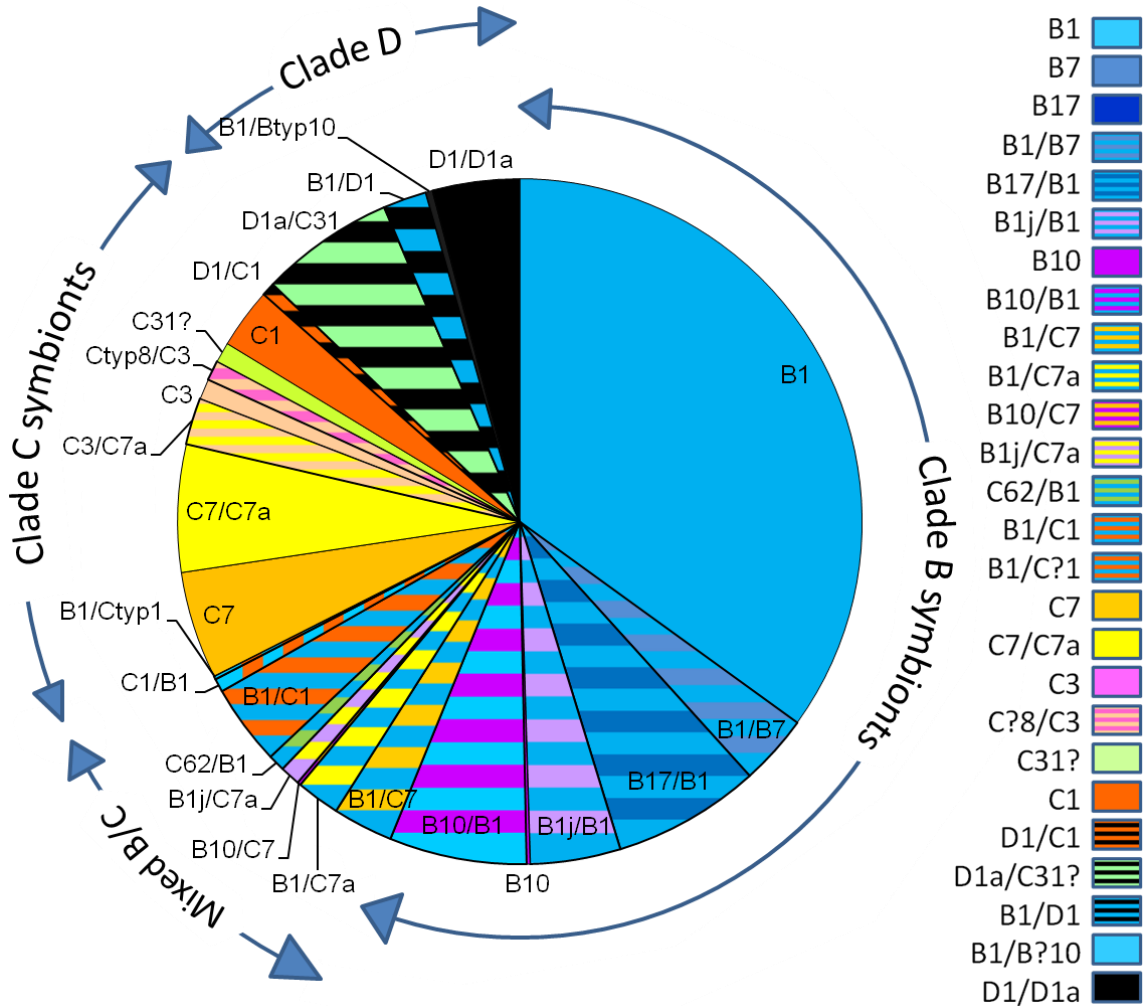


Figure 5.12: Pie-chart depicting the major symbionts, or pairs of symbionts (striped fill) found dominating *Montastraea annularis* endosymbiont communities. The sub-clade B1 most frequently was the most abundant *Symbiodinium* found harboured by the corals – usually exclusively, but sometimes in combination with other clade B, C or D symbionts. Where question marks are present ('?') symbiont type unable to be identified to sub-clade level with confidence.

another symbiont type, while in 5% of samples it was hosted in a background capacity. There were 26 commonly occurring dominant symbionts, or symbiont combinations, which appeared to dominate communities (see Fig. 5.12). B1 was the single most commonly occurring dominant symbiont, and was often found to be co-dominant with other B-types (e.g., B7, B17, B1j), also C (C1, C7 and C12) and D1a. C7, C12 and C1 were frequently seen to dominate communities. Clade C and B types were often found to exist co-dominantly, while D was co-dominant more often than not.

Mapping the spatial distribution of dominant sub-cladal types revealed considerable within-site species richness: at 30 out of 33 sites more than one dominant symbiont (or symbiont pair) was hosted (Fig. 5.13). The mean number of combinations hosted at any one site was three, with a maximum of six dominant banding patterns found at Rum Point in the Cayman Islands (Fig. 5.14). B-dominated communities appeared to have a westerly distribution, while C types appeared more frequently in the Eastern and Southern Caribbean marine ecoregions (Fig. 5.13).

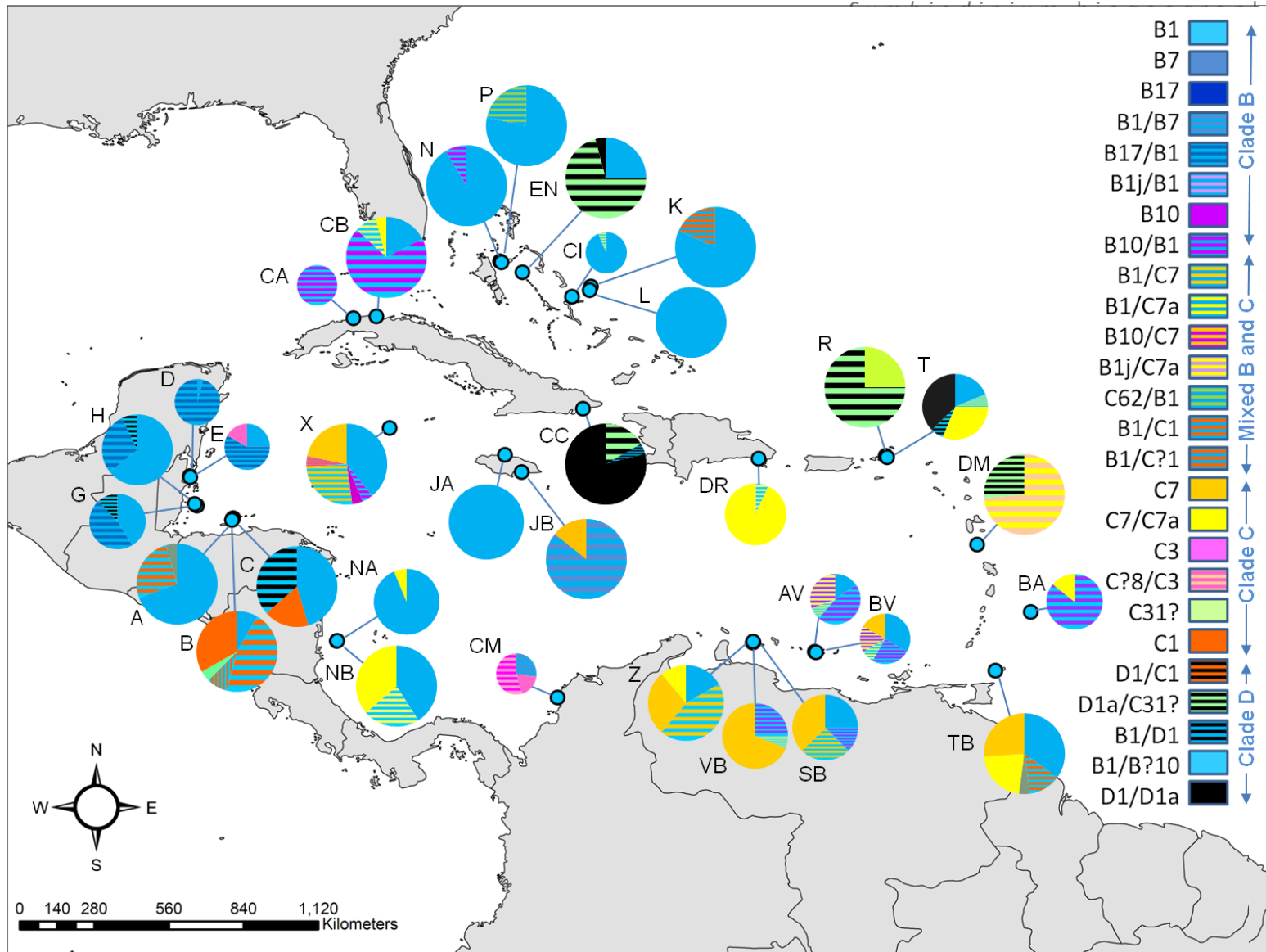


Figure 5.13: Map showing the distribution of the dominant symbiont types hosted by *Montastraea annularis* at 33 sites across the Caribbean and Bahamas. Pie charts represent the relative proportion of dominant symbiont (or pairs of symbionts) hosted at each site, with the colours representing various combinations. Striped patterns represent a co-dominant mix of two types. Letter identifies sample site and pie size reflects the number of coral samples successfully analysed (min=11, max=24).

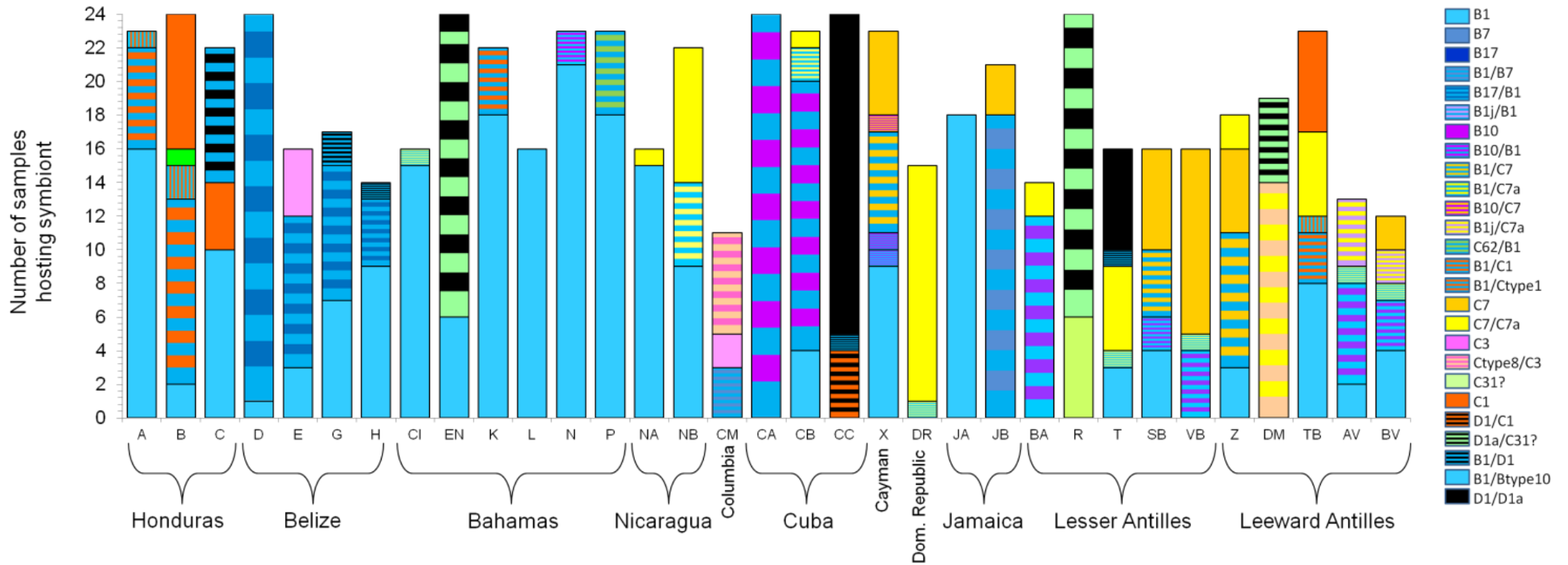


Figure 5.14: Bar chart describing the major symbiont sub-clades hosted by *Montastraea annularis* at 33 sites across the Caribbean and Bahamas. Communities of *Symbiodinium* were characterised to sub-cladal level for 11-24 coral samples from each site, with bars representing differing sample sizes. The dominant symbiont (in terms of abundance), or pair of symbionts, inhabiting each individual was recorded. Bold fills represent a community dominated by a single symbiont sub-clade, striped fills represent a mix of two or more.

Marine Ecoregion	Location	Site	Identifier	Sample size, n	Richness			Diversity	
					Species richness	Rarefaction (to n=11)	St Dev	Simpsons D Index	Simpson's Reciprocal Index 1 / D
Mesoamerican Barrier Reef	Honduras	Seaquest	A	23	3	3.89	0.02	0.42	2.39
	Honduras	Sandy Bay	B	24	6	1.46	0.38	0.20	4.99
	Honduras	Western Wall	C	22	3	2.45	0.00	0.42	2.38
	Belize	Coral Gardens	D	24	4	1.00	0.02	0.31	3.24
	Belize	Eagle Ray	E	16	5	2.39	0.13	0.23	4.44
	Belize	Long Cay	G	17	4	1.99	0.29	0.30	3.36
	Belize	West Reef	H	14	4	2.47	0.02	0.29	3.40
The Bahamas	Bahamas	Conception Island	CI	16	4	1.74	0.00	0.55	1.83
	Bahamas	Exumas North	EN	24	5	1.98	0.08	0.20	4.92
	Bahamas	Seahorse Reef	K	22	3	3.16	0.06	0.49	2.05
	Bahamas	Snapshot Reef	L	16	2	4.40	0.00	0.79	1.26
	Bahamas	Schoolhouse Reef	N	23	3	4.32	0.29	0.50	1.99
	Bahamas	Propeller Reef	P	23	3	2.95	0.09	0.57	1.75
Nicaragua/Columbia	Nicaragua	White Hole	NA	16	5	1.95	0.22	0.22	4.62
	Nicaragua	Chavo	NB	22	5	2.98	0.39	0.22	4.60
	Columbia	Palo 1	CM	11	4	1.91	0.00	0.27	3.66
Greater Antilles+ Cayman	Cuba	Baracoa	CA	24	3	2.00	0.00	0.47	2.13
	Cuba	Bacunayagua	CB	23	5	1.00	0.56	0.33	2.99
	Cuba	Siboney	CC	24	7	3.82	0.53	0.34	2.92
	Cayman	Rum Point	X	23	4	2.89	0.23	0.34	2.96
	Dominican Republic	Bayahibe	DR	15	5	2.98	0.70	0.29	3.43
	Jamaica	Drunkenmans Cay	JA	18	3	1.69	0.00	0.68	1.48
	Jamaica	Dairy Bull	JB	21	4	1.00	0.36	0.36	2.76
Lesser Antilles	Barbados	Victor's Reef	BA	14	4	1.69	0.06	0.38	2.64
	BVI	Ginger Island	R	24	6	4.36	0.13	0.22	4.51
	BVI	Beef Island	T	16	6	3.91	0.00	0.14	6.92
	Curacao	Snakebay	SB	16	5	2.68	0.20	0.31	3.26
	Curacao	Vaersensbay	VB	16	7	1.73	0.49	0.20	4.91
	Curacao	Buoy 1	Z	18	4	2.79	0.25	0.31	3.26
	Dominica	Grande Savane	DM	19	8	1.97	0.48	0.16	6.42
	Tobago	Buccoo Reef	TB	23	7	3.83	0.51	0.21	4.85
	Venezuela	Cayo de Agua	AV	13	6	4.92	0.52	0.20	4.99
	Venezuela	Dos Mosquises	BV	12	7	3.00	0.28	0.18	5.51

Table 5.3: Richness and diversity measures for *Symbiodinium* ITS2 at each of the 33 sites.

Not all clades displayed spatial distribution: clade D-dominated communities were spread across six widely dispersed sites: Honduras (C), the Bahamas (EN), Cuba (CC), the British Virgins Isles (R and T) and Dominica (DM). SADIE analyses were later used to test the degree of this observed spatial patterning of each symbiont sub-clade across the sites.

5.4.2.3 Symbiodinium richness

Margalef's species richness was employed to compute species richness for each site while taking into account variation in sample size (Table 5.3). Mean site species richness was 4.7 ± 1.5 , with a minimum of 2 (Snapshot Reef, in the Bahamas) and a maximum of 8 (the Dominican Republic).

Plotting symbiont richness (below) appeared to demonstrate some kind of spatial element to richness, with Bahamian, Honduran and Belizean corals showing lower richness than some of

the more easterly sites (Lesser and Leeward Antilles). In order to test whether observations about spatial patterning of species richness are genuine, a parametric SADIE analysis was performed on the total species counts per site, with an *iseed* of 30,000 and a maximum allowed number of randomisations *k5psim* of 156 selected. 5967 randomisations were executed. At each site, spatial pattern was measured through an index of clustering, with sites with counts greater than the overall mean assigned a patch cluster index, and those with counts less than the overall mean assigned a negative gap cluster index (Appendix Table 5.2).

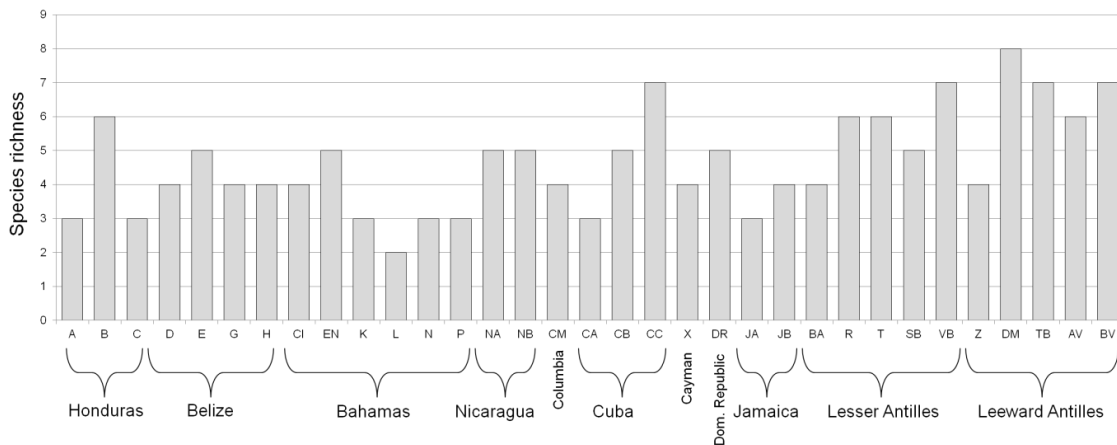


Figure 5.15: Bar chart comparing total species richness between sites.

The cluster index (v_{ij}) for each site was then mapped, producing a classed post map of the local degree of spatial patterning. Finally, universal kriging was used to interpolate between sample sites, and a contour map, with a contouring interval values of 1.5 and -1.5, chosen to reflect clustering that is half as large again as expected from a random arrangement of the counts - superimposed onto the classed post map (Fig. 5.16). The SADIE analysis produced an I_a (index of aggregation) of 2.2, that was shown to be significant ($P_a=0.001$). Both the patch ($v_i = 1.85$) and gap cluster indices ($v_j = -2.35$) were also shown to be significant, demonstrating richness data to show significant positive and negative clustering (Appendix Table 5.2). A second SADIE was performed on the rarefaction output for comparison, but was not significant (Appendix Table 5.2). The red-blue output map (Fig. 5.16) shows symbiont species richness (number of different *Symbiodinium* strains found per site) was clustered in many of the Lesser Antilles sites (eastern Caribbean), producing a significant patch of higher than expected richness of symbiont sub-clades in the east (red patch). Species richness was negatively clustered in the west (around the Bahamas, Jamaica and Mesoamerican Barrier Reef) producing a patch of lower than expected richness (blue patch). White areas were not significantly different to a random arrangement of symbiont richness.

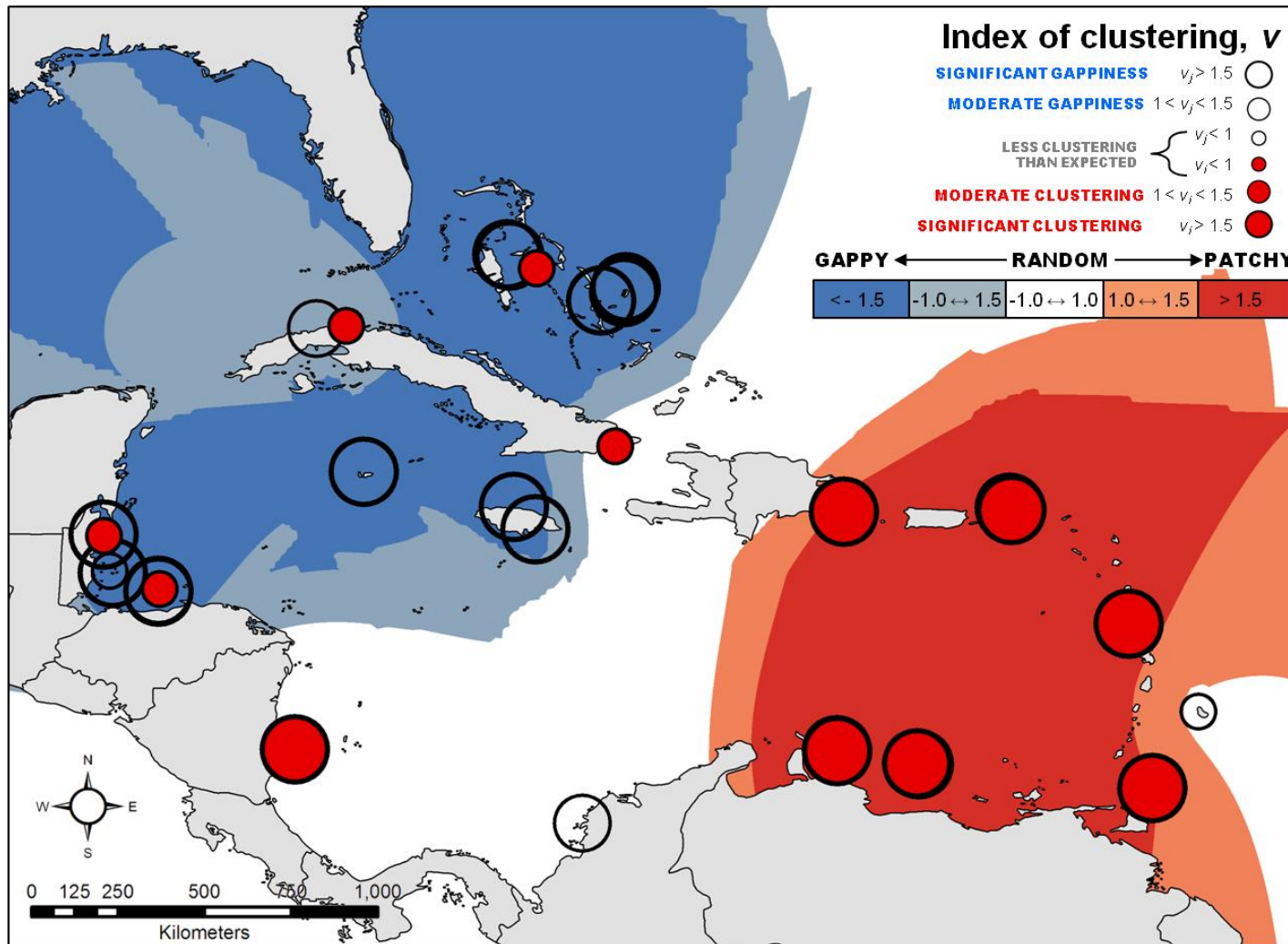


Figure 5.16: Red-blue plot showing clustering of data on *Symbiodinium* sub-cladal abundance, based on SADIE estimated indices of spatial clustering. For the classed post map, large filled circles represent a unit with clustering index that exceeds the 95th percentile for patches (red) or gaps (clear), from randomization distributions; medium-sized circles denote a unit that exceeds the 90th percentile; small circles denote unit with clustering below expectation (<1 or >-1). A contour plot has been superimposed, with coloured areas denoting richness clustering beyond expectation, and the darkest areas highly significant clustering of gappiness.

5.4.2.4 Symbiodinium diversity

The next step was to explore the symbiont diversity using calculated diversity indices. Simpson's Reciprocal Index was chosen as an appropriate diversity estimate, as the data fit the minimal assumptions of the index; the analysis is less sensitive to sample effort than other measures, and is weighed towards abundance rather than richness and is widely used. It was preferred to Shannon-Wiener, which is highly sensitive to n and influenced by rarity. The index was used to estimate diversity at each site (Table 5.3), and results plotted in a bar graph (Fig. 5.17).

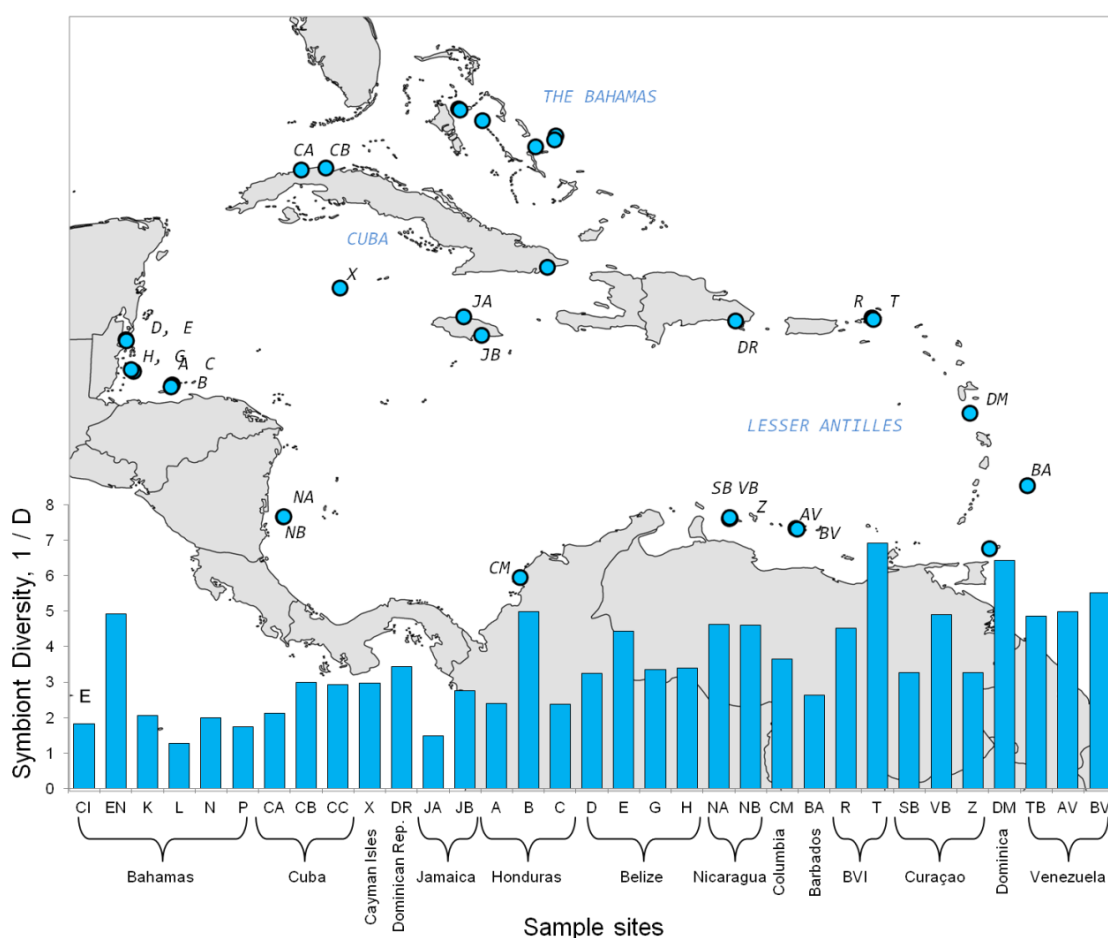


Figure 5.17: Bar graph representing symbiont diversity (Simpson's Reciprocal D) across the Caribbean. X-axis data arranged according to latitude.

5.4.2.5 Species clustering

A *species* similarity matrix was used to see if numbers of symbionts fluctuated in parallel across sites. Firstly, the number of species was reduced to those that only constituted more than 20% of the total abundance, and were found at more than one site, as cluster analyses with rarer species tends to confuse the picture. This left 13 species (B1, B7, B3, B17, B1j, B10, C1, C62, C3, C7, C12, Ctype3, D1 and D1a). A fourth root transformation was used to downweight high abundance species (this also improved the ordination stress), and a Bray-Curtis species

similarity matrix (most appropriate for ecological count data) generated to explore similarities in the distribution of species. Ordination was used to produce MDS plots (Fig. 5.18), with low stress (corresponding to a good ordination with no prospect of misinterpretation). The ordination was tested for consistency using a cluster analysis. This was used to produce a group-average linking cluster dendrograms (Fig. 5.18B) and clusters were superimposed onto ordination plots (see Fig. 5.18A). Plots revealed that D1 and D1a were found together most commonly. C7 and C12 were the only other clades found together at the 80% level.

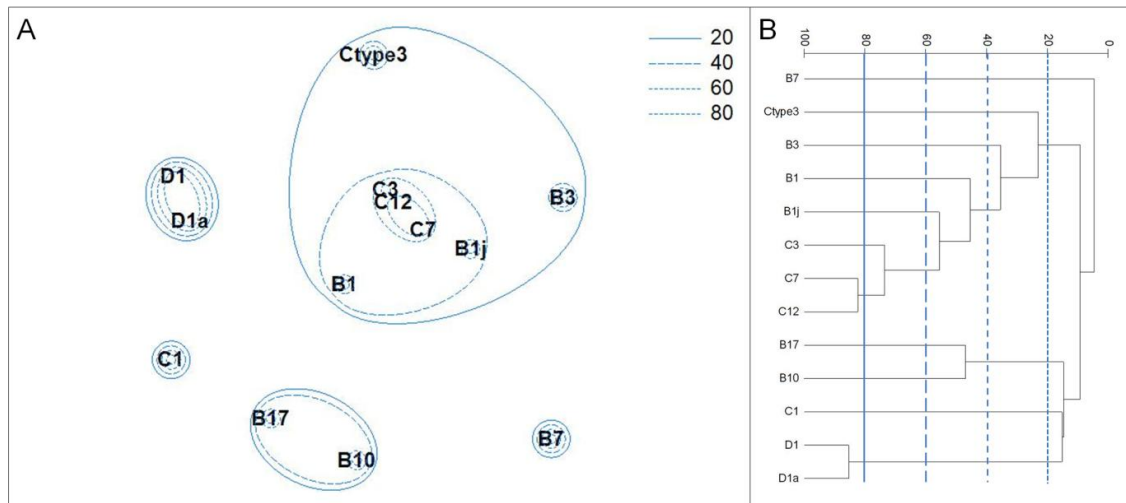


Figure 5.18: *Montastraea annularis* symbionts. **A)** 2-dimensional MDS configuration of the symbionts based on fourth-root transformed standardised abundances and Bray-Curtis similarities (stress < 0.1). Superimposed clusters from B) at similarity levels of 20, 40, 60 and 80% show grouping. **B)** Dendrogram of the species sub-clade similarities from standardised, fourth-root transformed abundance data (stress < 0.1).

5.4.2.6 Spatial analyses

PERMANOVA

A one-way PERMANOVA (see Chapter 6 for details) was used to assess the hypothesis of no differences in community structure among the thirty three sites (N=632 coral samples, p=22 symbiont types) (see 6.3.2.2). There was clearly a significant effect of the site groupings (pseudo-F = 36.1, P=0.0001), demonstrating that symbiont communities were similar within sites. A series of 528 pair-wise comparisons were then made between each site, to identify those that were not considered significantly different. Bonferroni was not required. Comparisons identified 501 of 528 as significantly different at the 5% level. A further 22 were not, although many of these were geographically close. For example, *M. annularis* from Curaçao sites Z and SB did not have significantly different symbiont communities (p=0.84, 2037 permutations), but were situated within 100 m of each other. Nearby Venezuelan sites AV and BV also (p=0.22, 8013 permutations), and SB and X (p=0.16, 5993 permutations) were also not deemed to host significantly varied symbiont communities.

Ordination

To further explore similarities between sites, a Bray Curtis similarity matrix was constructed between sites, based on root-transformed data symbiont sub-clade data. From this, ordination plots could be generated to explore the data. MDS ordination stress was 0.02, giving an excellent representation with no prospect of misinterpretation. A cluster analysis (Fig. 5. 19) revealed that sites divided into three main groups at the 40% similarity level: southwestern sites (including all southern ecoregion sites, all but one eastern site and all but one southwestern site); central and north western sites (all Cayman, Belize and Jamaican sites, all but one Bahamian and all but one Cuban site), and a final grouping of a BVI, Cuban and Bahamian site. In this final grouping, all sites hosted *D*. Finally, Columbian site Palo 1 formed a separate outlier, not related to any other site.

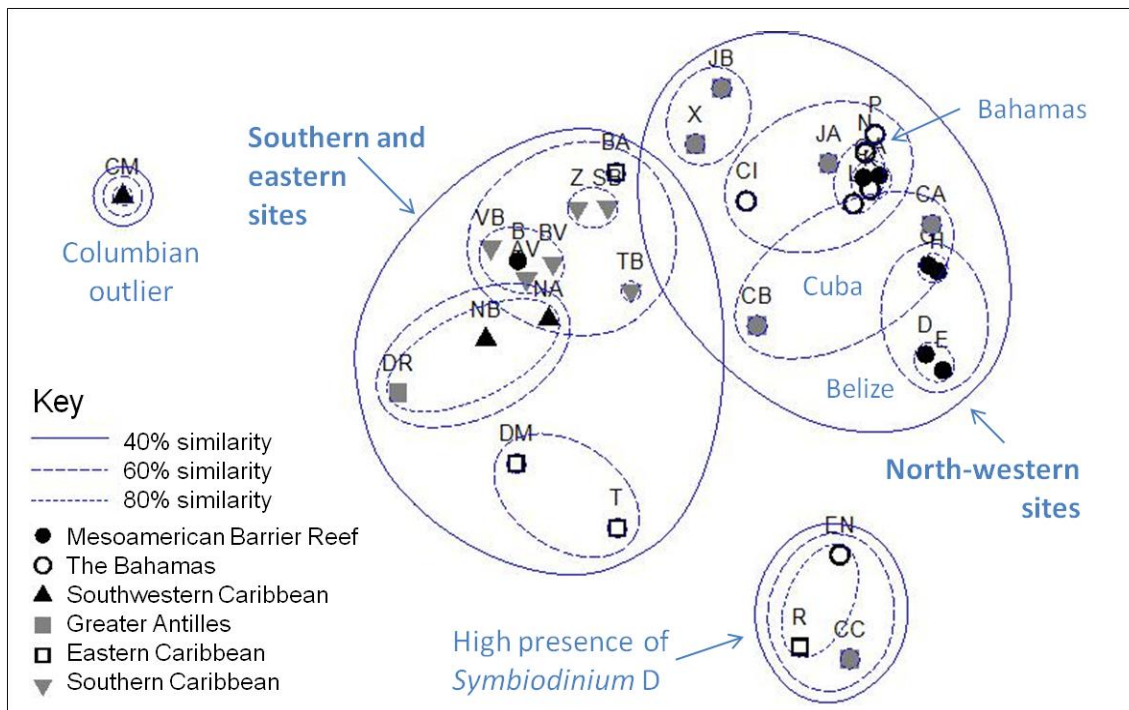


Figure 5.19: Caribbean reefs, *Montastraea annularis* symbionts. 2-dimensional MDS of square root transformed symbiont abundance data, based on Bray-Curtis similarities (stress= 0.12). Letters indicate site identifier code, site symbols denote eco-region. Superimposed clusters based on a dendrogram of the site similarities (see Appendix Figure 5.34).

At the 60% similarity level sites could be further clustered, with Belizean and Bahamian sites clustering in separate groups. One Jamaican site clustered with nearby Cayman, while the second was closer to the Bahamas in terms of symbionts. Nicaraguan sites grouped with the Dominican Republic, while all the Lesser Antilles sites (Venezuela, Curacao, Tobago and Barbados) formed another group. At the 80% level, geographic distance seemed important, with neighbouring sites less than 100 km from each other tending to cluster, for example Belizean sites D and E (located on Caye Caulker) and G and H (both from Glovers Atoll) grouped separately, as did Buoy 1 (Z) and Snake Bay (SB), neighbouring sites from Curacao. The third Curacao site, Varsenbay (VB) clustered with the two Venezuelan sites at this level. Sites located

more than 100 km from any other site, e.g. Barbados (BA), Tobago (TB), Cayman Islands (X), Jamaican sites (JA and JB) and Cuban site Siboney (CC) – did not cluster with other sites at this level. This hierarchy of clustering does suggest some geographic element to community structuring – although clearly sites hosting D are seen as more different. This was further explored in Chapter 6.

SADIE analysis

Two SADIE analyses – a distance to regularity, and a clustering analysis - were then used to assess the significance of the observed spatial patterns in distribution of *Symbiodinium* clades across the Caribbean, presented in Fig. 5.10. To account for variation in sample sizes, data on percentage membership of each type was employed, rather than actual count data. Separate analyses were performed on the count data for each cladal type; A, B, C and D, as well as mixed types. In each analysis, the *iseed* (integer acting as initial seed for SADIE's internal random number generator) was set to 30,000, and the maximum allowable number of randomisations was selected (k5psim=153), with 5796 randomised permutations of the data performed.

Distance-to-regularity analysis showed significant spatial patterning in the overall distribution of *Symbiodinium* B ($I_a=2.03$, $P_a=0.005$) and *Symbiodinium* C ($I_a=2.14$, $P_a=0.002$). Further examination of outputs of the cluster analysis showed that spatial patterns in B and C were manifested as both gaps and clusters. Clade D symbionts ($I_a=1.02$, $P_a=0.4$) and mixed assemblages ($P_a>0.05$) showed a random distribution with no evidence of Caribbean-wide spatial patterning (see Appendix Table 5.2)..

Site specific values generated by the cluster analysis (Table 5.4), revealed emergent patterns of clade distribution. Clade B was significantly clustered in all Western Caribbean (except Sandy Bay) and most Bahamian sites (except the Exhumas and Propeller reef), but were not found in greater-than-expected abundances in any other marine ecoregion (Table 5.4). Clade B was also noticeably lacking from the BVI and Curaçao sites. Meanwhile, clade C distribution only showed significant clustering in most Southern and Eastern Caribbean sites, but was even more apparent in its low abundance across all other ecoregions, with the exception of the Southwest. Only one site, Ginger Island (BVI) had a significantly high cluster value for D (Table 5.4), while samples hosting mixed clades produced high gap scores – although like clade D, these regional patterns were not deemed overall significant by the analysis. Site cluster values were then taken and used to map patterns of spatial distribution for each clade, with interpolation allowing regions of high clustering to be identified. The results (presented as red-blue plots. Fig. 5.20), further displayed significant biogeographic partitioning in the distribution of *Symbiodinium* B and *Symbiodinium* C, but a random distribution with no evidence of spatial patterning for clade D symbionts.

Area	Country	Reef	Site	Latitude	Longitude	B	C	D	A	B/C	B/D	C/D	B/C/D
Western Caribbean	Honduras	Seaquest	A	16.2940	-86.6000	3.66	-0.02	-1.66	0.00	0.06	-0.32	-1.61	-4.08
	Honduras	Sandy Bay	B	16.3340	-86.5680	-0.38	0.24	-2.14	0.98	0.40	-0.30	-1.55	-3.80
	Honduras	Western Wall	C	16.2710	-86.6040	3.67	-3.60	-2.42	-0.01	-0.41	-0.31	-2.61	-3.94
	Belize	Coral Gardens	D	17.7484	-88.0233	5.07	-5.42	0.66	-0.15	-0.56	1.85	-1.72	-2.04
	Belize	Eagle Ray	E	17.7203	-88.0136	6.52	-4.53	0.36	-0.14	-0.68	1.38	-1.67	-2.03
	Belize	Long Cay	G	16.7545	-87.7881	4.25	-2.17	-0.22	-0.09	-2.14	-0.16	-1.85	-2.45
	Belize	West Reef	H	16.8088	-87.8621	6.72	-1.26	-0.21	-0.10	-2.49	-0.15	-1.76	-2.12
The Bahamas	Bahamas	Conception Island	CI	23.8120	-75.1218	2.31	-3.10	-0.31	-1.30	-2.78	-2.08	-0.23	-0.28
	Bahamas	Exumas North	EN	24.6409	-76.7954	-0.29	0.26	0.54	-1.15	-4.00	0.92	1.12	1.10
	Bahamas	Seahorse Reef	K	24.1582	-74.4839	2.61	-3.06	-1.36	-1.34	0.04	-0.34	-1.44	-1.58
	Bahamas	Snapshot Reef	L	24.0314	-74.5297	2.63	-3.03	-2.02	-1.32	-3.17	-1.94	-1.41	-1.62
	Bahamas	Schoolhouse Reef	N	24.9734	-77.5051	4.40	-2.71	-0.16	-1.12	-1.49	-1.93	-0.10	-0.11
	Bahamas	Propeller Reef	P	25.0064	-77.5524	0.34	-0.30	-0.17	-1.11	0.02	-1.96	-0.11	-0.12
South West	Nicaragua	White Hole	NA	12.1881	-83.0518	0.70	1.39	-1.57	-0.44	1.23	-0.85	-2.04	-2.45
	Nicaragua	Chavo	NB	12.1835	-83.0670	0.00	1.34	-1.63	-0.43	1.24	-0.87	-2.12	-2.62
	Columbia	Palo 1	CM	10.2770	-75.6110	-1.16	1.37	-1.37	-1.04	1.14	-1.37	-1.29	-1.44
Greater Antilles	Cuba	Baracoa	CA	23.0871	-82.5077	1.49	-2.70	-0.92	-0.67	-1.23	-1.03	-0.73	-0.80
	Cuba	Bacunayagua	CB	23.1507	-81.7274	1.47	-3.93	-0.82	-0.71	-0.85	-1.15	-0.65	-0.70
	Cuba	Siboney	CC	20.0315	-74.7548	-0.96	-0.92	0.98	-1.29	-1.38	1.98	2.17	-1.34
	Cayman	Rum Point	X	19.3776	-81.2810	1.30	0.72	-0.91	-0.59	0.81	-0.92	-0.90	-0.94
	Dominican Rep.	Bayahibe	DR	18.3440	-88.8314	-1.35	1.07	-0.51	-1.57	-0.91	-0.71	-0.49	-0.51
	Jamaica	Drunkenmans Cay	JA	18.4688	-77.3856	1.36	-1.73	-0.43	-1.01	-1.38	-1.38	-0.37	-1.67
	Jamaica	Dairy Bull	JB	17.8876	-78.8288	1.24	-1.54	-0.39	-1.06	-1.34	-1.35	-1.39	-1.50
	Barbados	Victor's Reef	BA	13.1630	-59.6409	0.50	-0.51	-0.36	-1.51	-0.38	-1.60	-0.61	-0.26
Eastern Caribbean	Dominica	Grande Savane	DM	15.4369	-61.4485	-0.78	1.66	0.78	-1.59	-1.00	-1.45	-0.40	1.27
	BVI	Ginger Island	R	18.3915	-64.4838	-2.28	2.07	1.07	-1.63	-1.33	-1.26	0.96	1.43
	BVI	Beef Island	T	18.4395	-64.5351	-2.06	-0.01	1.89	-1.63	-1.27	-1.21	-0.01	-0.01
	Curaçao	Snakebay	SB	12.1390	-69.0021	-2.74	3.29	-1.35	-1.53	5.02	-2.77	-0.93	-1.09
Southern Caribbean	Curaçao	Vaersenbay	VB	12.1611	-69.0112	-3.81	2.19	-1.14	-1.51	3.20	-2.55	-0.90	-1.09
	Curaçao	Buoy 1	Z	12.1259	-69.0253	-5.58	4.15	-1.18	-1.52	2.12	-2.56	-0.89	-1.05
	Tobago	Buccoo Reef	TB	11.1831	-60.8334	0.70	0.46	-0.88	-1.51	0.45	-1.81	-0.68	-0.40
	Venezuela	Cayo de Agua	AV	11.8178	-66.9306	1.08	5.28	-1.17	-1.54	1.79	-2.91	-0.80	-0.87
	Venezuela	Dos Mosquises	BV	11.7958	-68.8842	1.49	5.21	-1.17	-1.57	1.51	-2.97	-0.82	-0.85

Table 5.4: Cluster indices generated by SADIE analysis for *Symbiodinium* clade distribution across sample sites. Blue cells indicate values with a significant v_j value (demonstrating negative clustering), while red cells (significant v_j) depict sites where symbiont appeared to be more clustered than would occur by random chance (measured against 5967 random permutations).

Non-parametric SADIE analyses (based on ranked symbiont count values) were performed to further explore spatial patterns in distribution of each individual symbiont type identified to sub-clade level (symbionts not successfully identified were omitted from the analysis) Table 5.5. Parametric methods were not appropriate in this instance, as data (particularly for rarer symbiont types) tended to be skewed, with variance much greater than the mean due to a few highly abundant types, limiting the ability of the data to detect spatial patterning – so data were transformed to rank abundances.

Symbiodinium ITS2 variants B1, B17, B1j, B10, C7 and C12 (C7a) all showed significantly high I_a values to indicate some kind of spatial patterning across the region (Table 5.5, Fig. 5.1). B1 showed a similar distribution to clade B (Fig. 5.20 and 5.21), though not all B variants followed the same spatial distribution: patch clusters of B1j appeared more similar to C7 and C12 spatial distributions, which showed a high abundance in the Lesser Antilles and low in the Bahamas (Fig. 5.21).

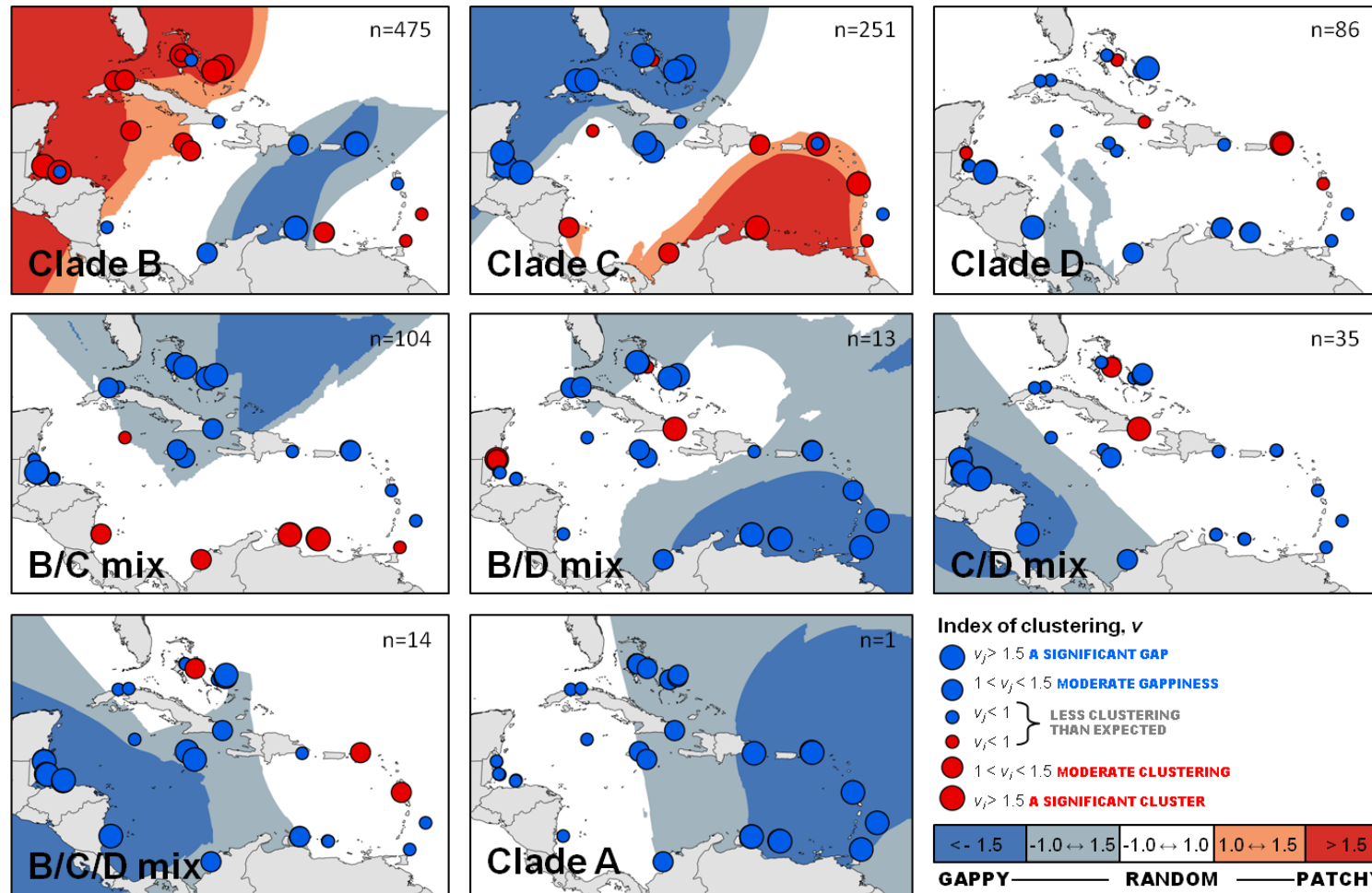


Figure 5.20: Red-blue plots highlighting areas and sites that showed significant positive (large red circles) and negative (large blue circles) clustering in terms of the abundance of *Symbiodinium* cladal types (presented in Fig. 41). Coloured areas highlight neighbouring groups of sites which share high (or low) degrees of clustering. Only Clades B and C (first two panels) were shown to have significant spatial patterning across the region. Clade B shows significant clustering in the Bahamian and Western ecoregions, while is notably less abundant in the Dominican Republic and Curaçao. Clade C shows an opposing spatial pattern, with a lack of C in the Bahamas, Greater Antilles and Western ecoregions, and an abundance in the Eastern and Southern Caribbean. Clade D shows no highly significant spatial patterning: it's distribution across the Caribbean no different than a random arrangement.

Symbiont type	Mean	Variance	Index of dispersion	δ	Distance to Regularity, D		Clustering indices			
					I_a	P_a	V_i		V_j	
					Index of aggregation	Significance of I_a	Patch cluster index		Gap cluster index	
							mean	p-value	mean	p-value
B1	34	363.6	342.2	1.91	1.72	0.02	1.78	0.02	-1.51	0.08
B17	34	169.3	159.3	1.08	1.63	0.03	2.15	0.01	-1.67	0.04
B1j	34	191.2	179.9	2.36	2.75	0.00	2.91	0.00	-3.21	0.00
B10	34	145.6	137.1	1.41	1.86	0.00	2.51	0.00	-1.72	0.03
C1	34	211.5	199.1	0.73	1.15	0.25	1.25	0.18	-1.08	0.34
C62	34	33.0	31.1	0.23	0.91	0.73	1.00	0.93	-0.87	0.72
C3	34	211.0	199.1	0.73	1.15	0.25	1.25	0.18	-1.08	0.34
C7	34	338.9	319.0	2.59	2.29	0.00	2.05	0.01	-2.93	0.00
C12	34	322.8	303.8	2.54	2.30	0.00	2.43	0.00	-2.74	0.00
B7	34	93.1	87.6	0.22	1.02	0.44	0.90	0.59	-1.01	0.46
B3?	34	145.6	137.1	0.64	1.15	0.25	1.12	0.28	-1.18	0.23
C31?	34	93.1	87.6	0.75	1.36	0.09	1.25	0.15	-1.43	0.08
D1a-like	34	64.0	60.2	0.71	1.50	0.05	1.62	0.00	-1.44	0.06
D1a	34	145.6	137.1	1.11	1.57	0.05	1.37	0.13	-1.78	0.03
A13	32	33.0	31.1	0.49	1.45	0.08	1.01	0.06	-1.52	0.00

Table 5.5: SADIE outputs, describing the indices for evaluating the spatial distribution of each observed *Symbiodinium* ITS2 type. Cells highlighted pink indicate significant values.

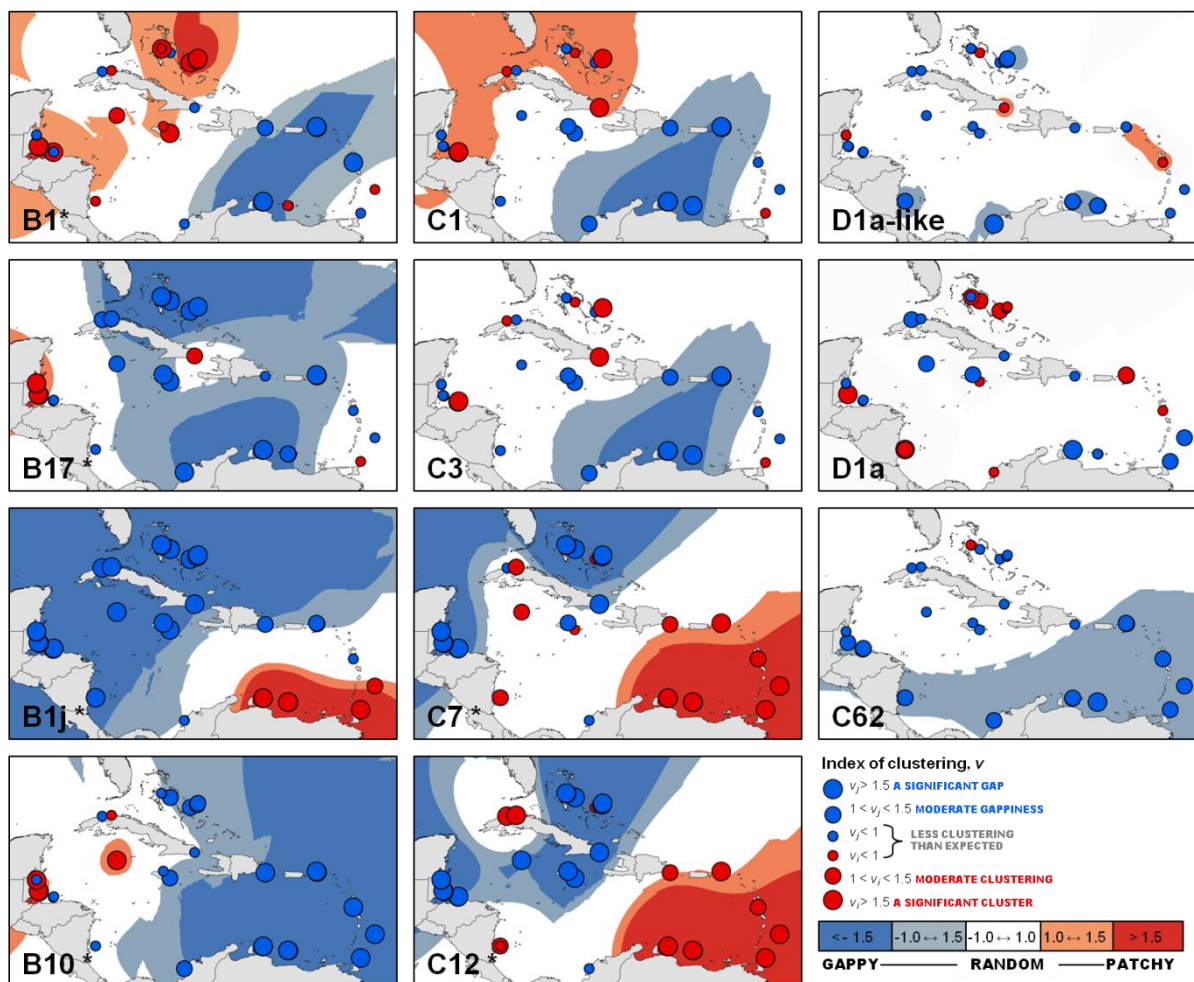


Figure 5.21: Red-Blue plot: A contour map based on SADIE analysis output, representing the location and extent of clusters in the data, based on a standardised and dimensionless indices of clustering, v_i (positive clustering, red) and v_j (negative clustering, blue), for *Symbiodinium* ITS2 variants. *=significant regional clustering based on Index of Aggregation.

5.5 Discussion

5.5.1 Diversity of *Symbiodinium* ITS2 types hosted

M. annularis was found to host a diverse range of endosymbionts, with 22 *Symbiodinium* ITS2 variants recorded, 16 of which were successfully identified as previously documented sub-cladial types. The high diversity hosted may be partly explained by the wide geographic range of the coral, and the fact that it is a hermaphroditic broadcast spawner (which tends to host higher symbiont diversity; LaJeunesse et al. 2004). Additionally, we sampled *M. annularis* from shallow depths: symbiont ITS2 diversity in *M. annularis* has been shown to be greater in shallow water (1-8 m) (Warner et al 2006). Finally, symbiont ITS2 diversity is known to be higher in the Caribbean than in other oceans (LaJeunesse et al. 2003); one proposed hypothesis for this being that an inverse relationship exists between host diversity and symbiont diversity (this is tested in Chapter 6).

5.5.1.1 Sub-clade B1

B1 was by far the most commonly occurring symbiont type, occurring in 72% of individuals (n=632). Clade B's Caribbean distribution proved influential in determining spatial patterning of symbiont communities in *M. annularis*. Not only was the taxon highly abundant, but it dominated communities in 35% of samples, and shared co-dominance with another clade in a further 32%. The widespread occurrence of B1 is unsurprising, a wealth of studies report dominance of *Symbiodinium* B in *M. annularis* at sites across the coral's entire latitudinal range e.g., Lee Stocking Island, Bahamas (LaJeunesse 2002); Mesoamerican Barrier Reef (Garren et al. 2006, Warner et al. 2006); offshore reefs of San Blas, Panama (Rowan et al. 1997). *Symbiodinium* B has also been reported to be more common in *M. annularis* than other *Montastraea* species (Garren et al. 2006). Dominance of B1 does not stop with *Montastraea*: it was found to be the most prevalent *Symbiodinium* species in the Caribbean in a study sampling multiple zooxanthellate hosts (LaJeunesse 2002), associating with nearly half of host invertebrate taxa surveyed in Belize and Barbados (Finney et al. 2010).

One proposed explanation for the high prevalence of B1 is that this symbiont may possess a greater ability to photo-acclimate to high and low irradiances (Iglesias-Prieto and Trench 1997a, although see Warner et al. 2001). Evidence suggests B1 is found harboured at all depths (Finney et al. 2010), making it a suitable symbiont for a coral which inhabits wide range of depth and turbidity. Prevalence at higher latitudes suggested B are generalists adapted to low irradiance and cooler seas (Rodriguez-Lanetty and Hoegh-Guldberg 2003), although as they are restricted to shallower depths of the range of some hosts (e.g. *Montastraea* spp.) clade B have also been described as 'sun specialists' (Rowan 1998) and 'narrowly adapted specialists' (Toller et al. 2001b). It is likely that corals acquiring symbionts from the environment may favour highly abundant generalist species like B1 (LaJeunesse et al. 2004).

Several studies that analysed B1 using finer resolution markers (e.g., microsatellite flanker regions) suggest that substantial cryptic diversity exists within B1, with at least three (maybe four) distinct lineages, analogous to species, existing within the sub-clade (Santos et al. 2004, Finney et al. 2010). Clade B *Symbiodinium* are understood to have a slower evolutionary rate of ITS genes compared to orthologs in clades A and C, meaning ITS2 B1 may be a taxonomic level above the other sub-clades (Santos et al. 2004). In a Caribbean study comparable to ours in geographic extent and sampling effort, B1 hosted by the sea fan *Gorgonia ventalina* was shown to have a high level of genetic structuring, with major biogeographic divisions between Florida, Bermuda and the Caribbean, and lesser divisions within the Caribbean, partitioning the Bahamas, Mesoamerican Barrier reef, Panama and the Southern/Eastern Caribbean (Andras et al. 2011). One concern is that by choosing ITS2 as a molecular marker, we may have missed important functional diversity within this clade, as well as skewing results to imply lower

ecological diversity in regions heavily dominated by B1 (i.e. the north west). However, B1 diversity at this finer scale level appears to have high host specificity, and investigations so far suggest that *M. annularis* exclusively hosts the B1 sub B1².

5.5.1.2 Sub-clade B10

B10 was an important symbiont in northern Cuban samples (CA and CB), also occurring in the Cayman Islands (X) and Honduras, although it was not a dominant type here. The distribution of B10 was shown to be significant ($I_a=1.86$, $P_a<0.005$), although spatial patterning consisted of a significant lack of B10 from the Eastern and Southern ecoregions, rather than any positive clustering (Fig. 5.20). Previous records of B10 in *M. annularis* come from one study in the Florida Keys, where B10 was reported to dominate colonies ($n=6$) at a shallow site (Little Grecian Reef) just 320 km north from our Cuban sites (Thornhill et al. 2006b) fitting in with our spatial distribution.

5.5.1.3 Sub-clade B17

B17 was found to dominate symbiont communities at Belizean sites (D, E, H and G), with an additional few cryptic occurrences in Cuba and Tobago. A previous study which isolated B17 from *Montastraea* in Belize, but not in Barbados, supports our finding of a significant patch cluster along the Mesoamerican Barrier Reef ($I_a=1.63$, $P_a=0.03$, Table 5.5), but a notable absence of this clade from large areas of the remainder of the Caribbean (Fig. 5.21). Clade B phylogenies based on microsatellite flanker regions (rather than ITS2, which has been criticised for failing to reveal true diversity in this lineage) have revealed B17 extracted from *M. annularis* may actually fall within two B1 ITS2 sub-taxa (Finney et al. 2010), suggesting this type to be closely related.

5.5.1.4 Sub-clade B1j

B1j showed the greatest degree of spatial structuring across the Caribbean within the B-clade (Table 5.5) although the pattern was almost the exact opposite of B1, B17 and B10 distribution. A patch cluster was revealed across the Southern Caribbean region, and a low level of abundance across almost the remainder of the region (with the exception of the Eastern ecoregion) (Fig. 5.21). Studies that have recorded B1j in *M. annularis* were also from this area of the Caribbean (LaJeunesse et al. 2009, Finney et al. 2010). B1j appeared to be spatially associated with C7 and C7a, with the variants showing a similar distribution (Fig. 5.18 and 5.21). Of all recorded occurrences of B1j, 28% of the time it was alongside C7a, and 40% of the time it was with C7 – this was again observed in studies recording this ITS2 type. In two Barbados studies (LaJeunesse et al. 2009, Finney et al. 2010), shallow (6-10 m) colonies contained a B1/C7a or B1j (high-light)/ C7a mix. B1j was also found to replace D1a after

bleaching on shallow Barbados reefs (LaJeunesse et al. 2009), and its prevalence in this area might be due to the severity of the bleaching that occurred in the Eastern Caribbean region prior to sampling (Oxenford et al 2008).

5.5.1.5 Clade C

Although *Symbiodinium* C is typically associated with deeper *M. annularis* colonies, C3, C7 and C7a (C12) were found in reasonable abundance. Of these variants, only C7 and C12 demonstrated significant spatial structuring. C12 is generally found in deeper or shaded corals: this type was found in all *M. annularis* colonies > 15 m deep in Barbados in a study focussed on bleaching (LaJeunesse et al. 2009), and again in all colonies deeper than <10 m in the same location (Finney et al. 2010). C12 was additionally shown to make up a small proportion of shallow water colony symbionts at South Perry reef in the Bahamas, reappearing and disappearing over a 5 year period (Thornhill et al. 2006b).

In a comparison of eastern and western Caribbean, Finney et al. (2010) noted that deeper *M. annularis* species complex from Barbados hosted C7a (C12), while their counterparts in the west (Belize) hosted C7 instead. This led the authors to suppose that corals in the east hosted counterparts in the west with similar ecological traits - finding several examples of parallels in *Porites* spp. However, we did not find a difference in the distribution of C7 and C12 – finding both more frequently in the east than the west (Fig. 5.2). This may be because Finney et al. (2010) sampled just six species and included *M. faveolata* and *M. franski*. *M. faveolata* appeared to drive the data (no C7 was actually detected in *M. annularis*).

5.5.1.6 Clade A

A13 (also known as A1.1), thought to be a highly opportunistic symbiont, was only found in one sample. Low abundance could have been predicted as A13 is ecologically rare; one study identified only four clade A *Symbiodinium* in over 476 Caribbean cnidarians (Finney et al. 2010); another only observed A once in very shallow (0-3 m) back reef habitats (LaJeunesse 2002, Garren et al. 2006), while a third demonstrated the type to associate with *M. annularis* only in severely bleached individuals (LaJeunesse et al. 2009). As bleached and very shallow colonies were not sampled, this might explain why our study found just one incidence.

5.5.1.7 Clade D

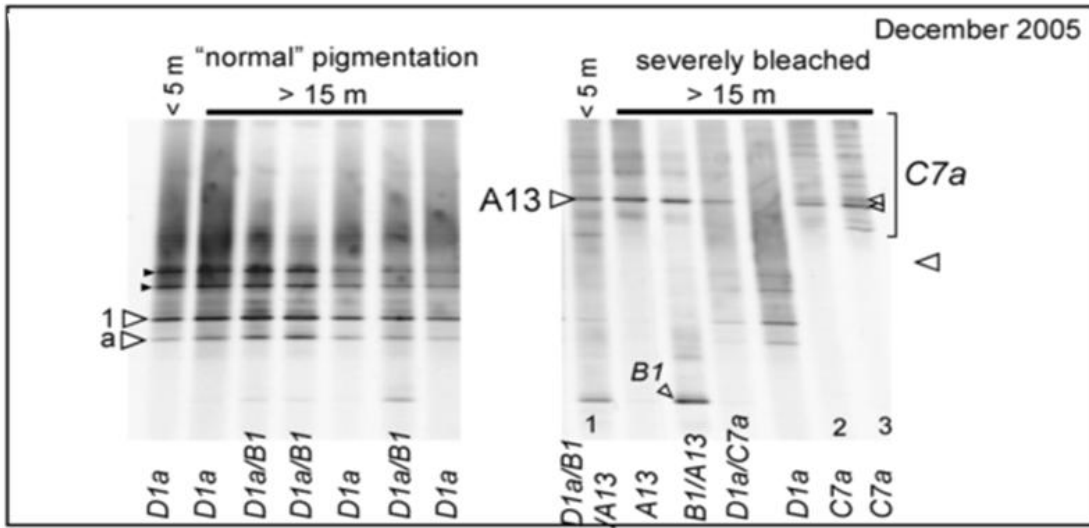
D1 and D1a showed no evidence of any spatial patterning at a regional level – although this does not rule out local scale patterning (Oliver & Palumbi 2009). The unique DGGE fingerprint – a bright D1 band with a D1a below - has been recorded previously from the Western Indian Ocean, central Pacific and Caribbean, found in a wide range of species and often, but not always, associated with shallow water depths (LaJeunesse 2002, LaJeunesse et al. 2004, see

Chapter 7). Although it only occurred in high numbers at fewer sites than B and C, Clade D was shown to have a homogenous distribution across the Caribbean (Fig. 5.20, panel 3), with no patches of significant clustering, although one site – Ginger Island (BVI) showed a higher than expected abundance of D (Table 3). *Symbiodinium* clade D is regarded as a rare generalist endosymbiont with a global distribution (Stat and Gates 2011). Our observation that D made up a minor component (13.6%) of the total surveyed Caribbean-wide community, falls in line with the conclusions of previous studies: namely that *Symbiodinium* D it is typically rare, (found in less than 10% of samples) and far less speciose than B and C (Stat and Gates 2011, review of D). Our observations (Fig. 5.13), revealed that D was numerically highly abundant (> 55%) at a seemingly sporadically-located seven of the 33 sampled sites, and absent from the remainder. At three of these locations - the Exhumas (Bahamas, EN), Ginger Island (BVI, R) southeast Cuba (CC) - D was found in 75%, 96% and 100% of samples, respectively, yet neighbouring sites rarely harboured D. The association of *Symbiodinium* D and *M. annularis* has previously been shown to be linked to habitats with high levels of sedimentation (Toller et al. 2001, Garren et al. 2006), and one possible explanation might be that these seven sites may be highly sedimented. D is known to have a stress-tolerance that exceeds that B and C clades, allowing it to proliferate in corals experiencing sub-optimal reef conditions, usually in terms of higher than average thermal stress, but in the case of *M. annularis*, also in turbid environments (Stat and Gates 2011). D also appears in *M. annularis* in the build up to bleaching events (LaJeunesse et al. 2009), and although *M. annularis* typically revert to pre-bleaching zooxanthallae communities (Toller et al. 2001b), after severe bleaching events this can take 2-3 years (Stat and Gates 2011).

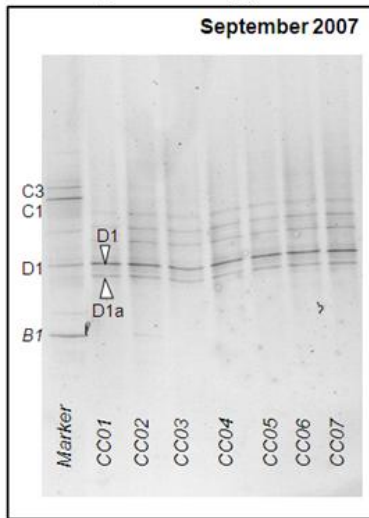
British Virgin Islands sites both hosted *Symbiodinium* communities which were heavily dominated by D1/D1a, and Ginger Island was the only site to generate a significant value of clustering for D ($v=1.89$) (Table 5.4, Fig. 5.20). One explanation for this may be the extreme bleaching experienced at these sites prior to sampling (Bouchon et al. 2005). Records show that at the time of sampling, in November 2006, coral communities were still in the process of recovering, with partial colony bleaching still prevalent (Bouchon et al. 2005). However, Tobago and Barbados were both also heavily impacted by the 2005 bleaching event, yet didn't harbour D1/D1a profiles. This could be due to the time of sampling/extent of recovery – both these sites were sampled in 2007, by which time *Symbiodinium* communities may have had time to recover fully. It was also noted that in Tobago, most bleaching occurred at deeper sites, whereas sampling took place at 3 m. Finally, the patchy nature of *M. annularis* bleaching recorded in Barbados (Bouchon et al. 2005) may have provided researchers with more opportunities to select healthy looking colonies for sampling. Given the “patchy” nature of the occurrences of D, exposure to a thermal stress event might be a more likely explanation for the occurrence of D. In fact, the authors of the review on *Symbiodinium* D (Stat and Gates 2009) suggest that the ‘patchy’ distribution of clade D may be explained by the hypothesis proposed by LaJeunesse that a substantial proportion of corals harbour cryptic clade D in their symbiont

community that later become temporarily dominated by D during or after a stress event (LaJeunesse et al. 2009). This is likely due to its role as an opportunist. In Chapter 7 we go on to examine the distribution of D in more detail, using rtPCR to quantify incidence of cryptic D in *M. annularis*.

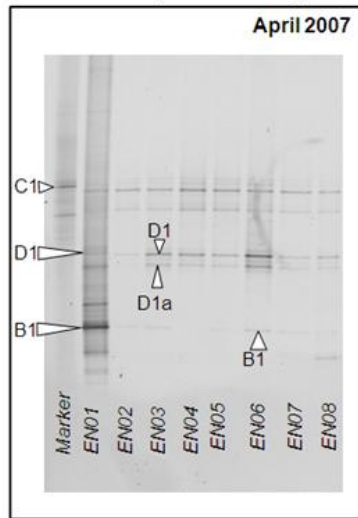
Barbados: bleaching event 2005 (LaJeunesse et al 2009)



Cuba (this study)



Bahamas (this study)



BVI (this study)

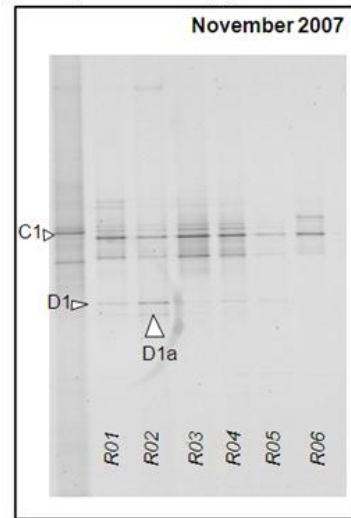


Figure 5.22: Investigating *Symbiodinium* D: three sites (CC, EN and R) were grouped differently from other reef sites in the MDS plots (Fig. 5.19). The DGGE banding profiles were comparable to those generated by *M. annularis* symbiont communities during a major bleaching event in Barbados – colonies that maintained ‘normal’ pigmentation while surrounding colonies bleached, but within 24 months these same colonies had reverted back to being dominated by C7a (LaJeunesse et al 2009).

In summary, the ITS2 types and the relative proportions recorded in this study were no different to the patterns of diversity anticipated from the findings of previous studies, leading us to accept our null hypothesis that the *Symbiodinium* ITS2 communities documented would not differ significantly from those recorded in previous surveys. Accepting the null hypothesis further supports the finding that *M. annularis* shows highly stable symbioses (Thornhill et al. 2006a).

5.5.2 Intra-site diversity

The finding that within-site diversity appeared lesser than within region and within study diversity is unsurprising (Fig. 5.19). Other studies have noted that members of a host taxon in a particular reef environment and geographic region usually possess the same symbiont type (Baker 1999, LaJeunesse 2002). Thornhill et al. 2006 note a reef ‘endemism’ at the reef scale level in *M. annularis* (Thornhill et al. 2009). However, Warner et al. 2006 described significant variability in the dominant types hosted by *M. annularis* within a reef site – particularly in shallow water colonies (8 m) like ours (Warner et al. 2006) – with variable mixes of dominant B1, C7 (and in one colony, C3).

Several other studies have investigated *Symbiodinium* diversity in *Montastraea* sp. at the intra-site level, and their findings generally corroborated with results - below are detailed comparison of findings from the Bahamas, Belize and Panama and Barbados.

5.5.2.1 Bahamas

Previous surveys found a dominance of *Symbiodinium* B1 in Bahamian *M. annularis*, similar to the study results (see section 5.4.1.2). At Lee Stocking Island (four years prior to the present study) B1 was present not just in *Montastraea*, but in over half of the host taxa (n=29 species) began (LaJeunesse 2002). A later study that sampled *M. annularis* from the nearby Exhumas between 2003 and 2005, also found every single Bahamian colony of *M. annularis* sampled hosted B1 (Thornhill et al. 2009). The 2003/2005 study additionally employed microsatellite loci to examine the population genetics of the B1 symbiont. The authors found low genotypic diversity across Bahamian reefs, with only 2-4 B1 genotypes found per reef (Thornhill et al. 2009). Although B1 genotypes tended to be site specific, this was much more apparent in the Floridian sites compared to the Bahamian sites, which showed a more diverse mix. Low diversity in the Bahamas extends beyond the cladal level, to population level. In addition to B1 dominating every colony, the authors recorded some C12 (also known as C7a) on colony sides, and D1a were recorded in Bahamian samples, concurring with our findings – D1a in the Exhumas, and C12 at Conception Island (Thornhill et al. 2009).

5.5.2.2 Belize

The symbiont diversity of the *M. annularis* species complex has been previously explored to cladal level for Belize, with *Symbiodinium* B comprising 79% of the samples, but A and C also recorded (Garren et al. 2006). While the present study improved the resolution of the *Symbiodinium* catalogue for this area, our findings of ITS2 diversity closely corresponded to those of SSU RFLP diversity in that previous report. In both studies, Belizean samples were shown to be dominated by *Symbiodinium* B (Garren et al. = 78.6%, n=103; this study = 90.1%,

n=71), with a comparable amount of C (9.7 vs. 5.6%), comparing dominant DGGE types. In our study, a B/D mix dominated the remaining 4.2% of samples (and in the case of Long Cay D was probably more prevalent than recorded), while no D types were found before. *Symbiodinium* A dominated the remaining 11.7% of samples, despite not being found in our surveys. However, in the previous study, A was only found ‘in the southern and atoll sites’, and the use of different molecular markers may have produced this result. Interestingly, Garren et al. found a high degree of symbiont specificity in Belize, never finding more than a single clade type in any one sample – a trait we also noted unique to Belize, with no B/C mixes: despite B/C mixes being common in the Caribbean in general (~50% of our samples).

5.5.2.3 Panama

Symbiodinium diversity within *M. annularis* has been surveyed in the Bocas del Toro region in Panama, which lies halfway between our Nicaraguan and Columbian sample sites (Garren et al. 2006). Here, the authors, identifying symbionts to cladal level, found greater diversity and evenness of symbiont types A, B, C, D and C’ (a new type) than in matched sampling efforts on the *Symbiodinium* B-dominated Mesoamerican Barrier Reef, with spatial patterns best explained by exposure (open ocean vs coastal) and total suspended solids.

A similar story emerged in our dataset, with a higher diversity recorded in the Southwestern ecoregion (Simpsons 1/D = 4.71) compared to the Western Caribbean (3.13), despite a similar number of symbiont taxa being recorded.

5.5.2.4 Barbados

M. annularis symbiont communities have been studied in Barbados in 2005 (LaJeunesse et al. 2009) and also in 2005-2007 (Finney et al. 2010). In both reports, shallow water samples contained B1j or B1, often mixed with C7a, while deeper samples contained only C7a profiles. Our DGGE profiles exactly mirrored those found published in Finney’s study, with the majority showing the B1j profile she described: a B1 band, a B1j band, and two B1 heteroduplexes above (Appendix Fig. 5.27). One coral hosted symbiont A13 – another sub-clade identified in previous Barbadian studies (Finney et al. 2010).

5.5.3 Within-colony variation/Host-specificity

Host specificity was fairly high at within colony level: it was recorded that 74% of samples hosted just one clade of symbiont, with the ratio of B:C:D as 7:2:1. This had been found previously (Goulet 2006). B1 was often found to co-occur with another B or a C-type. Similar intracolony zonation and intracladal variation of *Symbiodinium* rDNA “types” within *Montastraea* spp. has been documented (Rowan et al. 1997, Toller et al. 2001a, Garren et al. 2006, Thornhill et al. 2006b, Thornhill et al. 2009).

5.5.4 Spatial patterns of *Symbiodinium* distribution

M. annularis inhabiting the Lesser Antilles – particularly in an area eastwards and inclusive of the Dominican Republic and Curaçao, were shown to harbour demonstrably higher-than-average community richness (in terms of numbers of *Symbiodinium* sub-clades hosted), while those in the Bahamas, along the Mesoamerican Barrier Reef and in Jamaica made up an area of poorer-than-average symbiont communities. Diversity measures and counts of cladal types supplemented this spatial analysis, showing that eastern corals harboured more even mixes of B and C clades, and a higher number of sub-clades. SADIE analyses of clade B, C and D distribution revealed that both B and C both showed a significant and high degree of clustering across the range, while mixed cladal assemblages were generally rarer than might be expected, while showing no significant spatial structuring. While clade B was frequently hosted in the north-west, and occurred less commonly in the east, clade C showed almost the exact inverse of this spatial pattern. A study comparing eastern (Barbados) and western (Belize) Caribbean *Symbiodinium* ITS2 communities also commented on a major east-west division, with only a 20% overlap in the *Symbiodinium* ITS2 types found in each region (Finney et al. 2010). In contrast to the conclusions of this study, the study also found an comparable ratio of B : C clades in each region, but this may have been because multiple hosts (45 genera) were sampled.

The spatial patterning of species richness from north-west to southeast may also be largely explained by the patterns of B and C: the dominance of the B1 sub-clade in Bahamian, Jamaican, Belizean and Honduran reefs over other types will reduce the richness and diversity of these symbiont communities, while clade C sub-types appeared to be more even in terms of occurrence, leading to greater richness and diversity in the Lesser Antilles. This unique ecological success of *Symbiodinium* B in the north-west might be caused by responses to past environmental change (LaJeunesse 2005) – such as marine extinctions in the western tropical Atlantic at the Pliocene/Pleistocene boundary (Finney et al. 2010), a hypothesis supported by the low level of ITS2 sequence divergence recorded in B (Finney et al. 2010). Recent evidence identified a genetic break in the structuring of several different coral populations (shown in large scale studies in *Acropora* sp. (Baums et al. 2005, Vollmer and Palumbi 2007), *M. annularis* (Foster et al. 2012) and soft corals (Andras et al. 2013)), perhaps suggestive of a common biogeographic divide for Caribbean organisms, thought to occur around an area of strong current flow between Puerto Rico and Hispaniola (the Mona Passage). However, the precise positioning of this divide is controversial, and similar genetic partitioning was absent in conch, lobster, urchins and most reef fish (Andras et al. 2011). In addition, this break was not seen in *Symbiodinium* B1 at population level, in a study comparing genetic structuring of endosymbiont communities and their octocoral host, despite host genetics supporting the east-west genetic divide (Andras et al. 2013).

As SADIE analyses demonstrated significant clustering of B and C clades (into the north-west and east respectively) analogous to biogeographic partitioning, the second null hypothesis, which proposed that *M. annularis* would host a homogenous mix of *Symbiodinium* ITS2 types across its Caribbean range – can be rejected.

5.5.5 Wider implications of the finding

Although this study has demonstrated substantial spatial variability in the symbionts hosted by *M. annularis*, care must be taken when extrapolating this result. Other studies into symbiont biogeography, that have demonstrated comparable diversity in *M. annularis*, have also noted that host specificity and depth zonation are more important determinants (Warner et al. 2006). Only one host was investigated, but it is safe to say that the distributions recorded here are unlikely to be mirrored by other Caribbean corals, most of which are much more specific in the formation of symbioses. Secondly, spatial diversity of symbionts in *M. annularis* are considerably greater at shallower depths (<8m), and observed distributions are unlikely to be maintained in colonies residing at deeper depths, where C types tend to be harboured exclusively (Warner et al. 2006).

Changes in *M. annularis* 1995 bleaching incidences on the MBRS have been shown to be driven by variation in the observed distribution of zooxanthellae communities, with fore-reef *M. annularis* undergoing a higher percentage of bleaching compared to backreef habitats, as a greater proportion host stress-intolerant clade C (Walsh et al. in prep.). Knowing that bleaching varies under various *Symbiodinium* clades, and that (A>B>>C) (Rowan et al. 1997), we could extrapolate the results of this study to predict bleaching Caribbean wide bleaching patterns. In 2005 the Eastern Caribbean was more severely impacted than the West. This could be attributed to cladal distribution with *M. annularis*.

Having established a significant geographic spatial pattern of *Montastraea annularis* hosted *Symbiodinium* communities across the Caribbean and Bahamas, the next steps are to attempt to explain this patterning in terms of environmental parameters or host genetics (Chapter 6), and to establish whether this pattern is temporally stable (Chapter 8).

5.6 References

- Andras JP, Kirk NL, Drew Harvell C (2011) Range-wide population genetic structure of *Symbiodinium* associated with the Caribbean Sea fan coral, *Gorgonia ventalina*. *Molecular Ecology* **20**:2525-2542
- Andras JP, Rypien KL, Harvell CD (2013) Range-wide population genetic structure of the Caribbean sea fan coral, *Gorgonia ventalina*. *Molecular Ecology* **22**:56-73
- Baker AC (1999) *Symbiosis ecology of reef-building corals*. Ph.D thesis, University of Miami
- Baker AC (2003) Flexibility and specificity in coral-algal symbiosis: Diversity, ecology, and biogeography of *Symbiodinium*. *Annual Review of Ecology Evolution and Systematics* **34**:661-689
- Baker AC, Starger CJ, McClanahan TR, Glynn PW (2004) Coral reefs: Corals' adaptive response to climate change. *Nature* **430**:741-741
- Baums IB, Miller MW, Hellberg ME (2005) Regionally isolated populations of an imperiled Caribbean coral, *Acropora palmata*. *Molecular Ecology* **14**:1377-1390
- Berkelmans R, van Oppen MJH (2006) The role of zooxanthellae in the thermal tolerance of corals: a 'nugget of hope' for coral reefs in an era of climate change. *Proceedings of the Royal Society B-Biological Sciences* **273**:2305-2312
- Bouchon C, Portillo P, Bouchon-Navaro Y, Max L, Hoetjes P, Brathwaite A, Roach R, Oxenford HA, O'Farrell S, Day O (2005) Status of the coral reefs of the Lesser Antilles after the 2005 coral bleaching event. In: Wilkinson C, Souter D (eds) *Status of Caribbean coral reefs after bleaching and hurricanes in 2005*. GRCMN Report.
- Buddemeier RW, Baker AC, Fautin DG, Jacobs JR (2004) The adaptive hypothesis of bleaching. In: Rosenberg E, Loya Y (eds) *Coral health and disease*. Springer-Verlag, Berlin, Germany
- Burke L, Maidens J (2004) *Reefs at risk in the Caribbean*. Report, World Resources Institute
- Chollett I, Mumby PJ, Muller-Karger FE, Hu C (2012) Physical environments of the Caribbean Sea. *Limnology and Oceanography* **54**:1233-1244
- Coffroth MA (2005) Genetic diversity of symbiotic dinoflagellates in the genus *Symbiodinium*. *Protist* **156**:19-34
- Correa A, McDonald M, Baker A (2009) Development of clade-specific *Symbiodinium* primers for quantitative PCR (qPCR) and their application to detecting clade D symbionts in Caribbean corals. *Marine Biology* **156**:2403-2411
- Eakin CM, Morgan JA, Heron SF, Smith TB, Liu G, Alvarez-Filip L, Baca B, Bartels E, Bastidas C, Bouchon C, Brandt M, Bruckner AW, Bunkley-Williams L, Cameron A, Causey BD, Chiappone M, Christensen TRL, Crabbe MJC, Day O, de la Guardia E, Diaz-Pulido G, DiResta D, Gil-Agudelo DL, Gilliam DS, Ginsburg RN, Gore S, Guzman HM, Hendee JC, Hernandez-Delgado EA, Husain E, Jeffrey CFG, Jones RJ, Jordan-Dahlgren E, Kaufman LS, Kline DI, Kramer PA, Lang JC, Lirman D, Mallela J, Manfrino C, Marechal J-P, Marks K, Mihaly J, Miller WJ, Mueller EM, Muller EM, Orozco Toro CA, Oxenford HA, Ponce-Taylor D, Quinn N, Ritchie KB, Rodriguez S, Ramirez AR, Romano S, Samhoury JF, Sanchez JA, Schmahl GP, Shank BV, Skirving WJ, Steiner SCC, Villamizar E, Walsh SM, Walter C, Weil E, Williams EH, Roberson KW, Yusuf Y (2010) Caribbean corals in crisis: record thermal stress, bleaching, and mortality in 2005. *PLoS ONE* **5**:e13969
- Finney J, Pettay D, Sampayo E, Warner M, Oxenford H, LaJeunesse T (2010) The relative significance of host-habitat, depth, and geography on the ecology, endemism, and speciation of coral endosymbionts in the genus *Symbiodinium*. *Microbial Ecology* **60**:250-263
- Fitt W, Brown B, Warner M, Dunne R (2001) Coral bleaching: interpretation of thermal tolerance limits and thermal thresholds in tropical corals. *Coral Reefs* **20**:51-65
- Foster NL (2007) Population dynamics of the dominant Caribbean reef-building coral, *Montastraea annularis*. Ph.D, University of Exeter
- Foster NL, Paris CB, Kool JT, Baums IB, Stevens JR, Sanchez JA, Bastidas C, Agudelo C, Bush P, Day O, Ferrari R, Gonzalez P, Gore S, Guppy R, McCartney MA, McCoy C, Mendes J, Srinivasan A, Steiner S, Vermeij MJA, Weil E, Mumby PJ (2012) Connectivity of Caribbean coral populations: complementary insights from empirical and modelled gene flow. *Molecular Ecology* **21**:1143-1157
- Frankin EC, Stat M, Pochon X, Putnam HM, Gates RD (2012) GeoSymbio: a hybrid, cloud-based web application of global geospatial bioinformatics and ecoinformatics for *Symbiodinium*-host symbioses. *Molecular Ecology Resources* **12**:369-373
- Freudenthal HD (1962) *Symbiodinium* gen. nov. and *Symbiodinium microadriaticum* sp. nov., a zooxanthella: taxonomy, life cycle and morphology. *Journal of Protozoology* **9**:45-49

- Garren M, Walsh S, Caccone A, Knowlton N (2006) Patterns of association between *Symbiodinium* and members of the *Montastraea annularis* species complex on spatial scales ranging from within colonies to between geographic regions. *Coral Reefs* **25**:503-512
- Goulet TL (2006) Most corals may not change their symbionts. *Marine Ecology Progress Series* **321**:1-7
- Goulet TL (2007) Most scleractinian corals and octocorals host a single symbiotic zooxanthella clade. *Marine Ecology Progress Series* **335**:243-248
- Granados-Cifuentes C, Rodriguez-Lanetty M (2011) The use of high-resolution melting analysis for genotyping *Symbiodinium* strains: a sensitive and fast approach. *Molecular Ecology Resources* **11**:394-399
- Hoegh-Guldberg O (1999) Climate change, coral bleaching and the future of the world's coral reefs. *Marine and Freshwater Research* **50**:839-866
- Hoegh-Guldberg O, Mumby PJ, Hooten AJ, Steneck RS, Greenfield P, Gomez E, Harvell CD, Sale PF, Edwards AJ, Caldeira K, Knowlton N, Eakin CM, Iglesias-Prieto R, Muthiga N, Bradbury RH, Dubi A, Hatzioiols ME (2007) Coral reefs under rapid climate change and ocean acidification. *Science* **318**:1737-1742
- Jones L, Alcolado PM, Cala Y, Cobian D, Coelho V, Hernandez A, Jones R, Mallela J, Manfrino C (2008) The effects of coral bleaching in the Northern Caribbean and Western Atlantic. In: Wilkinson C, Souter D (eds) *Status of Caribbean coral reefs after bleaching and hurricanes in 2005*. GRCMN Report.
- Kirk N, Andras J, Harvell C, Santos S, Coffroth M (2009) Population structure of *Symbiodinium* sp. associated with the common sea fan, *Gorgonia ventalina*, in the Florida Keys across distance, depth, and time. *Marine Biology* **156**:1609-1623
- Knowlton N, Weil E, Weigt LA, Guzman HM (1992) Sibling species in *Montastraea annularis*, coral bleaching, and the coral climate record. *Science* **255**:330-333
- Lajeunesse TC (2001) Investigating the biodiversity, ecology, and phylogeny of endosymbiotic dinoflagellates in the genus *Symbiodinium* using the ITS region: In search of a "species" level marker. *Journal of Phycology* **37**:866-880
- Lajeunesse TC (2002) Diversity and community structure of symbiotic dinoflagellates from Caribbean coral reefs. *Marine Biology* **141**:387-400
- Lajeunesse TC (2005) "Species" radiations of symbiotic dinoflagellates in the Atlantic and Indo-Pacific since the miocene-pliocene transition. *Molecular Biology and Evolution* **22**:570-581
- Lajeunesse TC, Bhagooli R, Hidaka M, DeVantier L, Done T, Schmidt GW, Fitt WK, Hoegh-Guldberg O (2004) Closely related *Symbiodinium* spp. differ in relative dominance in coral reef host communities across environmental, latitudinal and biogeographic gradients. *Marine Ecology Progress Series* **284**:147-161
- Lajeunesse TC, Pettay DT, Sampayo EM, Phongsuwan N, Brown B, Obura DO, Hoegh-Guldberg O, Fitt WK (2010) Long-standing environmental conditions, geographic isolation and host-symbiont specificity influence the relative ecological dominance and genetic diversification of coral endosymbionts in the genus *Symbiodinium*. *Journal of Biogeography* **37**:785-800
- Lajeunesse TC, Smith RT, Finney J, Oxenford H (2009) Outbreak and persistence of opportunistic symbiotic dinoflagellates during the 2005 Caribbean mass coral 'bleaching' event. *Proceedings Biological Sciences* **276**:4139-4148
- Lajeunesse TC, Thornhill DJ (2011) Improved resolution of reef-coral endosymbiont (*Symbiodinium*) species diversity, ecology, and evolution through *psbA* non-coding region genotyping. *PLoS ONE* **6**:e29013
- Levitan DR, Fukami H, Jara J, Kline D, McGovern TM, McGhee KE, Swanson CA, Knowlton N (2004) Mechanisms of reproductive isolation among sympatric broadcast-spawning corals of the *Montastraea annularis* species complex. *Evolution* **58**:308-323
- McField M, Bood N, Fonseca A, Arrivillaga A, Rinos AF, Viruel RML (2008) Status of the Mesoamerican reef after the 2005 coral bleaching event. In: Wilkinson C, Souter D (eds) *Status of Caribbean coral reefs after bleaching and hurricanes in 2005*. GRCMN Report.
- Mieog JC, Oppen MJH, Cantin NE, Stam WT, Olsen JL (2007) Real-time PCR reveals a high incidence of *Symbiodinium* clade D at low levels in four scleractinian corals across the Great Barrier Reef: implications for symbiont shuffling. *Coral Reefs* **26**:449-457
- Miller J, Muller E, Rogers C, Waara R, Atkinson A, Whelan KRT, Patterson M, Witcher B (2009) Coral disease following massive bleaching in 2005 causes 60% decline in coral cover on reefs in the US Virgin Islands. *Coral Reefs* **28**:925-937
- Muscantine L, Porter JW (1977) Reef corals: mutualistic symbioses adapted to nutrient-poor environments. *Bioscience* **27**:454-460

- Oliver TA, Palumbi SR (2009) Distributions of stress-resistant coral symbionts match environmental patterns at local but not regional scales. *Marine Ecology Progress Series* **378**:93-103
- Ortiz JC (2008) Coral holobiont community structure: how much have we missed by focusing only in the coral host? *Proceedings of the International Society for Coral Reef Studies*, 2008, Miami, Florida
- Perry JN (1995) Spatial Analysis by Distance Indices. *Journal of Animal Ecology* **64**:303-314
- Perry JN, Winder L, Holland JM, Alston RD (1999) Red–blue plots for detecting clusters in count data. *Ecology Letters* **2**:106-113
- Petit RJ, El Mousadik A, Pons O (1998) Identifying populations for conservation on the basis of genetic markers. *Conservation Biology* **12**:844-855
- Pochon X, Gates RD (2010) A new *Symbiodinium* clade (Dinophyceae) from soritid foraminifera in Hawaii. *Molecular Phylogenetics and Evolution* **56**:492-497
- Rodriguez-Lanetty M, Loh WKW, Carter DA, Hoegh-Guldberg O (2001) Latitudinal variability in symbiont specificity within the widespread scleractinian coral *Plesiastrea versipora*. *Marine Biology* **138**:1175-1181
- Rowan R, Knowlton N (1995) Intraspecific diversity and ecological zonation in coral-algal symbiosis. *Proceedings of the National Academy of Sciences* **92**:2850-2853
- Rowan R, Knowlton N, Baker A, Jara J (1997) Landscape ecology of algal symbionts creates variation in episodes of coral bleaching. *Nature* **388**:265-269
- Rowan R, Powers DA (1991a) A molecular genetic classification of zooxanthellae and the evolution of animal-algal symbioses. *Science* **251**:1348-1351
- Sampayo EM, Dove S, Lajeunesse TC (2009) Cohesive molecular genetic data delineate species diversity in the dinoflagellate genus *Symbiodinium*. *Molecular Ecology* **18**:500-519
- Santos SR, Shearer TL, Hannes AR, Coffroth MA (2004) Fine-scale diversity and specificity in the most prevalent lineage of symbiotic dinoflagellates (*Symbiodinium*, Dinophyceae) of the Caribbean. *Molecular Ecology* **13**:459-469
- Silverstein RN, Correa AMS, Baker AC (2012) Specificity is rarely absolute in coral-algal symbiosis: implications for coral response to climate change. *Proceedings of the Royal Society B: Biological Sciences* **279**:2609-2618
- Spalding MD, Fox HE, Allen GR, Davidson N, Ferdana ZA, Finlayson MAX, Halpern BS, Jorge MA, Lombana AL, Lourie SA, Martin KD, McManus E, Molnar J, Recchia CA, Robertson J (2007) Marine ecoregions of the world: a bioregionalization of coastal and shelf areas. *Bioscience* **57**:573-583
- Stat M, Gates RD (2011) Clade D *Symbiodinium* in scleractinian corals: a nugget of hope, a selfish opportunist, an ominous sign, or all of the above? *Journal of Marine Biology* Article ID **730715**, 9 pages
- Thornhill D, Fitt W, Schmidt G (2006a) Highly stable symbioses among western Atlantic brooding corals. *Coral Reefs* **25**:515-519
- Thornhill DJ, LaJeunesse TC, Kemp DW, Fitt WK, Schmidt GW (2006b) Multi-year, seasonal genotypic surveys of coral-algal symbioses reveal prevalent stability or post-bleaching reversion. *Marine Biology* **148**:711-722
- Thornhill DJ, Xiang Y, Fitt WK, Santos SR (2009) Reef endemism, host specificity and temporal stability in populations of symbiotic dinoflagellates from two ecologically dominant Caribbean corals. *PLoS ONE* **4**:e6262
- Toller WW, Rowan R, Knowlton N (2001a) Zooxanthellae of the *Montastraea annularis* species complex: patterns of distribution of four taxa of *Symbiodinium* on different reefs and across depths. *Biological Bulletin* **201**:348-359
- Toller WW, Rowan R, Knowlton N (2001b) Repopulation of zooxanthellae in the Caribbean corals *Montastraea annularis* and *M. faveolata* following experimental and disease-associated bleaching. *Biological Bulletin* **201**:360-373
- Trench RK (1993) Microalgal-Invertebrate Symbioses - A Review. *Endocytobiosis and Cell Research* **9**:135-175
- van Hooidonk RJ, Manzello DP, Moye J, Brandt ME, Hendee JC, McCoy C, Manfrino C (2012) Coral bleaching at Little Cayman, Cayman Islands 2009. *Estuarine, Coastal and Shelf Science* **106**:80-84
- Van Oppen MJH, Gates RD (2006) Conservation genetics and the resilience of reef-building corals. *Molecular Ecology* **15**:3863-3883
- Vollmer SV, Palumbi SR (2007) Restricted gene flow in the Caribbean staghorn coral *Acropora cervicornis*: implications for the recovery of endangered reefs. *Journal of Heredity* **98**:40-50
- Walsh SM, McField M, Knowlton N (in prep.) Zooxanthellae community structure across the Mesoamerican Barrier Reef explains historical bleaching patterns.

- Warner ME, Fitt WK, Schmidt GW (1999) Damage to photosystem II in symbiotic dinoflagellates: A determinant of coral bleaching. *Proceedings of the National Academy of Sciences* **96**:8007-8012
- Warner ME, LaJeunesse TC, Robison JD, Thur RM (2006) The ecological distribution and comparative photobiology of symbiotic dinoflagellates from reef corals in Belize: Potential implications for coral bleaching. *Limnology and Oceanography* **51**:1887-1897
- Wilkinson C, Souter D (2008) *Status of Caribbean coral reefs after bleaching and hurricanes in 2005*. Global Coral Reef Monitoring Network, and Reef and Rainforest Research Centre, 152p, ISSN 1447 6185, Vol, Townsville, Australia

6

Exploring environmental, geographic and genetic drivers of Caribbean symbiont biogeography in a key reef building coral

6.1 Introduction

Understanding the spatial scaling of biodiversity is a key goal in ecology. Linking patterns in symbiont spatial distribution, such as those identified in Chapter 5, with independent predictors (e.g., geographic or environmental variation) is a critical step in enhancing knowledge about the underlying drivers of symbiont biogeography, as well as the functional significance of *Symbiodinium* diversity. For example, initial evidence that D1 is thermally tolerant and that C clades avoid high irradiance environments have emerged from spatial studies that have correlated occurrence of types to environmental heterogeneity between sampling locations, both on large (e.g., between oceans; B dominating the Caribbean, and C the Pacific; LaJeunesse 2002) and small scales (e.g., within colony; B on colony tops, C on colony sides; Rowan et al. 1997).

Montastraea annularis is flexible in terms of hosting symbiont associations (Toller et al. 2001b), and this makes it an ideal model to explore the relative importance of environmental, geographic and genetic drivers in shaping *Symbiodinium* distribution. Temperature and irradiance (including UV; Lesser 2000) - or proxies such as latitude and depth - are known to play a critical role in shaping symbiont community distribution, particularly at local scales. However many other factors, including salinity (Coles & Jokiel 1992), nutrients (Fagoonee et al. 1999) and turbidity (Toller et al. 2001b, Garren et al. 2006), and biological factors such as predation (Augustine and Muller-Parker 1998) and disease (Toller et al. 2001a, Correa et al. 2009) can affect symbioses. Few studies have attempted to explain broad-scale variability in *Symbiodinium* associations in terms of these other environmental metrics (Cooper et al. 2011).

Alternative drivers of spatial variability could include those determined by organism dispersal, or by patterns of colonisation (LaJeunesse 2005), both manifested as diminishing relatedness of communities as geographic distance increases (known as 'distance-decay'; Green and Bohannan 2006). Evidence for 'distance-decay' (or 'isolation-by-distance', IBD) of *Symbiodinium* communities is growing, with recent genetic work showing strong gradients of isolation-by-distance in *Symbiodinium* at population level, both in the Caribbean (Santos et al. 2003b, Andras et al. 2009, Thornhill et al. 2009) and the Pacific (Howells et al. 2009). These studies suggest that spatial patterns in *Symbiodinium* community may be principally driven by geographic dispersal rather than environmental heterogeneity and that environmental drivers might have a larger role in determining spatial distribution at the local scale (e.g., variability in irradiance may be more influential in determining bathymetric distribution than geographic distribution).

Host species is often described as the most important predictor of partitioning of symbiont clades, with host a more influential factor than environmental and geographic drivers (Finney et al. 2010, LaJeunesse et al. 2010, Cooper et al. 2011). More recently spatial structuring of algal communities has been correlated with genetic structuring *within* their coral symbiotic partners across several sites along the Great Barrier Reef (GBR), Australia (Bongaerts et al. 2010). It is not clear from examining distribution maps of *Symbiodinium* ITS2-types (Chapter 5, Figs 5.19, 5.20), whether the spatial patterns depicted – namely a significant east-west divide in species abundance - are a product of ecological radiations from different areas (i.e. distance decay), are driven by environmental heterogeneity, or are associated with *M. annularis* host populations. Identifying whether genetic, geographic or environmental factors make better predictors for the observed spatial patterns will help determine the major influences of *Symbiodinium* community structure. In this chapter, a variety of multivariate models are used to explain variation in the distribution of symbiont types hosted by *M. annularis* in the Caribbean basin, using an array of distance measures and environmental and genetic predictors, while controlling for potentially confounding variables.

6.2 Chapter Aims

The aim of this chapter is to identify the environmental, genetic and geographic variables that best explain *Symbiodinium* community spatial structuring across the Caribbean.

Null hypothesis: environmental, geographic and genetic-related explanatory variables included in the study (see section 6.3.2) do not explain the observed variation in symbiont distribution recorded in Chapter 5.

- a. H_1 = *Symbiodinium* spatial structuring is best explained by geographic distance measures.

- b. H_2 = *Symbiodinium* spatial structuring is best explained by environmental heterogeneity.
- c. H_3 = *Symbiodinium* community spatial structuring is most closely related to/can be best explained by *M. annularis* genetics.
- d. H_4 = *Symbiodinium* community spatial structuring is best explained by a combination of host genetics, environmental and geographic factors.

6.3 Overview of statistical model variables

6.3.1 Dependent variables: symbiont community

Analysis of spatial distribution of *Symbiodinium* cladal types in Chapter 5 revealed significant spatial structuring across the Caribbean region. A broad east-west divide was apparent, supporting reported Caribbean *Symbiodinium* partitioning in several cnidarian hosts between a western (Belize) and an eastern (Barbados) site (Finney et al. 2010). In our study, *Symbiodinium* C displayed a predominantly easterly distribution, while *Symbiodinium* B, found in 75% colonies, dominated communities in the north (Bahamas) and west (Mesoamerican Barrier Reef). At a higher taxonomic resolution, types B1, B17, B1j, B10, C7 and C12 revealed significant regional spatial patterning. In contrast, *Symbiodinium* D displayed a patchy distribution, although occurrences of clade D were shown to be randomly distributed geographically. A variety of metrics derived from this dataset were used to describe symbiont variability across the Caribbean basin (see 6.4.1).

6.3.2 Explanatory variables: geographic, environmental and genetic

6.3.2.1 Geographic distance

Substantial evidence for distance-decay exists for seemingly ‘panmictic’ free-living dinoflagellates (in the same class as *Symbiodinium*), who demonstrate isolation-by-distance genetic structuring (Green and Bohannan 2006, Nagai et al. 2007). *M. annularis* relies on algal acquisition from the environment (i.e., horizontal transmission of zooxanthellae), and subsequently its symbiont communities may be more likely to exhibit some form of distance-derived spatial structuring, than brooding host species that employ vertical transmission (Thornhill et al. 2006a).

The scale at which geographic distance may be influential in driving patterns of symbiont variability is not well established. At the reef scale (10s of meters), some studies document stability (even endemism; Thornhill et al. 2009), while others record significant variation in *M. annularis* symbiont communities (Warner et al. 2006). On larger scales, studies have detected patterns of isolation by distance in *Symbiodinium*, at spatial scales of 200 km (e.g., in B1 harboured by the sea fan *Gorgonia ventalina*; Kirk et al. 2009) to 450 km (e.g., in

Pseudopterogorgia elisabethae in the Bahamas; Santos et al. 2003b). Similar broad geographic spatial patterns have been documented on the GBR, over 1300 km (Howells et al. 2009). In *M. annularis*, populations of *Symbiodinium* B1 have been shown to display significant genetic structuring at spatial scales of 500 km (Thornhill et al. 2009).

To assess the ability of geographic distance to explain patterns of symbiont distribution, various distance measures were employed during analysis. At the colony-level analysis this involved inclusion of data on ‘reef’, ‘location’ and ‘eco-region’ (Spalding et al. 2007; Fig. 4.2, Chapter 4), reflecting spatial scales of meters to kilometres. At the population level, we compared geographic distance matrices with symbiont community resemblance matrices, and explored relationships with latitude and longitude with other symbiont community metrics. Distance measures were included in the environmental linear model.

6.3.2.2 Environmental conditions

Temperature

Temperature is generally regarded as the key driver of *Symbiodinium* distribution, as it is widely known to be influential in determining the coral-endosymbiont partnership both under typical circumstances (Rowan and Knowlton 1995) and disturbance conditions (Berkelmans and van Oppen 2006). Temperatures as little as 1 °C above the average annual maximum can trigger bleaching and associated community shifts, although bleaching threshold varies according to the duration of temperature stress and the stress history of the corals. No single temperature variable or index of thermal stress has been shown to adequately reflect the response of corals (Berkelmans 2002; Berkelmans et al. 2004; Manzello et al. 2007; McClanahan et al. 2007). Coral response will also depend on intrinsic factors, such as the reef community (McClanahan et al. 2007), species composition (Yee et al. 2008) or the shape of the coral (Jimenez et al. 2008). As a result, a variety of metrics are commonly used to approximate thermal stress experienced by corals (e.g., cumulative degree heating weeks (Liu et al. 2006), degree heating months (Barton and Casey 2005) or number of days above a threshold (Manzello et al. 2007)). A number of these thermal stress metrics were employed to examine for relationships with symbiont community data (for Methods see 6.4.1.1).

Irradiance

Irradiance is a vital determinant of *Symbiodinium* distribution, with one Caribbean study showing 40-50% of ITS2 types partitioned according either to shallow, high-irradiance, or deep, low-irradiance environments (Finney et al. 2010). Evidence from the Caribbean suggests irradiance may be more critical than temperature in triggering extreme symbiont shifts (Rowan and Knowlton 1995, Garren et al. 2006), with high doses of UV light, particularly UVB

radiation, implicated in coral bleaching events. For *M. annularis* inhabiting the range of depths employed in this study (i.e., 2 - 12 m), tissues exposed to high-intensity, downwelling irradiance have been associated with *Symbiodinium* B, or occasionally A (Toller et al. 2001b). Meanwhile, *Symbiodinium* C dominates colony sides and shaded tops, with unshaded columns creating gradients of irradiance (Rowan et al. 1997).

a) *Irradiance vs turbidity*

Irradiance is associated with water clarity: any factor that reduces photosynthesis of algal symbionts may achieve the same result as physiological bleaching (Fitt et al. 2001), and it follows that variation in turbidity may influence partitioning in symbiont distribution. A study on *M. annularis* in Belize and Panama revealed that symbiont community variation could be partly explained by total suspended solids (Garren et al. 2006), while an Australian study also related relative abundance of types to locations with high water quality indices (Cooper et al. 2011). However, it should also be noted that cases have been reported where turbid environments, often considered marginal, can buffer against environmental stress of elevated irradiance and SSTs (Smith et al. 2008).

b) *Irradiance vs depth*

Irradiance also interacts with water depth: in high-light, shallow water (1-3 m) *M. annularis* associate almost exclusively with *Symbiodinium* B across all parts of a colony (Rowan et al. 1997, LaJeunesse et al. 2009); from 4 -10 m there is an interaction with irradiance, *Symbiodinium* B are frequently found on the tops of colonies, with C on the deeper, shaded sides – although this is more likely due to irradiance than bathymetry (Rowan 1997, Toller et al. 2001). However, at deeper depths (generally > 8 m; Rowan and Knowlton 1995, Toller et al. 2001a), only *Symbiodinium* C are found. Bathymetry is known to be a fundamental driver of Caribbean symbiont spatial partitioning (Rowan et al. 1997, Finney et al. 2010), and diversity (Warner et al. 2006) particularly in *M. annularis* (Rowan and Knowlton 1995), where the relationship between depth and symbiont clade has been demonstrated even at intra-colony (cm) level (Rowan et al. 1997). Symbiont communities demonstrate distinct but overlapping habitats within a colony (Rowan et al. 1997). Depth is also a dominant driver of partitioning: in sea fans in the Florida Keys, depth produced sharper differentiation in *Symbiodinium* B1 at the population level than geographic distance (Kirk et al. 2009). Although this study aimed to control for depth, samples were taken in a depth range from 2 – 12 m (mean = 5.95(±3.4) m), therefore this variable was included in the model because of its potential confounding effects: clearly even small variations in depth can influence the structuring of symbiont communities.

Since data on irradiance was unavailable, depth and turbidity was used as proxies for irradiance examining the role of light in determining symbiont biogeography (for Methods see 6.4.1.2).

Nutrients

‘Water quality’, based on combined nutrient and irradiance measures (including dissolved inorganic nitrogen, phosphorus and organic nutrients), was able to explain 37.6% of variation in *Acropora millepora* symbiont community along the length of the GBR (Cooper et al. 2011). In the Caribbean, total suspended solids and proximity to coastal regions – measures that the authors link to nutrients and sedimentation – were deemed influential in determining symbiont communities in *M. annularis* (Garren et al. 2006). Although few other studies have investigated the influence of nutrients on *Symbiodinium* biogeography, symbiont population growth has been shown to be nutrient limited, both in field (Fagoonee et al. 1999) and laboratory studies (Dubinsky et al. 1990). Seasonal changes in nitrate concentrations correlate with fluctuating *Symbiodinium* densities, (Marubini and Davies 1996, Fagoonee et al. 1999), and can even affect bleaching susceptibility (Wooldridge 2009). It follows that spatial heterogeneity in inorganic nitrate and phosphate concentrations may provide some insight into symbiont community variation, and reef-level estimates for concentrations of both these nutrients were involved in the analysis (for Methods see 6.4.1.4).

Salinity

Freshwater is the second most commonly cited cause of reported coral bleaching, after temperature induced bleaching (Coles and Jokiel 1992). Experimental and observational studies have shown that reduced salinity can affect algal endosymbiont functioning, causing a decline in photosynthetic efficiency of endosymbionts, and a sub-lethal bleaching response (Kerswell and Jones 2003). However, scleractinian corals can survive in salinities ranging from 23.3 to 41.8 (Kleypas et al. 1999), suggesting that some endosymbionts/coral partnerships may show differential tolerances to salinity. Salinity was included in the explanatory model (see 6.4.1.3).

Mechanical disturbance regime

Marine organisms living in shallow coastal habitats are strongly influenced by the mechanical disturbance regime. Two principal types of mechanical disturbance can be distinguished: chronic exposure to waves and acute, episodic physical disturbance from tropical cyclones (Chollett et al. 2012). Exposure to waves has been linked to ecological traits, such as duration of spawning time (van Woesik 2010) and the Caribbean distribution of the *M. annularis* host (Chollett and Mumby 2012). Partitioning in symbioses hosted by *M. annularis* in inner, lagoonal reef sites and outer, coastal reef sites have been repeatedly identified (Toller et al. 2001b, Garren et al. 2006). ‘Enclosure’, a quantitative measure of the relative influence of open ocean versus coastal areas, employed by Garren *et al.* was identified as the most important driver of variation in *M. annularis* symbiont communities in Panama and Belize (Garren et al. 2006). Differential thermal histories of inshore lagoonal reefs and offshore fore-reefs have been

shown to influence bleaching susceptibility (Castillo and Helmuth 2005). Finally, hurricane frequency has been associated with host genetic variability (Foster et al. 2013). Three descriptors of the mechanical disturbance regime – wave exposure, hurricane frequency and enclosure – were used to explore community spatial patterns of *Symbiodinium*.

6.3.2.3 Host population genetics

Host is frequently reported as the most important determinant of symbiont partitioning (Finney et al. 2010, Cooper et al. 2011). Acquisition of symbionts is largely determined by coral host reproductive mode (Thornhill et al. 2006a), and as hermaphroditic broadcast spawners (Szmant 1991) *M. annularis* are more flexible in their symbioses than brooding corals (Thornhill et al. 2006). It might therefore follow that *M. annularis* symbiont communities will be less likely to be associated with host population genetic structure and perhaps more determined by local availability of free-living symbionts (LaJeunesse et al. 2004b) (see 6.3.2.1). However, within a single host, few studies have attempted to examine *Symbiodinium* communities with coral host population structure (Ortiz 2008). Genetic structuring was reported in brooding coral *Seriatopora hystrix* and its symbiont community across several habitats and locations on the GBR (Bongaerts et al. 2010). Another study that looked at the sea fan *Gorgonia ventalina*, which, like *M. annularis*, acquires zooxanthellae through horizontal transmission, also correlated symbiont structure with its Caribbean host (although symbionts exhibited a higher degree of genetic structuring; Andras et al. 2011). Another argument for examining the role played by host genetics is that the patterns in symbiont distribution described in Chapter 5 appear to mirror a genetic break described in coral populations between eastern and western portions of the Caribbean (Baums et al. 2006, Foster et al. 2012). The Mona Passage between Puerto Rico and the Dominican Republic has been proposed as break between east and west in *Acropora palmata* and *A. cervicornis* (Baums et al. 2005, Vollmer and Palumbi 2007) although data based on *M. annularis* suggests the break might lie further west with a second break isolating the British Virgin Isles and Dominica from the east and west populations (Foster et al. 2012). This region also appears to be a break between clade B dominated west and the more speciose clade C dominated east. Finally, some studies have proposed that symbiont diversity is inversely proportional to host diversity, as an explanation for the relatively low symbiont diversity of the Caribbean compared to the Pacific (LaJeunesse et al. 2003; 2004a). Examination of host diversity compared to symbiont diversity may be able to elucidate these patterns on a smaller scale.

Within the study area, *M. annularis* shows weak, but significant IBD based on variability at six polymorphic microsatellite loci (Foster et al. 2012). Caribbean *M. annularis* form three distinct genetic clusters: a central cluster, a western cluster (including the Bahamas, Cuba, Jamaica and Belizean sites) and an eastern cluster (Tobago, Venezuela, Dominica and Barbados). Further

sub-divisions were also supported. Given this evidence, and the patterns observed in the previous chapter that suggest spatial symbiont patterning, it is likely that the distance element to community diversity may be one of the more important factors in explaining distribution.

Various metrics were used to explore host genotypic patterning at the population level, including univariate host genotypic richness and diversity at each reef site – which were also included in the environmental model. At the individual level, multivariate data on genetic distance measures were compared with Sorenson resemblance matrices for presence/absence of different symbiont types (6.4.1.8).

6.3.2.4 Confounding factors

Confounding factors such as collection date and season (and to an extent, depth) also require consideration when attempting to derive conclusions about partitioning of variability.

Collector

Strong partitioning of *Symbiodinium* B and C on the tops and sides of *M. annularis* colonies (see *Colony depth* and *Irradiance*) emphasise the need for a clear and consistent sampling method. Fifteen different collectors assisted with the sampling for this research. At 16 of the 33 sites, the scientific project lead (N. Foster) was present during sampling, reducing the effect of collection bias. However, these 16 sites comprised the entire Mesoamerican Barrier Reef and Bahamian eco-regions, (along with Nicaragua and Barbados): areas of higher community homogeneity where B1 was shown to consistently dominate *M. annularis* communities. Four researchers undertook sampling in the Greater Antilles and two in the south-western Caribbean. Six different scientific teams sampled in the Lesser Antilles region – the area that generated the greatest amount of symbiont diversity, and also produced more *Symbiodinium* C, associated with the sides of colonies. Although a single factor ANOVA showed no significant difference in the recorded sampling depths with collector ID ($F=0.007$, $p=0.932$), suggesting that all researchers adhered to sampling instructions, it remains important to verify whether the factor ‘collector’ helps explain observed variability in the symbiont communities, to be confident that results were not unconsciously influenced by collection bias.

Collection month and year

Inclusion of the month and year of collection as variables in the statistical model was necessary, given evidence for temporal dynamics of many symbiont communities with season (Fagoonee et al. 1999), and across years (Cooper et al. 2011). In addition, the Caribbean experienced a widespread and severe bleaching event in the middle of the sampling period (Wilkinson and Souter 2008, Eakin et al. 2010) which may have affected symbiont patterns.

6.4 Methodology

Twenty-three environmental parameters (Table 6.1) were determined for each reef site using a combination of remote sensing data and environmental data gathered during sample collection (see Chapter 5 for more details). These were all considered for inclusion in a distance-based multiple linear regression model (DISTLM), designed to partition variability in hosted symbiont communities according to regression (see 6.4.2.2). For details of how data on *M. annularis* symbiont communities were collected, see section 5.3 (Chapter 5).

6.4.1 Dependent variables

Colony-level data on the presence/absence of symbiont clades, and population-level data on the relative proportions of colonies hosting different clades per reef site, were used to investigate the broad-scale partitioning in host-symbiont associations. Resemblance measures (e.g., Sorenson's similarity for colony-level binary data, Bray-Curtis similarity for population-level count data) were used to evaluate variability in occurrence/proportions of each of the different clades within a colony/site simultaneously. *Symbiodinium* variability was additionally investigated at a finer taxonomic resolution, by examining variability in the distribution of sub-cladal types (B1, B17, B1j, C7 etc). Finally, univariate metrics such as symbiont community richness and diversity, and relative proportions of different cladal types were used to further explore particularly interesting relationships.

6.4.2 DISTLM model explanatory variables

6.4.2.1 Thermal stress metrics

A suite of thermal stress proxies were generated for each reef site, using available NOAA datasets from the AVHRR pathfinder dataset v 5.2 (Casey et al. 2010), <http://www.nodc.noaa.gov/SatelliteData/pathfinder4km/>. For each of the 33 sites, the monthly climatological mean was calculated (1981-2010) for the datapoint closest to the site location (4 km resolution, Table 6.1). In addition, maximum values were selected for each year in the record in order to calculate maximum monthly means. Maximum monthly mean was used as a proxy for chronic thermal stress – an average summer maximum - at each site (*ts_chron*). In order to further characterize the thermal stress regime, warm anomalies were calculated for each period, using HotSpots (calculated by subtracting the maximum monthly climatological mean SST from the current value; Liu et al. 2006). Degree Heating Weeks (DHW), a measurement of accumulated thermal stress incorporating all hotspots above 1°C for the last 12 weeks, were then calculated.

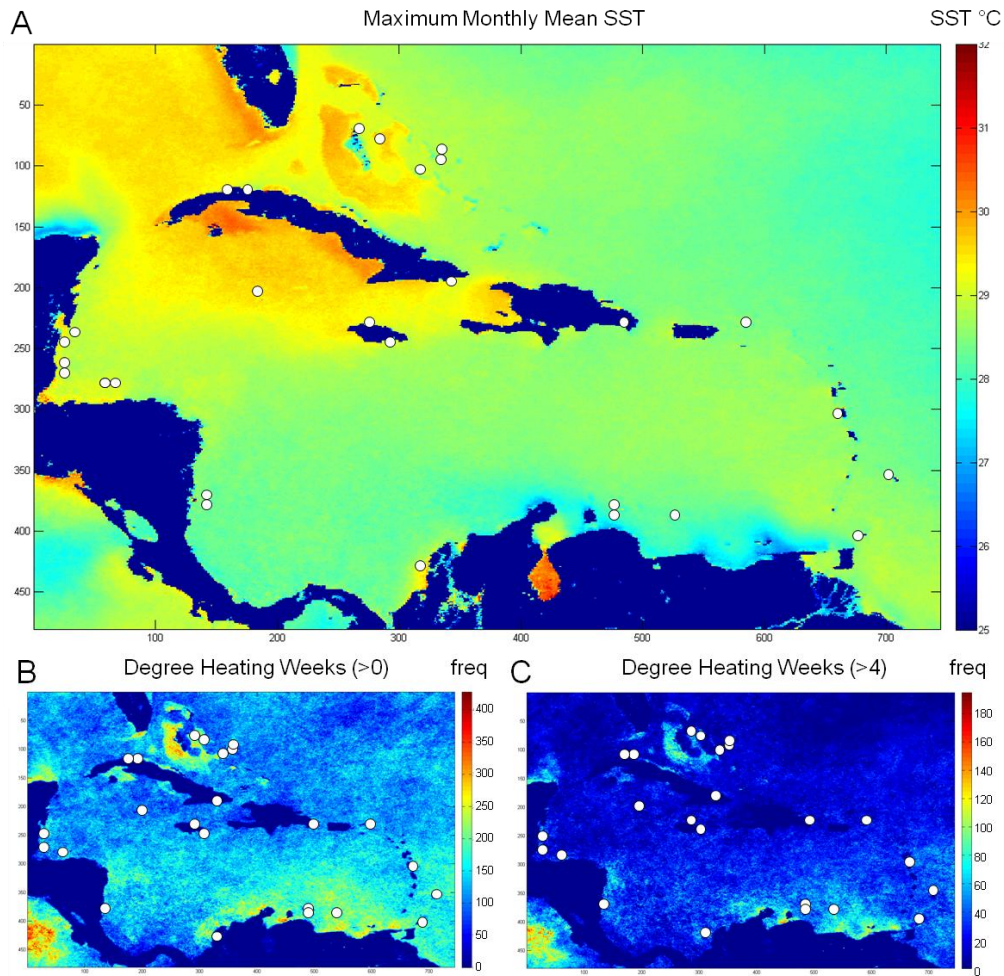


Figure 6.1: Thermal stress metrics used to inform the statistical model **A)** Chronic thermal stress shown by maximum monthly mean sea surface temperatures (1981-2010) from the AVHRR Pathfinder dataset. White circles represent sampling sites ('reefs'). **B)** History of thermal stress: number of DHWs since 1981 **C)** History of severe thermal stress: map of frequency of DHWs above 4, since 1981.

Two measures of acute thermal stress were generated for each site: the first was the frequency of DHW above zero for the year preceding collection (*ts_acute_0*), the second the frequency of DHW above four (*ts_acute_4*). Finally, long-term thermal history at each site was approximated by taking the number of DHW from the start of the dataset (1981) until the year preceding sampling at each site. Again, two measures of thermal stress history were employed, one generated by summing all DHW > 0 and one by DHW > 4 (*ts_history_0*, *ts_history_4*).

6.4.2.2 Irradiance proxies

Both depth at the location and light attenuation in the water column (approximated by chlorophyll-*a* concentrations) were used as proxies for irradiance.

Depth

Collection depths ranged from 2 - 12 m (Chapter 5). Absolute depth was included as an

Variable	ID	Description	Units	Spatial resolution	Source	
Geographic	Latitude	lat	Latitudinal location of reef site (decimal degrees)	decimal °	11 m	Foster et al. 2007
	Longitude	long	Longitudinal location of reef site (decimal degrees)	decimal °	11 m	Foster et al. 2007
	Geographic proximity	dist	PCO1 estimate of the resemblance (derived from lat-long data)	none	>0.1 km	This study
Environmental	Acute thermal stress	ts_acute_0	Number of DHW above zero, for the year prior to sampling	frequency	4 km	AVHRR pathfinder v5.2
	Acute thermal stress (severe)	ts_acute_4	Number of DHW above four, for the year prior to sampling	frequency	4 km	AVHRR pathfinder v5.2
	Chronic thermal stress	ts_chron	Maximum of monthly mean SST for all years in record (1981-2010)	°C	4 km	AVHRR pathfinder v5.2
	History of thermal stress	ts_histor_0	Number of DHW above zero from 1981 until one year prior to sampling	frequency	4 km	AVHRR pathfinder v5.2
	History of severe thermal stress	ts_histor_4	Number of DHW above four from 1981 until one year prior to sampling	frequency	4 km	AVHRR pathfinder v5.2
	Turbidity	chla_1y	Average chlorophyll-a concentration during the year of sampling	mg m ³	4 km	MODIS daily Chlor_a
	Turbidity	chla_avg	Average chlorophyll-a concentration for entire data set	mg m ³	4 km	MODIS daily Chlor_a
	Salinity	sal_avg	Climatological average of surface salinity	no units	0.25°	World Ocean Atlas 2009
	Nitrate concentration	nit_avg	Climatological average of surface nitrate concentration	μ mol l ⁻¹	1°	World Ocean Atlas 2009
	Phosphate concentration	pho_avg	Climatological average of surface phosphate concentration	μ mol l ⁻¹	1°	World Ocean Atlas 2009
	Silicate concentration	sil_avg	Climatological average of surface silicate concentration	μ mol l ⁻¹	1°	World Ocean Atlas 2009
	Wave exposure	wave_avg	Natural log of the climatological average of wave exposure	Ln(j m ⁻³)	1 km	Chollett et al. 2012
	Enclosure	encl	Reciprocal of the sum of the distance to land in cardinal directions	1/m	0.1 km	Adapted from Garren et al. 2006
	Hurricane frequency	hurr	Total hurricane incidences, category 1-5 (1853-2004)	frequency	100 km	Chollett et al. 2012, Foster et al. 2013
	Depth	depth	Mean depth of the reef site	m	1 m	Foster et al. 2007
Genetic	Host genotypic richness	coral_S	Number of independent colonies per reef site	frequency	10 m	Foster et al. 2012
	Host genotypic diversity	coral_D	Clonal diversity: number of genotypes/number of samples	frequency	10 m	Foster et al. 2012
	Host heterozygosity (HE)	coral_HE	Genetic variation in a population, based on the squared allele frequencies		n/a	This study / Foster et al. 2007
Temporal	Sampling year	year	Year (2003-2007) that sampling took place	1 year	n/a	Foster et al. 2007
	Sampling month	month	Month that sampling took place	1 month	n/a	Foster et al. 2007

Table 6.1: List of the environmental, geographic and genetic parameters considered for inclusion in statistical model designed to explain *M. annularis* symbiont biogeography

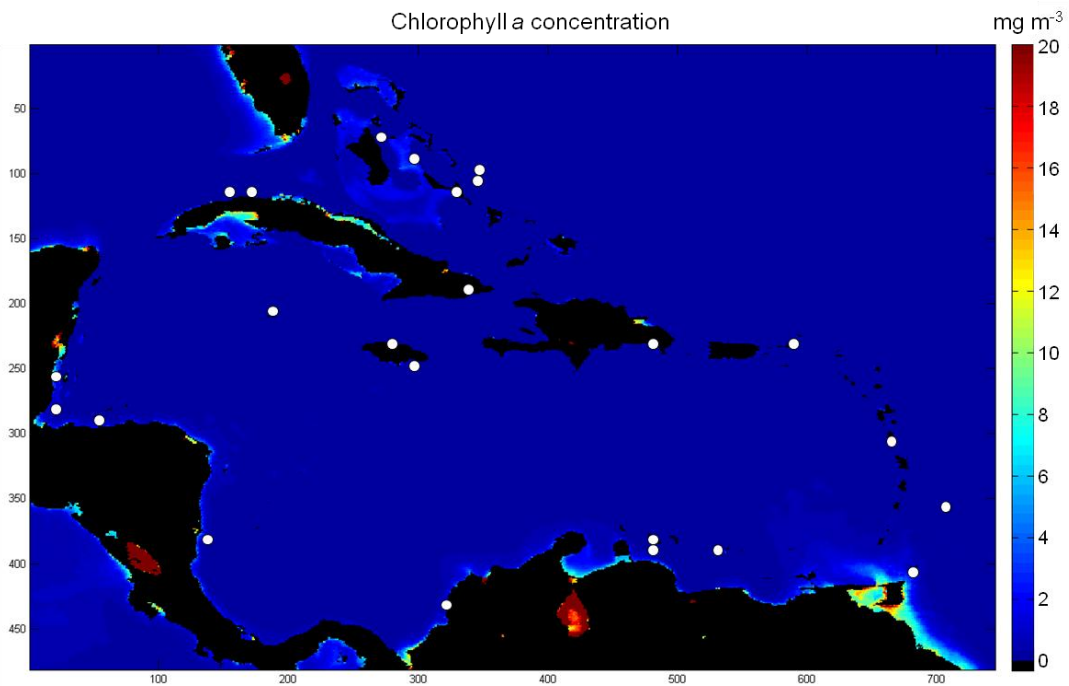


Figure 6.2: Average chlorophyll-a concentration (mg m^{-3}) derived from MODIS satellite data: this was used as a proxy for turbidity/irradiance in the model.

environmental covariate in the linear model, but was also used as a factor with two ‘shallow, S’ (< 8 m) and ‘deep, D’ (> 8 m) based on work in Belize (Warner et al. 2006) and Panama (Rowan et al. 1997, Toller et al. 2001b) that all identified 8 m as being a threshold at which significant partitioning in *Symbiodinium* species richness in *M. annularis* occurred. In our dataset, 72% of populations were sampled from shallow depths, compared to 28% from deep.

Chlorophyll-a concentration

MODIS data (available at 4 km resolution) from the Aqua satellite was used to identify sites with a high chlorophyll concentration (<http://oceandata.sci.gsfc.nasa.gov/MODISA/Mapped/Daily/4km/chlor/>). Datasets of the daily concentration of chlorophyll a pigments (g m^{-3}) in the surface water were averaged for the year preceding sampling (*chla_1y*) – as well as averaging across the entire dataset (2003 – 2007) (*chla_ave*) so that the site norm could be seen (Fig. 6.2).

6.4.2.3 Salinity

Salinity data for each site (psu) were downloaded from the WODselect (online World Ocean Database 09) retrieval system – the best available compendium of *in situ* salinity and nutrient data (Table 6.1), <http://www.nodc.noaa.gov/OC5/SELECT/woaselect/woaselect.html>.

Because of the coarse resolution of the dataset (0.25°), bilinear interpolation between salinity datapoints was required when sampling sites were located too close to land. The climatological

average for each site was used (*sal_avg*), as the dataset lacked temporal resolution to explore patterns in salinity across time in more detail (Figure 6.3).

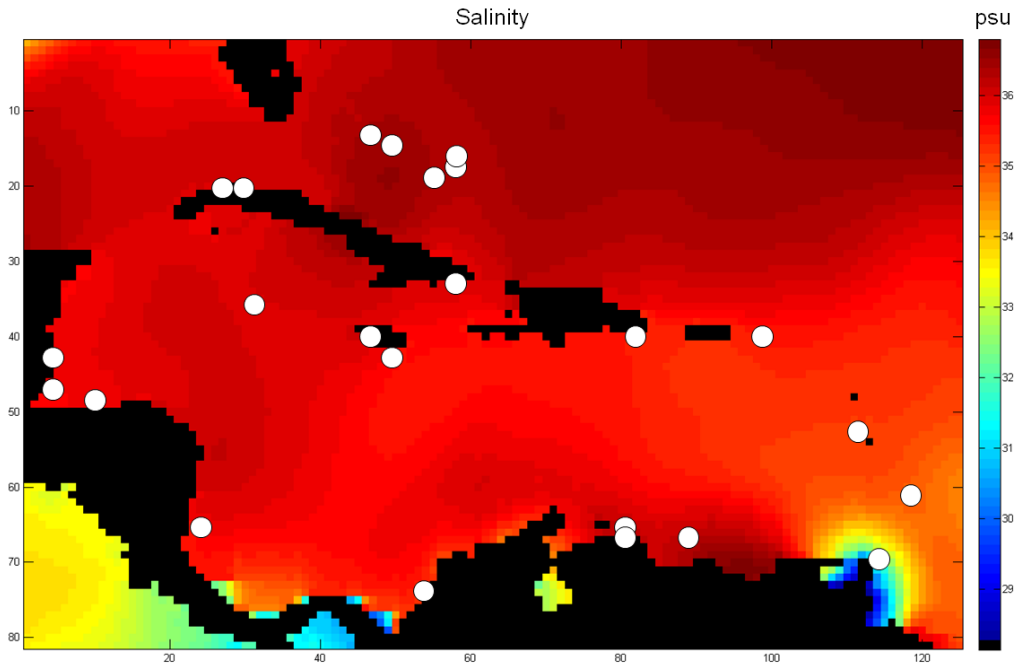


Figure 6.3: Average salinity at the sea surface, from the online world database 2009. These data were used to inform the statistical model. White circles represent sampling locations.

6.4.2.4 Nutrients

WODselect was again used to access Caribbean nutrient data, and average surface nitrate (*nit_avg*), phosphate (*pho_avg*) and silicate (*sil_avg*) concentration ($\mu\text{mol l}^{-1}$) were calculated for each site (Fig. 6.4). Mean climatological values were used because temporal and spatial resolution (1° latitude-longitude) of this dataset is fairly limited.

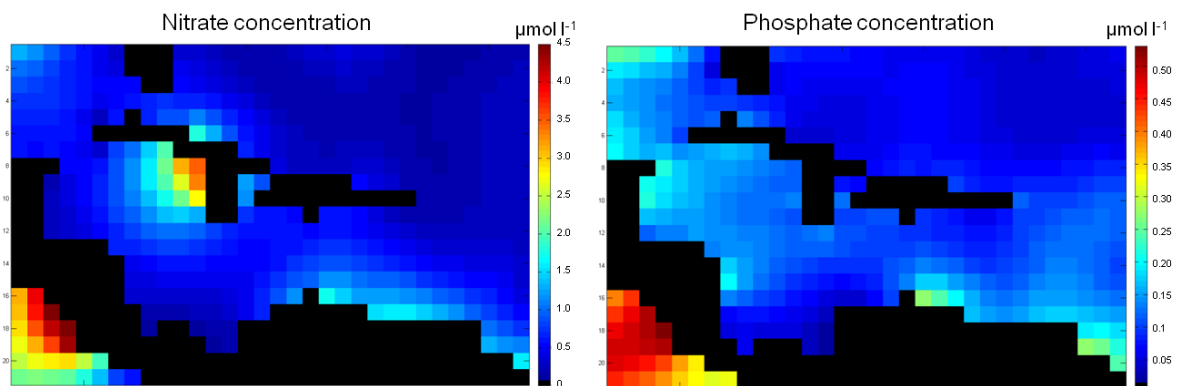


Figure 6.4: Mean inorganic nutrient concentrations of NO_3^- and PO_4^{3-} . These data were used to inform the statistical model.

6.4.2.5 Wave exposure

Wave exposure at each site was estimated from coastline data and QuickSCAT satellite wind speed and direction (Chollett et al. 2012). Waves can be attenuated not only by islands but by

reef crests that protect back areas from the direct influence of waves. In the Caribbean, this is an issue only in the Mesoamerican Barrier Reef system. Therefore wave exposure for this area was calculated using a more detailed analysis including this factor (Chollett and Mumby 2012), but incorporated into the main dataset (*wave_avg*).

6.4.2.6 Enclosure

Enclosure, (*encl*), was calculated using the reciprocal of the sum of the distance of the site to land in four (cardinal) directions, following the methodology of Garren *et al* (Garren *et al.* 2006). A low value represents greater influence by open ocean (Appendix Table 6.4).

6.4.2.7 Hurricanes

The sampling region was divided into three latitudinal bands (high, medium and low intensity) based on the average number of hurricanes to strike an area in any given year, Appendix Table 6.1 (Gardner *et al.* 2005, Foster 2007). Each reef site was then designated a hurricane score (*hurrr*), based on the total number of storms (category 1-5) recorded between 1893 and 2004 (Foster *et al.* 2013).

6.4.2.8 Coral host metrics

Six polymorphic microsatellite loci (Severance and Karl 2006), were used to describe the genetic structure of the *M. annularis* host (Foster *et al.* 2007). This involved amplification of target loci using fluorescently labelled primers in two multiplex PCR reactions. PCR product was visualised as electropherograms on a CEQ 8000 (Beckman Coulter) sequencer, and alleles were scored based on amplicon size. Identical multilocus genotypes found within some sites, with Foster *et al* (2012) showing the probability of these genotypes occurring by chance (rather than by descent) was low, suggesting they indicate clonemates. Clonal diversity for each site (*coral_D*) was calculated using the proportion of indistinguishable genotypes (N_g/N_i) (Ellstrand and Roose 1987), where N_g is the number of unique multilocus genotypes and N_i is the number of individuals sampled. This metric was used in the DISTLM linear model, along with the number of independent colonies per site, as a measure of host genotypic richness (*coral_S*), and expected heterozygosity (*coral_HE*), a measure of genetic diversity at each site based on squared allele frequencies.

6.4.2.9 Geographic distance measures

Distances between sites (km) were calculated based on geographic co-ordinates, and a distance matrix generated (Ersts Available from http://biodiversityinformatics.amnh.org/open_source/gdmg), Appendix Table 6.2. PCO1 scores from a PCO run on the distance matrix accounted for 79.4% of spatial variation between sites, were included in the multiple regression analysis as a univariate proxy for the relative proximity

of reef sites to each other. Other spatial metrics – site latitude, longitude and depth – collected at the time of sampling were considered for inclusion in the linear regression, and those that weren't used as univariate metrics to explore data.

6.4.3 Statistical methods

6.4.3.1 Data exploration

Data exploration was performed in order to select which of the 23 variables measured in this to include in the statistical multivariate model. Collinearity between covariate variables (such as between thermal stress metrics) can produce type II errors (failure to reject an untrue NH) (Zuur et al. 2010). Pair-wise scatter plots (Draftsman plots, Fig 6.5) and correlation estimates (Appendix Table 6.2) were used to compare the distributions of all environmental quantitative variables under consideration for inclusion in the model – as well as some temporal (month, year) and spatial variables (latitude, longitude, distance).

Twenty-three variables in total were included in the exercise (Fig. 6.5), allowing inspection for outliers (which can distort the results) and examination of the general distribution of the covariates, in addition to identification of colinearity. Eight collinear (>60%) covariates (longitude, latitude, sample month, average chlorophyll *chl_a_avg*, silicate *sil_avg*, host genetic richness *coral_S*, one thermal stress metric *ts_histor_4* and hurricane frequency *hurr*) were subsequently dropped from the analysis, leaving just 15 explanatory variables (Appendix Table 6.2). Latitude and longitude were both highly informative variables, correlating >45% with nine of the 20 environmental covariates between them (Appendix Table 6.2). The decision to remove latitude and longitude (rather than correlated variables) was based on attempting to explain symbiont variability at a finer resolution as possible. Due to the spatial distribution of hurricanes (occur more frequently in the north) this variable was correlated with phosphate (>60%) as well as acute, chronic and historic temperature stress (>50%) and was also removed.

DISTLM also requires covariate data with approximately symmetric distributions that are normal, with no extreme outliers (Clarke and Gorley 2006). Several of the remaining parameters did not fit these assumptions. Inspection of the draftsman plots (Fig. 6.5) enabled selection of an appropriate transformation. Acute thermal stress *ts_acute_4*, enclosure *encl* and chlorophyll parameters *chl_a_1y*, showed right-skewed distributions (Fig. 6.5), so a square root transformation was applied to *chl_a_1y* and a log ($c+y$) (required for data with many 'zeros') transform applied to *ts_acute_4* and *encl*. Since several other SST-related variables were based on DHW metrics, it seemed logical to treat them in the same way as *ts_acute_4*. A final inspection of draftsman plots based on the retained, transformed variables revealed satisfactory fitted assumptions (Appendix Fig. 6.5).

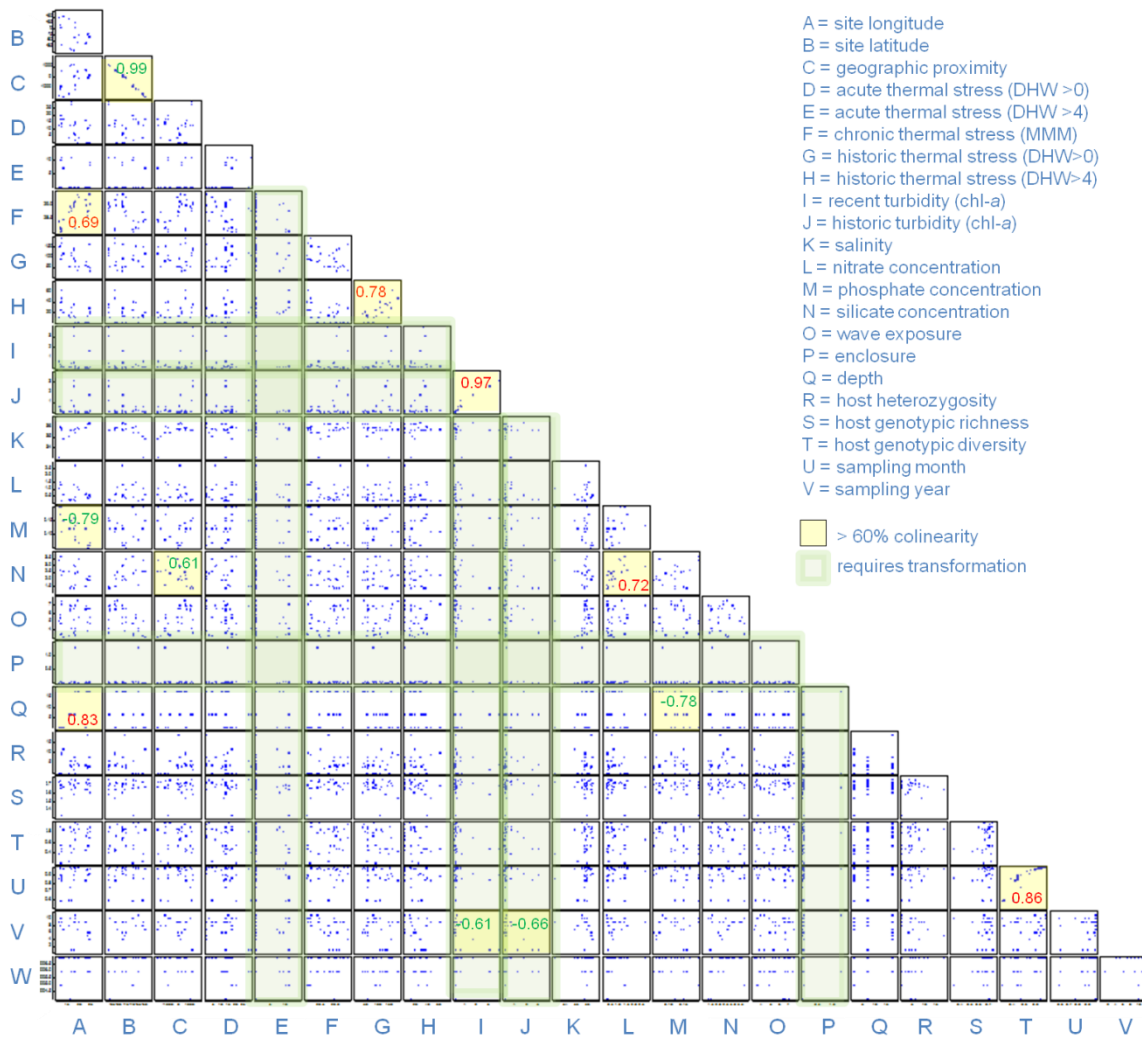


Figure 6.5. Draftsman plots of all environmental covariates. Examination of scatter plots between all covariables allowed identification of a) outliers b) data requiring transformation (in green) and c) variable collinearity (in yellow), prior to analysis. Red (positive) and green (negative) values indicate strength and direction of the correlation (see also Appendix table 6.2). Variables E, I, J and P showed skewed distributions and were subsequently transformed.

Data on symbiont abundances (i.e. dependent variables) were pooled and standardised, to give a percentage presence/absence for each site. Rare symbionts that were found only at one site were removed from the dataset, as the model can be sensitive to low abundances, although later comparisons showed that this made little difference to stability of outcomes. Prior to creating a Bray-Curtis similarity matrix for DISTLM, symbiont abundances were root transformed to down-weight the importance of heavily dominant B1. Bray-Curtis is the most appropriate similarity measure for ecological count data. From the similarity matrix generated, ordination plots could be generated to explore the data (see Chapter 5).

6.4.3.2 DISTLM multiple regressions

A distance-based linear model (DISTLM) was selected as a regression approach that can model the relationship between multivariate response variables (e.g., communities of symbionts comprising various proportions of sub-clades), as described by a resemblance matrix, and one or

more predictors (Legendre and Anderson 1999). Regression models suit quantitative and continuous data such as environmental data. Unlike most regression models p-values are obtained through permutation, avoiding the usual assumptions that errors be normally distributed. Predictor variables can be fit individually or together in specified sets.

The DISTLM regression analysis was performed using an add-on PERMANOVA+ (specifically designed for multivariate resemblance-based methods) in ecological software package PRIMER (PRIMER-E Ltd, Plymouth Marine Laboratory). A Bray-Curtis similarity matrix was generated based on resemblance measures between all sites, on the square root transformed abundance data. The model contained 15 unrelated variables (selected in 6.4.3.1), including environmental (*ts_acute_0*, *ts_acute_4*, *ts_chron*, *ts_histor_0*, *chla_avg*, *sal_avg*, *pho_avg*, *nit_avg*, *wave_avg*, *depth*, *encl*), geographic (*dist*), genetic (*coral_D*, *coral_HE*) and temporal (*year*) see Table 6.1, Appendix Table 6.4 and 6.5). Marginal tests explored the amount of variability explained by each parameter considered independently. In order to identify the combination of available predictor variables that best explained symbiont community partitioning, we employed a ‘BEST’ model selection procedure, which examines the value of the selection criterion for ALL possible combinations of the 15 variables. The ten most informative models were selected on the basis of AIC (Akaike Information Criterion) scores of model fit, which takes into account the number of predictors in each model as well as the R^2 value. Finally, in order to explicitly examine the proportion of variance attributable to environmental variables compared to the amount explained by spatial or genetic variables, predictors each were assigned to one of four indicator sets (environmental, geographic, genetic, temporal), and the analyses re-run to explain community partitioning in response to multiple sets of variables.

6.4.3.3 Additional analyses

PERMANOVA (Scales of spatial partitioning of variability at the colony level)

DISTLM analyses were performed at the level of reef site, because most environmental data, (1-4 km resolution) were available at this resolution. However, more response variables were available at the colony level. A fully hierarchical (nested) PERMANOVA (permutational multivariate analysis of variance; Anderson et al. 2008) was used to assess the hypothesis of no differences in community structure among the sites, locations and eco-regions (N=632 coral samples, p=22 symbiont types). Unlike MANOVA, PERMANOVA uses permutations, making it suitable for our symbiont count that do not comply with assumptions of normality, and for which Euclidian distance-based measures (used by MANOVA) are not appropriate (Anderson et al. 2008). Sorenson’s similarity measures were used to compare the symbiont taxa count data within each coral; it is the most appropriate resemblance measure for binary presence/absence

data as it weights variables in common higher than species absences (Kent and Coker 1992). The PERMANOVA design (type III (partial) sum of squares, permutation of residuals under a reduced model) included reef sites (33 levels) nested within locations (15) within eco-regions (6). Categorical variable ‘collector’ and ‘year’ were also included in this analysis. The test was designed and run in PRIMER, and observations were compared to expected results from over 9900 random permutations of the data.

RELATE (Relating coral host genetic distances to symbiont spatial structuring)

A RELATE statistical test, (similar to a Mantel test) was used to explore the relationship between coral host diversity and symbiont community diversity at the colony level (i.e. at a higher resolution than in the environmental linear regression model). RELATE produces a measure of how closely related the data are, with probabilities based on the number of permuted statistics greater than or equal to Rho. Two multivariate datasets for a matching set of samples: one containing pairs of genetic distance scores for the six microsatellite loci (12 allele scores, 567 individuals) belonging to the host colony (see 6.4.1.9), and one describing the presence/absence of each *Symbiodinium* sub-cladal ITS2-type for the same colony’s endosymbiont community (see 6.3.1) were compared using Spearman’s Rank correlation coefficients. This was done by first generating two resemblance matrices, using a Sorenson coefficient to generate a matrix for symbiont count data (18 variables, 567 samples) and a matrix based on pair-wise individual genetic distance (estimated in GENALEX (Peakall and Smouse 2006)) for the microsatellite allele score data (12 variables, 567 samples). Variation between elements in the first matrix were then compared to those in the second by calculating a rank correlation coefficient (Spearman’s ρ) the two, and the coefficient value compared to 9999 permutations of matrix data (significance level of sample statistic: 0.01%), using PRIMER.

RELATE was additionally used to explore the relationship between geographic distance between sites (6.4.1.9), and symbiont community composition.

6.5 Results

6.5.1 DISTLM analyses

Only three of the 15 explanatory covariates included in the multiple regression model were able to explain variation in symbiont community when unaccompanied by other variables in marginal tests (Table 6.2). Chronic temperature stress (*ts_chron*) was the best predictor, explaining 19% of the community variability (pseudo-F=7.25, $p < 0.001$). Geographic distance (*dist*, pseudo-F=5.89, $p < 0.001$) and phosphate concentration (*pho_avg*, pseudo-F=3.54,

Model type	AIC score	R ²	RSS	No. of variables	Variables included
Best overall model	230.83	0.54	26347	7	dist, ts_acute_0, ts_chron, chla_ave, nit_ave, pho_ave, year
One term model	236.61	0.19	45927	1	ts_chron
Two term model	234.89	0.28	40891	2	ts_acute_0, ts_chron
Three term model	233.37	0.36	36627	3	ts_acute_0, ts_chron, pho_ave
Four term model	232.33	0.42	33305	4	ts_acute_0, ts_chron, chla_ave, pho_ave
Five term model	231.59	0.46	30576	5	dist, ts_acute_0, ts_chron, chla_ave, pho_ave
Six term model	231.62	0.50	28750	6	dist, ts_acute_0, ts_chron, chla_ave, nit_ave, pho_ave
Seven term model	230.83	0.54	26347	7	dist, ts_acute_0, ts_chron, chla_ave, nit_ave, pho_ave, year
Eight term model	231.13	0.56	24988	8	dist, ts_acute_0, ts_chron, chla_ave, nit_ave, pho_ave, depth, year
Nine term model	231.61	0.58	23826	9	dist, ts_acute_0, ts_chron, ts_histor_0, chla_ave, nit_ave, pho_ave, depth, year
Ten term model	232.52	0.60	23028	10	dist, ts_acute_0, ts_chron, ts_histor_0, chla_ave, nit_ave, pho_ave, encl, depth, year

Table 6.3: Summary of DISTLM population-scale outputs. Includes the best identified explanation of *Symbiodinium* community variance, and best result for each number of variables (only 1-10 variables shown). AIC = score of model fit (selection criterion), R² = coefficient of determination (% variance explained), RSS= residual sum of squares.

Variable	SS(trace)	Pseudo-F	P	Prop.
dist	9356	5.89	0.0009	0.16
ts_acute_0	1358.7	0.73	0.5744	<0.1
ts_acute_4	2311.1	1.27	0.2703	<0.1
ts_chron	11106	7.25	0.0001	0.19
ts_histor_0	3996	2.26	0.0651	<0.1
chla_avg	3821.6	2.15	0.0775	<0.1
sal_avg	2846.7	1.58	0.1655	<0.1
nit_avg	3118.5	1.74	0.1336	<0.1
pho_avg	6028.3	3.55	0.0114	0.11
wave_avg	2783.7	1.54	0.1873	<0.1
encl	2302.5	1.26	0.1773	<0.1
depth	3353.7	1.87	0.1147	<0.1
coral_HE	647.59	0.34	0.8978	<0.1
coral_D	526.72	0.28	0.9168	<0.1
year	1402.2	0.76	0.5588	<0.1

Table 6.2: Summary of DISTLM population-scale marginal tests, examining the relationship between *Symbiodinium* communities and explanatory covariates. Significant variables highlighted in blue. 'SS' = sums of squared deviations (partitioning of variance), Pseudo-F = test statistic, P(permutation)=interpretation of test stat (p-value). 'Prop' = proportion of variance explained by model term. Residual df=30).

p=0.011) were also identified as predictors. They were able to explain 16% and 10% of symbiont community variation respectively.

In the multiple regression analyses, the single best combination of predictors identified by the BEST algorithm (based on AIC scores), contained seven variables (*dist*, *ts_acute_0*, *ts_chron*, *chla_ave*, *nit_ave*, *pho_ave*, *year*) and explained 53% of the variation (Table 6.3). Each of the ten best models selected contained between 5 and 9 variables, with the average model comprising > 7 explanatory variables, explaining 46 - 58% of variance. The high number of variables included in each of these selected explanatory model indicates the complex nature of symbiont community partitioning. SST metric *ts_chron* was consistently selected as an informative variable, occurring in every one of the best models selected for each of an increasing number of terms, from 1 to 10 terms (Table 6.5). None of the best fit models contained the variables *ts_acute_4*, *sal_avg*, *coral_D*, *coral_HE* or *wave_avg*.

6.5.1.1 Environmental vs genetic vs geographic variation

For regression models with variables fitted in specified sets, marginal tests revealed that only groups of geographic (pseudo-F=3.66, p<0.001) and environmental (pseudo-F=2.34, p<0.001) factors could significantly explain variation. Environmental factors were more informative than geographic, explaining 53%. This compared to just 20% of variation accounted for by geographic distance measures (Table 6.4). Host genetic factors and temporal factors were not

Group	SS(trace)	Pseudo-F	P	Prop.	res.df	regr.df
Temporal	1402.2	0.76	0.5557	<0.1	30	2
Geographic	11492	3.66	0.0012	0.20	29	3
Environmental	29980	2.34	0.0011	0.53	21	11
Genetic	1173.7	0.30	0.9791	<0.1	29	3

Table 6.4: Summary of DISTLM population-scale marginal test outputs, examining the relationship between *Symbiodinium* communities and four sets of explanatory covariates. Significant sets highlighted in blue.

able to adequately explain any variation when considered independently. The best model identified for the variable sets explained contained a combination of environmental, geographic and temporal factors (i.e. year), and explained 63% of the variation (AIC score=235.63, RSS=21042). The set containing variables associated with host genetics was not included as a factor in any of the ten best models identified by the BEST algorithm, indicating the redundancy of this variable set.

6.5.2 Additional analyses

6.5.2.1 PERMANOVA

Source	df	SS	MS	Pseudo-F	P (perm)	Unique perms	% variation explained
Eco-region	5	2.70×10^5	53983	1.184	0.369	9924	11.2
Location(Eco-region)	9	3.27×10^5	36356	0.923	0.160	9926	<0.1
Site(Location(Eco-region))	18	3.10×10^5	17241	18.367	0.001	9856	28.9
Collector(Location(Eco-region))	1	2.66×10^3	2662	2.836	0.123	9994	30.3
Residual	598	5.61×10^5	938				30.6
Total	631	1.65×10^6					

Table 6.5: Summary of population-scale analyses for model selection to examine the relationship between *Symbiodinium* communities and environmental variables. 'df' = degrees of freedom, 'SS' = sums of squared deviations (partitioning of variance) per degree of freedom, 'MS' = mean squares, Pseudo-F = test statistic, P(perm)=interpretation of test stat (p-value), % variation explained was interpreted from square root of estimates of components of variation.

Results for the fully hierarchical (nested) PERMANOVA design (used to investigate spatial variability of *M. annularis* symbiont communities at the individual level) showed significant variability at the level of site (pseudo-F=18.37, p=0.0001, Table 6.3). Neither location, nor ecoregion had a significant effect (p>0.05). Collector was also shown to be non-informative (p=0.123). The model compared composition of *Symbiodinium* communities in terms of presence of absence of 22 different ITS2-types, in 632 coral samples.

6.5.2.2 RELATE (exploring host diversity)

Five-hundred and eighty-eight of the 632 individual *M. annularis* coral colonies whose symbiont communities were analysed were also successfully genotyped (Foster 2007), covering 32 of the 33 sites (Columbia site CM had missing microsatellite data). Three-hundred and

ninety-seven individual multi-locus genotypes (genets) were identified. Of these, 86 genets occurred in more than one sample, and in three cases, identical genets occurred in > 10 sampled colonies. Identical genotypes were only shared within sites, never between sites. No significant association was detected by a regression analysis (with CM, DM and R removed from the analysis due to insufficient data) which compared symbiont richness with host genotypic richness ($F=0.65$, $R^2=0.023$, $p=0.322$ $df=29$).

Contrasting levels of host clonality were observed within each reef site; the Cayman Islands (X) displayed the greatest diversity, with 22 out of 23 samples having unique genotypes (Table 6.6). Regionally, greatest genotypic richness was found in the Bahamas; the poorest area in terms of symbiont diversity. Meanwhile the poorest genotypic richness was found in the Southern and Eastern Caribbean -in TB (Tobago), Z (Curaçao) and DM (Dominica) >80% of colonies shared genotype with at least one other sample - although these spatial patterns were shown to be non-significant. Only at three sites (CM, DR and R) were no identical genotypes found – but this is likely because <5 samples were successfully genotyped at these sites.

Of the 86 host identical multilocus genotypes that were found on multiple occasions, just over half (58%) of genotypes were found to be dominated by the same ITS2 symbiont (or pair of symbionts) in all occurrences of the clone. In most cases, this was two or three samples, but at Cuban site CA, nine identical clonemates were all found to harbour the same B10/B1 mix. However, this occurred at a site where B10/B1 was the only types hosted by any coral. In a further 42% of cases, more than two different symbiont communities inhabited identical clonemates, with 4% showing at least three different dominant symbionts. One clone in Curaçao was found hosting either B1, C7, C12 or a B1/C7 co-dominant mix.

Spatial Analyses for Distance Indices (SADIE) analysis showed no overall spatial patterns in the distribution of host clonality across the Caribbean ($I_a=1.042$, $P_a=0.37$); although cluster analysis revealed Bahamian sites CI, EN, N and P to have a greater than expected level of clonal diversity, while Nicaraguan site NB, and Belizean sites D and E were identified as having a low level – in all three of these sites 50% of sampled hosts shared identical multilocus genotypes with at least one other type. These patterns of distribution agree with the findings of Foster et al (2013), who showed sites in Belize and Curaçao to be genetically depauperate.

A RELATE non-parametric comparison of a haplotype genetic distance matrix (generated by GENALEX (Peakall and Smouse 2006)) with our geographic distance matrix (based on site lat-long values) displayed a weak (Spearman's $\rho=0.17$) but significant ($p=0.007$) correlation.

The RELATE analysis generated a Spearman's ρ of -0.12 to describe the relationship between the symbiont community similarity (i.e. presence/absence of 18 different symbiont taxa) and host genetic distance matrices (Fig. 6.13). GENALEX genetic distances produce a score of '0'

Region	Location	Reef site	Identifier	Sample number	No. unique genets	Genotypic diversity	% samples with clonemates	Identical genotypes	Max clonemates	Simpsons Diversity
Mesoamerican Barrier Reef	Honduras	Seaquest	A	23	21	0.91	26%	3	2	0.99
	Honduras	Sandy Bay	B	22	20	0.91	18%	2	2	0.99
	Honduras	Western Wall	C	22	12	0.55	50%	1	11	0.76
	Belize	Coral Gardens	D	22	11	0.50	68%	4	5	0.90
	Belize	Eagle Ray	E	16	8	0.50	75%	4	6	0.85
	Belize	Long Cay	G	17	14	0.82	35%	3	2	0.98
	Belize	West Reef	H	14	6	0.43	64%	1	9	0.60
The Bahamas	Bahamas	Conception Island	CI	16	14	0.88	25%	2	2	0.98
	Bahamas	Exumas North	EN	24	17	0.71	38%	2	7	0.92
	Bahamas	Seahorse Reef	K	22	12	0.55	64%	4	6	0.90
	Bahamas	Snapshot Reef	L	16	13	0.81	31%	2	3	0.97
	Bahamas	School House Reef	N	23	19	0.83	30%	3	3	0.98
	Bahamas	Propeller Reef	P	23	21	0.91	22%	2	3	0.98
	Nicaragua	White Hole	NA	16	7	0.44	75%	3	5	0.84
Southern Caribbean	Nicaragua	Chavo	NB	22	11	0.50	68%	4	6	0.89
	Columbia	Palo 1	CM	11	n/a	n/a	0%	n/a	n/a	n/a
	Cuba	Baracoa	CA	24	11	0.46	71%	4	9	0.84
Greater Antilles	Cuba	Bacunayagua	CB	23	17	0.74	43%	4	3	0.97
	Cuba	Siboney	CC	24	21	0.88	25%	3	2	0.99
	Cayman	Rum Point	X	23	22	0.96	9%	1	2	0.99
	Dominican Rep.	Bayahibe	DR	5	5	1.00	0%	0	0	1.00
	Jamaica	Drunkenmans Cay	JA	18	12	0.67	61%	5	3	0.95
	Jamaica	Dairy Bull	JB	21	18	0.86	29%	3	2	0.99
	Barbados	Victor's Reef	BA	14	12	0.86	14%	2	2	0.98
Lesser Antilles	BVI	Ginger Island	R	2	2	1.00	0%	0	0	1.00
	BVI	Beef Island	T	16	13	0.81	38%	3	2	0.98
	Curaçao	Snakebay	SB	16	9	0.56	69%	4	4	0.91
	Curaçao	Vaersenbay	VB	16	8	0.50	69%	3	5	0.87
	Curaçao	Buoy 1	Z	18	4	0.22	94%	3	11	0.59
	Dominica	Grande Savane	DM	19	5	0.26	95%	4	12	0.60
	Tobago	Buccoo Reef	TB	23	9	0.39	83%	5	7	0.86
	Venezuela	Cayo de Agua	AV	13	12	0.92	31%	2	2	0.99
	Venezuela	Dos Mosquises	BV	12	11	0.92	17%	1	2	0.98

Table 6.6. Host genotype data by site

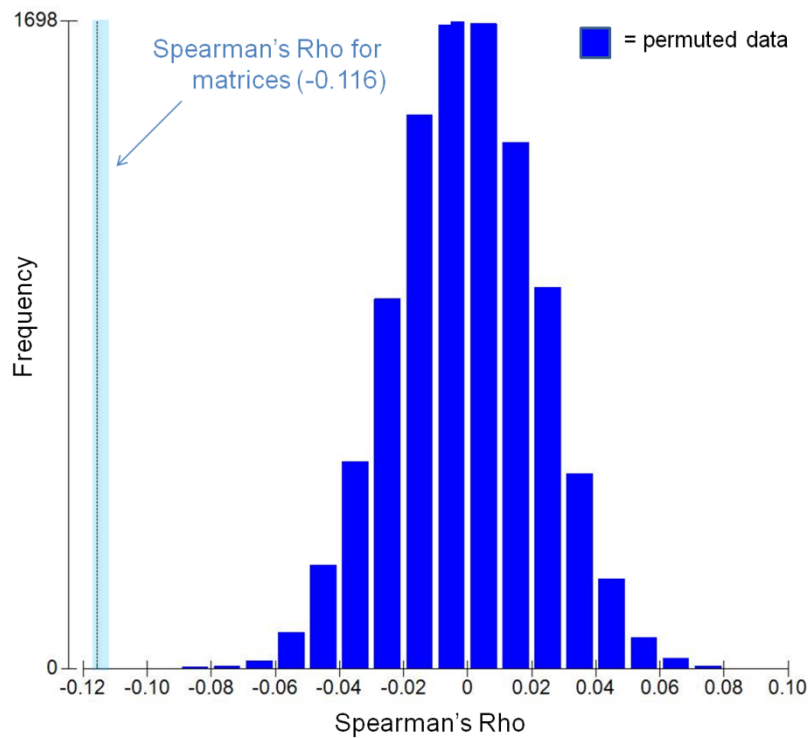


Figure 6.6: RELATE output, showing the significant ($p < 0.001$, as p sits outside the distribution of random permutations) Spearman's ρ value (-0.12) generated for genetic and geographic matrix comparisons (for resemblance matrices for 567 *M. annularis* colonies) compared with 9999 permutations (plotted in blue). This indicates host genetics of a colony is correlated (12%) with symbiont diversity.

for identical genotypes, while Sorensens similarity generates a score of '100' for identical community composition, meaning that the negative ρ can be interpreted as a positive relationship between host genetic and symbiont community similarity. Although the correlation was small, the p value was shown to be significant ($p < 0.001$) at the 0.01% level, with none of the 9999 permutations under the null hypothesis exceeding the threshold value.

Re-running the RELATE analysis using different measures of symbiont community (e.g., dominant symbiont types, clade level) produced comparable results.

The RELATE analysis produced a positive correlation of 0.244 between geographic distance matrices and Bray-Curtis symbiont community composition resemblance matrices (6.4.3.2). This was highly significant ($p = 0.0002$), with only two permuted ρ values generating greater correlations, out of 9999 permutations (Fig. 6.6).

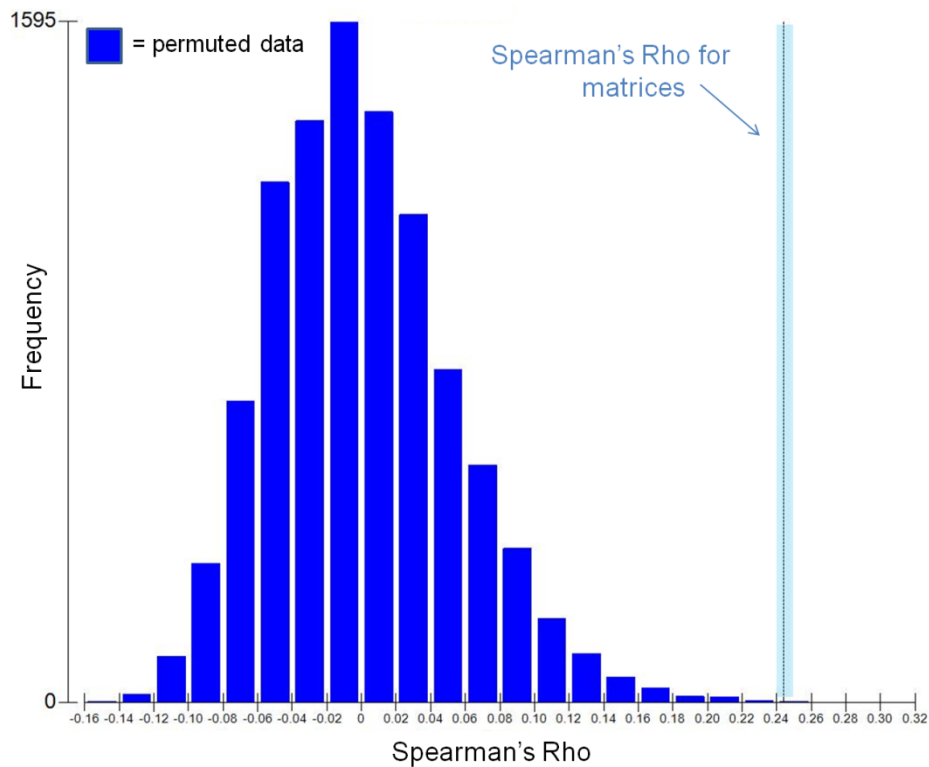


Figure 6.7: RELATE output, showing the significant Spearman's ρ value generated for matrix comparisons (for distance and community resemblance matrices for 33 Caribbean sites) compared with 9999 permutations

6.6 Discussion

In this chapter, geographic distance has been shown to play a significant role in partitioning of *Symbiodinium* community variation at the colony level in *M. annularis* (Fig. 6.7). At the population level, distance remained important in explaining symbiont variation in a single regression (explaining 16% community variability, Table 6.2). Geographic distance was selected as a variable in the best fit regression model (alongside environmental parameters explaining 53% of variability), and was frequently included as a predictor in the suite of models generated by DISTLIM (Table 6.3). Although not as able to explain as much diversity as environmental variables, combined, distance parameters were able to account for 20% of variability, and were more important than host genetic or temporal variability (Table 6.4).

Host genotype was considerably less informative in explaining variation in symbiont community: there was no clear relationship between genetic diversity of the coral and the richness of its symbiont community, although a weak but significant association was shown to exist between genetic distance and community similarity at the individual level (Fig. 6.6). At the population level, variables associated with the host (i.e., expected heterozygosity `coral_HE`, clonal diversity `coral_D`) were not able to explain symbiont community diversity in marginal tests (Table 6.2). In addition, they were not selected as useful predictors in the DISTLM multiple regression models (Table 6.3), and remained non-significant in explaining symbiont

diversity when combined (Table 6.4). On this basis, it seems feasible that the correlation observed at the individual level may be a coincident effect driven by common underlying environmental/geographical variation.

Finally, two environmental parameters: chronic temperature stress (*ts_chron*) and phosphate concentration (*pho_avg*) were identified as being important drivers in terms of the *Symbiodinium* community variability at the population level. In marginal regression tests (Table 6.2), these parameters explained 19% and 11% of variation respectively. A strong association ($F=12.87$, $R^2=0.30$, $p=0.0011$) was observed between the proportion of colonies hosting *Symbiodinium* clade C at each site, and the long term temperature maxima recorded for that site (Fig. 6.10). It is this relationship with chronic temperature stress – a metric correlates positively with latitude (Fig. 6.5) – that we hypothesise may provide the main driving force behind the observed patterns of symbiont diversity and distribution (Chapter 5).

Geographic distance and environmental factors (long term thermal stress and phosphate concentrations) clearly have an influential role to play in determining *Symbiodinium* communities across the Caribbean, allowing us to reject our null hypothesis, NH (section 6.2). We can also reject hypothesis H₃, as host genetics – although significant – clearly are not the main driver of patterns of symbiont biogeography. Despite this, our *M. annularis* symbiont communities were shown to display a substantial variability - particularly at intra-site level – that the environmental, genetic and geographic parameters tested were unable to adequately explain, and further work should aim to explore this.

6.6.1 Partitioning of symbiont communities by geographic distance

Significant effect of site groupings, determined by the hierarchical PERMANOVA, supported the findings of Chapter 5 that used SADIE analyses to explore spatial patterning. In this chapter we found that variability between individual colonies was large (31%) - and comparable to that between sites (29%) (Table 6.5) – but at larger scales location (scale: 100's kms) eco-region (scale: 1000's of km's) were less able to explain community diversity. High variability between symbiont communities within a coral species has also been observed in a Hawaiian coral species, where the majority of the variability partitioned at colony level (~80%), some at site level (~20%) and none at wider spatial scales (Stat et al. 2011). In a study into the population genetics of *Symbiodinium* B1 in *M. annularis* across the Bahamas and Florida, it was found that regional differences explained 40% of observed variation, site differences 47% and colony differences 14% (Thornhill et al. 2009). These findings were comparable to the results of this study, given that their 'region' level was similar to this study's 'location' level. However, in this study higher estimates of variability explained at small spatial scales (e.g. 31% vs 14%), and lower values at bigger spatial scales (29% vs 47%) suggest geographic distance is *less* important in structuring communities as it is populations of *Symbiodinium*. The authors suggested, given

multiple strands of evidence both in the Caribbean (Santos et al. 2003b, Kirk et al. 2009) and Pacific (Howells et al. 2009) that a potentially ubiquitous feature of *Symbiodinium* populations is high levels of structure over spatial distances as small as 10's of km (Oliver and Palumbi 2009). We suggest this statement may also hold true, but perhaps to a lesser extent, at the *Symbiodinium* community level.

Another finding of the PERMANOVA was that of no significant effect of 'collector' (10 levels) on symbiont biogeography ($p=0.123$, Table 6.5), providing confidence that observer bias did not affect the results of this study. Despite being non-significant, collector did correlate with community, and potentially explained 30% of variation. This could be explained by the fact that collector was closely linked to location (with collectors often sampling within a country) and eco-region, as researchers concentrated on sets of sites in their jurisdiction.

The direct RELATE comparison of geographic distance data and Bray-Curtis community resemblance measures at the population level revealed a positive correlation of 0.24 (Fig. 5.6). This recorded association between distance and *Symbiodinium* community further emphasises the importance of geographic distance in structuring communities.

6.6.2 Environmental partitioning of symbiont communities

Environmental factors combined explained >50% of variation in symbiont biogeography (53%; Table 6.4), leaving us unable to satisfactorily reject hypothesis H_2 (section 6.2). The fact that the best DISTLM models incorporated 7-9 different explanatory factors (Table 6.3) demonstrates the complex and multi-faceted nature of the environmental drivers of symbiont biogeography. Although *ts_chron* and *pho_avg* were both identified as important drivers (Table 6.2), it appears likely that biogeographic symbiont patterns observed were determined by a combination of contributing environmental factors (Table 6.3). Disentangling the relative effects of the environment is difficult using these modelling approaches, and ideally would require experimental work. One metric that encompassed a range of environmental variables was latitude (correlates with multiple factors, Fig. 6.5). Plotting symbiont diversity for each site against latitude revealed a negative linear correlation ($F=13.8$, $R^2=0.31$, $p=0.001$, Fig. 6.8), with northern sites (e.g. the Bahamas) having less diversity (nb/ longitude explained less diversity; $F=4.52$, $R^2=0.13$, $p=0.042$). Symbiont partitioning correlating with latitude (Fig. 6.8) are likely driven by a combination of environmental factors.

6.6.2.1 Thermal stress

Chronic thermal stress was the single most informative environmental covariate identified, accounting for 19% of observed variation in *M. annularis* symbiont communities (Table 6.2). It was included as a predictor in all multiple regression models, explaining up to 60% of variation

when combined with other covariates (Table 6.3). Other temperature metrics, namely *ts_acute_0*, but also *ts_historic_0*, were also frequently included in multiple regression models. Although unable to explain symbiont diversity on its own, when combined with *ts_chron*, *ts_acute_0* was able to explain 45% of diversity and these SST-related parameters produced the best fit two-variable model. This temperature-related finding is directly comparable to the finding of a study into variability of symbiont associations with *Acropora millepora* on the GBR (Cooper et al. 2011). Here the authors, investigating diversity at a similar regional scale (1400 km), were able to explain an equivalent 51.3% of their observed community diversity, with ‘long term’ (nine-year average) SSTs explaining 10.8% of variation, and summer SST and SST anomalies explaining a further 6.9 and 5.4% respectively.

The acute temperature stress (*ts_acute_4*) variable was unable to explain community biogeography, perhaps because only eight of the 33 sites had experienced $DHW > 4$ (three from Curaçao (Z, SB, VB, all sites experience > 10 DHWs), one from Barbados (DHW=7), two Bahamian sites (N and P), a Belizeian site (H) and a Nicaraguan site (NB)). There was no apparent spatial patterning with no differences between eco-regions (ANOVA, $F=1.63$, $df=5$, $p < 0.189$).

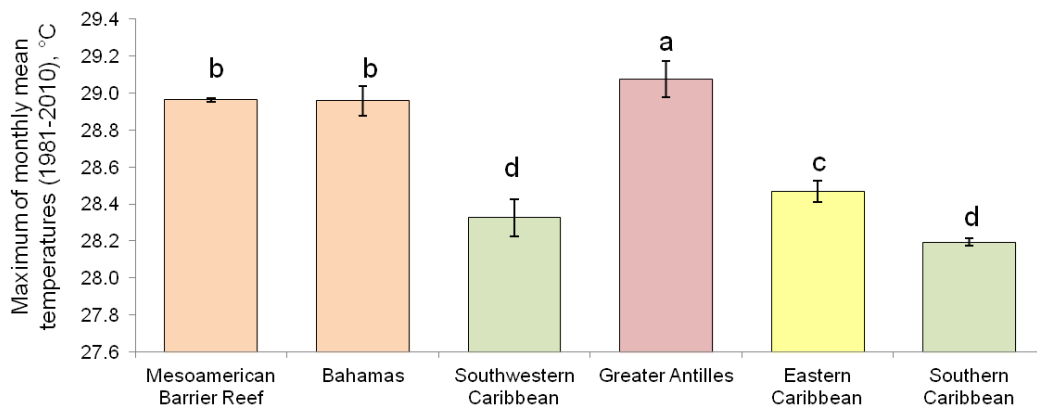


Figure 6.9: Maximum monthly mean SST (°C) by Caribbean eco-region. Post-hoc Tukey's HSD scores reveal four significantly different groupings based on MMM temperature (a,b,c,d)

SSTs are one of the major characteristics differentiating Caribbean high latitude cooler regions from the generally warmer central and south west (Chollett et al. 2012) (Fig. 6.9). In Chapter 5, symbiont sub-clade distributions were frequently shown to be concentrated in either the northwest or south east. For example, *Symbiodinium* B1j and C12 commonly populated *M. annularis* at Lesser Antilles sites, while B10 was limited in range to northern Cuba and the Bahamas (e.g. Fig. 4.13). However, chronic temperature stress (an indicator of routine ambient summer temperature) varies significantly with latitude and is clearly lower around the southern Venezuelan and Curaçao sites, and eastern Lesser Antilles (Fig. 6.1, 6.9). The influential role of long-term temperature in determining symbiont distribution in *M. annularis* might be

considered intuitive, as *Symbiodinium* are known to be temperature sensitive, and a range of temperature tolerances have been recorded in different taxa (see Chapter 7). However, although temperature/irradiance has been shown to effect symbiont communities at local scales, very little evidence (besides Cooper et al. 2011) exists to directly demonstrate the role of temperature in driving wider biogeographic patterns. The few large-scale spatial studies simply linked symbiont community variability to latitudinal and onshore-offshore gradients (Rodríguez-Lanetty et al. 2001, LaJeunesse et al. 2004a, LaJeunesse et al. 2010).

6.6.2.2 Nutrient concentrations

The identification of phosphate concentration as a driver of symbiont variation agrees with studies in the Caribbean and GBR that identified water quality factors (including nutrient concentrations) as being important drivers of symbiont community partitioning (Garren et al. 2006, Cooper et al. 2011). All reef sites had $<2.0 \mu\text{mol l}^{-1}$ phosphate, with the eastern Caribbean countries (Curaçao, Venezuelan and Tobago) having greater than average concentrations, and Bahamian sites experiencing low values (<0.07). More detailed exploration of symbiont community variables revealed that clade B symbionts appeared to loosely drive this relationship, with sub-clade B1j showing the strongest association with phosphate concentration (F=6.86, df=1, $R^2=0.19$, $p=0.013$): this type was found in greater abundance in southerly Caribbean sites where phosphate levels were higher, suggesting this algae is nutrient limited. Phosphates are known to inhibit calcification in corals, with experiments showing that enrichment ($>2 \mu\text{mol l}^{-1}$) inhibited reef growth by 43% on the GBR (Kinsey and Davis 1979), while organic phosphates also caused a 36% inhibition of calcification in *Stylophora pistillata* at $10 \mu\text{m}$, (Yamashiro, 1995). Zooxanthellae are thought to remove phosphate that inhibits calcification (Simkiss, 1964) and addition of phosphate *with* nitrate can boost zooxanthalle numbers (Muscatine et al 1989).

Nitrate, although not informative on its own, was included in the best DISTLM model. Nitrates were highest at Jamaican site JA ($2.75 \mu\text{mol l}^{-1}$), with Southern Caribbean locations (Curaçao, Venezuela, and Tobago) consistently having high nitrate levels ($>1.0 \mu\text{mol l}^{-1}$). All other sites had $< 1.0 \mu\text{mol l}^{-1}$ with the exceptions of all sites in Cuba ($1.04 \mu\text{mol l}^{-1}$), Cayman ($1.19 \mu\text{mol l}^{-1}$) and JB in Jamaica ($1.36 \mu\text{mol l}^{-1}$).

6.6.2.3 Other environmental factors

Chlorophyll-*a* was consistently used in the best explanatory models, agreeing with studies that identified turbidity/water quality as important drivers of symbiont variability. Sites D and E in Belize had higher chlorophyll content than other sites (3.94 and 3.15 mg m^{-3} , respectively – Caribbean-wide average 0.46 mg m^{-3}) in the year preceding sampling, with Exhumas North (1.67 mg m^{-3}) the next highest and several other sites (G, JB, TB and VB) falling above average.

The factor `chl_a_1y` was repeatedly identified as important in determining symbiont diversity, and it may be that clade B is associated with greater turbidity/lower irradiance. This may help explain the observation that *M. annularis* in Mexico have shown increased calcification rates along a gradient of turbidity, with both skeletal density and calcification declining with increased turbidity (Carricart-Ganivet and Merino 2001).

Salinity and wave exposure were rarely identified as good predictors. Wave exposure varied between sites, with the minimum at our Barbados site, and the maximum measured at Rum Point in Grand Cayman (Cayman Isles). All Bahamian reef sites experienced above average salinity (>36.3 psu), while eastern Caribbean sites Barbados, Tobago and Dominica all had low salinity (<35.3 psu). Salinity (`sal_avg`) was rarely identified as an important factor.

Bathymetry generates substantial partitioning in endosymbiont community composition (Rowan and Knowlton 1995) and diversity (Warner et al. 2006) in *M. annularis*, with colonies inhabiting deeper habitats hosting less diverse communities that tend to be dominated by clade C (Rowan et al. 1997, Toller et al. 2001b). Although more colonies hosted C at deep sites (45% compared to 35% in shallow sites), the depth effect was found to be non-significant in this instance. Neither could significant differences be detected in the symbiont diversity, richness of other aspects of the community collected from deep or shallow sites. This may be due to successful standardisation during collection, overlapping boundaries of symbiont zonation (Rowan et al. 1997), differences in depth zonation of communities on different reefs, or the fact that the mean depth of the site recorded did not accurately reflect the within-site variability of collection depths for individual colonies.

6.6.2.4 Latitude

Latitude was able to explain 31% of variation in symbiont diversity (Fig. 6.8) complying with the fundamental ecological hypothesis of a global latitudinal gradient in biodiversity with more species found towards the tropics (MacArthur and MacArthur 1961, Brown et al. 2004). Other Caribbean studies have recorded differential diversity of *Symbiodinium* ITS2 types in the north and south. A 2002 study comparing Bahamian and Mexican *Symbiodinium* diversity attributed the observed differential to sampling effort (LaJeunesse 2002), while a comparison of *M. annularis* endosymbiont communities in Belize and Panama found a greater diversity and evenness in the southerly Panamanian samples (Garren et al. 2006). However, in both studies, comparison of just two data points meant that this pattern could not be confidently attributed to a Caribbean latitudinal gradient. Stronger evidence for latitudinal gradients have been observed across 2500 km in north-east Australia (where *Plesiastrea versipora* inhabiting high latitude sites hosted *Symbiodinium* 18S rDNA B clades, and those in low latitude sites hosted more C) (Rodriguez-Lanetty et al. 2001), and in *Symbiodinium* C diversity in a range of host species

along the GBR (LaJeunesse et al. 2004b). At a finer genetic resolution, population diversity within the sub-clade B1 hosted by the sea fan *G. ventalina* was shown to negatively correlate with latitude across the Caribbean ($R^2=0.18$) (Andras et al. 2011). It appears an inherent latitude-related pattern in host-symbiont partnerships across coral communities may exist (LaJeunesse and Trench 2000, Loh et al. 2001, Rodriguez-Lanetty et al. 2001), although it should be noted that these patterns exist only in corals that acquire their endosymbionts from the environment (LaJeunesse et al. 2004b). An explanation for the existence of this latitudinal gradient could be multi-factorial: either driven by spatial heterogeneity in the physical environment (e.g. temperature), climatic stability at lower latitudes (related to the stability of primary production); because of host-specificity (although apparently not in *M. annularis*, see 6.5.3); a gradient in availability of *Symbiodinium*, bleaching history at the site or some phylogeographic phenomena.

6.6.2.5 Clade C

Further exploration into the nature of the relationship between long-term temperature stress and endosymbiont community variability, revealed a negative correlation with the proportion of *M. annularis* colonies hosting clade C and site long-term SST maxima (Fig. 6.10). Further analysis additionally identified sub-clade C7 in being particularly highly negatively correlated with `ts_chron` ($F=13.84$, $R^2=0.42$, $p<0.001$), likely driving this relationship. Distributions of thermally tolerant symbionts have previously been associated with high temperature habitats (Oliver and Palumbi 2011) but clade C types are often reported as generalists, though considered intolerant to high irradiance. The results presented here provide important evidence for acclimation of this clade to cooler summer temperatures, as *M. annularis* acclimated to cooler conditions fare worse under stress (Castillo and Helmuth 2005). An alternative explanation for the difference in C distribution between east and west Caribbean are that distributions are determined by radiations during the Pleistocene (Finney et al. 2010) and perhaps maintained by geographic barriers (such as the Mona passage). However, the fact that many clade B symbionts (in particular B1) were detected across the entire Caribbean range suggests that this hypothesis may not be plausible. Clade C may be more restricted in its distribution by thermal sensitivity than B clades when hosted by *M. annularis*. Latitudinal partitioning in the distribution of clade C types has been identified previously, between central and southern regions of the GBR (LaJeunesse et al. 2004b). The partitioning of C according to temperature may explain the observed relationship between latitude and diversity, as clade C is known to host the greatest diversity (LaJeunesse 2005).

6.6.3 Symbiont partitioning among coral hosts

Results of the RELATE analysis suggest a very weak but significant association between *M. annularis* genotype and its symbiont community. Although a real association clearly exists (Fig.

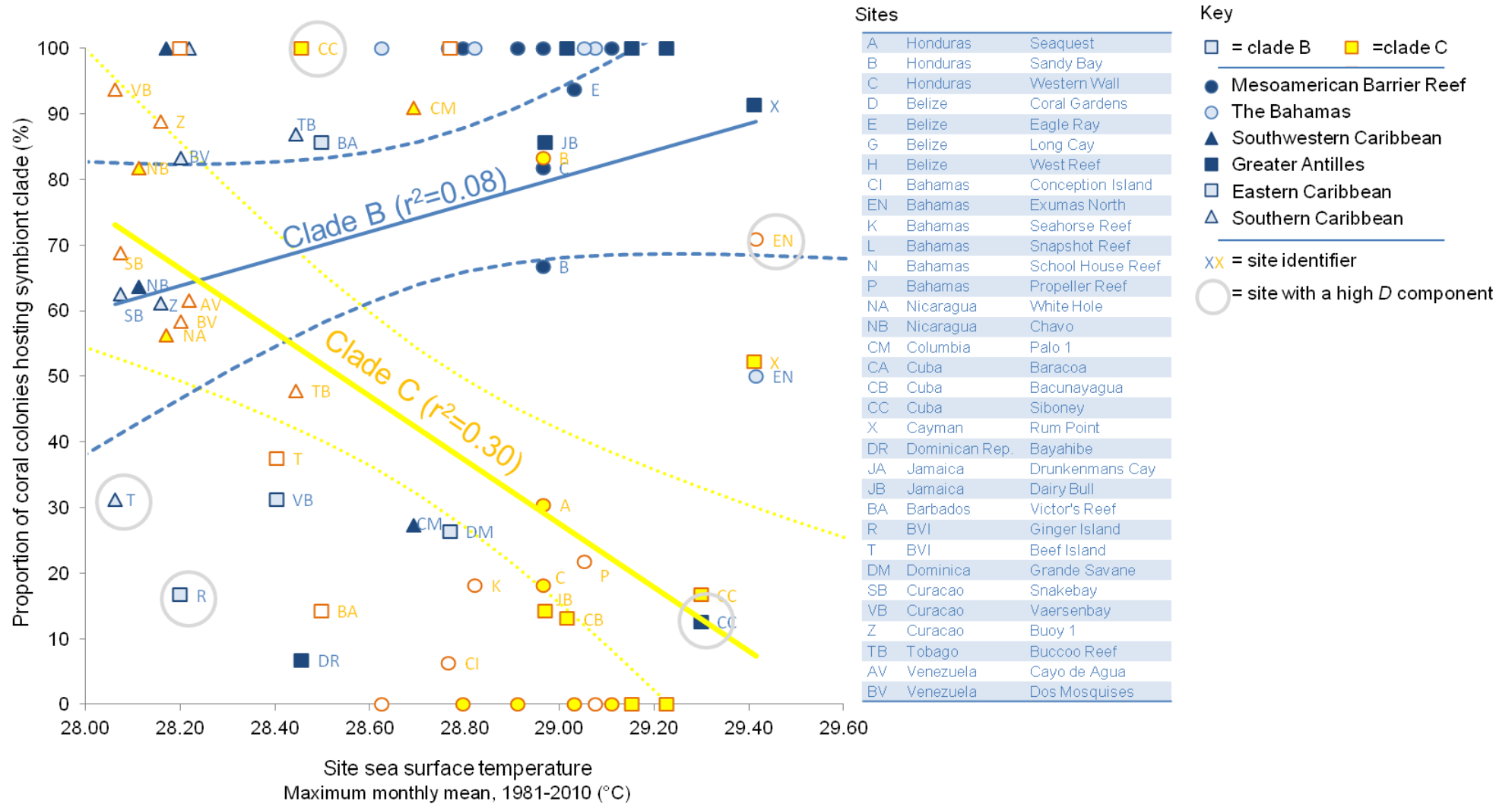


Figure 6.10: Scatter graph showing the relationship between chronic temperature stress (*ts_chron* in the PERMANOVA statistical model) and two important components of symbiont community variation: the relative proportion of colonies hosting *Symbiodinium* clade B (in blue) and clade C (in yellow) at each site. There is a clear association between the proportion of *M. annularis* colonies hosting clade C, and the long term temperature trends at each site. In addition, sites that contain a relatively large proportion of rare symbiont D often produced outliers.

6.7), its weakness could be interpreted as insufficient evidence to demonstrate the presence of a causal relationship, suggesting instead an underlying environmental variable indirectly driving both factors. The association might be generated by broad-scale patterns of connectivity (e.g., both host genetic distance and symbiont community variation correlated somewhat with geographic distance ($\rho=0.17$ and $\rho=0.24$, respectively both $p<0.01$) – for example the east-west break described both in coral populations (Fukami et al. 2004, Foster et al. 2012) and symbiont biogeography (Finney et al. 2010) – or an association between different drivers of host and endosymbiont diversity, for example spatial correlation between hurricane incidence (which explains 64% of variation in *M. annularis* genetic diversity (Foster et al. 2013) and also positively correlated with latitude, e.g., decreasing frequency from north to south) and temperature (also linked to latitude positively correlated with chronic thermal stress, Fig. 6.5).

Other studies that have compared the population structures of Caribbean cnidarian hosts and their endosymbiotic partners have also revealed congruence between the partner distributions, but failed to find a clear link between host and symbiont distributions (Andras et al. 2011), with *Symbiodinium* populations connected across geographic regions that divide the host (Andras et al. 2013). Faced with the evidence from this study it would be difficult to describe the similarity in the apparent ‘east-west’ division in *M. annularis* population genetics and symbiont communities as causal, and the spawning nature of the species makes it difficult to conceive a mechanism for this being a causal effect.

6.6.4 Unexplained variation

A significant amount of symbiont community variation was evident at the colony scale (Table 6.3), supporting published studies that have documented substantial within-site variability in *M. annularis* endosymbiont communities (Rowan and Knowlton 1995, Toller et al. 2001b). A similar degree of Caribbean within-site variation (31%), inter-site (29%) and inter-region (29%) was identified (Table 6.3), agreeing with Warner et al (2006), who recorded strong differentiation in the dominant symbionts hosted by *M. annularis* at spatial scales of meters, particularly at the shallow and intermediate depths analogous to those sampled in this study (Warner et al. 2006). Identification of drivers of colony-scale variation is beyond the remit of this study, but perhaps more detailed collection of data on environmental heterogeneity at smaller spatial scales may have facilitated better exploration intra-site variation; although much work already exists showing irradiance to be a highly influential driver at these scales (Rowan et al. 1997). Meanwhile, a closer inspection of inter-site variability at the local scale is the logical next step with this dataset. Data exist on the relative spatial patterning of colonies within sites, and further work should examine this within-site variation, perhaps with particular emphasis on size and positioning of colony.

At population level, even the best models were only able to explain 48-56% of the symbiont variability. Other factors, overlooked by this study but that may help explain partitioning include sediment type (Littman et al. 2008) and seawater pH (Reynaud et al. 2003). Sediment type may play a role in determining symbiont community of *M. annularis*, as free living symbionts predominantly associate with the benthos (Littman et al. 2008). Cooper *et al* (2011) discovered that the mud content of the surrounding sediment could explain 80% of variation in symbiont community in *Acropora millepora* on the GBR. Seawater pCO₂ has also been shown to affect symbiont densities and influence community dynamics. Symbiont densities in *Porites* and *S. pistillata* declined as pH was experimentally reduced from 8.09 (around 3.99 Ω_{ar}) to 7.19 (0.65 Ω_{ar}), although chlorophyll concentration per cell increased (Krief et al. 2010). Other studies documented an opposing effect: increasing pCO₂ (pH 8.0 to pH 7.8), boosted symbiont densities by a factor of 1.70 (Reynaud et al. 2003). Further observations prompted these authors to suggest that increasing pCO₂ disrupts the growth rates of the algal cells (Reynaud et al. 2003). Symbiont community composition may also be affected by ocean acidification: experiments showed that photosynthesis and growth of four phylotypes (ITS2 A1, A13, A2, and B1) were differentially affected by a doubling of pCO₂, with the growth rate of A13 and photosynthetic capacity of A2 increasing, while others remained unaffected. This provides a mechanism by which the phylotypes available in free-living populations may change, affecting corals that rely on horizontal transmission (Brading et al. 2011). Since *M. annularis* communities were shown to be heavily dominated by B1 (Chapter 5), perhaps pCO₂ may not be so important in the Caribbean – however lack of data on seawater pH meant that this could not be tested.

6.7 Conclusion

Only a few other studies have attempted to explain the ecological dominance and diversity of coral endosymbionts in terms of environmental conditions, geographic isolation and host genetics, across such a broad geographic scale (LaJeunesse et al. 2010, Cooper et al. 2011). Like these studies, we demonstrate that heterogeneity in the Caribbean temperature regime – particularly chronic and acute temperature stress (together explaining almost half of diversity, Table 6.3) - is the primary driver of symbiont distributions at a regional scale, with geographic distance also playing a role (albeit comparatively less informative, Table 6.4). On this basis we were unable to reject hypothesis H₄ (section 6.2). However, unlike other studies, we show a multitude of environmental factors (including phosphate levels) were able to contribute to explaining biogeography (Table 6.3): inclusion of seven variables in the best fit model indicates the complex nature of the community partitioning. As a result we were unable to reject hypothesis H₂ (section 6.2). We show that patterns of *M. annularis* genetic diversity were related to symbiont community differences, but were unable to explain variability to the same

extent as environmental and geographic predictors. Finally, we present a clear relationship between clade C distribution and chronic temperature stress on a regional scale, and suggest that clade C types (in particular C7) are acclimated to lower chronic temperature stress. This has important implications for regions – such as the Lesser Antilles and Venezuelan and Curaçao – where *M. annularis* host substantially more clade C, and emphasises the need for consideration of coral acclimation and thermal stress in marine reserve design (Mumby et al. 2011). An improved understanding of the specific environmental drivers of *Symbiodinium* biogeography is fundamental for prediction of coral community responses to a changing climate. However, caution should be taken when interpreting these biogeographic patterns, as they are very specific to the symbioses between *Symbiodinium* and our study species, *M. annularis*. It would be unwise to extrapolate conclusions about environmental, geographic and genetic drivers of *Symbiodinium* partitioning to either to other Caribbean host species, or depths.

6.8 References

- Anderson MJ, Gorley RN, Clarke KR (2008) *PERMANOVA+ for PRIMER: guide to software and statistical methods*. Plymouth Marine Lab, PRIMER-E Ltd.
- Andras JP, Kirk NL, Coffroth MA, Harvell CD (2009) Isolation and characterization of microsatellite loci in *Symbiodinium* B1/B184, the dinoflagellate symbiont of the Caribbean sea fan coral, *Gorgonia ventalina*. *Permanent Genetic Resources* **9**:989-993
- Andras JP, Kirk NL, Drew Harvell C (2011) Range-wide population genetic structure of *Symbiodinium* associated with the Caribbean Sea fan coral, *Gorgonia ventalina*. *Molecular Ecology* **20**:2525-2542
- Andras JP, Rypien KL, Harvell CD (2013) Range-wide population genetic structure of the Caribbean sea fan coral, *Gorgonia ventalina*. *Molecular Ecology* **22**:56-73
- Augustine L, Muller-Parker G (1998) Selective predation by the mosshead sculpin *Clinocottus globiceps* on the sea anenome *Anthopleura elegantissima* and its two algal symbionts. *Limnology and Oceanography* **43**:711-715
- Baums IB, Miller MW, Hellberg ME (2005) Regionally isolated populations of an imperiled Caribbean coral, *Acropora palmata*. *Molecular Ecology* **14**:1377-1390
- Baums IB, Miller MW, Hellberg ME (2006) Geographic variation in clonal structure in a reef-building Caribbean coral, *Acropora palmata*. *Ecological Monographs* **76**:503-519
- Berkelmans R, van Oppen MJH (2006) The role of zooxanthellae in the thermal tolerance of corals: a 'nugget of hope' for coral reefs in an era of climate change. *Proceedings of the Royal Society B-Biological Sciences* **273**:2305-2312
- Bongaerts P, Riginos C, Ridgway T, Sampayo EM, van Oppen MJH, Englebert N, Vermeulen F, Hoegh-Guldberg O (2010) Genetic divergence across habitats in the widespread coral *Seriatopora hystrix* and its associated *Symbiodinium*. *PLoS ONE* **5**:e10871
- Brading P, Warner ME, Davey P, Smith DJ, Achterberg EP, Suggett DJ (2011) Differential effects of ocean acidification on growth and photosynthesis among phylotypes of *Symbiodinium* (Dinophyceae). *Limnology and Oceanography* **56**:927-938
- Carricart-Ganivet JP, Merino M (2001) Growth responses of the reef-building coral *Montastraea annularis* along a gradient of continental influence in the southern Gulf of Mexico. *Bulletin of Marine Science* **68**:133-146
- Casey KS, Brandon TB, Cornillon P, Evans R (2010) The past, present and future of the AVHRR Pathfinder SST program. In: Barale V, Gower J, Albertotanza L (eds) *Oceanography from space, revisited*. Springer, New York, p 273-288.
- Castillo KD, Helmuth BST (2005) Influence of thermal history on the response of *Montastraea annularis* to short-term temperature exposure. *Marine Biology* **148**:261-270
- Chollett I, Mumby PJ (2012) Predicting the distribution of *Montastraea* reefs using wave exposure. *Coral Reefs* **31**:493-503
- Chollett I, Mumby PJ, Muller-Karger FE, Hu C (2012) Physical environments of the Caribbean Sea. *Limnology and Oceanography* **54**:1233-1244
- Clarke KR, Gorley RN (2006) *PRIMER v6: User Manual/Tutorial*. Plymouth Marine Lab, PRIMER-E, Plymouth
- Coles S, Jokiel P (1992) Effects of salinity on coral reefs. In: Connell D, Hawker D (eds) *Pollution in tropical aquatic systems*. CRC Press, Boca Raton, Florida, p 147-166
- Cooper TF, Berkelmans R, Ulstrup KE, Weeks S, Radford B, Jones AM, Doyle J, Canto M, O'Leary RA, van Oppen MJH (2011) Environmental factors controlling the distribution of *Symbiodinium* harboured by the coral *Acropora millepora* on the Great Barrier Reef. *PLoS ONE* **6**:e25536
- Correa AMS, Brandt ME, Smith TB, Thornhill DJ, Baker AC (2009) *Symbiodinium* associations with diseased and healthy scleractinian corals. *Coral Reefs* **28**:437-448
- Dubinsky Z, Stambler N, Ben-Zion M, McCloskey LR, Muscatine L, Falkowski PG (1990) The effect of external nutrient resources on the optical properties and photosynthetic efficiency of *Stylophora pistillata*. *Proceedings of the Royal Society of London Series B, Biological Sciences* **239**:231-246
- Eakin CM, Morgan JA, Heron SF, Smith TB, Liu G, Alvarez-Filip L, Baca B, Bartels E, Bastidas C, Bouchon C, Brandt M, Bruckner AW, Bunkley-Williams L, Cameron A, Causey BD, Chiappone M, Christensen TRL, Crabbe MJC, Day O, de la Guardia E, Diaz-Pulido G, DiResta D, Gil-Agudelo DL, Gilliam DS, Ginsburg RN, Gore S, Guzman HM, Hendee JC, Hernandez-Delgado EA, Husain E, Jeffrey CFG, Jones RJ, Jordan-Dahlgren E, Kaufman LS, Kline DI, Kramer PA, Lang JC, Lirman D, Mallela J,

- Manfrino C, Marechal J-P, Marks K, Mihaly J, Miller WJ, Mueller EM, Muller EM, Orozco Toro CA, Oxenford HA, Ponce-Taylor D, Quinn N, Ritchie KB, Rodriguez S, Ramirez AR, Romano S, Samhoury JF, Sanchez JA, Schmahl GP, Shank BV, Skirving WJ, Steiner SCC, Villamizar E, Walsh SM, Walter C, Weil E, Williams EH, Roberson KW, Yusuf Y (2010) Caribbean corals in crisis: record thermal stress, bleaching, and mortality in 2005. *PLoS ONE* **5**:e13969
- Ellstrand NC, Roose ML (1987) Patterns of genotypic diversity in clonal plant species. *American Journal of Botany* **74**:123-131
- Ersts PJ (Available from http://biodiversityinformatics.amnh.org/open_source/gdmg) *Geographic Distance Matrix Generator (version 1.2.3)*. In: American Museum of Natural History CfBaC (ed)
- Fagoonee I, Wilson HB, Hassell MP, Turner JR (1999) The dynamics of zooxanthellae populations: a long-term study in the field. *Science* **283**:843-845
- Finney J, Pettay D, Sampayo E, Warner M, Oxenford H, LaJeunesse T (2010) The relative significance of host-habitat, depth, and geography on the ecology, endemism, and speciation of coral endosymbionts in the genus *Symbiodinium*. *Microbial Ecology* **60**: 250-263
- Fitt W, Brown B, Warner M, Dunne R (2001) Coral bleaching: interpretation of thermal tolerance limits and thermal thresholds in tropical corals. *Coral Reefs* **20**:51-65
- Foster NL (2007) Population dynamics of the dominant Caribbean reef-building coral, *Montastraea annularis*. Ph.D, University of Exeter
- Foster NL, Baums IB, Mumby PJ (2007) Sexual vs. asexual reproduction in an ecosystem engineer: the massive coral *Montastraea annularis*. *Journal of Animal Ecology* **76**:384-391
- Foster NL, Baums IB, Sanchez JA, Paris CB, Chollett I, Agudelo CL, Vermeij MJA, Mumby PJ (2013) Hurricane-driven patterns of clonality in an ecosystem engineer: the Caribbean coral *Montastraea annularis*. *PLoS ONE* **8**:e53283
- Foster NL, Paris CB, Kool JT, Baums IB, Stevens JR, Sanchez JA, Bastidas C, Agudelo C, Bush P, Day O, Ferrari R, Gonzalez P, Gore S, Guppy R, McCartney MA, McCoy C, Mendes J, Srinivasan A, Steiner S, Vermeij MJA, Weil E, Mumby PJ (2012) Connectivity of Caribbean coral populations: complementary insights from empirical and modelled gene flow. *Molecular Ecology* **21**:1143-1157
- Fukami H, Budd AF, Levitan DR, Jara J, Kersanach R, Knowlton N (2004) Geographic differences in species boundaries among members of the *Montastraea annularis* complex based on molecular and morphological markers. *Evolution* **58**:324-337
- Gardner TA, Côté IM, Gill JA, Grant A, Watkinson AR (2005) Hurricanes and Caribbean coral reefs: impacts, recovery patterns and role in long-term decline. *Ecology* **86**:174-184
- Garren M, Walsh S, Caccone A, Knowlton N (2006) Patterns of association between *Symbiodinium* and members of the *Montastraea annularis* species complex on spatial scales ranging from within colonies to between geographic regions. *Coral Reefs* **25**:503-512
- Green J, Bohannan BJM (2006) Spatial scaling of microbial biodiversity. *Trends in Ecology and Evolution* **21**:501-507
- Howells EJ, Oppen MJH, Willis BL (2009) High genetic differentiation and cross-shelf patterns of genetic diversity among Great Barrier Reef populations of *Symbiodinium*. *Coral Reefs* **28**:215-225
- Jimenez IM, Kuhl M, Larkum AWD, Ralph PJ (2008) Heat budget and thermal microenvironment of shallow-water corals: do massive corals get warmer than branching corals? *Limnology and Oceanography* **53**:1548-1561
- Kent A, Coker P (1992) *Vegetation description and analysis - a practical approach*, Vol. John Wiley & Sons, New York
- Kerswell AP, Jones RJ (2003) Effects of hypo-osmosis on the coral *Stylophora pistillata*: nature and cause of 'low-salinity bleaching'. *Marine Ecology Progress Series* **253**:145-154
- Kinsey DW, Davis PJ (1979) Effect of elevated nitrogen and phosphorus on coral reef growth. *Limnology and Oceanography* **25**:935-940
- Kirk N, Andras J, Harvell C, Santos S, Coffroth M (2009) Population structure of *Symbiodinium* sp. associated with the common sea fan, *Gorgonia ventalina*, in the Florida Keys across distance, depth, and time. *Marine Biology* **156**:1609-1623
- Kleypas JA, Mcmanus JW, Menez LAB (1999) Environmental limits to coral reef development: where do we draw the line? *American Zoologist* **39**:146-159
- Krief S, Hendy EJ, Fine M, Yam R, Meibom A, Foster GL, Shemesh A (2010) Physiological and isotopic responses of scleractinian corals to ocean acidification. *Geochimica et Cosmochimica Acta* **74**:4988-5001

- LaJeunesse T, Thornhill D, Cox E, Stanton F, Fitt W, Schmidt G (2004a) High diversity and host specificity observed among symbiotic dinoflagellates in reef coral communities from Hawaii. *Coral Reefs* **23**:596-603
- LaJeunesse TC (2002) Diversity and community structure of symbiotic dinoflagellates from Caribbean coral reefs. *Marine Biology* **141**:387-400
- LaJeunesse TC (2005) "Species" radiations of symbiotic dinoflagellates in the Atlantic and Indo-Pacific since the miocene-pliocene transition. *Molecular Biology and Evolution* **22**:570-581
- LaJeunesse TC, Bhagooli R, Hidaka M, DeVantier L, Done T, Schmidt GW, Fitt WK, Hoegh-Guldberg O (2004b) Closely related *Symbiodinium* spp. differ in relative dominance in coral reef host communities across environmental, latitudinal and biogeographic gradients. *Marine Ecology Progress Series* **284**:147-161
- LaJeunesse TC, Loh WKW, van Woesik R, Hoegh-Guldberg O, Schmidt GW, Fitt WK (2003) Low symbiont diversity in southern Great Barrier Reef corals, relative to those of the Caribbean. *Limnology and Oceanography* **48**:2046-2054
- LaJeunesse TC, Pettay DT, Sampayo EM, Phongsuwan N, Brown B, Obura DO, Hoegh-Guldberg O, Fitt WK (2010) Long-standing environmental conditions, geographic isolation and host-symbiont specificity influence the relative ecological dominance and genetic diversification of coral endosymbionts in the genus *Symbiodinium*. *Journal of Biogeography* **37**:785-800
- LaJeunesse TC, Smith RT, Finney J, Oxenford H (2009) Outbreak and persistence of opportunistic symbiotic dinoflagellates during the 2005 Caribbean mass coral 'bleaching' event. *Proceedings of the Royal Society - Biological Sciences* **276**:4139-4148
- LaJeunesse TC, Trench RK (2000) Biogeography of two species of *Symbiodinium* (Freudenthal) inhabiting the intertidal sea anemone *Anthopleura elegantissima* (Brandt). *Biological Bulletin* **199**:126-134
- Lesser MP (2000) Depth-dependent photoacclimatization to solar ultraviolet radiation in the Caribbean coral *Montastraea faveolata*. *Marine Ecology Progress Series* **192**:137-151
- Littman RA, van Oppen MJH, Willis BL (2008) Methods for sampling free-living *Symbiodinium* (zooxanthellae) and their distribution and abundance at Lizard Island (Great Barrier Reef). *Journal of Experimental Marine Biology and Ecology* **364**:48-53
- Liu G, Strong AE, Skirving WJ, Arzayus LF (2006) Overview of NOAA Coral Reef Watch Program's near-real-time satellite global coral bleaching monitoring activities. *Proceedings of the 10th International Coral Reef Symposium*, Okinawa, Japan, p 1738-1793
- Loh WKW, Loi T, Carter D, Hoegh-Guldberg O (2001) Genetic variability of the symbiotic dinoflagellates from the wide ranging coral species *Seriatopora hystrix* and *Acropora longicyathus* in the Indo-West Pacific. *Marine Ecology Progress Series* **222**:97-107
- Marubini F, Davies PS (1996) Nitrate increases zooxanthellae population density and reduces skeletogenesis in corals. *Marine Biology* **127**:319-328
- McClanahan TR, Ateweberhan M, Ruiz Sebastian C, Graham NAJ, Wilson SK, Bruggemann JH, Guillaume MMM (2007) Predictability of coral bleaching from synoptic satellite and in situ temperature observations. *Coral Reefs* **26**:695-701
- Mumby PJ, Elliott IA, Eakin CM, Skirving W, Paris CB, Edwards HJ, Enríquez S, Iglesias-Prieto R, Cherubin LM, Stevens JR (2011) Reserve design for uncertain responses of coral reefs to climate change. *Ecology Letters* **14**:132-140
- Nagai S, Lian C, Yamaguchi S, Hamaguchi M, Matsuyama Y, Itakura S, Shimada H, Kaga S, Yamauchi H, Sonda Y, Nishikawa T, Kim C-H, Hogetsu T (2007) Microsatellite markers reveal population genetic structure of the toxic dinoflagellate *Alexandrium tamarense* (Dinophyceae) in Japanese coastal waters. *Journal of Phycology* **43**:43-54
- Oliver TA, Palumbi SR (2009) Distributions of stress-resistant coral symbionts match environmental patterns at local but not regional scales. *Marine Ecology Progress Series* **378**:93-103
- Oliver TA, Palumbi SR (2011) Many corals host thermally resistant symbionts in high-temperature habitat. *Coral Reefs* **30**:241-250
- Ortiz JC (2008) Coral holobiont community structure: how much have we missed by focusing only in the coral host? *Proceedings of the International Society for Coral Reef Studies*, 2008, Miami, Florida
- Peakall ROD, Smouse PE (2006) GENALEX 6: genetic analysis in Excel. Population genetic software for teaching and research. *Molecular Ecology Notes* **6**:288-295
- Reynaud S, Leclercq N, Romaanie-Lioud S, Ferrier-Pagés C, Jaubert J, Gattuso JP (2003) Interacting effects of CO₂ partial pressure and temperature on photosynthesis and calcification in a scleractinian coral. *Global Change Biology* **9**:1660-1668

- Rodriguez-Lanetty M, Loh WKW, Carter DA, Hoegh-Guldberg O (2001) Latitudinal variability in symbiont specificity within the widespread scleractinian coral *Plesiastrea versipora*. *Marine Biology* **138**:1175-1181
- Rowan R, Knowlton N (1995) Intraspecific diversity and ecological zonation in coral-algal symbiosis. *Proceedings of the National Academy of Sciences* **92**:2850-2853
- Rowan R, Knowlton N, Baker A, Jara J (1997) Landscape ecology of algal symbionts creates variation in episodes of coral bleaching. *Nature* **388**:265-269
- Santos SR, Gutiérrez-Rodríguez C, Lasker HR, Coffroth MA (2003b) *Symbiodinium* sp. associations in the gorgonian *Pseudopterogorgia elisabethae* in the Bahamas: high levels of genetic variability and population structure in symbiotic dinoflagellates. *Marine Biology* **143**:111-120
- Severance E, Karl S (2006) Contrasting population genetic structures of sympatric, mass-spawning Caribbean corals. *Marine Biology* **150**:57-68
- Smith DJ, Etienne M, Springer N, Suggett DJ (2008) Tolerance, refuge and recovery of coral communities to thermal bleaching: evidence from reefs of the Seychelles. *Proceedings of the 11th International Coral reef Symposium*, Fort Lauderdale, Florida
- Spalding MD, Fox HE, Allen GR, Davidson N, Ferdana ZA, Finlayson MAX, Halpern BS, Jorge MA, Lombana AL, Lourie SA, Martin KD, McManus E, Molnar J, Recchia CA, Robertson J (2007) Marine ecoregions of the world: a bioregionalization of coastal and shelf areas. *Bioscience* **57**:573-583
- Stat M, Bird CE, Pochon X, Chasqui L, Chauka LJ, Concepcion GT, Logan D, Takabayashi M, Toonen RJ, Gates RD (2011) Variation in *Symbiodinium* ITS2 sequence assemblages among coral colonies. *PLoS ONE* **6**:e15854
- Szmant AM (1991) Sexual reproduction by the Caribbean reef corals *Montastraea annularis* and *M. cavernosa*. *Marine Ecology Progress Series* **74**:13-25
- Thornhill D, Fitt W, Schmidt G (2006a) Highly stable symbioses among western Atlantic brooding corals. *Coral Reefs* **25**:515-519
- Thornhill DJ, LaJeunesse TC, Kemp DW, Fitt WK, Schmidt GW (2006) Multi-year, seasonal genotypic surveys of coral-algal symbioses reveal prevalent stability or post-bleaching reversion. *Marine Biology* **148**:711-722
- Thornhill DJ, Xiang Y, Fitt WK, Santos SR (2009) Reef endemism, host specificity and temporal stability in populations of symbiotic dinoflagellates from two ecologically dominant Caribbean corals. *PLoS ONE* **4**:e6262
- Toller WW, Rowan R, Knowlton N (2001a) Repopulation of zooxanthellae in the Caribbean corals *Montastraea annularis* and *M. faveolata* following experimental and disease-associated bleaching. *Biological Bulletin* **201**:360-373
- Toller WW, Rowan R, Knowlton N (2001b) Zooxanthellae of the *Montastraea annularis* species complex: patterns of distribution of four taxa of *Symbiodinium* on different reefs and across depths. *Biological Bulletin* **201**:348-359
- van Woesik R (2010) Calm before the spawn: global coral spawning patterns are explained by regional wind fields. *Proceedings of the Royal Society B: Biological Sciences* **277**:715-722
- Vollmer SV, Palumbi SR (2007) Restricted gene flow in the Caribbean staghorn coral *Acropora cervicornis*: implications for the recovery of endangered reefs. *Journal of Heredity* **98**:40-50
- Warner ME, LaJeunesse TC, Robison JD, Thur RM (2006) The ecological distribution and comparative photobiology of symbiotic dinoflagellates from reef corals in Belize: potential implications for coral bleaching. *Limnology and Oceanography* **51**:1887-1897
- Wilkinson C, Souter D (2008) *Status of Caribbean coral reefs after bleaching and hurricanes in 2005*. Global Coral Reef Monitoring Network, and Reef and Rainforest Research Centre, 152p, ISSN 1447 6185, Vol, Townsville, Australia
- Wooldridge SA (2009) Water quality and coral bleaching thresholds: Formalising the linkage for the inshore reefs of the Great Barrier Reef, Australia. *Marine Pollution Bulletin* **58**:745-751
- Yee SH, Santavy DL, Barron MG (2008) Comparing environmental influences on coral bleaching across and within species using clustered binomial regression. *Ecological Modelling* **218**:162-174
- Zuur AF, Ieno EN, Elphick CS (2010) A protocol for data exploration to avoid common statistical problems. *Methods in Ecology and Evolution* **1**:3-14

7

Prevalence of cryptic *Symbiodinium* D in *Montastraea annularis*

Kennedy EV, Stevens JR, Mumby PJ (in prep.)
*High prevalence of cryptic thermally tolerant symbionts
in the key Caribbean reef builder, Montastraea annularis*
Coral Reefs

7.1 Abstract

Emerging evidence demonstrates that thermally tolerant *Symbiodinium* D1-4 (formerly D1a; (LaJeunesse 2002) also known as *Symbiodinium trenchii* (LaJeunesse 2005)) may regularly comprise a cryptic member of coral endosymbiont communities (Loram et al. 2007, Mieog et al. 2007, Correa et al. 2009a, Silverstein et al. 2012). This provides a foundation for the theory of inferred bleaching resilience through rapid modification of the symbiont community (symbiont ‘shuffling’) (Baker et al. 2004, Berkelmans and van Oppen 2006, LaJeunesse et al. 2009). Real-time PCR (RT-PCR) is sufficiently sensitive to detect symbiont background levels of <5-10% (Mieog et al. 2007). In the current study, it was employed to screen 552 samples of the key reef builder *Montastraea annularis* from across a ~1700 km Caribbean range for the presence of cryptic *Symbiodinium* D1-4. All but one out of 33 populations analysed were found to host cryptic D clade *Symbiodinium*, with an average of >30% of individuals per site found to contain the symbiont. This compared to 12% in just 12 populations detected by the conventional screening technique – denaturing gradient gel electrophoresis (DGGE) – run concurrently on the same sample set. Detectable levels of D were variable, with gene copy number (relative to copy number of other symbionts in the community) ranging over a magnitude of nine. Distribution of background D showed a mainly uniform spread across the Caribbean and Bahamas, although Mesoamerican Barrier Reef corals hosted cryptic D more frequently than might be expected by chance. Background levels of D were also highest in Belizean sites. Widespread prevalence of background *Symbiodinium* D levels in *M. annularis* may well reflect a greater than expected potential capacity for the coral to respond to environmental threats through symbiont shuffling. The ecological implications in terms of reef conservation are complex: even if shuffling of D can confer temporary thermal tolerance to the host during bleaching events (not all communities hosting multiple clades shuffle symbionts (McGinley et al. 2012), and temperatures may exceed

tolerance limits (Hoegh-Guldberg et al. 2002), its dominance has been associated with decreased coral growth rates (Little et al. 2004), at a time when maintaining reef structure is vital to maintain reef ecosystem function.

7.2 Introduction

Bleaching-induced coral mortality is the single biggest threat facing Caribbean reefs today (Hoegh-Guldberg 1999, Frieler et al. 2013). Bleaching incidences are predicted to increase in both intensity and frequency, as global sea surface temperatures (SSTs) rise producing temperature anomalies. Climate models propose the global 1.5°C threshold could be exceeded between 2023 and 2050 (under ‘business as usual’ trajectories), forcing Caribbean SSTs up by as much as 1.3°C (Simpson et al. 2009). This is enough to increase the frequency of Caribbean >2°C thermal stress events by 0.4 - 0.7 year⁻¹: well above the critical limit for long term coral reef degradation (Frieler et al. 2013).

Coral bleaching is a phenomenon involving the dissociation of the symbiotic relationship between a cnidarian host and the photosynthetic dinoflagellates residing within its gastrodermal cells (Brown 1997). When corals are healthy, the dinoflagellate populations fluctuate at densities of around $\sim 2 \times 10^6 \text{ cm}^{-2}$ (Fagoonee et al. 1999), giving the host tissue a brown colouration and contributing to host metabolism and skeletogenesis which ultimately sustain the coral reef ecosystem. Bleaching is triggered by environmental stressors, most commonly in the form of SST elevated above the local average maxima (Fitt et al. 2001) and irradiance (Lesser 2000); but also through but also through reduced SST, salinity (Kerswell and Jones 2003), disease (Toller et al. 2001a, although see Correa et al. 2009b) and other water quality factors. Symbionts may lose pigmentation, be degraded *in situ* or be expelled from the host (Brown 1997). If not reinstated within a specified time period (dependent on host species, severity of bleaching and other environmental factors), corals will experience partial and occasionally full colony mortality. The probability of Caribbean mass mortality events are increasing as global climate change drives SSTs further above the regional norms, and recovery periods become ever more limited by bleaching frequency. In 2005, the biggest recorded Caribbean mass mortality to date was observed with 80% of corals bleaching and 40% of these going on to die (Eakin et al. 2010).

A ‘nugget of hope’ for the continued persistence of reefs as we know them may stem from the phenotypic diversity exhibited by algal endosymbionts (Baker et al. 2004, Berkelmans and van Oppen 2006). Molecular techniques have revealed a suite of symbiont ITS2-based endosymbiont haplotypes, classified into nine clades named A-I (Pochon and Gates 2010). Clades A-D, F and G generally associate with scleractinian corals, with clades B and C being dominant in the Caribbean. Experimental and observational work has shown a variety of

physiological properties can be attributed to different haplotypes (Rowan et al. 1997, Stat et al. 2008). In particular, some zooxanthellae display differential susceptibilities to thermal damage to the PSII reaction centre (involved in photosynthesis) which leads to expulsion of symbionts (Tchernov et al. 2004, Warner et al. 2006). In coral colonies associated with more than one symbiont haplotype, symbiont shuffling – a change in the relative abundance of different resident algal populations within a colony – provides a mechanism by which a holobiont may adjust its capacity to respond to environmental change (Baker et al. 2004, LaJeunesse et al. 2009). This may allow a coral species to be adapted to a range of environmental gradients (bathymetry, temperature, latitude, irradiance), as well as enabling positive responses to environmental perturbations. For example, a shift in dominance towards *Symbiodinium* D in stressed *Acropora millepora* was associated with an acquired tolerance of 1-1.5°C (Berkelmans and van Oppen 2006), and it has been suggested that the symbiont may indirectly confer disease resistance in Caribbean corals (Correa et al. 2009b).

Some evidence from early molecular studies pointed to a high degree of host specificity and fidelity in cnidarian-dinoflagellate symbioses (Goulet 2006, 2007). However, subsequent work has strongly refuted this – particularly for scleractinian corals – citing evidence of multiple symbiont clades within species, dynamism in symbiont communities and the existence of ‘cryptic’ symbiont taxa (found at low abundance within colonies) as support for the shuffling hypothesis (Baker and Romanski 2007). Other recent work has further demonstrated that the conventional techniques (e.g., DGGE, RFLPs) used to catalogue endosymbionts in corals may have limited capacity to detect low abundances, meaning coral symbiont diversity may have been consistently underestimated (Loram et al. 2007, Mieog et al. 2007, McGinley et al. 2012, Silverstein et al. 2012). These studies continue to identify ‘cryptic’ endosymbionts in a number of coral species, again demonstrating that the complexity of symbiont communities, especially in corals (Baker and Romanski 2007), has been underestimated. Thus evidence from several different studies provides support for the simultaneous occurrence of multiple symbionts within a variety of coral species, suggesting that specificity in coral-algal symbioses is rarely absolute (Baker and Romanski 2007, Silverstein et al. 2012), and adaptation by shuffling is a realistic possibility (Buddemeier and Fautin 1993). Understanding the scope for coral adaptation or acclimation is a key requirement for future conservation strategies (Mumby et al. 2011).

7.2.1 *Symbiodinium* D

Clade D has been described as a relatively rare symbiont with a global distribution, which has attracted interest due to its thermal tolerance (Stat and Gates 2011). It has been mainly found in reefs that experience unusually high SSTs (Baker et al. 2004, Oliver and Palumbi 2011), and colonies recently impacted by bleaching events (Jones et al. 2008, LaJeunesse et al. 2009), suggesting temperature stress can favour this symbiont. *Symbiodinium* D may also be associated

with other ‘stressful’ environmental conditions, including high sedimentation levels (Garren et al. 2006), turbidity (LaJeunesse et al. 2010) and cool water bleaching events (McGinley et al. 2012). The property of thermal tolerance is linked to symbiont taxa with high thylakoid membrane lipid concentrations. Lipids are hypothesised to protect against irreversible membrane disruption caused by high temperatures (Tchernov et al. 2004), although not all members of clade D possess this thermal property (and high lipid content is not restricted to clade D alone). In the Caribbean, the only members of D that occur (ITS2-type D1 and D1a – also known as *Symbiodinium trenchii*) have shown evidence of thermal tolerance (LaJeunesse et al. 2009, Wang et al. 2012). This has led to them being described by some as a ‘safety-parachute’ in the face of rising SSTs (Stat and Gates 2011). A pivotal study that monitored incidence of D in Barbadian *M. annularis* pre-, during and post-bleaching helped validate the shuffling theory by demonstrating that corals that harboured cryptic clade D endosymbionts later became dominated by them during and after a stress event, and that colonies dominated by D remained unbleached (Toller et al. 2001a, LaJeunesse et al. 2009). D has also been shown to be present in a low-abundance, background capacity on the Great Barrier Reef (GBR), where it was detected in 71% of colonies of four coral species tested (Mieog et al. 2007); in the eastern Pacific, where it was present at almost imperceptible levels in 40% of the *Pocillopora* screened (McGinley et al. 2012), and the Caribbean, where cryptic levels were found in five of six coral genera tested, many of which had never been observed previously to host D (Correa et al. 2009a). These recent studies strengthen the argument for an innate capacity to respond positively to thermal stress events in many corals, although the mechanism is clearly complex and real world evidence of implementation is far from unanimous (McGinley et al. 2012).

7.2.2 *Montastraea annularis*

M. annularis is a coral species known to host a variety of symbiont types, commonly clades B and C, but also A and D (Rowan and Knowlton 1995, Toller et al. 2001b, Garren et al. 2006). As a spawning coral, *M. annularis* must acquire endosymbionts from the environment (horizontal transmission; Szmant 1991), which partly explains its ability to host a wide variety of types (LaJeunesse et al. 2003). Flexibility in forming symbioses may explain why this coral is adapted to a larger range of bathymetric, latitudinal and water quality gradients than other Caribbean species (Weil and Knowlton 1994). This makes it the most important reef builder in the Caribbean, with *Montastraea* spp. reefs exemplifying Caribbean diversity (Mumby et al. 2008), although these reefs were also built by corals in the genus *Acropora* which remains depauperate on reefs today (see Chapter 4). Although host flexibility and the ability to acquire symbionts from the environment may infer an innate capacity for symbiont shuffling (Toller et al. 2001a, LaJeunesse et al. 2009), the window of opportunity for uptake may be limited (Little et al. 2004), and evidence suggests that symbiont communities hosted by *M. annularis* colonies show a high degree of temporal stability (Toller et al. 2001a, Thornhill et al. 2009), with little

evidence for symbiont ‘switching’ (i.e., changes brought about by uptake of new symbionts from the environment; Baker 2003). Only severe bleaching events are capable of disrupting the community and post-disruption most colonies regain their original community balance within a matter of months to years (Toller et al. 2001a, Thornhill et al. 2006, LaJeunesse et al. 2009). As the key reef builder in the Caribbean, understanding the symbiont community of this species is critical for making predictions about the ecological response of the region to climate change.

7.2.3 Real-time PCR

Commonly used survey techniques for detecting and identifying coral endosymbionts (namely PCR-DGGE, SSCP, RFLP analysis and DNA fingerprinting (Sampayo et al. 2009) have been successfully used to detect clades A, B, C and D in *M. annularis*, but are not capable of detecting symbionts at abundances below 5-10% of the total symbiont population, while direct sequencing of PCR product only identifies the dominant symbiont. RT-PCR is as much as 1,000-fold more sensitive than DGGE and SSCP (Mieog et al. 2007), and subsequently has the potential to improve estimates of the diversity of coral-*Symbiodinium* (Correa et al. 2009a). Other advantages of RT-PCR, including its ability to quantify abundance of types (Correa et al. 2009a), and the ease and speed of the technique (which is faster and less complicated than DGGE; Granados-Cifuentes and Rodriguez-Lanetty 2011) means it is increasingly being employed as a method for detecting low background levels of symbionts (Silverstein et al. 2012).

7.2.4 Aims

After characterising the dominant endosymbiont taxa using DGGE, RT-PCR was used to specifically screen for and quantify background levels of D clade endosymbionts in *M. annularis* colonies, across almost the entire Caribbean range of the coral. Evidence of naturally occurring symbiont shuffling in *M. annularis* has previously been documented at just one Caribbean site (LaJeunesse et al. 2009): by screening samples from across the whole region, we can demonstrate the prevalence (or absence) of the capability for thermal adaptation of Caribbean reefs. Our aim is to build on the work of recent studies that have revealed complexity in symbiont communities and increasing prevalence of cryptic D, as well as refining our understanding of *M. annularis* symbiont communities.

7.3 Materials and Methods

7.3.1 Sample collection and DNA extraction

Thirty 1 cm³ fragments of *M. annularis* tissue were collected from 33 sites spanning over 1700 km (including 15 countries and six ecoregions) across the Caribbean and Bahamas between

2003 and 2007 (Fig. 7.2) (Foster 2007). Sites were accessed using scuba, and approximately 30 small (1 cm³) fragments were chiselled from the edge of spatially independent ramets, before being placed and stored in 90% ethanol at 4°C, *sensu* Foster *et al* (2012). As bathymetry and irradiance are known to influence the *M. annularis* symbiont community, all collections were limited to between 2 and 6 m and only the tops of colonies were sampled. A mix of coral and symbiont DNA was extracted from a 1 cm² square of tissue using the DNeasy tissue kit (Qiagen), (with extended centrifugation at step five) and then stored at -20°C.

7.3.2 Symbiont screening using DGGE

Extracted DNA was amplified in a PCR reaction using *Symbiodinium*-specific rDNA primers ‘ITS2 Clamp’ and ‘ITSintfor2’ using a PCR protocol (95°C × 5 minutes; followed by 30 cycles of 94°C (45s), 57°C (45s), 72°C (60s); with a final annealing step of 59°C for 20 minutes), based on LaJeunesse (2002). The resulting PCR products were electrophoresed on a polyacrylamide denaturing gradient gel (40 to 60% denaturant) for 14 h at 114 V (Ingeny System). Imaged gels were examined by eye and scored for types, with comparison to a database of other gels used to help identify haplotypes. Dominant bands were excised and sent for sequencing (Macrogen) to resolve ITS2 type (see Chapter 5, section 5.3.3 for further details).

Primer name	Direction	Primer sequence (5'–3')	Primer size (bp)	Primer melting temperature (T _m)	Primer GC content (%)	Product size (bp)
D (external)	Forward	CCCAGGTGAGAATCCTGTGT	20	59.96	55	411
	Reverse	GGTCGAAAGGAACCACTGAA	20	60.09	50	
D (internal)*	Forward	GCCGTGTACGGTGCTCGCTCTCAA	24	72.25	62.5	312
	Reverse	GGCCACTCGCAAATGGACAGC	21	67.26	61.9	

Table 7.1. Clade-specific nuclear rDNA primer sets developed to amplify portions of the multi-copy ribosomal gene family in *Symbiodinium* clade D using qPCR. The external primers were developed to amplify a larger fragment to create standards. *Primers designed by Correa *et al* 2009.

7.3.3 RT-PCR analysis

A 312 base pair target region specific to *Symbiodinium* clade D, located in domain 2 of the LSU gene (Table 7.1), was amplified using published qPCR primers (Correa *et al.* 2009a). A 10µl reaction mix containing 1 mM of both forward and reverse primers; 1 µl DNA template; 2 x Absolute qPCR SYBR Green Fluorescein Mix (Thermo Scientific) and made up with dH₂O was amplified in qPCR reactions (CFX96 real-time PCR detection system, Bio-Rad Laboratories, Inc.) using the FAM filter. Reaction conditions were an initial denaturing step of 95°C for 10 min, followed by 50 PCR cycles of 95°C, 61°C and 72°C for 30 seconds each (Correa *et al.* 2009a). A final high-resolution melting (HRM) step entailed a 55°C to 95 °C temperature ramp, of 0.2°C every 2 seconds. Fluorescence data were collected during each PCR annealing step, and each temperature step of the HRM melt cycle. Each DNA sample was run in duplicate for

the clade D primer set, and positive (standard) and negative controls were included on every plate.

As DNA quantity may vary, an estimate for the abundance of total *Symbiodinium* was required to derive meaningful information about the proportional abundance of *Symbiodinium* D in each individual. The internal transcribed spacer region, ITS2, was selected as a suitable marker to assess total symbiont abundance, as this gene borders the LSU tandem repeats used to identify D (see Fig. 5.2, Chapter 5) and therefore should be directly comparable, and because reliable primers exist for ITS2 that can amplify all known *Symbiodinium* clades. Every sample that was screened for D was subsequently run through qPCR (again in duplicate) using the ITS2 primer set (cycling conditions: 98°C × 2 min, 45 cycles of 98°C × 5 s, 55°C × 5s and 72°C × 5s; Granados-Cifuentes and Rodriguez-Lanetty 2011). In addition to being used to estimate relative abundance of D, outputs generated here were used to assess DNA quality. Any samples that failed to generate positive ITS2 amplifications or produced poor quality melt curves, were removed from the dataset to avoid false negative D.

Selection of a fixed fluorescent threshold in the exponential phase of the reaction allowed comparable C_T values to be calculated. Where C_T values differed by > 1, data were discarded; otherwise, an average was generated from duplicate samples. C_T is directly proportional to the original quantity of DNA template, but in order to quantify copy number, an external standard of known concentration was required. To create a standard, new primers that amplified a region 20 base pairs up-and downstream from the D and ITS2 primer binding sites were designed using Primer-BLAST (NCBI), to generate PCR product that could be used as a standard (Ye et al. 2012). DNA samples from individual colonies that DGGE-sequencing had identified as containing D were selected. These samples were amplified under PCR conditions as described in 7.3.2, but with the annealing temperature based on the melt temperature of the newly designed primers (Table 7.1). The final concentration of the product was measured using spectrophotometric determination of DNA concentration. The copy number of standard DNA molecules could then be calculated using the following equation:

Number of molecules (μL^{-1}) = $(X \text{ g } \mu\text{L}^{-1} \text{ DNA} / \text{PCR product length} \times 660) \times \text{Avagadro constant}$

Where X is DNA concentration, the length of the PCR product is 312 base pairs (for LSU) and

320 base pairs for (for ITS2), and the Avogadro constant is 6.022×10^{23} . A series of twelve standards of known concentration were then generated using serial dilution (500, 250, 100, 50.0, 10.0, 5.00, 1.00, 0.50, 0.10, 0.05, 0.01, 5×10^{-3} , 1×10^{-3} , 5×10^{-4} , 1×10^{-4} , 5×10^{-5} , 1×10^{-5}), and eight of these were included on each plate.

7.3.4 Data analysis

C_T values were used to estimate starting quantities of D, and of ITS2, based on the standard series (see above). Examination of melt curves allowed purity of the reaction products to be assessed, providing an extra level of confidence in the results: amplified product generated a melt peak at the correct temperature range (e.g., 84.4°C (±0.5) for D target fragments), whereas melting at lower temperatures was indicative of primer dimer.

Non-parametric spatial analysis was performed on the geographical dataset using SADIE (Spatial Analysis for Distance IndicEs), with red-blue plots used to identify areas of significant clustering (Perry 1995, Perry et al. 1999).

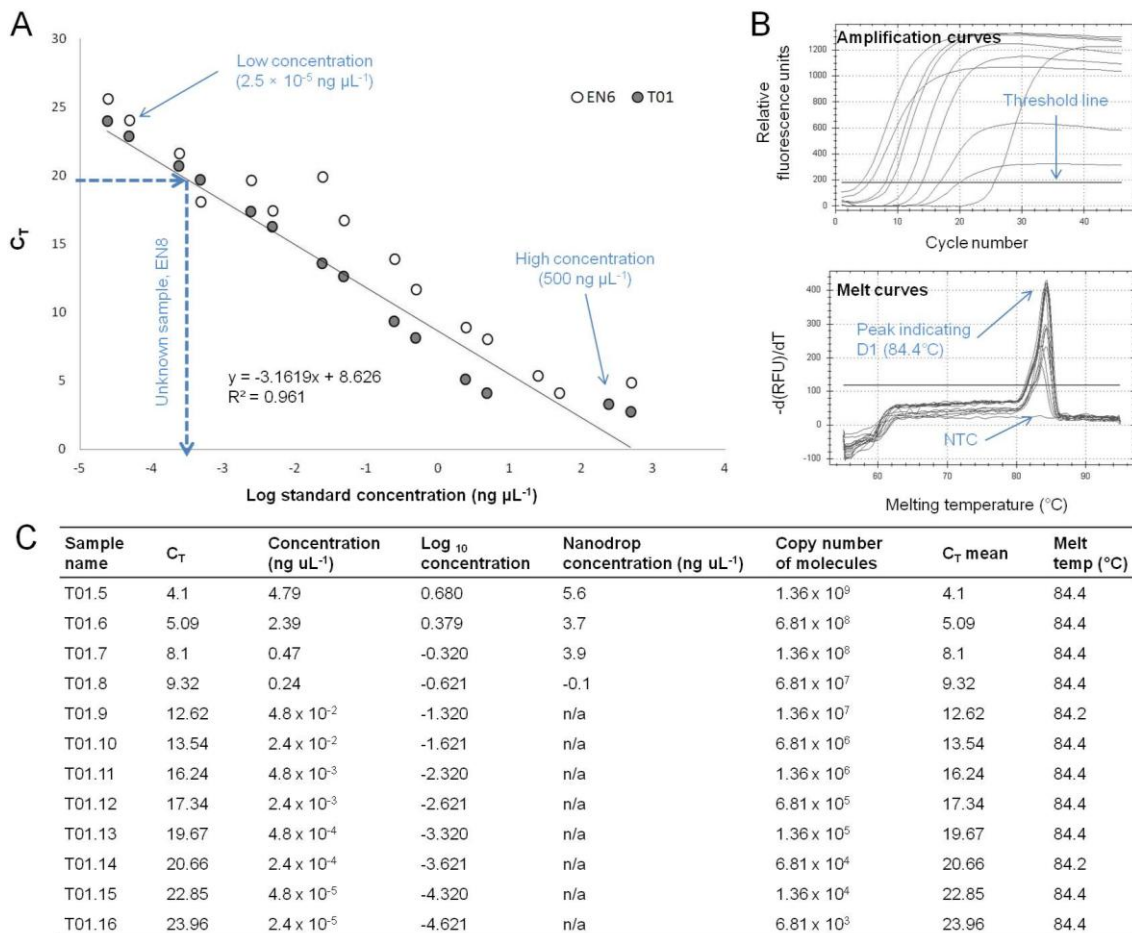


Figure 7.1: Standard curves for absolute quantification of *Symbiodinium* D clade DNA using RT-PCR. A) Standard curve graph, showing curves for two different standards. Curve based on the T01 sample gave the best result ($r^2 = 0.96$). B) Amplification curves and melt curves generated on the same run. C) Best data were used to generate standards.

7.4 Results

7.4.1 Assessment of symbiont communities by DGGE

Five-hundred and fifty-two coral colonies were successfully screened for *Symbiodinium* D. Within this dataset, DGGE distinguished 22 different ITS2 sub-clades, nested within four clades: *Symbiodinium* A, B, C and D. Sixty-five percent of colonies exclusively harboured clade B, and a further 17% hosted a mix of B and C. ITS2-B1 was the most frequently occurring sub-clade, found in 71% of colonies, with sub-clades B10 and B17 occurring less frequently. Thirty-one percent of samples harboured clade C (13% exclusively), with C7, C12 and C1 the most commonly occurring sub-clades. *Symbiodinium* D was found in 12.5% of corals (69 colonies), more commonly in a mixed assemblage (70%) than alone (30%). Colonies containing D were found in just 12 of the 33 sites. When examined independently, the spatial distribution of *Symbiodinium* D detected by DGGE alone (taking into account site location) was close to random (SADIE Index of Aggregation, $I_a=1.57$, $P_a=0.05$).

7.4.2 Assessment of symbiont communities by RT-PCR

RT-PCR produced positive amplifications (indicating presence of *Symbiodinium* D) in 170 colonies (31% of all corals). Low-abundance D was present at 97% (32/33) of sampling sites (Fig. 7.2). Examination of melt curves revealed almost all (>98%) samples with positive amplifications had a characteristic dissociation signature with melting point at 84.4°C; specific to the melting temperature of the target fragment (Fig. 7.1B). Those that did not were removed from the dataset, as melt curves particularly below 80°C can reflect primer dimer.

The proportion of spatially independent coral samples hosting cryptic D ranged from 0–100%, with an average of 30% of samples hosting cryptic D per site ($se=4.67$). Only Drunkenman's Cay in Jamaica (site JA) was found to have no cryptic D ($n=14$), despite these samples having a good quantity of starting DNA template (ITS2 = 12.8 ng μL^{-1}).

7.4.3 Quantifying background abundance of D

The quantity of D detected in samples extended over several orders of magnitude, with estimated starting quantities (SQ) ranging from 2.41×10^{-11} to 4.37×10^{-2} ng μL^{-1} . The average (3.33×10^{-2} ng μL^{-1}) is equivalent to a copy number of 9.75×10^8 molecules, although the multicopy nature of rDNA means that this value is unlikely to reflect the actual abundance of individual zooxanthellae. A relative quantity of *Symbiodinium* D gene copies, based on the ratio of D:ITS2 was estimated independently (Fig. 7.3). Some sites, (e.g. all Belizean sites, Bahamian sites CI and EN, the Dominican Republic and Dominica in the Lesser Antilles) had much higher relative abundance of background D to other sites.

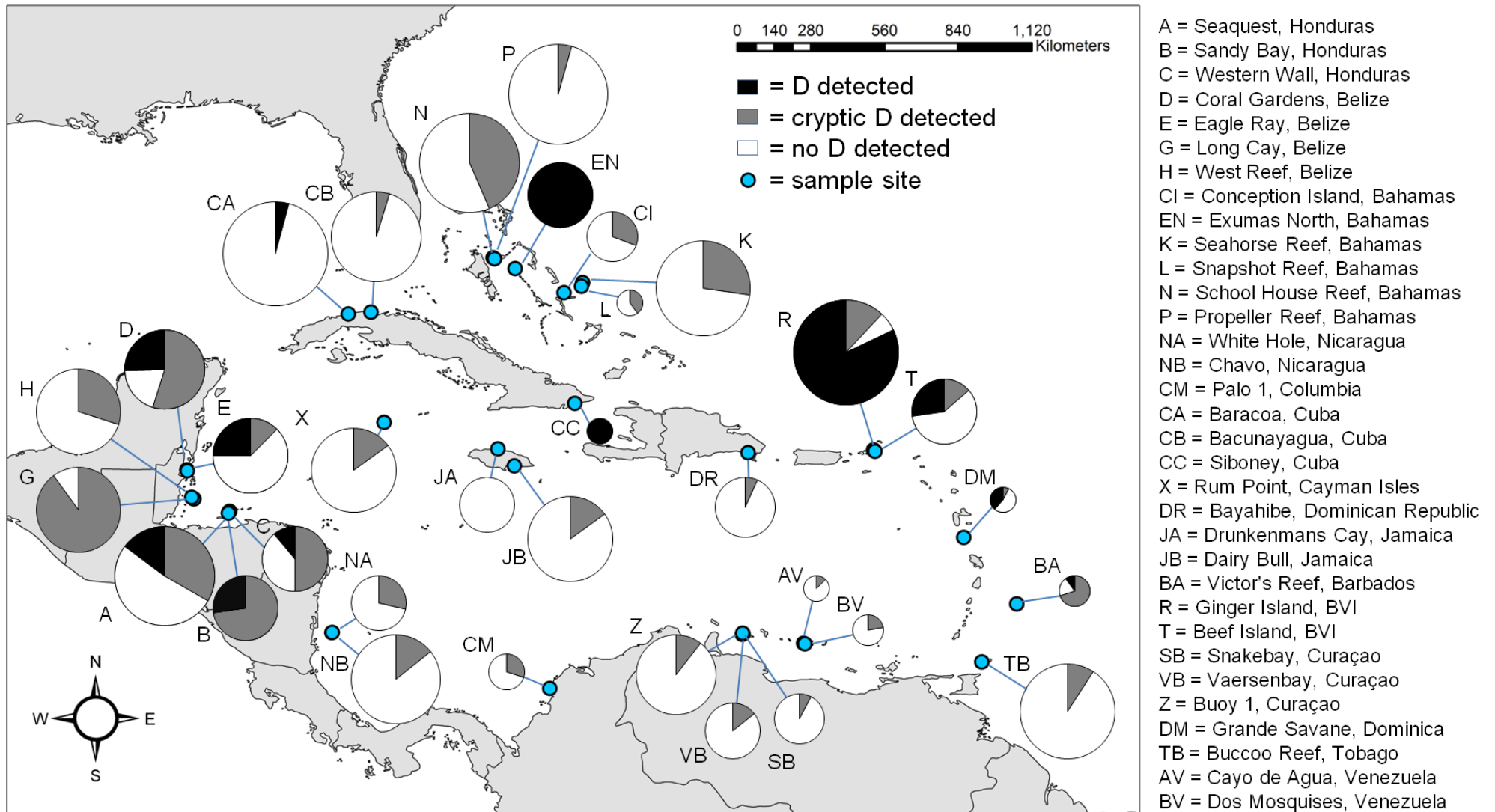


Figure 7.2. Proportion of *M. annularis* population harbouring *Symbiodinium* D. Thirty-three sites tested. Pie chart size reflects sample size (min=5, max=23), dark shading reflects proportion of samples hosting D detectable by DGGE, pale shading corresponds to low-abundance D, detected only by more sensitive RT-PCR.

In some cases, (e.g. sites EN, DM, D and E), these were sites where D had been detected by DGGE. In others (e.g., sites CC, R and T), background abundance was not greater, despite DGGE detecting clade D *Symbiodinium*.

The ability of DGGE to detect D appeared unrelated to the absolute starting quantity (SQ) of D. The samples in which D was detected actually had slightly lower SQ than the samples where D remained cryptic (mean SQ of D detected by DGGE = 9.12×10^{-6} ng μL^{-1}) compared to dataset mean (3.33×10^{-4} ng μL^{-1}), while the minimal quantity of D detected (2.41×10^{-11} ng μL^{-1} equivalent to a copy number of 70) was close to the minimum detected by DGGE (5.50×10^{-13} ng μL^{-1} ; copy number of 160).

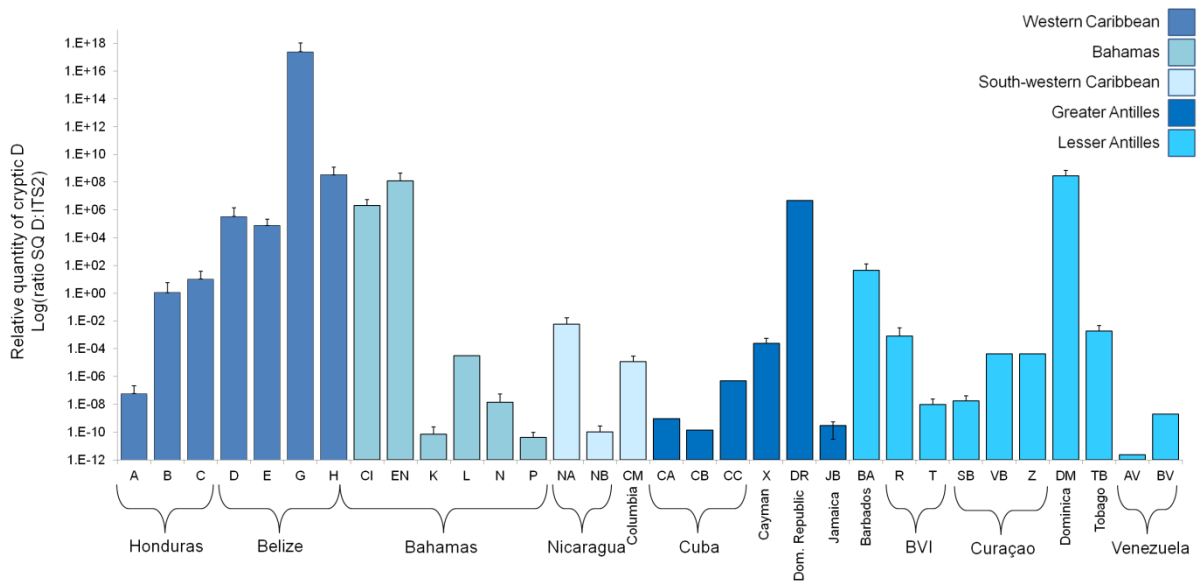


Figure 7.3. Relative quantities of *Symbiodinium* D gene copies found at each site (ratio of D:ITS2). Detectable background levels of D varied by an order of magnitude of nine between the 33 sites (designated by letters), but remained similar within sites. Locations (countries) and ecoregions (colours) to which the sites belong are also described. The D: ITS2 displayed here should be viewed as ‘order of magnitude’ estimates only. Site JA is excluded as it was not found to host D.

7.4.4 Spatial distribution of *Symbiodinium* D

Spatial analysis of the data revealed that the overall pattern of distribution of low-abundance D across the Caribbean and Bahamas was close to random ($I_a = 1.42$, $P_a = 0.09$), just as DGGE detectable levels had been. However, a high SADIE patch cluster index (v_i) of 2.22 ($p = 0.01$) revealed some clustering in the regional distribution of cryptic *Symbiodinium* D. Exploration of data through a cluster analysis identified several sites as containing a higher occurrence of D than expected (all three Honduran sites, two out of four Belizean sites and a Bahamian site in San Salvador), driving this significant cluster value. The location of these sites identified a patch cluster around the Mesoamerican Barrier Reef. A northern Cuba site, Beef Island in the BVI, two Curaçao sites and Dos Mosquises (a Venezuelan site) hosted less D than might be expected by chance, producing a significant gap cluster around the southern Caribbean (see

Appendix Fig. 7.1), although there were no significant gaps in the overall distribution ($v_i = -1.25$, $p = 0.192$).

Caribbean eco-region	Site identifier	Reef site	Sample size	% colonies hosting D (RT-PCR)	% colonies hosting D (DGGE)	Dominant symbiont	Copy number of D gene copies μL^{-1}	Copy number of ITS2 gene copies μL^{-1}
Mesoamerican Barrier Reef	A	Seaquest, Honduras	23	39	17	B1	8.12×10^3	7.08×10^{12}
	B	Sandy Bay, Honduras	16	100	38	B1/C1	9.33×10^6	1.19×10^{13}
	C	Western Wall, Honduras	16	56	13	B1	5.91×10^4	1.3×10^{15}
	D	Coral Gardens, Belize	19	74	26	B17	5.29×10^5	1.5×10^{13}
	E	Eagle Ray, Belize	18	17	28	B1/B17	9.68×10^6	9.27×10^9
	G	Long Cay, Belize	20	90	0	B1/B17	5.40×10^6	1.87×10^{11}
	H	West Reef, Belize	20	30	0	B1/B17	1.16×10^6	6.39×10^{10}
	The Bahamas	CI	Conception Island, Bahamas	13	31	0	B1	4.68×10^4
EN		Exumas North, Bahamas	16	56	100	D1	1.51×10^6	8.6×10^{12}
K		Seahorse Reef, Bahamas	22	27	0	B1	2.50×10^{10}	1.1×10^{17}
L		Snapshot Reef, Bahamas	5	40	0	B1	6.87×10^4	9.46×10^9
N		School House Reef, Bahamas	23	43	0	B1	3.41×10^4	1.81×10^{16}
South-western	P	Propeller Reef, Bahamas	23	4	0	B1	3.85×10^2	8.34×10^{16}
	NA	White Hole, Nicaragua	14	29	0	B1	2.41×10^6	5.89×10^{15}
	NB	Chavo, Nicaragua	21	14	0	B1/C12	8.63×10^5	1.7×10^{16}
Greater Antilles	CM	Palo 1, Columbia	10	30	0	C?	3.04×10^4	2.51×10^{11}
	CA	Baracoa, Cuba	24	4	4	B10	4.57×10^5	1.53×10^{15}
	CB	Bacunayagua, Cuba	21	5	0	B10	1.38×10^6	2.68×10^{17}
	CC	Siboney, Cuba	22	5	100	D1a	2.39×10^3	1.92×10^{13}
	X	Rum Point, Cayman	20	15	0	B1/C7	4.36	3.19×10^{16}
	DR	Bayahibe, Dominican Republic	15	7	0	C12	2.46×10^7	1.34×10^{11}
	JA	Drunkenmans Cay, Jamaica	14	0	0	B1	n/a	n/a
Lesser Antilles	JB	Dairy Bull, Jamaica	20	15	0	B1/B8	3.88	5.51×10^{13}
	BA	Victor's Reef, Barbados	9	78	11	B1j/B1	1.18×10^7	1.04×10^{13}
	R	Ginger Island, BVI	24	67	96	D1a	4.06×10^7	4.6×10^{13}
	T	Beef Island, BVI	16	19	38	B1/D1a	4.81×10^3	7.07×10^{13}
	SB	Snakebay, Curacao	13	8	0	C7	5.12×10^4	1.25×10^{11}
	VB	Vaersensbay, Curacao	14	14	0	C7	1.41×10^5	8.78×10^{10}
	Z	Buoy 1, Curacao	19	11	0	B1/C7	1.41×10^5	8.78×10^{10}
	DM	Grande Savane, Dominica	8	13	63	C12	1.42×10^1	2.04×10^{10}
	TB	Buccoo Reef, Tobago	22	9	0	C1	1.61×10^6	3.13×10^{10}
	AV	Cayo de Agua, Venezuela	8	13	0	B1j/C12	3.52×10^2	4.33×10^{13}
BV	Dos Mosquises, Venezuela	9	22	0	B1j/C12	1.13×10^3	4.03×10^{10}	

Table 7.2: Summary of RT-PCR and DGGE outputs by site, grouped by marine eco-region. Dominant symbiont represents the main symbiont type (or types) that occurred at a site – little within-site variability was detected. Copy number of D is essentially meaningless, given the multicopy nature of the gene and differing quality of the DNA samples. Copy number of ITS2 represents occurrences of all cladal symbionts, but, again, is quantitatively meaningless for the same reasons. A relative proportion of D (ratio of D : ITS2) is used as a proxy for D abundance throughout the paper.

7.5 Discussion

The Discussion section summarises the findings from the DGGE analysis (7.5.1), specifically *Symbiodinium* D abundances, which are then compared to D abundances detected by the more sensitive screening technique, RT-PCR (7.5.2). As well as presenting the total number of *M. annularis* colonies harbouring clade D, we present our attempts to quantify the relative abundance of the symbiont hosted within each colony's symbiont community (7.5.3). This leads us to a discussion on the potential for *Symbiodinium* D to 'save' coral reefs (7.5.4 and 7.5.5).

7.5.1 Dominance of B1 in *M. annularis* (DGGE)

DGGE revealed *M. annularis* communities to be dominated by *Symbiodinium* B1. This supports literature showing this symbiont to be the most common Caribbean type, hosted by a variety of cnidarian genera (LaJeunesse 2002), and particularly abundant in our study species (Thornhill et al. 2009). The distribution and abundances of other observed types, namely B (including B17, B10) and C clades (e.g., C7, C12, C3 and C1), corroborate well with the findings of numerous smaller scale studies into *M. annularis* symbiont community composition (Rowan and Knowlton 1995, Rowan et al. 1997, Toller et al. 2001b, Garren et al. 2006, LaJeunesse et al. 2009, Thornhill et al. 2009). At least 27% of colonies tested hosted >3 subclades, (max= 7), providing additional evidence for host flexibility in *M. annularis* (see also Chapter 5).

DGGE detected *Symbiodinium* D in just 12% of samples, with D appearing dominant in just 4% (21 samples). Other studies have shown similar prevalence of D, which generally represents <10% of the endosymbiotic community in the host population (Stat and Gates 2011). Previous work has found mixed evidence for D in *M. annularis*. Findings from studies in Belize (Garren et al. 2006), Panama (Rowan and Knowlton 1995, Rowan et al. 1997) and in the Bahamas and Florida (Thornhill et al. 2009) resembled those from the majority of our sites (21 out of 33) in failing to detect D in *M. annularis*. Where D has been detected using comparable low-resolution methods (DGGE and RFLPs), e.g., at Lee Stocking Island, Bahamas (LaJeunesse 2002), in Panama (Garren et al. 2006) and Barbados (LaJeunesse et al. 2009) it has often presented at similar frequencies to the 12.6% of colonies in this study (12.5%, 11% and 3% respectively). Where higher dominant abundances of D have been found, these are associated with corals stressed by temperature (e.g., >60% in Barbados and Florida during bleaching) (Thornhill et al. 2006, LaJeunesse et al. 2009, Finney et al. 2010), and/or disease (e.g., 100% in Panama; (Toller et al. 2001a). In our study, sporadic response to stress events could explain the high dominance of D (90-100%) detected in the Exhumas (EN), the British Virgin Isles (R) and Cuba (CC).

7.5.2 Prevalence of low-abundance *Symbiodinium* D (RT-PCR)

RT-PCR revealed that all sites but one had colonies (~30%) harbouring *Symbiodinium* D at low

abundances, despite DGGE only detecting its presence at 12 of 33 sites. Of the 553 individuals screened, DGGE detected only 69 instances of *Symbiodinium* D, meaning this technique failed to detect D in a further 101 colonies. Low-level (i.e. RT-PCR detectable) occurrence in an average of 29.8% of colonies per site agreed with recent evidence from Barbados that found 28% of healthy *M. annularis* colonies contained D that was detectable only by RT-PCR (LaJeunesse et al. 2009). Correa *et al.* (2009) also recorded low levels of *Symbiodinium* D in 21% of all Caribbean corals (including *Acropora cervicornis*, *Colpophyllia natans*, *Montastraea cavernosa*, *Agaricia* spp., and *Madracis* spp.) analysed, across a geographic range comparable with this study, although *M. annularis* was not sampled. Our findings compliment the conclusions of both studies, by demonstrating the breadth of the association of *M. annularis* with D shown in Barbados, across a Caribbean scale comparable to Correa's study.

At more than half the sites, between 11 and 40% of *M. annularis* colonies sampled harboured low levels of D. Spatial analyses revealed some variation in the number of occurrences of cryptic D. Twelve sites were identified as hosting D more or less frequently than expected, with more frequent occurrences in the Mesoamerican Barrier Reef region (Appendix Fig. 1). To a lesser extent, the southern Caribbean (Curaçao and Venezuelan sites) revealed a scarcity of D (Appendix Figure 1). The overall spatial arrangement across the region was fairly uniform, agreeing with the consensus that *Symbiodinium trenchii* exhibits random geographic distribution (Stat and Gates 2011).

7.5.3 Quantification of background abundance of D

In this study, relative abundance of D ranged over nine orders of magnitude, supporting studies that found a similar range in the abundance of detectable D (e.g., seven (Correa et al. 2009a) to eight orders (Mieog et al. 2007)). Any C_T over 45 were discarded from the analysis, as although ~70 samples detected D and produced clear melt up until $C_T = 50$, at a level of C_T of >45 (equivalent to < 70 copies per μL^{-1} , i.e. one cells worth of zooxanthellae (Loram et al. 2007)) rare cells could be contaminants, either on the surface of the host or collected in the seawater sampled with the holobiont. This also improved reproducibility estimates by >10%. Although signals were often low (again common in mixed assemblages), template-free controls were consistently negative. In future, it may also be pertinent to run additional controls to test seawater collected from the site at the time of sampling for contamination.

It was found (in this study) that DGGE detection limits were affected by the total copy number of ITS2 (i.e. number of symbiont types) rather than the absolute starting quantity of D. Smaller ratios of D:ITS2 were related to inability of DGGE to detect D, even if the absolute molecular quantity of D was comparable between samples. This may be due to a swamping effect of other symbiont types during PCR for DGGE, or preferential amplification of alternative clades, a problem reported in other critiques of the DGGE technique. The genomes of clade D

Symbiodinium are known to have a relatively low ribosomal copy number (e.g. 3-5 times less than clade C), making them harder to detect in mixed samples (Smith, 2008); e.g., in one study ITS-DGGE fingerprinting could detect presence of C3-e at proportions as low as 1%, but only detected D1a when it existed in proportion > 20% (LaJeunesse et al. 2009). Precision of qPCR is known to be lower in samples hosting multiple clades (e.g., precision 12% and reproducibility 19%; Loram et al. 2007). Despite a large proportion of our samples *M. annularis* colonies hosting multiple clades (see Chapter 5), in this study our reproducibility (among replicates) was 63%.

7.5.4 Invasion of a competitive opportunist?

The widespread presence of D at most Caribbean locations might reflect the presence of D at the time of symbiont uptake during coral settlement (e.g., due to symbiont switching), which may mirror observed geographic distributions. This would suggest an innate low-level presence of D1 which could infer a natural ability to respond to future warming events, though shuffling. However, until *Symbiodinium* can be successfully isolated from seawater this theory cannot be tested.

As an opportunistic symbiont, site variability in both incidence of occurrence and abundance level of D may well be further explained by thermal stress history at different Caribbean locations. Bleaching history has been proposed as an explanation for the occurrence of D, with higher incidence of D in a diversity of hosts sampled from reefs with a history of bleaching (Baker et al. 2004). The notably high abundance and occurrence of D observed at Mesoamerican Barrier reef sites may reflect the severity of the 1995 mass bleaching event in the region, where 76% of *M. annularis* were reported to have experienced bleaching (McField 1999). Latterly, bleaching would allow D to become established in the *M. annularis* community. Studies have shown that time spans ranging from months to years may be required for original symbiont communities to re-establish dominance, following bleaching associated increases in clade D in *M. annularis* (Thornhill et al. 2006, LaJeunesse et al. 2009). In one study it took up to five years for *M. annularis* symbiont communities to revert to pre-bleaching status (Thornhill et al. 2006). In another, *M. annularis*, along with another bleaching susceptible coral *Siderastraea siderea*, still contained D1a two years following the 2005 bleaching event in Barbados, while other species (*Diploria* spp., *Agaricia* spp. and *Meandrina meandrites*) had managed to purge themselves of the symbiont by November 2007 (LaJeunesse et al. 2009). The detection of higher levels of low-abundance D may be the remnants of past bleaching events in this region. Temporal analyses would be needed to resolve the stability of cryptic D at each site, thus giving a better indication of whether shuffling or uptake explains the spatial patterns of distribution.

7.5.5 A mechanism for symbiont shuffling?

Evidence from Barbados confirms shuffling of cryptic *Symbiodinium* D in *M. annularis* in apparent response to a thermal stress event (LaJeunesse et al. 2009). The abundance of D increased in colonies in response to bleaching, with the symbiont becoming dominant in 60% of colonies. Colonies harbouring D remained unbleached, clearly demonstrating the ability of *M. annularis* to adapt through symbiont shuffling. The finding of this study, that background levels of D can be expanded to the entire Caribbean region, provides insight into the potential for shuffling to act as a widespread mechanism by which Caribbean reefs might respond positively to increasing thermal stress. The inference is that the demonstrated capacity for *M. annularis* to recover from severe bleaching events may be more geographically extensive than first supposed.

However, there are several caveats for predicting response to climate change based on prevalence of background D. Firstly, the flexibility of *M. annularis* in hosting symbionts does not appear to confer a greater diversity of potential responses to environmental threats in this important reef builder: it remains ranked among the most bleaching-susceptible of Caribbean species (Manzello et al. 2007, Yee et al. 2008, van Hooidonk et al. 2012), and has experienced a 72% Caribbean-wide population decline in fifteen years (Edmunds and Elahi 2007). In the Barbados shuffling study, *M. annularis* was among the worst affected by bleaching, despite the apparent protection of D. When considering bleaching, the symbiont community can only go part way to explaining holobiont vulnerability: coral host itself also plays a role, with other host related factors, such as abundance of UV-absorbing compounds and the ability of coral to mop up hydrogen peroxide that triggers the response to expel, partially determining differential bleaching responses (Baird et al. 2009, Császár et al. 2010).

Secondly, controversy still reigns over the widespread ecological significance of background levels of *Symbiodinium* D. In the Barbados study, only half of the species surveyed (*M. annularis*, *M. cavernosa*, *Agaricia* sp. and *Meandrina meandrites*) demonstrated a significant shift in prevalence of cryptic D – in other species D did not vary significantly over the bleaching event (LaJeunesse et al. 2009). Another study has shown limited shift in community dominance in *Pocillopora* during a cold water bleaching event, despite detecting background levels of D that at higher abundances could prevent bleaching, as shown by McGinley *et al.* (McGinley et al. 2012). In this case, the authors argued that shuffling events may be rare, despite background levels of D remaining high. Additionally the relationship between B1 and Caribbean corals has been shown to exist since the Pleistocene, and recovery of ITS2 B1 sequences from gorgonians >100 years old have been used to argue that there is little evidence for symbiont shuffling in the past (Baker et al. 2013).

Thirdly, symbiont shuffling will not be a solution for all Caribbean corals. Not all species are as flexible in their associations as *Montastraea* spp.: many are ‘specifist’, exhibiting low flexibility and hosting taxonomically narrow assemblages (Putnam et al. 2012). As a spawning species, *M. annularis* can uptake symbionts from the environment, but brooders (including common Caribbean species (e.g., *Agaricia* sp., *Siderastrea* sp. and *Porites* sp.) will inherit symbionts from parents, usually resulting in more specific and highly stable symbioses, implying fewer opportunities for shuffling (Thornhill et al. 2006a).

Fourthly, the benefits inferred by hosting D in terms of resilience to thermal stress may be counteracted by severe costs in terms of tradeoffs. The opportunistic symbiont may see stressful conditions as an opportunity to exploit the host as a habitat rather than engage in an interactive and mutually beneficial partnership. Not all clades are equally valuable, e.g., clade A is understood to be functionally less beneficial to *Acropora* in Hawaii than clade C (Stat et al. 2008). The ability of scleractinian corals to form calcium carbonate skeletal structures is linked to symbiosis, and clade D is thought to be linked to the efficiency of colony calcification, with colonies harbouring mainly D growing more slowly (Little et al. 2004, Jones and Berkelmans 2010). For example *Acropora millepora* harbouring D grow 38% slower than colonies harbouring C (Little et al. 2004, Jones and Berkelmans 2010). Moreover, temporary dominance of an uncommon opportunistic symbiont post-bleaching event may have costs to reefs in times of low thermal stress (Thornhill et al. 2006a, Jones et al. 2008, LaJeunesse et al. 2009). Even if the benefits outweigh the costs, corals have to bleach before background symbionts can become established (Buddemeier and Fautin 1993, Berkelmans and van Oppen 2006). The bleaching process in itself is stressful, reducing skeletal extension rates in *M. annularis* by up to > 50%, for six months following bleaching as well as affecting reproduction (Mendes and Woodley 2002). This ultimately affects the ability of reefs to grow, with associated long-term implications for the survival of reefs (Chapter 4).

Finally, the ability to shuffle may not be enough to cope with the rapid changes expected to occur in the mid- to near future. Even the most optimistic of future projections that include some assumption of coral thermal adaptation through symbioses still project one third of global reefs to experience long term degradation (Frieler et al. 2013).

7.6 Conclusion

A gap in the scientific knowledge (referred to in a recent review; Stat and Gates 2011) identifies limited understanding of biogeography in *Symbiodinium* in general – and that most studies distinguish only the dominant endosymbionts in corals. Here we were able to explore diversity of *Symbiodinium* D to a greater resolution across a larger geographic scale than previously attempted. Whether observable patterns have been established as a result of past

thermal stress events, and whether they can provide hope for Caribbean reefs in the face of global climate change remains to be seen. Despite the caveats, presence of low levels of different symbionts in the coral host provides an additional tool in the toolbox of environmental responses for *M. annularis*. Most Caribbean coral reefs will need to adapt to 0.2 to 0.3°C per decade over the next 30 to 50 years to prevent bleaching more than once every five years (Simpson et al. 2009). Whether the widespread prevalence of D is enough to achieve this remains to be seen. Shedding light on the spatial distribution of this key endosymbiont form may have implications for predicting future occurrences of Caribbean bleaching events in the face of global climate change, and aid reserve design (Mumby et al. 2011). However, greater understanding of the true ecological implications of low-level D,– including the real incidence of symbiont shuffling, may be required to draw firm conclusions from our findings.

7.7 References

- Baird AH, Bhagooli R, Ralph PJ, Takahashi S (2009) Coral bleaching: the role of the host. *Trends in Ecology and Evolution* **24**:16-20
- Baker AC (2003) Flexibility and specificity in coral-algal symbiosis: Diversity, ecology, and biogeography of *Symbiodinium*. *Annual Review of Ecology Evolution and Systematics* **34**:661-689
- Baker AC, Romanski AM (2007) Multiple symbiotic partnerships are common in scleractinian corals, but not in octocorals: Comment on Goulet (2006). *Marine Ecology Progress Series* **335**:237-242
- Baker AC, Starger CJ, McClanahan TR, Glynn PW (2004) Coral reefs: Corals' adaptive response to climate change. *Nature* **430**:741-741
- Baker DM, Weigt L, Fogel M, Knowlton N (2013) Ancient DNA from coral-hosted *Symbiodinium* reveal a static mutualism over the last 172 years. *PLoS ONE* **8**:e55057
- Berkelmans R, van Oppen MJH (2006) The role of zooxanthellae in the thermal tolerance of corals: a 'nugget of hope' for coral reefs in an era of climate change. *Proceedings of the Royal Society B-Biological Sciences* **273**:2305-2312
- Brown BE (1997) Coral bleaching: causes and consequences. *Coral Reefs* **16**:S129-S138
- Buddemeier RW, Fautin DG (1993) Coral bleaching as an adaptive mechanism - a testable hypothesis. *Bioscience* **43**:320-326
- Correa A, McDonald M, Baker A (2009a) Development of clade-specific *Symbiodinium* primers for quantitative PCR (qPCR) and their application to detecting clade D symbionts in Caribbean corals. *Marine Biology* **156**:2403-2411
- Correa AMS, Brandt ME, Smith TB, Thornhill DJ, Baker AC (2009b) *Symbiodinium* associations with diseased and healthy scleractinian corals. *Coral Reefs* **28**:437-448
- Császár NBM, Ralph PJ, Frankham R, Berkelmans R, van Oppen MJH (2010) Estimating the potential for adaptation of corals to climate warming. *PLoS ONE* **5**:e9751
- Eakin CM, Morgan JA, Heron SF, Smith TB, Liu G, Alvarez-Filip L, Baca B, Bartels E, Bastidas C, Bouchon C, Brandt M, Bruckner AW, Bunkley-Williams L, Cameron A, Causey BD, Chiappone M, Christensen TRL, Crabbe MJC, Day O, de la Guardia E, Diaz-Pulido G, DiResta D, Gil-Agudelo DL, Gilliam DS, Ginsburg RN, Gore S, Guzman HM, Hendee JC, Hernandez-Delgado EA, Husain E, Jeffrey CFG, Jones RJ, Jordan-Dahlgren E, Kaufman LS, Kline DI, Kramer PA, Lang JC, Lirman D, Mallela J, Manfrino C, Marechal J-P, Marks K, Mihaly J, Miller WJ, Mueller EM, Muller EM, Orozco Toro CA, Oxenford HA, Ponce-Taylor D, Quinn N, Ritchie KB, Rodriguez S, Ramirez AR, Romano S, Samhoury JF, Sanchez JA, Schmahl GP, Shank BV, Skirving WJ, Steiner SCC, Villamizar E, Walsh SM, Walter C, Weil E, Williams EH, Roberson KW, Yusuf Y (2010) Caribbean corals in crisis: record thermal stress, bleaching, and mortality in 2005. *PLoS ONE* **5**:e13969
- Edmunds PJ, Elahi R (2007) The demographics of a 15-year decline in cover of the Caribbean reef coral *Montastraea annularis*. *Ecological Monographs* **77**:3-18
- Fagoonee I, Wilson HB, Hassell MP, Turner JR (1999) The dynamics of zooxanthellae populations: a long-term study in the field. *Science* **283**:843-845
- Finney J, Pettay D, Sampayo E, Warner M, Oxenford H, LaJeunesse T (2010) The relative significance of host-habitat, depth, and geography on the ecology, endemism, and speciation of coral endosymbionts in the genus *Symbiodinium*. *Microbial Ecology* **60**:250-263
- Fitt W, Brown B, Warner M, Dunne R (2001) Coral bleaching: interpretation of thermal tolerance limits and thermal thresholds in tropical corals. *Coral Reefs* **20**:51-65
- Foster NL (2007) Population dynamics of the dominant Caribbean reef-building coral, *Montastraea annularis*. Ph.D, University of Exeter
- Foster NL, Paris CB, Kool JT, Baums IB, Stevens JR, Sanchez JA, Bastidas C, Agudelo C, Bush P, Day O, Ferrari R, Gonzalez P, Gore S, Guppy R, McCartney MA, McCoy C, Mendes J, Srinivasan A, Steiner S, Vermeij MJA, Weil E, Mumby PJ (2012) Connectivity of Caribbean coral populations: complementary insights from empirical and modelled gene flow. *Molecular Ecology* **21**:1143-1157
- Frieler K, Meinshausen M, Golly A, Mengel M, Lebek K, Donner SD, Hoegh-Guldberg O (2013) Limiting global warming to 2°C is unlikely to save most coral reefs. *Nature Climate Change* **3**:165-170
- Garren M, Walsh S, Caccone A, Knowlton N (2006) Patterns of association between *Symbiodinium* and members of the *Montastraea annularis* species complex on spatial scales ranging from within colonies to between geographic regions. *Coral Reefs* **25**:503-512
- Goulet TL (2006) Most corals may not change their symbionts. *Marine Ecology Progress Series* **321**:1-7

- Goulet TL (2007) Most scleractinian corals and octocorals host a single symbiotic zooxanthella clade. *Marine Ecology Progress Series* **335**:243-248
- Granados-Cifuentes C, Rodriguez-Lanetty M (2011) The use of high-resolution melting analysis for genotyping *Symbiodinium* strains: a sensitive and fast approach. *Molecular Ecology Resources* **11**:394-399
- Hoegh-Guldberg O (1999) Climate change, coral bleaching and the future of the world's coral reefs. *Marine and Freshwater Research* **50**:839-866
- Jones A, Berkelmans R (2010) Potential costs of acclimatization to a warmer climate: growth of a reef coral with heat tolerant vs. sensitive symbiont types. *PLoS ONE* **5**:e10437
- Jones AM, Berkelmans R, van Oppen MJH, Mieog JC, Sinclair W (2008) A community change in the algal endosymbionts of a scleractinian coral following a natural bleaching event: field evidence of acclimatization. *Proceedings of the National Academy of Sciences* **275**:1359-1365
- Kerswell AP, Jones RJ (2003) Effects of hypo-osmosis on the coral *Stylophora pistillata*: nature and cause of 'low-salinity bleaching'. *Marine Ecology Progress Series* **253**:145-154
- Lajeunesse TC (2002) Diversity and community structure of symbiotic dinoflagellates from Caribbean coral reefs. *Marine Biology* **141**:387-400
- Lajeunesse TC (2005) "Species" radiations of symbiotic dinoflagellates in the Atlantic and Indo-Pacific since the miocene-pliocene transition. *Molecular Biology and Evolution* **22**:570-581
- Lajeunesse TC, Loh WKW, van Woesik R, Hoegh-Guldberg O, Schmidt GW, Fitt WK (2003) Low symbiont diversity in southern Great Barrier Reef corals, relative to those of the Caribbean. *Limnology and Oceanography* **48**:2046-2054
- Lajeunesse TC, Pettay DT, Sampayo EM, Phongsuwan N, Brown B, Obura DO, Hoegh-Guldberg O, Fitt WK (2010) Long-standing environmental conditions, geographic isolation and host-symbiont specificity influence the relative ecological dominance and genetic diversification of coral endosymbionts in the genus *Symbiodinium*. *Journal of Biogeography* **37**:785-800
- Lajeunesse TC, Smith RT, Finney J, Oxenford H (2009) Outbreak and persistence of opportunistic symbiotic dinoflagellates during the 2005 Caribbean mass coral 'bleaching' event. *Proceedings of the Royal Society - Biological Sciences* **276**:4139-4148
- Lesser MP (2000) Depth-dependent photoacclimatization to solar ultraviolet radiation in the Caribbean coral *Montastraea faveolata*. *Marine Ecology Progress Series* **192**:137-151
- Little AF, van Oppen MJH, Willis BL (2004) Flexibility in algal endosymbioses shapes growth in reef corals. *Science* **304**:1492-1494
- Loram JE, Boonham N, O'Toole P, Trapido-Rosenthal HG, Douglas AE (2007) Molecular quantification of symbiotic dinoflagellate algae of the genus *Symbiodinium*. *Biological Bulletin* **212**:259-268
- Manzello DP, Berkelmans R, Hendee JC (2007) Coral bleaching indices and thresholds for the Florida Reef Tract, Bahamas, and St. Croix, US Virgin Islands. *Marine Pollution Bulletin* **54**:1923-1931
- McGinley MP, Aschaffenburg MD, Pettay DT, Smith RT, Lajeunesse TC, Warner ME (2012) *Symbiodinium* spp. in colonies of eastern Pacific *Pocillopora* spp. are highly stable despite the prevalence of low-abundance background populations. *Marine Ecology Progress Series* **462**:1-7
- Mendes JM, Woodley JD (2002) Effect of the 1995-1996 bleaching event on polyp tissue depth, growth, reproduction and skeletal band formation in *Montastraea annularis*. *Marine Ecology Progress Series* **235**:93-102
- Mieog JC, Oppen MJH, Cantin NE, Stam WT, Olsen JL (2007) Real-time PCR reveals a high incidence of *Symbiodinium* clade D at low levels in four scleractinian corals across the Great Barrier Reef: implications for symbiont shuffling. *Coral Reefs* **26**:449-457
- Mumby PJ, Broad K, Brumbaugh DR, Dahlgren C, Harborne AR, Hastings A, Holmes KE, Kappel CV, Micheli F, Sanchirico JN (2008) Coral reef habitats as surrogates of species, ecological functions, and ecosystem services. *Conservation Biology* **22**:941-951
- Mumby PJ, Elliott IA, Eakin CM, Skirving W, Paris CB, Edwards HJ, Enríquez S, Iglesias-Prieto R, Cherubin LM, Stevens JR (2011) Reserve design for uncertain responses of coral reefs to climate change. *Ecology Letters* **14**:132-140
- Oliver TA, Palumbi SR (2011) Many corals host thermally resistant symbionts in high-temperature habitat. *Coral Reefs* **30**:241-250
- Perry JN (1995) Spatial Analysis by Distance Indices. *Journal of Animal Ecology* **64**:303-314
- Perry JN, Winder L, Holland JM, Alston RD (1999) Red-blue plots for detecting clusters in count data. *Ecology Letters* **2**:106-113
- Pochon X, Gates RD (2010) A new *Symbiodinium* clade (Dinophyceae) from soritid foraminifera in Hawaii. *Molecular Phylogenetics and Evolution* **56**:492-497

- Putnam HM, Stat M, Pochon X, Gates RD (2012) Endosymbiotic flexibility associates with environmental sensitivity in scleractinian corals. *Proceedings of the Royal Society B: Biological Sciences* **279**:4352-4361
- Rowan R, Knowlton N (1995) Intraspecific diversity and ecological zonation in coral-algal symbiosis. *Proceedings of the National Academy of Sciences* **92**:2850-2853
- Rowan R, Knowlton N, Baker A, Jara J (1997) Landscape ecology of algal symbionts creates variation in episodes of coral bleaching. *Nature* **388**:265-269
- Sampayo EM, Dove S, Lajeunesse TC (2009) Cohesive molecular genetic data delineate species diversity in the dinoflagellate genus *Symbiodinium*. *Molecular Ecology* **18**:500-519
- Silverstein RN, Correa AMS, Baker AC (2012) Specificity is rarely absolute in coral-algal symbiosis: implications for coral response to climate change. *Proceedings of the Royal Society B: Biological Sciences* **279**:2609-2618
- Simpson MC, Scott D, New M, Sim R, Smith D, Harrison M, Eakin CM, Warrick R, Strong AE, Kouwenhoven P, Harrison S, Wilson M, Nelson GC, Donner S, Kay R, Gledhill DK, Liu G, Morgan JA, Kleypas JA, Mumby PJ, Palazzo A, Christensen TRL, Baskett ML, Skirving WJ, Elrick C, Taylor M, Magalhaes M, Bell J, Burnett JB, Ruttly MK, Overmas M, Robertson R (2009) *An overview of modelling climate change impacts in the Caribbean region with contribution from the Pacific Islands*. United Nations Development Programme (UNDP) Report, Barbados, West Indies
- Stat M, Gates RD (2011) Clade D *Symbiodinium* in scleractinian corals: a nugget of hope, a selfish opportunist, an ominous sign, or all of the above? *Journal of Marine Biology* Article ID 730715, 9 pages
- Stat M, Morris E, Gates RD (2008) Functional diversity in coral-dinoflagellate symbiosis. *Proceedings of the National Academy of Sciences* **105**:9256-9261
- Szmant AM (1991) Sexual reproduction by the Caribbean reef corals *Montastraea annularis* and *M. cavernosa*. *Marine Ecology Progress Series* **74**:13-25
- Tchernov D, Gorbunov MY, de Vargas C, Narayan Yadav S, Milligan AJ, Haggblom M, Falkowski PG (2004) Membrane lipids of symbiotic algae are diagnostic of sensitivity to thermal bleaching in corals. *Proceedings of the National Academy of Sciences of the United States of America* **101**:13531-13535
- Thornhill D, Fitt W, Schmidt G (2006a) Highly stable symbioses among western Atlantic brooding corals. *Coral Reefs* **25**:515-519
- Thornhill DJ, LaJeunesse TC, Kemp DW, Fitt WK, Schmidt GW (2006) Multi-year, seasonal genotypic surveys of coral-algal symbioses reveal prevalent stability or post-bleaching reversion. *Marine Biology* **148**:711-722
- Thornhill DJ, Xiang Y, Fitt WK, Santos SR (2009) Reef endemism, host specificity and temporal stability in populations of symbiotic dinoflagellates from two ecologically dominant Caribbean corals. *PLoS ONE* **4**:e6262
- Toller WW, Rowan R, Knowlton N (2001a) Repopulation of zooxanthellae in the Caribbean corals *Montastraea annularis* and *M. faveolata* following experimental and disease-associated bleaching. *Biological Bulletin* **201**:360-373
- Toller WW, Rowan R, Knowlton N (2001b) Zooxanthellae of the *Montastraea annularis* species complex: Patterns of distribution of four taxa of *Symbiodinium* on different reefs and across depths. *Biological Bulletin* **201**:348-359
- van Hooidonk RJ, Manzello DP, Moye J, Brandt ME, Hendee JC, McCoy C, Manfrino C (2012) Coral bleaching at Little Cayman, Cayman Islands 2009. *Estuarine, Coastal and Shelf Science* **106**:80-84
- Wang J-T, Meng P-J, Chen Y-Y, Chen CA (2012) Determination of the thermal tolerance of *Symbiodinium* using the activation energy for inhibiting photosystem II activity. *Zoological Studies* **51**:137-142
- Warner ME, LaJeunesse TC, Robison JD, Thur RM (2006) The ecological distribution and comparative photobiology of symbiotic dinoflagellates from reef corals in Belize: Potential implications for coral bleaching. *Limnology and Oceanography* **51**:1887-1897
- Weil E, Knowlton N (1994) A multi-character analysis of the Caribbean coral *Montastraea annularis* (Ellis and Solander, 1786) and its two sibling species, *M. faveolata* (Ellis and Solander, 1786) and *M. franksi* (Gregory, 1895). *Bulletin of Marine Science* **55**:151-175
- Ye J, Coulouris G, Zaretskaya I, Cutcutache I, Rozen S, Madden T (2012) Primer-BLAST: A tool to design target-specific primers for polymerase chain reaction. *BMC Bioinformatics* **13**:134-139
- Yee SH, Santavy DL, Barron MG (2008) Comparing environmental influences on coral bleaching across and within species using clustered binomial regression. *Ecological Modelling* **218**:162-174

8

Temporal stability of *Montastraea annularis* symbioses: a Bahamian case study

8.1 Introduction

Montastraea annularis is unusual among Caribbean corals in the flexibility it displays in its symbioses in terms of *Symbiodinium* taxa it can associate with (Toller et al. 2001a). Chapters 5 and 6 explored the extent of this flexibility across a large spatial scale (almost the entire species range), describing symbioses with 22 clades and discussing them in the context of environmental variability, geographic distance and in comparison with host genetic structuring. However, *Symbiodinium* communities within an *M. annularis* colony have also been shown to fluctuate both in terms of density (e.g., seasonal fluctuations in abundance; Warner et al. 2002), and in response to environmental stressors (sporadic changes in abundance and in community composition; Rowan et al. 1997, LaJeunesse et al. 2009) on a temporal scale. Some corals, such as *Acropora millepora*, demonstrate very variable communities from year to year (Cooper et al. 2011). In order to explore how robust the observed spatial patterns recorded in Chapter 5 are, it is necessary to investigate temporal stability in symbiont communities. This chapter describes a small scale study that attempts to assess stability of symbiont communities in *M. annularis* at four sites in the Bahamas, over a total period of six years.

8.1.1 Stability of coral-algal symbioses over time: a contentious issue

Seasonal fluxes in zooxanthellae densities are common, and have been recorded in *M. annularis* in the Bahamas, with higher densities occurring during cooler periods, and lower during warmer summer months (Warner et al. 2002). Changing densities have been positively correlated with host tissue mass (Fitt et al. 2001), irradiance, temperature (Warner et al. 2002) and seawater nitrate concentration (Fagoonee et al. 1999). Whether or not the *composition* of symbiont communities is also flexible on a temporal scale remains contentious. The issue is critical, particularly in the context of projected climate change, as the ability to form flexible symbioses

provides a mechanism for adaptation or acclimation, which may ultimately determine the future of reefs in a changing environment (Baker 2003, Berkelmans & van Oppen 2006). Protagonists, arguing that cnidarian species predominantly associate with just one endosymbiont clade (or a narrow subset) (Goulet 2007), provide evidence that these symbioses remain highly stable even when faced with environmental stressors or transplantation (Goulet 2006, McGinley et al. 2012). One study that investigated symbioses of ancient Caribbean corals suggested stable symbioses with Symbiodinium B1 have lasted >100 years (Baker et al. 2013). In contrast, sceptics of the one-symbiont-per-host hypothesis cite incidences of coral species that, like *M. annularis*, may host multiple endosymbiont clades within a single coral colony (see Chapter 5) (Toller et al. 2001a, Garren et al. 2006, Baker & Romanski 2007), and/or possess substantial diversity of cryptic clades (see Chapter 7) (Mieog et al. 2007, Correa et al. 2009a, Silverstein et al. 2012). Moreover, supporters of the multiple-endosymbiont-clades-per-host theory propose that taxa comprising the symbiont community show dynamic responses to factors such as disease (Toller et al. 2001b although see Correa et al. 2009b) and environmental stress (Kinzie et al. 2001, Toller et al. 2001b, Baker et al. 2004, Berkelmans & van Oppen 2006), that result in either ‘switching’ or ‘shuffling’ their relative abundances (Baker 2003). One study showed a change in the dominant symbiont taxa hosted by *M. annularis* during a period of high thermal stress (LaJeunesse et al. 2009). While evidence exists to support both sides of the argument, it appears that, for corals at least, the question of symbiont community dynamism is complex and likely to vary widely among species (Thornhill et al. 2006a).

8.1.2 Temporal dynamism of *M. annularis* symbiont communities?

M. annularis is atypical among Caribbean corals in displaying temporal changes in symbiont partners (Thornhill et al. 2006b). Over short timescales (days to weeks) the relative proportions of B, C and A and D have been shown to experience appreciable shifts in response to natural (Rowan et al. 1997, LaJeunesse et al. 2009) and experimentally induced (Toller et al. 2001b) bleaching events. Recovering corals may also exhibit ‘successional’ shifts in symbiont populations over timeframes of months (Toller et al. 2001b, LaJeunesse et al. 2009) to years (Thornhill et al. 2006b). Finally, competitive interactions among symbiont taxa occur may over longer timeframes (i.e. years to decades) within colonies as coral growth causes slow changes in microenvironments (such as corallites shifting from the tops to the sides of ramets; Toller et al. 2001b). This has been demonstrated by experimental manipulations of irradiance gradients in *M. annularis*, producing changes in the distribution of clade B and C symbionts within a colony in the space of six months (Rowan et al. 1997).

Substantial field and laboratory evidence exists for varying degrees of symbiont shuffling in *M. annularis* in response to mild to severe environmental change. Does this mean that the distributions of communities observed in Chapter 5 reflect only a snapshot in time? Although

M. annularis is capable of shuffling, a case can be made for a relatively high degree of temporal fidelity in symbiont partnerships in the majority of individual hosts. *M. annularis* has been compared to Caribbean brooding corals (e.g., *Agaricia agaricites*, *Porites astreoides* and *Siderastrea radians*) in terms of the substantial stability in symbiont communities it experiences over longer time periods (Thornhill et al. 2006a). Rowan et al. (1997) reported temporal stability of clade type in their field control *M. annularis* colonies over periods of six months. Toller et al. (2001b)'s experimental manipulations revealed that recovering *M. annularis* generally showed identical zooxanthellae clades as they did prior to treatment, except for in the cases of severe depletion (caused by disease or temperature induced bleaching) where new clades would become established. Thornhill et al. (2006b) went on to demonstrate that even in severely bleached colonies, symbiont communities tended to slowly revert to their original symbioses, with up to five years required for complete post-bleaching reversion. On two reefs, tagged *M. annularis* colonies showed gradual changes in both the identity and proportion of symbiont types D1a, C3 and B1 at one reef, and D1a, B1 and B10 in another until 2002, when a stable dominance of B1 or B10 was eventually re-established (Thornhill et al. 2006b). Another study, which examined population genetic variation in *Symbiodinium* clade B populations hosted by *M. annularis* at two sites in the Bahamas, reported a high degree of reef endemism at the B1 population level, with little evidence of temporal change in endosymbiont type during a two year sampling period (Thornhill et al. 2009).

8.2 Chapter aims

The main aim of this focused study was to assess temporal stability of *M. annularis* symbiont communities across the Bahamian archipelago. From this, we might surmise whether Caribbean partitioning of *Symbiodinium* diversity as presented in Chapter 5 represents a snapshot in time of a dynamic partnership, or a suite of more stable symbioses, from which conclusions about symbiont traits can be derived, and better informed decisions regarding placement of marine reserves and other conservation actions can be formulated (Mumby et al. 2011).

Symbiont communities inhabiting *M. annularis* colonies at two sampling locations adjacent to two Bahamian islands were sampled four times between 2006 and 2012. During this period, several thermal stress events occurred, which may have disrupted the balance of symbionts.

H₀ = the relative proportions of dominant symbionts hosted by Bahamian M. annularis populations at New Providence (Propeller and School House reefs) and San Salvador (Seahorse and Snapshot reefs) remain independent of sampling year, over a six year time period.

Secondly, every sampled *M. annularis* colony was screened for low-abundance *Symbiodinium* D using a high sensitivity method (Chapter 7).

H₀ = detectable background occurrences of Symbiodinium D hosted by Bahmanian M. annularis populations at New Providence (Propeller and School House reefs) and San Salvador (Seahorse and Snapshot reefs) remain independent of sampling year, over a six year time period.

8.3 Methodology

8.3.1 Sampling sites

Four patch reefs, established as sites during a project in 2006 (Foster 2007), were revisited between 2010–2012 for sampling. Propeller reef (Lat (°): 25.0046, Long(°): -77.3309) and School House reef (Lat(°): 24.588, Long(°): -77.3005) are located ~6 km apart on the southwest of New Providence Island (Fig. 8.1). Propeller reef is located 1 km from a power station wastewater outflow pipe, and was dominated by large colonies of *M. annularis*. School House, a similar (but slightly smaller) patch reef east of Propeller, lies further (~3.5 km) offshore.

Snapshot and Seahorse reefs are located on San Salvador Island, lying southeast of New Providence on the eastern limit of the Bahamas archipelago, and more exposed to the open waters of the Atlantic Ocean. Seahorse reef (Lat(°): 24.0878, Long(°): -74.2852), an extensive patch reef with a number of large gorgonians and several *Acropora* spp. across the site, is located 4.5 km off the most northerly tip of San Salvador. Snapshot reef (Lat(°): 24.0230, Long(°): -74.3158), on the western leeward side of San Salvador is slightly more sheltered. Again, the site was dominated by *M. annularis*. All sites were between 3 – 4 m deep.

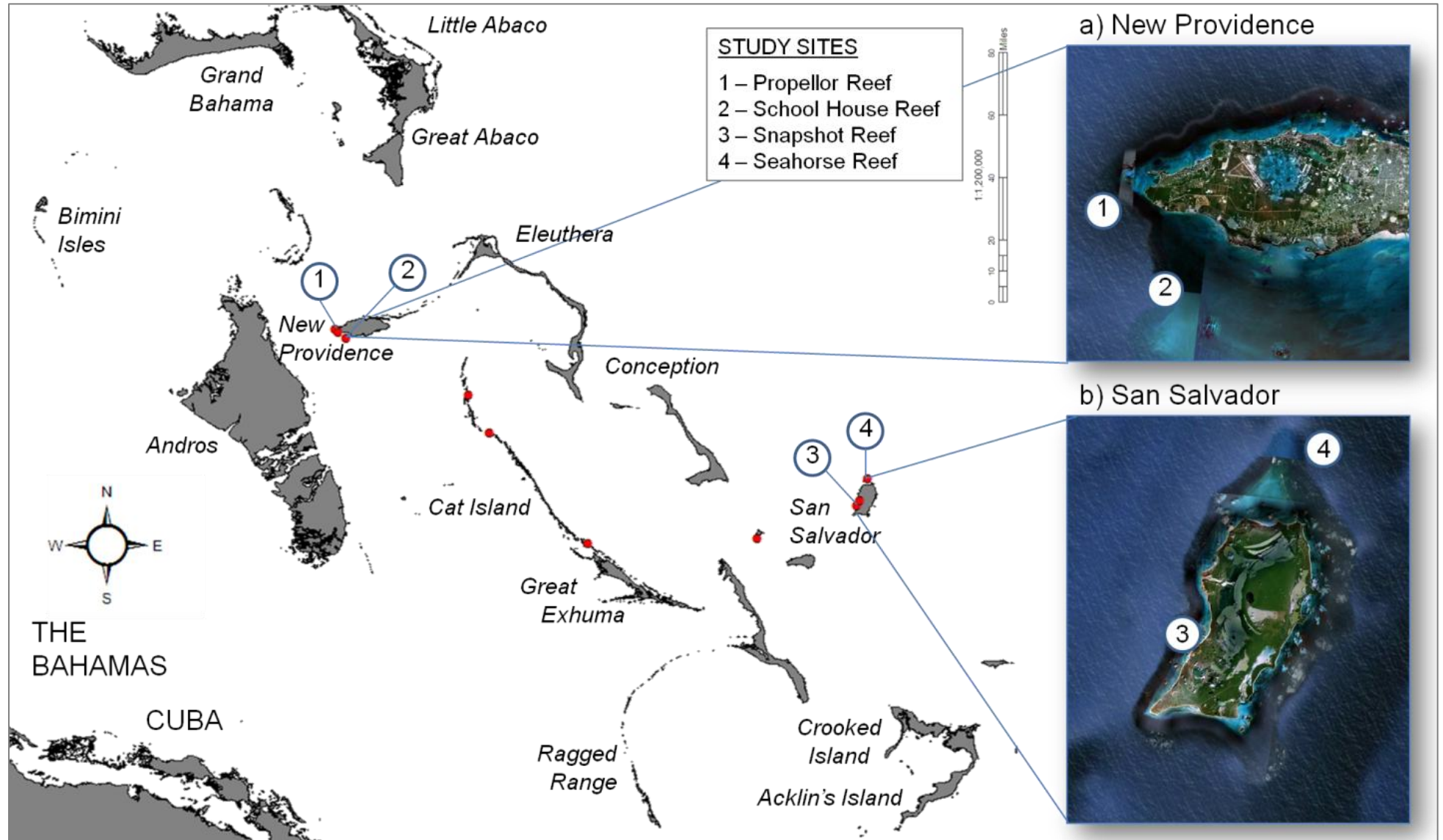


Figure 8.1: Map of the Bahamian archipelago, showing study site locations. Inset a) New Providence Island, b) San Salvador Island

*red dots marked in red indicate sites sampled in 2006 only, see Chapter 5 and Foster 2007.

8.3.2 Sample collection

Field sites, established as part of a study on *Montastraea annularis* (Foster 2007), were accessed using SCUBA, during the third week in June in 2006, and again in 2010, 2011 and 2012. A 10 m wide circular sampling plot (Fig. 8.2), was assembled at each location *sensu* Foster (Foster 2007). The radius of the sampling plot was extended beyond 5 m if less than 30 colonies were found in the initial plot. Thirty separate *M. annularis* ramets within each plot were sampled, the location of each mapped by recording distance (to the nearest 5 cm) from the centre of the sampling plot (marked with a fixed stake), and bearing ($^{\circ}$) (Fig. 8.3). A $\sim 1\text{cm}^2$ sample was gently chipped from the edge of each lobe on each colony using a hammer and a small chisel. Samples were collected in separate labelled plastic ziplock bags, and on returning to the shore were preserved in 90% ethanol and stored at 4°C . A GPS waypoint, time, weather conditions and reef position of each site were also recorded.

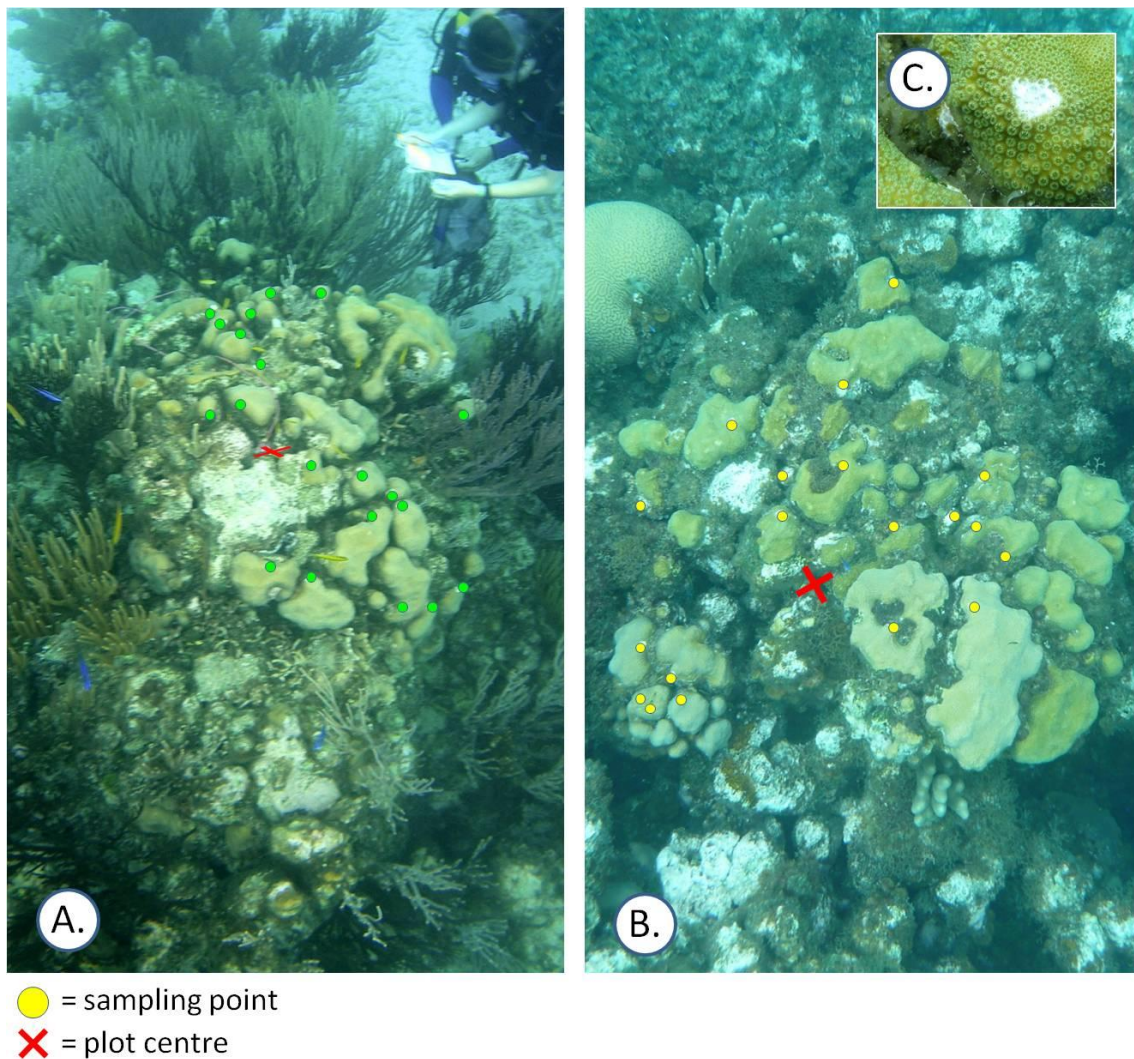


Figure 8.2: Sampling *Montastraea annularis* colonies in the field in San Salvador at A) Snapshot reef and B) Seahorse reef, in 2012. Inset C) shows close up of chisel scrape following polyp removal. Scars were not visible by the following year.

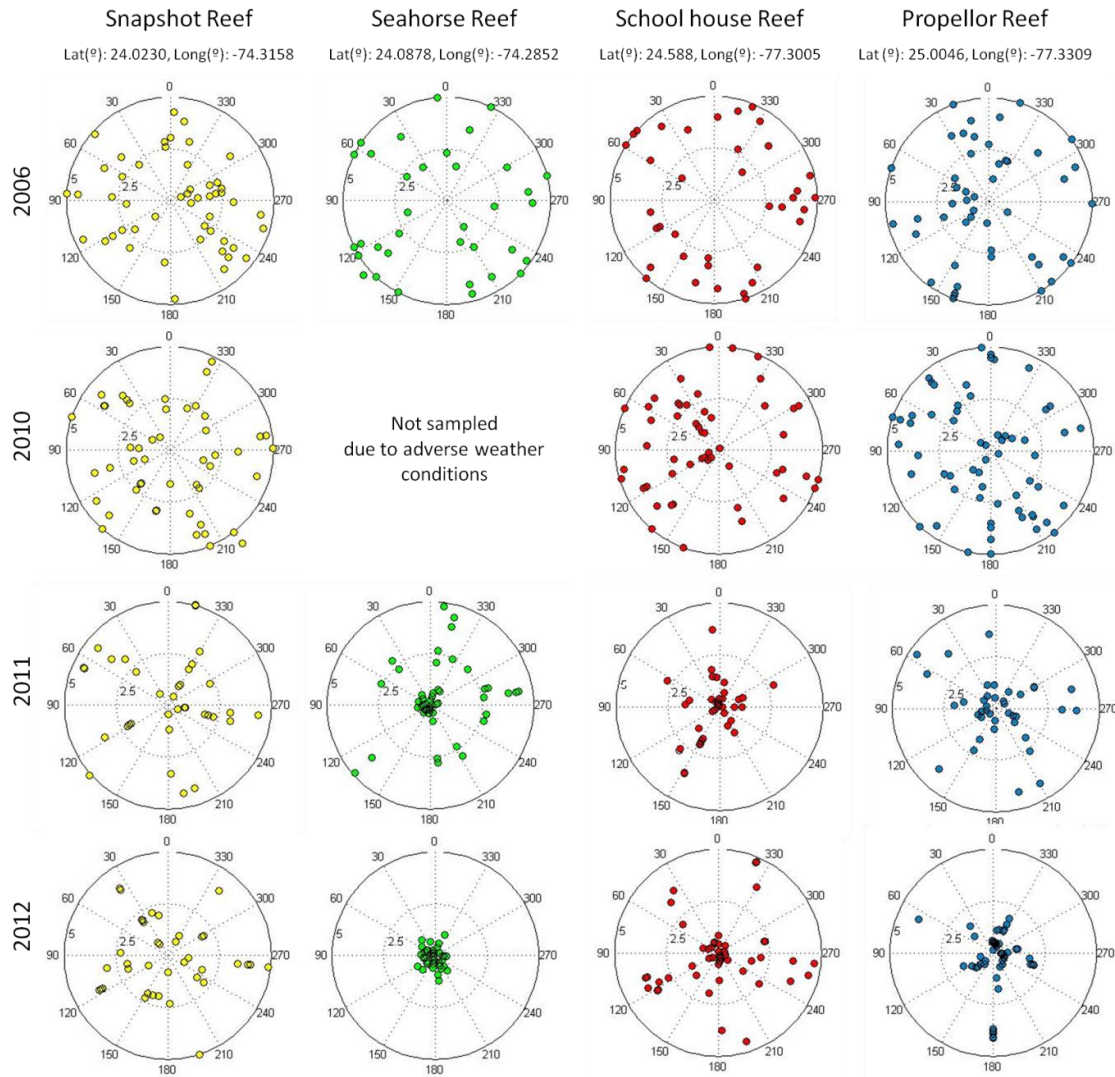


Figure 8.3: Sampling plots for the four sites, during four sampling years.

8.3.3 DNA extraction

Holobiont tissue was homogenised and both host and symbiont DNA extracted overnight using Qiagen DNEasy Blood and Tissue kits. Roughly 1 cm² of tissue was removed from the skeleton using a scalpel, and overnight lysis performed as per the manufacturer's instructions. The following day, purification protocol was followed, with extension at most centrifugation steps owing to the 'gloopy' nature of the lysed product. One µl of the final eluate was used as a template for amplification. The quality of the final eluate was tested using the nanodrop.

8.3.4 DGGE and sequencing

Denaturing gel gradient electrophoresis ('DGGE') was used to identify bands representing zooxanthellae sub-clades within the PCR product for each individual (see Chapter 5, section 5.3.3: *Denaturing Gel Gradient Electrophoresis (DGGE) and sequencing analysis* for full method). Bands were sequenced to confirm identity of sub-clades, and added to an alignment, which was

compared to a database of all known Caribbean *Symbiodinium* ITS2-types extracted from the open access web-resource GeoSymbio (Frankin et al. 2012), see Appendix Table 8.1.

8.3.5 Screening for *Symbiodinium* D

Real-time PCR in conjunction with high resolution melt (HRM) analysis were used to screen each *M. annularis* colony specifically for the presence or absence of low abundance *Symbiodinium* D (see Chapter 7, section 7.3.3: *RT-PCR analysis* for full method).

8.3.6 Statistical analyses

Zooxanthellae communities and occurrences of low-abundance D could then be compared within and between sites, and between years. An extended Fisher Exact Test of independence was used to determine shuffling between dominant *Symbiodinium* sub-types at each of the four locations, as well as for the region overall (Freeman & Halton 1951). Chi-squared was not appropriate for the site-level analyses due to sample size. Seahorse reef was excluded from the regional analysis as some time-point data were missing.

8.4 Results

8.4.1 Temporal stability of dominant symbionts

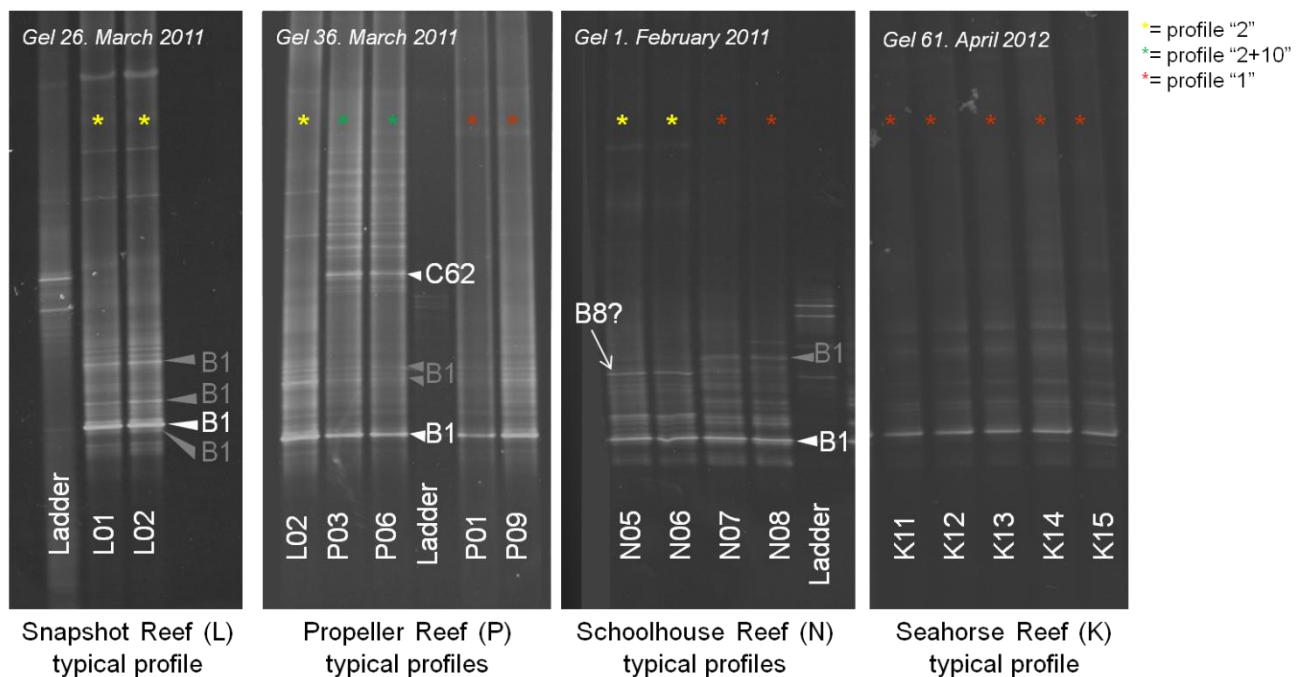


Figure 8.4 DGGE gel images revealing the most common banding patterns found at each site

The symbiont communities sampled from 248 spatially independent *M. annularis* ramets were categorised using a combination of PCR-DGGE fingerprinting and sequencing. Every

individual generated one bright further-migrating band on the gel, corresponding to the B1 symbiont (Fig. 8.4). In many lanes, additional bands were present. Sequencing revealed these either to be B1 heteroduplexes, or other B or C clade types.

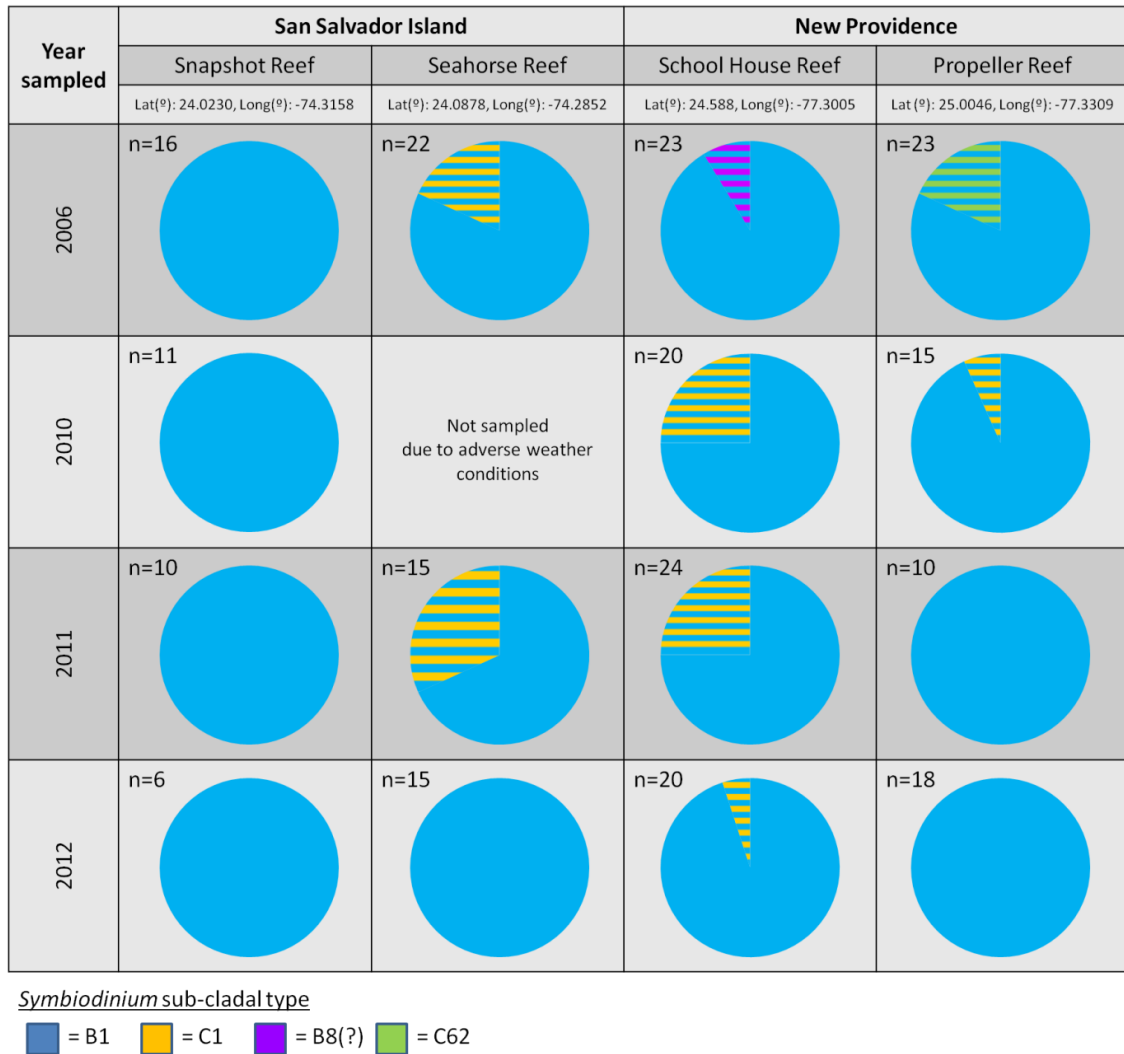


Figure 8.5 Pie charts representing dominant *Symbiodinium* types harboured by *M. annularis* ramets across four Bahamian reefs (Snapshot, Seahorse, School House and Propeller reefs) at four time points: 2006, 2010, 2011 and 2012. Striped pie sections represent a pair of co-dominant types.

Snapshot reef samples generated homogenous profiles, comprising one bright low molecular weight B1 band on a gel, and two or more slightly larger bands a short way above, in a smear (Fig 8.4). In several samples there was a faint band directly below the B1 band. Sequencing revealed all three of these bands to be B1 heteroduplexes, in addition to confirming the dominant band as B1. Limited change was observed across the four time points, with B1 dominating every sample tested (Fig. 8.5).

Propeller reef (P) displayed more variable *Symbiodinium* DGGE profiles, although every sample had a dominant B1 band, and many showed heteroduplexes similar to those generated from Snapshot reef *Symbiodinium* samples (Profile 2). An additional slower migrating band was

present in several 2006 samples, P03, P06, P16 and P17 (Fig. 8.4). Although these bands appeared in a ‘C7’ position (a sub-clade commonly found in *M. annularis*, see Chapter 5), sequencing of this band revealed a different endosymbiont type, which aligned best with sub-clade C62 in alignments with all known types (GeoSymbio; Frankin et al. 2012). This type has not been previously reported to inhabit *M. annularis*. Snapshot and Propeller reef samples shared the higher of the heteroduplexes present in Snapshot samples, but several samples (P12, P13) also showed a slower-migrating band in the approximate D1a position. Symbiont communities sampled in 2010 were all dominated by the B1 band, but again were quite varied, with P17 and P07 generating an uncommon lower band, and P20 and P53 also showed unusual bands here – although these were not dominant. The 2011 and 2012 samples appeared more uniform with little difference between communities hosted by each colony (Fig. 8.5).

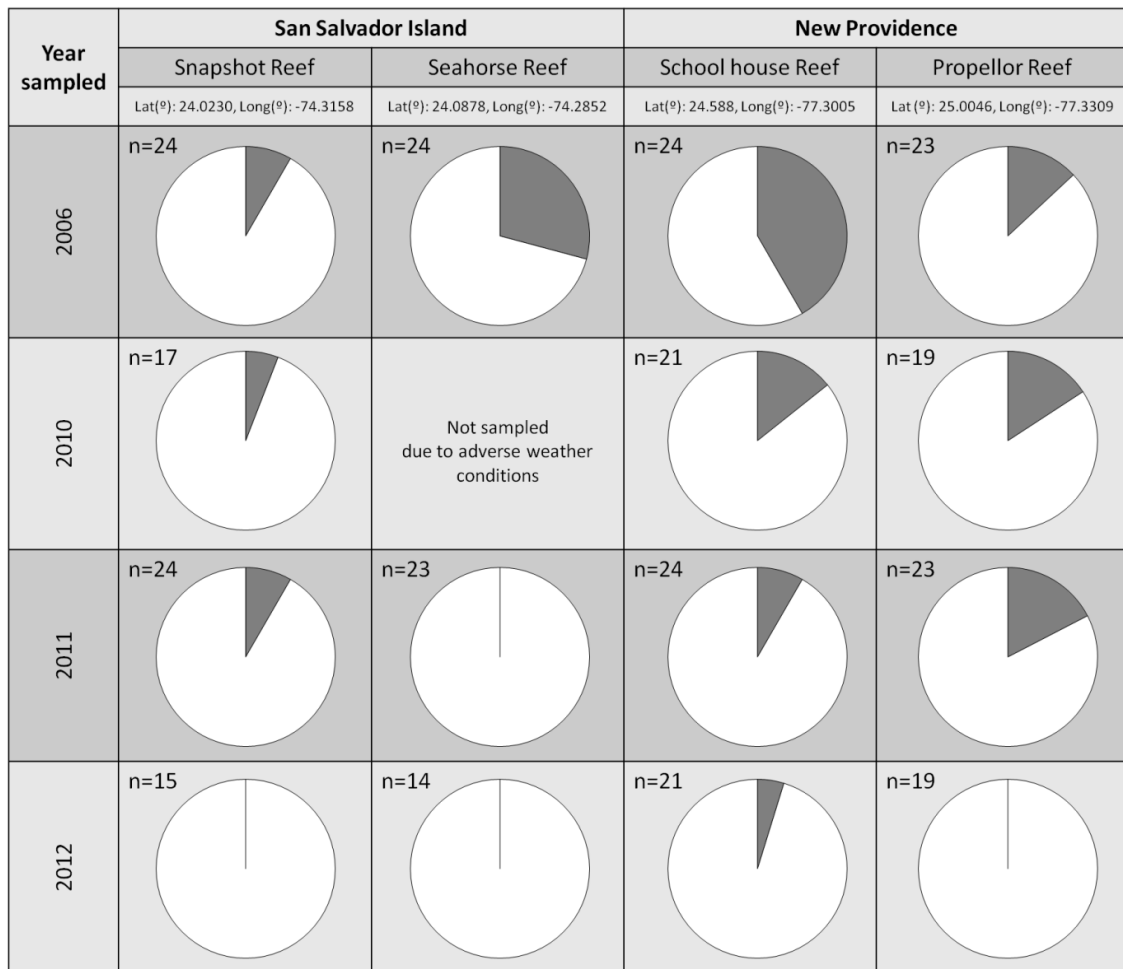
Location	df	Fishers Exact p-value
Snapshot reef	0	1.000
Seahorse reef	2	0.042
School House reef	6	0.152
Propeller reef	6	0.215
Bahamas (total)*	3	0.088

Table 8.1 Results of Fisher’s Exact Test comparing temporal changes in the dominant symbiont hosted at each location, demonstrates that relative proportions of dominant symbionts remain independent from year to year at the 1% significance level. *Seahorse reef was excluded from the Bahamas total calculation, as data were missing from 2010.

School House reef (N) DGGE fingerprints revealed fairly uniform communities, with most samples (e.g. N07 and N08) exhibiting profiles similar to Snapshot reef, with a band below B1 (B10?) and a few N05 and N06, showing slightly different banding, with a higher band around the D1 position. However, re-running some School House samples adjacently on the same gel (gel 41) to some from Snapshot indicated the paler bands from School House were consistently in a different fingerprint position – slightly higher than in the Snapshot profile (2). Sequencing of the dominant band and heteroduplexes revealed all to be B1 or heteroduplexes. The unusual band in N05 and N06 also had a different sequence (Fig. 8.4); temporarily named “Btype10”, but the method was unable to confidently identify this symbiont: a BLAST search revealed B8 to be a similar. The 2010, 2011 and 2012 samples all generated a mix of profiles, with some co-dominant for B1 and C1, but most exclusively dominant for B1. Seahorse reef (K) showed relatively simple profiles dominated by a single band in the B1 position. Occasionally, e.g. in sample K29, a much higher band (C1) was co-dominant with B1.

An extended Fisher Exact Test confirmed that the relative proportion of dominant C and B clades observed remained independent of the sampling time point ($p=0.088$). This result was also confirmed at site level, except for at Seahorse Reef, where a significant change in the proportion of C clade symbionts hosted between 2011 and 2012 meant that community composition was not independent of time ($p=0.042$). Overall, these results demonstrate temporal stability in the dominant types hosted by *M. annularis* across the Bahamas, and at all reef sites included in this study, with the exception of Seahorse Reef.

8.4.2 Temporal stability of cryptic *Symbiodinium D*



Symbiodinium detected

Figure 8.6 Pie charts displaying changes in the relative number of *Montastraea annularis* ramets found to host low abundances of *Symbiodinium D*, at four different sites in the Bahamas (Snapshot, Seahorse, School House and Propeller reefs), at four time points (June of 2006, 2010, 2011, 2012)

Symbiodinium D was detected in *M. annularis* colonies at all four sites, and also at all four time points (Fig 8.6). Where D was present at a site, it was harboured by 5% to 42% of colonies. Over time, there appeared to be a decline in the number of colonies hosting low abundances of D, from an average 23% of colonies (across all sites) hosting D in 2006, to 12% in 2010, to 9%

in 2011 and just 1% in 2012. In 2012 D was only detected in just one colony at School House reef (Fig. 8.6).

Extended Fisher Exact Tests revealed temporal differences in the number of colonies hosting D at two of the sites – Seahorse reef and School House reef, but not at Snapshot or Propeller Reefs (Table 8.2).

Location	df	Fishers Exact p-value
Snapshot reef	3	0.859
Seahorse reef	2	0.002
School House reef	3	0.006
Propeller reef	3	0.306
Bahamas (total)	3	<0.001

Table 8.2 Results of Fisher’s Exact Test comparing temporal changes in *Symbiodinium* D hosted by *M. annularis* ramets at four Bahamian locations, showing that the relative proportions of colonies hosting D were dependent on sampling year. Seahorse and School House reef symbiont communities were deemed independent between years at the 1% level (significant differences in bold).

8.5 Discussion

8.5.1 Temporal stability of symbiont communities

In this chapter the apparent temporal stability in the endosymbionts dominating *M. annularis* ramets at three out of four Bahamian reef sites, over a six-year period has been demonstrated. At all four study sites, at all sampling time points, symbiont ITS2-type B1 was found to be dominant, and was hosted by 100% of colonies. Snapshot reef showed a stable community of B1, in all samples, over the entire sampling period. At the remaining three sites more variation in community composition was evident. At Propeller, Seahorse and School House reefs B1 was shown to share dominance with C1 in a proportion of colonies, while in 2006, B1 from four colonies at Propeller and two colonies at School House reef was co-dominant with C and B symbiont types that could not be confidently identified (possibly C62 and B8, respectively). However, annual variation in the absolute number of ramets hosting a dominant pair of symbionts (as opposed to exclusively B1) were not deemed significant by Fisher Exact Tests ($p > 0.01$). This implies substantial temporal stability over a six year time period, meaning that the first null hypothesis (of no observable change in symbiont dominance over the study period) cannot be rejected (Section 8.2), although more data and a most robust study design would be desirable to fully test the null hypothesis and draw conclusions with confidence (Section 8.5.3).

It is difficult to explain the difference between Seahorse Reef and the other sites: this offshore reef site was considerably more exposed than the others, and differences between inner and outer reefs (generally driven by water quality factors) are consistently identified as important in driving symbiont community partitioning (Garren et al. 2006, LaJeunesse et al. 2010, Cooper et al. 2011). One explanation for the difference observed in temporal stability between *M. annularis* on Seahorse reef – an exposed, offshore reef location – and the other more sheltered sites may be driven by local scale variation in *Symbiodinium* communities.

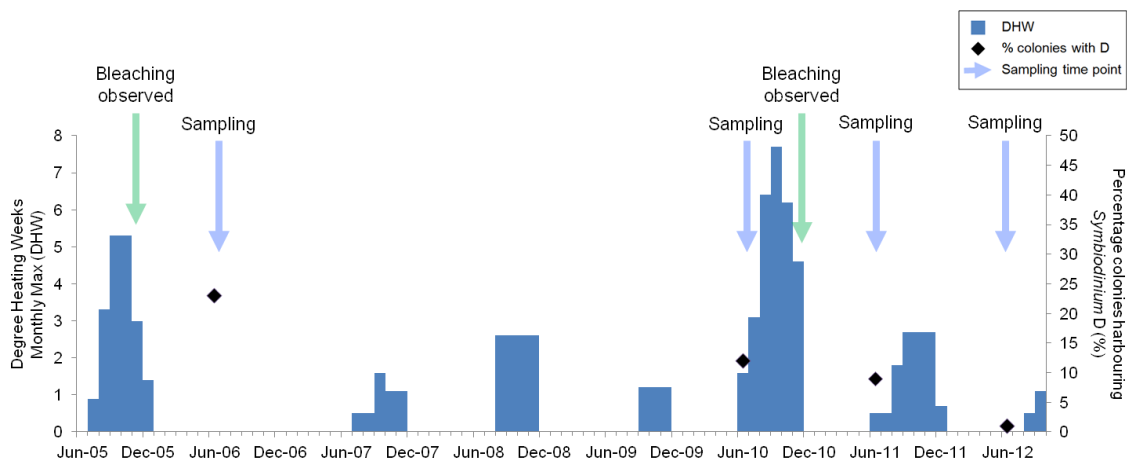


Figure 8.7. Bar chart showing accumulated degree heating weeks (a measure of thermal stress) in the Bahamas (Data from the Bahamas monitoring station, Lee Stocking Island (Long – 76.500, Lat 23.500: approx 200 km from both sampling sites). Bleaching commonly occurs when DHWs exceed 4. Percentage of *M. annularis* colonies harbouring low levels of D are also plotted. Data extracted from ReefBase.

Overall, the result appears to agree with the other studies that have demonstrated overall temporal stability of *M. annularis* symbiont communities – in the absence of severe thermal stress events - over comparable time periods e.g., two years (Warner et al. 2006) to five years (Thornhill et al. 2006b). Researchers who sampled twelve tagged *M. annularis* colonies in the Bahamas 15 times between August 2000 and August 2004 also found all colonies were dominated by B1 throughout the duration of sampling – although a few deeper colonies (12 m) had several instances of mixed B1 and C12 (Thornhill et al. 2006b). In another study, the same researchers found that none of the genetic variation within the *Symbiodinium* B1 populations was attributable to sampling time points from *M. annularis* (or *M. faveolata*) across the Bahamas (or Florida) (Thornhill et al. 2009), with reef location more important in explaining diversity (in *M. annularis* all genotypes were site specific).

However, two severe thermal stress events – one in November 2005, just eight months prior to the first sampling point, and a second in October 2010, between the second and third time points, occurred in the region (Fig 8.7). These SST anomalies might have been expected to influence symbiont community composition, especially if bleaching was triggered in our colonies. Bleaching events near the study sites were described by local scientists and dive operators, although no quantitative estimates exist during these periods. On San Salvador during November 2005, the Bahamian Reef Survey team (Earthwatch Institute) noted that “bleaching

was evident primarily on *Agaricia* sp., *Favia fragum*, and *Porites* sp. ... limited bleaching of *Montastraea annularis* was also observed; however, many coral heads of this species displayed significant blanching” (source: Coral-List posting). Bleaching here does not appear to be as severe as the 1998 event, where 60% of all *M. annularis* bleached on San Salvador Island (McGrath and Smith 2005) (Peckol et al. 2003). The principal scientist from the Earthwatch team, John Rollino, compared his observations to the milder 1995/6 bleaching event, where just 2% of *M. annularis* colonies bleached (McGrath & Smith 2005). Bleaching was described in San Salvador by the same team in December 2010, again noting *Agaricia agaricites* colonies bleaching over 75% of their surface, and mortality in their 15-month old *Acropora palmata* transplants, although it was noted that *Montastraea* sp. exhibited “little, if any, ill effects”. Meanwhile, bleaching was also reported in October 2010 by Stuarts Cove Dive Operators at sites around the south east of New Providence (School House and Propeller reefs). “All sites exhibited some bleaching”, although more detailed information on the bleaching severity and impact on different species was not provided.

Thermal stress events clearly affected the reefs of San Salvador and New Providence during the period of our study. However, the lack of a severe bleaching response in *M. annularis* may explain why dominant symbionts hosted by were maintained throughout the study period. Whether comparable temporal stability in symbiont dominance would have been maintained throughout a more severe bleaching event – such as observed in 1998 – is unknown. B1 has clearly maintained its dominance over several stressful periods (Fig. 8.7) demonstrating a high degree of temporal stability in our holobiont.

8.5.2 Temporal stability of low-abundance D

The second part of the study focussed on a thermally tolerant symbiont known to be present in relatively low densities of *M. annularis* colonies. *Symbiodinium* D was detected in a proportion of colonies at all sites (at at least one time point), but occurrence diminished over the study, with just one colony (out of 69 sampled in 2012) observed to contain D in 2012, compared to 22 colonies (out of 95) sampled in 2006. At Seahorse and School House reefs, observed differences between sampling time points were shown to be significant by Fisher Exact Tests ($p < 0.01$).

This result agrees with findings of studies that have reported an eventual post-bleaching reversion to original symbiont communities, which involves a reduction of *Symbiodinium* D (thought to incur tradeoffs in terms of calcification efficiency) following increases in density during (or in the build up to) bleaching (Thornhill et al. 2006b, LaJeunesse et al. 2009). It has been suggested that D may naturally persist at trace background levels within symbiont communities, and that stress events – such as elevated SSTs – may trigger a shift in relative abundance to detectable levels (Smith, PhD thesis). Perhaps the ‘blanching’ observed by John Rollino in Bahamian *M. annularis* in November 2005 facilitated shuffling of low *Symbiodinium*

D abundances to detectable levels seven months later, in our 2006 survey. Other studies show high amount of D prior to, during and immediately after bleaching (Thornhill et al. 2006b, LaJeunesse et al. 2009). In a Barbadian study, levels of D remained high for at least seven months following a bleaching event in October 2005, and were still comparable with bleaching levels in April/May 2006, only dropping off after 24 months (LaJeunesse et al. 2009). In a Florida study, D1a was detected in the tops of *M. annularis* colonies prior to the 1998 bleaching event, and remained detectable (by DGGE) in a community of six coral colonies until May 2002, after which it was not again detected (the study ended in August 2004) (Thornhill et al. 2006b). Without sampling prior to 2005 it cannot be known whether these levels (23% of colonies) are normal for the Bahamas or not, although Chapter 6 suggests at least 30% of colonies across the Caribbean contain cryptic D, and 28% of healthy *M. annularis* colonies contained cryptic D in Barbados (LaJeunesse et al. 2009).

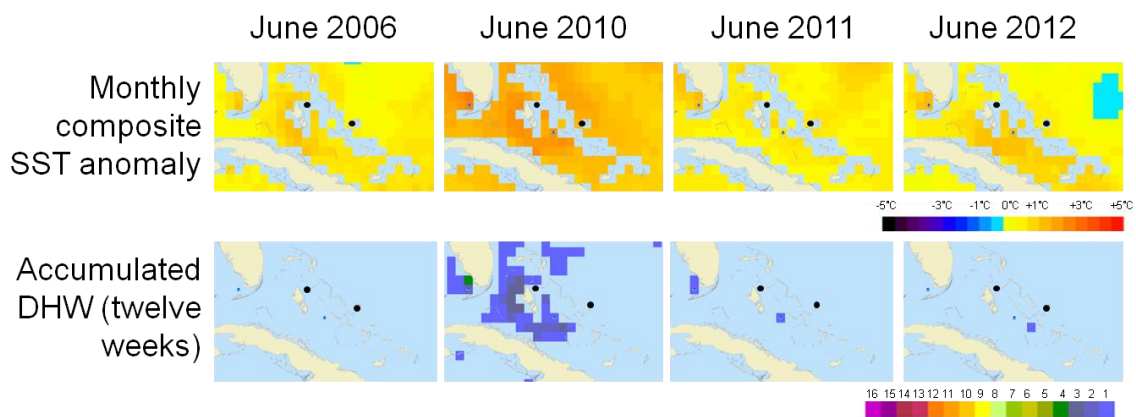


Figure 8.8. Maps showing SST anomalies, and DHWs (both measures of thermal stress) for the Bahamas during sampling months. Maps provided by ReefBase. Black dots represent sampling site locations.

Lack of survey data from 2007 – 2009 creates uncertainty as to whether prevalence of D declined, or was maintained, between our first two sampling time points. If thermal stress is important in influencing D, the 2008 accumulated Degree Heating Weeks (DHWs) (Fig. 8.7) may have affected the number of colonies hosting D, although no bleaching reports were found for our sites in 2008. The colonies from 2010 were sampled six months prior to reported reef bleaching, although incidences of low abundance D have been shown to accumulate in *M. annularis* in the build up to bleaching events (LaJeunesse et al 2009). The 12% prevalence of D we recorded in 2010 may be a legacy from the 2005 (or possible 2008) thermal stress events, or as an immediate response to the elevated temperatures observed in June 2010 (Fig. 8.7). The latter seems more likely, as if the declining trends we observe are true, then D densities are clearly able to drop to undetectable levels within the space of a year (e.g., 2011 to 2012) if environmental conditions are correct.

In 2011 D was detected at three of the four sites: again six months after an observed bleaching event (albeit one where *M. annularis* did not appear to bleach). *Symbiodinium* D was barely

detected in 2012: if abundances are linked to thermal stress events this may be due to more stable temperature conditions enabling other symbionts to gradually re-establish full dominance, and supporting previous studies suggesting post-bleaching reversion in *M. annularis* (Thornhill et al. 2006b).

Two of our study sites – Snapshot and Propeller reef – did not show significant changes in the number of ramets hosting D, while Seahorse and School House reef clearly did. Propeller reef – situated by a warm water outflow – may have maintained a high level of background D for this reason. It is impossible to reliably attribute the decline in the number of ramets hosting detectable D to thermal stress events, however it seems likely that thermal stress may be providing a mechanism by which low level densities of different symbiont taxa are in a continual state of flux. *M. annularis* is documented as being one of the first species to bleach on the reef and has been shown to be more susceptible to water temperature increases than other corals (Fitt et al 1995, McField 1999). Perhaps a fluctuating presence of D reported in this study may explain why, in 2005 and 2010, *M. annularis* in the Bahamas appeared to avoid bleaching.

8.5.3 Study limitations

This short term study served its purpose by demonstrating annual stability in populations from year to year, but had some severe limitations. Although sampling at the same location gave a good impression of the behaviour of the population at each site – and in many cases photographs taken during sampling meant it was known that the exact same colony was sampled – refinement of the study design to tagging colonies so that the exact same ramet was re-sampled at each time point would have provided interesting data on how individual colonies were behaving. Without sampling the exact same colony, we cannot be confident that the minor changes in symbiont community observed reflect symbiont shuffling within a single colony, or naturally occurring variation in stable symbiont communities among colonies. Secondly, expansion of the study both spatially – to include sites known to host more diverse and co-dominant symbiont communities (e.g., eastern Caribbean communities, see Chapter 4) – and temporally – to sample at more frequent time points (weekly to monthly) - would be a requirement before any firm conclusions were drawn about community stability. Many of the documented responses to elevated SST have occurred over timescales of weeks to months (Toller et al 2001, LaJeunesse et al 2009), while symbiont densities in Bahamian *M. annularis* are known to fluctuate seasonally (Warner et al. 2002). In Chapter 5 we discussed how high amount of variability in symbiont communities can be partitioned to colony level: adopting a sampling methodology to test samples from multiple locations on the same coral colony can help resolve spatial heterogeneity of *Symbiodinium* assemblages in *Montastraea* (Kemp et al. 2008).

One way to improve the study's resolution might be to examine the population dynamics of the most dominant clade B1 (present in 100% of our Bahamian samples). Microsatellites have been characterised for this symbiont (also known as *Symbiodinium trenchii*, LaJeunesse et al 2005) (Appendix Table 8.4). As a preliminary exercise seven polymorphic microsatellite loci were selected – based on a study into B1 diversity in the common sea fan, *Gorgonia ventalina*, across the Florida Keys (Kirk et al. 2009) – a multiplex designed, primers optimised and used to amplify the seven regions in selected samples from four Bahamian populations, and a Jamaican outgroup. One locus appeared to be monomorphic for our populations, but the other primer sets amplified between three and 14 alleles. This could form the basis of further work into understanding of B1 population diversity.

8.5.4 Conclusions

In this chapter we were able to show temporal stability of dominant symbionts in *M. annularis* over a six year time period, suggesting that spatial patterns in symbiont biogeography observed in Chapter 5 are likely to be fairly robust over time periods of five to ten years. This stability appears to be a feature of not just *M. annularis*, but other Caribbean species (Warner et al. 2006, Thornhill et al. 2006a). However, instability in background abundances of D at two sites suggest that while it might take an extreme environmental perturbation to trigger a shift in the dominant symbiont, or symbiont pair, at a low level symbiont taxa within a community are likely to be experiencing mild but continual shuffling in their relative abundances, as they jostle in response to seasonal or environmental changes.

8.6 Acknowledgements

Many thanks to Nicola Foster, for donating the 2006 samples; Tom Rothfus and Rochelle Hanna at the Gerace Centre, San Salvador, for assistance with permits and equipment; Jan and Phil Shears for sampling assistance; Riding Rock dive outfit, San Salvador; Fran and Monty at Custom Aquatics, New Providence, and the Bahamian Dept of Fisheries for access. All diving adhered to the University of Exeter code of conduct and complied with Gerace Research Centre scientific diving regulations.

8.7 References

- Baker AC (2003) Flexibility and specificity in coral-algal symbiosis: Diversity, ecology, and biogeography of *Symbiodinium*. *Annual Review of Ecology Evolution and Systematics* **34**:661-689
- Baker AC, Romanski AM (2007) Multiple symbiotic partnerships are common in scleractinian corals, but not in octocorals: Comment on Goulet (2006). *Marine Ecology Progress Series* **335**:237-242
- Baker AC, Starger CJ, McClanahan TR, Glynn PW (2004) Coral reefs: corals' adaptive response to climate change. *Nature* **430**:741-741
- Baker DM, Weigt L, Fogel M, Knowlton N (2013) Ancient DNA from coral-hosted *Symbiodinium* reveal a static mutualism over the last 172 years. *PLoS ONE* **8**:e55057
- Berkelmans R, van Oppen MJH (2006) The role of zooxanthellae in the thermal tolerance of corals: a 'nugget of hope' for coral reefs in an era of climate change. *Proceedings of the Royal Society B-Biological Sciences* **273**:2305-2312
- Cooper TF, Berkelmans R, Ulstrup KE, Weeks S, Radford B, Jones AM, Doyle J, Canto M, O'Leary RA, van Oppen MJH (2011) Environmental factors controlling the distribution of *Symbiodinium* harboured by the coral *Acropora millepora* on the Great Barrier Reef. *PLoS ONE* **6**:e25536
- Correa A, McDonald M, Baker A (2009a) Development of clade-specific *Symbiodinium* primers for quantitative PCR (qPCR) and their application to detecting clade D symbionts in Caribbean corals. *Marine Biology* **156**:2403-2411
- Correa AMS, Brandt ME, Smith TB, Thornhill DJ, Baker AC (2009b) *Symbiodinium* associations with diseased and healthy scleractinian corals. *Coral Reefs* **28**:437-448
- Fagoonee I, Wilson HB, Hassell MP, Turner JR (1999) The dynamics of zooxanthellae populations: a long-term study in the field. *Science* **283**:843-845
- Fitt W, Brown B, Warner M, Dunne R (2001) Coral bleaching: interpretation of thermal tolerance limits and thermal thresholds in tropical corals. *Coral Reefs* **20**:51-65
- Foster NL (2007) Population dynamics of the dominant Caribbean reef-building coral, *Montastraea annularis*. Ph.D, University of Exeter
- Frankin EC, Stat M, Pochon X, Putnam HM, Gates RD (2012) GeoSymbio: a hybrid, cloud-based web application of global geospatial bioinformatics and ecoinformatics for *Symbiodinium*-host symbioses. *Molecular Ecology Resources* **12**:369-373
- Freeman GH, Halton JH (1951) Note on an Exact Treatment of contingency, Goodness of Fit and other problems of significance. *Biometrika* **38**:141-149
- Garren M, Walsh S, Caccone A, Knowlton N (2006) Patterns of association between *Symbiodinium* and members of the *Montastraea annularis* species complex on spatial scales ranging from within colonies to between geographic regions. *Coral Reefs* **25**:503-512
- Goulet TL (2006) Most corals may not change their symbionts. *Marine Ecology Progress Series* **321**:1-7
- Goulet TL (2007) Most scleractinian corals and octocorals host a single symbiotic zooxanthella clade. *Marine Ecology Progress Series* **335**:243-248
- Kemp D, Fitt W, Schmidt G (2008) A microsampling method for genotyping coral symbionts. *Coral Reefs* **27**:289-293
- Kinzie RA, Takayama M, Santos SR, Coffroth MA (2001) The Adaptive Bleaching Hypothesis: experimental tests of critical assumptions. *Biological Bulletin* **200**:51-58
- Kirk N, Andras J, Harvell C, Santos S, Coffroth M (2009) Population structure of *Symbiodinium* sp. associated with the common sea fan, *Gorgonia ventalina*, in the Florida Keys across distance, depth, and time. *Marine Biology* **156**:1609-1623
- LaJeunesse TC, Pettay DT, Sampayo EM, Phongsuwan N, Brown B, Obura DO, Hoegh-Guldberg O, Fitt WK (2010) Long-standing environmental conditions, geographic isolation and host-symbiont specificity influence the relative ecological dominance and genetic diversification of coral endosymbionts in the genus *Symbiodinium*. *Journal of Biogeography* **37**:785-800
- LaJeunesse TC, Smith RT, Finney J, Oxenford H (2009) Outbreak and persistence of opportunistic symbiotic dinoflagellates during the 2005 Caribbean mass coral 'bleaching' event. *Proceedings of the Royal Society B: Biological sciences* **276**:4139-4148
- McGinley MP, Aschaffenburg MD, Pettay DT, Smith RT, LaJeunesse TC, Warner ME (2012) *Symbiodinium* spp. in colonies of eastern Pacific *Pocillopora* spp. are highly stable despite the prevalence of low-abundance background populations. *Marine Ecology Progress Series* **462**:1-7
- McGrath TA, Smith GW (2005) Variations in scleractinian coral populations on patch reefs around San Salvador Island, Bahamas 1992 - 2002. In: Buckner SD, McGrath TA (eds) *Proceedings of the 10th Symposium on the Natural History of the Bahamas*, San Salvador, Bahamas

- Mieog JC, Oppen MJH, Cantin NE, Stam WT, Olsen JL (2007) Real-time PCR reveals a high incidence of *Symbiodinium* clade D at low levels in four scleractinian corals across the Great Barrier Reef: implications for symbiont shuffling. *Coral Reefs* **26**:449-457
- Mumby PJ, Elliott IA, Eakin CM, Skirving W, Paris CB, Edwards HJ, Enríquez S, Iglesias-Prieto R, Cherubin LM, Stevens JR (2011) Reserve design for uncertain responses of coral reefs to climate change. *Ecology Letters* **14**:132-140
- Peckol PM, Curran HA, Greenstien BJ, Floyd EY, Robbart ML (2003) Assessment of coral reefs off San Salvador Island, Bahamas (stony corals, algae and fish populations). In: Lang JC (ed) *Status of coral reefs in the Western Atlantic: results of initial surveys*. AGRRA program, p 124-144
- Rowan R, Knowlton N, Baker A, Jara J (1997) Landscape ecology of algal symbionts creates variation in episodes of coral bleaching. *Nature* **388**:265-269
- Silverstein RN, Correa AMS, Baker AC (2012) Specificity is rarely absolute in coral-algal symbiosis: implications for coral response to climate change. *Proceedings of the Royal Society B: Biological Sciences* **279**:2609-2618
- Thornhill D, Fitt W, Schmidt G (2006a) Highly stable symbioses among western Atlantic brooding corals. *Coral Reefs* **25**:515-519
- Thornhill DJ, LaJeunesse TC, Kemp DW, Fitt WK, Schmidt GW (2006b) Multi-year, seasonal genotypic surveys of coral-algal symbioses reveal prevalent stability or post-bleaching reversion. *Marine Biology* **148**:711-722
- Thornhill DJ, Xiang Y, Fitt WK, Santos SR (2009) Reef endemism, host specificity and temporal stability in populations of symbiotic dinoflagellates from two ecologically dominant Caribbean corals. *PLoS ONE* **4**:e6262
- Toller WW, Rowan R, Knowlton N (2001a) Zooxanthellae of the *Montastraea annularis* species complex: patterns of distribution of four taxa of *Symbiodinium* on different reefs and across depths. *Biological Bulletin* **201**:348-359
- Toller WW, Rowan R, Knowlton N (2001b) Repopulation of zooxanthellae in the Caribbean corals *Montastraea annularis* and *M. faveolata* following experimental and disease-associated bleaching. *Biological Bulletin* **201**:360-373
- Warner M, Chilcoat G, McFarland F, Fitt W (2002) Seasonal fluctuations in the photosynthetic capacity of photosystem II in symbiotic dinoflagellates in the Caribbean reef-building coral *Montastraea*. *Marine Biology* **141**:31-38
- Warner ME, LaJeunesse TC, Robison JD, Thur RM (2006) The ecological distribution and comparative photobiology of symbiotic dinoflagellates from reef corals in Belize: potential implications for coral bleaching. *Limnology and Oceanography* **51**:1887-1897

9

General Discussion

9.1 Project evaluation

This project makes several contributions to the field of coral reef research and environmental change; the most important of which relate to past and future changes in the ability of Caribbean reefs to maintain structural growth (9.1.1), but also the distribution and diversity of *Symbiodinium* in *Montastraea annularis* across its Caribbean range (9.1.2).

9.1.1 Caribbean carbonate budgets and reef growth

The primary contribution of Chapters 3 and 4 are the integration of ecological and geological processes into a complex theoretical carbonate budget model, subsequently used to assess Caribbean reef functioning from the recent ecological past into the future. Using documented ecological perturbations on reefs across the region, past reef construction and bioerosion is simulated: the key finding from this being that over the last 50 years Caribbean reefs have likely transitioned from states characterized by high rates of carbonate production (“healthy” reefs in the 1960s and 70s) to an increasingly fragile state, hovering between net reef accretion and erosion (“degraded” reefs of the 2000s). These changes have been principally driven by coral cover loss, changes in the biomass of *Diadema antillarum* and parrotfish, sedimentation and nutrient pollution. However, the stressors affecting Caribbean reefs today are shifting, with the dominant threat evolving from simply local pressures (sedimentation, nutrient pollution, fishing, disease) to include global-scale stressors (coral bleaching; Hoegh-Guldberg et al. 2007). This will necessitate a change in the scaling of reef management strategies (Côté and Darling 2010). By directly addressing the growing concern over the efficacy of local management under projected climate change impacts, this work has shown that for “business as usual” carbon emissions scenarios, local conservation measures are unlikely to prevent Caribbean reefs from experiencing prolonged net reef erosion over the next 70 years (although conservation of herbivores alone might delay net reef erosion by a decade). Importantly, the budget modelling

work showed that when local management efforts are combined with an aggressive CO₂ reduction plan (RCP2.6), reefs are likely to at least remain at carbonate budget equilibrium states or possibly return to states of net carbonate production over the next 70 years. These findings, although theoretical, are convincing and will hopefully stimulate additional research and policy discussion.

9.1.1.1 Further work

As well as keeping the model updated as scientific progress adds to ecological understanding of coral reef constituents, the next logical step would be to adapt this model for other environments. The Caribbean hosts a range of other reefs beside *Montastraea* forereefs, and these are known to host different abundances and diversity of bioeroding taxa, as well as being dominated by different calcifying communities. Beyond this, reefs of the Pacific and Caribbean function very differently (Roff and Mumby 2012) and it would be both interesting and informative to expand this model to much more complicated Pacific reef system in order to compare and contrast contemporary reef growth in these diverse regions.

9.1.2 *Symbiodinium* diversity

In the second part of the thesis, I adjusted the focus from an ecosystem-level view of coral reefs to a detailed empirical examination of just one relevant ecological process. Although any number of the many (>115) ecological and biological processes included in the model would have been appropriate, I chose to focus on symbiotic dinoflagellates because of the strategic importance of understanding their contribution towards coral bleaching and thermal adaptation. In the field of coral-algal symbiosis, cataloguing symbionts across the Caribbean is an essential first step in improving the baseline from which scientific research can build and evolve. Few equivalently sized (over >1000 km²) multi-site datasets exist for a single scleractinian species (Rodriguez-Lanetty et al. 2001, Cooper et al. 2011) (except for octocorals, Goulet et al. 2008, Andras et al. 2011), and the primary contribution of Chapter 5 comes from the wide scale (and high resolution) of the analysis. It is hoped that the datasets size and quality means it will make a substantial and informative contribution to the global geospatial database GeoSymbio, a hybrid web application of spatial bioinformatics for *Symbiodinium*-host symbioses based on ITS2 gene sequences, and an invaluable free resource for coral scientists (Frankin et al. 2012). Additional products of Chapter 5 included the discovery of several potential ‘new’ species that warrant further investigation, as well as the assessment of HRM techniques as a tool for detecting symbiont sub-clades. Unfortunately in the case of *M. annularis*, we found the technique lacked the resolution to identify *Symbiodinium* reliably to sub-clade level, as recently claimed (Granados-Cifuentes and Rodriguez-Lanetty 2010) although it was sensitive and fast in deciphering clade-level assemblages. Nevertheless the data on *Symbiodinium* diversity provide a

vital foundation, from which more advanced hypotheses about the effect of climate change on Caribbean reefs can be tested.

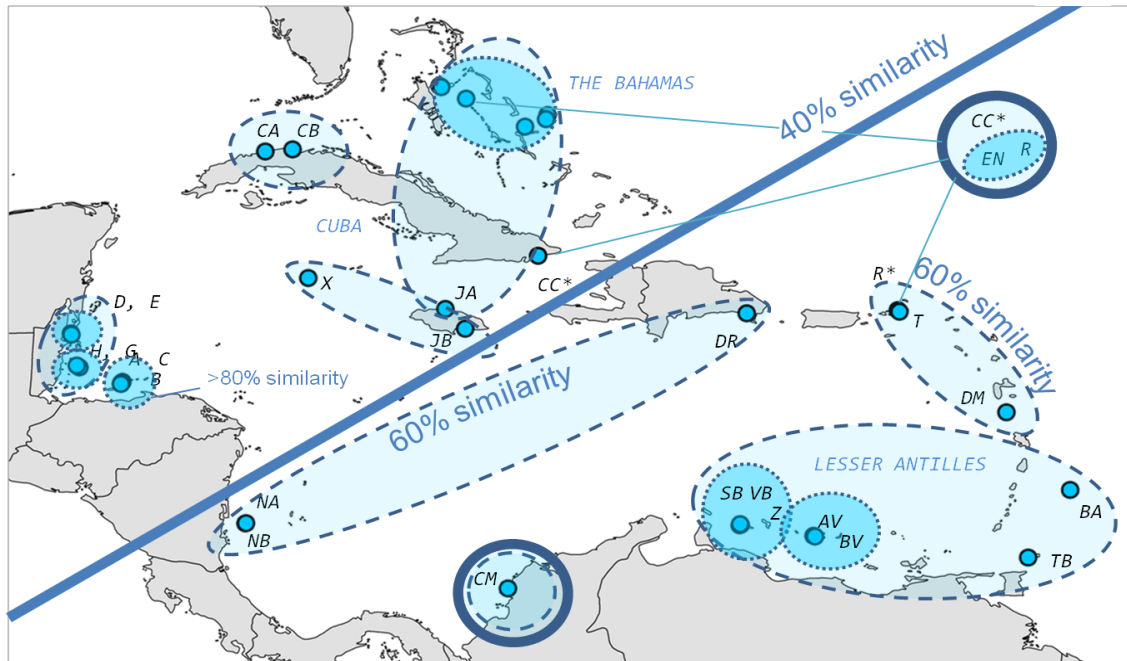


Figure 9.1. Map depicting partitioning of *Montastraea annularis* symbiont communities based on ordination (dotted lines encompass groups with 60% similarity, darker circles 80% similarity and bold lines partitioning at 40% similarity. Chapter 5 presented an east-west divide in symbiont community composition.

In Chapter 6 I investigated *Symbiodinium* diversity (Fig 9.1) in the context of Caribbean environmental heterogeneity, demonstrating that as well as distance, temperature played an important role in determining the east-west *Symbiodinium* biogeography in our coral host, *M. annularis*. Only two other studies have attempted biogeographical comparisons of symbiont communities on a comparative scale, while considering an equivalent number of environmental (and other) factors in their analyses (LaJeunesse et al. 2010, Cooper et al. 2011). Links between coral-algal symbioses and temperature are well established, but the majority of studies that sample across such large latitudinal gradients only consider one explanatory factor (usually temperature) as the driver (e.g., Silverstein et al. 2011). The findings of Chapter 6 clearly emphasise the importance of, not just one, but a combination of environmental factors in driving patterns of symbiont biogeography. The adaptive bleaching hypothesis (Buddemeier et al. 2004) focuses on temperature induced improvement of fitness, but results here show that drivers are probably more holistic.

Beyond this finding, Chapter 6 revealed associations between certain symbiont strains and particular environmental drivers. A negative relationship was observed between the proportion of sub-clade C7 (and to a lesser extent, all C clades) hosted and chronic thermal temperature stress (Fig. 9.2a). This provides the first evidence of association of this sub-clade to sites of relatively low chronic temperature stress: something that has not been explicitly demonstrated before (except in *Symbiodinium* D1a (which is associated with sites of chronically high thermal

stress; Oliver and Palumbi 2011, Silverstein et al. 2011)). Weaker links were also established between B1j and phosphate levels (Fig. 9.2b). Although these observations require further empirical testing, this information contributes to the little that is known about the various physiological properties which symbiont clades impart to the holobiont.

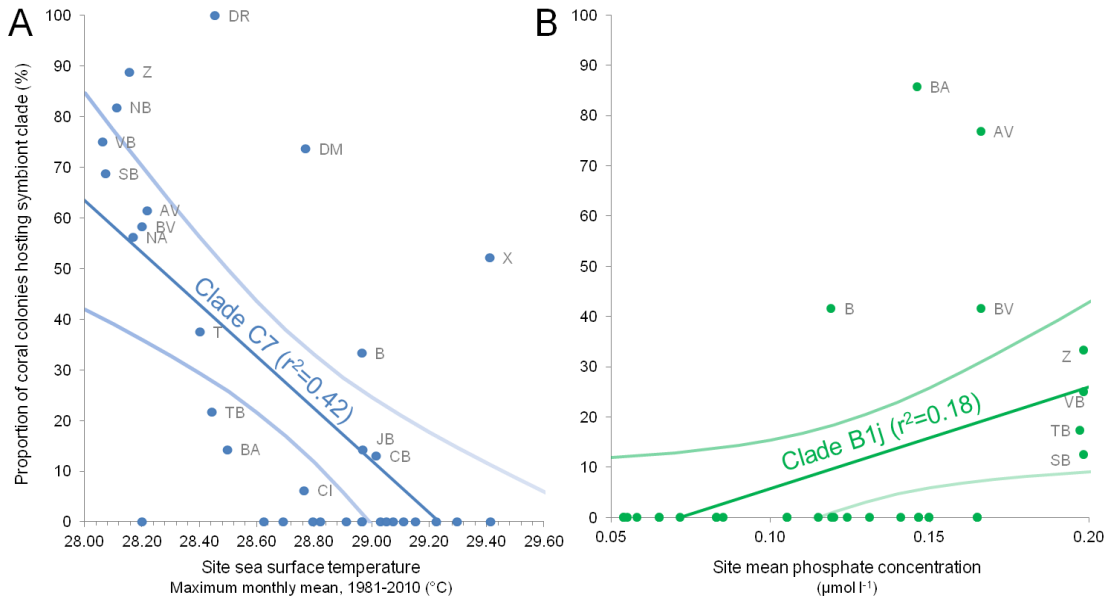


Figure 9.2. Scatter plots showing the associations derived between specific symbiont strains and environmental parameters (described in Chapter 5). **A**) A negative regression between C7 and reef chronic SST ($p=0.0007$), suggests this clade may be acclimated to cooler areas, while **B**) a positive relationship between B1j and phosphate suggest this symbiont is nutrient limited. Bars show 95% confidence limits. Letters indicate reef site (refer to Chapter 4)

Chapter 7 employed novel genetic techniques to explore one aspect of the *Symbiodinium* community—the prevalence of low abundance thermally tolerant *Symbiodinium* D—with results discussed in the context of global climate change. Discovery of a widespread Caribbean prevalence of this symbiont (previously only recorded in Barbados; LaJeunesse et al. 2009) has important implications for coral adaptation: understanding adaptive potential of scleractinians is a key requirement of conservation strategies (Mumby et al. 2011).

In Chapter 8, the temporal stability of the symbioses described in Chapter 5 were explored, by means of an investigation into Bahamian *M. annularis* colonies over a six year period. Demonstrating temporal stability, like many other studies, adds gravitas to the patterns of symbiont biogeography in Chapter 5. However, the additional detection of very low-levels of other symbionts using the techniques from Chapter 7, suggests that the temporal ‘stability’ recorded by many other symbiont studies may be facet of the resolution of the screening technique employed. It is likely ‘dominance’ by one or two clades will still encompass a degree of continuous shuffling of background symbiont abundances.

9.1.2.1 Further work

In terms of the current dataset, the next logical step would be further investigation of the

population genetics of *Symbiodinium* B1, both temporally (for the Bahamas samples) and spatially. A key goal of the field is to better understand the traits conferred by different symbionts to their hosts, so some experimental work to test the effects of different communities hosted by *M. annularis* on both calcification rate and thermal tolerance (lethal and sub-lethal) would be very exciting. More work is needed to resolve the symbiont clades that were not successfully identified in Chapter 5, while further development of the RT-PCR and HRM techniques could be very beneficial for the field, enabling processing of large sample sets quickly and efficiently. Finally, monitoring the background field levels of ‘disaster taxa’ (Correa and Baker 2011) like *Symbiodinium* D in *M. annularis* over longer time periods will aid understanding of the environmental responses of these important symbionts, and whether they can really facilitate coral survival under rapid environmental change.

9.2 Synthesis of project strands

There is a strong case to be made for giving equal consideration to a corals endosymbiont community (i.e. treating as a holobiont), rather than focussing exclusively on the host species. The tight association between coral calcification and the photosynthetic efficiency of zooxanthellae is well established (Gattuso et al. 1999, Allemand et al. 2004), but it is only recently that empirical evidence demonstrating variation in the *Symbiodinium* harboured produces intra-specific variation in both bleaching susceptibility (Toller et al. 2001, LaJeunesse et al. 2009) and calcification rates (Little et al. 2004, Cantin et al. 2009). However, without robust data regarding how different *Symbiodinium* strains quantitatively affect *M. annularis* bleaching thresholds and calcification rates, it would be a stretch to incorporate *Symbiodinium* into our comprehensive reef model at present.

9.2.1 Linking symbiont diversity to *M. annularis* calcification rate

Gaps in the scientific knowledge regarding traits conferred by symbionts are being addressed (Ortiz et al. 2013), while *Symbiodinium* D is shown to affect calcification in juvenile *Acropora* (Little et al. 2004, Cantin et al. 2009) and other species (Robin Smith, pers. comm.). Chapter 7 explored how the widespread prevalence of clade D might affect bleaching susceptibility and calcification of *M. annularis* communities. But a more apposite question might be how the east-west partitioning of symbiont communities across the Caribbean (Chapter 5) might manifest itself in *M. annularis* calcification. To investigate this I performed some simple data exploration, linking symbiont type (generated as part of Chapter 5) and *M. annularis* linear extension rates (LER) (gathered from the literature as part of Chapters 2 and 3).

Data collated on *M. annularis* extension rates as part of model in Chapter 3 (Appendix Table 9.1), included >30 published references to *M. annularis* calcification, from a range of Caribbean

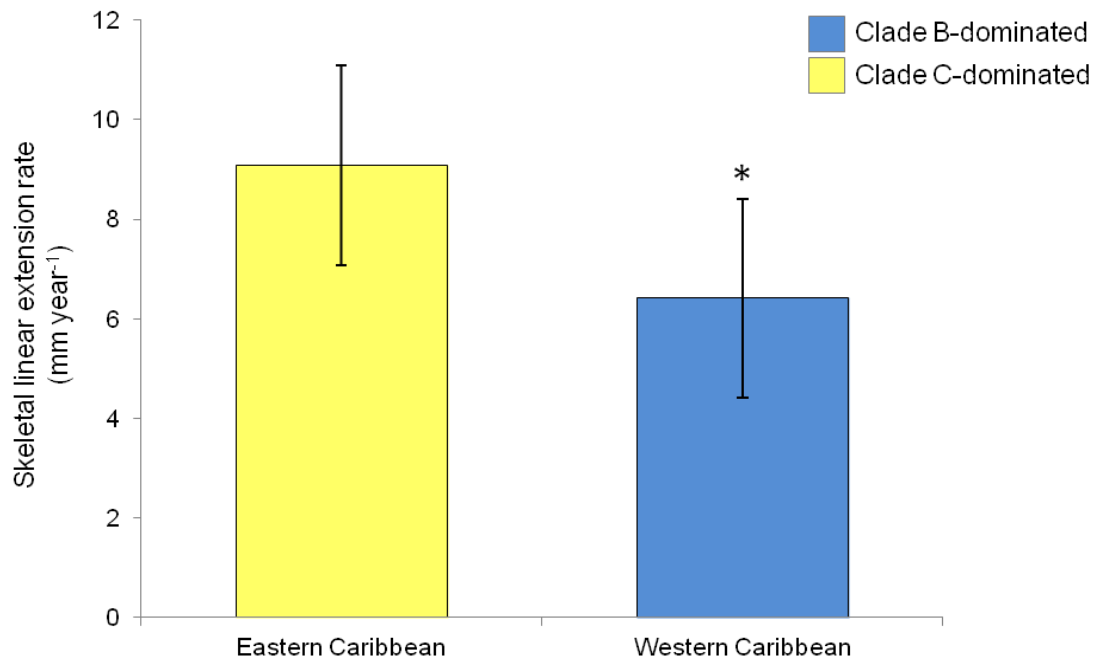


Figure 9.3. Linking east-west *Symbiodinium* partitioning to host calcification rates. Bar chart shows the mean skeletal linear extension rate estimates of *Montastraea annularis* in two regions of the Caribbean known to differ significantly in terms of symbiont community representation (error bars represent one standard deviation).

reef sites. Avoiding any pre-1990 references that did not explicitly refer to ‘columnar’ *M. annularis* (these could include *M. faveolata* and *M. franski* growth estimates; Knowlton et al. 1992), as well as removing those collected at depths > 20 m (an important determinant in coral LER; Baker and Weber 1975) and atypical reef conditions such as sedimentation (Dodge and Thomson 1974, Mallela and Perry 2007) left a smaller dataset. After testing the effect of sampling year (1915 - 2007: no significant relationship), skeletal extension rate data were then stratified according to those that fell into the eastern (i.e., Curaçao, Barbados, US Virgin Isles, Chapter 4 Fig. 4.16, 4.19) and western ‘patch’ (Belize, Honduras, Jamaica, Bahamas, Florida). Mexican samples were removed from the dataset as we did not sample symbionts in the Mexican Gulf. Based on the assumption that symbiont communities remain stable over time (see Chapter 8) we found a significant difference in the LER in our eastern (9.09 mm year⁻¹, n=22) and western (6.41 mm year⁻¹, n=25) *M. annularis* mean estimates (ANOVA, F=13.8, p<0.001, df = 1). Although further testing would be required to establish that this difference was not caused by environmental variables, as symbiont community is closely linked to calcification, we tentatively suggest that dominance of *Symbiodinium* C clades in the east facilitate the greater *M. annularis* linear extension rates observed here.

Explicit differences between calcification in corals hosting predominantly *Symbiodinium* C compared to B have not previously been demonstrated, although several lines of published evidence may support this association. In Mexico, *M. annularis* LER was shown to decline along environmental gradients, away from turbidity (Carricart-Ganivet and Merino 2001). Corresponding parallels were recorded in the *M. annularis* symbiont communities in Panama,

with colonies hosting more C also found closer to shore with higher turbidity scores (Garren et al. 2006). Together, these studies perhaps suggesting that change in LER may be mediated by zooxanthellae. With long term temperature stress identified as an important predictor of symbiont communities - particularly distribution of *Symbiodinium* clade C (Chapter 5), implications for this temperature-sensitive clade under predicted regional warming may have significant knock-on effects on for Caribbean carbonate budgets (Chapter 4), particularly if loss of C implies a reduced calcification ability of *M. annularis*, especially in terms of projected sea level rise (Simpson et al. 2009).

This tentative finding, although requiring further testing, demonstrates the type of advances that would need to be made towards to characterising effects of symbiont sub-clades, in order to bring the two strands of the thesis together. To incorporate variation in holobiont growth rates to usefully inform the accretory part of the carbonate budget model should be a future goal. Our possible link between *Symbiodinium* C and faster skeletal extension also further highlights the importance of considering the holobiont, rather than the coral host and endosymbiont community separately, and provides hope for eventual inclusion of symbionts in a fully comprehensive version of our ecological Caribbean model.

9.3 A ‘nugget of hope’ for the future?

There are several reasons to hold out hope for the future of Caribbean reefs. Ecosystem dynamics are complicated (Nyström et al. 2000), but model outputs of Chapter 4 show a degree of ecosystem resilience to projected climate change: with function maintained to the end of the century with improved management and global climate mitigation. The models suggest that the effects of projected OA – at the community scale at least, may not affect ecosystem functioning to the same degree as projected SST, and, on its own, are unable to prevent reef functioning (similar results found by Chan and Connolly 2013). Changing focus from reef-scale to colony-scale, *M. annularis* is described as having several traits (e.g., massive morphology, slow grow, spawning reproduction) that have made this coral resilient against Caribbean extinctions in the geological past (van Woesik et al. 2012). One ‘tolerance’ trait requirement described by van Woesik et al is a >10% association with *Symbiodinium* D. The finding of comparable background levels of this symbiont in Chapter 8, provides slim hope for the continued survival of this key remaining reef builder.

Scientific research is essential for the continual discovery of new elements of resilience: recently it was demonstrated that some CCA skeletons contained dolomite, a mineral 6-10 fold more resistant to chemical dissolution than calcite (Nash et al. 2013). Meanwhile the sudden and unexpected return of *Diadema antillarum* to half of their pre-mortality in Dairy Bull Reef, Jamaica (Edmunds and Carpenter 2001) have led to a reported return to coral dominated state at

the site (Carpenter and Edmunds 2006, Crabbe 2009). While events like these are rare, modeling the wider return of *D. antillarum*– and that of *Acropora* spp. - in Chapter 4 produced positive budget forecasts for Caribbean reefs. Other work has shown that restoring grazing pressure can reverse the shift from coral to macroalgal dominance (Mumby and Harborne 2010).

Although the global CO₂ trajectory commits us to a period of warming over the next 20-30 years, *Symbiodinium* are frequently proposed as a mechanism of adaptation to warmer temperatures (Berkelmans and van Oppen 2006). Variation among symbiont populations may expand the functional diversity of the intact symbiotic association (holobiont) and genetic diversity among corals and zooxanthellae can potentially enable adaptation, and thereby enhance resilience (van Oppen et al. 2011). Responses might involve range shifts (Serrano et al. 2013), or an increase in the temperature tolerance of individual colonies in situ by a shift to relatively heat-tolerant clades of zooxanthellae in surviving colonies (Maynard et al. 2008, LaJeunesse et al. 2009). Although the speed at which climate change is impacting reef ecosystems makes adaptation very unlikely (Hoegh-Guldberg et al. 2007, Ortiz et al. 2013), some field evidence suggests supports adaptation to stress in *M. annularis* (Castillo and Helmuth 2005). This may be facilitated by *Symbiodinium* D; in Chapter 7 we report evidence that *M. annularis* (often described as a ‘bleaching vulnerable coral’) failed to bleach on San Salvador in 2005, despite bleaching in 1998. Improved understanding of coral and symbiont tolerances may allow more sophisticated placement of MPA’s may help counteract the negative effects of warming (Côté and Darling 2010, Selig et al. 2012), if reefs previously exposed to thermal stress are chosen (thought to increase adaptive capacity of corals).

Management interventions that reduce non-climatic stressors (e.g. pollution, siltation, over-fishing) could play a significant role in increasing the survival and recovery of corals after bleaching events and in improving their ability to adapt to warmer conditions (Hughes et al. 2010). In surveys of coral scientists, lack of laws and enforcement was seen as one of the greatest threats to coral reefs (Kleypas and Eakin 2007), but increasing numbers of fishing bans e.g., in the Bahamas, Belize, Netherlands Antilles and Nicaragua (McManus and Lacambra 2005). Supporting our Chapter 4 outputs, other studies show that well implemented local management can aid the survival prospects of reefs facing global climate change (Wooldridge 2009, Mumby and Harborne 2010), as well as benefiting surrounding areas (Harrison et al. 2012). Under certain conditions, reefs can recover rapidly: for example in Kaneohe Bay, Hawaii, removal of two sewage outfalls led to decline in nutrient concentrations and rapid return to coral dominance (Maragos et al. 1985). Management may help delay more severe climate impacts, buying time for the global community to act (Chapter 4).

Tackling changing climate on a global scale requires commitment of governments and is harder to achieve than local management. The Wider Caribbean alone, home to 238 million people, is geopolitically complex with 35 countries (including 27 island states) spanning a broad range of wealth and politics (Simpson et al. 2009). Although awareness and concern about climate change has increased, with the majority of scientists and members of the wider global community now viewing climate change as a serious global threat (Lorenzoni and Pidgeon 2006), instigating a socio-political response across governments remains a challenge. In response to this challenge, the role of scientists is evolving, with advocacy becoming more widely acceptable, giving the scientific community a louder voice. In 2012, in an unprecedented move by the international scientific coral reef community, a Consensus Statement endorsed by over 3000 reef scientists was issued calling on governments to work together to take action on climate change. We can only hope.

9.4 References

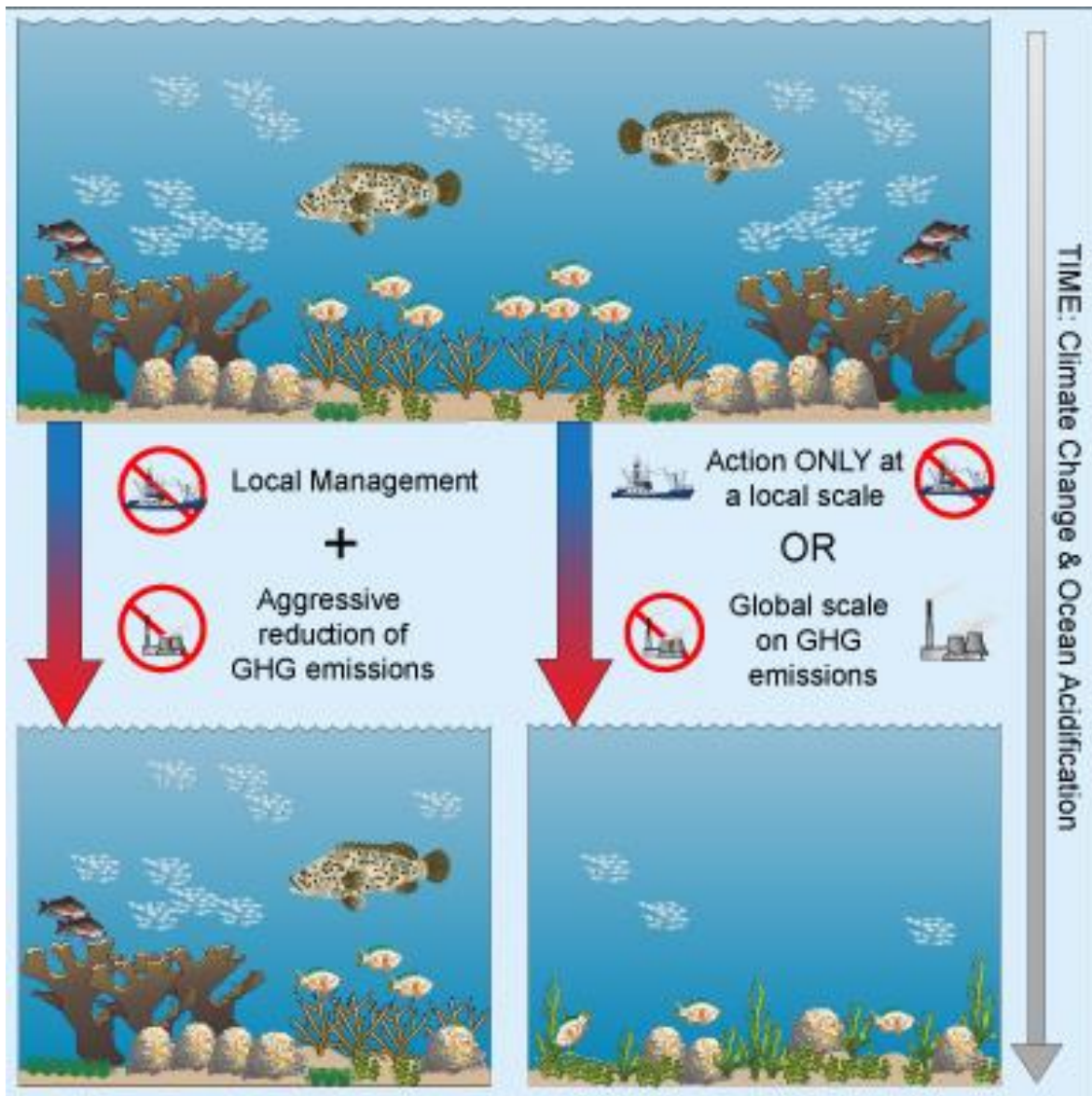
- Allemand D, Ferrier-Pages C, Furla P, Houlbrequé F, Puverel S, Reynaud S, Tambutte E, Tambutte S, Zoccola D (2004) Biomineralisation in reef-building corals: from molecular mechanisms to environmental control. *Comptes Rendus Palevol* **3**:453-467
- Andras JP, Kirk NL, Drew Harvell C (2011) Range-wide population genetic structure of *Symbiodinium* associated with the Caribbean Sea fan coral, *Gorgonia ventalina*. *Molecular Ecology* **20**:2525-2542
- Baker PA, Weber JN (1975) Coral growth rate: variation with depth. *Earth and Planetary Science Letters* **27**:57-61
- Berkelmans R, van Oppen MJH (2006) The role of zooxanthellae in the thermal tolerance of corals: a 'nugget of hope' for coral reefs in an era of climate change. *Proceedings of the Royal Society B-Biological Sciences* **273**:2305-2312
- Buddemeier RW, Baker AC, Fautin DG, Jacobs JR (2004) The adaptive hypothesis of bleaching. In: Rosenberg E, Loya Y (eds) *Coral health and disease*. Springer-Verlag, Berlin, Germany
- Cantin N, Oppen M, Willis B, Mieog J, Negri A (2009) Juvenile corals can acquire more carbon from high-performance algal symbionts. *Coral Reefs* **28**:405-414
- Carpenter RC, Edmunds PJ (2006) Local and regional scale recovery of *Diadema* promotes recruitment of scleractinian corals. *Ecology Letters* **9**:271-280
- Carricart-Ganivet JP, Merino M (2001) Growth responses of the reef-building coral *Montastraea annularis* along a gradient of continental influence in the southern Gulf of Mexico. *Bulletin of Marine Science* **68**:133-146
- Castillo KD, Helmuth BST (2005) Influence of thermal history on the response of *Montastraea annularis* to short-term temperature exposure. *Marine Biology* **148**:261-270
- Chan NCS, Connolly SR (2013) Sensitivity of coral calcification to ocean acidification: a meta-analysis. *Global Change Biology* **19**:282-290
- Cooper TF, Berkelmans R, Ulstrup KE, Weeks S, Radford B, Jones AM, Doyle J, Canto M, O'Leary RA, van Oppen MJH (2011) Environmental factors controlling the distribution of *Symbiodinium* harboured by the coral *Acropora millepora* on the Great Barrier Reef. *PLoS ONE* **6**:e25536
- Correa AMS, Baker AC (2011) Disaster taxa in microbially mediated metazoans: how endosymbionts and environmental catastrophes influence the adaptive capacity of reef corals. *Global Change Biology* **17**:68-75
- Côté IM, Darling ES (2010) Rethinking ecosystem resilience in the face of climate change. *PLoS Biology* **8**:e1000438
- Crabbe MJC (2009) Scleractinian coral population size structures and growth rates indicate coral resilience on the fringing reefs of North Jamaica. *Marine Environmental Research* **67**:189-198
- Dodge RE, Thomson J (1974) The natural radiochemical and growth records in contemporary hermatypic corals from the Atlantic and Caribbean. *Earth and Planetary Science Letters* **23**:313-322
- Edmunds PJ, Carpenter RC (2001) Recovery of *Diadema antillarum* reduces macroalgal cover and increases abundance of juvenile corals on a Caribbean reef. *Proceedings of the National Academy of Sciences of the United States of America* **98**:5067-5071
- Frankin EC, Stat M, Pochon X, Putnam HM, Gates RD (2012) GeoSymbio: a hybrid, cloud-based web application of global geospatial bioinformatics and ecoinformatics for *Symbiodinium*-host symbioses. *Molecular Ecology Resources* **12**:369-373
- Garren M, Walsh S, Caccone A, Knowlton N (2006) Patterns of association between *Symbiodinium* and members of the *Montastraea annularis* species complex on spatial scales ranging from within colonies to between geographic regions. *Coral Reefs* **25**:503-512
- Gattuso J-P, Allemand D, Frankignoulle M (1999) Photosynthesis and calcification at cellular, organismal and community levels in coral reefs: a review on interactions and control by carbonate chemistry. *American Zoologist* **39**:160-183
- Goulet TL, Simmons C, Goulet D (2008) Worldwide biogeography of *Symbiodinium* in tropical octocorals. *Marine Ecology Progress Series* **355**:45-58
- Granados-Cifuentes C, Rodriguez-Lanetty M (2010) The use of high-resolution melting analysis for genotyping *Symbiodinium* strains: a sensitive and fast approach. *Molecular Ecology Resources* **11**:394-399
- Harrison HB, Williamson DH, Evans RD, Almany Glenn R, Thorrold Simon R, Russ Garry R, Feldheim Kevin A, van Herwerden L, Planes S, Srinivasan M, Berumen Michael L, Jones Geoffrey P (2012)

- Larval export from marine reserves and the recruitment benefit for fish and fisheries. *Current Biology* **22**:1023-1028
- Hoegh-Guldberg O, Mumby PJ, Hooten AJ, Steneck RS, Greenfield P, Gomez E, Harvell CD, Sale PF, Edwards AJ, Caldeira K, Knowlton N, Eakin CM, Iglesias-Prieto R, Muthiga N, Bradbury RH, Dubi A, Hatziolos ME (2007) Coral reefs under rapid climate change and ocean acidification. *Science* **318**:1737-1742
- Hughes TP, Graham NAJ, Jackson JBC, Mumby PJ, Steneck RS (2010) Rising to the challenge of sustaining coral reef resilience. *Trends in Ecology and Evolution* **25**:633-642
- Kleypas J, Eakin CM (2007) Scientists perceptions of the threats to coral reefs: results of a survey of coral reef researchers. *Bulletin of Marine Science* **80**:419-436
- Knowlton N, Weil E, Weigt LA, Guzman HM (1992) Sibling species in *Montastraea annularis*, coral bleaching, and the coral climate record. *Science* **255**:330-333
- LaJeunesse TC, Pettay DT, Sampayo EM, Phongsuwan N, Brown B, Obura DO, Hoegh-Guldberg O, Fitt WK (2010) Long-standing environmental conditions, geographic isolation and host-symbiont specificity influence the relative ecological dominance and genetic diversification of coral endosymbionts in the genus *Symbiodinium*. *Journal of Biogeography* **37**:785-800
- LaJeunesse TC, Smith RT, Finney J, Oxenford H (2009) Outbreak and persistence of opportunistic symbiotic dinoflagellates during the 2005 Caribbean mass coral 'bleaching' event. *Proceedings of the Royal Society B-Biological Sciences* **276**:4139-4148
- Little AF, van Oppen MJH, Willis BL (2004) Flexibility in algal endosymbioses shapes growth in reef corals. *Science* **304**:1492-1494
- Lorenzoni I, Pidgeon N (2006) Public views on climate change: European and USA perspectives. *Climatic Change* **77**:73-95
- Mallela J, Perry CT (2007) Calcium carbonate budgets for two coral reefs affected by different terrestrial runoff regimes, Rio Bueno, Jamaica. *Coral Reefs* **26**:129-145
- Maragos J, Evans C, Holthus P (1985) Reef corals in Kaneohe Bay six years before and after termination of sewage discharges (Oahu, Hawaiian Archipelago). In: Gabrie C, Salvat B (eds) *Proceedings of the 5th International Coral Reef Symposium*, Tahiti
- Maynard JA, Anthony KRN, Marshall PA, Masiri I (2008) Major bleaching events can lead to increased thermal tolerance in corals. *Marine Biology* **155**:173-182
- McManus E, Lacambra C (2005) *Fishery regulations in the Wider Caribbean Region*, UNEP Report, Cambridge, UK
- Mumby PJ, Elliott IA, Eakin CM, Skirving W, Paris CB, Edwards HJ, Enríquez S, Iglesias-Prieto R, Cherubin LM, Stevens JR (2011) Reserve design for uncertain responses of coral reefs to climate change. *Ecology Letters* **14**:132-140
- Mumby PJ, Harborne AR (2010) Marine reserves enhance the recovery of corals on Caribbean reefs. *PLoS ONE* **5**:e8657
- Nash MC, Opdyke BN, Troitzsch U, Russell BD, Adey WH, Kato A, Diaz-Pulido G, Brent C, Gardner M, Prichard J, Kline DI (2013) Dolomite-rich coralline algae in reefs resist dissolution in acidified conditions. *Nature Climate Change* **3**:268-272
- Nyström M, Folke C, Moberg F (2000) Coral reef disturbance and resilience in a human-dominated environment. *Trends in Ecology and Evolution* **15**:413-417
- Oliver TA, Palumbi SR (2011) Many corals host thermally resistant symbionts in high-temperature habitat. *Coral Reefs* **30**:241-250
- Ortiz JC, González-Rivero M, Mumby PJ (2013) Can a thermally tolerant symbiont improve the future of Caribbean coral reefs? *Global Change Biology* **19**:273-281
- Rodriguez-Lanetty M, Loh WKW, Carter DA, Hoegh-Guldberg O (2001) Latitudinal variability in symbiont specificity within the widespread scleractinian coral *Plesiastrea versipora* *Marine Biology* **138**:1175-1181
- Selig ER, Casey KS, Bruno JF (2012) Temperature-driven coral decline: the role of marine protected areas. *Global Change Biology* **18**:1561-1570
- Serrano E, Coma R, Ribes M, Weitzmann B, Garcia M, Ballesteros E (2013) Rapid northward spread of a zooxanthellate coral enhanced by artificial structures and sea warming in the western Mediterranean. *PLoS ONE* **8**:e52739
- Silverstein R, Correa A, LaJeunesse T, Baker A (2011) Novel algal symbiont (*Symbiodinium* spp.) diversity in reef corals of Western Australia. *Marine Ecology Progress Series* **422**:63-75
- Simpson MC, Scott D, New M, Sim R, Smith D, Harrison M, Eakin CM, Warrick R, Strong AE, Kouwenhoven P, Harrison S, Wilson M, Nelson GC, Donner S, Kay R, Gledhill DK, Liu G, Morgan JA, Kleypas JA, Mumby PJ, Palazzo A, Christensen TRL, Baskett ML, Skirving WJ, Elrick C, Taylor

- M, Magalhaes M, Bell J, Burnett JB, Ruttly MK, Overmas M, Robertson R (2009) *An overview of modelling climate change impacts in the Caribbean region with contribution from the Pacific Islands*. United Nations Development Programme (UNDP), Barbados, West Indies
- Toller WW, Rowan R, Knowlton N (2001) Repopulation of zooxanthellae in the Caribbean corals *Montastraea annularis* and *M. faveolata* following experimental and disease-associated bleaching. *Biological Bulletin* **201**:360-373
- van Oppen MJH, Souter P, Howells EJ, Heyward A, Berkelmans R (2011) Novel genetic diversity through somatic mutations: fuel for adaptation of reef corals? *Diversity* **3**:405-423
- van Woesik R, Franklin EC, O'Leary J, McClanahan TR, Klaus JS, Budd AF (2012) Hosts of the Plio-Pleistocene past reflect modern day coral vulnerability. *Proceedings of the Royal Society B: Biological Sciences* **279**:2448-2456
- Wooldridge SA (2009) Water quality and coral bleaching thresholds: formalising the linkage for the inshore reefs of the Great Barrier Reef, Australia. *Marine Pollution Bulletin* **58**:745-751

Appendices

Chapter 4 Appendix



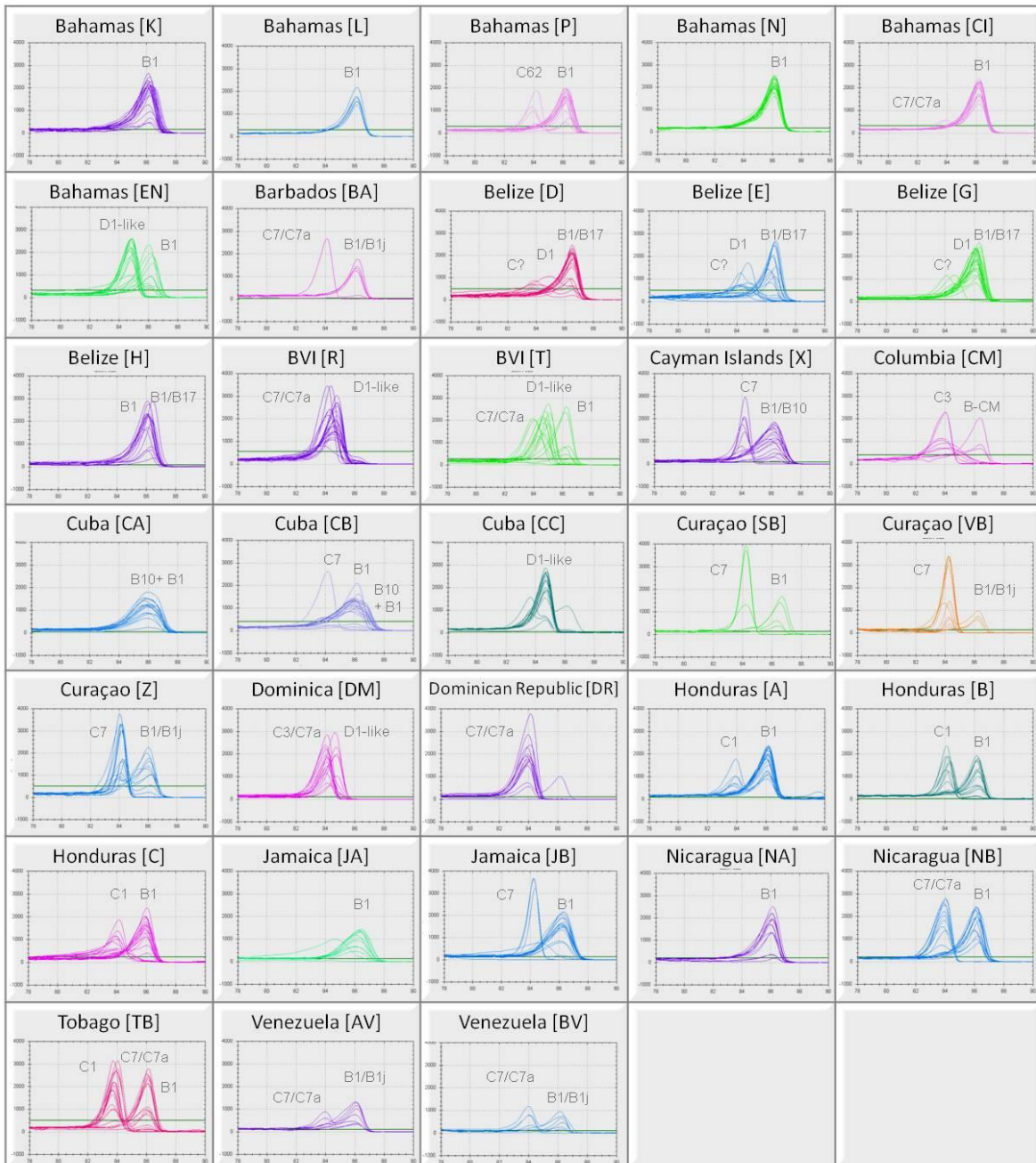
Appendix Figure 4.1: Graphical abstract summarizing the main finding of Chapter 4. (Credit: G. Roff)

Abundance data	Mean	Variance	δ	Distance to Regularity, D				Clustering indices			
				I_a		P_a		V_i		V_j	
				Index of aggregation	Significance of I_a	Patch cluster index		Gap cluster index			
						mean	p-value	mean	p-value		
Species Richness	4.67	2.23	1.49	2.20	0.001	1.85	0.025	-2.35	0.003		
Rarefaction	2.65	1.14	1.14	1.43	0.086	1.89	0.024	-1.92	0.022		
Clade B	74.73	981	1.75	2.03	0.005	2.55	0.001	-1.78	0.038		
Clade C	40.76	1350	4.08	2.14	0.002	2.05	0.017	-2.25	0.006		
Clade D	11.73	744	4.10	1.02	0.400	0.90	0.506	-1.02	0.421		
Clade A	0.03	0.03	10.74	1.01	0.428	0.98	0.907	-1.01	0.409		
Clade B + C	16.94	415	3.01	1.38	0.095	1.36	0.140	-1.51	0.085		
Clade C + D	4.42	262	6.82	1.06	0.336	1.41	0.108	-1.07	0.296		
Clade D + B	1.91	35.3	8.76	1.43	0.066	1.53	0.096	-1.39	0.089		
Mixed B + C + D	1.94	40.1	8.78	1.37	0.085	1.27	0.151	-1.46	0.065		

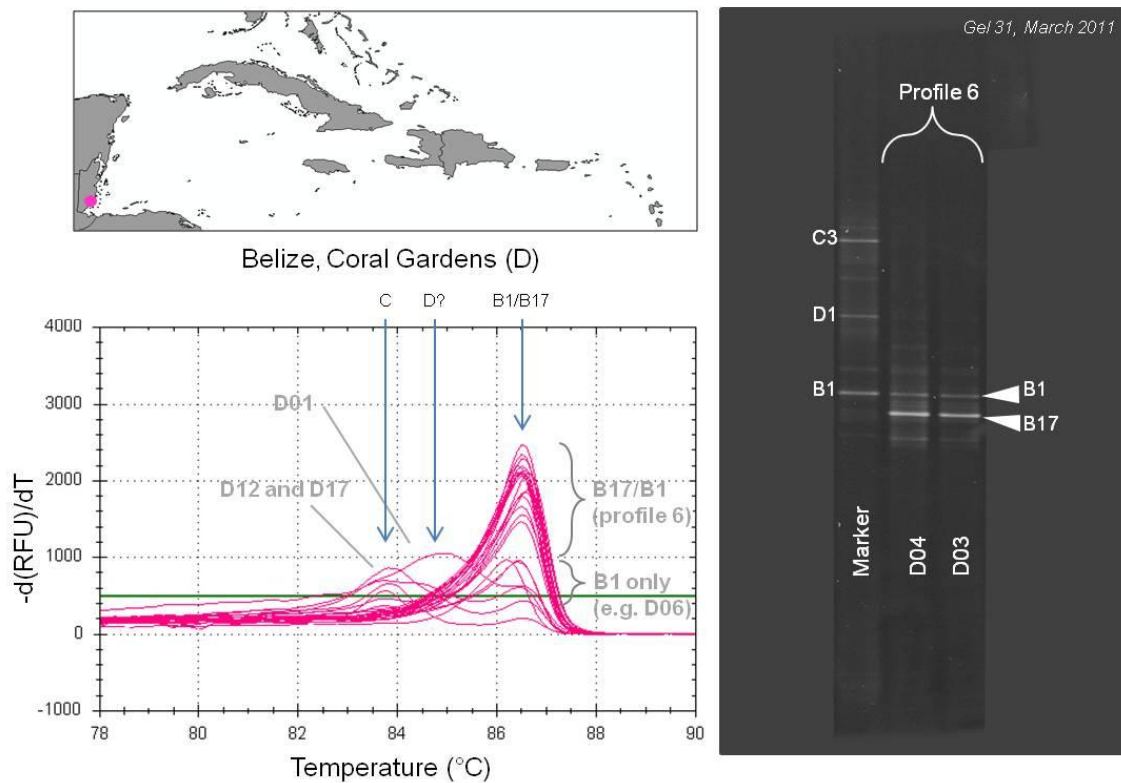
Appendix Table 5.2: Outputs generated by the SADIE analyses, for *Symbiodinium* clade and species richness measures.

Area	Country	Reef	Site	Latitude	Longitude	A13	B1	B10	B17	B1j	B3?	B7	C1	C12	C3	C62	C7	C31?	D1?	D1a
Mesoamerican Barrier Reef	Honduras	Seaquest	A	16.2940	-86.6000	-2.18	4.39	-0.30	-0.32	-4.77	-0.01	-0.99	0.42	-1.51	0.42	-0.96	-4.25	-3.61	-0.25	-3.96
	Honduras	Sandy Bay	B	16.3340	-86.5680	-2.15	0.00	-0.27	-0.26	-3.78	0.20	-1.00	2.13	-2.08	2.13	-1.01	-3.56	-3.63	-0.25	-2.55
	Honduras	Western Wall	C	16.2710	-86.6040	-2.16	-0.39	-0.30	-0.31	-4.41	-0.02	-0.96	2.01	0.01	2.01	-1.01	0.00	-3.51	-0.24	-5.15
	Belize	Coral Gardens	D	17.7484	-88.0233	-2.17	-0.12	-0.01	2.27	-4.92	-1.78	-1.07	-0.51	-2.39	-0.51	-0.94	-2.38	-2.04	1.63	-2.69
	Belize	Eagle Ray	E	17.7203	-88.0136	-2.11	0.01	3.87	2.69	-5.43	-0.44	-1.08	-0.62	-6.81	-0.62	-0.95	-6.52	-2.09	1.62	-2.97
	Belize	Long Cay	G	16.7545	-87.7861	-2.12	4.82	1.53	1.66	-6.04	-0.32	-1.08	-0.41	-2.35	-0.41	-0.99	-2.29	-2.11	-0.12	-3.55
	Belize	West Reef	H	16.8088	-87.8621	-2.15	2.86	4.50	4.37	-6.02	-0.35	-1.09	-0.45	-2.59	-0.45	-1.01	-2.43	-2.12	-0.11	-3.55
The Bahamas	Bahamas	Conception Island	CI	23.8120	-75.1218	-1.77	2.44	-1.35	-2.92	-3.90	-2.85	-0.91	-0.39	0.45	-0.39	-0.25	0.47	-0.28	-1.63	-2.41
	Bahamas	Exumas North	EN	24.6409	-76.7954	-1.88	-0.24	-1.13	-3.18	-5.13	-3.45	-0.99	0.78	-3.14	0.78	-0.08	-2.55	1.08	-1.55	1.31
	Bahamas	Seahorse Reef	K	24.1582	-74.4839	-1.67	2.67	-1.32	-3.05	-3.83	-2.63	-0.95	1.73	-2.97	1.73	-0.29	-3.27	-1.63	-1.66	-2.09
	Bahamas	Snapshot Reef	L	24.0314	-74.5297	-1.71	2.95	-1.34	-1.48	-3.79	-2.62	-0.93	-0.03	-4.01	-0.03	-0.29	-3.08	-1.64	-1.67	-2.09
The Bahamas	Bahamas	School House Reef	N	24.9734	-77.5051	-1.87	3.01	-0.98	-3.03	-4.18	-3.51	-1.02	-0.22	-3.94	-0.22	-0.01	-6.24	-0.11	-1.50	-0.16
	Bahamas	Propeller Reef	P	25.0064	-77.5524	-1.91	0.95	-0.96	-2.73	-3.96	-1.75	-1.02	-0.23	-3.66	-0.23	1.00	-5.75	-0.12	-1.49	-0.17
	Bahamas	White Hole	NA	12.1881	-83.0518	-1.91	0.83	-0.80	-0.87	-1.97	-1.69	-0.92	-0.78	0.92	-0.78	-1.14	1.13	-2.40	-0.75	-2.34
Mesoamerica & Columbia	Nicaragua	Chavo	NB	12.1835	-83.0670	-1.89	0.00	-0.82	-0.90	-2.13	-1.75	-0.94	-0.87	1.17	-0.87	-1.14	1.19	-2.67	-0.76	-2.41
	Columbia	Palo I	CM	10.2770	-75.6110	-1.34	-0.94	-1.45	-1.50	-0.97	-0.72	0.96	-1.38	-0.95	-1.38	-1.22	-0.73	-1.46	-1.32	-1.45
Greater Antilles & Caymans	Cuba	Baracoa	CA	23.0871	-82.5077	-2.10	-0.88	-0.72	-1.24	-3.35	-1.00	-0.56	0.82	1.84	0.82	-0.45	-0.18	-0.83	-0.90	-0.86
	Cuba	Bacunayagua	CB	23.1507	-81.7274	-2.09	0.17	0.83	-1.39	-3.42	-1.01	-0.53	-0.14	2.03	-0.14	-0.40	1.13	-0.73	-0.99	-0.82
	Cuba	Siboney	CC	20.0315	-74.7548	-1.73	-0.59	-0.89	1.22	-1.56	-1.31	-0.40	1.51	-2.38	1.51	-0.59	-1.58	-1.40	-1.52	1.35
	Cayman	Rum Point	X	19.3776	-81.2810	-2.20	1.22	1.80	-1.03	-2.22	-0.58	0.88	-0.85	-2.35	-0.85	-0.66	1.22	-0.98	-0.94	-0.96
	Dominican Republic	Bayahibe	DR	18.3440	-68.8314	-0.93	-1.16	-1.57	-0.80	-1.37	-0.83	-0.98	-1.18	1.21	-1.18	-0.98	1.06	-0.52	-2.18	-0.53
	Jamaica	Drunkenmans Cay	JA	18.4688	-77.3856	-1.97	0.90	-0.75	-1.57	-1.91	0.80	-0.11	-1.11	-2.79	-1.11	-0.69	-1.16	-1.68	-1.29	-0.43
	Jamaica	Dairy Bull	JB	17.8876	-76.8288	-1.88	1.65	-1.50	-1.53	-1.69	-0.11	0.86	-1.43	-1.76	-1.43	-0.76	0.14	-1.56	-1.24	-1.64
	Barbados	Victor's Reef	BA	13.1630	-59.6409	1.01	0.52	-3.43	-0.30	1.36	-0.89	-1.50	-0.36	3.84	-0.36	-1.20	3.79	-0.27	-2.14	-0.34
	BVI	Ginger Island	R	18.3915	-64.4838	-0.51	-2.27	-2.26	-1.56	-1.13	-0.96	-1.50	-1.95	-0.92	-1.95	-1.05	-0.87	1.60	-2.36	1.93
	BVI	Beef Island	T	18.4395	-64.5351	-0.52	-2.15	-2.22	-1.53	-1.06	-0.95	-1.48	-1.87	2.29	-1.87	-1.06	2.27	-0.01	-2.36	1.49
Lesser Antilles	Curacao	Snakebay	SB	12.1390	-69.0021	-0.78	-6.26	-3.30	-3.88	4.71	0.00	-0.94	-2.81	7.22	-2.81	-1.29	5.39	-1.13	-2.16	-1.37
	Curacao	Vaersenbay	VB	12.1611	-69.0112	-0.79	-2.29	-3.08	-3.51	3.48	1.12	-0.96	-1.87	3.47	-1.87	-1.29	2.64	-1.13	-2.22	-1.22
	Curacao	Buoy 1	Z	12.1259	-69.0253	-0.79	-4.36	-3.00	-3.36	2.81	-0.01	-0.91	-3.47	4.95	-3.47	-1.29	2.12	-1.11	-2.12	-1.20
	Dominica	Grande Savane	DM	15.4369	-61.4485	-0.18	-2.05	-3.46	-0.62	-0.45	-0.84	-1.64	-0.71	1.32	-0.71	-1.15	1.06	1.08	-2.28	0.76
	Tobago	Buccoo Reef	TB	11.1831	-60.8334	-0.13	-0.42	-3.56	0.66	2.50	-0.77	-1.39	0.62	2.99	0.62	-1.24	4.12	-0.41	-2.13	-0.54
	Venezuela	Cayo de Agua	AV	11.8178	-66.9306	-0.57	0.89	-3.68	-1.15	2.88	2.20	-1.18	-2.11	2.99	-2.11	-1.29	2.93	-0.86	-2.29	-1.14
	Venezuela	Dos Mosquises	BV	11.7958	-66.8842	-0.56	-0.01	-3.74	-1.16	2.65	1.28	-1.18	-1.19	2.19	-1.19	-1.29	4.20	-0.87	-2.28	-1.17

Appendix Table 5.3: Cluster indices generated by SADIE analysis for symbionts at each site. Blue cells indicate values with a significant v_j value (demonstrating negative clustering), while red cells (significant v_i) depict sites where symbiont appeared to be more clustered than would occur by random chance (measured against 5000+ random permutations).



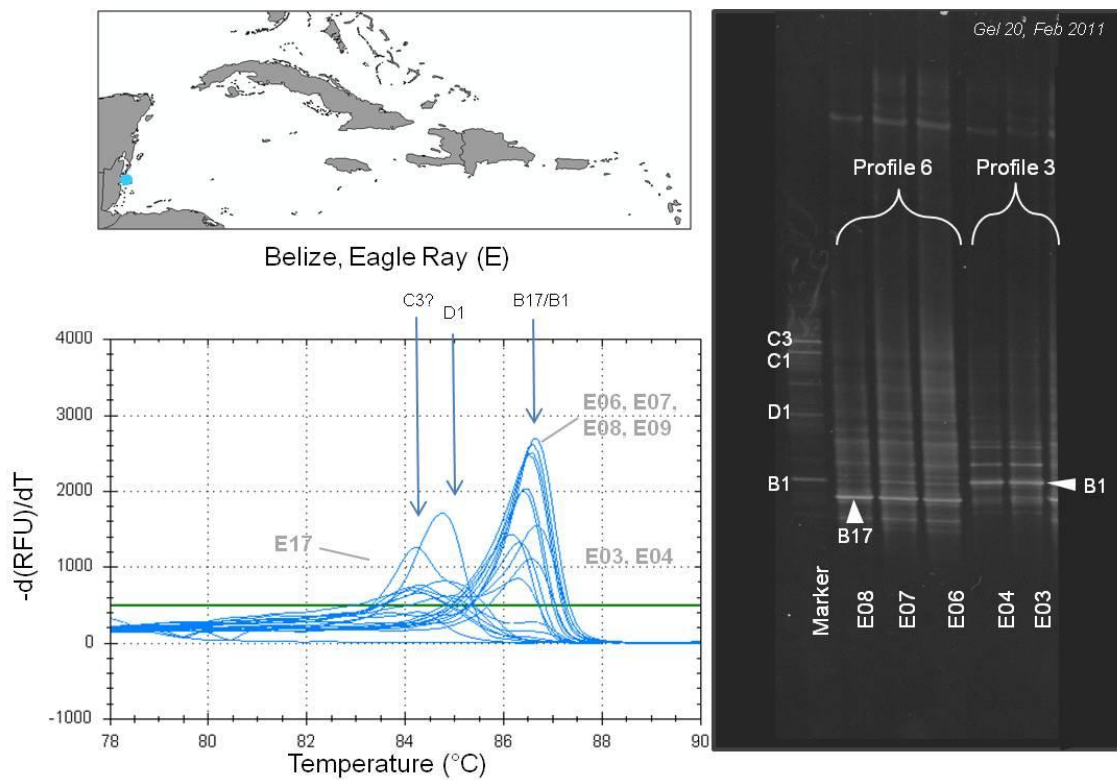
Appendix Figure 5.1: HRM outputs for all sampled populations of *Montastraea annularis* endosymbionts.



Appendix Figure 5.2: Selected DGGE gel images and HRM outputs for Belizean site D, Coral Gardens.

DGGE profiles (profile '6') D01 to D05, D07 and D08 were not unique to the site, but also presented in three samples from other Belizean sites Eagle Ray (E) and Glovers Reef (H). Sequencing revealed this fingerprint's dominant band is B17, a low migrating band that lies below a pale B1, with three SNP differences between the ITS2 types. B1 was present in all 10 samples, with the exceptions of D01 and D10, where only the B17 could be seen. D06 was the only sample to show a completely different profile, with no B17 (profile '1').

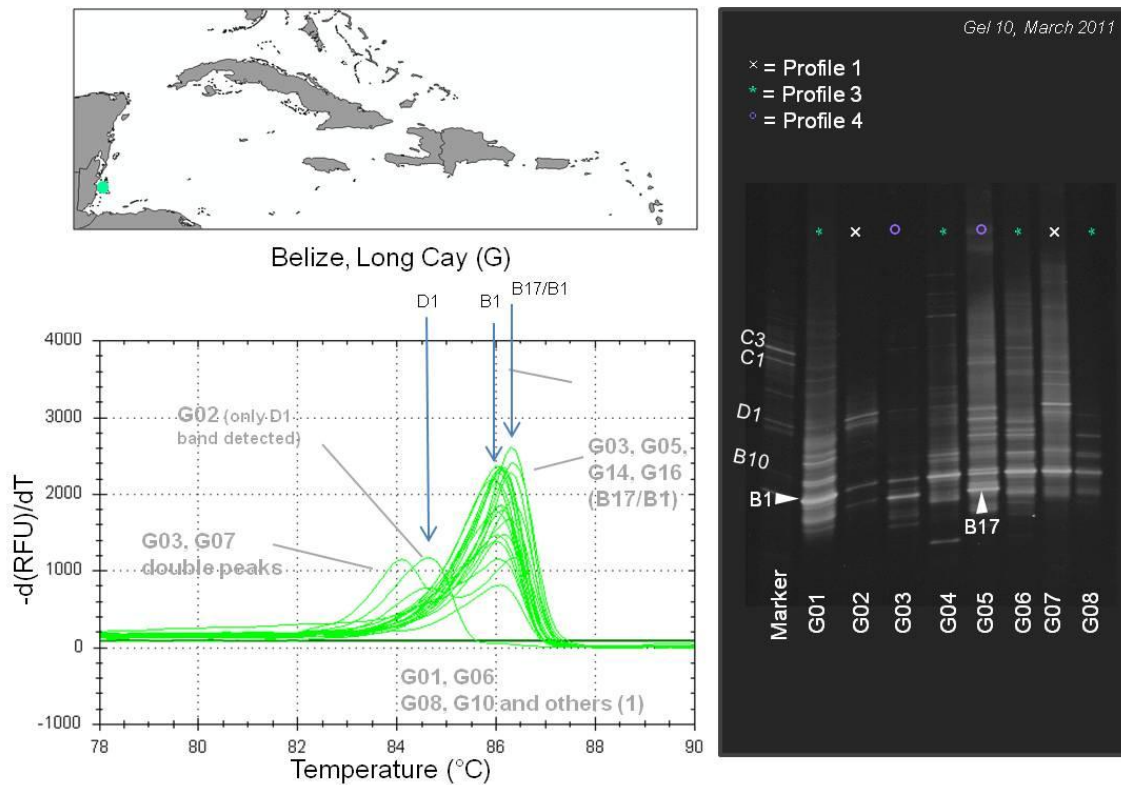
The HRM analysis produced a single large (3000) melt peak, around 86.3°C, representing the B17/B1 mix (Fig. 5). Sample D06 produced an indistinguishable melt peak, revealing that the technique was unable to distinguish B17 and B1 ITS2 types, although samples hosting the B17/B1 mix tended produce a higher fluorescence (2000 units) compared to those just hosting B1 (500-800 units). A few samples (e.g., D10, D11, D12, D17 and D30) produced a secondary melt peak around 83.8°C – although it is unknown which symbiont sub-clade this melt peak represents, the temperature suggests it's a C-type – the temperature is close to that found in CC samples.



Appendix Figure 5.3: Selected DGGE gel images and HRM outputs for Belizean site E, Eagle Ray.

Eagle Ray (E) samples produced a range of DGGE profiles (Fig. 6). The majority (e.g., E02, E06, E07, E08, E09) generated B17-dominated profiles identical to those prevalent at neighbouring site Coral Gardens (D) (profile ‘6’ see Fig. 5). In E03, E04 and E05, the B1 band was brightest, with a second band above, which sequencing revealed to be a heteroduplex. This profile (profile ‘3’) was also found at sites H and G, and at a Honduran site. E01 and E10 produced one very faint high band, in the C3 position.

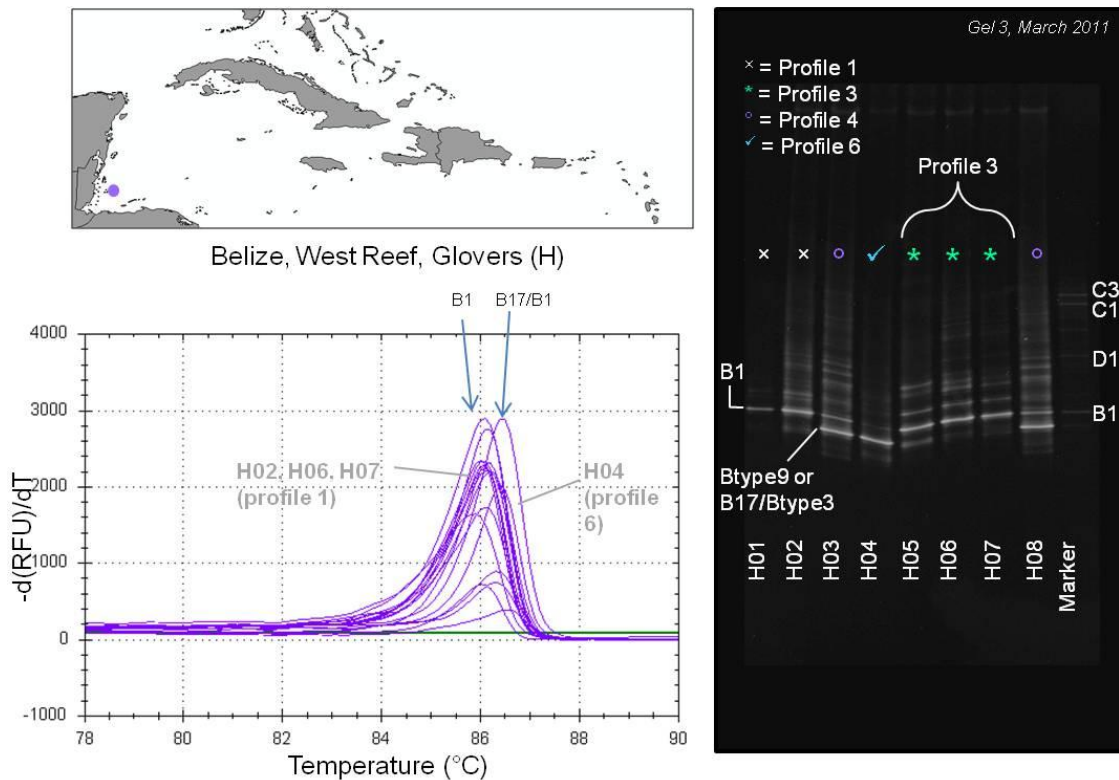
For the HRM analysis, samples with profile ‘6’ (dominated by B17) all produced melt peaks at 86.4°C, just as in H, D and G samples with the same DGGE profile. Again, HRM is unable to resolve the three SNP difference between B17 and B1. Several samples (E02, E06, E07, E08 and E09) generated an additional peak at 84.8°C, which may correspond to D1a, but was unable to be resolved (recorded as D1a-like). E01 also produced just one peak at 83.8°C, that corresponds to the C3 band. This peak was also observed in further samples (e.g., E07 and E09) indicating presence of this type in amounts small enough not to be detected by DGGE.



Appendix Figure 5.4: Selected DGGE gel images and HRM outputs for Belizean site G, Long Cay.

Long Cay (G) samples hosted diverse communities, displaying real mix of DGGE ribotypes – most of which matched those occurring at nearby site H. The most prolific DGGE profile (‘3’), consisted of a dominant B1 band, along with two paler bands above, understood to be heteroduplexes, and was also found at Belizean sites E and H, and at a nearby Honduras site, C. G03 and G05 appeared to follow the other Belizean profile, (‘6’), dominated by the B17 ITS2 type. G02, G03, G05 and G07 produced a band in the D1 position, although sequencing was unable to confirm this as D1.

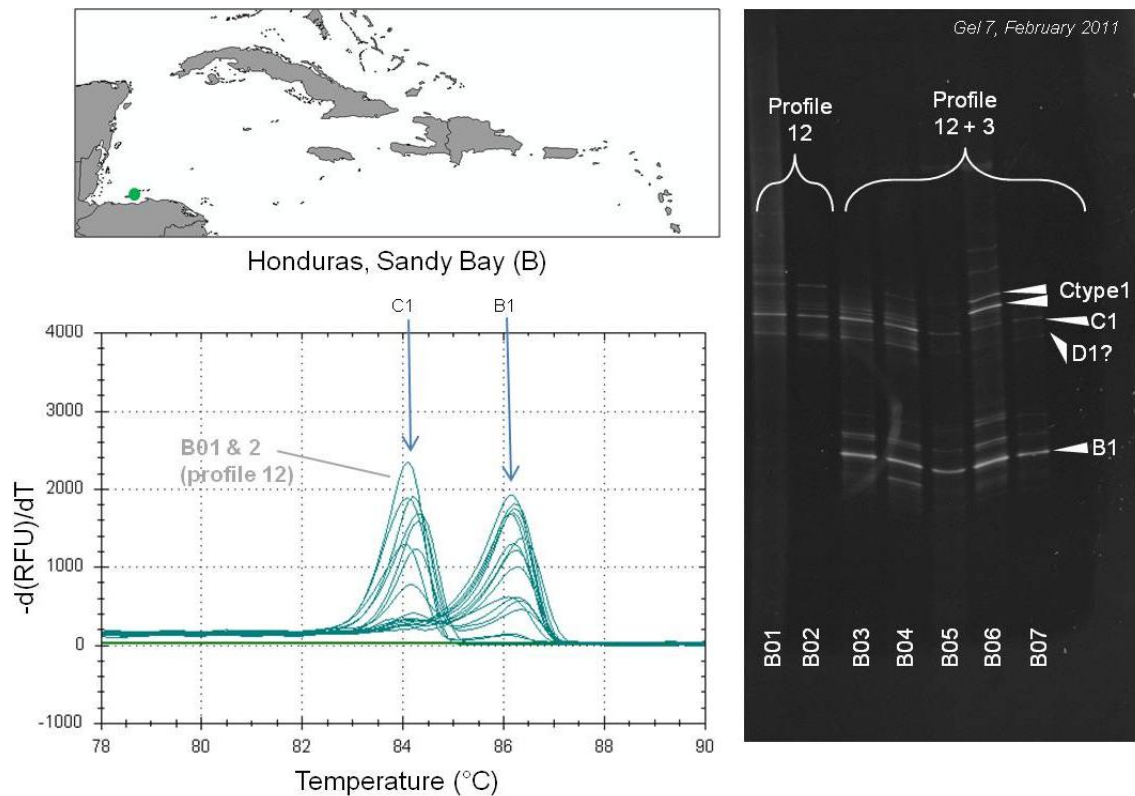
Samples with a large (1000+) melt peak at 86.0°C (e.g., G01, G04, G06, G08, G09) were assumed to be dominated by B1, the symbiont type that melts at this temperature, and this agrees with the DGGE patterns. G07, which was also dominated by B1 in DGGE, also contained this peak, but had another peak at 84.5°C, thought to be representative of D1a. G02 was unique in generating a single low (400) melt peak of 84.6°C, again reflecting the dominance of the D1a-like band alone. G03 produced a double melt peak too: one at 86.3°C (representing the B17/B1 mix found in all Honduran D samples), and a second at 84.6°C (D1-like). Samples G14, G16, G19, G20, G23 and G24 all produced this 86.3-4 band, again representing B17/B1). Although DGGE suggested four of the ten (G02, G03, G05 and G07) Long Cay samples contained D1/D1a, and HRM confirmed that G02, G03 and G07 to have melt peaks at the appropriate temperature for D1 (84.6°C±0.1) (nb/ G05 failed), screening samples from G using QPCR using more sensitive D-specific primers (in chapter X) revealed a further 9/10 samples contained low levels of D1a.



Appendix Figure 5.5: Selected DGGE gel images and HRM outputs for Belizean site H, West Reef.

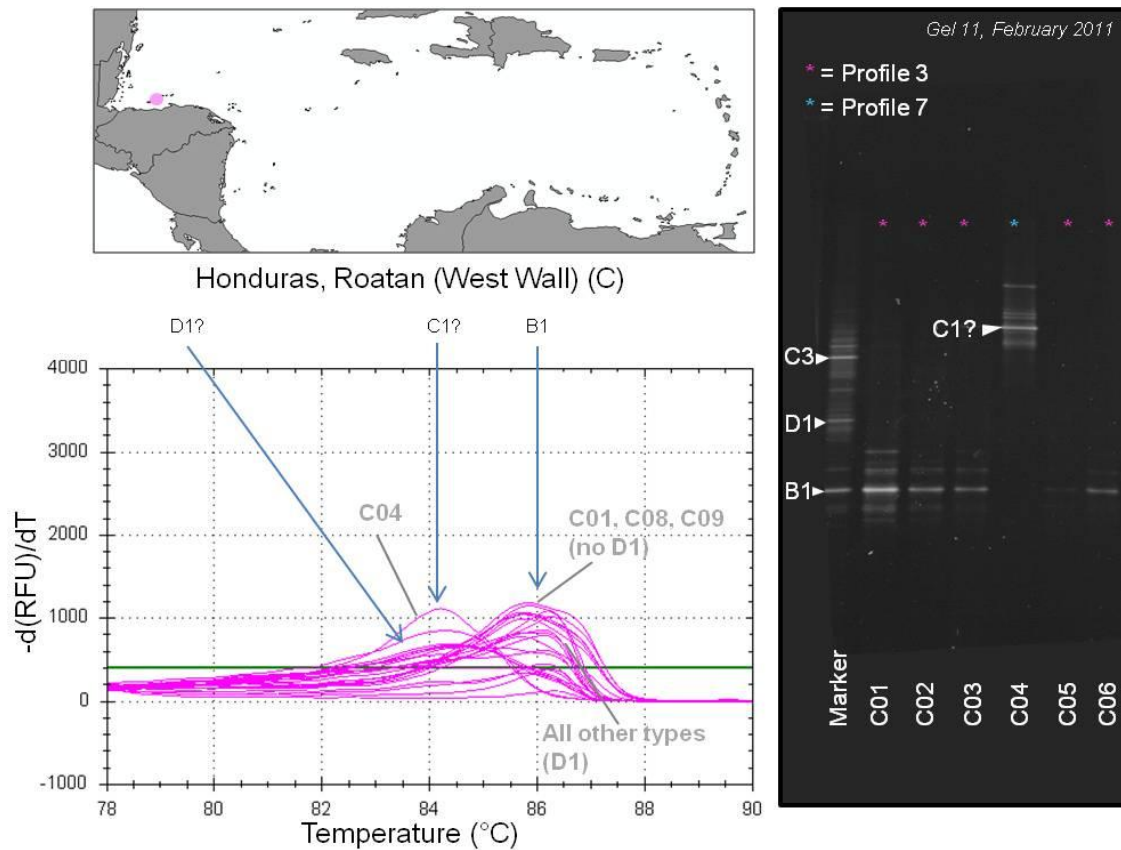
Like Long Cay, West Reef (H), a sheltered reef slope site with a dense population of *M. annularis*, produced a bigger variety of profiles than D and E. West Reef shared profiles 1, 3 and 4 with Long Cay, and also 6 (also present in E and D). B1 tended to be the dominant band in most of the H samples (H01, H02, H05-H07, H09, H10), and where it was not dominant, was still present in all except H04 (faintly). H03, H04, H05 and H08 contained a lower band, in a similar position to B17: in H03, H04 and H08, this was the dominant band.

H04 produced a peak at 86.4°C, which corresponds to the B17/B1 melt peak also seen in all D samples and majority of G samples too. Where B1 dominated, the peak was seen at 86.0°C, whereas where a B1/B17 mix occurred, a 86.4°C melt peak was observed. However, these differences could not be used to conclusively screen remaining samples, as peaks overlapped to a large extent.



Appendix Figure 5.6: Selected DGGE gel images and HRM outputs for Honduran site B, Sandy Bay.

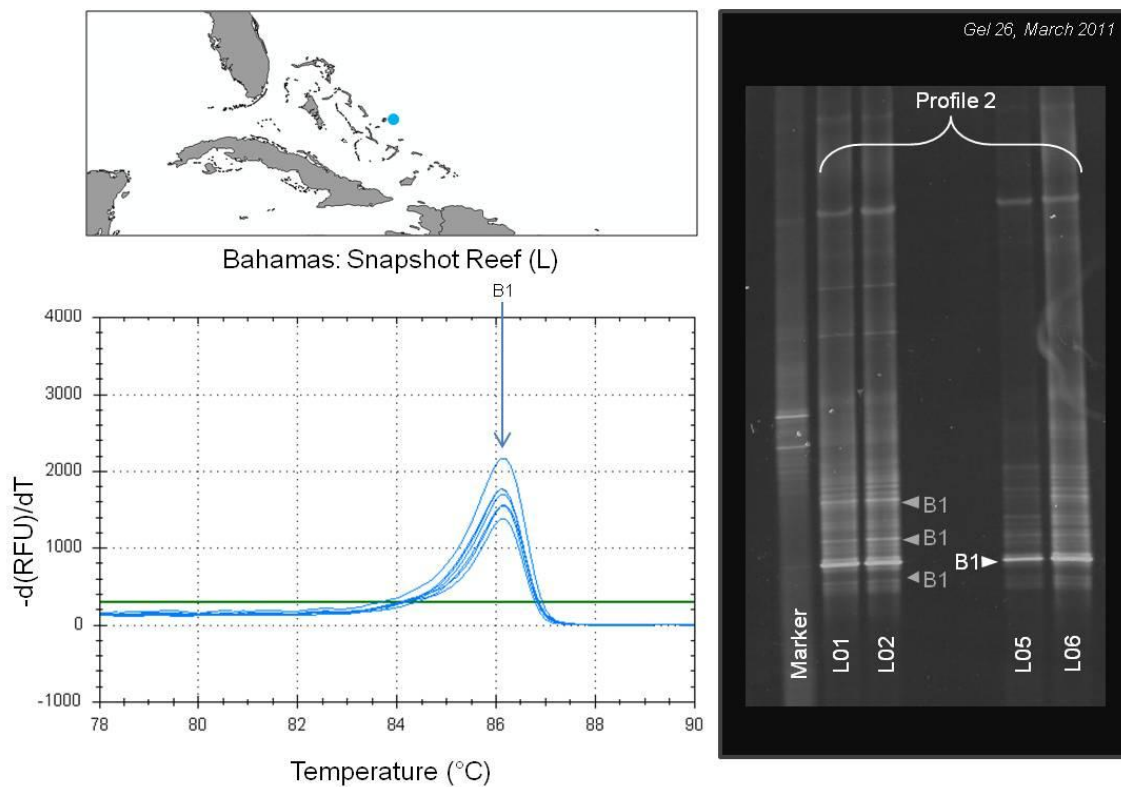
Sandy Bay (B), Roatan was the most diverse of the Honduran sites ($1/D = 4.99$) revealing four combinations of profile types. All profiles contained a C1 band, and for some (e.g., B01 and B02) this was the dominant band, with a paler heteroduplex below (profile '12'). These same samples generated tall (>1000) HRM peaks at 84.0°C , clearly representing C1. Most of the remaining samples produced double melt peaks: one at $84.1\text{--}2$ and one at 86.3 (e.g., B05 – B10) – presumably representing the two main bands of the profile. DGGE revealed these samples to possess a co-dominant B1 band. B06 was unusual as it had two even higher bands. Sequencing was not able to resolve this type, which has temporarily been named Ctype1. HRM was unable to distinguish this unidentified band from C1, producing one identical melting peak for this sample. This suggesting either that this type is very close to C1.



Appendix Figure 5.7: Selected DGGE gel images and HRM outputs for Honduran site C, Western Wall.

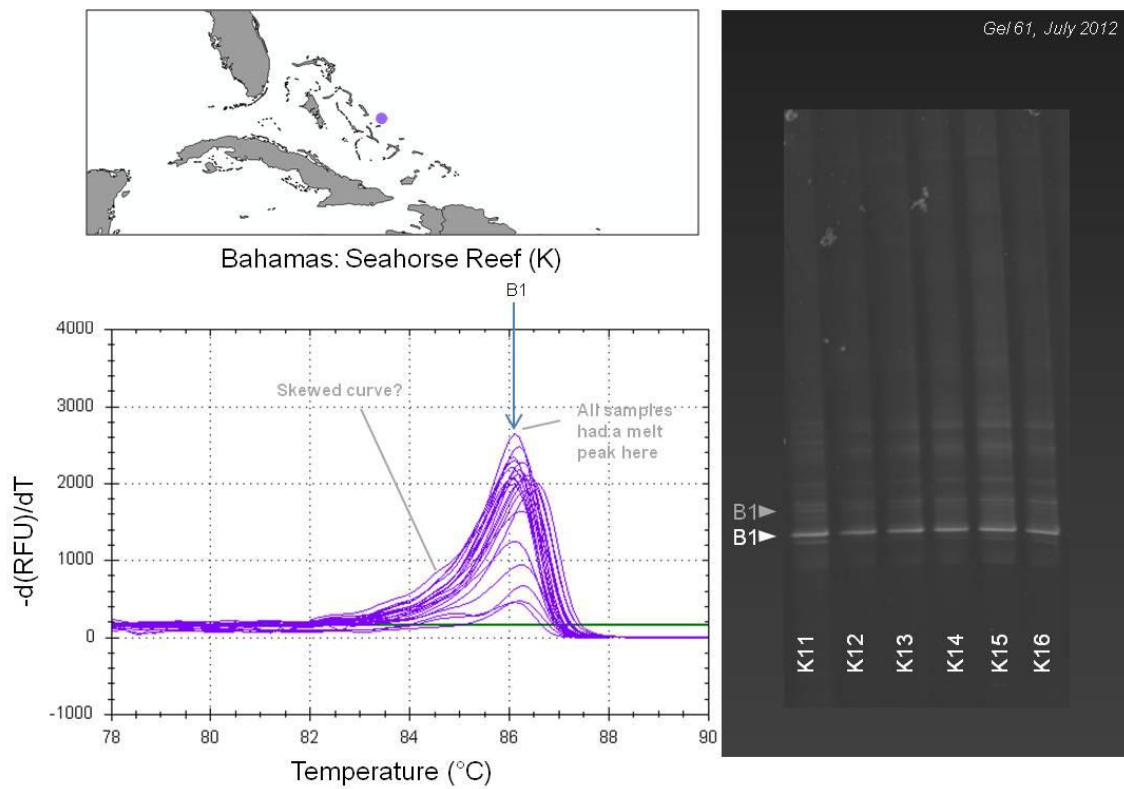
Western wall (C) revealed a fairly homogenous set of simple DGGE ribotypes. These were dominated (88%) by profile ‘3’, consisting of a dominant B1 band, with two fainter B1 heteroduplexes spaced above – similar to B07 found at Sandy Bay (B). In two out of three gels these paler bands were too faint to be seen. C04 was an exception, with no B1 and a high band, probably C1, as commonly found at other Honduran sites.

HRM analysis concurred with the DGGE, while providing some further resolution, with some samples generating two peaks instead of one. While C01 showed one peak at 86.1°C, representative of B1, others that were shown to reveal B1 by the DGGE analysis also showed peaks at 86.2°C, but also showed additional melt peaks around 84.3°C – not present on the DGGE gel. Further investigation revealed these samples were all individuals that were shown to contain D1a in a separate analysis. Those that did not contain D1a did not have the second melt peak. Curiously, samples from nearby site B were also shown to contain D1a, but did not show these peaks – possibly the amount of D lay below the detection limit for this technique. Finally, two samples (C04 and C14) had a much lower peak at 84.1°C, which neatly corresponds to the C1 band present in DGGE gels.



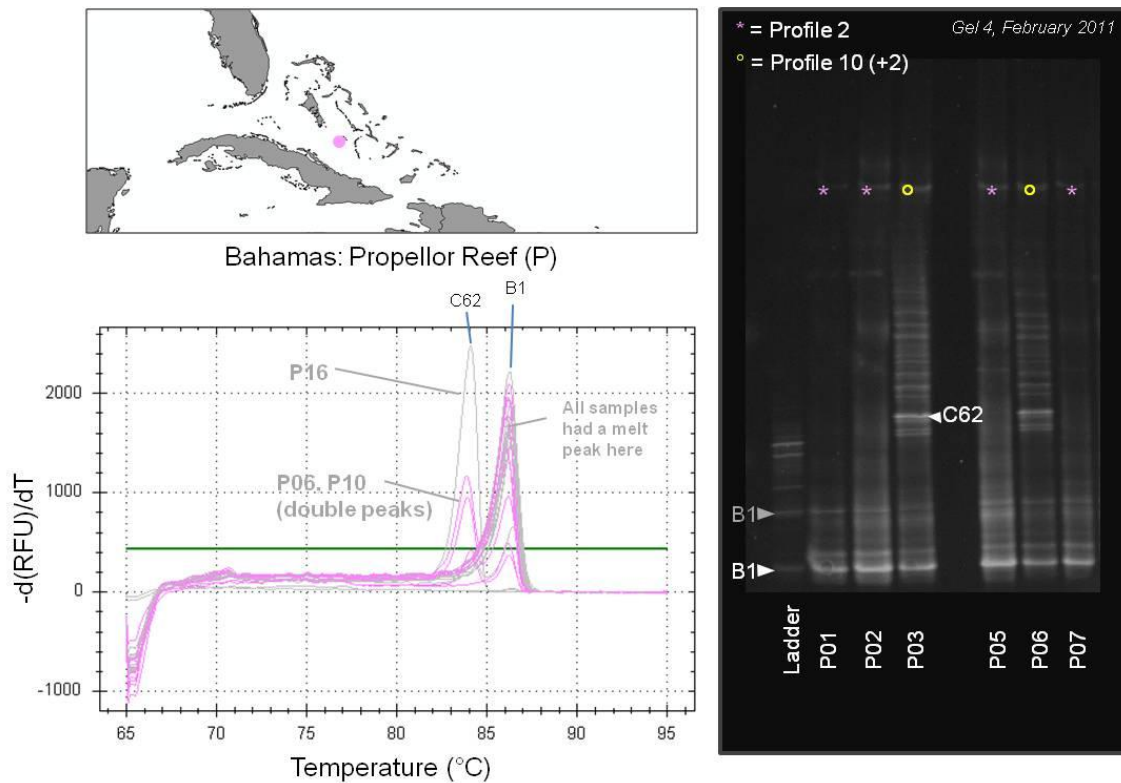
Appendix Figure 5.8: Selected DGGE gel images and HRM outputs for Bahamian reef L, Snapshot.

Snapshot reef (L) hosted the lowest *Symbiodinium* ITS2 diversity of all the sites sampled (Simpsons $1/D = 1.26$) with every sample producing an identical DGGE ribotype (profile '2'), with a dominant B1 band, and several fainter bands (two above, one below) which appeared to varying degrees (Fig. 12). Sequencing of all bands in samples L01 and L02 revealed these bands to be B1 heteroduplexes. HRM analysis supported the DGGE evidence: all samples to produced a single melt peak at 86.1°C , confirming presence of B1 in all samples. Some samples (e.g., L05 and L11) were also shown to have low amounts of D1, but this was not detected on DGGE.



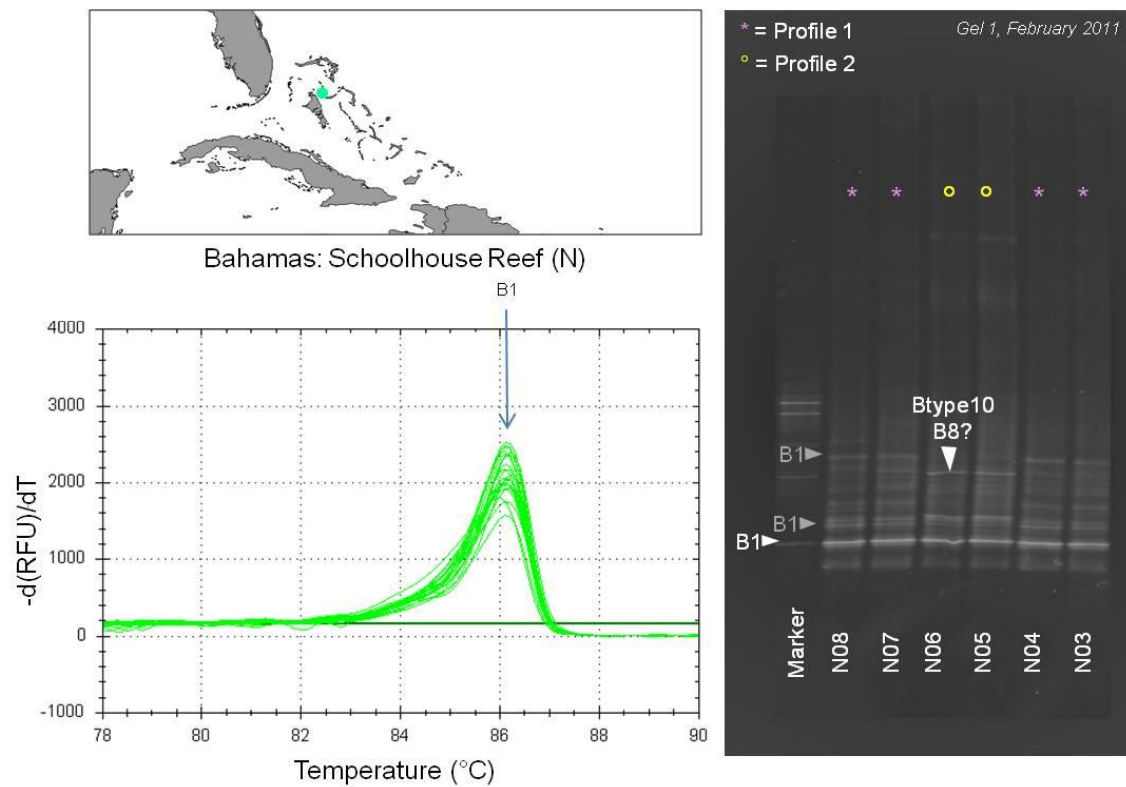
Appendix Figure 5.9: Selected DGGE gel images and HRM outputs for Bahamian reef K, Seahorse.

Seahorse Reef (K) was the most exposed of the Bahamian sites, located off the north of San Salvador Island about 40 km from the more sheltered leeward Snapshot Reef (L). Along with Snapshot, B1 was dominant in all samples, with a few showing a co-dominant C1 band (Fig. 11). HRM produced melt curves at the B1 temperature, although no secondary melt peaks showing that HRM wasn't able to detect or distinguish C1 here (Fig. 13).



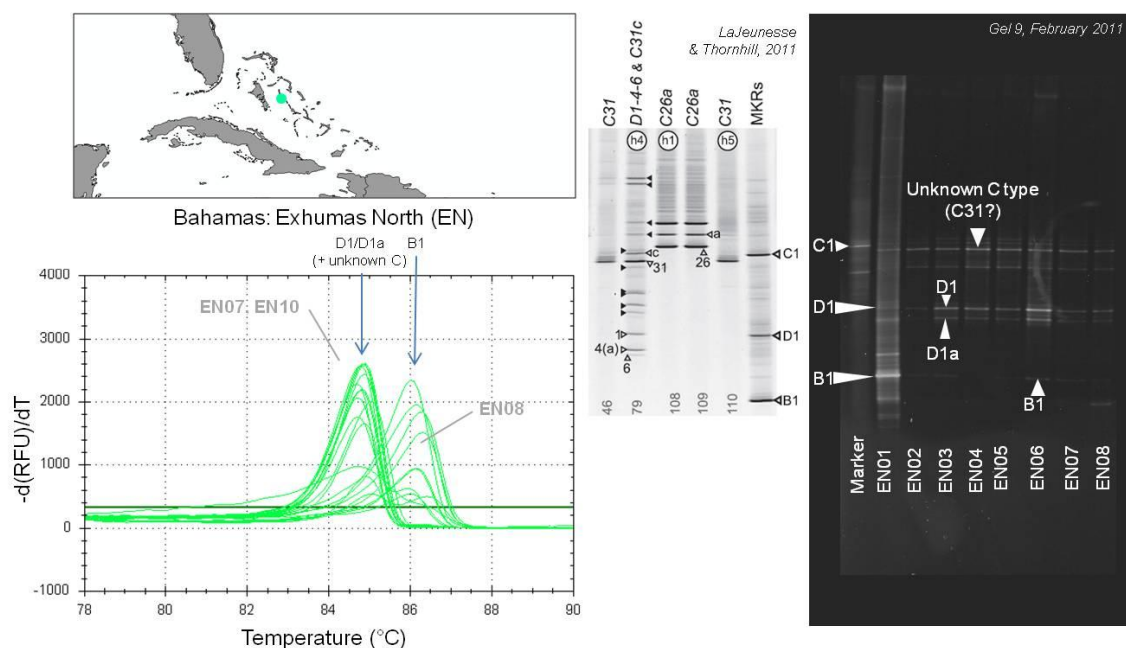
Appendix Figure 5.10: Selected DGGE gel images and HRM outputs for Bahamian reef P, Propellor Reef.

The majority of Propellor Reef (P) samples adhered to a simple B1-dominated ribotype (profile '2') evident at Snapshot reef (L), consisting of a bright B1 band (Fig. 14). A slightly higher band in some samples was almost close to being a D1 band, but a combination of sequencing and direct comparison with EN samples revealed it to be a B1 heteroduplex, migrating further than D1. Three samples, P03, P06 and P16 produced additional higher migrating bands, which sequencing revealed to be an unknown type. The positioning of the band appeared similar to C12, but lay slightly higher on the gel and had 7 SNPs different to the normal C1 sequence. An alignment with all major published ITS2 types extracted from the GeoSymbio database (Frankin, Stat et al. 2012) showed C62 to be the closest, but not perfect, match to this symbiont, so it has temporarily tentatively been called 'C62' until further resolution is possible. HRM revealed three melt profiles. The majority of samples displayed the first: a tapered peak around 86.2°C, corresponding to B1. Several samples (P06, P10, P11, P23) showed a double peak, with co-dominant bands at 83.9°C as well as the 86.1°C. 83.9°C melt peak produced by a few samples (P16, P06) corresponds to 'C62'.



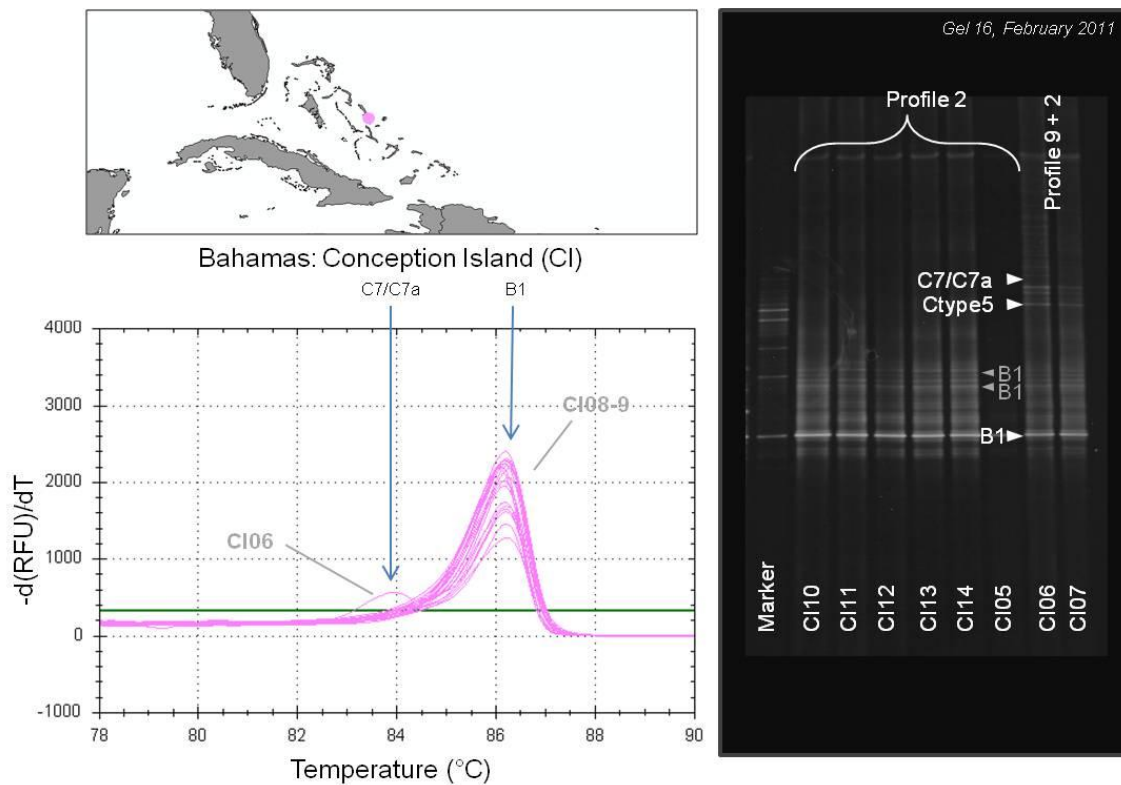
Appendix Figure 5.11: Selected DGGE gel images and HRM outputs for Bahamian reef N, Schoolhouse Reef.

Almost all Schoolhouse Reef samples showed identical banding profiles (profile '1'), dominated by B1, with a pale band below and several bands above, which sequencing revealed to be B1 heteroduplexes (Fig. 15). A minority of samples (e.g., N05 and N06) showed a slightly different banding pattern (profile '2'), which couldn't be aligned with any other sequences in the GeoSymbio alignment file sequence most similar to B8 (or B34) in the alignment, but that couldn't be identified with confidence. HRM failed to distinguish between profiles 1 and 2 with all samples producing a single melt peak at the B1 position ($86.1 \pm 0.1^{\circ}\text{C}$) although closer inspection revealed samples potentially hosting B8 appeared to have a small bump around 84.9°C .



Appendix Figure 5.12: Selected DGGE gel images and HRM outputs for Bahamian reef EN, from the Exhumas National Park. *Inset* shows image taken from another study, showing D1a and C31.

The Exhumas samples displayed remarkably different DGGE profiles to other Bahamian sites, and showed significantly higher species richness compared to the rest of the Bahamas (Simpsons 1/D = 4.92, vs. Bahamian mean of 1.78 ± 0.31). The majority produced a fingerprint with a dominant band pair in the D1/D1a position, and a higher migrating pair of C-type bands above, just below C1 (Fig. 16). Sequencing of this pale band was unsuccessful, the position on the gel looks similar to C31+C31b (although Pacific only) perhaps C1k, or Caribbean C1a & C1i?. This DGGE fingerprint, named ‘profile 14a’, dominated a variety of other sites, including Dominican (DM) and BVI (R) sites. Other samples produced B1 dominated profiles (e.g., EN01) while most other samples had a low amount of B1 present – a very faint band could just be observed in most lanes. EN08 produced a band that migrated lower than B1, although this band could not be identified. HRM produced five distinct profiles. The majority of samples showed a peak around $84.7 - 84.8^\circ\text{C}$, which corresponds to the DGGE profile containing D1/D1a/unknown C-type bands, and was also observed in the HRM output from Dominican (DM) and BVI (R) samples. Here, HRM was evidently unable to distinguish between the D1/D1a and slightly higher unidentified C-band.

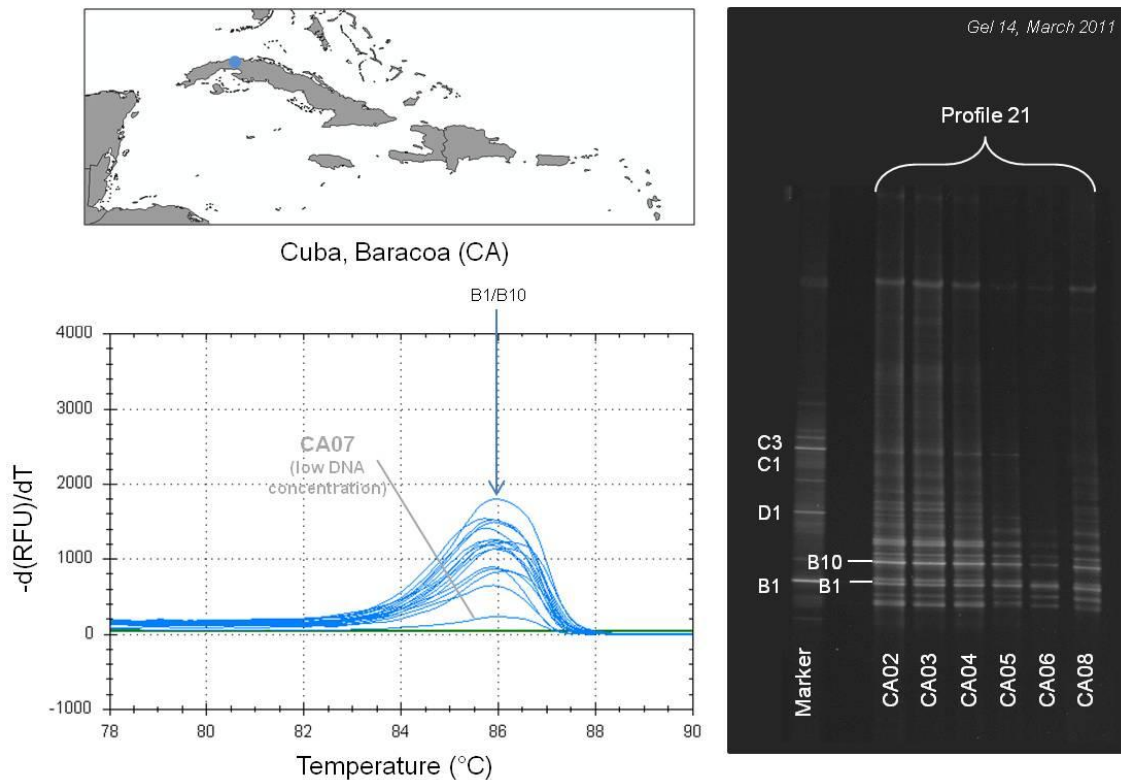


Appendix Figure 5.13: Selected DGGE gel images and HRM outputs for Bahamian reef CI, from Conception Island.

All Conception Island (CI) samples were dominated by the B1 band, displaying similar DGGE profiles to that of Propellor Reef (Fig. 17). Two higher migrating bands were also present which were shown to be B1 heteroduplexes. In sample CI06, three high bands were also observed, a pair that are comparable with the double C7/C7a bands – similar to some Tobagan, Dominican and Nicaraguan samples and Barbadian found in the eastern Caribbean region, and a lower unidentified band (“Ctype5”).

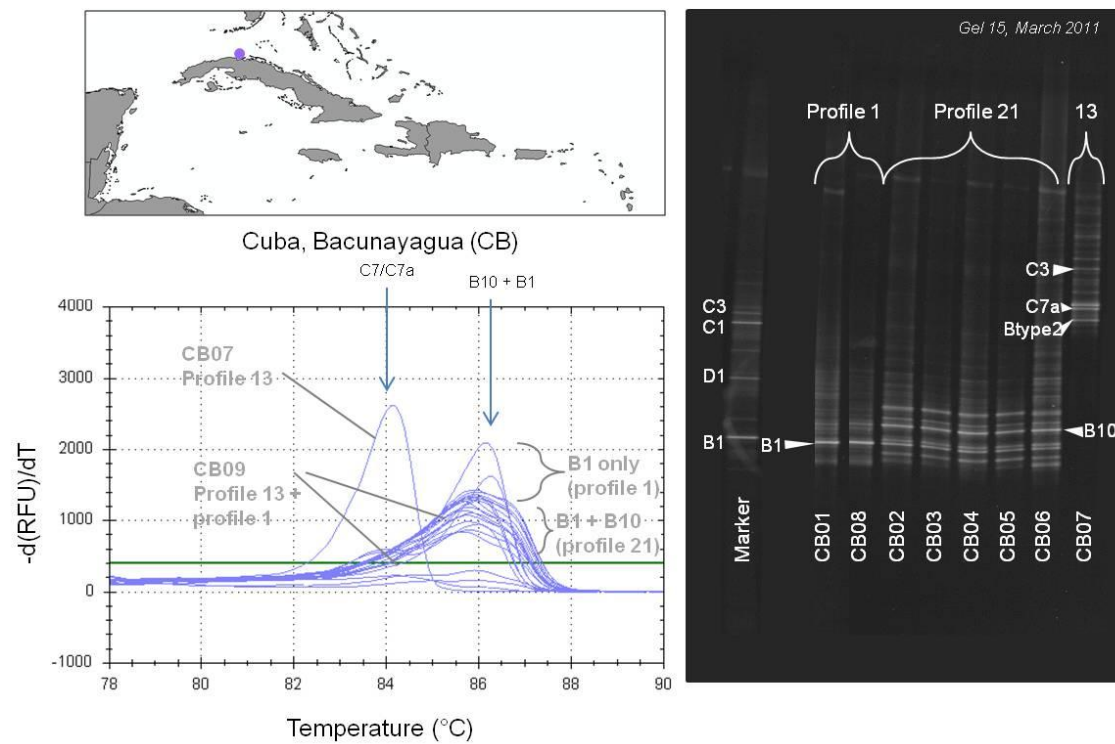
HRM produced two melt peak profiles; the most common consisted of a single peak consistently found at 86.2°C (corresponding to B1), but the left-hand skew of the peak suggests

it might be combined with another type (for example some samples CI19, CI20, CI23) had a little bump at around 84.5°C. The second ribotype also had 86.2°C peak, but a second peak at 84.1°C suggesting a C type.



Appendix Figure 5.14: Selected DGGE gel images and HRM outputs for Cuban reef CA, Baracoa.

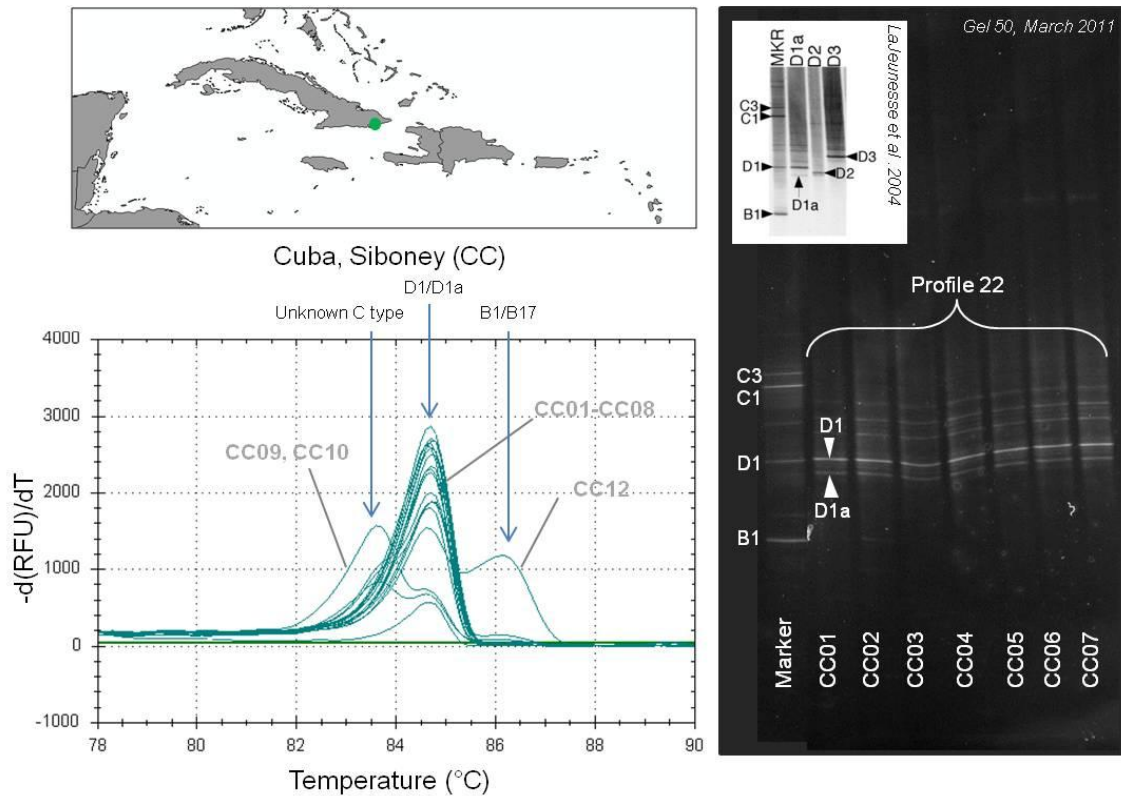
Baracoa (CA) samples were uniformly made up of what sequencing revealed to be a B10 dominated fingerprint (profile '21'), a profile that appears to be unique to Cuban sites CA and CB. Located just above the B1 band, the B10 sub-type was shown to have just one base pair different to B1. In the majority of cases either B10 (e.g., CA02, CA03, CA04, CA09) or a B10/B1 (e.g., CA05, CA08) was dominant (Fig. 19). The only other place that B10 occurred in our dataset was on Grand Cayman, and in a background capacity in Honduras, although B10 appeared in *M. annularis* samples from nearby Floridian reefs 320 km due north of our Cuban sites in a published study from 2003-2005 (Thornhill, Xiang et al. 2009). A few samples appeared to have just a dominant B1 (e.g., CA06). The HRM analysis appeared to be unable to resolve the small differences between B1 and B10, with all samples producing a single melt peak at 85.8°C (± 0.1), representative of the B1/B10 mix. Curiously, instead of tapering these melt peaks were skewed to the right, and also showed a lower fluorescence that other peaks on the same plate, flaring at < 1000 fluorescence units, compared to 2000. This might be explained by the fact a single melt curve was representing two similar ITS2 types. The only DGGE ribotype to show a dominant B1 band instead of a B10/B1 band, was later shown to contain D1a using qPCR (Chapter X).



Appendix Figure 5.15: Selected DGGE gel images and HRM outputs for Cuban reef CB, Bacunayagua.

Bacunayagua (CB), just 82 km east of Baracoa (CA) hosted a range of three DGGE profile types, demonstrating greater *Symbiodinium* diversity than its homogenous neighbour. The most commonly occurring type - the B10/B1 profile '21' - was identical to that found at Baracoa, and unique to these Cuban sites (Fig. 20). Other samples (e.g., CB01, CB08 and CB10) produced simpler banding profiles, dominated by B1 alone (profile '1'). CB07 had a different fingerprint (profile '13', with higher bands), which matched that of Dominican Republic sample DR01. Sequencing revealed this community to be dominated by *C7/C7a*, with an unidentified band below ('Btype2'), and a C3 band above. CB09 had a combination of both profile 13 and profile 1.

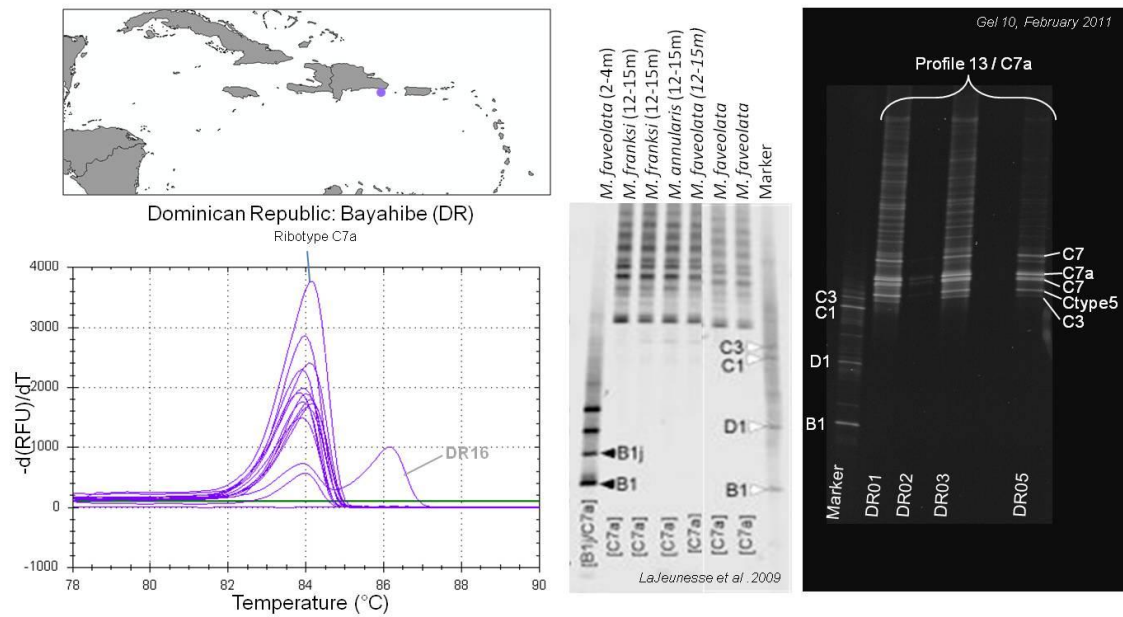
The HRM analysis supported conclusions from the DGGE. Just as in Baracoa, most samples produced just one melting peak around 85.8°C (± 0.1), as the HRM appeared unable to distinguish closely related ITS2 sequences B1 and B10. However, closer inspection of the plot revealed that the relative fluorescence of CB01, CB08 and CB10 – the three individuals hosting only B1 – was almost 500 units higher, and more tapered, possibly causing a distinction between profile '1' (B1 only) and smaller (1000 units), more skewed and flatter curves of profile '21' (B1/B10) – Fig.20. The clearer flare produced by just one clear B1 band, showing the technique may be able to resolve B1 vs B1/B10 differences. CB09 produced a mix of profile '13' and profile '21' on the gel: it produced a double melt peak. Finally CB07 ('13') produced a completely different peak at 84.1°C.



Appendix Figure 5.16: Selected DGGE gel images and HRM outputs for Cuban reef CC, Siboney. Inset: D1a banding from the Pacific, from LaJeunesse *et al.* 2004.

Siboney (CC) symbiont communities appeared very different to other Cuban (CA, CB) samples, perhaps unsurprisingly coming from over > 800 km away. None shared the unique B1/B10 Cuban profile '21', instead producing fingerprints with five faint bands (profile '22'). The brightest band in each case was a D1 band, with a D1a below, and three further bands above (Fig. 21). This fingerprint has been recorded previously from the Western Indian Ocean, central Pacific and Caribbean, found in a wide range of species and often, but not always, associated with shallow water depths (LaJeunesse 2002, LaJeunesse *et al.* 2004). (LaJeunesse, Bhagooli *et al.* 2004). In our dataset, this profile is shared by a BVI sample (T01), a single Jamaican sample (JB2) and seven Bahamian samples from one site in the Exhumas (EN). As well as the D1a band, a few samples showed additional bands: CC12 had low bands in the B1 position and B17 position, while CC09, CC10, CC13 and CC21 showed a possible C-type band (C1?) above the main D1 that was unidentifiable.

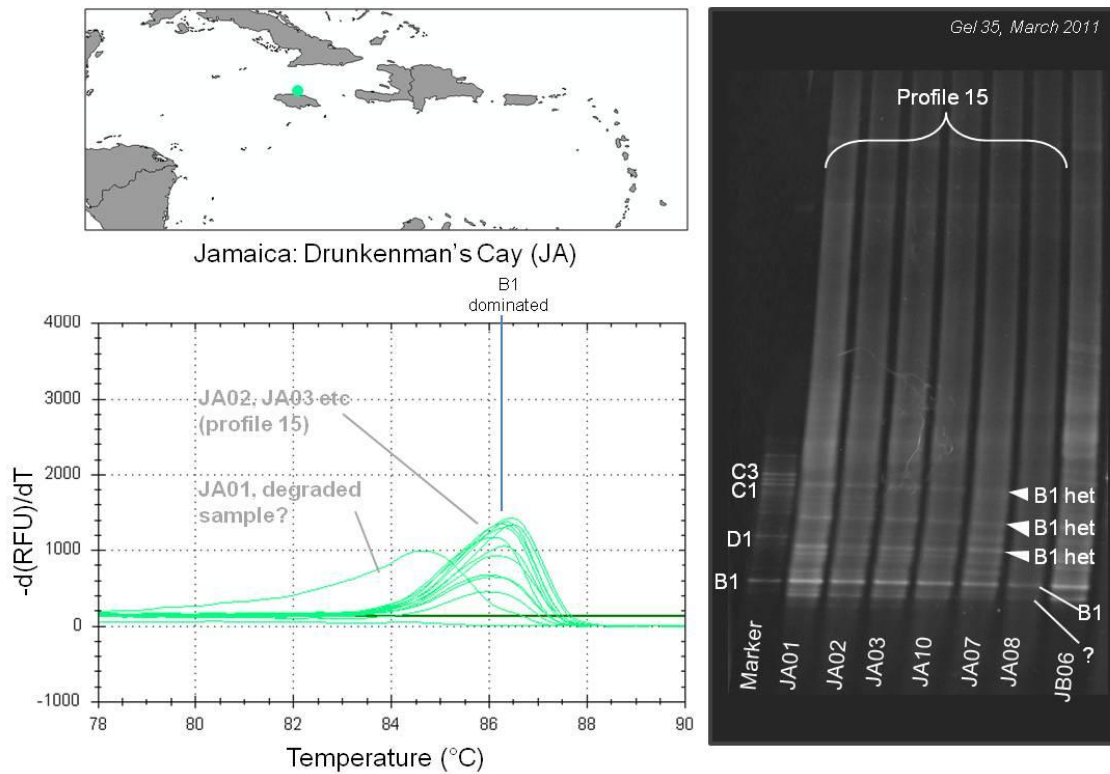
HRM melt profiles corroborated the DGGE ribotypes, with the majority showing a melt peak around 84.7°C, representative of the dominant D1/D1a bands. This is a similar melt peak to those found in D1/D1a dominated EN (84.7-8°C) and CC samples (84.8°C). Exceptions to the normal melt peak profile included CC09, CC10, CC13 and CC21, which had two melt peaks, one at 83.7°C, as well as the 84.7°C (D1/D1a). This 83.7°C is thought to be C1. Sample CC12 had a dominant D1/D1a band, but also a second peak at 86.2°C, the normal melt profile for B1/B17. This agrees with the DGGE profiles.



Appendix Figure 5.17: Selected DGGE gel images and HRM outputs for the Dominican Republic.

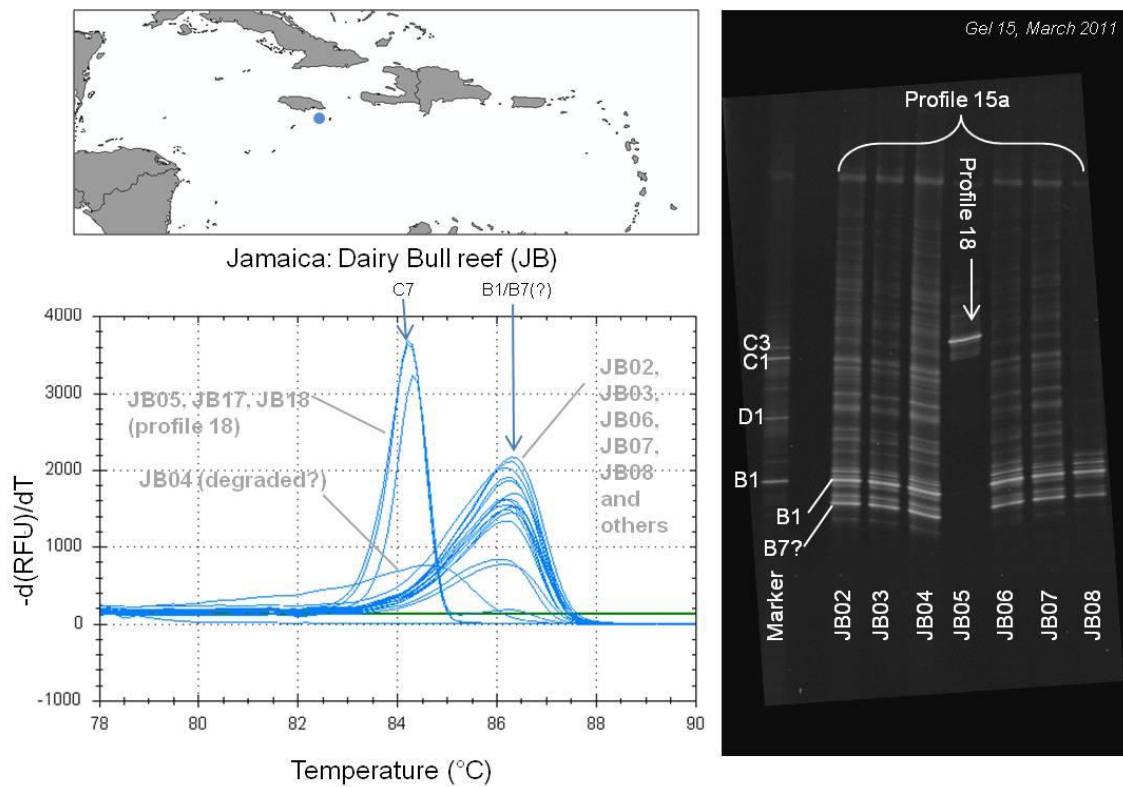
Bayahibe (DR) samples (which were degraded) all produced a banding pattern (profile ‘13’) very similar to that described in *M. annularis* symbiont ITS2 types in Barbados (LaJeunesse, Smith et al. 2009). The profile is dominated by a pair of bright bands: C7 and C7a (also known as C12) (Fig. 22). Above this band pair lie several C7 heteroduplexes. Below the band pair lies a very faint C3 band. The difference between the published profile and ours is a bright C-type band between C3 and C7, which sequencing was unable to identify. Sequencing revealed only one base pair difference between this new type (‘Ctype5’) and C3.

HRM analysis showed melt peaks for profiles at 83.8-84.0°C, for all samples where DGGE had shown a C7/C7a + C3 (profile ‘13’) DGGE ribotype. This melt peak value lies halfway between recorded melt peak values for C7/C7a (e.g. 84.1°C) and C3 (83.9°C), perhaps reflecting the mix of types. Comparing melt profiles to those with similar DGGE fingerprints showed that the DR (with the additional unidentified C band) had a slightly lower melting peak, and also appeared skewed to the right, than those dominated by C7/C7a and C3 alone (e.g. Dominican samples). One sample showed an unusual double peak, with the second peak at 86.2°C. This was the only sample that contained D1a.



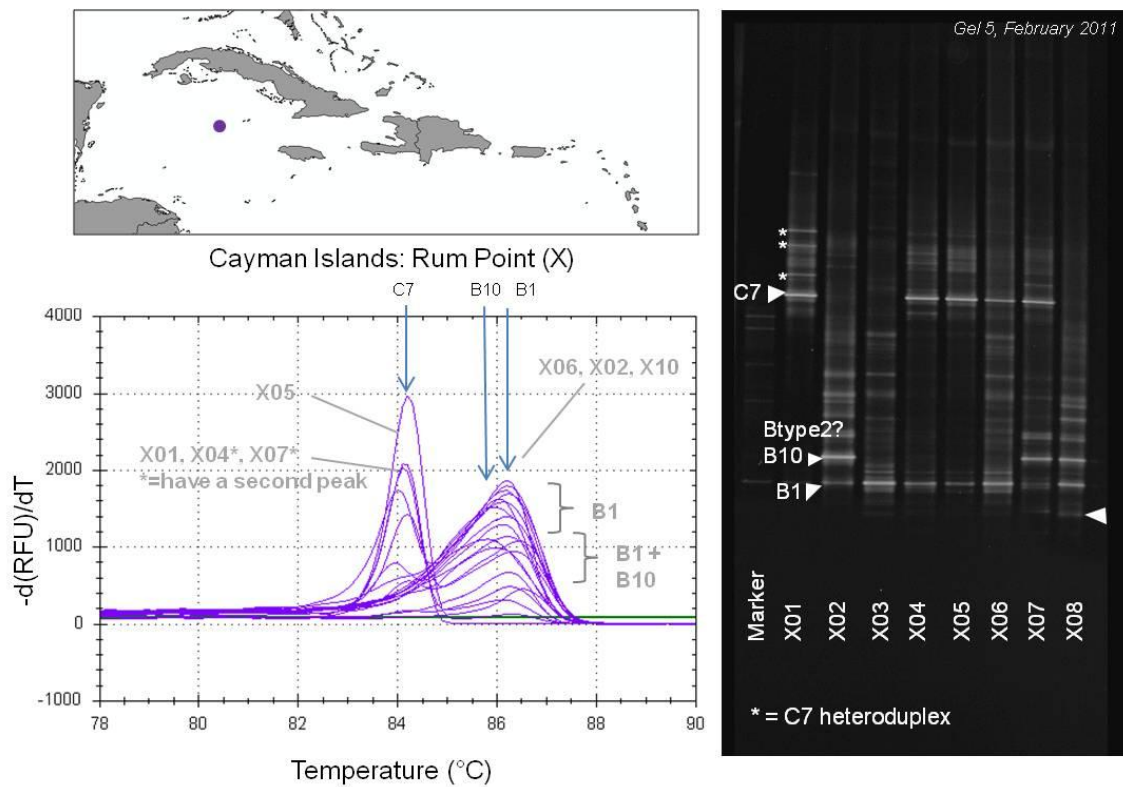
Appendix Figure 5.18: Selected DGGE gel images and HRM outputs for the Jamaican site, Drunkenmans Cay (JA).

Samples from Drunkenman's Cay (JA) had the lowest diversity in the Greater Antilles (Simpsons $1/D = 1.48$) with all samples producing a B1 dominated fingerprint (profile '15'). The profile also harboured several higher migrating bands (sequencing revealed the brightest four of these to be B1 heteroduplexes) and a paler B7 band lying just below, in a similar, but slightly lower position that B17 (direct comparison with E types) (Fig. 23). HRM analysis produced just one set of melt peaks at 86.0-86.3°C, thought to be analogous to the B1 banding profile for 15. JA01 and JA09 produced peaks at 84.5°C despite showing identical banding on the DGGE – perhaps these are degraded samples, as they also show low fluorescence.



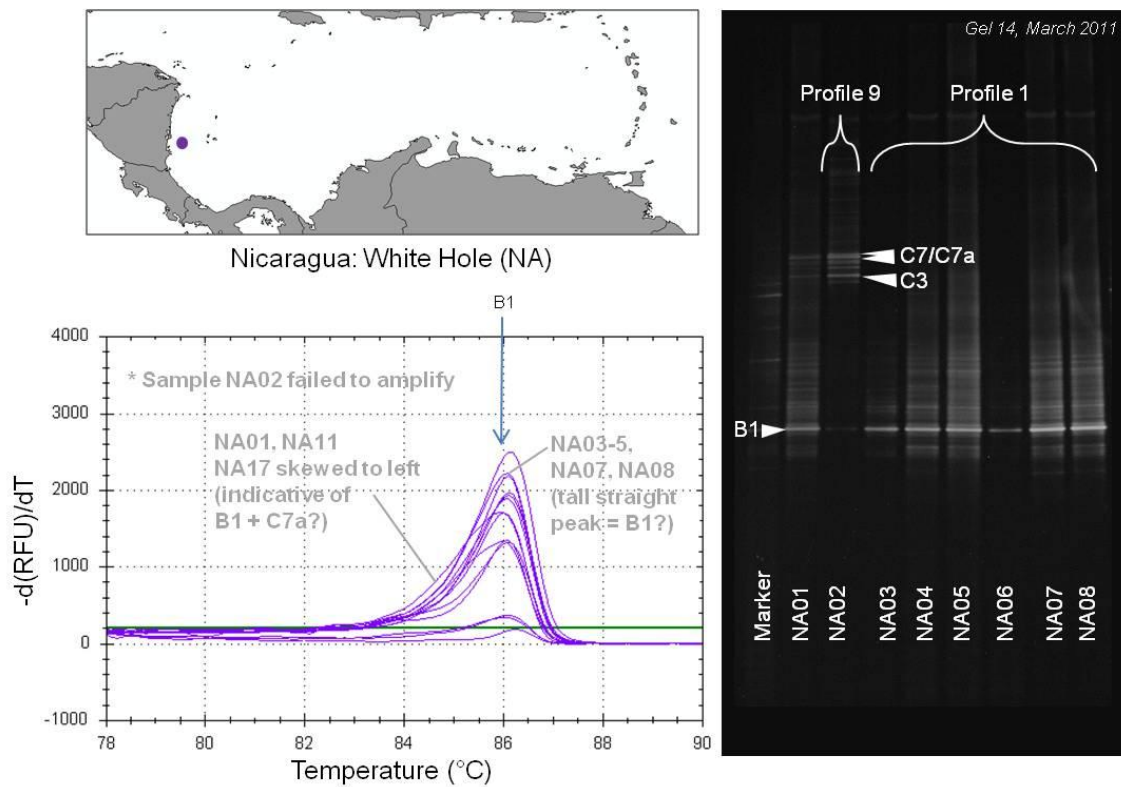
Appendix Figure 5.19: Selected DGGE gel images and HRM outputs for Jamaican reef JB, Dairy Bull reef.

The majority of Dairy Bull (JB) reef samples produced similar profiles to Jamaican site Drunkenman's Cay, with a bright B1 band and a co-dominant B7 band, although the B7 band is as bright as the B1 (Fig. 24). This B1/B7 mix was also found in Columbia (CM) samples. A few samples (e.g., JB05) produced an alternative profile, which appears to host a single symbiont, C7. This profile is also common to all Curaçao populations (Z, VB and SB samples) and one of the Venezuelan sites (BV). HRM melt profiles revealed two melt peaks – one broad peak (86.0-86.2°C) corresponding to the B1/B7 mix, and the other (84.3°C), corresponding to the alternative C7 band. Samples produced either one, or the other.



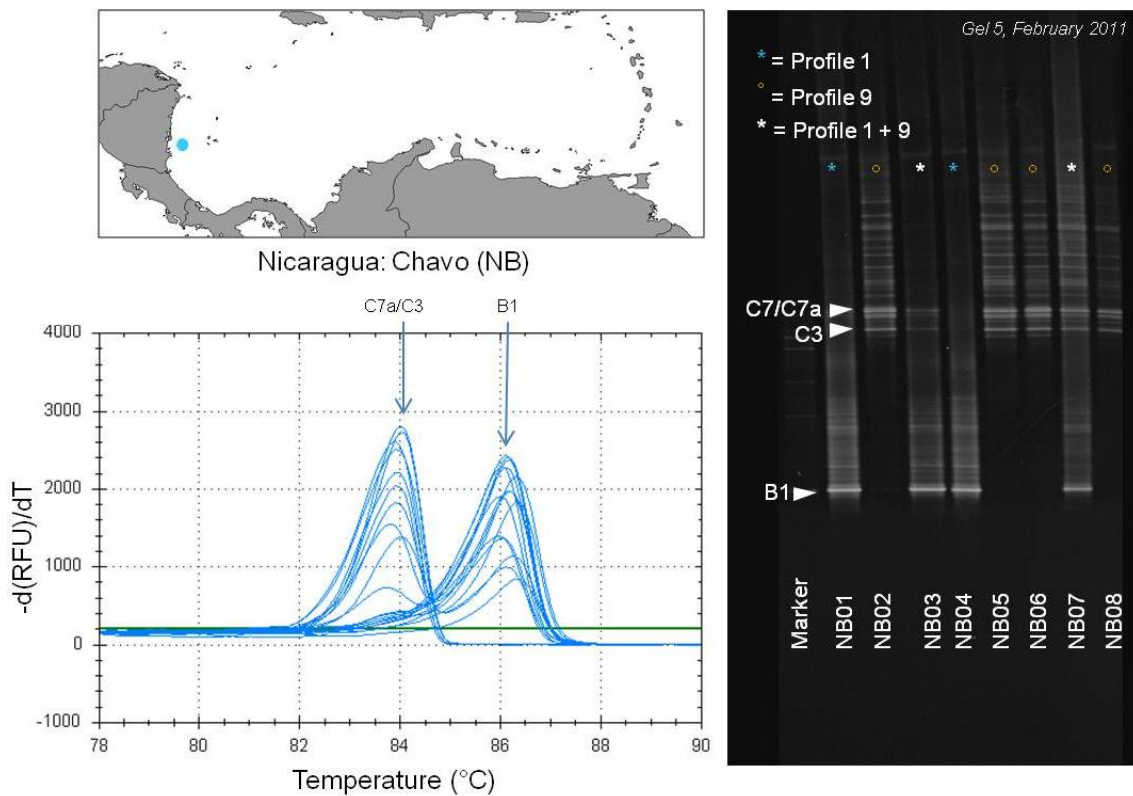
Appendix Figure 5.20: Selected DGGE gel images and HRM outputs for Grand Cayman Reef X, Rum Point.

Rum Point samples hosted a variety of *Symbiodinium* types (Fig 25). All individuals hosted various combinations of either C7, B1 or B10. Sample X07, for example, was populated exclusively by B10, X10 by B1, and X08 by C7. Samples X04 and X05 were co-dominant for C7/B1, X07 for C7/B10 and X08 for B1/B10. Most other DGGE bands tested were heteroduplexes, although a faint band present in many samples (X07, X06, X20, X15, X12) appeared similar to the B7 band found present in Jamaican samples, although unfortunately this could not be confirmed. HRM analysis corroborated DGGE observations. Samples identified as hosting C7 produced a melt peak at 84.1°C, and those that had additional B1 or B10 bands showed a second peak around 86.0°C. HRM was not able to resolve B1/B10 differences conclusively, although samples hosting purely B1 had a higher melting temperature than those hosting B10 only (86.2°C for B1, compared to 85.8°C for B10), many of the samples contained a mix of B10 and B1, leading to a mass of peaks at 86.0°C around 1500. Where samples contained both B1 and B10, melt peak of 86.0 was observed.



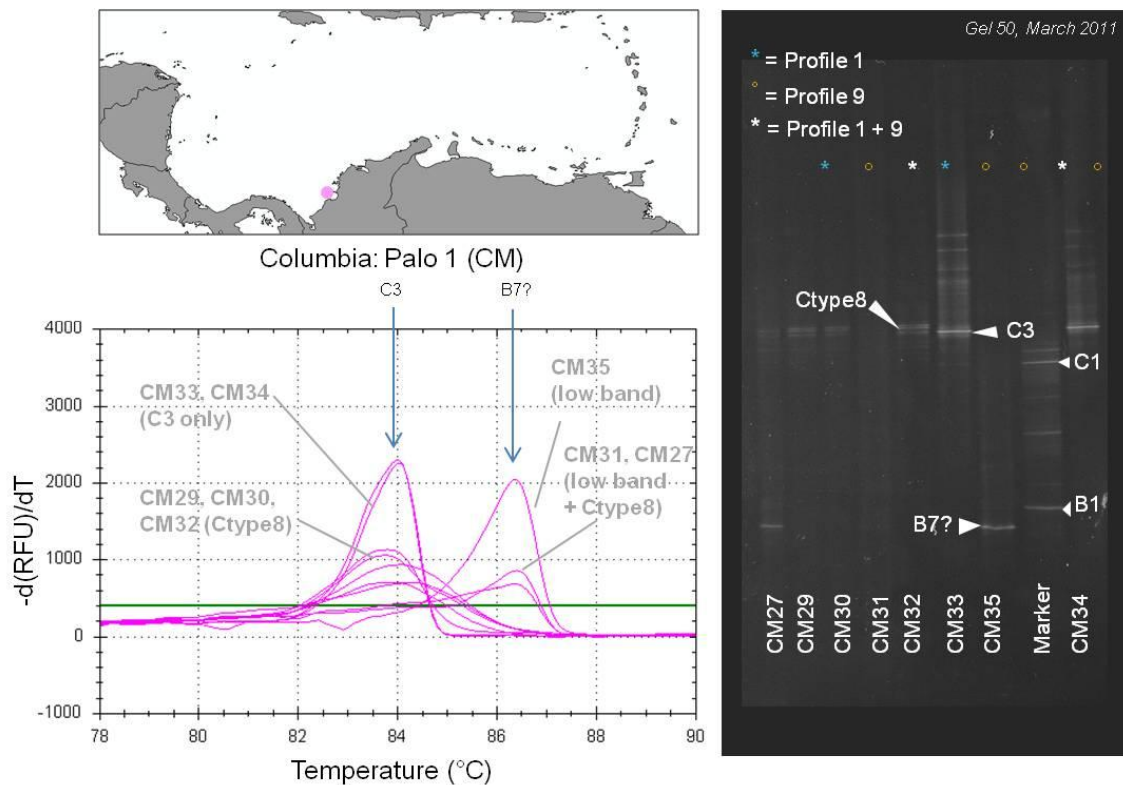
Appendix Figure 5.21: Selected DGGE gel images and HRM outputs for Nicaraguan site NA, White Hole.

Most White Hole (NA) samples were dominated exclusively by B1 (profile '1'), with a few samples (e.g., NA02) showing additional three higher bands (profile '9'), consisting of a lower C3, 'Ctype5', a C7a and a C7 (Fig. 27). HRM revealed a single melt peak at 86.1°C in almost all individuals, corresponding with the B1 band. Unfortunately, after running successfully on the DGGE gel sample NA02 failed to amplify during qPCR in three instances, most likely due to degradation of the genetic material. We assume that the technique was unable to detect low levels (i.e. fainter bands) of profile '9' in other samples, with the B1 shading it. However, while many of the 86.1 °C melt peaks (e.g., NA03, NA04, NA07, NA08) showed a neatly tapered peak up to 2500 RFU units, some peaks (e.g., NA01, NA09, NA10, NA11, NA17 and NA19) displayed a shorter (~1000 units), broader peak, with a bulge to the left hand side (usually peaking around 83.9°C), perhaps indicative of a dominant B1 with some additional C7a/C7 banding. This phenomena is also commonly found in nearby site NB (Fig. 27).



Appendix Figure 5.22: Selected DGGE gel images and HRM outputs for Nicaraguan site NA, White Hole.

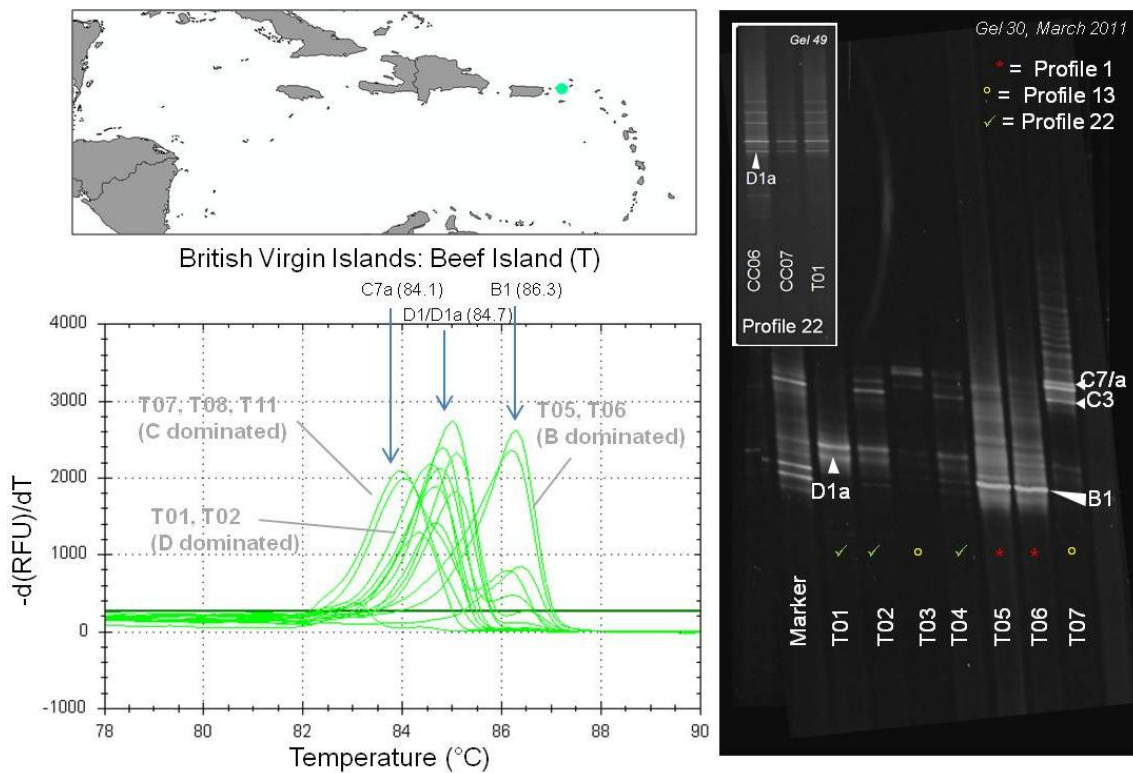
Chavo (NB) samples showed two DGGE ribotypes identical to neighbouring site NA (just 1.73 km away). Approximately 40% of samples were dominated by B1 (profile '1'), the most commonly occurring type in NA samples. In the HRM analysis, these produced a clear peak at 86.1°C (Fig. 28). A further 38% exclusively harboured C-types, including C7a/C7/C3 mix – again found in one sample (NA02) at the neighbouring White Hole site. These types produced a melt peak of 83.9°C (Fig. 28). The remaining 22% were a mix of profiles 1 and 9, harbouring roughly equal amounts of C and B types. These produced a double melt peak in HRM (86.1°C and 83.9°C). As in nearby NA samples, some of the B1 peaks showed a slight skew to the left, possibly indicating additional low level presence of the profile '9' C-dominated ribotype in the B1 dominated sample.



Appendix Figure 5.23: Selected DGGE gel images and HRM outputs for Columbian site CM, Palo 1.

Columbia samples had degraded in storage, but those that could be successfully amplified showed an interesting variety of DGGE ribotypes (Fig. 29). Some (e.g., CM33, CM34) were dominated by a single high band, which sequencing revealed to be C3. The majority of samples showed a different very pale double band in a similar position, but that had migrated slightly higher on the gel. An alignment showed the closest type to this was C38 – previously only found in *Acropora* in the Eastern Caribbean (LaJeunesse 2005). A lower migrating band was present in CM35, the B7 band also present in Jamaican samples, and some samples, (e.g., CM26) displayed both the C38(?) and B7 band.

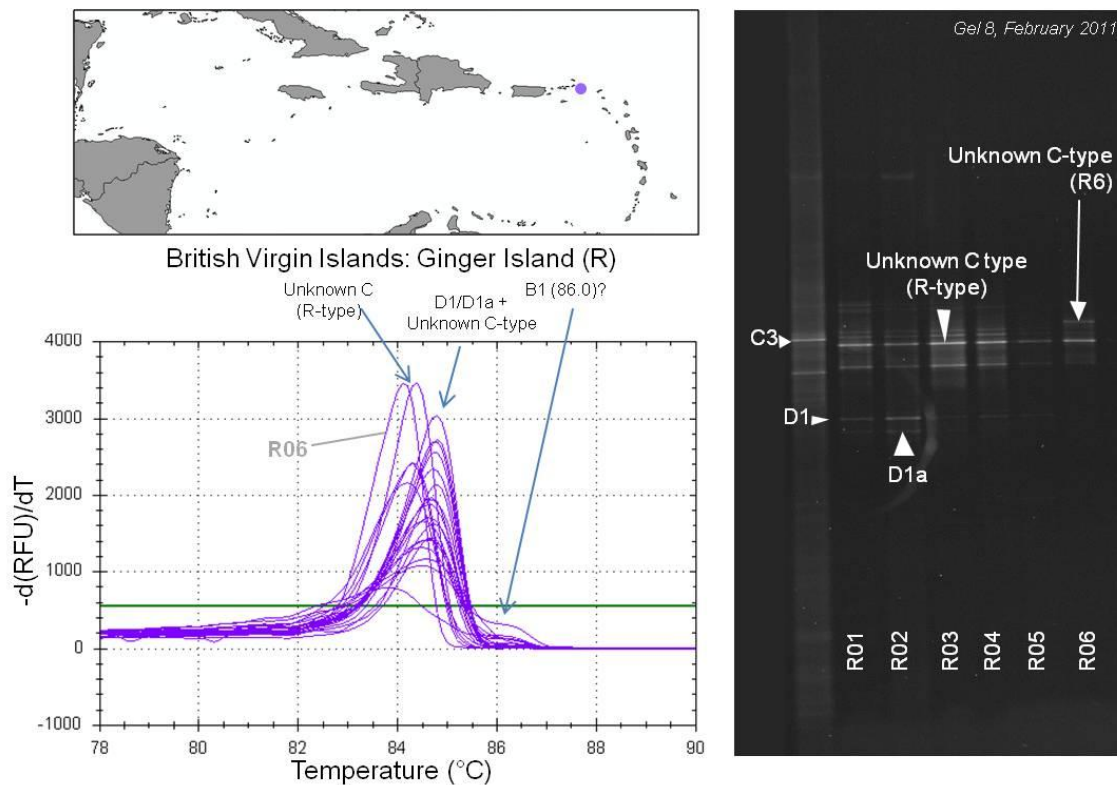
HRM analysis supported the DGGE outcome. C3 dominated profiles (CM33 and CM34) showed a unmistakable fluorescent peak (2500) at 84.0°C, while the B7 dominated profile, CM35, showed a similarly clear-cut fluorescent peak at 2000, at 86.4°C (a little higher than the melt peak for B1 of 86.1°C, as expected). Other samples that contained a mix of B7 and C38 – e.g., CM32 and CM27 – still generated a melt peak at the B-type melt temperature, but the curve was <1000 and spanned a broader temperature range. Samples harbouring exclusively C38(?) were almost indistinguishable from C3 in terms of melting point, this could be expected, given these ITS2 types travelled a similar distance on the gel. However C38 had a consistently lower melting point than C3 (83.6-83.8°C compared to 84.0-84.1°C) and could be differentiated by the fact they showed much less fluorescence and had a broader curve.



Appendix Figure 5.24: Selected DGGE gel images and HRM outputs for BVI site T, Beef Island.

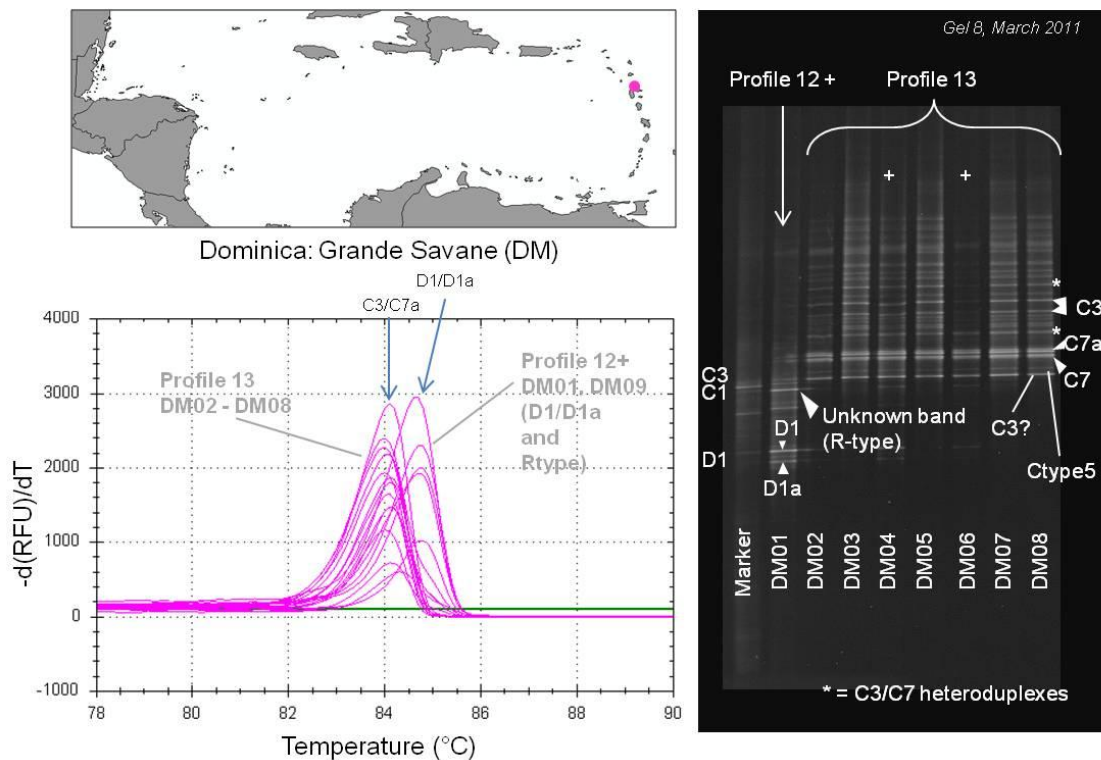
Beef Island (T) samples showed more variable symbiont communities than their Ginger Island counterparts. Individuals fell into one of three main DGGE ribotypes, each dominated by a different cladal type: profile ‘22’ (in T01, T02, T04), identical to the principal ribotype found at the Cuban site (CC), consisted of a bright band that sequencing revealed to D1a, and a fainter band well spaced above (D1) – see Fig. 31. Other samples (T05, T06) appeared to show a simple, B1 dominated profile of banding (profile 1), while T03, T07 and T08 presented the typical profile ‘13’ (a low C3 band, a double C7/C7a band, and several heteroduplexes above). The recent severe bleaching event may go some way to explaining the high prevalence of D1a in these samples.

All samples adhering to profile ‘22’ (dominated by D1/D1a) had a single melt peak at 84.7°C – this concurs with D1 dominated samples from Belize (G) and Cuba (CC) which produced similar sized melt peaks at 84.6°C and 84.8°C respectively. Communities dominated by B1 (e.g. T05, T06) produced a melt peak at 86.2°C, fitting in with the B1 dominated samples. The final set of samples (e.g. T07) produced a peak at 84.1°C, agreeing with other profile ‘22’ samples (Fig. 31).



Appendix Figure 5.25: Selected DGGE gel images and HRM outputs for BVI site R, Ginger Island.

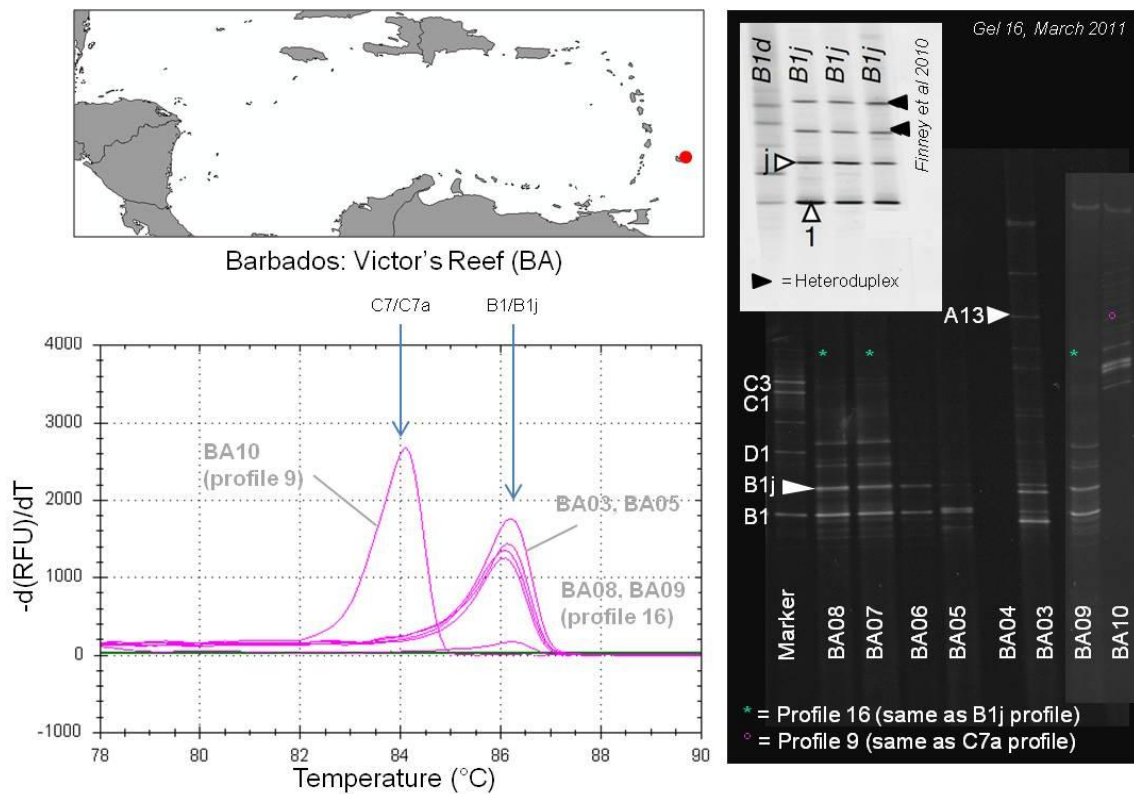
Like neighbouring Beef Island (Fig. A24), Ginger Island samples were dominated by D1/D1a - perhaps related to the recent bleaching event - although the site hosted less diversity. Samples were homogenous within site, but the profile generated (profile '14a') was also seen in the Bahamas (EN) and shared with a few samples from Dominica (DM). Profiles consisted of a bright C band (thought to be C31) - present in all samples - which lies just below the C1 band. A second, paler band is well spaced below, lying above the D1 band in several samples, (e.g., R01-R04, R06, R07, R09). In some samples a faint D1 band is also present in the usual place, with a D1a below (e.g., R01, R02, R04). These samples are identical to those DM01 and DM09 samples from Dominica (DM). And R06 showed had an additional unusual C band, above the dominant C31 and C3, but below C7 - and hasn't been identified. HRM analysis was unable to resolve differences in D1/D1a and C31 band mix, producing just one peak for each individual. The positioning of the melt peak suggests that the D1/D1a mix is masking the signal of the unidentified C-type (C31?). We hypothesise that the several samples with melt peaks at precisely 84.7°C (e.g., R05, R11-15, R26 and R27) might reflect those with a mixed C31(?) band and D1/D1a profile, as Sibony (CC) samples (also containing D1/D1a) produced similar melt peaks. We then suggest that overlapping peaks that closer to 84.5°C may just contain the single dominant C band (C31), who's melt profile is slightly higher on the DGGE gel. Some samples (e.g., R01, R04) showed a more lumpy peak (< 800 fluorescence units), with possibly a secondary melt peak at 86°C, which could represent samples with a faint B1 component. R06 - with a unique unidentified band - had a different looking peak at 84.2°C, perhaps reflecting the mix of two different types.



Appendix Figure 5.26: Selected DGGE gel images and HRM outputs for BVI site R, Ginger Island.

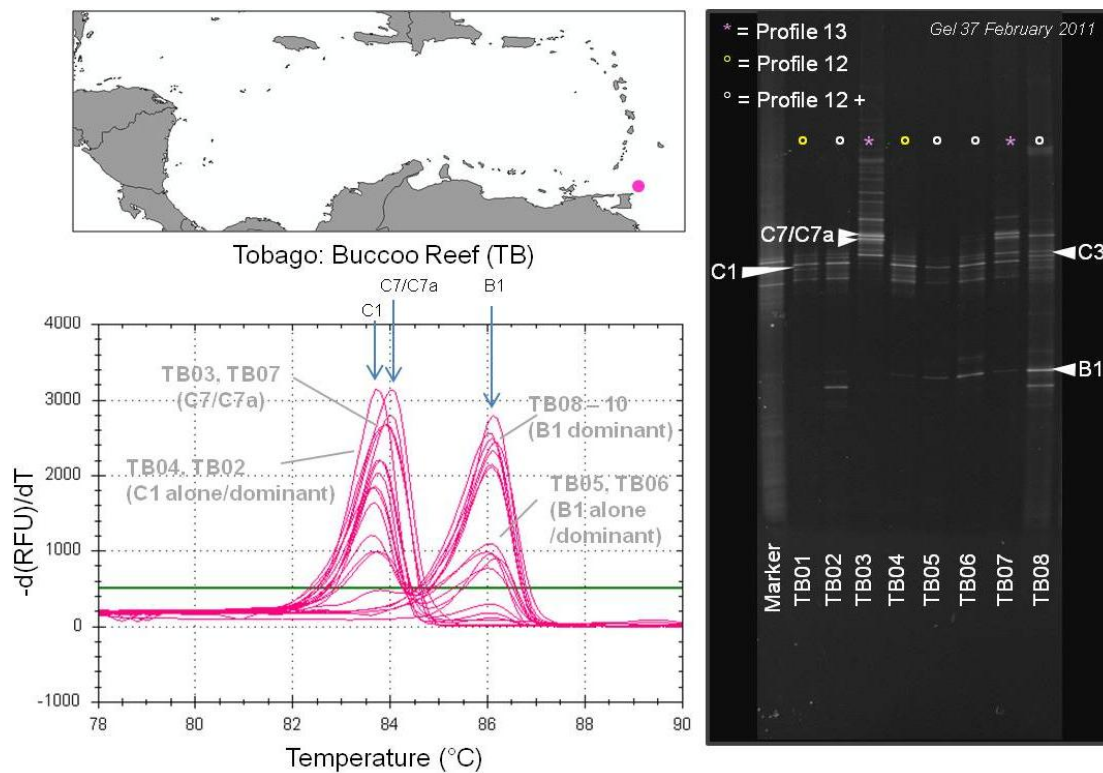
Dominica was unusual in being one of the only sites (along with Cuban CC site, and Ginger Island, R) that no individuals screened were dominated by a B-type – in most other sites at least one or two individuals were dominated by sub-clade B1. Only 5 of the 19 samples screened even contained a weak amount of B1 (Fig. 33). Eight of the ten samples displayed profile ‘13’, (also present in one Tobago, one Barbados, a Dominican Republic and several Nicaraguan samples). This fingerprint is dominated by two bright C7 parallel bands (a C7 and C7a above), with a faint unidentified band (‘Ctype5’), and a bright C3 band below this (Fig. 33). Sequencing revealed this new C-band, shared by the Dominican Republic, (where it was dominant), to have 1 base pair difference from C38 and from C7. Above the C7/C7a double bands, are a double C3 band, and an array of C7 heteroduplexes. This ribotype is very similar to the C7a profile previously been described in Barbados (Finney et al 2010). DM01 and DM09 were the exceptions in this group, showing lower B1 bands and the brightest band in an unusual position, just below the C1, with a band below this, closer to the D1 (these bands are mostly likely to be a C-type (C31). Lower down, these profiles all contained the D1/D1a banding, as seen in Cuban (CC) and Bahamian (EN) sites. DGGE gels showed these DM profiles are identical to those found in the BVI (site R, Ginger Island), profile ‘14a’ (Fig. 32).

HRM profiles fell into one of two melt peaks: 84.0°C and 84.7°C (Fig. 33). DM01 and DM09 followed the 84.7°C, identical to the C31(?) melt peaks of Ginger Island samples, but also similar to the D1/D1a dominated samples (e.g., Cuban CC samples), which also contain D1/D1a mix but not the C above (C31). Evidently the D1/D1a signal is masking that of the other C bands. All other samples were between 84.0 and 84.1°C, corresponding to the C3/C7 declaration.



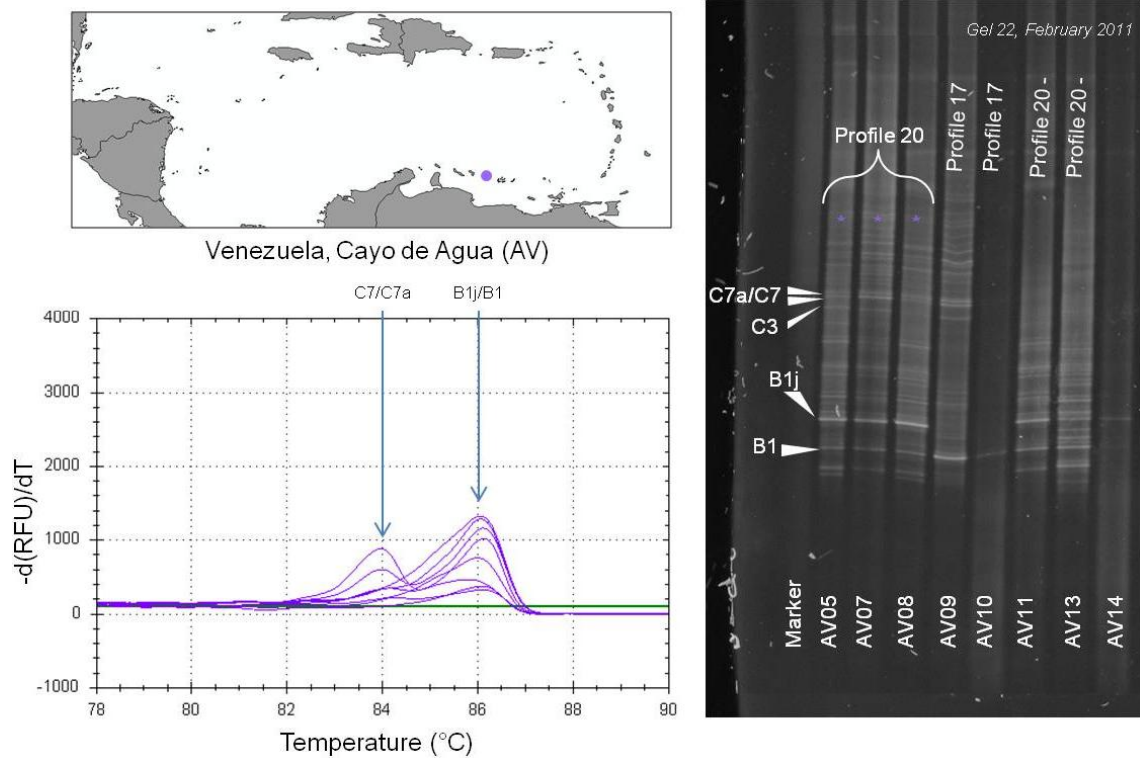
Appendix Figure 5.27: Selected DGGE gel images and HRM outputs for Barbados site BA, Victors Reef.

M. annularis symbiont communities have been studied in Barbados in 2005 (LaJeunesse, Smith et al. 2009) and also in 2005-2007 (Finney, Pettay et al. 2010). In both reports, shallow water samples contained B1j or B1, often mixed with C7a, while deeper samples contained only C7a profiles. Our DGGE profiles mirrored those found published in Finney's study, with the majority showing the B1j profile she described: (profile '16': a B1 band, a B1j band, and two B1 heteroduplexes above) (Fig. 34). One sample – BA10 – had the C7a profile (profile 9), with two bright parallel C7 and a C7a bands. This was also seen faintly in BA03. BA03 also possibly contained some A13 – another symbiont identified at this site in previous studies – although this band was in the correct position, it was too weak to be successfully sequenced (Finney, Pettay et al. 2010). Most samples produced one HRM peak around 76 $^{\circ}C$, which probably represents the B1/B1j mix (Fig. 34). BA03 and BA05 produced taller peaks, as they had simpler mixes. BA10 produced a strong flare at 84.1 $^{\circ}C$, representing the C7/C7a flare.



Appendix Figure 5.28: Selected DGGE gel images and HRM outputs for Tobago site TB, Buccoo Reef .

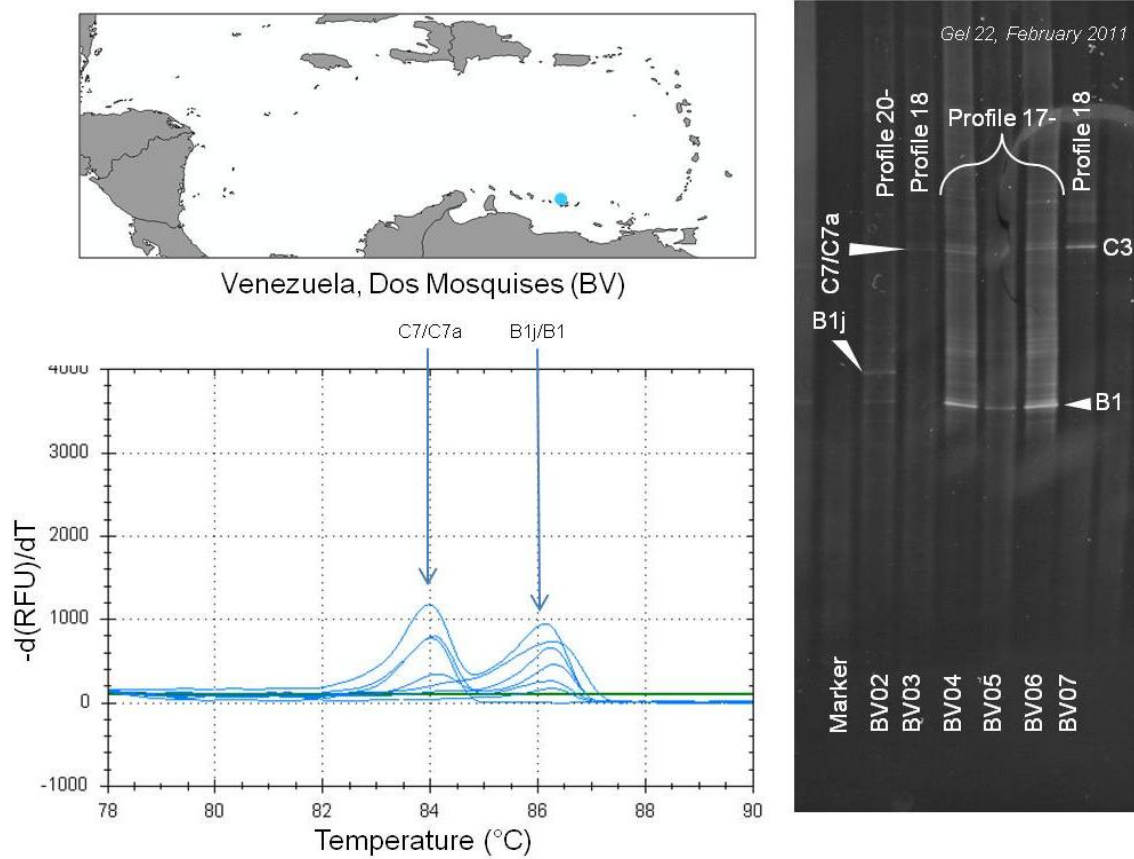
All Tobagan DGGE ribotypes contained what was understood to be C1 band (in most cases the dominant band), along with a lower, unidentified band (could be a C1 heteroduplex), identical to those found in Honduras site B. In some cases (e.g., TB02, TB05-TB06, TB08-10) a band was also observed in the B1 position. An alternative profile (e.g., TB03, TB07) with higher bands, specifically C7/C7a, was also recorded (Fig 35). HRM melt peaks fell into 5 categories. The simplest, had one peak at 83.9°C (e.g., TB03, TB07, TB14, TB23), representing the higher C7/C7a double band (profile '13') usually accompanied by C3 (although one peak shows that HRM is unable to resolve differences in these two types). Some types, e.g. TB20 and TB15, had two equally sized melt peaks - one at 83.7°C and one at 86.1°C. The 83.7°C melt peak, very similar to 83.9°C, but slightly lower fluorescence (e.g. 1500 compared to 2500 units), probably represents the C1 double band found in almost every sample, while 86.1°C corresponds to *Symbiodinium* B1. Two further variations on this melt profile, are those that share the double peak, but have either the C1 (e.g. TB07, TB12, TB04) or B1 (TB10, TB11, TB15) significantly greater in size. Finally, some samples (TB08, TB09) simply had the 86.1°C alone, exclusively hosted B1 (Fig. 35).



Appendix Figure 5.29: Selected DGGE gel images and HRM outputs for Venezuelan site AV, Cayo de Agua.

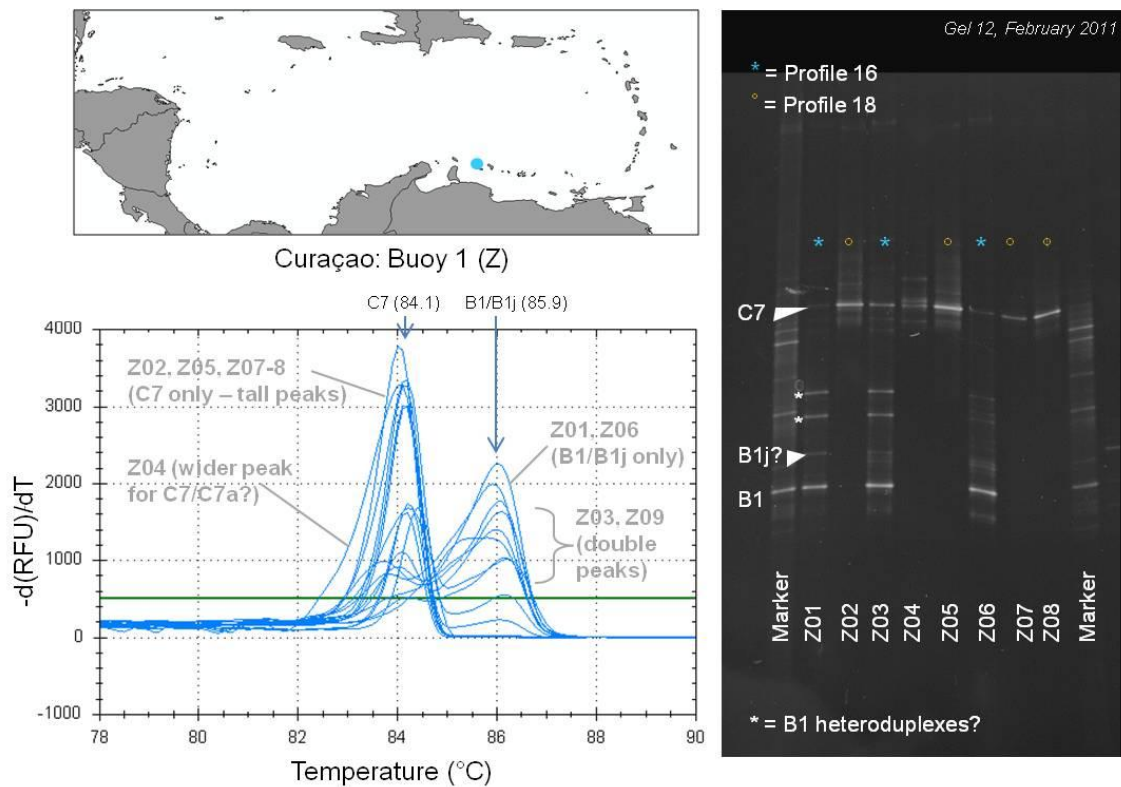
In Cayo de Agua (AV), the most commonly occurring DGGE banding pattern (AV05, AV07, AV08, AV14) revealed a mix of types (profile '20'), dominated by a bright B1j along with a double C7/C7a band, a pale B1 band, a double band below B1, and other pale banding throughout the profile. AV11 and AV13 and AV15 show variations on this profile, all are missing the C7/C7a, and AV13 and AV15 have additional bands. AV10, AV09 and AV16 show a markedly different profiles, dominated by B1, but AV09 and AV16 also present C7/C7a bands. This was more similar to the Dos Mosquises samples, most of which were dominated by B1.

In the HRM analysis, AV09 and AV16 presented two distinct melt peaks, representing the B1 (86.2°C) and C7/C7a (84.0°C) strains. Supporting this, AV10 also shows a single B1 peak at 86.2°C. AV15 also shows a mild double peak, although the C7/C7a flare is smaller – perhaps indicating that this C7 was missed on the gel. AV08 and AV14 show one clear peak at 86.0°C – representing B1j – the fact that the T_m is slightly below that of the T_m for B1 reflects the fact this band doesn't travel as far on the gel. BV01 showed a peak at 86.0°C, suggestive of B1j/B1 mix. BV04 showed a double peak of B1 (86.2°C) and C3 (84.0°C) strains, similar to AV09 and AV16 which showed a similar DGGE fingerprint (profile '17'). BV03, which only showed C7/C7a banding, showed one peak at the C7a temperature (84.0°C). AV05, AV11, AV13 didn't work.



Appendix Figure 5.30: Selected DGGE gel images and HRM outputs for Venezuelan site BV, Dos Mosques.

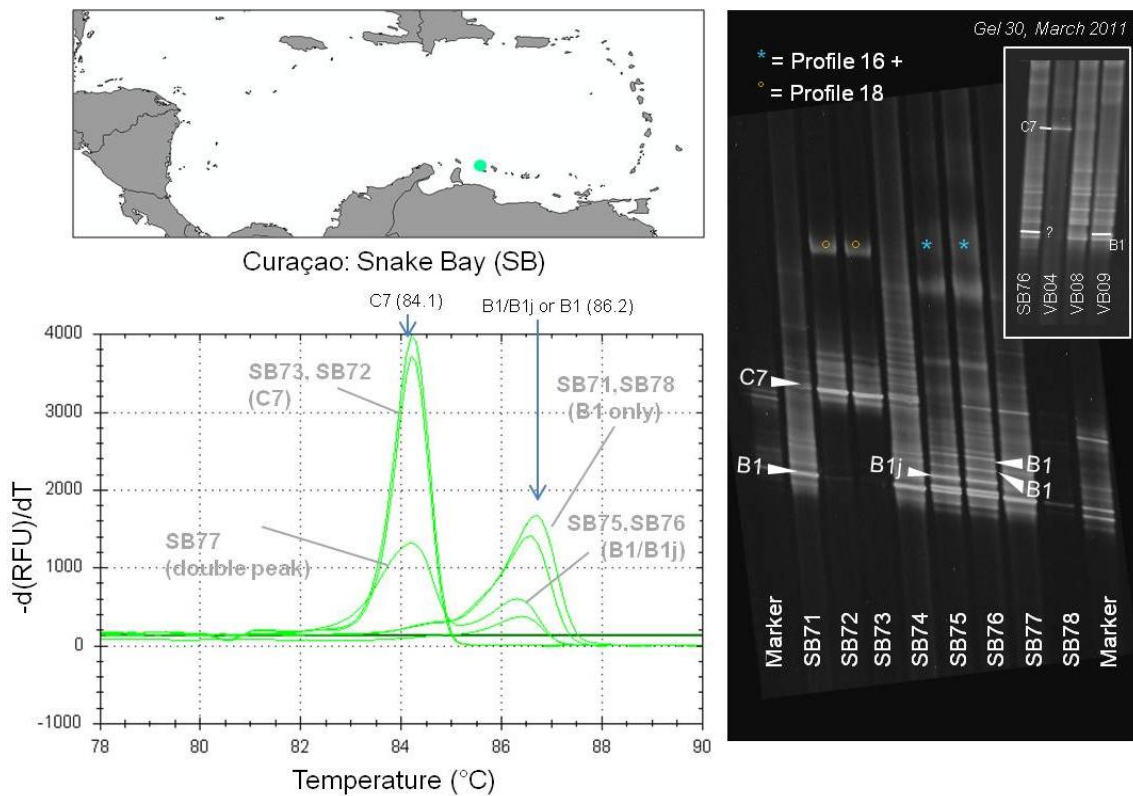
Dos Mosques (BV) symbiont communities were dominated by B1, and had an additional double C7/C7a band as in AV samples profile '17' (Fig. 37). BV04, BV05 and BV06 all followed this profile. BV02 had a strong B1j and a B1 – like AV11 (profile '20'). BV03 and BV07 only showed the C7 (profile '18'). BV07 had a C3 rather than a C7 band. HRM analysis produced similar melt profiles to the AV site (Fig. 36).



Appendix Figure 5.31: Selected DGGE gel images and HRM outputs for Curaçao Z, Buoy 1.

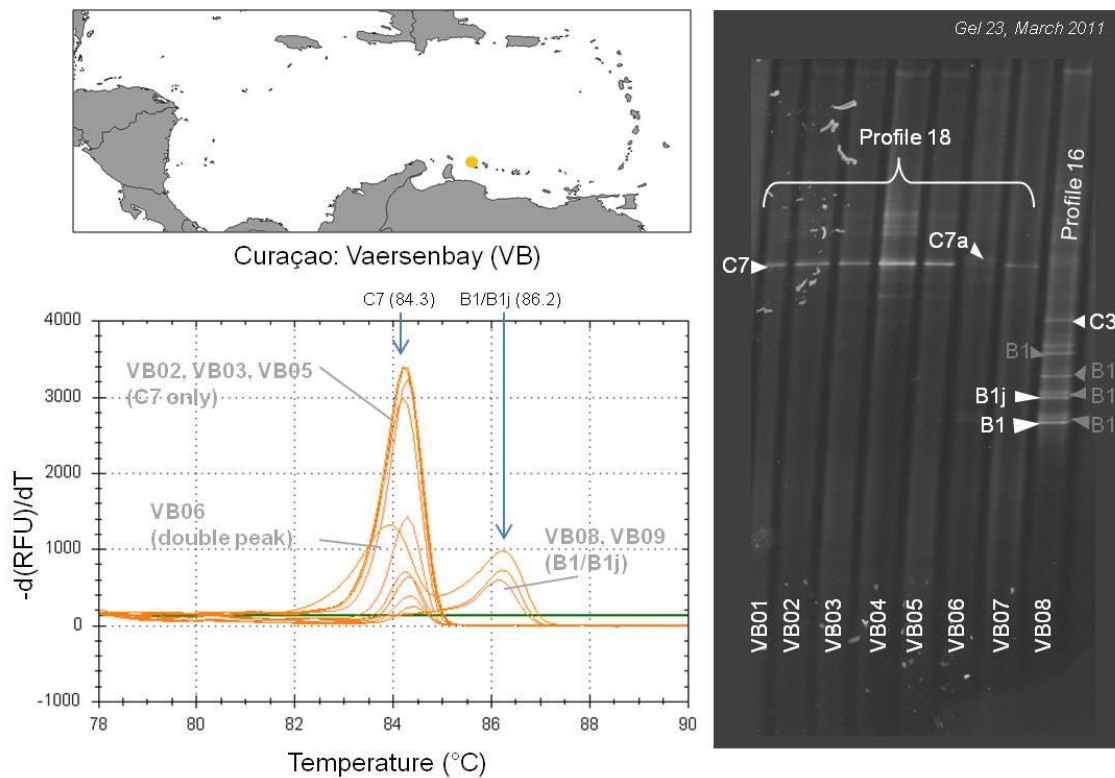
Buoy 1 (Z) samples were either dominated by B1/B1j (e.g. Z01, Z06, profile '16'), C7 (e.g., Z02, Z04, Z05, profile '18'), or a combination of both (e.g., Z03), Fig. 38. In occasional samples, (e.g. Z04), a double C7/C7a band was apparent instead of the single C7. The B1/B1j profile, common at a variety of other Lesser Antilles sites, consists of a bright B1, a paler B1j above, and two B1 heteroduplexes above this (Finney, Pettay et al. 2010). This profile (16) was also found in the Bahamas – again in combination with C7, and was also common in both other Curaçao sites – Vaersenbay (VB) and Snake Bay (SB).

HRM corroborated DGGE observations, although an amorphous peak in the B1 position (86.0°C) suggests that this melt profile reflects more than simply B1, but a B1/B1j mix (Fig. 38). Consistent tall (4000) peaks at 84.1°C were thought to contain only C7, while shorter, broader peaks hosted C7/C7a, although this could not be used reliably as a diagnostic tool. Double melt peaks occurred where both B1/B1j and C7 profiles were found, with peak size varying in proportion to the brightness of the DGGE band image were consistent with the DGGE results (Fig. 38).



Appendix Figure 5.32: Selected DGGE gel images and HRM outputs for Curaçao site SB, Snake Bay.

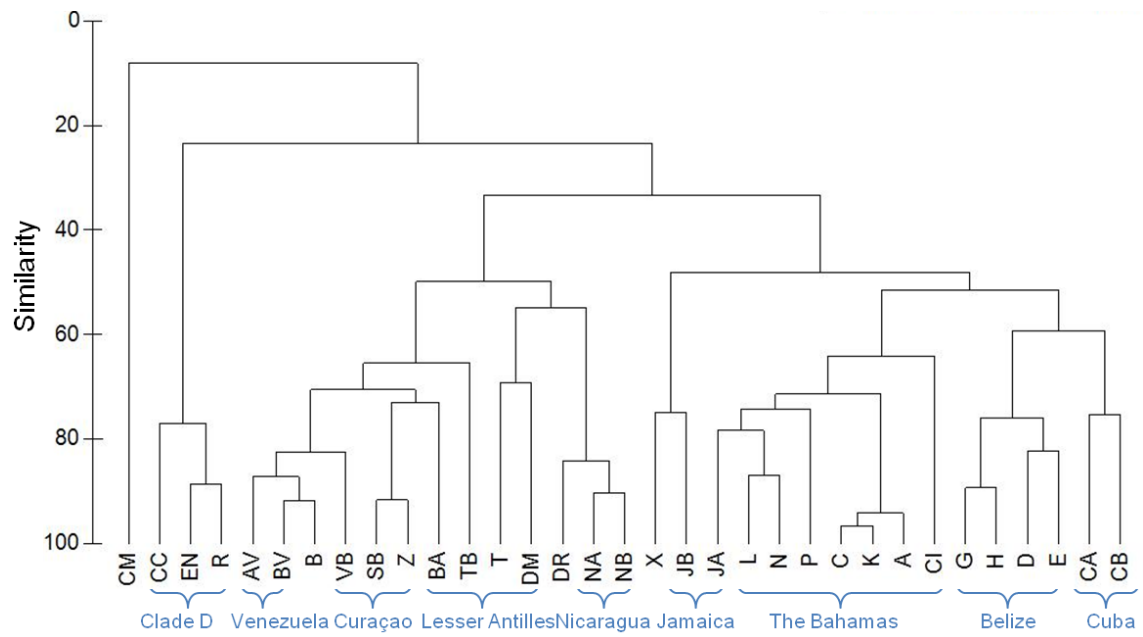
Snake Bay samples, which were degraded, tended to be dominated by B1, C7 or both – similar to neighbouring Buoy 1 (Z) and Vaersenbay (VB) communities. Several (although not all) of the samples dominated by B1 revealed a DGGE profile similar to that of profile ‘16’ (common at Buoy 1), with a B1j above, and two heteroduplexes above that (e.g., SB75 and SB76) although others (e.g., SB71) presented a single B1 band. One difference is this profile appeared to show an additional bright band immediately above the B1 (see inset), possibly representing B3. This was also observed in Vaersenbay samples (e.g., VB09). SB74 showed the double C7/C7a instead of just one bright C7 band – just as occasional samples in Z04) and VB (VB06). For the HRM analysis, just as in other Curaçao sites, individuals harbouring C7 produced a tall (2000) melt peak at 84.2 $^{\circ}\text{C}$, while those with B1 or B1/B1j produced peaks at 86.2 $^{\circ}\text{C}$ (nb/standards on both plates (6.1 and 10.1) were exactly 0.2 $^{\circ}\text{C}$ apart, suggesting the 0.3 $^{\circ}\text{C}$ difference between the C7 melt peaks (and B1 melt peaks) on this plate (SB) and the (Z) plate was due to plate differences). HRM was unable to clearly resolve differences between samples hosting B1 and a B1/B1j (profile ‘16’) combination – with both producing melt peaks at 86.2 $^{\circ}\text{C}$ – however those hosting B1 only appeared to show a slightly taller peak, while those hosting B1/B1j a stunted, more amorphous peak, fractionally more skewed to the left. This agrees with previous findings that suggest B1/B1j tend to melt at slightly lower temperatures (e.g., 85.9 $^{\circ}\text{C}$), and makes sense as a melt peak representing several bands (i.e. B1 and B1j) is less likely to produced a clear result. Samples hosting both C7 and B1 showed double melt peaks (e.g., SB77) while SB117 and SB122 produced mysterious high melt peaks at 86.7 $^{\circ}\text{C}$.



Appendix Figure 5.33: Selected DGGE gel images and HRM outputs for Curaçao site VB, Vaersenbay.

Like other Curaçao communities sampled from Snake Bay (SB) and Buoy 1 (Z), Vaersenbay (VB) samples primarily hosted C7 types (Fig. 40). Some samples (e.g., VB06) produced a double C7/C7a band, while others just hosted C7. A few individuals (e.g., VB08) showed profile '16', dominated by B1, but consisting of several bands above, including B1j and several B1 heteroduplexes. Unlike usual profile '16' patterns (e.g., Barbados (BA) samples and other Curaçao (Z) samples, that show 4 clear bands, VB samples had additional bands – up to 8, which sequencing revealed to be heteroduplexes. VB08 also produced a C3 band above the B1, and very pale C7/C7a double band was also present in this sample. VB09 – similar to VB08, had a bright additional band like those in SB, which might be B3.

As in SB samples, HRM was unable to distinguish between samples hosting B1/B1j mix or simply B1: both generated a melt peak around 86.2°C, although the melt profiles of those hosting the mixed assemblage were slightly reduced in peak size (e.g., VB08, VB09). Samples hosting C7 only produced clear 4000 tapered peaks at 84.3°C, in accordance with samples from Z and SB demonstrating the same profile. HRM was unable to distinguish C7 from C7/C7a double bands, producing identical melt profiles. Unfortunately, VB08 failed to work, so the presence of the C3 band could not be verified, and it didn't appear in the VB09 sample (although this was very pale on the DGGE).



Appendix Figure 5.34: Caribbean reefs, *Montastraea annularis* symbionts. Dendrogram of square root transformed symbiont abundance data, based on Bray-Curtis similarities. Letters indicate site identifier code. Used to inform Figure 5.19, Chapter 5.

Chapter 6 Appendix

Site identifier	Location	Reef site	Hurricane frequency
A	Honduras	Seaquest	Medium
B	Honduras	Sandy Bay	Medium
C	Honduras	Western Wall	Medium
D	Belize	Coral Gardens	Medium
E	Belize	Eagle Ray	Medium
G	Belize	Long Cay	Medium
H	Belize	West Reef	Medium
CI	Bahamas	Conception Island	High
EN	Bahamas	Exumas North	High
K	Bahamas	Seahorse Reef	High
L	Bahamas	Snapshot Reef	High
N	Bahamas	School House Reef	High
P	Bahamas	Propeller Reef	High
NA	Nicaragua	White Hole	Low
NB	Nicaragua	Chavo	Low
CM	Columbia	Palo 1	Low
CA	Cuba	Baracoa	Low
CB	Cuba	Bacunayagua	High
CC	Cuba	Siboney	High
X	Cayman	Rum Point	High
DR	Dominican Rep.	Bayahibe	Medium
JA	Jamaica	Drunkenmans Cay	Medium
JB	Jamaica	Dairy Bull	Medium
BA	Barbados	Victor's Reef	Low
R	BVI	Ginger Island	High
T	BVI	Beef Island	High
SB	Curaçao	Snakebay	Low
VB	Curaçao	Vaersenbay	Low
Z	Curaçao	Buoy 1	Low
DM	Dominica	Grande Savane	Medium
TB	Tobago	Buccoo Reef	Low
AV	Venezuela	Cayo de Agua	Low
BV	Venezuela	Dos Mosquises	Low

Appendix Table 6.1: Hurricane frequency for each reef site.
These data were used to inform the statistical model.

	Latitude (lat)	Longitude (long)	Geographic proximity (dist)	Acute thermal stress (ts_acute_0)	Acute thermal stress (ts_acute_4)	Chronic thermal stress (ts_chron)	Historic thermal stress (ts_histor_0)	Historic thermal stress (ts_histor_4)	Turbidity (chla_ave_1y)	Turbidity (chla_ave)	Salinity (sal_ave)	Nitrate concentration (nit_ave)	Phosphate conc. (pho_ave)	Silicate concentration (sil_ave)	Wave exposure (wave_ave)	Enclosure (encl)	Hurricane frequency (hurr)	Depth (depth)	Host heterozygosity (coral_HE)	Host genotypic richness (coral_S)	Host genotypic diversity (coral_D)	Sampling month (month)	
long	-0.27																						
dist	0.36	-1.00																					
ts_acute_0	-0.46	-0.08	0.03																				
ts_acute_4	-0.25	0.08	-0.10	0.49																			
ts_chron	0.69	-0.54	0.58	-0.42	-0.38																		
ts_histor_0	-0.57	0.04	-0.09	0.28	0.07	-0.45																	
ts_histor_4	-0.55	-0.11	0.05	0.39	0.46	-0.50	0.78																
chla_ave_1y	0.02	-0.31	0.30	-0.01	-0.20	0.25	0.44	0.34															
chla_ave	0.02	-0.33	0.32	0.04	-0.23	0.26	0.49	0.35	0.97														
sal_ave	0.49	-0.38	0.42	-0.11	0.11	0.21	-0.25	0.08	-0.04	-0.02													
nit_ave	-0.26	0.32	-0.34	-0.10	0.07	-0.09	0.01	-0.06	-0.17	-0.18	-0.01												
pho_ave	-0.79	0.06	-0.14	0.49	0.28	-0.36	0.37	0.37	0.17	0.16	-0.40	0.40											
sil_ave	-0.43	0.59	-0.61	-0.12	0.32	-0.38	0.12	0.09	-0.28	-0.29	-0.20	0.72	0.37										
wave_ave	0.14	-0.57	0.56	-0.17	-0.33	0.39	0.05	-0.05	-0.12	-0.04	0.21	0.09	-0.12	-0.19									
encl	0.02	0.24	-0.23	0.07	-0.08	-0.16	-0.03	-0.18	-0.05	-0.05	-0.05	-0.12	-0.15	-0.15	-0.20								
hurr	0.83	-0.08	0.17	-0.51	-0.27	0.51	-0.54	-0.55	-0.05	-0.05	0.38	-0.28	-0.78	-0.32	0.07	0.22							
depth	0.24	-0.29	0.31	-0.35	-0.09	0.26	0.02	0.03	-0.03	0.00	0.15	-0.13	-0.36	-0.17	0.20	-0.21	0.11						
coral_HE	0.15	0.03	-0.01	-0.18	-0.45	0.27	-0.13	-0.37	-0.04	0.01	-0.13	-0.05	-0.18	-0.17	0.23	-0.03	0.20	0.01					
coral_S	0.32	0.05	-0.02	-0.26	-0.31	0.18	-0.27	-0.31	-0.20	-0.15	0.26	0.01	-0.40	-0.19	0.09	0.10	0.46	0.22	0.29				
coral_D	0.29	0.03	0.00	-0.31	-0.34	0.14	-0.10	-0.23	-0.03	0.01	0.17	0.09	-0.35	-0.10	0.19	0.12	0.36	0.25	0.18	0.86			
month	-0.29	0.45	-0.46	-0.20	-0.01	-0.40	-0.21	-0.23	-0.61	-0.66	-0.17	0.28	0.06	0.41	0.04	0.21	-0.16	-0.20	-0.05	0.11	0.12		
year	0.18	0.37	-0.34	-0.39	-0.23	0.07	0.21	-0.05	0.03	0.06	-0.15	0.24	-0.29	0.21	-0.03	-0.03	0.16	0.22	0.22	0.16	0.20	-0.12	

Appendix Table 6.2. Pearson correlation between transformed environmental covariates.
Any factors correlated by more than 0.6 are highlighted (positive correlation = red, negative = green)

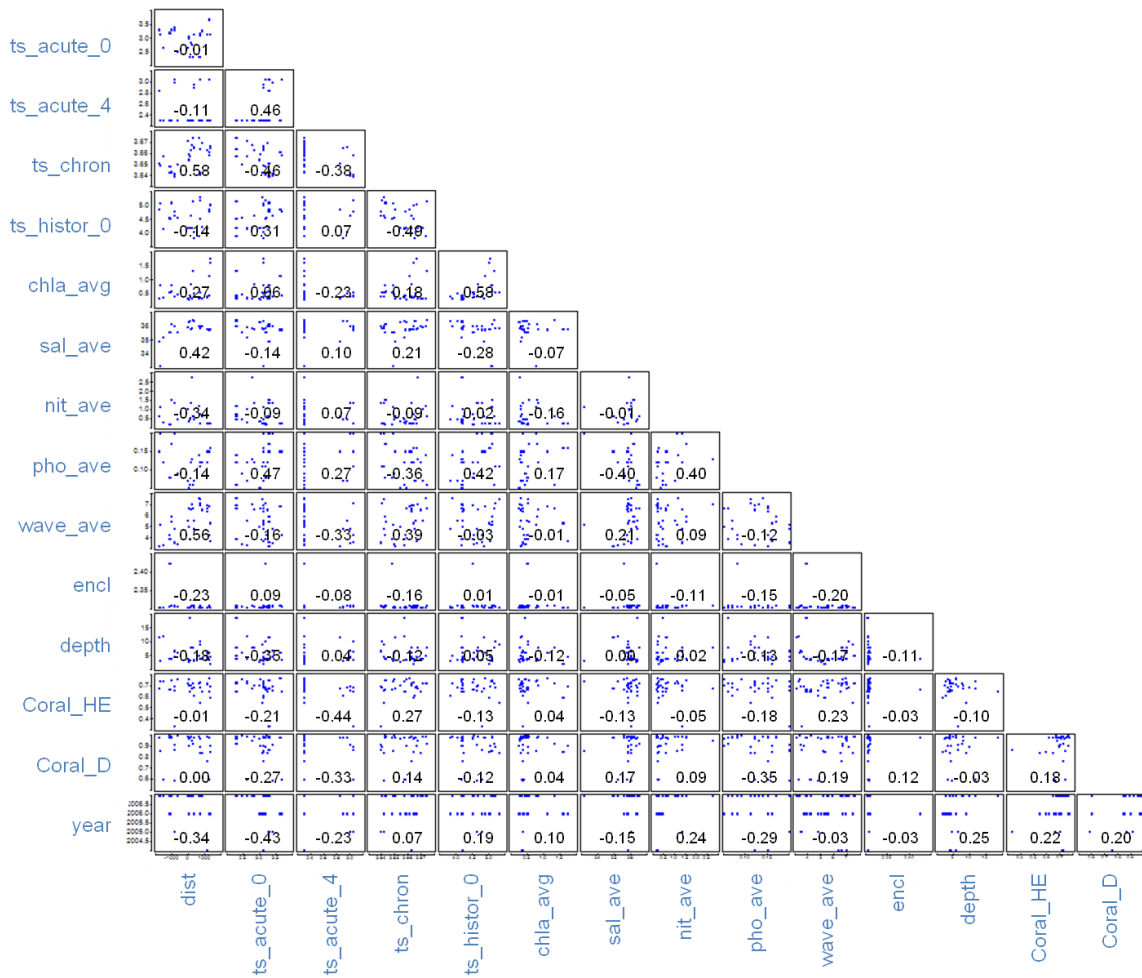
	Mesoamerican Barrier Reef							The Bahamas					Southern			Greater Antilles						Lesser Antilles												
	A	B	C	D	E	G	H	CI	EN	K	L	N	P	NA	NB	CM	CA	CB	CC	X	DR	JA	JB	BA	R	T	SB	VB	Z	DM	TB	AV		
A	0.0																																	
B	5.6	0.0																																
C	2.6	8.0	0.0																															
D	221.7	220.9	223.3	0.0																														
E	218.8	217.9	220.3	3.3	0.0																													
G	136.6	138.2	137.2	113.5	110.2	0.0																												
H	146.4	147.8	147.0	106.0	102.7	10.1	0.0																											
CI	1462.1	1456.7	1463.9	1501.8	1502.4	1536.9	1540.4	0.0																										
EN	1380.6	1375.0	1382.7	1394.2	1395.2	1441.2	1443.7	193.3	0.0																									
K	1537.5	1532.1	1539.4	1576.7	1577.4	1612.2	1615.8	75.5	240.4	0.0																								
L	1526.0	1520.6	1527.9	1566.7	1567.3	1601.5	1605.1	65.0	239.6	14.9	0.0																							
N	1352.3	1346.7	1354.4	1354.0	1355.1	1406.3	1408.2	274.0	80.7	319.0	319.1	0.0																						
P	1351.4	1345.8	1353.5	1352.1	1353.3	1404.8	1406.8	280.0	86.6	324.7	324.8	6.0	0.0																					
NA	596.2	597.4	594.5	817.7	814.7	720.2	730.2	1541.4	1534.9	1610.2	1596.0	1538.3	1539.8	0.0																				
NB	595.5	596.7	593.8	817.1	814.0	719.4	729.4	1542.7	1536.1	1611.5	1597.3	1539.4	1540.8	1.7	0.0																			
CM	1365.4	1364.5	1364.6	1576.6	1574.1	1501.3	1511.3	1507.6	1603.9	1549.9	1535.4	1648.2	1652.5	839.8	841.3	0.0																		
CA	869.2	863.7	871.7	827.0	828.6	895.4	895.5	758.5	606.6	826.9	820.7	550.2	547.1	1214.6	1215.2	1603.6	0.0																	
CB	918.1	912.5	920.5	890.2	891.6	953.0	953.8	678.4	528.6	747.0	740.7	474.7	471.9	1228.4	1229.1	1573.8	80.2	0.0																
CC	1319.7	1315.0	1321.0	1420.0	1419.6	1423.5	1429.5	422.6	554.4	460.2	445.9	618.5	624.0	1244.2	1245.7	1089.7	871.6	800.7	0.0															
X	659.9	654.6	661.6	734.2	734.0	747.7	752.7	806.1	746.6	881.2	869.2	734.4	734.9	822.5	823.3	1182.2	432.1	422.6	687.8	0.0														
DR	1901.3	1897.2	1902.1	2031.5	2030.7	2018.7	2025.9	892.7	1082.0	873.1	866.1	1161.2	1167.2	1672.8	1674.5	1157.6	1517.8	1444.3	650.4	1316.2	0.0													
JA	1008.2	1003.8	1009.3	1128.2	1127.5	1119.7	1126.5	639.5	689.8	701.1	686.4	724.2	728.0	926.5	928.0	931.7	740.5	689.6	326.7	422.5	903.6	0.0												
JB	1054.6	1050.4	1055.5	1186.3	1185.4	1171.1	1178.3	683.0	751.8	739.3	724.4	791.9	796.0	921.8	923.3	857.3	827.8	777.1	323.5	498.0	847.6	87.5	0.0											
BA	2921.1	2918.0	2921.4	3084.5	3083.2	3050.6	3059.0	2016.1	2208.9	1984.3	1979.9	2289.3	2295.3	2544.0	2545.7	1769.7	2654.4	2582.5	1783.0	2411.3	1140.7	1988.9	1916.0	0.0										
R	2360.1	2356.1	2361.0	2490.5	2489.7	2478.0	2485.2	1258.2	1451.4	1219.2	1216.3	1532.0	1537.9	2108.3	2110.0	1501.0	1946.2	1869.8	1094.8	1771.9	459.3	1362.3	1306.9	779.5	0.0									
T	2354.9	2350.9	2355.8	2484.9	2484.1	2472.6	2479.8	1250.8	1444.0	1211.8	1208.9	1524.7	1530.5	2104.6	2106.4	1499.7	1939.3	1862.9	1088.5	1766.0	454.0	1356.7	1301.5	787.1	7.6	0.0								
SB	1953.6	1951.1	1953.5	2137.4	2135.7	2087.9	2097.1	1451.4	1615.8	1457.7	1446.8	1685.8	1691.5	1528.7	1530.4	750.8	1878.7	1821.2	1072.3	1541.6	691.0	1142.7	1056.8	1023.1	848.3	849.5	0.0							
VB	1952.0	1949.5	1951.9	2135.7	2133.9	2086.2	2095.4	1448.7	1613.2	1455.0	1444.1	1683.1	1688.8	1527.7	1529.3	750.5	1876.4	1818.8	1069.7	1539.4	688.6	1140.3	1054.5	1023.8	846.8	848.0	2.7	0.0						
Z	1951.6	1949.1	1951.5	2135.5	2133.8	2085.9	2095.1	1451.6	1615.9	1458.0	1447.1	1685.7	1691.4	1526.3	1527.9	748.0	1877.9	1820.4	1072.1	1540.3	692.5	1141.6	1055.8	1025.8	850.9	852.2	2.9	4.2	0.0					
DM	2693.2	2689.7	2693.7	2844.4	2843.3	2818.8	2826.8	1708.4	1901.6	1673.5	1669.8	1982.3	1988.2	2362.0	2363.7	1640.1	2367.9	2294.0	1500.0	2150.4	850.3	1729.5	1662.2	319.5	461.1	468.8	895.2	895.1	898.1	0.0				
TB	2841.4	2838.6	2841.4	3017.0	3015.4	2974.1	2983.0	2065.0	2254.8	2042.0	2036.0	2333.9	2340.0	2424.0	2425.6	1619.2	2653.7	2585.6	1786.6	2374.8	1172.8	1955.5	1876.8	255.8	893.3	900.5	896.9	898.1	899.2	478.2	0.0			
AV	2180.5	2177.9	2180.4	2362.4	2360.6	2314.4	2323.5	1591.4	1766.1	1588.5	1578.9	1839.8	1845.6	1755.6	1757.3	963.7	2073.0	2012.0	1239.3	1752.3	754.6	1344.7	1260.7	806.3	777.5	780.7	228.4	229.8	230.7	716.9	668.8	0.0		
BV	2186.0	2183.5	2185.9	2367.9	2366.2	2320.0	2329.1	1596.2	1771.0	1593.1	1583.6	1844.7	1850.6	1760.8	1762.4	968.3	2078.4	2017.4	1244.5	1757.9	758.4	1350.3	1266.3	801.8	778.2	781.4	233.8	235.2	236.1	714.1	663.6	5.6		

Appendix Table 6.3. Geographic distances measures (km) between sites

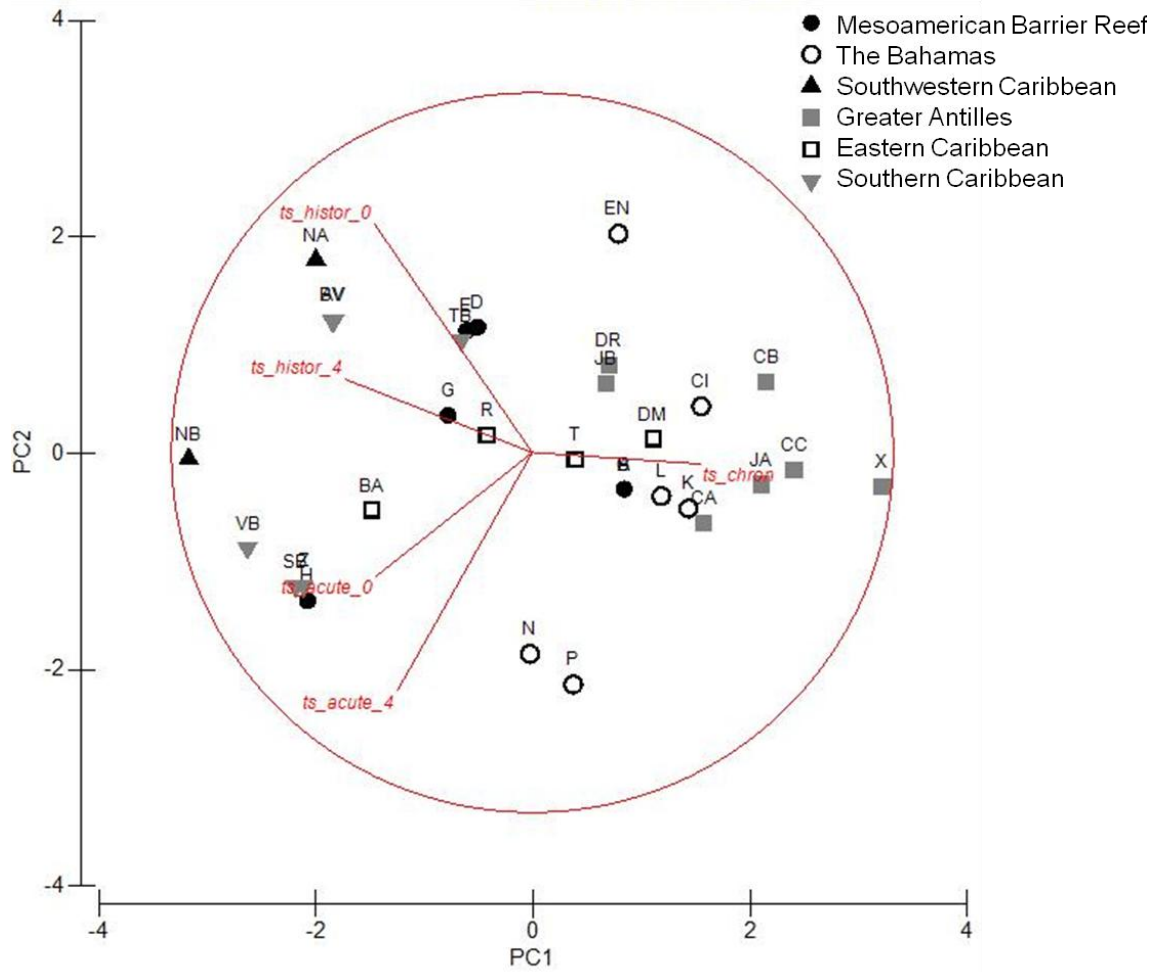
Identifier	Location	Reef site	dist	ts_acute_0	ts_acute_4	ts_chron	ts_histor_0	chla_avg	sal_avg	nit_avg	pho_avg	wave_avg	encl	depth	coral_HE	coral_D	year
A	Honduras	Seaquest	1106	13	0	28.97	56	0.14	35.81	0.25	0.15	6.38	0.02	4.0	0.723	0.99	2004

B		Sandy Bay	1103	13	0	28.97	56	0.13	35.81	0.22	0.12	6.98	0.02	6.0	0.713	0.99	2004
C		Western Wall	1106	13	0	28.97	56	0.14	35.8	0.25	0.15	6.62	0.02	4.5	0.721	0.76	2004
D	Belize	Coral Gardens	1278	13	0	29.11	142	3.09	35.79	0.27	0.16	3.71	0.02	4.5	0.692	0.9	2006
E		Eagle Ray	1277	13	0	29.03	136	2.58	35.79	0.27	0.16	5.31	0.02	2.0	0.591	0.85	2006
G		Long Cay	1238	28	0	28.91	120	1.25	35.74	0.26	0.15	6.87	0.07	6.0	0.764	0.98	2006
H		West Reef	1247	30	11	28.8	109	0.18	35.74	0.26	0.15	4.22	0.05	3.5	0.649	0.6	2006
CI		Conception Island	60	0	0	28.77	55	0.19	36.36	0.49	0.06	3.91	0.02	18.6	0.646	0.98	2007
EN	Bahamas	Exumas North	244	0	0	29.42	161	1.77	36.48	0.61	0.06	6.63	0.07	7.9	0.72	0.92	2007
K		Seahorse Reef	3	11	0	28.82	55	0.07	36.33	0.37	0.05	6.63	0.02	3.4	0.76	0.9	2006
L		Snapshot Reef	5	10	0	28.63	56	0.09	36.33	0.37	0.05	5.01	0.02	2.7	0.703	0.97	2006
N		School House Reef	322	13	9	29.08	47	0.24	36.39	0.49	0.07	5.54	0.06	3.5	0.687	0.98	2006
P		Propeller Reef	327	13	8	29.05	35	0.15	36.39	0.49	0.07	4.8	0.03	3.0	0.609	0.98	2006
NA	Nicaragua	White Hole	658	12	0	28.17	191	0.28	35.82	0.23	0.11	7.46	0.02	9.0	0.542	0.84	2006
NB		Chavo	659	14	11	28.11	166	0.28	35.82	0.23	0.11	7.12	0.03	10.0	0.687	0.89	2007
CA	Cuba	Baracoa	791	16	0	29.23	59	0.1	35.97	0.62	0.12	6.52	0.02	4.0	0.643	0.84	2007
CB		Bacunayagua	712	0	0	29.02	81	0.12	36.01	0.72	0.12	6.94	0.06	4.0	0.728	0.97	2007
CC		Siboney	-60	4	0	29.3	56	0.1	35.9	1.04	0.07	5.54	0.02	4.0	0.72	0.99	2007
X	Cayman Isles	Rum Point	600	0	0	29.41	39	0.1	35.99	1.19	0.14	7.56	0.02	5.0	0.724	0.99	2007
DR	Dominican Rep.	Bayahibe	-709	2	0	28.46	84	0.21	35.55	0.48	0.09	3.43	0.04	6.0	0.758	1	2007
JA	Jamaica	Drunkenmans Cay	179	6	0	29.15	55	0.09	35.88	2.75	0.13	6.99	0.07	8.0	0.675	0.95	2007
JB		Dairy Bull	109	7	0	28.97	94	0.7	35.75	1.36	0.12	6.58	0.03	8.0	0.705	0.99	2007
BA	Barbados	Victor's Reef	-1805	17	7	28.5	117	0.1	34.91	0.64	0.15	3.19	0.02	11.8	0.672	0.98	2007
R	BVI	Ginger Island	-1154	15	0	28.2	84	0.27	35.57	0.21	0.08	4.25	0.04	4.0	0.666	1	2007
T		Beef Island	-1147	14	0	28.4	81	0.27	35.57	0.21	0.08	3.91	1.28	4.0	0.67	0.98	2006
SB	Curaçao	Snakebay	-845	20	10	28.07	92	0.15	36.00	1.38	0.2	3.47	0.06	6.7	0.698	0.91	2005
VB		Vaersenbay	-844	17	11	28.06	109	0.14	36.00	1.38	0.2	3.56	0.06	6.5	0.333	0.87	2005
Z		Buoy 1	-843	20	10	28.16	92	0.15	36.00	1.38	0.2	4.79	0.05	4.7	0.657	0.59	2005
DM	Dominica	Grande Savane	-1550	4	0	28.77	54	0.12	35.17	0.31	0.12	3.34	0.02	12.0	0.738	0.6	2007
TB	Tobago	Buccoo Reef	-1736	13	0	28.44	150	0.63	33.11	1.12	0.2	5.18	0.02	3.0	0.74	0.86	2007
AV	Venezuela	Cayo de Agua	-1073	17	0	28.22	153	0.32	36.15	1.54	0.17	5.48	0.06	4.0	0.752	0.99	2007
BV		Dos Mosquises	-1079	17	0	28.2	153	0.65	36.15	1.54	0.17	5.91	0.06	4.0	0.747	0.98	2007

Appendix Table 6.4. Data on environmental variables (pre-transformation) included in the final model (see Table 6.1 for environmental covariate descriptors)

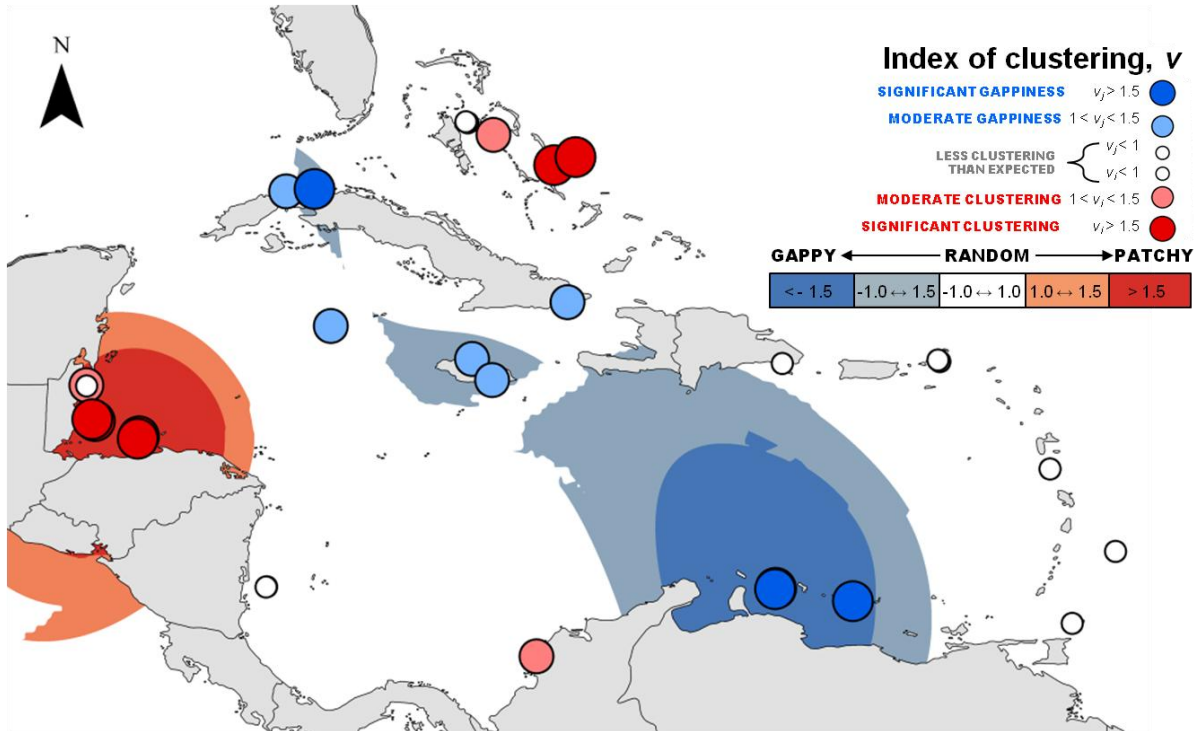


Appendix Table 6.5. PCA ordination plot of Caribbean sites based on normalised temperature stress indices. Two dimensional PCA is not a good description of structure in higher space with PC1 describing only 36.3% of variability and PC2 a further 23.2%. Superimposed vectors (in green) show the varying nutrient concentrations and exposure.



Appendix Figure 6.1. PCA ordination plot of Caribbean sites based on normalised temperature stress indices. Two dimensional PCA is a fair description of structure in higher space with PC1 describing only 54.3% of variability and PC2 a further 20.2%. Superimposed vectors (in red) show the changing temperature stress experienced by sites.

Chapter 7 Appendix



Appendix Figure 7.1: Red-blue plot indicating spatial clustering in the D distribution. Red data points indicate higher than expected occurrences of D, while red areas delineate patch clusters – an area of clustered D1. Blue data points indicate sites with significant dearth of D1, than would be expected by chance, while blue shaded areas gap clusters. The large amount of white space indicates that the distribution of D1 is not different than might be expected in a random distribution, leading to the overall spatial distribution being non-significant: i.e. D1 is fairly uniformly distributed across the region.

Chapter 8 Appendix

Clade	Type	Genbank no.	Country	Region	Latitude	Longitude	Min Depth	Max Depth	Collection date	Reference
A	A13	AF333504	Barbados	n/a	13.07	-59.39	0	5	2005	LaJeunesse, 2009
A	A13	AF333504	Barbados	n/a	13.07	-59.39	15	15	2005	LaJeunesse, 2009
B	B1	AY074981	U.K.	Bermuda	32.37	-64.79	n/a	n/a	n/a	Savage, 2002
B	B1	AF333511	United States	US Virgin Islands	18.30	-64.89	8	8	2007	Correa, 2009
B	B1	AF333511	Barbados	Eastern Caribbean	13.11	-59.32	6	10	2005	Finney, 2010
B	B1	AF333511	Bahamas	Exuma Islands	23.77	-76.09	4	4	1998	LaJeunesse, 2002
B	B1	AF333511	Bahamas	Exuma Islands	23.77	-76.09	14	14	1998	LaJeunesse, 2002
B	B1	AF333511	Barbados	n/a	13.07	-59.39	0	5	2005	LaJeunesse, 2009
B	B1	AF333511	Barbados	n/a	13.07	-59.39	15	15	2005	LaJeunesse, 2009
B	B1	AF333511	Bahamas	Exuma Islands	23.77	-76.09	4	4	2000	Thornhill, 2006
B	B1	AF333511	Bahamas	Exuma Islands	23.77	-76.09	12	12	2000	Thornhill, 2006
B	B1	AF333511	United States	Florida Keys	24.59	-80.22	3	3	1998	Thornhill, 2006
B	B1	AF333511	United States	Florida Keys	24.59	-80.22	12	12	2000	Thornhill, 2006
B	B1	AF333511	United States	Florida Keys	24.59	-80.22	1	2	2000	Thornhill, 2006
B	B1	AF333511	Bahamas	Exuma Islands	24.35	-75.35	12	15	2003	Thornhill, 2009
B	B1	AF333511	Bahamas	Exuma Islands	25.03	-77.40	2	4	2003	Thornhill, 2009
B	B1	AF333511	United States	Florida Keys	25.04	-80.39	1	2	2003	Thornhill, 2009
B	B10	AF499787	United States	Florida Keys	25.03	-80.39	3	4	2003	Thornhill, 2009
B	B17	AY074987	Panama	n/a	8.50	-80.50	n/a	n/a	n/a	Savage, 2002
B	B1j	GU907637	Barbados	Eastern Caribbean	13.11	-59.32	6	10	2005	Finney, 2010
B	B1j	GU907637	Barbados	n/a	13.07	-59.39	0	5	2005	LaJeunesse, 2009
C	C1	AF333515	United States	US Virgin Islands	18.30	-64.89	4	4	2007	Correa, 2009
C	C1	AF333515	United States	US Virgin Islands	18.30	-64.89	8	8	2007	Correa, 2009
C	C12	AF499801	Bahamas	Exuma Islands	23.77	-76.09	12	12	2000	Thornhill, 2006
C	C12	AF499801	Bahamas	Exuma Islands	24.35	-75.35	12	15	2003	Thornhill, 2009
C	C3	AF499789	United States	US Virgin Islands	18.30	-64.89	4	4	2007	Correa, 2009
C	C3	AF499789	Bahamas	Exuma Islands	23.77	-76.09	4	4	1998	LaJeunesse, 2002
C	C3	AF499789	United States	Florida Keys	24.59	-80.22	1	2	2000	Thornhill, 2006
C	C3	AF499789	United States	Florida Keys	25.04	-80.39	1	2	2003	Thornhill, 2009
C	C7	AF499797	United States	US Virgin Islands	18.30	-64.89	4	4	2007	Correa, 2009
C	C7	AF499797	Barbados	Eastern Caribbean	13.11	-59.32	6	10	2005	Finney, 2010
C	C7	AF499797	Barbados	Eastern Caribbean	13.11	-59.32	10	20	2005	Finney, 2010
C	C7	AF499797	Barbados	n/a	13.07	-59.39	0	5	2005	LaJeunesse, 2009
C	C7	AF499797	Barbados	n/a	13.07	-59.39	15	15	2005	LaJeunesse, 2009
C	C7a	n/a	Barbados	Eastern Caribbean	13.11	-59.32	6	10	2005	Finney, 2010
C	C7a	n/a	Barbados	Eastern Caribbean	13.11	-59.32	10	20	2005	Finney, 2010
C	C7a	n/a	Barbados	n/a	13.07	-59.39	0	5	2005	LaJeunesse, 2009
C	C7a	n/a	Barbados	n/a	13.07	-59.39	15	15	2005	LaJeunesse, 2009
D	D1	AF334660	United States	US Virgin Islands	18.30	-64.89	4	4	2007	Correa, 2009
D	D1	AF334660	United States	US Virgin Islands	18.30	-64.89	4	4	2007	Correa, 2009
D	D1	AF334660	United States	US Virgin Islands	18.30	-64.89	8	8	2007	Correa, 2009
D	D1	AF334660	Belize	South Yucatan	16.48	-88.05	1	5	2002	Finney, 2010
D	D1	AF334660	Bahamas	Exuma Islands	23.77	-76.09	n/a	n/a	1998	LaJeunesse, 2002
D	D1	AF334660	Barbados	n/a	13.07	-59.39	15	15	2005	LaJeunesse, 2009
D	D1	AF334660	United States	Florida Keys	24.59	-80.22	1	2	2000	Thornhill, 2006
D	D1	AF334660	United States	Florida Keys	24.59	-80.22	3	3	1998	Thornhill, 2006
D	D1a	AF499802	Bahamas	Exuma Islands	23.77	-76.09	n/a	n/a	1998	LaJeunesse, 2002
D	D1a	AF499802	United States	US Virgin Islands	18.30	-64.89	4	4	2007	Correa, 2009
D	D1a	AF499802	United States	US Virgin Islands	18.30	-64.89	4	4	2007	Correa, 2009
D	D1a	AF499802	United States	US Virgin Islands	18.30	-64.89	8	8	2007	Correa, 2009
D	D1a	AF499802	Belize	South Yucatan	16.48	-88.05	1	5	2002	Finney, 2010
D	D1a	AF499802	Barbados	n/a	13.07	-59.39	15	15	2005	LaJeunesse, 2009
D	D1a	AF499802	United States	Florida Keys	24.59	-80.22	1	2	2000	Thornhill, 2006
D	D1a	AF499802	United States	Florida Keys	24.59	-80.22	3	3	1998	Thornhill, 2006

Appendix Table 8.1: Database excerpt from GeoSymbio alignment file: records of *Symbiodinium* ITS2 gene isolated from *Montastraea annularis* corals only, *in hospite*

	2006					2010			2011			2012		
	B1	C1	B8(?)	C62	cryptic D1	B1	C1	cryptic D1	B1	C1	cryptic D1	B1	C1	cryptic D1
Snapshot reef	100%	0%	0%	0%	8%	100%	0%	6%	100%	0%	8%	100%	0%	0%
Seahorse reef	100%	18%	0%	0%	29%	n/a	n/a	n/a	100%	47%	0%	100%	0%	0%
School House reef	100%	0%	9%	0%	42%	100%	25%	14%	100%	25%	8%	100%	5%	5%
Propeller reef	100%	0%	0%	11%	13%	100%	7%	16%	100%	0%	17%	100%	0%	0%

Appendix Table 8.2: Percentage of *M. annularis* sampled colonies containing each symbiont taxa.

Dominant clade type

Observed: contingency table (total number of colonies sampled)

	2006	2010	2011	2012	Total
Clade B	53	33	33	43	162
Clade C	4	6	6	1	17
	57	39	39	44	179

Expected: contingency table

	2006	2010	2011	2012
Clade B	51.6	35.3	35.3	39.8
Clade C	5.4	3.7	3.7	4.2

Fishers exact test $p=0.088$ **Symbiodinium D**

Observed: contingency table (total number of colonies sampled)

	2006	2010	2011	2012	Total
D present	20	6	6	1	33
D absent	51	34	34	52	171
	71	40	40	53	204

Expected: contingency table

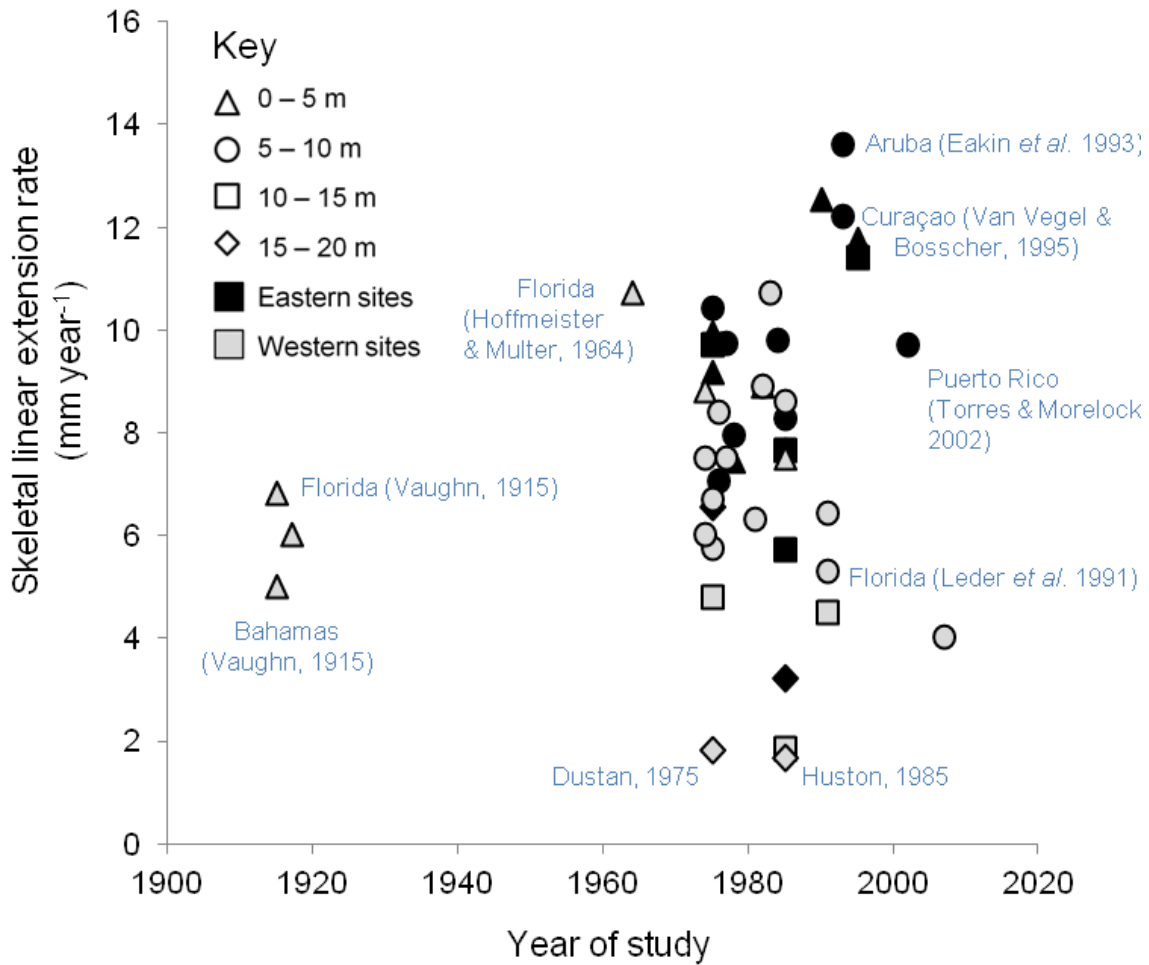
	2006.0	2010.0	2011.0	2012.0
D present	11.5	6.47	6.47	8.57
D absent	59.5	33.5	33.5	44.4

Fishers exact test $P<0.001$ **Appendix Tables 8.3:** Contingency tables for the Fisher Exact Test for temporal variation across the Bahamas

Locus	Motif	Number of alleles	Size of alleles (bp)	Genbank number	Primer sequence (5'-3')	Repeat sequence	T _r	Size (bp)
CA6.38	2	8	96–114		F: 5'-CAAAGAATATTCGGGGTCA-3' R: 5'-AGTTGATACGCCGGATGTGT-3'	(CA) ₈ CG(CA) ₄	56	112
Gv2	2	8	189–205	FJ390034	F: PET-TGTAGATGAGGTGCGGTCAG R: ACAATGATAGGGGGCTCACA	(CT) ₁₂	52	160–202
Gv42	2	5	156–164	FJ390038	F: 6FAM-ACTTCCTTTGTTGTGCGTCA R: GCGGGTACTTTTGAAGGT	(GA) ₁₃	54	153–165
Sym155	3	21	239–299	FJ390041	F: 6FAM-GTCCCTTCTCTGCTTACCTGTTTAGGAGA R: AGGACCCCTCATGCTGGAAGAGC	(CAA) ₅ 5bp(CAA) ₈ TAA(CAA) ₁₀	54	222–277
Sym254	3	16	154–202	FJ390042	F: VIC-TGAAAAGTTCGAAGTAAGTACCCAAAAGAAGAAC R: TGTGCGGCAGTGAACCCATCGTG	(CAA) ₁₈	54	136–189
Gv100	3	21	270–342	FJ390036	F: VIC-TATCAAGGTCCTATTTTCACAGCACAA R: ACAGCGAGGTATAGTATTGAGTAAAGAA	(GTT)3GAT(GTT) ₂₄ 11bp(GTT) ₁₉	54	252–282
GV44	2	0	116–175	FJ390039	F: PET-AATCGTTTTTGGGTGGTCTC R: TCAATTCGTACCCGACAATG	(CT)10(GT)2(CT)13(GT)2	54	116–175

Appendix Table 8.4 Characterisation and PCR amplification conditions of the seven *Symbiodinium* clade B microsatellite loci, that could be used in future work. Adapted from Santos and Coffroth (2003) and Andras *et al* 2009.

Chapter 9 Appendix



Appendix Figure 9.1. Scatter plot of published *Montastraea annularis* skeletal linear extension rates, taken from > 30 studies. Note that black symbols (depicting eastern Caribbean sites) appear to have higher LER estimates on average than grey (Western Caribbean) samples.

Site	Linear extension rate (mm year ⁻¹)	Depth	Publication
Florida	6.8	0 - 5 m	Vaughn, 1915
Bahamas	5.0	0 - 5 m	
Jamaica	6.0	5 m	Vaughn, 1917
Florida	10.7	3 m	Hoffmeister & Multer, 1964
Jamaica	6.2 - 8.8	0 - 15 m	Aller & Dodge, 1974
Jamaica	6.2 - 8.8	2 - 4 m	Dodge et al. 1974
Florida	6.0	n/a	MacIntyre & Smith, 1974
Jamaica	4.8 - 6.7	10 m	Dustan, 1975
	1.5 - 2.1	20 m	
US Virgin Isles	9.2	0 m	Baker & Weber, 1975
	9.9	4 m	
	10.4	9 m	
	9.7	13 m	
	6.5	18 m	
Jamaica	6.7	10 m	Dustan, 1975
	4.8	15 m	
Curaçao	6.3 - 7.8	10 m	Bak, 1976
Florida	8.4	n/a	Shinn, 1976
Barbados	9.7	0 - 10 m	Stearn <i>et al.</i> 1977
Honduras	4.0 - 11.0	n/a	Weber & White, 1977
Panama	5.0	n/a	
US Virgin Isles	6.6 - 8.3	5 m	Gladfelter <i>et al.</i> 1978
	7.0 - 8.9	10 m	
Belize	6.30	n/a	Highsmith, 1981
Belize	6.6 - 12.8	0 - 5 m	Graus & Macintyre, 1982
	5.2 - 11.2	5 - 10 m	
Florida	10.70	n/a	Davis, 1983
Bermuda	8.10	n/a	
US Virgin Isles	6.1 - 14.4	3 - 8 m	Dodge & Brass, 1984
US Virgin Isles	7.5 - 10.7	3 m	Hubbard & Scaturro, 1985
	5.8 - 8.9	6 m	
	6.8 - 9.3	9 m	
	6.7 - 10.2	12 m	
	3.4 - 7.4	15 m	
	2.4 - 4.2	18 m	
Jamaica	2.8 - 12.2	5 m	Huston, 1985
	5.9 - 11.3	10 m	
	1.0 - 2.7	15 m	
	1.2 - 2.1	20 m	
Barbados	9.8 - 15.5	5 m	Tomascik, 1990
Panama	8.5	1 - 3 m	Guzman <i>et al.</i> 1991
Florida	5.2 - 5.4	9 m	Leder <i>et al.</i> 1991
	5.2 - 7.2	10 m	
	4.5	14 m	
Panama	7.4 - 8.3	3 - 14 m	Knowlton <i>et al.</i> 1992
Aruba	12.2	0 - 10 m	Eakin <i>et al.</i> 1993
	13.6	0 - 10 m	
Curaçao	10.6 - 12.9	5 m	Van Vegel & Bosscher, 1995
	11.5 - 11.3	15 m	
Mexico	8.2	2 m	Carricart-Ganivet, 2000
	9.1	10 m	
Mexico	6.8 - 10.3	10 m	Carricart-Ganivet & Merino, 2001
Puerto Rico	9.7	7 m	Torres & Morelock 2002
Mexico	4.8 - 6.0	1 - 2 m	Cruz-Pinon <i>et al.</i> 2003
Mexico	7.80	2 - 10 m	Carricart-Ganivet, 2004
Jamaica	4.00		Mallela & Perry, 2007

Appendix Table 9.1: Data collated on *Montastraea annularis* skeletal linear extension rate from > 30 publications (see also Fig. 9.1 and 9.2)